An examination of peripheral blood to reflect transcriptomic adaptation to physical exercise training in sedentary men compared with sex-matched athletic phenotypes

by

Sergio Marin

B. Biology. (Hons)

Master Biomedicine

Submitted in Total Fulfilment of the Requirement for the

Doctor of Philosophy – Molecular Physiology

School of Science, Psychology and Sport

Federation University Australia

September, 2021

Statement of Authorship and Originality

Except where explicit reference is made in the text of the thesis, this thesis contains no material published elsewhere or extracted in whole or in part from a thesis by which I have qualified for or been awarded another degree or diploma. No other person's work has been relied upon or used without due acknowledgement in the main text and the list of references of the thesis. No editorial assistance has been received in the production of the thesis without due acknowledgement. Except where duly referred to, the thesis does not include material with copyright provisions or requiring copyright approvals.

Signature: _____

Date: 17/09/2021

Ethical approval declaration

Experimental studies within this thesis were approved by Federation University Human Research Ethics Committee (ID number: A17-134, see Appendix O), and complies with Federation University reporting process.

Thesis abstract

There is renewed interest in exercise genomics that peripheral blood RNA expression may be important to understand exercise mediated adaptations to exercise. However, there is little direct supporting evidence. Therefore, this thesis involved two studies to examine the relationship between RNA expression and exercise, and two experimental studies to examine relationships and adaptive response of peripheral blood RNA in sedentary compared with athletic phenotypes. In the first two studies, we conducted both meta-analysis and network meta-analysis to examine current randomised controlled trial (RCT) evidence to determine current best evidence on the link between RNA expression and athletic phenotype in addition to head-to-head comparison of different exercise types to induce differential expression of RNA transcripts in sedentary compared with athletic phenotypes. We observed that current available body of RCTs in peripheral blood exercise genomics presents too large heterogeneity in study design, methodological and data reporting aspects. Thus, we concluded that peripheral blood cannot be established as a valid source for identifying, neither the effect of physical exercise training on transcriptomic markers nor the distinction of divergent transcriptomic profiles in response to different exercise modalities.

In the third and fourth studies, we aimed to determine whether peripheral blood RNA and circular RNA (circRNA) expression was different between sedentary and athletic phenotypes, and whether these transcripts were consistent in response to exercise training in exercise-naïve men. To achieve this, we conducted two STROBE compliant observational experiments of n=71 participants with distinct athletic phenotypes. We concluded that peripheral blood transcriptome expression might allow for identification of divergent athletic phenotypes, although this is not supported by further examination of peripheral blood RNA expression levels in response to an exercise training intervention.

The sum of works presented in this thesis does not agree with many propositions relating to the strength of evidence in peripheral blood transcriptomics literature. This is principally due to the heterogeneity and lack of consistency of research in this field which is currently insufficient to provide any strong conclusions. In conclusion, peripheral blood RNA and circRNA do not yet offer useful avenues to predict the adaptive response to different exercise types in athletic and non-athletic men.

Acknowledgments

This thesis would have not been completed without the guidance and support from a team of colleagues, friends, and most importantly, family. I would like to thank my team of colleagues in the lab and in the faculty. All of you have contributed with your grain of sand, which has been paramount for the completion of this project. Specifically, thanks to the Federation University academics who engaged with me during my studies. Itemising thoughtful discussions with so many is only prevented by the frequency of positive engagement and the present thesis' word count.

The support of my supervisory team has been crucial to orientate me on the difficult endeavour that a PhD represents. To my associate supervisor, Dr. Kyle J Miller, your attention to detail has been remarkably valuable to polish the final result that is presented in this document. To my principal supervisor, Prof. Fergal Grace, you have been a tremendous support and pillar throughout this journey. Thanks to you I have deepened my understanding of research, science, and I have acquired knowledge and skills that go beyond the spectre of science. You have provided crucial support and confidence in difficult times and I am very grateful I have been able to share this path with a supervisor whom I now consider a friend.

I also want to thank all my friends, those from Australia and those back home for providing me with the fundamental social structure that helped me keep moving forward. You have helped to ease the otherwise difficult journey that this accomplishment represents.

Finally, but most importantly, I want to acknowledge the incredible support of my family, specially my parents. *Siempre he estado orgulloso de mi familia y en casos como estos es cuando recuerdo el porqué. Especialmente, mis padres. Habéis realizado un esfuerzo y trabajo tremendos para apoyarme incluso desde la enorme distancia a la que estaba. No solamente esta tesis, sino toda mi carrera como investigador, no podría haber sido posible*

sin vosotros. Vuestro papel ha sido imprescindible y vuestro apoyo irremplazable a la hora de apoyarme en este viaje. Muchas gracias.

Table of Contents

1 INTRODUCTION 26

1.1 References 32

2 GENERAL METHODOLOGY 36

2.1 Study design 36

2.2 Participants 37

2.3 Experimental group classification 38

2.4 Body composition 38

2.5 Blood collection 39

2.6 1 Repetition Maximum test (1RM) 39

2.7 Assessment of Cardiorespiratory fitness 40

2.8 Exercise intervention 41

2.8.1 Mixed exercise training (MET) program 41

2.8.2 STRENGTH exercise training (RET) program 41

2.8.3 AEROBIC exercise training (AET) program 42

2.8.4 AEROBIC and STRENGTH protocols during the study. 42

2.9 RNA extraction protocol 42

2.10 Library preparation and RNA sequencing 42

2.11 Statistical power and sample size calculation 43

2.12 Physiological data analysis 43

2.13 RNA-seq bioinformatical analysis 44

2.14 Circular RNA (circRNA) bioinformatical analysis 46

2.15 References 47

3 AN EXAMINATION OF CHRONIC AEROBIC OR RESISTANCE EXERCISE TRAINING ON PERIPHERAL BLOOD TRANSCRIPTOMICS IN HEALTHY MALES: A SYSTEMATIC REVIEW AND META-ANALYSIS OF CANDIDATE SIGNATURES FROM RANDOMISED CONTROLLED TRIALS (RCTS) 49

3.1 ABSTRACT 50

3.2 INTRODUCTION 53

3.3 MATERIALS AND METHODS 55

3.3.1 Protocol and registration 55

3.3.2 Eligibility criteria 55

3.3.3 Study selection and data collection process 55

3.3.4 Risk of bias in individual studies 57

3.3.5 Summary of outcomes 57

3.3.6 Synthesis of results 58

3.4 RESULTS 58

3.4.1 Study selection 58

3.4.2 Study characteristics 59

3.4.3 Risk of bias within studies 60

3.4.4 Results of individual studies 60

3.4.5 Synthesis of results 61

3.5 DISCUSSION 62

3.5.1 Summary of main findings 62

3.5.2 Summary of studies meeting eligibility 63

3.5.3 Study design 65

3.5.4 Methodology 67

3.5.5 Data reporting 69

3.5.6 Strengths and limitations 69

3.6 CONCLUSION 70

3.7 REFERENCES 71

4 COMPARATIVE EFFICACY OF DIFFERENT EXERCISE TYPES TO CHARACTERISE PERIPHERAL BLOOD TRANSCRIPTOMICS IN HUMANS: A SYSTEMATIC REVIEW AND NETWORK META-ANALYSIS OF CANDIDATE SIGNATURES FROM RANDOMISED CONTROLLED TRIALS (RCTS) 82

4.1 ABSTRACT 83

4.2 INTRODUCTION 85

4.3 METHODS 87

4.3.1 Protocol and registration 87

4.3.2 Eligibility criteria 87

4.3.3 Study selection and data collection process 88

4.3.4 Risk of bias in individual studies 89

4.3.5 Summary of outcomes 90

4.3.6 Synthesis of results 90

4.4 RESULTS 91

4.4.1 Study selection 91

4.4.2 Study characteristics 92

4.4.3 Exercise type characteristics 93

4.4.4 Risk of bias within studies 93

4.4.5 Results of individual studies 94

4.4.6 Synthesis of results 95

4.5 DISCUSSION 95

4.6 CONCLUSSION 98

4.7 REFERENCES 99

5 EXAMINATION OF PERIPHERAL BLOOD TRANSCRIPTOME (PBT) EXPRESSION TO CHARACTERISE TRANSCRIPTOMIC ADAPTATION OF SEDENTARY MALE PARTICIPANTS TO SUPERVISED EXERCISE TRAINING COMPARED WITH ATHLETIC PHENOTYPES: A STROBE COMPLIANT OBSERVATIONAL STUDY. 118

5.1 ABSTRACT 119

5.2 INTRODUCTION 121

5.3 METHODS 124

5.3.1 Participants 124

5.3.2 Study design 124

5.3.3 Body composition 124

5.3.4 Blood collection 125

5.3.5 Determination of muscular strength 125

5.3.6 Determination of maximal oxygen consumption ($\dot{V}O_{2max}$) 125

5.3.7 RNA extraction 126

5.3.8 Library preparation and RNA sequencing 126

5.3.9 Mixed exercise training (MET) 126

5.3.10 Resistance exercise training (RET) 126

5.3.11 Aerobic exercise training (AET) 126

5.3.12 RNA sequencing profiling 127

5.3.13 Statistical analysis 127

5.4 RESULTS 128

5.4.1 CRF and Muscular Strength 129

5.4.2 Transcriptome Expression 130

5.5 DISCUSSION 132

Main findings 132

5.6 CONCLUSION 142

5.7 REFERENCES 143

6 PERIPHERAL BLOOD CIRCRNA MAY DIFFERENTIATE ATHLETIC PHENOTYPE BUT DOES NOT CHARACTERISE ADAPTATION TO MIXED EXERCISE TRAINING IN SEDENTARY PHENOTYPE: A STROBE COMPLIANT OBSERVATIONAL STUDY. 154

6.1 ABSTRACT 155

6.2 INTRODUCTION 157

6.3 METHODS 159

6.3.1 Participants 159

6.3.2 Study design 159

6.3.3 Body composition 160

6.3.4 Blood collection 160

6.3.5 Determination of muscular strength 160

6.3.6 Determination of maximal oxygen consumption ($\dot{V}O_{2max}$) 160

6.3.7 RNA extraction 161

6.3.8 Library preparation and RNA sequencing 161

6.3.9 Mixed exercise training (MET) 161

6.3.10 CircRNA microarray expression profiling 161

6.3.11 Statistical analysis 162

6.4 RESULTS 163

6.4.1 Athletic Phenotype Characterisation 163

6.4.2 Athletic circRNA Expression Profile Characterisation 164

6.5 DISCUSSION 164

6.6 CONCLUSION 168

6.7 REFERENCES 169

7 REALISATION OF AIMS AND HYPOTHESES 185

List of tables

Table 3-1 Participants, protocol, exercise characteristics, and outcomes of the studies included in this review. 75

Table 4-1 Participants, protocol, exercise characteristics, and outcomes of the RCTs included in this review. 102

Table 4-2 List of transcripts examined in at least 2 RCTs. 110

Table 5-1 Participants characteristics at enrolment. 148

Table 5-2 Physiological measurements after 4 weeks of MET for SEDENTARY and the same period for STRENGTH and AEROBIC. 149

Table 5-3 Physiological measurements after 4 weeks of AET for SEDENTARY AEROBIC and RET for SEDENTARY STRENGTH, and the same period for STRENGTH and AEROBIC; 150

Table 6-1 Participants characteristics at enrolment. 181

Table 6-2 Physiological measurements after 4 weeks of MET for SEDENTARY and the same period for normal training in STRENGTH and AEROBIC. 182

List of figures

Figure 1-1 PubMed search (July 2021) conducted using search terms: ‘physical activity’, ‘exercise’, ‘blood’, ‘gene expression’. 28

Figure 2-1 Example of protocol design and testing points for a given sedentary participant..37

Figure 2-2 Example of protocol design and testing points for a given trained athlete..... 37

Figure 2-3. List of biotype proportions in the refseq for hg38 (GCA_000001405.15)..... 45

Figure 3-1 Number of publications per year using "physical activity OR exercise AND blood AND gene expression" as boolean operators (PubMed search (July 2021)..... 76

Figure 3-2 Flowchart of screening process. 77

Figure 3-3 Example PubMed search string used for this meta-analysis. 78

Figure 3-4 Summary of the exercise intervention for Thompson et al. study. (Adapted from Thompson et al., 2010)..... 79

Figure 3-5 Risk of bias chart of studies included in the review. 80

Figure 4-1 Example search string Network Meta-analysis in PubMed..... 111

Figure 4-2 Schematic of exercise types compared within this review. 112

Figure 4-3 Flowchart of screening process. 113

Figure 4-4 Risk of bias charts of studies included in the review. 114

Figure 4-5 Forest plot of individual and pooled effect size estimates for IL-10 expression after moderate/high-intensity exercise training..... 115

Figure 4-6 Forest plot of individual and pooled effect size estimates for TNF-α expression after moderate/high-intensity exercise training..... 116

Figure 5-1 Flow of Participants through the study..... 151

Figure 5-2 TRNH expression in AEROBIC compared with sedentary participants throughout the study. 152

Figure 6-1 Flow of participants through the study..... 183

List of appendices

	Title	Page
Appendix A	Data collection form	188
Appendix B	Differential gene expression AEROBIC vs SEDENTARY at enrolment	193
Appendix C	Differential gene expression STRENGTH vs SEDENTARY at enrolment	203
Appendix D	Differential gene expression AEROBIC and STRENGTH vs SEDENTARY at enrolment	204
Appendix E	Differential gene expression in SEDENTARY after 4 weeks of MET	205
Appendix F	Differential gene expression AEROBIC vs SEDENTARY after 4 weeks of MET	206
Appendix G	Differential gene expression STRENGTH vs SEDENTARY after 4 weeks of MET	212
Appendix H	Differential gene expression AEROBIC vs SEDENTARY AEROBIC after 4 weeks of specific training	213
Appendix I	Differential gene expression STRENGTH vs SEDENTARY STRENGTH after 4 weeks of specific training	217
Appendix J	Differential circRNA expression AEROBIC vs SEDENTARY at enrolment	219
Appendix K	Differential circRNA expression STRENGTH vs SEDENTARY at enrolment	275
Appendix L	Differential circRNA expression in SEDENTARY after 4 weeks of MET	289

Appendix M	Differential circRNA expression AEROBIC vs SEDENTARY after 4 weeks of MET	290
Appendix N	Differential circRNA expression STRENGTH vs SEDENTARY after 4 weeks of MET	364
Appendix O	Ethical Approval statement	395

List of abbreviations

Abbreviation	Description
$\Delta \dot{V}O_{2max}$	Delta $\dot{V}O_{2max}$
1RM	1 Repetition Maximum
ACSM	The American College of Sports Medicine
AdipoR1	Adiponectin Receptor 1
AdipoR2	Adiponectin Receptor 2
ADP	Adenosine Diphosphate
AET	Aerobic Exercise Training
AGRF	Australian Genome Research Facility
APSS	Adult Pre-Exercise Screening System
ATGL	Adipose Triglyceride Lipase
ATP	Adenosine Triphosphate
BAX	Bcl-2-associated X protein
BCL2	B-cell lymphoma 2
BM	Body Mass
BMI	Body Mass Index
C9orf16	Chromosome 9 open reading frame 16
$Ca2^{+}$	Calcium Ion
CACNA1A	Calcium Voltage-Gated Channel Subunit Alpha1 A
cAMP	Cyclic Adenosine Monophosphate
CD34	Cluster of Differentiation 34
CD83	Cluster of Differentiation
cDNA	Complementary DNA
CG	Control Group

CI	Confidence Interval
CircRNA	Circular RNA
CIRI	Circular RNA Identifier
CLC	Charcot-Leyden Crystal Galectin
CONSORT	CONsolidated Standards Of Reporting Trials
CPM	Counts Per Million
CRF	Cardiorespiratory Fitness
CS	Compound Symmetry
DE	Differential Expression
DEFA1	Defensin Alpha 1
DEFA1	Defensin Alpha 3
DEFA1B	Defensin Alpha 1B
dTTP	Deoxythymidine Triphosphate
dUTP	Deoxyuridine Triphosphate
EMI-II	Exercise Motivations Inventory-II
ESSA	Exercise & Sports Science Australia
FC	Fold Change
FDR	False Discovery Rate
FOSB	FosB Proto-Oncogene, AP-1 Transcription Factor Subunit
G0S2	G0/G1 Switch 2
Gdown1	GRINL1A Complex Locus Protein 1
glmQL	Generalized Linear Models with Quasi-Likelihood Test
GPR20	G Protein-Coupled Receptor 20
GTF	Gene Transfer Format
HBA1	Haemoglobin Subunit Alpha 1

HBG2	Haemoglobin Subunit Gamma 2
HR_{max}	Heart Rate Maximum
ICD	International Classification of Disease
IG	Intervention Group
IL-10	Interleukin-10
IL-1B	Interleukin 1 Beta
IL-6	Interleukin-6
IL8	Interleukin-8
LMM	Linear Mixed Model
lncRNA	Long non-coding RNA
LOC100996740	Uncharacterized LOC100996740 pseudogene
LOC101929887	Uncharacterized LOC101929887 pseudogene
MeSH	Medical Subject Headings
MET	Mixed Exercise Training
miRNA	Micro RNA
NECTIN2	Nectin Cell Adhesion Molecule 2
NG-Seq	Next Generation-Sequencing
NK	Natural Killer
OXPHOS	Oxidative Phosphorylation
PBMC	Peripheral Blood Mononuclear Cell
PBT	Peripheral Blood Transcriptome
PCA	Principal Component Analysis
PDI	Disulfide Isomerase
PICOS	Popoulation Intervention Comparison Outcome Study type
POLR2M	RNA Polymerase II Subunit M

PRISMA	Preferred Reporting Items for Systematic Reviews and Meta-analyses
PROSPERO	International Prospective Register of Systematic Reviews
PVRL2	Nectin Cell Adhesion Molecule 2
QC	Quality Control
qPCR	Quantitative Polymerase Chain Reaction
RABT	Reference Annotation Based Assembly Option
RCT	Randomised Controlled Trial
RER	Respiratory Exchange Ratio
RET	Resistance Exercise Training
RNA	Ribonucleic Acid
RNF17	Ring Finger Protein 17
Rob tool	Cochrane Collaboration's Tool for Assessing Risk of Bias
ROS	Reactive Oxygen Species
RPE	Rating of Perceived Exertion
RPL13AP5	Ribosomal Protein L13a Pseudogene 5
rRNA	Ribosomal RNA
RUVr	Remove Unwanted Variation Using Residuals
SD	Standard Deviation
SF-36	36-Item Short Form Survey
SMA	Sports Medicine Australia
STROBE	STrengthening the Reporting of OBservational studies in Epidemiology
SV	Surrogate Variable
TMM	Trimmed Mean of M Values
TNF-a	Tumor Necrosis Factor Alpha
TRNA	Mitochondrially Encoded TRNA-Alanine

TRNE	Mitochondrially Encoded TRNA-Glutamic Acid
TRNF	Mitochondrially Encoded TRNA-Phenylalanine
TRNH	Mitochondrially Encoded TRNA-Histidine
TRNQ	Mitochondrially Encoded TRNA-Glutamine
TXNDC5	Thioredoxin Domain Containing 5
$\dot{V}O_{2max}$	Maximal Oxygen Consumption

Format and organisation of this thesis

The present document is prepared according to the “sandwich thesis” format. Thus, this thesis is comprised of a general introduction, four original research papers (Chapters 3 to 6) and accompanied by general conclusion which addresses a realisation of thesis aims. All experimental chapters are formatted according to an intended peer-reviewed journal outlet. Each is currently being prepared for publication in peer reviewed journals with the candidate as first author.

Contributions to Thesis Chapters with Multiple Authors

Study 1 (Chapter 3)

The original idea for this study was conceived by SME and FG. PROSPERO registration of meta-analysis study was conducted by SME and FG. Screening process of articles was done by SME and DH, and discordance solved by FG. Data analysis was conducted by SME and confirmed by FG and KJM. Interpretation of data and findings was done by SME and FG. SME and FG prepared the first draft of the chapter. SME, KJM and FG contributed to the final version of the thesis chapter.

Study 2 (Chapter 4)

SME and FG conceived the original idea from which this study follows. SME and FG registered the Network Meta-Analysis at PROSPERO database. Original articles were screened by SME and DH, and when in disagreement, discordance was solved by FG. SME and KJM conducted analysis of the data, and it was confirmed by FG. Interpretation of data and findings was conducted by SME and FG. First draft was prepared by SME and FG, and SME, KJM and FG contributed to the final version of the thesis chapter.

Study 3 (Chapter 5)

The original idea for this experimental study was conceived by SME and FG. Ethics approval for the trial was obtained by FG and SME. Data analysis and interpretation of findings was conducted by SME, KJM, and FG. First draft of the chapter was prepared by SME and FG. SME, KJM, and FG contributed to the final version of the chapter.

Study 4 (Chapter 6)

SME and FG conceived the original idea for the experimental study described in this chapter. Ethical approval for the trial was obtained by FG and SME. SME performed data analysis which was confirmed by FG and KJM. SME and FG interpreted study findings. Preparation of the first draft was conducted by SME and supported by FG. SME, KJM, and FG each contributed to the final version of this thesis chapter.

Original research chapters within this thesis are compliant with COPE guidelines on publication ethics, where each co-author met adequate contribution relating to intellectual content and approved the final manuscripts. (https://doi.org/10.24318/cope.2018.1.1)

1 INTRODUCTION

Complete sequencing of the Human Genome was achieved in April 2003, which offered valuable information and established *de novo* human genetic pathways with a long-term goal of achieving personalised medicine [1]. In the interim, the field of genetics has expanded with a requirement to consider genomic variants in concert with environmental stimuli and differential expression of transcripts which coalesce to determine athletic phenotypes. Protein coding RNAs (mRNA) have been identified as key protein synthesising molecules that ultimately determine phenotype characterisation. As such, these molecules are now acknowledged as key players in gene expression and exercise proteomics.

Perhaps the greatest revelation from the Human Genome Project, and counter to *a priori* expectations of sizeable gene counts, was that the entire coding sequences constitute a mere 20,000 - 25,000 protein-coding genes and comprises less than 2% of the entire human genome [1]. This required a renewed focus on what was formerly termed ‘junk DNA’ and subsequent research during the past decade uncovered that prior genetic research may have been overly cavalier with terminology. There has been subsequent and gradual acceptance for contributory importance of non-coding genomic material to, at least in part, dictate important phenotypic outcomes. Indeed, we have recently witnessed a broader interrogation of human transcriptomes with emphasis on non-coding RNA (ncRNA) architecture, including microRNAs (miRNAs) and long noncoding RNAs (lncRNAs) [2-5]. Specifically, lines of inquiry have predominated in discovery research of dysregulation within human gene networks relevant for clinical and hereditary disease. Within these disease models, non-coding material are emerging as fundamental components of networked gene regulation across

diverse biological processes, where both regulation and dysregulation of their expression is being identified in human health and disease [6-10].

Compared with linear RNA transcripts, circular RNAs (circRNAs) are receiving attention as a novel class of endogenous ncRNAs which offer a greater degree of stability than their linear counterparts as a consequence of their unique circular covalently bonded structure, thus offering greater protection from cleavage and subsequent degradation by exonucleases [11]. circRNAs may have key roles in human gene expression and signalling pathways and because they are present in multiple human sample-site tissues (blood, saliva, exomes) they are gaining credibility as potential biomarkers in disease and health [12-14]. Physical exercise is a stimulus which promotes complex physiological adaptations within the human body. Moreover, repetitive exercise training develops particular phenotypes and are characterised by numerous physiological changes which improve physical capacity and contribute to disease prevention. These physiological adaptations have been well studied [15-23]. However, while these effects are well known, the genetic transcripts which dictate optimal adaptation to exercise (or individual exercise types) are not well understood. Similarly, genetic mechanisms which drive metabolic processes and adaptation to exercise training are yet to be established.

This complex field of research is perhaps the most exciting unresolved scientific challenge for researchers and stakeholders in health optimization and human performance. Uncovering key aspects of exercise genetics, gene discovery, regulatory ncRNAs, and expression patterns offer further potential to identify individual predisposition for high performance within a given sport discipline. Moreover, as different types of exercise modalities confer different phenotypic adaptation [24, 25], it stands to reason that ncRNA expression profiles likely express transcript mechanisms which may be dependent on exercise modality [26-28]. It is of noteworthy importance to highlight that this field remains in its

infancy, thus, before moving into attempting a deeper understanding of the genetic mechanisms responsible for the physiological processes that we see in adaptation to exercise, there are some key fundamentals which must be established in order to pursue this ambitious task.

To date, researchers undertaking exercise genomics research have predominantly leaned towards the investigation of biopsy techniques of skeletal muscle to characterise the transcriptomic responses to exercise training [29-35]. More recently, peripheral blood has been proposed as a novel method to employ in this type of research, as observed by increased research output within the exercise genetics scientific community (**Fig. 1-1**). As such, the underlying principle is that peripheral blood may reflect systemic responses [36] as a surrogate downstream reflection of genomic processes within skeletal muscle during biological adaptation to physical exercise [37, 38]. In context with many questions which remain unresolved in the field of exercise genetics, this thesis will pursue multiple lines of enquiry confined within an overarching investigation for the utility of peripheral blood

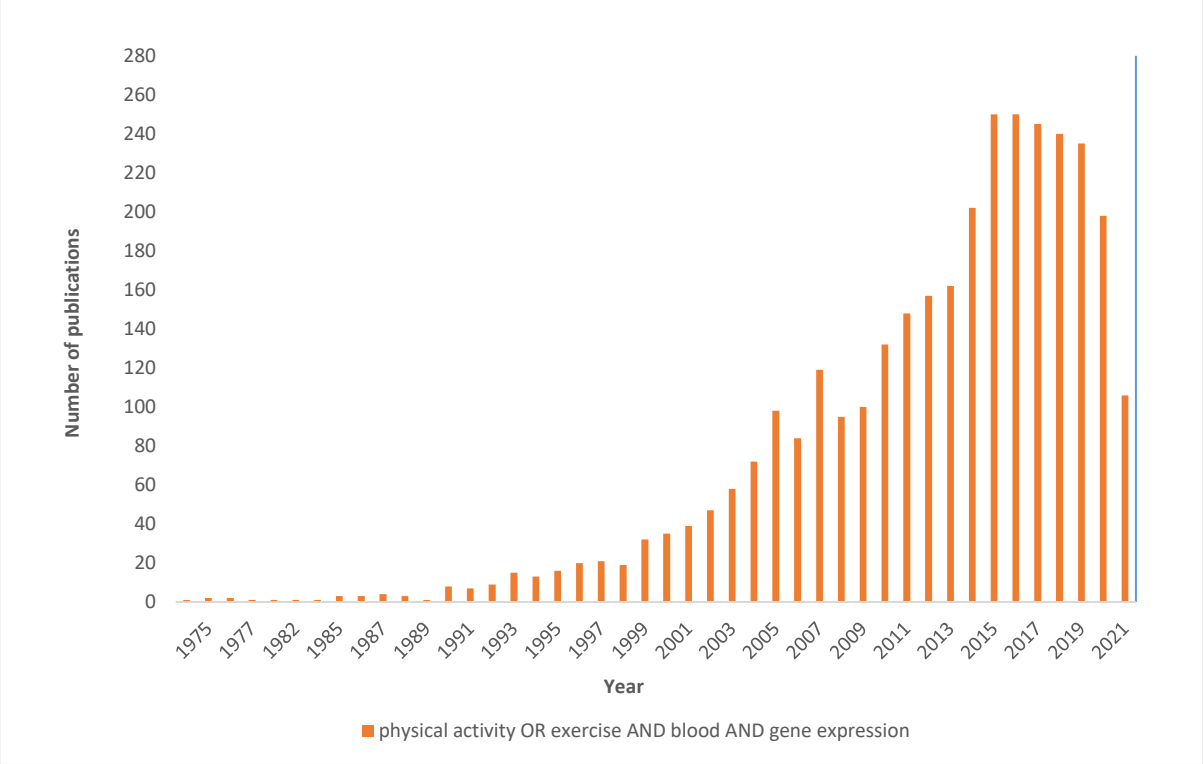

Figure 1-1 *PubMed search (July 2021) conducted using search terms: 'physical activity', 'exercise', 'blood', 'gene expression'.*

transcriptome (PBT) expression analysis to characterise exercise adaptation in apparently healthy sedentary humans. The foundations of this thesis are centered on four main research questions, with corresponding hypotheses;

i) **Does current randomised controlled trial (RCT) evidence identify peripheral blood transcriptomic signatures to characterise athletic phenotype in men?**

Hypothesis 1

(H_0): Peripheral blood is not a valid source for identifying the effect of physical exercise training on transcriptomic markers of apparently healthy males in (RCTs).

(H_1): Peripheral blood can be considered a valid source for identifying the effect of physical exercise training on transcriptomic markers of apparently healthy males in (RCTs).

ii) **Does RCT evidence identify different exercise types (head-to-head comparison) to differentiate peripheral blood transcriptome (PBT) expression in divergent athletic phenotypes?**

Hypothesis 2

(H_0): Peripheral blood is not a valid source for identification of differential effects of divergent physical exercise training on transcriptomic markers of apparently healthy exercise-naïve participants in Randomised Controlled Trials (RCTs).

(H_1): Peripheral blood can be considered valid source for identification of differential effects of divergent physical exercise training on transcriptomic markers of apparently healthy exercise-naïve participants in Randomised Controlled Trials (RCTs).

iii) **Can a structured supervised exercise training program identify different PBT characteristics in sedentary male participants compared with athletic phenotypes?**

Hypothesis 3a

(H_0): Peripheral Blood Transcriptome (PBT) expression would not discriminate between exercise-naïve sedentary males (SEDENTARY) compared with either AEROBIC or STRENGTH athletic phenotypes.

(H_1): Peripheral Blood Transcriptome (PBT) expression could discriminate between exercise-naïve sedentary males (SEDENTARY) compared with either AEROBIC or STRENGTH athletic phenotypes.

Hypothesis 3b

(H_0): 4 weeks of Mixed Exercise Training (MET) would not identify unique adaptive Peripheral Blood Transcriptome (PBT) expression changes within SEDENTARY compared with either AEROBIC or STRENGTH athletic phenotypes.

(H_1): 4 weeks of Mixed Exercise Training (MET) will identify unique adaptive Peripheral Blood Transcriptome (PBT) expression changes within SEDENTARY compared with either AEROBIC or STRENGTH athletic phenotypes.

iv) **Can a supervised mixed exercise training (MET) program identify non-coding PBT (circRNA) characteristics in sedentary male participants compared with athletic phenotypes?**

Hypothesis 4a

(H_0): Peripheral blood circRNA expression would not discriminate between SEDENTARY, AEROBIC and STRENGHT phenotypes.

(H_1): Peripheral blood circRNA expression will discriminate between SEDENTARY, AEROBIC and STRENGHT phenotypes.

Hypothesis 4b

(H_0): Peripheral blood circRNA expression would not be different in SEDENTARY undergoing four weeks of Mixed Exercise Training (MET), compared with AEROBIC and STRENGTH athletes.

(H_1): Peripheral blood circRNA expression will change in SEDENTARY undergoing four weeks of Mixed Exercise Training (MET), compared with AEROBIC and STRENGTH athletes.

1.1 REFERENCES

1. Heilig R, Eckenberg R, Petit J, Fonknechten N, Silva C, Cattolico L, et al. International Human Genome Sequencing Consortium. Nature 431, 931-945. Nature. 2004;431(7011):931-45. Epub 2004/10/22. doi: 10.1038/nature03001. PubMed PMID: 15496913.
2. Cabili MN, Trapnell C, Goff L, Koziol M, Tazon-Vega B, Regev A, et al. Integrative annotation of human large intergenic noncoding RNAs reveals global properties and specific subclasses. Genes & development. 2011;25(18):1915-27. Epub 2011/09/06. doi: 10.1101/gad.17446611. PubMed PMID: 21890647; PubMed Central PMCID: PMCPMC3185964.
3. Derrien T, Johnson R, Bussotti G, Tanzer A, Djebali S, Tilgner H, et al. The GENCODE v7 catalog of human long noncoding RNAs: analysis of their gene structure, evolution, and expression. Genome research. 2012;22(9):1775-89. Epub 2012/09/08. doi: 10.1101/gr.132159.111. PubMed PMID: 22955988; PubMed Central PMCID: PMCPMC3431493.
4. Bartel DP. MicroRNAs: genomics, biogenesis, mechanism, and function. Cell. 2004;116(2):281-97. Epub 2004/01/28. PubMed PMID: 14744438.
5. Sood P, Krek A, Zavolan M, Macino G, Rajewsky N. Cell-type-specific signatures of microRNAs on target mRNA expression. Proceedings of the National Academy of Sciences of the United States of America. 2006;103(8):2746-51. Epub 2006/02/16. doi: 10.1073/pnas.0511045103. PubMed PMID: 16477010; PubMed Central PMCID: PMCPMC1413820.
6. Tijsen AJ, Creemers EE, Moerland PD, de Windt LJ, van der Wal AC, Kok WE, et al. MiR423-5p as a circulating biomarker for heart failure. Circulation research. 2010;106(6):1035-9. Epub 2010/02/27. doi: 10.1161/circresaha.110.218297. PubMed PMID: 20185794.
7. Fichtlscherer S, De Rosa S, Fox H, Schwietz T, Fischer A, Liebetrau C, et al. Circulating microRNAs in patients with coronary artery disease. Circulation research. 2010;107(5):677-84. Epub 2010/07/03. doi: 10.1161/circresaha.109.215566. PubMed PMID: 20595655.
8. Long G, Wang F, Duan Q, Chen F, Yang S, Gong W, et al. Human circulating microRNA-1 and microRNA-126 as potential novel indicators for acute myocardial infarction. International journal of biological sciences. 2012;8(6):811-8. Epub 2012/06/22. doi: 10.7150/ijbs.4439. PubMed PMID: 22719221; PubMed Central PMCID: PMCPMC3372885.
9. Niu ZY, Sun SY, Li GX. The polymorphism at the miRNA binding site of GOLGA(7) is associated with the Non-Hodgkin's lymphoma cancer risk. Int J Clin Exp Pathol. 2017;10(3):3735-8. PubMed PMID: WOS:000399083300149.
10. Li Z, Niu YJ. Association between lncRNA H19 (rs217727, rs2735971 and rs3024270) polymorphisms and the risk of bladder cancer in Chinese population. Minerva Urologica E Nefrologica. 2019;71(2):161-7. Epub 2018/03/30. doi: 10.23736/s0393-2249.18.03004-7. PubMed PMID: WOS:000469464100008.
11. Memczak S, Jens M, Elefsinioti A, Torti F, Krueger J, Rybak A, et al. Circular RNAs are a large class of animal RNAs with regulatory potency. Nature. 2013;495(7441):333-8. Epub 2013/03/01. doi: 10.1038/nature11928. PubMed PMID: 23446348.
12. Memczak S, Papavasileiou P, Peters O, Rajewsky N. Identification and Characterization of Circular RNAs As a New Class of Putative Biomarkers in Human Blood. PloS one. 2015;10(10):e0141214. Epub 2015/10/21. doi: 10.1371/journal.pone.0141214. PubMed PMID: 26485708; PubMed Central PMCID: PMCPMC4617279 covering the use of

blood circular RNAs as biomarkers in neurological diseases. This did not alter the authors' adherence to PLOS ONE policies on sharing data and materials.
13. Koh W, Pan W, Gawad C, Fan HC, Kerchner GA, Wyss-Coray T, et al. Noninvasive in vivo monitoring of tissue-specific global gene expression in humans. Proceedings of the National Academy of Sciences of the United States of America. 2014;111(20):7361-6. Epub 2014/05/07. doi: 10.1073/pnas.1405528111. PubMed PMID: 24799715; PubMed Central PMCID: PMCPMC4034220.
14. Zhang Z, Yang T, Xiao J. Circular RNAs: Promising Biomarkers for Human Diseases. EBioMedicine. 2018;34:267-74. Epub 08/02. doi: 10.1016/j.ebiom.2018.07.036. PubMed PMID: 30078734; PubMed Central PMCID: PMCPMC6116471.
15. Booth FW, Roberts CK, Laye MJ. Lack of exercise is a major cause of chronic diseases. Comprehensive Physiology. 2012;2(2):1143-211. Epub 2012/04/01. doi: 10.1002/cphy.c110025. PubMed PMID: 23798298; PubMed Central PMCID: PMCPMC4241367.
16. Lear SA, Hu W, Rangarajan S, Gasevic D, Leong D, Iqbal R, et al. The effect of physical activity on mortality and cardiovascular disease in 130 000 people from 17 high-income, middle-income, and low-income countries: the PURE study. Lancet (London, England). 2017;390(10113):2643-54. Epub 2017/09/26. doi: 10.1016/s0140-6736(17)31634-3. PubMed PMID: 28943267.
17. Thompson PD, Eijsvogels TH. New physical activity guidelines: A call to activity for clinicians and patients. Jama. 2018. Epub 2018/11/13. doi: 10.1001/jama.2018.16070. PubMed PMID: 30418469.
18. Blair SN, Kampert JB, Kohl HW, 3rd, Barlow CE, Macera CA, Paffenbarger RS, Jr., et al. Influences of cardiorespiratory fitness and other precursors on cardiovascular disease and all-cause mortality in men and women. Jama. 1996;276(3):205-10. Epub 1996/07/17. PubMed PMID: 8667564.
19. Blair SN, Kohl HW, 3rd, Paffenbarger RS, Jr., Clark DG, Cooper KH, Gibbons LW. Physical fitness and all-cause mortality. A prospective study of healthy men and women. Jama. 1989;262(17):2395-401. Epub 1989/11/03. PubMed PMID: 2795824.
20. Gulati M, Black HR, Shaw LJ, Arnsdorf MF, Merz CN, Lauer MS, et al. The prognostic value of a nomogram for exercise capacity in women. The New England journal of medicine. 2005;353(5):468-75. Epub 2005/08/05. doi: 10.1056/NEJMoa044154. PubMed PMID: 16079370.
21. Kokkinos P, Myers J, Kokkinos JP, Pittaras A, Narayan P, Manolis A, et al. Exercise capacity and mortality in black and white men. Circulation. 2008;117(5):614-22. Epub 2008/01/24. doi: 10.1161/circulationaha.107.734764. PubMed PMID: 18212278.
22. Mora S, Redberg RF, Cui Y, Whiteman MK, Flaws JA, Sharrett AR, et al. Ability of exercise testing to predict cardiovascular and all-cause death in asymptomatic women: a 20-year follow-up of the lipid research clinics prevalence study. Jama. 2003;290(12):1600-7. Epub 2003/09/25. doi: 10.1001/jama.290.12.1600. PubMed PMID: 14506119.
23. Braith RW, Stewart KJ. Resistance exercise training: its role in the prevention of cardiovascular disease. Circulation. 2006;113(22):2642-50. Epub 2006/06/07. doi: 10.1161/CIRCULATIONAHA.105.584060. PubMed PMID: 16754812.
24. Egan B, Zierath J. Exercise Metabolism and the Molecular Regulation of Skeletal Muscle Adaptation. Cell metabolism. 2013;17(2):162-84. Epub 2013/02/12. doi: 10.1016/j.cmet.2012.12.012. PubMed PMID: 23395166.
25. Hughes DC, Ellefsen S, Baar K. Adaptations to Endurance and Strength Training. Cold Spring Harbor perspectives in medicine. 2018;8(6):a029769. Epub 2017/05/12. doi: 10.1101/cshperspect.a029769. PubMed PMID: 28490537; PubMed Central PMCID: PMCPMC5983157.

26. Laine S, Högel H, Ishizu T, Toivanen J, Yli-Karjanmaa M, Grönroos TJ, et al. Effects of Different Exercise Training Protocols on Gene Expression of Rac1 and PAK1 in Healthy Rat Fast- and Slow-Type Muscles. Frontiers in physiology. 2020;11(1448):584661. Epub 2020/12/18. doi: 10.3389/fphys.2020.584661. PubMed PMID: 33329033; PubMed Central PMCID: PMCPMC7711069.
27. Pillon NJ, Gabriel BM, Dollet L, Smith JAB, Sardón Puig L, Botella J, et al. Transcriptomic profiling of skeletal muscle adaptations to exercise and inactivity. Nature communications. 2020;11(1):470. Epub 2020/01/26. doi: 10.1038/s41467-019-13869-w. PubMed PMID: 31980607; PubMed Central PMCID: PMCPMC6981202.
28. Olioso D, Dauriz M, Bacchi E, Negri C, Santi L, Bonora E, et al. Effects of Aerobic and Resistance Training on Circulating Micro-RNA Expression Profile in Subjects With Type 2 Diabetes. J Clin Endocrinol Metab. 2019;104(4):1119-30. Epub 2018/11/18. doi: 10.1210/jc.2018-01820. PubMed PMID: WOS:000469813500017.
29. O'Neill DS, Zheng D, Anderson WK, Dohm GL, Houmard JA. Effect of endurance exercise on myosin heavy chain gene regulation in human skeletal muscle. The American journal of physiology. 1999;276(2):R414-9. Epub 1999/02/10. doi: 10.1152/ajpregu.1999.276.2.R414. PubMed PMID: 9950919.
30. Wadley GD, Tunstall RJ, Sanigorski A, Collier GR, Hargreaves M, Cameron-Smith D. Differential effects of exercise on insulin-signaling gene expression in human skeletal muscle. Journal of applied physiology (Bethesda, Md : 1985). 2001;90(2):436-40. Epub 2001/02/13. doi: 10.1152/jappl.2001.90.2.436. PubMed PMID: 11160039.
31. Welle S, Bhatt K, Thornton CA. Stimulation of myofibrillar synthesis by exercise is mediated by more efficient translation of mRNA. Journal of applied physiology (Bethesda, Md : 1985). 1999;86(4):1220-5. Epub 1999/04/08. doi: 10.1152/jappl.1999.86.4.1220. PubMed PMID: 10194206.
32. Bamman MM, Roberts BM, Adams GR. Molecular Regulation of Exercise-Induced Muscle Fiber Hypertrophy. Cold Spring Harbor perspectives in medicine. 2018;8(6). Epub 2017/05/12. doi: 10.1101/cshperspect.a029751. PubMed PMID: 28490543; PubMed Central PMCID: PMCPMC5983156.
33. Williams RS, Neufer PD. Regulation of Gene Expression in Skeletal Muscle by Contractile Activity. Comprehensive Physiology. Sumplement 29: Handbook of Physiology1996. p. 1124-50.
34. Damas F, Ugrinowitsch C, Libardi CA, Jannig PR, Hector AJ, McGlory C, et al. Resistance training in young men induces muscle transcriptome-wide changes associated with muscle structure and metabolism refining the response to exercise-induced stress. European journal of applied physiology. 2018. Epub 2018/09/10. doi: 10.1007/s00421-018-3984-y. PubMed PMID: 30196447.
35. Timmons JA, Knudsen S, Rankinen T, Koch LG, Sarzynski M, Jensen T, et al. Using molecular classification to predict gains in maximal aerobic capacity following endurance exercise training in humans. Journal of applied physiology (Bethesda, Md : 1985). 2010;108(6):1487-96. Epub 2010/02/06. doi: 10.1152/japplphysiol.01295.2009. PubMed PMID: 20133430; PubMed Central PMCID: PMCPMC2886694.
36. Liew C-C, Ma J, Tang H-C, Zheng R, Dempsey AA. The peripheral blood transcriptome dynamically reflects system wide biology: a potential diagnostic tool. The Journal of Laboratory and Clinical Medicine. 2006;147(3):126-32. doi: 10.1016/j.lab.2005.10.005.
37. Zeibig J, Karlic H, Lohninger A, Damsgaard R, Smekal G. Do blood cells mimic gene expression profile alterations known to occur in muscular adaptation to endurance training? European journal of applied physiology. 2005;95(1):96-104. Epub 2005/04/09. doi: 10.1007/s00421-005-1334-3. PubMed PMID: 15815935.

38. Broadbent J, Sampson D, Sabapathy S, Haseler LJ, Wagner KH, Bulmer AC, et al. Gene networks in skeletal muscle following endurance exercise are coexpressed in blood neutrophils and linked with blood inflammation markers. Journal of applied physiology (Bethesda, Md : 1985). 2017;122(4):752-66. Epub 2017/01/21. doi: 10.1152/japplphysiol.00114.2016. PubMed PMID: 28104750.

2 GENERAL METHODOLOGY

Disclaimer: Chapters 5 and 6 are experimental studies conducted in the same cohort of participants. In order to avoid repetition and redundancy throughout the thesis, the general methodology shared by these two studies is provided in this section. Additionally, sufficient methodology details are provided within each of those chapters, so they can act as independent "stand alone" studies.

2.1 STUDY DESIGN

For chapters 5 and 6, participants were asked to report to the Federation University Exercise Physiology Laboratory for a briefing session before study enrolment. They received detailed information on the study enrolment and were informed of their rights to withdraw at any time. Participants were screened before participation by the Adult Pre-exercise Screening System (APSS) screening tool (https://www.essa.org.au/Public/ABOUT_ESSA/Adult_Pre-Screening_Tool.aspx) to ensure that they were free from any medical condition that would disqualify them from participating in the study. Once written informed consent was obtained, participants returned to the laboratory after 5-7 days for the first testing session. Measurements were taken at enrolment, 4 weeks after enrolment (follow-up 1) and 8 weeks after enrolment (follow-up 2). The standard testing diagrams for the participants are shown in **Figure 2-1** and **2-2**. Measurements consisted of standard anthropometric measurements (height, weight, body mass index, and body fat composition), cardiovascular measures (max heart rate and resting blood pressure), blood sample from antecubital vein for gene and circular RNA (circRNA) expression analysis, 1 repetition maximum test (1RM), cardiorespiratory fitness test ($\dot{V}O_{2max}$ test, defined by reaching at least three of the following criteria: volitional exhaustion, RER>1.15, blood lactate>7mmol/l, HR_{max}= 220-age, Rating of Perceived Exhaustion (RPE)>7, or plateau in $\dot{V}O_2$). All procedures were approved by Federation University Human Research Ethic Committee.

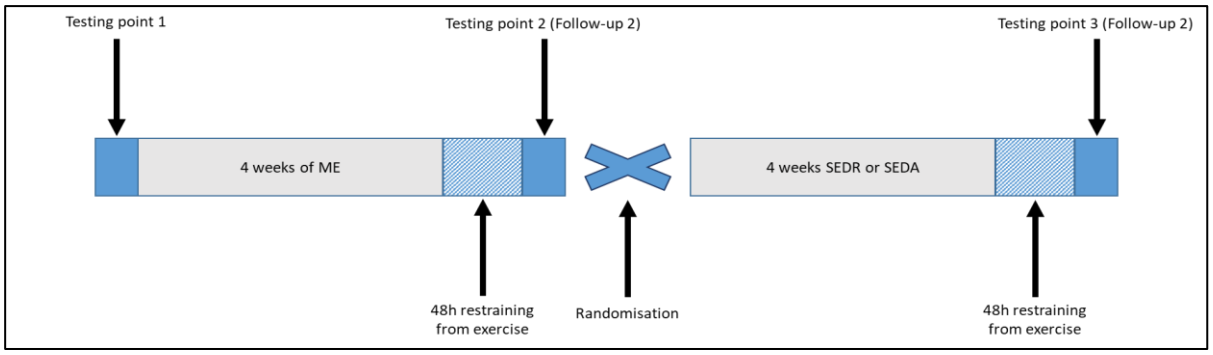

Figure 2-1 Example of protocol design and testing points for a given sedentary participant. *ME: Mixed Exercise training; SEDR: Sedentary STRENGTH training; SEDA: Sedentary AEROBIC training.*

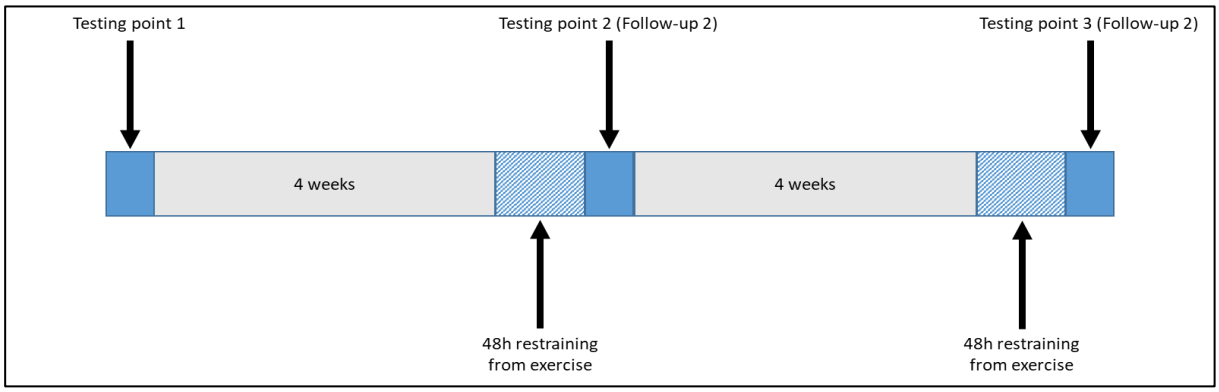

Figure 2-2 Example of protocol design and testing points for a given trained athlete*. Participants were asked to continue with their normal exercise regime during the length of the study.*

2.2 PARTICIPANTS

Seventy-nine participants were screened for eligibility. Eight participants were excluded (one for having a genetic disorder, four did not meet the performance criteria for AEROBIC/STRENGTH trained groups, one did not meet criteria for sedentary group, two did not meet age criteria). Seventy-one participants aged 18-45 years were recruited for this study consisting divergent athletic phenotypes; SEDENTARY exercise-naive (*n*=31) and two positive control groups of AEROBIC (*n*=20) and STRENGTH (*n*=20) trained athletes. SEDENTARY (*n*=28) underwent a crossover exercise program consisting mixed exercise training (MET) (4 weeks) before random allocation to SEDENTARY STRENGTH (*n*=14) or SEDENTARY AEROBIC (*n*=14) training (4 weeks). Participants were recruited from poster advertisement in local gymnasiums and phone calls to local organisations. When enrolled,

participants completed STAGE 1 section of the APSS screening tool. The APSS is a standardised way of pre-exercise screening in Australian health and fitness industry, developed by Fitness Australia, Exercise and Sports Science Australia (ESSA) and Sports Medicine Australia (SMA). The aim of this section was to identify individuals with a known disease, or signs or symptoms of disease, who may be at a higher risk of an adverse event during physical activity/exercise in order to exclude them from the study. All seventy-one participants were enrolled to the study.

2.3 EXPERIMENTAL GROUP CLASSIFICATION

Participants were assigned to one of three distinct groups which consisted either STRENGTH, AEROBIC, or SEDENTARY. STRENGTH were classified on their capability to perform on a strength test (one repetition maximum [1RM]; Bench press ≥ 1.25x body mass [BM]; Squat ≥ 1.75xBM & Deadlift ≥ 1.85xBM; Combined total of ≥ 4.86xBM). AEROBIC and SEDENTARY were classified on the determination they could not lift the combined bench press, deadlift and squat total of ≥ 4.86xBM. They were also classified according to their $\dot{V}O_{2max}$ ($\dot{V}O_{2max} \geq 60$ mL·Kg^{-1}·min^{-1} for AEROBIC and $VO_{2max} < 35$ mL·Kg^{-1}·min^{-1} for SEDENTARY).

2.4 BODY COMPOSITION

Participants arrived at the laboratory following an overnight fast and at least 48 hours after doing any kind of physical activity to avoid the presence of acute response signals to exercise. They had standard anthropometric (height, weight, body mass index, body fat) and cardiovascular measurements (resting blood pressure and resting heart rate) taken following clinical guidelines. Body mass was measured with participants in minimal clothing and using a balanced weighing scale (Seca, Cardiokinetics, Salford, UK), balanced before each round of weighting with a 5kg free mass. Height was measured with a stadiometer (Seca, Cardiokinetics, Salford, UK).

2.5 BLOOD COLLECTION

Blood was collected at the same time period of the day to account for the effect of any circadian rhythms on gene expression. After laying down in supine position for 15 minutes, a trained phlebotomist collected 3ml of peripheral blood into a Tempus Blood RNA Tube (Life Technologies™) via a venous catheter inserted into an antecubital forearm vein on the participant's non-dominant arm. Following blood collection, the tube was shaken vigorously for 10-15 seconds before being transferred to -80˚C freezer until biochemical processing.

2.6 1 REPETITION MAXIMUM TEST (1RM)

To be included, prospective participants were required to (a) have a minimum of 3 years of experience performing high-bar back squat exercise and bench press technique and (b) be able to perform a deep squat with a minimum barbell load of ≥2 times their body mass. Prospective participants were excluded if they had current or previous musculoskeletal injuries that would prevent them from performing squatting exercise or strength tests safely. Participants' muscular strength was tested by one repetition maximum (1RM) test. The muscular strength test consisted of three different exercises: bench press, deadlift and squats. Participants started with a general aerobic warm-up. Before attempting the 1RM for each exercise, participants carried out a specific warm-up consisting of 40-60% of their estimated 1RM for a maximum of 10 repetitions. After a minimum of 2 minutes recovery, participants advanced to 60-80% of their estimated 1RM for a maximum of five repetitions. Following this, there was another rest of at least 2 min, then a subsequent 90% of their estimated 1RM for a maximum of three repetitions and an extended rest of at least 5 min prior to the 1RM test. Participants completed 1-RM, strength assessments in random order with a minimum of 48 hours between strength assessments. During each session, participants performed strength assessments for the bench press and squat exercise in random order. Participants lifted a free

weight Olympic bar with weighted plates. During the bench press and incline press assessments, subjects laid with their back flat on the bench and their feet in full contact with the floor throughout the lift. Subjects grasped the bar with a thumb-lock grip at a position slightly greater than shoulder width. Trained spotters assisted with deploying the bar from the support rack, and participants were required to lower the bar in line with the areola of the chest before returning the bar to full arm extension. Barbell load was increased incrementally until the participants reached a load where failure (i.e., inability to lift the weight) occurred. Thus, 1RM was recorded as the heaviest barbell load to be that was successfully lifted. Verbal encouragement was provided for all participants participanting in 1RM attempts. The tests were carried out according to standards approved by the Australian Institute of Sports [36].

2.7 ASSESSMENT OF CARDIORESPIRATORY FITNESS

Maximal Oxygen Consumption Test ($\dot{V}O_{2max}$) was measured on a cycle ergometer (Velotron® Pro, Seattle, WA, USA). Expired gases were sampled every 30s using Moxus Modular $\dot{V}O_2$ System (AEI Technologies). Prior to conducting the test, gas analysers were calibrated using a gas bottle with exact known concentrations (4.05% CO_2 and 15.6% O_2, 0.3% CO_2 and 20.9% O_2) and inspired volume was calibrated using a 3 litre Hans Rudolph Series 5530 calibration syringe. Initial resistance at the electromagnetically braked cycle ergometer was set at 120W for AEROBIC and STRENGTH, and 100W for SEDENTARY, SEDENTARY AEROBIC, and SEDENTARY STRENGTH. Participants were required to maintain a peddling cadence of 90rpm during the duration of the test. Exercise work-rates progressed in increments every minute from moderate to maximal intensity. After 2 minutes of warming up, resistance was elevated by 20W every minute until volitional exhaustion. Heart rate at peak $\dot{V}O_{2max}$ was obtained.

2.8 EXERCISE INTERVENTION

In order to control exercise compliance, quality and standardisation, all exercise sessions were supervised by a qualified Exercise Physiologist (ESSA)/Practitioner at Federation University, Australia gymnasium and exercise physiology laboratory.

2.8.1 Mixed exercise training (MET) program

Participants allocated to SEDENTARY underwent four weeks of MET as follows; 2 sessions of AEROBIC exercise training (AET) and 1 session of STRENGTH exercise training (RET) during weeks 1 and 3, and 1 session of AET and 2 sessions of RET during weeks 2 and 4. This distribution was selected so there is an equal number of each type of exercise training during the duration of the MET. Participants trained three times a week, with at least 48 hour separating exercise sessions. Subjects were asked to work at 80% of their peak heart rate (HR) determined during $\dot{V}O_{2\ max}$ assessment during the AET sessions, and conversely, with 80% of their 1RM during the RET sessions.

2.8.2 STRENGTH exercise training (RET) program

After randomization, SEDENTARY STRENGTH completed four weeks of RET. Participants trained three times a week, with at least 48 hour separating exercise sessions. The training emphasized compound movements aimed at major muscle groups. The STRENGTH training load was guided by percentage of 1RM testing and rating of perceived exertion. The initial week commenced at estimated 70% and gradually increased to 85%. The training load of each exercise was increased when participants were able to safely complete the full amount of sets and repetitions for that exercise. A typical session duration was approximately 45-60 minutes which incorporated a warm-up followed by six exercises of 3-5 sets with 3-12 repetitions per set.

2.8.3 AEROBIC exercise training (AET) program

After randomization, SEDENTARY AEROBIC underwent four weeks of AET. Participants trained three times a week, with at least 48 hour separating exercise sessions. The modes of training consisted of alternating cycling on ergometers and running on treadmills. During their sessions, participants exercised at 80% of their peak HR (determined from the $\dot{V}O_{2\,max}$ test). The exercise session duration was typically 45-60 minutes, inclusive of warm up, workout and cool-down regimen.

2.8.4 AEROBIC and STRENGTH protocols during the study.

During the whole length of the study, AEROBIC and STRENGTH continued with their normal exercise-training regimens that they were doing prior to enrolling to the study.

2.9 RNA EXTRACTION PROTOCOL

Blood samples were removed from the freezer and thawed on ice for 30 minutes. After this time, they were shaken vigorously again for 15 seconds and incubated overnight at room temperature. 24 hours later, whole RNA extraction was performed using MagMAX for Stabilized Blood Tubes RNA Isolation Kit™ (Thermo Fisher Scientific™) according to the manufacturer instructions [37]. Purified RNA samples were then quantified using Nanodrop 2000 (Thermo Fisher Scientific™), and stored at -80˚C until sequencing.

2.10 LIBRARY PREPARATION AND RNA SEQUENCING

RNA Library preparation was completed using the TruSeq Stranded Total RNA Sample Preparation Guide (Illumina®) according to manufacturer instructions [38]. Library preparation, RNA sequencing and RNA sequencing analysis was performed by AGRF (Australian Genome Research Facility). A second sequencing of replicates was undertaken due to library quality. The best sample from each run was chosen for analysis. Human TrueSeq

stranded RNA samples were sequenced on an Illumina NovaSeq platform. Briefly, samples were treated with the Ribo-Zero Gold preparation to deplete ribosomal RNA (rRNA). The purified RNA was fragmented with divalent cations and heat. Synthesis of the first strand cDNA was conducted with random primers, followed by a second strand synthesis with "marking" (incorporation of dUTP in place of dTTP). After this, there was an A-tailing and A-dapter ligation step. Finally, there was a selective enrichment for the non-uracil containing first cDNA strand by use of a uracil-sensitive polymerase. The Illumina NovaSeq RNA-seq sequence production of a 100bp single end was generated.

2.11 STATISTICAL POWER AND SAMPLE SIZE CALCULATION

Cardiorespiratory fitness has been used as the base to calculate the power of this study because it is the largest determinant of morbidity and mortality [13, 15, 16, 18, 19, 39]. Based on previous data from our laboratory, with an alpha coefficient of 0.05 and a beta value of 0.8, and considering that >7% increase (conservative) in $\dot{V}O_{2max}$ can be achieved within 4 weeks in exercise-naïve participants, 16 participants were required for each group. Accounting for the randomization and likelihood of withdrawals within the sedentary cohort, this resulted in a sample population of 72 participants.

2.12 PHYSIOLOGICAL DATA ANALYSIS

Means and standard deviations (SD) or confidence intervals (CI) are presented for descriptive data, unless otherwise stated. Quantitative primary variables were analysed using linear mixed model (LMM). Unlike repeated measures analysis of variance, LMMs allow the use of cases with missing data, the incorporation of time-varying covariates and the testing of difference within-subjects correlation structures. The LMM for each dependent variable ($\dot{V}O_{2max}$ and 1RM) included one between-subjects factor (group) and one within-subjects factor (time). Interactions between group and time were also included. Models were compared using

likelihood ratio tests. Three error covariance structures were tested: 1) independence (zero covariance) and two repeated measures structures; 2) compound symmetry (covariance constant over time); 3) first order autoregressive (covariance diminishing with time). Compound symmetry (CS) produced the best fitting models and was used throughout. The parameters of the best fitting models were estimated using restricted maximum likelihood. Paired t-tests with Bonferroni correction were completed to determine the significance of pair-wise differences. Assumptions of normality and homogeneous variance of errors were tested by analysis of residuals. As an intention to treat analysis, the Last Observation Carried Forward method was used to address missing data in the analysis of physiological characteristics. When there were missing data in follow-ups 1 or 2, the last known measurement was used, if available, and was treated to assume possible change according to the trend of the group. Analysis was conducted on SPSS software Version 25. Significance was assumed at the 0.05 level.

2.13 RNA-SEQ BIOINFORMATICAL ANALYSIS

The primary bioinformatics analysis involved demultiplexing and quality control (QC). The readings were screened for the presence of any Illumina adapter/overrepresented sequences and cross-species contamination. The data was processed through an RNA-seq expression analysis workflow, which includes alignment, transcript assembly, quantification and normalisation. Cleaned sequences were aligned against the Homo sapiens genome (Build version hg38). The STAR aligner (v2.5.3a) was used to map reads to the genomic sequences. The counts of reads mapping to each known gene were summarised. Counts were summarised at gene level using the featureCounts v1.5.3 utility of the subread package. Transcripts were assembled with the Stringtie tool v1.3.3b utilising the reads alignment with hg38 and reference annotation-based assembly option (RABT) yielding assembly for known and potentially novel transcripts. Results were written to GTF format.

Differential expression (DE) analysis was applied using EdgeR. Raw counts were filtered to counts per million (CPM) greater than 0.5, and genes not scored in more than 5 of the replicates of 3 or more groups were removed from the analysis. Counts were normalised using the TMM normalisation of edgeR. The EDAseq package was used to assess bias due to gene length and gene GC content. Between lanes normalisation was also applied. The contribution of known covariates was assessed with variance estimation in the samples. Treatment, replicate, lane, time and flow cell were fitted as random effects. Mavric software was used to estimate the contribution of known covariates to top Principal Components (PC). All samples and covariates were applied. To determine the treatment effect the analysis was restricted to sedentary

Biotype	No. exons	Pct exons
misc_RNA	63326	6.59%
mRNA	866473	90.22%
ncRNA - antisense RNA	66	0.01%
ncRNA - lncRNA	28190	2.94%
ncRNA - Rnase MRP	1	0.00%
ncRNA - RNAse P	1	0.00%
ncRNA - snoRNA	388	0.04%
ncRNA - snRNA	105	0.01%
ncRNA - TERC	1	0.00%
miRNA	1834	0.21%
rRNA	21	0.00%

Figure 2-3. *List of biotype proportions in the refseq for hg38 (GCA_000001405.15).*

participants only. Surrogate variables (SV) analysis was undertaken to identify unknown confounders. The number of estimated SV were 84, so we decided to model 5 and 10 SV. The RUVSeq Bioconductor package was used to remove background variation observed in the data. Flow cell was fitted to the model as a covariate to determine the residuals. Effects of sequencing run (flow cell) and sequencing lane were corrected using ComBat-seq. Then, batch effects were removed using the LIMMA tools. Normalised counts with the “remove unwanted variation using residuals” correction (RUVr) were used to assess structures in the lower dimensions of the principle components. Common dispersion of the averaged, filtered, RUVr corrected counts were estimated and confirmed to be <0.1. A Generalized Linear Models with Quasi-Likelihood

Test (glmQL) was applied for pairwise contrasts on the RUVr corrected counts with and without flow cell effects to quantify the differential expression between and within groups. Features were quantified and annotated by their relevant biotype. The proportions of each biotype contained in the refseq for hg38 (GCA_000001405.15) are listed in table 3. To avoid false positives and to select only transcripts highly impacted by the intervention, and therefore more likely to being relevant in the adaptation to exercise training, we selected a restrictive FC threshold of 2 for up-regulation and 0.5 for down-regulation. Differential expression was significant when FDR<0.05.

2.14 CIRCULAR RNA (CIRCRNA) BIOINFORMATICAL ANALYSIS

CircRNA were assessed using CIRI (version 2.0.6) (Gao et al., 2015). First, reads were aligned using BWA v0.7.17. CIRI was executed in high-stringency mode using default settings and the resulting counts merged to a ‘counts matrix’ of each back spliced junction location and sample. The circRNA junctions were converted to a counts matrix using in-house scripts. At this stage junctions were removed if <5 samples contained a count, to reduce the size of the matrix. The counts matrix was read into R for differential gene expression analysis. After exploring the data patterns, junctions supported by more than 3 replicates in 3 groups were retained. Counts were filtered for CPM < 0.5 and RUVr analysis applied. Results of RUVr suggested that dispersions were not adequately reduced. The unadjusted counts were chosen for differential expression analysis. Differential expression analysis was conducted as described in Section 3.12 - RNA-seq bioinformatical analysis, and outputs follow the same structure.

2.15 References

1. Tanner RK, Gore CJ. Physiological tests for elite athletes. Champaign, IL : Human Kinetics. 2013.
2. Thermo Fisher Scientific. MagMAX for Stabilized Blood Tubes RNA Isolation Kit. Available from: https://bit.ly/3jIv8V4.
3. Illumina. TruSeq Stranded Total RNA Reference Guide Document # 1000000040499 v00 2017. Available from: https://bit.ly/3w6ZjYV.
4. Blair SN, Kohl HW, 3rd, Paffenbarger RS, Jr., Clark DG, Cooper KH, Gibbons LW. Physical fitness and all-cause mortality. A prospective study of healthy men and women. Jama. 1989;262(17):2395-401. Epub 1989/11/03. PubMed PMID: 2795824.
5. Blair SN, Kampert JB, Kohl HW, 3rd, Barlow CE, Macera CA, Paffenbarger RS, Jr., et al. Influences of cardiorespiratory fitness and other precursors on cardiovascular disease and all-cause mortality in men and women. Jama. 1996;276(3):205-10. Epub 1996/07/17. PubMed PMID: 8667564.
6. Kokkinos P, Myers J, Kokkinos JP, Pittaras A, Narayan P, Manolis A, et al. Exercise capacity and mortality in black and white men. Circulation. 2008;117(5):614-22. Epub 2008/01/24. doi: 10.1161/circulationaha.107.734764. PubMed PMID: 18212278.
7. Mora S, Redberg RF, Cui Y, Whiteman MK, Flaws JA, Sharrett AR, et al. Ability of exercise testing to predict cardiovascular and all-cause death in asymptomatic women: a 20-year follow-up of the lipid research clinics prevalence study. Jama. 2003;290(12):1600-7. Epub 2003/09/25. doi: 10.1001/jama.290.12.1600. PubMed PMID: 14506119.
8. Lear SA, Hu W, Rangarajan S, Gasevic D, Leong D, Iqbal R, et al. The effect of physical activity on mortality and cardiovascular disease in 130 000 people from 17 high-income, middle-income, and low-income countries: the PURE study. Lancet (London, England). 2017;390(10113):2643-54. Epub 2017/09/26. doi: 10.1016/s0140-6736(17)31634-3. PubMed PMID: 28943267.
9. Kodama S, Saito K, Tanaka S, Maki M, Yachi Y, Asumi M, et al. Cardiorespiratory fitness as a quantitative predictor of all-cause mortality and cardiovascular events in healthy men and women: a meta-analysis. Jama. 2009;301(19):2024-35. Epub 2009/05/21. doi: 10.1001/jama.2009.681. PubMed PMID: 19454641.

3 AN EXAMINATION OF CHRONIC AEROBIC OR RESISTANCE EXERCISE TRAINING ON PERIPHERAL BLOOD TRANSCRIPTOMICS IN HEALTHY MALES: A SYSTEMATIC REVIEW AND META-ANALYSIS OF CANDIDATE SIGNATURES FROM RANDOMISED CONTROLLED TRIALS (RCTS)

"The following experimental chapter is presented in accordance with author guidance procedures for the journal ***Biology of Sport***".

https://www.termedia.pl/Journal/Biology_of_Sport-78/Infoe

ISSN: 2083-1862; ISSN: 0860-021X

3.1 ABSTRACT

Background Physiological adaptation to exercise has been well studied. However, the molecular mechanisms underpinning such adaptation are not well understood. Currently, the body of knowledge is mainly compounded by research focusing on skeletal muscle and overweighted towards associative studies. Analysis of Peripheral Blood Transcriptome (PBT) has been proposed as an alternative method but Randomised Controlled Trials (RCTs) in this field have not been quantitatively summarised.

Aims The present study aims to primarily (i) use Meta-analytical techniques to quantitatively summarise and compare existing literature on RCTs studying the effect of exercise training on the PBT expression of sedentary males, to secondarily (ii) interrogate the usefulness of peripheral blood as a biomarker to characterise transcriptome expression response to chronic exercise.

Methods PRISMA compliant, systematic review and meta-analysis was conducted to quantitatively characterise PBT expression for response to chronic exercise. Inclusion criteria was RCTs analysing RNA expression in peripheral blood, in sedentary males over 18 years, with an aerobic or resistance exercise training during at least 4 weeks with a minimum of 10 sessions.

Results Two RCTs met inclusion criteria for meta-analysis. Both studies were successful to increase Cardiorespiratory Fitness (CRF) after aerobic exercise. Among these two studies, 2 transcripts were shared in the analysis of expression: Adiponectin Receptor 1 (AdipoR1) and Adiponectin receptor 2 (AdipoR2). However, expression response was different in these studies: Thompson et al. AdipoR1 and AdipoR2 ↔ after 24wk aerobic training; Lee et al. AdipoR1 and AdipoR2 ↑ after 12wk aerobic exercise. Due to large heterogeneity in study design, methodology and data reporting between studies, it was unviable to conduct meta-analytical techniques for quantitative summarise. Alternatively, we analysed the current state

of the field and the different aspects of study design, methodology and data reporting, in the spirit of good scientific practice for researchers aiming to study PBT expression of sedentary males in response to exercise training.

Conclusion Due to extensive heterogeneity in key study design, methodology, and data reporting aspects of existing RCTs in this field, it was not possible to draw any strong evidence which would recommend the use PBT expression analysis to characterise adaptation to exercise training in sedentary compared with athletic male phenotypes.

Keywords: Systematic review, meta-analysis, peripheral blood, gene expression, transcriptome, exercise training.

3.2 INTRODUCTION

Physical exercise increases circulation of Peripheral Blood Mononuclear Cells (PBMCs) originating from bone marrow hematopoietic stem cells, and an accumulating body of RCTs investigating exercise genomics propose PBMCs utility to reflect genetic expression in RCTs [1-10].

In April 2003, the human genome project was completed two years ahead of schedule [11], making the entire human genetic blueprint available for the first time in history. This major breakthrough allowed for a better study of the relationship between genetic signatures and their effect to determine particular phenotypes. Moreover, exercise training develops particular phenotypes characterised by numerous physiological changes that contribute to improve health [12-19]. However, while these effects are well known, the genetic mechanisms underpinning these benefits are not well understood.
Research investigating gene expression in response to exercise training predominantly employs muscle biopsy techniques. Early muscle biopsy studies focused on genes coding for specific proteins with a key role in the adaptation of muscle to exercise training, with subsequent research emphasis to examining the relationship between long-term training-induced physiological changes in skeletal muscle and the regulation in gene expression [20-22]. Overall, it has been shown that resistance and aerobic exercise modulate the expression of genes involved in muscle hypertrophy, and mitochondria function and number.
However, one restriction with the advancement of exercise genomics is that muscle biopsies involve a highly invasive procedure and leave participants with a long recovery time. Additionally, multiple muscle biopsies cause similar response in terms of infiltrating neutrophils and macrophages, satellite cells and IL-1B detection in skeletal muscle than eccentric exercise [23]. On the other hand, peripheral blood has been proposed as an alternative method to examine the molecular mechanisms underpinning the physiological

benefits of exercise. It is easy, fast, and simple to obtain, and significantly less invasive for the patient than the biopsy. Additionally, the capacity to characterise phenotypic markers from peripheral blood offers greater commercial opportunities in the domain of personalised medicine. However, the relative utility of blood to mimic the gene expression obtained from muscle biopsy has not been adequately established.

Two previous reviews provide insight on gene expression in peripheral blood in response to exercise training. Gjevestad et al. conducted a systematic review, with no quantitatively compared pooled evidence, on all types of studies, of males and/or females, any type of physical exercise (acute or chronic), focusing on the gene expression of human blood cells (excluding Natural Killer cells) [24]. A more recent one, conducted by Amar et al., did an extensive review quantitatively comparing pooled evidence of publicly available transcriptomic data on males and females, in any type of physical exercise or training, in blood and skeletal muscle, including any intervention study [25]. However, despite the tremendous work and effort put into their study, no data about RCTs on the chronic response of gene expression in peripheral blood in sedentary participants were included. Thus, up to date no systematic review that quantitatively compares pooled evidence focused on RCTs examining the effect of physical exercise training on PBT expression in apparently healthy sedentary males has been conducted.

Additionally, since the early 2000s there has been an exponential rise in studies using PBT expression analysis (**Fig. 3-1**), thus evidencing the necessity to quantitatively summarise RCTs in the field with the aforementioned characteristics.

With these aspects in mind, the present study set out to systematically review and quantitatively compare current RCT evidence for a magnitude response of PBT expression in apparently health males in response to exercise programs (aerobic or resistance). The primary aim was to compare the change in the expression of transcripts analysed in the selected

studies included in this review. Secondary aim was to provide current best evidence on the use of peripheral blood as a genetic biomarker of response to exercise training, from RCTs. Therefore, we tested the hypothesis that peripheral blood is a valid medium to identify the effect of physical exercise training on transcriptomic markers of apparently healthy males utilizing the available peer reviewed RCTs.

3.3 MATERIALS AND METHODS

3.3.1 Protocol and registration

This review was prospectively registered in the PROSPERO database (registration number: CRD42020171206). We used the Preferred Reporting Items for Systematic Reviews and Meta-Analyses (PRISMA) guidelines [26].

3.3.2 Eligibility criteria

We restricted records to those (i) using a randomised control trial (RCT) protocol; (ii) using sedentary, apparently healthy (absent of any clinical described in the International Classification of Disease or ICD) male participants; 3) using participants over the age of 18 years; 4) conducting a structured aerobic or resistance exercise intervention for a duration of at least 4 weeks, with a minimum of 10 sessions; 5) where peripheral blood was used to determine the effect of exercise in the RNA expression at least before and after the intervention; and 6) published in peer reviewed journals in English language.

3.3.3 Study selection and data collection process

PubMed, Web of Science, CINAHL and SPORTDiscus were searched from inception to May 21st, 2020. In compliance with PICOS (participants, interventions, matched control groups, outcomes, and study design) criteria, we searched Medical Subject Headings (MeSH),

abstract, title, and keywords, using a combination of Boolean operators and key search terms (See **Fig. 3-2**). We screened reference lists from relevant studies and existing review articles for potentially eligible studies. Study characteristics and outcome data were extracted by two independent researchers (SM and DH) using a standardised data collection form (Appendix A), and results were compared. Discrepancies were resolved by discussion with a third researcher (FG). The authors were contacted if a complete report of the data was not available.

Control group was classified as two types, active control or waiting list. Participants included in a waiting list group did not undertake any intervention during the duration of the trial. Participants in an active control group conducted a different kind of intervention that did not incorporate any physical activity and/or exercise. Participant characteristics were coded according to age, body mass, and BMI. Type of exercise was categorised as aerobic exercise or resistance exercise. Length of the intervention was coded as total number of days. Intensity was categorised as percentage of maximal oxygen uptake ($\dot{V}O_{2max}$) or heart rate maximum (HR_{max}) for aerobic exercise intervention, and percentage of one-repetition maximum (1RM) for muscular strength. Frequency was coded as number of sessions per week, and volume of exercise as minutes per week. Exercise supervision was coded as yes, no, or partially. Retention to the study was assessed as a percentage for the control and exercise groups separately when possible, or for the total. Methodological characteristics were coded according to the intention-to-treat procedures used, type of statistical analysis, inclusion/exclusion criteria, time of blood collection, source of RNA from peripheral blood (PMBC, buffy coat, whole blood, or a particular cell subset), methodology for RNA extraction, and method for transcript identification (targeted genes by PCR, microarray, or Next Generation-sequencing).

3.3.4 Risk of bias in individual studies

Risk of bias will be assessed using the Cochrane Collaboration's Tool for Assessing Risk of Bias [27] (RoB tool). Criteria includes random sequence generation, allocation concealment, blinding of participants and personnel, blinding of outcome assessment, incomplete outcome data, selective outcome reporting, and other sources of bias. Other sources of bias were based on factors that are specific for studies mixing physical exercise interventions and gene expression analysis , i.e.: comparison of the changes in the exercise group with the changes in the control group, supervision of the exercise intervention, type of control group, the selection of a subset of participants within the study to examine the gene expression, timing for the collection of the post-treatment sample (immediately after, 24h after, 48h after…), the criteria for the selection of a particular Fold Change (FC) and p value threshold for a significant change in gene expression, time of the day for blood collection, ethnicity differences, age differences, sex, appropriate representation of peripheral blood as a sample (using PBMCs, buffy coat, or a particular subset of blood cells as a source for RNA), and gene expression being the primary outcome of the study. RoB assessments were conducted by two researchers (SM and DH) and consensus was reached by a third researcher (FG).

3.3.5 Summary of outcomes

Systematic review and meta-analysis were conducted using STATA (version 14.1) to assess the average FC of each of the transcripts reported in at least two studies. Fold change is described as the ratio between the expression of a transcript before and after and intervention. Therefore, when FC was not provided, it was calculated in order to include it in the pool of studies. We listed the transcripts that were up-regulated, down-regulated, or that did not change, for each of the studies that reported this information. If a study reported more than

one post-treatment value, only the assessment time-point immediately following the conclusion of the intervention phase was considered.

3.3.6 Synthesis of results

If FC was not available, effects sizes were calculated in order to compare between studies. When possible, pooled data would be used to complete the meta-analysis using a random-effects model to investigate differences between exercise interventions and control. Standardized difference in means (Hedges' g)/effect sizes are calculated for each individual study and a summary with overall effect size is recorded for each group of studies. Effect sizes in a positive direction determines a more favourable outcome from exercise training, whereas a negative direction determines a more favourable outcome in the respective control group.

3.4 RESULTS

3.4.1 Study selection

Following the removal removing duplicates (*n*=529), the systematic search process identified 1,252 articles which met eligibility for individual screening. Two independent researchers (SM and DH) screened the titles and abstracts of records with an agreement of 97.6%. A total of 1,215 articles were excluded at this stage (See **Fig. 3-2**). Full-texts of the remaining 37 articles were screened (SM and DH) with an agreement of 78.4%, yielding 7 articles that fulfilled all eligibility criteria. However, because 5 of those 7 articles included data for men and women, authors were contacted twice throughout a period of 2 weeks requesting the data separately for men and women. It was not possible to obtain the data from the authors, therefore the 2 articles with only males as participants were included in the systematic review. A third reviewer (FG) participated in the screening to give consensus in case of discrepancies.

3.4.2 Study characteristics

Data were extracted by two independent researchers (SM and DH) with a total agreement of 96 %. Across the two included studies, there were a total of 36 participants (21 intervention and 15 control) both involving aerobic training. Thompson and colleagues included sedentary participants recruited from the local community, aged 54±5 years for the intervention group and 52±4 in the waiting list control group. The intervention for this study was unsupervised aerobic exercise training. Physical activity was recorded using a combination of accelerometer and heart rate with branched-equation modelling systems. The length of the exercise program was 24wks with a frequency of 3 sessions/wk during weeks 1 and 2, and 4 sessions/wk during the remaining weeks. Duration and intensity of the sessions followed an incremental trend starting from 30min at 50% $\dot{V}O_{2max}$ during weeks 1 and 2 and reaching 60min at 70% $\dot{V}O_{2max}$ in weeks 23 and 24 (A detailed summary of the exercise intervention can be found in **Figure 3-4**). Compliance to the intervention was 83.67%. The participants included in the gene expression analysis were six of the men with high serum IL-6 at baseline in that study, with no intention to treat. Blood was collected at least 36h after undergoing any type of physical activity, but there was no information on the time of the day when it was done. RNA was extracted from PBMCs, and the transcripts were identified using a Microarray platform [1].

Lee and colleagues recruited sedentary participants, students from the institution where the study was conducted, aged between 20-30 years. The control group was a waiting list. The exercise intervention in this study consisted of a supervised jogging and/or running programme on a motor-driven treadmill. The length of the intervention was 12wks with a frequency of 5 sessions/wk. Each session had a duration of 40min and was conducted at an intensity of 60-70% of their age-based HR_{max}. Study compliance was 100%. In this case, all participants included in the study were also included in the gene expression analysis.

However, they did not report any information about how many hours passed between the last bout of exercise prior to blood collection, or at what time of the day it was collected. The researchers extracted the RNA from PBMCs and used qPCR to identify the transcripts of interest [3]. A complete description of the characteristics of these studies can be found in **Table 3-1**.

3.4.3 Risk of bias within studies

Due to the nature of the studies, it was not possible to blind participants for the exercise intervention, resulting in a high risk of performance bias. Excluding the Other sources of Bias criteria, the remaining four risk of bias category in these two studies was generally low-to-moderate, with the exception of a high risk of attrition bias in the case of Thompson et al. (**Fig. 3-5**). The Other sources of Bias criteria resulted as follows. Both studies were considered to present a low risk of bias for sex, age, supervision of the exercise intervention, type of control group, and appropriate representation of peripheral blood as a sample, and a high risk of value for gene expression being the primary outcome of the study. Timing for the collection of the post-treatment sample resulted in low in the case of Thompson et al. [1] and high for Lee et al. [3]. The participants used in the gene expression analysis and the comparison of the changes in the exercise group with the changes in the control group were considered high for Thompson et al. and low for Lee et al. The criteria for the selection of a particular Fold Change (FC) and p value threshold for a significant change in gene expression was judged as unclear in the case of Thompson et al. and low in Lee and colleagues. Finally, ethnicity differences and time of the day for blood collection were determined as unclear for both studies.

3.4.4 Results of individual studies

Both studies measured CRF after an aerobic exercise intervention. In the case of Thomson et al. [1], $\dot{V}O_{2max}$ was reported, and determined using a progressive incline test to

volitional fatigue on a treadmill, whereas Lee et al. [3] did not detail the measurement of aerobic capacity. In both studies, the exercise intervention was successful to increase CRF compared with control participants. Thompson and colleagues used a Microarray to interrogate the expression of multiple transcripts at a time. They found that after 24wk of intervention, 53 probes were differentially expressed in the subset of participants used in their study (6 participants with a high IL-6 blood levels at baseline), after selecting a threshold of FC<2.0 and a $p<0.05$. Contrastingly, Lee et al. utilised qPCR to target specific transcripts, AdipoR1 and AdipoR2. They reported an increased expression of AdipoR1 ($p<0.001$) and AdipoR2 ($p=0.001$) compared with control, following 12wk of intervention. A more detailed analysis can be found in **Table 3-1**.

3.4.5 Synthesis of results

Due to the heterogeneity in **study design, methodology, and data reporting** among the limited number of studies meeting the inclusion criteria, and the fact that those studies analysed different outcome data, it was not possible to quantitatively summarise studies as seen in traditional meta-analysis [28].

3.5 DISCUSSION

3.5.1 Summary of main findings

The main findings from this study highlight the current limitations of RCTs using PBT expression analysis to reflect to exercise training adaptation, such that only two RCTs were successful in meeting modest inclusion criteria for quantitative comparison. Thus, meta-analysis was prohibited in this instance. Taking into consideration this outcome, the consistency thus utility of peripheral blood as a useful medium to identify candidate gene signatures is not borne out by the available data. In light of this, the following discussion provides a narrative summary with substantive attention on aspects of observed inconsistencies which should be considered by researchers wishing to employ randomised controlled trial to study exercise transcriptomics from peripheral blood.

Meta-analysis is a quantitative progression to systematic review that offers great potential to derive consolidated knowledge from individual RCTs of PBT. The present meta-analysis identified 1,252 original research articles across multiple electronic databases meeting keyword search criteria (**Fig. 3-3**), which were screened in duplicate, in compliance with formal Cochrane guidelines [26]. This resulted in a subsequent and inexorable fact that none of these RCTs were eligible for quantitative pooling. Contrary to the opportunity of leveraging increased statistical power, our major discovery is that the degree of heterogeneity between individual studies is so great that any generalised conclusion in PBT research cannot be achieved. Our original hypothesis originated from a recent plethora of RCTs which utilise the medium of peripheral blood to examine genomic response to exercise training (**Fig. 3-1**). Similarly, as each relevant study requires the utilisation of standard exercise interventions to identify significance of genomic outcomes, it was reasonable to hypothesise the presence of sufficient quantity and consistency within this literature for meaningful pooling of uniform

PBT expression towards characterising the phenotypic response to exercise training using whole blood measures. Similarly, should there have been some reliability and consistency amongst candidate signatures, the potential for continuous data would allow some early determination as to the magnitude of response. Unfortunately, lack of uniformity amongst (*n*=11) studies was such that two studies met eligibility criteria [1, 3] wherein, reported outcomes could not be combined meaningfully. In light of limitations to empirically examine the potential magnitude and variation of transcriptomic response to exercise training in males, the following section will provide a narrative synthesis of the two eligible studies before proceeding to substantive attention to key areas of inherent inconsistency within the literature with the intention of informing future research.

3.5.2 Summary of studies meeting eligibility

In accordance with accepted guidelines on quantitative comparison of polled research trials, two studies are enough to conduct a meta-analysis, as long as those studies' information can be pooled and that their results are similar enough (Ryan R; Cochrane Consumers and Communication Review Group. 'Cochrane Consumers and Communication Group: meta-analysis. http://cccrg.cochrane.org, December 2016 (accessed DATE)). Two studies each met our criteria for qualitative summary [1, 3]. Notably, there are characteristic similarities in both RCTs, which enrolled male participants to aerobic exercise interventions which were successful to improve CRF (7.8%; 18.7% respectively) and each derived AdipoR1 and AdipoR2 from RNA. Thompson et al. examined the effect of 24wks of unsupervised high/moderate-intensity aerobic exercise training on markers of chronic inflammation in peripheral blood of *n*=27 healthy sedentary males compared with *n*=27 controls. These researchers further examined microarray gene expression analysis from a biased subset of *n*=6 participants exhibiting the highest serum levels of IL-6 in systemic PBMCs at enrolment. Lee et al. examined whether 12wks of supervised high-to-moderate

intensity aerobic training altered the expression of adiponectin receptors AdipoR1 and AdipoR2 genes within PBMCs, and further examined whole body insulin sensitivity in *n*=15 healthy male participants compared with *n*=15 controls. However, both studies also have a notable lack of conformity which should likewise be appreciated. For instance, Thompson and colleagues restricted Microarray gene expression analysis of *n*=6 participants with the highest circulating IL-6 at enrolment whereas Lee and co-workers employed qPCR to derive gene expression from *n*=30 males. Furthermore, Thompson et al. did not report adiponectin receptor data within their manuscript, rather, this data was identified from examining probes' information of the microarray used in their study, where both were unchanged. Conversely, whereas Lee et al. reported an upregulation of both AdipoR1 and AdipoR2 following 12 weeks of aerobic exercise, the other study did not find significant change after 24wk of moderate/high-intensity aerobic exercise. Taken together, the body of available evidence in exercise PBT expression from RCTs is limited and while there were some similarities to be found from two available RCTs, outcomes of interest for the present study were equivocal, such that their inconsistencies outweigh any meaningful coalition of study outcomes.

To confront the problem of replicability in phenotype-genotype association studies, Chanok and colleagues published recommendations for researchers undertaking such work [29]. However, to our knowledge, similar recommendations do not exist for PBT exercise research. Given the findings from the present study, this is more than semantics, as there are several important aspects that should be taken into consideration when designing RCTs in PBT expression analysis, each of which increases the risk of Type I or Type II error. Important considerations such as; type of control group, supervision of exercise intervention, bias in candidate selection used in analysis, timing for collection of pre- and post-intervention samples, comparison of changes between intervention group and control group, chrono-biological variations, and statistical benchmark criteria in selecting fold change (FC)

threshold and criterion alpha (*p*-value's) employed to identify significance of gene expression comparisons.

3.5.3 Study design

3.5.3.1 Type of control group

The basis of a RCT is the use of a control group that does not undertake the intervention of interest in the study (i.e. a structured exercise training) in order to compare the effect of said intervention with a scenario where that intervention does not have an effect (control group). However, this control group can sometimes be an active control, which is a group of participants that do not undertake the intervention of interest, but do undertake a different intervention, i.e. stretching [2]. Since a control group allows for minimising the risk of factors other than the intervention having an effect on the observed outcome, additional interventions in the control group (in particular those involving any type of physical exercise) may contribute to confusion or misinterpretation of the results. There are no current studies examining the effect of an active control group compared with a waiting list in gene expression of peripheral blood in exercise training. However, it is an aspect of debate in exercise training studies examining the effect on physiological traits. To this regard, we recommend researchers conducting studies in this field, to include an inactive control group that refrains from any sort of physical exercise during the duration of the study.

3.5.3.2 Supervision of exercise intervention

Although it appears there are no studies comparing the effect of supervised vs unsupervised physical exercise training in gene expression, research has been conducted examining the effect of those types of exercise interventions in performance and physiological outcomes, as discussed previously in this section. An observational study conducted by Curtis et al. suggests that overall fitness can be successfully improved in

previously sedentary individuals conducting supervised exercise programs, but a period of unsupervised exercise may produce a decrease in muscular endurance and cardiovascular health due to less physical activity [30]. On another instance, Lacroix et al. run a RCT to study the effects of a combination of balance and strength training [31]. Their results indicated that the supervised group showed improvements for different physical tests after 12 weeks compared with the unsupervised group. Regarding the examination of gene expression in peripheral blood in exercise, some studies do not supervise the exercise intervention [1, 6, 32], or simply they do not report it [4, 9]. Because, as discussed previously, exercise genomics is based on the idea that physiological adaptations are led by gene expression response to exercise training, those differences between supervised and unsupervised exercise programmes should be of concern to a researcher conducting a study in this field. We recommend the supervision of the exercise programme, if possible, by a qualified personal trainer or an exercise physiologist, to obtain an appropriate representation of an exposition to an exercise intervention program.

3.5.3.3 Selection bias (of a subset of participants for gene expression analysis)

Appropriate selection of participants included in the study is a major aspect for conducting a correct RCT in exercise science [33]. A thoughtful selection process, with criteria that aligns with the research question, has to be conducted in order to choose the most appropriate population for the study. Thus, this intention has to be carried on throughout all the steps of the study, including data analysis. In some instances, researchers will select a bias subset of participants included in the study (i.e. only those who show a particular characteristic at baseline), to conduct the gene expression analysis. This approach might be justified in a particular study aiming to ask a specific question [1]. However, to objectively interrogate the effect of exercise on gene expression of peripheral blood, this is a bias approach that should be avoided. Furthermore, it supresses the effect of randomisation

included in a RCT, as the subset of participants is not selected randomly anymore. Therefore, we suggest that researchers adhere to CONSORT guidelines when selecting the participants, including those included in gene expression analysis [34].

3.5.4 Methodology

3.5.4.1 Timing for collection of pre- and post- intervention samples

The anticipatory rise in exercise is a well-known concept that has been established for a long time [35]. It consists on a rise in heart rate before an expected physical activity. Since it is impossible to blind participants for the intervention in the cases of physical exercise studies, it is important to take this concept into account. Baseline samples should be collected in a control day were no exercise is expected. Regarding post-intervention sample timing, the acute gene expression response to acute bouts of exercise was first studied using microarray by Connolly et al. [36], observing a differential response between 30min pre-, immediately after and 60min post-exercise. From pre- to immediately after exercise there was an up-regulation of PBMCs genes associated with stress and inflammation. During the recovery phase 60min post-exercise, these genes changed their expression back to the levels observed at baseline. Subsequent studies' outcomes agree with these results [37, 38]. These findings suggest an acute response that is characteristic of the minutes close to the finalisation of exercise. Furthermore, another study [39] found differential gene expression after aerobic exercise even at 24h post-exercise, which was going back to baseline levels 48h after exercise. With this strong evidence, one would assume that researchers adequately time the blood collection in their studies, although some of them do not report this information [3, 6, 10, 32, 40].Therefore, in spirit of good scientific practice, we propose to refrain from any type of physical activity for at least 48h before the collection of a blood sample if aiming to investigate chronic effects of exercise programmes. Most importantly, to report this in the study.

3.5.4.2 Comparison of changes between intervention group and control group

One notable inconvenience observed in studies examining the effect of an exercise intervention in gene expression in peripheral blood is the incomplete reporting of the data. This is especially concerning when there is an absence of statistical comparison between the changes in gene expression in the control group and the intervention group. By conducting a RCT, the researcher adheres to Bradford Hills's criteria to avoid misinterpretation of causative inference where it should not be declared. Although the study may initially be designed accordingly, including an intervention group and a control group, this absence of data for both intervention and control groups at enrolment and during follow-up, can misrepresent generalisability of study findings and precludes viability for meta-analysis. There are a number of such instances of declared RCTs in PBT expression analysis [1, 6, 8] and researchers are encouraged to consider this during RCT design.

3.5.4.3 Chrono biological variation

Another important factor that contributes to gene expression in blood are the circadian rhythms, as significant variations in gene expression between morning and evening have been reported from peripheral blood [41]. This will be the case in studies studying gene expression in exercise, therefore affecting the outcome. It is recommended that all the samples be collected at similar times of the day for all the participants to be able to compare between groups, and repeated measures for the same participants also to be collected at the same time of the day in different day, for within group comparisons. In the case that this is not possible, authors should report the different collection times and acknowledge this risk of bias in the study. In some cases, authors do not even report the time of the day when samples are collected [1-4, 6, 7, 40]. The appropriate reporting of this information will allow researchers conducting reviews in the field to take into account this factor and conduct a better analysis and conclusion.

3.5.5 Data reporting

3.5.5.1 Criteria for selection of FC and p value threshold for significant change in gene expression

There are no requisite standards of threshold FC or p-values to define threshold for differential expression, thus significance in PBT studies. Resultant heterogeneity of RCT data prevents the correct comparison between studies that is required in meta-analysis studies. It also presents the possibility that those results might not be accurate or reflect the true effect of the intervention. Although the discussion of what are the appropriate FC or p-value required for a proper analysis of the data is not a topic of this review and requires a more in-depth examination of the matter, we argue that a standardised system would increase the consistency between studies and allows for a more accurate comparison between them. However, we suggest that researchers present all the raw data to allow other researchers to do conduct their own analyses.

3.5.6 Strengths and limitations

There are a number of notable limitations when conducting a meta-analytical review and the present study is no different. First, this review was restricted to RCTs enrolling male participants, thus limiting the available pool of studies. However, we rationalised that sex differences would elevate heterogeneity of interpretation. This may have been overcome by subgroup-analysis, yet would require a large body of RCTs to account for this covariate. Discrete differences in PBT expression should be acknowledged when conducting this type of trials as there is some evidence to support differences amongst elite female athletes compared with male counterparts [41]. Perhaps the greatest limitation towards resolving our hypothesis relates to the absence of any RCT to be pooled for meta-analytical summary. Despite this, it does raise attention on the lack of consistency of RCTs investigating PBT. To support the caution which should be exercised by researchers wishing to conduct PBT

research, we direct attention to some key aspects for consideration in RCT design of PBT expression studies.

3.6 CONCLUSION

This study revealed significant heterogeneity among RCTs employing peripheral blood to examine candidate transcript expression in exercise studies of sedentary males. Reasons for this lack of consistency relate to incongruences and lack of standardisation in study design, methodological differences, and data reporting. It is therefore safe to conclude that peripheral blood transcriptomics does not currently offer consistent or useful information. In light of this, the present chapter has offered systematic guidelines in clear areas of importance for those wishing to undertake exercise transcriptomic research.

3.7 REFERENCES

1. Thompson D, Markovitch D, Betts JA, Mazzatti D, Turner J, Tyrrell RM. Time course of changes in inflammatory markers during a 6-mo exercise intervention in sedentary middle-aged men: a randomized-controlled trial. Journal of Applied Physiology. 2010;108(4):769-79. doi: 10.1152/japplphysiol.00822.2009. PubMed PMID: WOS:000276324200003.
2. Iyalomhe O, Chen YX, Allard J, Ntekim O, Johnson S, Bond V, et al. A standardized randomized 6-month aerobic exercise-training down-regulated pro-inflammatory genes, but up-regulated anti-inflammatory, neuron survival and axon growth-related genes. Experimental gerontology. 2015;69:159-69. Epub 2015/05/20. doi: 10.1016/j.exger.2015.05.005. PubMed PMID: WOS:000360320200021; PubMed Central PMCID: PMCPMC4553116.
3. Lee SH, Hong HR, Han TK, Kang HS. Aerobic training increases the expression of adiponectin receptor genes in the peripheral blood mononuclear cells of young men. Biology of sport. 2015;32(3):181-6. Epub 2015/10/02. doi: 10.5604/20831862.1150298. PubMed PMID: 26424919; PubMed Central PMCID: PMCPMC4577554.
4. Schenk A, Pulverer W, Koliamitra C, Bauer CJ, Ilic S, Heer R, et al. Acute Exercise Increases the Expression of KIR2DS4 by Promoter Demethylation in NK Cells. International journal of sports medicine. 2019;40(1):62-70. Epub 2018/12/07. doi: 10.1055/a-0741-7001. PubMed PMID: WOS:000454222500009.
5. Butcher LR, Thomas A, Backx K, Roberts A, Webb R, Morris K. Low-intensity exercise exerts beneficial effects on plasma lipids via PPARgamma. Medicine & Science in Sports & Exercise. 2008;40(7):1263-70. Epub 2008/06/27. doi: 10.1249/MSS.0b013e31816c091d. PubMed PMID: 105658595. Language: English. Entry Date: 20081003. Revision Date: 20150711. Publication Type: Journal Article.
6. Sen S, Witkowski S, Lagoy A, Islam AM. A Six-Week Home Exercise Program Improves Endothelial Function and CD34(+) Circulating Progenitor Cells in Patients With Pre-Diabetes. Journal of Endocrinology and Metabolism. 2015;5(1-2):163-71. doi: 10.14740/jem273w. PubMed PMID: WOS:000360177700002.
7. Henagan TM, Phillips MD, Cheek DJ, Kirk KM, Barbee JJ, Stewart LK. The melanocortin 3 receptor: a novel mediator of exercise-induced inflammation reduction in postmenopausal women? J Aging Res. 2011;2011:512593. Epub 2011/01/22. doi: 10.4061/2011/512593. PubMed PMID: 21253483; PubMed Central PMCID: PMCPMC3022199.
8. Macêdo Santiago LÂ, Neto LGL, Borges Pereira G, Leite RD, Mostarda CT, de Oliveira Brito Monzani J, et al. Effects of Resistance Training on Immunoinflammatory Response, TNF-Alpha Gene Expression, and Body Composition in Elderly Women. Journal of Aging Research. 2018;2018:1-10. Epub 2018/12/05. doi: 10.1155/2018/1467025. PubMed PMID: 132650858. Language: English. Entry Date: 20181030. Revision Date: 20181030. Publication Type: Article. Journal Subset: Biomedical; PubMed Central PMCID: PMCPMC6230406.
9. Rodriguez-Miguelez P, Fernandez-Gonzalo R, Almar M, Mejias Y, Rivas A, de Paz JA, et al. Role of Toll-like receptor 2 and 4 signaling pathways on the inflammatory response to resistance training in elderly subjects. Age. 2014;36(6):9734. Epub 2014/11/28. doi: 10.1007/s11357-014-9734-0. PubMed PMID: WOS:000346770900016; PubMed Central PMCID: PMCPMC4245402.
10. Streese L, Khan AW, Deiseroth A, Hussain S, Suades R, Tiaden A, et al. High-intensity interval training modulates retinal microvascular phenotype and DNA methylation of p66Shc gene: a randomized controlled trial (EXAMIN AGE). Eur Heart J.

2020;41(15):1514-9. Epub 2019/07/20. doi: 10.1093/eurheartj/ehz196. PubMed PMID: 31323685.
11. Heilig R, Eckenberg R, Petit J, Fonknechten N, Silva C, Cattolico L, et al. International Human Genome Sequencing Consortium. Nature 431, 931-945. Nature. 2004;431(7011):931-45. Epub 2004/10/22. doi: 10.1038/nature03001. PubMed PMID: 15496913.
12. Lear SA, Hu W, Rangarajan S, Gasevic D, Leong D, Iqbal R, et al. The effect of physical activity on mortality and cardiovascular disease in 130 000 people from 17 high-income, middle-income, and low-income countries: the PURE study. Lancet (London, England). 2017;390(10113):2643-54. Epub 2017/09/26. doi: 10.1016/s0140-6736(17)31634-3. PubMed PMID: 28943267.
13. Thompson PD, Eijsvogels TH. New physical activity guidelines: A call to activity for clinicians and patients. Jama. 2018. Epub 2018/11/13. doi: 10.1001/jama.2018.16070. PubMed PMID: 30418469.
14. Blair SN, Kampert JB, Kohl HW, 3rd, Barlow CE, Macera CA, Paffenbarger RS, Jr., et al. Influences of cardiorespiratory fitness and other precursors on cardiovascular disease and all-cause mortality in men and women. Jama. 1996;276(3):205-10. Epub 1996/07/17. PubMed PMID: 8667564.
15. Blair SN, Kohl HW, 3rd, Paffenbarger RS, Jr., Clark DG, Cooper KH, Gibbons LW. Physical fitness and all-cause mortality. A prospective study of healthy men and women. Jama. 1989;262(17):2395-401. Epub 1989/11/03. PubMed PMID: 2795824.
16. Gulati M, Black HR, Shaw LJ, Arnsdorf MF, Merz CN, Lauer MS, et al. The prognostic value of a nomogram for exercise capacity in women. The New England journal of medicine. 2005;353(5):468-75. Epub 2005/08/05. doi: 10.1056/NEJMoa044154. PubMed PMID: 16079370.
17. Kokkinos P, Myers J, Kokkinos JP, Pittaras A, Narayan P, Manolis A, et al. Exercise capacity and mortality in black and white men. Circulation. 2008;117(5):614-22. Epub 2008/01/24. doi: 10.1161/circulationaha.107.734764. PubMed PMID: 18212278.
18. Mora S, Redberg RF, Cui Y, Whiteman MK, Flaws JA, Sharrett AR, et al. Ability of exercise testing to predict cardiovascular and all-cause death in asymptomatic women: a 20-year follow-up of the lipid research clinics prevalence study. Jama. 2003;290(12):1600-7. Epub 2003/09/25. doi: 10.1001/jama.290.12.1600. PubMed PMID: 14506119.
19. Braith RW, Stewart KJ. Resistance exercise training: its role in the prevention of cardiovascular disease. Circulation. 2006;113(22):2642-50. Epub 2006/06/07. doi: 10.1161/CIRCULATIONAHA.105.584060. PubMed PMID: 16754812.
20. O'Neill DS, Zheng D, Anderson WK, Dohm GL, Houmard JA. Effect of endurance exercise on myosin heavy chain gene regulation in human skeletal muscle. American Journal of Physiology-Regulatory, Integrative and Comparative Physiology. 1999;276(2):R414-R9. doi: 10.1152/ajpregu.1999.276.2.R414. PubMed PMID: 9950919.
21. Wadley GD, Tunstall RJ, Sanigorski A, Collier GR, Hargreaves M, Cameron-Smith D. Differential effects of exercise on insulin-signaling gene expression in human skeletal muscle. Journal of applied physiology (Bethesda, Md : 1985). 2001;90(2):436-40. Epub 2001/02/13. doi: 10.1152/jappl.2001.90.2.436. PubMed PMID: 11160039.
22. Welle S, Bhatt K, Thornton CA. Stimulation of myofibrillar synthesis by exercise is mediated by more efficient translation of mRNA. Journal of applied physiology (Bethesda, Md : 1985). 1999;86(4):1220-5. Epub 1999/04/08. doi: 10.1152/jappl.1999.86.4.1220. PubMed PMID: 10194206.
23. Malm C, Nyberg P, Engstrom M, Sjodin B, Lenkei R, Ekblom B, et al. Immunological changes in human skeletal muscle and blood after eccentric exercise and multiple biopsies. The Journal of physiology. 2000;529 Pt 1(Pt 1):243-62. Epub 2000/11/18.

doi: 10.1111/j.1469-7793.2000.00243.x. PubMed PMID: 11080266; PubMed Central PMCID: PMCPMC2270185.
24. Gjevestad G, Holven K, Ulven S. Effects of Exercise on Gene Expression of Inflammatory Markers in Human Peripheral Blood Cells: A Systematic Review. Current Cardiovascular Risk Reports. 2015;9(7):1-17. doi: 10.1007/s12170-015-0463-4.
25. Amar D, Lindholm ME, Norrbom J, Wheeler MT, Rivas MA, Ashley EA. Differential response trajectories to acute exercise in blood and muscle. bioRxiv. 2019:863100. doi: 10.1101/863100.
26. Moher D, Liberati A, Tetzlaff J, Altman DG, The PG. Preferred Reporting Items for Systematic Reviews and Meta-Analyses: The PRISMA Statement. PLOS Medicine. 2009;6(7):e1000097. doi: 10.1371/journal.pmed.1000097.
27. Higgins JPT, Altman DG, Gøtzsche PC, Jüni P, Moher D, Oxman AD, et al. The Cochrane Collaboration's tool for assessing risk of bias in randomised trials. BMJ. 2011;343:d5928. Epub 2011/10/20. doi: 10.1136/bmj.d5928. PubMed PMID: 22008217; PubMed Central PMCID: PMCPMC3196245.
28. Valentine JC, Pigott TD, Rothstein HR. How Many Studies Do You Need?: A Primer on Statistical Power for Meta-Analysis. Journal of Educational and Behavioral Statistics. 2010;35(2):215-47. doi: 10.3102/1076998609346961.
29. Chanock SJ, Manolio T, Boehnke M, Boerwinkle E, Hunter DJ, Thomas G, et al. Replicating genotype–phenotype associations. Nature. 2007;447(7145):655-60. Epub 2007/06/08. doi: 10.1038/447655a. PubMed PMID: 17554299.
30. Curtis Fennell KP, Ellen L Glickman. Effects of Supervised Training Compared to Unsupervised Training on Physical Activity, Muscular Endurance, and Cardiovascular Parameters. MOJ Orthop Rheumatol. 2016;5(4). doi: 10.15406/mojor.2016.05.00184.
31. Lacroix A, Kressig RW, Muehlbauer T, Gschwind YJ, Pfenninger B, Bruegger O, et al. Effects of a Supervised versus an Unsupervised Combined Balance and Strength Training Program on Balance and Muscle Power in Healthy Older Adults: A Randomized Controlled Trial. Gerontology. 2016;62(3):275-88. Epub 2015/12/10. doi: 10.1159/000442087. PubMed PMID: 26645282.
32. Black DS, Cole SW, Irwin MR, Breen E, St Cyr NM, Nazarian N, et al. Yogic meditation reverses NF-κB and IRF-related transcriptome dynamics in leukocytes of family dementia caregivers in a randomized controlled trial. Psychoneuroendocrinology. 2013;38(3):348-55. Epub 2012/07/17. doi: 10.1016/j.psyneuen.2012.06.011. PubMed PMID: 22795617; PubMed Central PMCID: PMCPMC3494746.
33. Hecksteden A, Faude O, Meyer T, Donath L. How to Construct, Conduct and Analyze an Exercise Training Study? Frontiers in physiology. 2018;9:1007-. Epub 2018/08/25. doi: 10.3389/fphys.2018.01007. PubMed PMID: 30140237; PubMed Central PMCID: PMCPMC6094975.
34. Schulz KF, Altman DG, Moher D. CONSORT 2010 Statement: Updated Guidelines for Reporting Parallel Group Randomized Trials. Ann Intern Med. 2010;152(11):726-32. Epub 2010/03/26. doi: 10.7326/0003-4819-152-11-201006010-00232. PubMed PMID: 20335313.
35. Skubic V, Hilgendorf J. Anticipatory, exercise, and recovery heart rates of girls as affected by four running events. Journal of Applied Physiology. 1964;19(5):853-6. Epub 1964/09/01. doi: 10.1152/jappl.1964.19.5.853. PubMed PMID: 14207732.
36. Connolly PH, Caiozzo VJ, Zaldivar F, Nemet D, Larson J, Hung SP, et al. Effects of exercise on gene expression in human peripheral blood mononuclear cells. Journal of applied physiology (Bethesda, Md : 1985). 2004;97(4):1461-9. Epub 2004/06/15. doi: 10.1152/japplphysiol.00316.2004. PubMed PMID: 15194674.

37. Carlson LA, Tighe SW, Kenefick RW, Dragon J, Westcott NW, Leclair RJ. Changes in transcriptional output of human peripheral blood mononuclear cells following resistance exercise. European journal of applied physiology. 2011;111(12):2919-29. Epub 03/25. doi: 10.1007/s00421-011-1923-2. PubMed PMID: 21437602; PubMed Central PMCID: PMCPMC4358769.
38. Buttner P, Mosig S, Lechtermann A, Funke H, Mooren FC. Exercise affects the gene expression profiles of human white blood cells. Journal of applied physiology (Bethesda, Md : 1985). 2007;102(1):26-36. Epub 2006/09/23. doi: 10.1152/japplphysiol.00066.2006. PubMed PMID: 16990507.
39. Kawai T, Morita K, Masuda K, Nishida K, Sekiyama A, Teshima-Kondo S, et al. Physical exercise-associated gene expression signatures in peripheral blood. Clinical journal of sport medicine : official journal of the Canadian Academy of Sport Medicine. 2007;17(5):375-83. Epub 2007/09/18. doi: 10.1097/JSM.0b013e31814c3e4f. PubMed PMID: 17873550.
40. Creswell JD, Irwin MR, Burklund LJ, Lieberman MD, Arevalo JM, Ma J, et al. Mindfulness-Based Stress Reduction training reduces loneliness and pro-inflammatory gene expression in older adults: a small randomized controlled trial. Brain Behav Immun. 2012;26(7):1095-101. Epub 2012/07/24. doi: 10.1016/j.bbi.2012.07.006. PubMed PMID: 22820409; PubMed Central PMCID: PMCPMC3635809.
41. Whitney AR, Diehn M, Popper SJ, Alizadeh AA, Boldrick JC, Relman DA, et al. Individuality and variation in gene expression patterns in human blood. Proceedings of the National Academy of Sciences of the United States of America. 2003;100(4):1896-901. Epub 2003/02/13. doi: 10.1073/pnas.252784499. PubMed PMID: 12578971; PubMed Central PMCID: PMCPMC149930.

Table 3-1 *Participants, protocol, exercise characteristics, and outcomes of the studies included in this review.*

Study	Participants	Protocol	Exercise intervention	Changes in phenotype	Source of RNA	Methodology for transcripts identification	Transcripts investigated	Regulation after exercise
Thompson et al. (2010) [1]	IG = SED 27 men (54±5 years) CG = SED 27 men (52±4 years) **1^0: -** **2^0:** √	Sedentary male volunteers were recruited from the local community. Participants were randomised to IG or CG (waiting list) using a sealed envelope. Participants in both groups reported to the laboratory at baseline, 4, 12, 24, and 26 wk later, each time following a 12h overnight fast. Before blood sampling, volunteers were asked to refrain from strenuous physical activity for at least 36 h. Participants were also asked whether they had experienced any symptoms of illness in the past 3 days or had taken any medication in the past 48 h. Microarray conducted in six of the men in the IG with high serum IL-6 at baseline.	24 wk of unsupervised aerobic exercise training, 3 days/wk during the first 2 wk and 4 days/wk for the rest. Duration started as 30min during the first wk and increased 5min every 4 wk. Intensity started as 50% $\dot{V}O_{2max}$ during the first wk and increased in 5% every 6 wk.	CG-pre $\dot{V}O_{2max}$: 35.2±4.7 (mL*Kg-1*min^{-1}) CG-post $\dot{V}O_{2max}$: 34.0±3.8 (mL*Kg-1*min^{-1}) ($p \geq 0.02$) IG-pre $\dot{V}O_{2max}$: 34.5±4.2 (mL*Kg-1*min^{-1}) IG-post $\dot{V}O_{2max}$: 37.2±4.0 (mL*Kg-1*min^{-1})($p \leq 0.02$)‡ $\dot{V}O_{2max}$ was determined using a progressive incline test to volitional fatigue on a treadmill, consisting of 3-min exercise stages with the gradient increasing by 3% at the end of each stage (Woodway, ELG 70, Weiss, Germany).	PBMC	Microarray Agilent Human Oligo Arrays (catalogue no. G4112F, Agilent Technologies UK)	41,267	53 probes differentially regulated by training in subjects with high baseline IL-6 (FC<2.0 and $p<0.05$) after 24 wk. Of those 53 probes, 31 were no longer significantly differentially expressed and 22 were still differentially expressed after 2 wk of retraining ($p<0.05$)
Lee et al. (2015) [3]	IG = SED 15 men CG = SED 15 men Students between 20-30 years old. **1^0: -** **2^0:** √	Participants were randomised to IG or CG (waiting list). Blood samples were available from 15 participants in the exercise-training group and 15 participants in the control group.	12 wk of supervised jogging and/or running programme on a motor-driven treadmill (Quinton, USA). Volume of 5min warm-up, 30 min exercise and 5min cool down, 5 days/wk. Volume was 200min/wk. Intensity of 60-75%$HR_{max.}$ Subjects maintained their exercise HR within 5 beats/min of their targeted HR by using a heart rate monitor (POLAR Accurex Plus, Finland). As the fitness level of each subject improved, the running velocity required to maintain the desired exercise intensity was increased.	CG-pre VO_2: 46.8±3.2 (mL*Kg-1*min^{-1}) CG-post VO_2: 47.8±3.0 (mL*Kg-1*min^{-1}) IG-pre VO_2: 45.9±2.10 (mL*Kg-1*min^{-1}) IG-post VO_2: 54.5±2.2 (mL*Kg-1*min^{-1}) Significant treatment effects post-pre ($p<0.001$)‡	PBMC	qPCR	AdipoR1, AdipoR2	AdipoR1 ↑ ($p<0.001$)‡, AdipoR2 ↑ ($p = 0.001$)‡ after 12wk.

IG=Intervention Group; CG= Control Group; SED= Sedentary; wk= Weeks; h=hours; IL-6= Interleukin-6; $\dot{V}O2max$= maximal oxygen uptake;mL= milliliters; Kg= kilograms; min= minutes; PBMC= Peripheral Blood Mononuclear Cell; FC= Fold Change; HR_{max}= Maximum Heart Rate; HR= Heart Rate; qPCR= quantitative Polymerase Chain Reaction; AdipoR1= Adiponectin Receptor 1; AdipoR2= Adiponectin Receptor 2 ; ↑ indicates upregulation of gene expression, ↓ indicates down-regulation of gene expression, and ↔ indicates no changes in gene expression. ‡ indicates that the p-value refers to the comparison of changes in intervention group with changes in control group. √ indicates whether gene expression is the primary (1^0) or secondary (2^0) outcome of the study.

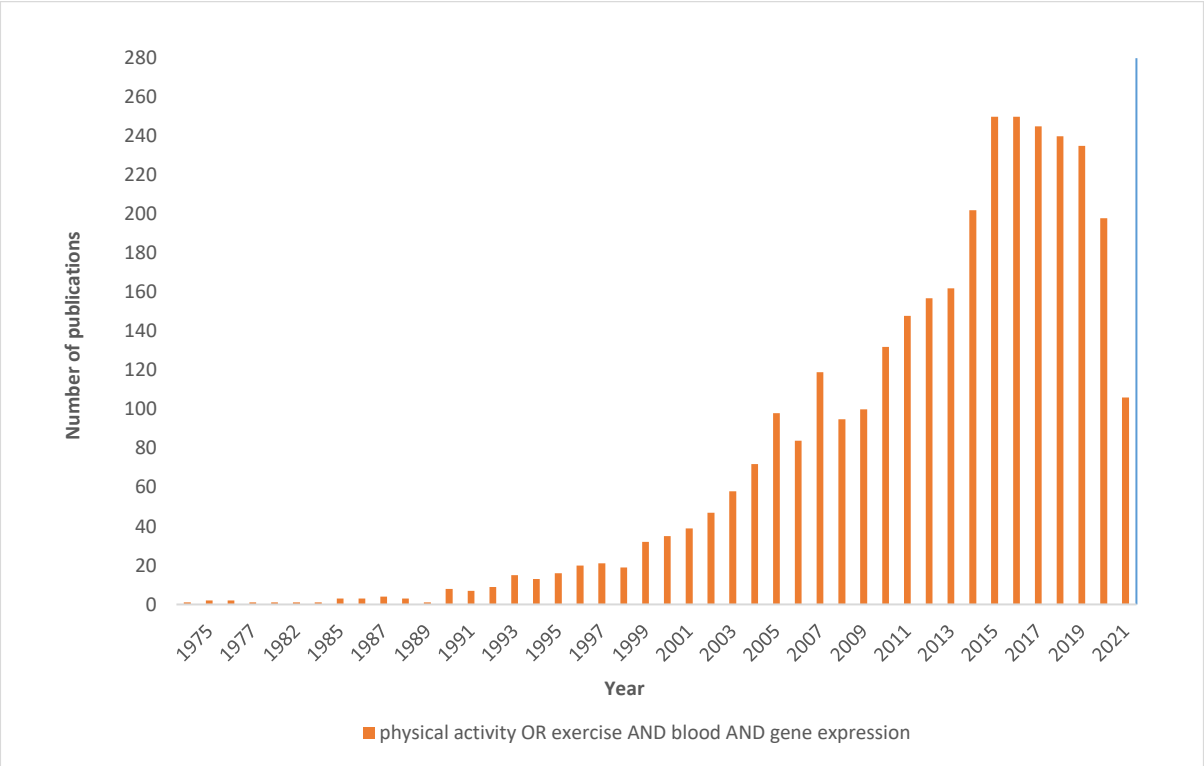

Figure 3-1 *Number of publications per year using "physical activity OR exercise AND blood AND gene expression" as boolean operators (PubMed search (July 2021).*

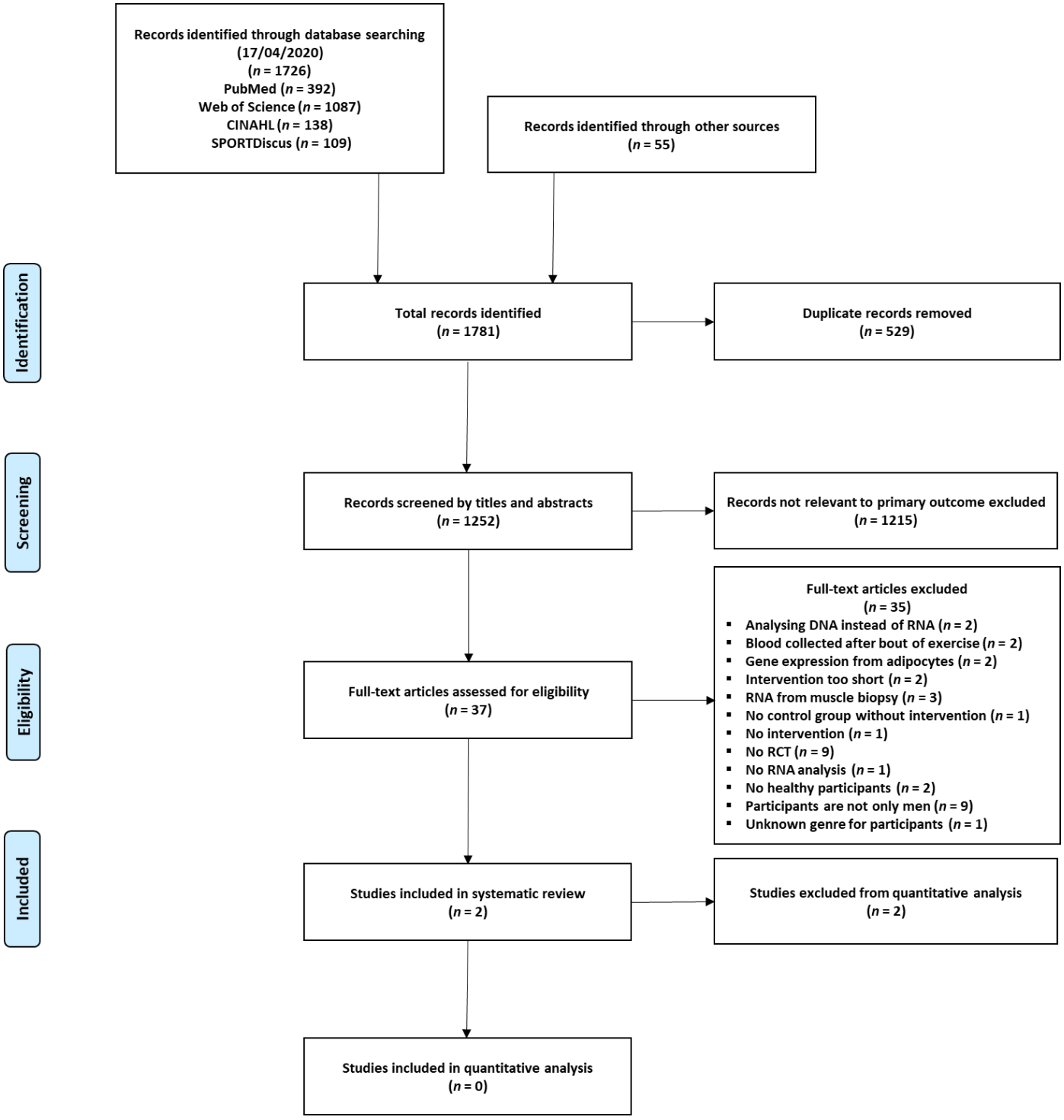

Figure 3-2 *Flowchart of screening process.*

(exercise[MeSH Terms]) OR resistance train*[Title/Abstract]) OR aerobic train*[Title/Abstract]) OR weight train*[Title/Abstract]) OR interval train*[Title/Abstract]) OR endurance[Title/Abstract]) OR strength[Title/Abstract]) OR athletes[Title/Abstract]) OR weight lift*[Title/Abstract]) OR anaerobic train*[Title/Abstract]) OR walk*[Title/Abstract]) OR jog*[Title/Abstract]) OR swim*[Title/Abstract]) OR marathon[Title/Abstract] **AND** gene expression[Title/Abstract] OR mRNA[Title/Abstract] OR messenger RNA[Title/Abstract] OR lncRNA[Title/Abstract] OR long non coding RNA[Title/Abstract] OR miRNA[Title/Abstract] OR micro RNA[Title/Abstract] OR circRNA[Title/Abstract] OR circular RNA[Title/Abstract] OR transcript*[Title/Abstract] OR ncRNA[Title/Abstract] OR non coding RNA[Title/Abstract] **AND** randomised controlled trial[Title/Abstract] OR controlled trial[Title/Abstract] OR controlled study[Title/Abstract] OR controlled clinical trial[Title/Abstract] OR controlled clinical study[Title/Abstract] OR RCT[Title/Abstract] OR randomi*[Title/Abstract]

Figure 3-3 *Example PubMed search string used for this meta-analysis.*

Table 1. *Summary of the exercise intervention*

Week	Days Per Week	Duration, min	Intensity, $\%\dot{V}O_{2max}$
1 and *2*	3	30	50
3 and *4*	4	30	50
5 and *6*	4	35	50
7	4	35	55
8 and *9*	4	40	55
10	4	40	55
11 and *12*	4	45	55
13 and *14*	4	45	60
15 and *16*	4	50	60
17 and *18*	4	50	65
19–21	4	55	65
22	4	60	65
23 and *24*	4	60	70

Intensity was calculated using initial baseline maximal oxygen consumption ($\dot{V}O_{2max}$).

Figure 3-4 *Summary of the exercise intervention for Thompson et al. study. (Adapted from Thompson et al., 2010).*

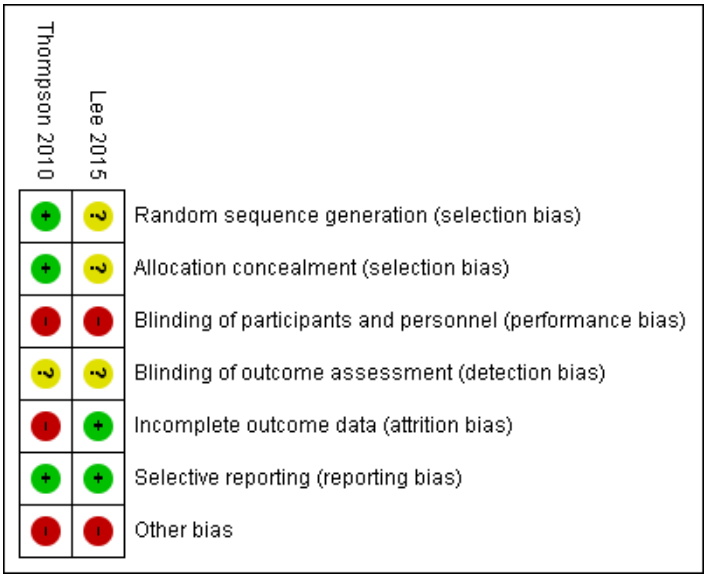

Figure 3-5 *Risk of bias chart of studies included in the review.*

4 COMPARATIVE EFFICACY OF DIFFERENT EXERCISE TYPES TO CHARACTERISE PERIPHERAL BLOOD TRANSCRIPTOMICS IN HUMANS: A SYSTEMATIC REVIEW AND NETWORK META-ANALYSIS OF CANDIDATE SIGNATURES FROM RANDOMISED CONTROLLED TRIALS (RCTS)

"The following experimental chapter is presented in accordance with author guidance procedures for the journal ***F1000***".

https://f1000research.com/

ISSN: 20461402

4.1 ABSTRACT

BACKGROUND: During the past decade, there have been substantial innovations in the exercise genomics and a plethora of *de novo* RCTs seeking to progress personalised medicine and optimising exercise prescription using peripheral blood transcriptomics using different exercise programming.

METHODS: Studies published through June 6, 2019, were identified from PubMed, Web of Science, CINAHL and SPORTDiscus electronic databases of English-language RCTs investigating the efficacy divergent exercise training modes in healthy sedentary participants were included in this analysis. Two investigators independently reviewed abstracts and full-text articles and extracted data from relevant studies (concordance 96.2%). Exercise modalities were classified into flexibility exercise, mind-body exercise, low-intensity aerobic exercise, moderate/high-intensity aerobic exercise, low-intensity resistance exercise, or moderate/high-intensity resistance exercise, or their combination for comparative analysis. Outcome included the expression of transcripts analysed in the RCTs, expressed as Fold Change (FC) or logFC.

RESULTS: 12 RCTs enrolling (*n*=392) participants, where (*n*=357) were analysed, and (~*n*=270) participants underwent peripheral blood transcriptomics. Following systematic scrutiny, only 2 transcripts were eligible for comparison (*TNF-a*, and *IL-10*). Remarkable heterogeneity between studies precluded network meta-analysis. From the 2 eligible RCTs (*n*=43, n=19 controls) provided data for basic pooled comparison of *IL-10* expression; 1.3 FC (95% CI [0.35, 5.02]) being upregulated following moderate/high-intensity resistance exercise training. Similarly, 2 RCTs (*n*=35, *n*=16 controls) provided eligible data for *TNF-a*; 0.4 FC (95% CI [0.06, 2.79]) which was down-regulated following moderate/high-intensity resistance exercise. Notable heterogeneity and absence of coherent presentation of data

prevented head-to-head comparison of exercise transcriptomics from different exercise modes.

CONCLUSIONS: Current RCT evidence relating to PBT expression analysis fails to meet the standards for meaningful head-to-head comparison of exercise modalities. Thus, evidence based personalised exercise prescription derived from RCTs utilising PBT analysis is not currently possible.

4.2 INTRODUCTION

Exercise genomics is a new field of research that has leveraged innovative technologies such as high throughput DNA sequencing achieved in coalition with machine learning to manage massive datasets. The ambition of this predictive analytics phenomenon is to identify specific exercise-related genes where an individual's genomic information could ultimately be used to customise exercise training. This potential to realise predictive exercise transcriptomics for personalised exercise prescription benefits from a body of well-established exercise physiology research. Yet, many key concepts such as the influence of different modes of exercise on differential gene expression, have not been adequately established.

Muscle biopsies have long been used to scrutinise the intricacies of gene expression regulation in skeletal muscle in response to exercise training. However, muscle biopsy involves an aggressive procedure, requiring patients to recover from the intervention. Due to that, over the past decade, peripheral blood has been proposed as a surrogate tissue to study the systemic effect of exercise training [1], and some research supports the idea of being able to pick up physiological adaptations to exercise training examining the peripheral blood transcriptome (PBT) [2].

There are two previous reviews which summarise existing literature on the effects of mind-body exercise on peripheral blood transcriptomics. Bower et al. narratively summarised Randomised Control Trial (RCT) evidence relating to the effects of mind-body exercise therapy to impact genetic markers of inflammation [3]. However, this study also included studies of both circulating and cellular markers of inflammation and studies were not restricted to RCTs enrolling healthy individuals. Buric et al. conducted a systematic review about gene expression changes induced by meditation and related practices [4]. The authors included a combination of clinical and non-clinical samples and were liberal with including

heterogeneous research design. Similarly, two further reviews have attempted to summarise the transcriptomic effect of either aerobic or resistance exercise from systemic blood. However, Gjevestad and colleagues (2015) did not discriminate between various research designs and restricted their study to human white blood cells. In this case, the search also included all types of study designs [5]. Another recent pairwise meta-analytical review conducted by Amar and colleagues (2019) utilised publicly available transcriptomic databases for studies including both aerobic and resistance exercise modalities on gene expression within both peripheral blood and skeletal muscle, irrespective of duration or intensity of exercise programming, in acute and chronic exercise, and conducting subgroup analysis such sex, age, divergent exercise histories [6].

To date, no review has attempted to utilise network meta-analytical techniques to interrogate the differential impact of RCTs of different types of exercise on gene expression within peripheral blood of exercise naive participants undertaking one or more formal exercise programs. In opposition to pairwise meta-analysis which depicts pooled effects sizes from individual studies, network meta-analysis derives effect sizes which allows head-to-head comparisons between divergent treatments from homogenous RCTs. Network meta-analysis facilitates the mathematical creation of a network from RCTs where all the trials share at least one common treatment of interest [7], further establishing indirect treatment comparisons that are absent from individual RCTs. Chapter two of this thesis utilised pairwise meta-analysis of RCTs examining PBT of sedentary males undertaking resistance/aerobic exercise, and identified distinct heterogeneity of methodology and study design of eligible studies. This coalition of limiting factors preclude the utility of pairwise meta-analytics of RCTs using best-fit literature until such time as there is coherency of RCTs that allows quantitative pooling of transcriptomic outcomes.

With these aspects in mind, the present study used a more expansive search criteria in order to systematically review and quantitatively compare RCTs to establish (head-to-head) relative effect of divergent exercise modalities that examine transcriptomic expression limited to peripheral blood amongst male and female participants. We utilized RCT evidence to test the hypothesis that peripheral blood is a valid medium to identify differential effects of divergent physical exercise training regimens on transcriptomic markers in apparently healthy exercise-naïve participants.

4.3 METHODS

4.3.1 Protocol and registration

This study was prospectively registered with PROSPERO database (registration number: CRD42020187182), in compliance with the Preferred Reporting Items for Systematic Reviews and Meta-Analyses (PRISMA-NMA) guidelines [8].

4.3.2 Eligibility criteria

From learnings derived from "*Chapter 2 - An examination of chronic aerobic or resistance exercise training on peripheral blood transcriptomics in healthy males: a (narrative) systematic review and meta-analysis of candidate signatures from randomized controlled trials (RCTs)*", this study utilised broader search criteria to include RCTs enrolling both female participants enrolled to a broader range of exercise studies in an attempt to capture a more comprehensive pool of eligible PBT studies.

Studies were deemed eligible when meeting the following criteria: 1) studies RCT design; 2) from studies enrolling either sedentary, apparently healthy males or females (absent of any clinical described in the International Classification of Disease or ICD) participants; 3) where participants were aged greater than 18 years; and where 4) studies

conducted one or more structured aerobic, resistance, flexibility, or mind-body exercise interventions lasting 5) >4 weeks, with a minimum of 10 sessions; and where 6) studies utilised peripheral blood to examine the effect RNA expression 7) before and after each exercise intervention; and were 8) published in peer reviewed journals published in English language.

4.3.3 Study selection and data collection process

Electronic databases: PubMed, Web of Science, CINAHL and SPORTDiscus were searched from inception to May 21st, 2020. The search utilised Medical Subject Headings (MeSH), abstract, title, and keywords, using a combination of Boolean operators and key search terms in compliance with PICOS criteria; participants, interventions, matched control groups, outcomes, and study design (an example Pubmed search strategy can be found in **Fig. 4-1**). Reference lists from relevant studies and past review articles were also screened for potentially relevant studies. Two independent researchers (SM and DH) extracted study characteristics and outcome data using a standardised data collection form (Appendix A), and results were compared. Discrepancies were resolved by discussion with a third researcher (FG). When a complete report of the data was not available for a particular study, the authors were contacted. The type of control group was classified as waiting list or active control. Participants in a waiting list group did not engage in any intervention during the length of the study. Participants in an active control group underwent a different type of intervention, which did not incorporate any physical activity and/or exercise. Participant characteristics were coded according to age, body mass, and BMI. Type of exercise was categorised as flexibility exercise, mind-body exercise, low-intensity aerobic exercise, moderate/high-intensity aerobic exercise, low-intensity resistance exercise, or moderate/high-intensity resistance exercise (described in detail in **Fig. 4-2**). Length of the intervention was coded as total number of days. Intensity was categorised as percentage of maximal oxygen uptake

($\dot{V}O_{2max}$) or heart rate maximum (HR_{max}) for aerobic exercise intervention, and percentage of one-repetition maximum (1RM) for muscular strength. Intensity was not assessed for mind-body or flexibility exercise. Frequency was coded as number of sessions per week, and volume of exercise as minutes per week. Exercise supervision was coded as yes, no, or partially. Retention to the study was described as a percentage for the control and exercise groups, independently when possible, or for the total. Methodological characteristics were coded according to the intention-to-treat procedures used, type of statistical analysis, inclusion/exclusion criteria, time of blood collection, source of RNA from peripheral blood (PMBC, buffy coat, whole blood, or a particular cell subset), methodology for RNA extraction, and method for transcript identification (targeted genes by qPCR, microarray, or Next Generation-sequencing).

4.3.4 Risk of bias in individual studies

We assessed the risk of bias in the included studies using the Cochrane Collaboration's Tool for Assessing Risk of Bias [9] (RoB tool). Two independent researchers (SM and DH) assessed the Risk of Bias, and consensus was reached by a third researcher (FG). Criteria includes random sequence generation, allocation concealment, blinding of participants and personnel, blinding of outcome assessment, incomplete outcome data, selective outcome reporting, and other sources of bias. Other source of bias were based on factors that are specific for studies mixing physical exercise interventions and gene expression analysis , i.e.: comparison of the changes in the exercise group with the changes in the control group, supervision of the exercise intervention, type of control group, the selection of a subset of participants within the study to examine the gene expression, timing for the collection of the post-treatment sample (immediately after, 24h after, 48h after…), the criteria for the selection of a particular Fold Change (FC) and *p* value threshold for a significant change in gene expression, time of the day for blood collection, ethnicity

differences, age differences, sex, appropriate representation of peripheral blood as a sample (using PBMCs, buffy coat, or a particular subset of blood cells as a source for RNA), and gene expression being the primary outcome of the study.

4.3.5 Summary of outcomes

We assessed the average FC (the ratio between the transcript expression before and after the intervention) for both control group and exercise treatment groups for each of the transcripts reported in >2 studies of utilising exercise interventions. Where FC was unavailable, this was calculated using available data from individual of studies. When data was not depicted numerically, figures were interrogated using ImageJ software to obtain requisite data [10]. Transcripts that were identified as being either up-regulated, down-regulated, or unchanged when this information was reported. In instances where individual RCTs reported more than one post-treatment value, the assessment time-point immediately following the conclusion of the intervention were used as criterion values.

4.3.6 Synthesis of results

In this network meta-analysis, divergent exercise treatments (mind-body, low-intensity aerobic, moderate/high-intensity aerobic, moderate/high-intensity resistance) compared with control conditions (either waiting list or active control) were classified into separate network estimates to account for between-study variation of known effect modifiers, to allow assumption of transitivity between treatment comparisons.

Data were analysed and figures generated using STATA/SE 15 (StataCorp, 2017). FC and 95% Confidence Intervals (CIs) for intervention and control groups were used for the analysis of gene expression outcome data, and depicted in forest plots as logFC. LogFC values below 0 would favor down-regulation of the transcript, whereas logFC values above 0 would favor up-regulation of the requisite transcripts compared with the control conditions. I^2 statistic was calculated to determine heterogeneity which is proportional to statistical

variability between individual studies. Values approximating ~50% would indicate moderate heterogeneity whereas >75% was considered to identify substantial heterogeneity.

Contribution plots were generated to illustrate direct and indirect contributions within each network model. Publication bias was evaluated using funnel plots method and inconsistency factor plots and inconsistency models were used to respectively test both loop-specific and global consistency.

Subgroup analyses were performed by separating studies according to their categorical/dichotomous variable categories when sufficient data for a given transcript was available: specifically, participant sex, supervision of exercise (yes, no, partially), source of RNA from blood (PBMCs, leukocytes, NK cells, others), and techniques utilised for transcript identification (PCR, microarray, or NG-Seq). Meta-regression analysis of data were conducted for continuous variables when data for a given transcript were available: age, performance level for a given type of exercise type at study enrolment, magnitude of change in athletic performance for a given exercise type. Statistical significance was accepted when $\alpha<0.05$.

4.4 RESULTS

4.4.1 Study selection

Systematic search in the literature yielded 1781 articles. After removing duplicates (n=529), 1252 were eligible for individual screening. Title and abstract screening was conducted by two independent researchers (SM and DH), with concordance of 97.6%, resulting in 1215 articles being excluded. 37 full text articles underwent detailed screening for eligibility, where 25 were excluded from the systematic review. Finally, 12 studies were eligible for inclusion in the final analysis. Again, two independent researchers (SM and DH) conducted the full text screening with concordance of 70.2%. Discrepancies were resolved by

consensus with a third researcher (FG). Procedural screening of RCTs can be found in **Fig. 4-3**.

4.4.2 Study characteristics

Data were extracted by two independent researchers (SM and DH) with agreement of 96.2 %. Subsequently, *n*=392 participants (CG=188, IG=204) across 12 studies were eligible for systematic scrutiny. From these, n=357 participants (CG=171, IG=186), where *n*=270 participants (*n*=125 controls) were included in respective PBT analysis, with transcripts-of-interest being study dependent. 2 studies were restricted to enrolling male participants [11, 12], and 3 studies solely enrolled female participants [13-15], 1 study did not specify participants sex [16]. 6 studies enrolled both males and female participants [17-22]. Amongst mixed sex studies, 3 did not specify proportional sex enrolment [17, 21, 22]. No single study compared PBT expression between males and females. Authors were contacted on >1 occasion during a 2 weeks period from initial request for sex balancing of RCT arms, and for any transcriptomic data which was not reported within the published articles (i.e. data for non-differentially expressed transcripts). 5 studies conducted a supervised exercise intervention [11, 14, 15, 19, 20], whereas 3 studies were unsupervised [12, 16, 17], with 2 studies being partially supervised [18, 22]. 2 studies did not report whether exercise was supervised [13, 21]. Across each of 12 studies deemed suitable for quantitative analysis, there were 4 different types of exercise, identified as; Low-intensity aerobic (*n*=1) [19], Moderate/high-intensity aerobic (*n*= 6) [11-13, 16, 20, 22], Moderate/high intensity-resistance (*n*=3) [14, 15, 21], and Mind-body (*n*=2) [17, 18].

RNA was extracted from different cell types within peripheral blood. The most common one was PBMCs, with 6 studies [11, 12, 17, 18, 20, 21]. The remaining 2 studies employed buffy coat techniques [19, 22], and 1 study employed RNA extraction from whole blood [14], 1 study used $CD34^+$ cells [16], 1 study used leukocytes [15], and 1 study extracted

RNA from NK cells [13]. Furthermore studies used different methods to identify the change in transcripts expression with 4 studies conducted Microarray analysis [12, 17, 18, 22], and 8 studies used PCR technique to identify target transcripts [11, 13-16, 19-21]. Notably, no studies used NG-seq as a form to interrogate gene expression.

4.4.3 Exercise type characteristics

The average length (days) for exercise programs per participant was longer for moderate/high-intensity aerobic (N=100; M=95.78, SD=48.09) than for low-intensity aerobic (N=17; M=56, SD=0), mind-body (N=38, M=56, SD=0), or moderate/high-intensity resistance (N=37; M = 41.72, SD =13.26). Detailed description of study characteristics are shown in **Table 4-1**.

4.4.4 Risk of bias within studies

Risk of bias within each study was generally low-to moderate, with the exception of two studies showing high risk of bias in four of the seven categories [12, 17]. Details on risk of bias for each study can be found in **Fig. 4-4**. Due to the nature of the studies, it was not possible to blind participants for the exercise intervention, resulting in a high risk of performance bias for all of them. Random sequence generation was low in half of the studies [12, 15-18, 22] and unclear on the other half [11, 13, 14, 19-21]. Allocation concealment was predominately moderate with 3 studies showing low risk of bias [12, 17, 22] and 9 showing unclear [11, 13-16, 18-21]. Blinding of outcome assessment was unclear in all the studies. Incomplete outcome data was identified as low in 8 of the studies [11, 13-16, 18, 19, 21], unclear in 1 [22], and high in 3 of them [12, 17, 20]. Selective reporting was low in 7 [11, 13-15, 19-21] and high in 5 [12, 16-18, 22]. The assessment of the Other risk of bias was overall high in all cases, and resulted as follows. Comparison of the changes in the exercise group with the changes in the control group was described as low in 9 [11, 13-15, 17-21] of the

studies and high in 3 [12, 16, 22]. Eight studies were considered to show low risk of bias for the Supervision of exercise [11, 12, 14, 15, 18-20, 22], whereas 3 were considered unclear [13, 16, 21] and 1 high [17]. Type of control group was found low for 9 of the studies [11-13, 15-19, 21], and high for 4 of them [14, 17, 20, 22]. Selection of a subset of participants within the study to examine the gene expression, was reported as low in 8 cases [11, 13, 17-22], unclear in 1 [16], and high 3 [12, 14, 15]. Timing for the collection of the post-treatment sample was considered low in 4 studies [12, 15, 19, 21], unclear in 7 [13, 14, 16-18, 20, 22], and high in 1 [11]. The criteria for the selection of a particular FC and p value threshold for a significant change in gene expression was judged low in 8 studies [11, 13-16, 19-21] and unclear in 4 [12, 17, 18, 22]. Time of the day for blood collection resulted in low in 4 of the studies [15, 17, 20, 21], and unclear in the other 8 [11-14, 16, 18, 19, 22]. Ethnicity was predominately categorised as unclear in all of the studies [11-17, 19-22], except for one of them that was low [18]. In the case of age, all the studies were reported as low [11-16, 18-22] except for one of them that was reported high [17]. Sex was depicted as low in 5 studies [11-15] and high in 7 studies [16-22]. As per the appropriate representation of peripheral blood as a sample we considered 9 studies to have a low risk of bias [11, 12, 14, 17-22] and 3 to have a high risk of bias [13, 15, 16]. Finally, gene expression being the primary outcome of the study was assessed low in 5 studies [13, 14, 16, 21, 22] and high in 7 of them [11, 12, 15, 17-20].

4.4.5 Results of individual studies

A detailed description of the results of individual studies included in this review is presented in **Table 4-1**, and grouped according to exercise modality employed. The majority of the studies employing q-PCR as a method for transcript identification reported data for each transcript under examination [11, 13-16, 19, 21]. In the case of the studies employing microarray, only data for the differentially expressed transcripts were reported [12, 17, 18,

22]. Pooled comparison identified 41 unique transcripts that were examined in >1 RCT. From these RCTs, only 12 had concordant transcript data in >2 studies. From those 12 RCTs, *IL-10* [14, 21], *CLC* [12, 17], *IL8* [12, 17], *CD83* [17, 18], *DEFA1* [17, 18], *DEFA1B* [17, 18], *FOSB* [17, 18], *HBA1* [17, 18], and *HBG2* [17, 18] was reported in 2 studies. 3 studies described data for *G0S2* [12, 17, 18] and *DEFA3* [17, 18, 22], and 4 studies reported *TNF-α* outcome data [14-16, 21]. This information is depicted in **Table 4-2.**

4.4.6 Synthesis of results

Two transcripts had data available for both control group and intervention group. Data from a total of 43 participants (19 control and 24 intervention) across two RCTs [14, 21] were included for *IL-10* meta-analysis, and data from 35 participants (16 control and 21 intervention) across two RCTs [15, 21] were included for *TNF-α*. Meta-analysis of *IL-10* resulted 1.3 FC (95% CI [0.35, 5.02]) up-regulation after moderate/high-intensity exercise training compared with control (**Fig. 4-5**). In the case of *TNF-α*, meta-analysis showed that it was down-regulated 0.4 FC (95% CI [0.06, 2.79]) after moderate/high-intensity exercise training compared with control (**Fig. 4-6**). All 3 studies conducted a moderate/high-resistance exercise intervention, therefore precluding the implementation of Network meta-analytical techniques.

4.5 DISCUSSION

The main finding from this study relates to the existence of a high magnitude of heterogeneity amongst exercise studies employing RCT design to examine peripheral blood transcriptomics. Indeed, the variability across RCT studies was such that only three studies were eligible for network meta-analysis. From the three studies eligible for NMA, investigation of *IL-10* and *TNF-α*, were most prominent. In addition to significant heterogeneity, outcome bias and incomplete reporting of data within the eligible RCTs

(*n*=12) was such that head-to-head comparison of individual study outcomes was impossible. In light of this, the following discussion is confined to summarizing key findings from studies eligible for systematic review and provide utility for researchers wishing to pursue similar lines of research enquiry.

The most commonly identified transcripts were *TNF-α* [14-16, 21], followed by *G0S2* [12, 17, 18], and *DEFA3* [17, 18, 22] and *IL-10* [14, 21]. Speculatively, *G0S2* is a gene coding for G0/G1 switch protein 2, which promotes apoptosis by binding to BCL2, hence preventing the formation of protective BCL2-BAX heterodimers. This mediates re-entry of cells from the G0 to G1 phase of the cell cycle. More specifically, it directly inhibits the adipose triglyceride lipase (ATGL) enzyme from degrading triacylglycerol in adipocytes [23] and is known to play an important role in energy metabolism. *DEFA3* is a gene that encodes for the protein defensin alpha 3, which is a member of a family of antimicrobial and cytotoxic peptides. It is found in the microbicidal granules of neutrophils and likely plays a role in phagocyte-mediated host defence [24]. TNF-α is a cytokine with a major role in the acute inflammatory response, has a major implication in the inflammatory process. Some studies suggest that resistance exercise training decreases circulating levels of this molecule, promoting and anti-inflammatory environment [15, 25, 26]. On the other hand *IL-10* gene encodes for a cytokine with the same name (IL-10). IL-10 has multiple, pleiotropic functions in inflammation and immunoregulation [27]. Furthermore, IL-10 role in response to exercise has been well studied [28-30], although the complex structure of the immune system network in coalition with RCT heterogeneity, preclude worthwhile interpretation.

To exemplify the lack of congruence within relevant RCTs, **Figures 4-5 and 4-6** identify two transcripts; *TNF-α* and *IL-10*, which identifies the only consistency between studies. Of further note, there is an emphasis exercise transcriptomic RCTs to examine immune adaptive response within individual studies, wherein a targeted gene approach was

undertaken to identify predetermined immune-response cytokines. Therefore, this approach to examine exercise transcriptomics in RCTs presents congruence heuristic bias which precludes any generalised discovery for the present review.

Type of exercise in RCTs included in this review

A priori rationale of the present review was that different exercise types (i.e. strength training, aerobic training) have observable phenotypic differences, presenting a logical rationale that gene expression patterns from RCTs of exercise transcriptomics would be different and that 'head-to-head' comparison of these exercise training modalities, might identify consistent transcripts of interest. Aerobic exercise interventions predominated within the studies meeting eligibility for systematic review (n=7), compared with strength training interventions (n=3) and mind body exercise (n=2). However, no single RCT compared different exercise modes on transcriptomic outcomes. This was surprising, in light that it is broadly appreciated that (ie) strength and aerobic phenotypes are characteristically different. Similarly, the degree of inconsistency between eligible RCTs (ie, source of RNA, analytical differences and research design approach) were a magnitude that precluded network meta-analytics in the present review. It seems that endorsement of this important rationale is not forthcoming and that reliable application of PBT research should not be expected in the immediate future.

Limitations

The present study is not without limitation. For instance, a broader approach to study inclusion which may have incorporated clinical populations and broad range of age and sex groups. Albeit, this is likely to have amplified heterogeneity and limit direct application and utility to identify important transcriptomic phenomena in healthy adults undertaking structured exercise training.

4.6 CONCLUSSION

There is significant heterogeneity amongst RCTs which examine peripheral blood exercise transcriptomics such that network meta-analytic interrogation was not possible. Studies meeting eligibility presented with numerous sources of bias and with limited consistency. This review supports the tenet that the application peripheral blood transcriptomics should not be expected in the near future.

4.7 REFERENCES

1. Zeibig J, Karlic H, Lohninger A, Damsgaard R, Smekal G. Do blood cells mimic gene expression profile alterations known to occur in muscular adaptation to endurance training? European journal of applied physiology. 2005;95(1):96-104. Epub 2005/04/09. doi: 10.1007/s00421-005-1334-3. PubMed PMID: 15815935.
2. Liu D, Wang R, Grant AR, Zhang J, Gordon PM, Wei Y, et al. Immune adaptation to chronic intense exercise training: new microarray evidence. BMC Genomics. 2017;18(1):29. Epub 2017/01/07. doi: 10.1186/s12864-016-3388-5. PubMed PMID: 28056786; PubMed Central PMCID: PMCPMC5216585.
3. Bower JE, Irwin MR. Mind–body therapies and control of inflammatory biology: A descriptive review. Brain, Behavior, and Immunity. 2016;51:1-11. Epub 2015/06/28. doi: 10.1016/j.bbi.2015.06.012. PubMed PMID: 26116436; PubMed Central PMCID: PMCPMC4679419.
4. Buric I, Farias M, Jong J, Mee C, Brazil IA. What Is the Molecular Signature of Mind-Body Interventions? A Systematic Review of Gene Expression Changes Induced by Meditation and Related Practices. Frontiers in Immunology. 2017;8:670. Epub 2017/07/04. doi: 10.3389/fimmu.2017.00670. PubMed PMID: WOS:000403397000001; PubMed Central PMCID: PMCPMC5472657.
5. Gjevestad G, Holven K, Ulven S. Effects of Exercise on Gene Expression of Inflammatory Markers in Human Peripheral Blood Cells: A Systematic Review. Current Cardiovascular Risk Reports. 2015;9(7):1-17. doi: 10.1007/s12170-015-0463-4.
6. Amar D, Lindholm ME, Norrbom J, Wheeler MT, Rivas MA, Ashley EA. Differential response trajectories to acute exercise in blood and muscle. bioRxiv. 2019:863100. doi: 10.1101/863100.
7. Mavridis D, Giannatsi M, Cipriani A, Salanti G. A primer on network meta-analysis with emphasis on mental health. Evidence-based mental health. 2015;18(2):40-6. Epub 2015/04/25. doi: 10.1136/eb-2015-102088. PubMed PMID: 25908686.
8. Moher D, Liberati A, Tetzlaff J, Altman DG, The PG. Preferred Reporting Items for Systematic Reviews and Meta-Analyses: The PRISMA Statement. PLOS Medicine. 2009;6(7):e1000097. doi: 10.1371/journal.pmed.1000097.
9. Higgins JPT, Altman DG, Gøtzsche PC, Jüni P, Moher D, Oxman AD, et al. The Cochrane Collaboration's tool for assessing risk of bias in randomised trials. BMJ. 2011;343:d5928. Epub 2011/10/20. doi: 10.1136/bmj.d5928. PubMed PMID: 22008217; PubMed Central PMCID: PMCPMC3196245.
10. Schneider CA, Rasband WS, Eliceiri KW. NIH Image to ImageJ: 25 years of image analysis. Nature Methods. 2012;9(7):671-5. Epub 2012/08/30. doi: 10.1038/nmeth.2089. PubMed PMID: 22930834; PubMed Central PMCID: PMCPMC5554542.
11. Lee SH, Hong HR, Han TK, Kang HS. Aerobic training increases the expression of adiponectin receptor genes in the peripheral blood mononuclear cells of young men. Biology of sport. 2015;32(3):181-6. Epub 2015/10/02. doi: 10.5604/20831862.1150298. PubMed PMID: 26424919; PubMed Central PMCID: PMCPMC4577554.
12. Thompson D, Markovitch D, Betts JA, Mazzatti D, Turner J, Tyrrell RM. Time course of changes in inflammatory markers during a 6-mo exercise intervention in sedentary middle-aged men: a randomized-controlled trial. Journal of Applied Physiology. 2010;108(4):769-79. doi: 10.1152/japplphysiol.00822.2009. PubMed PMID: WOS:000276324200003.
13. Schenk A, Pulverer W, Koliamitra C, Bauer CJ, Ilic S, Heer R, et al. Acute Exercise Increases the Expression of KIR2DS4 by Promoter Demethylation in NK Cells. International

journal of sports medicine. 2019;40(1):62-70. Epub 2018/12/07. doi: 10.1055/a-0741-7001. PubMed PMID: WOS:000454222500009.
14. Henagan TM, Phillips MD, Cheek DJ, Kirk KM, Barbee JJ, Stewart LK. The melanocortin 3 receptor: a novel mediator of exercise-induced inflammation reduction in postmenopausal women? J Aging Res. 2011;2011:512593. Epub 2011/01/22. doi: 10.4061/2011/512593. PubMed PMID: 21253483; PubMed Central PMCID: PMCPMC3022199.
15. Macêdo Santiago LÂ, Neto LGL, Borges Pereira G, Leite RD, Mostarda CT, de Oliveira Brito Monzani J, et al. Effects of Resistance Training on Immunoinflammatory Response, TNF-Alpha Gene Expression, and Body Composition in Elderly Women. Journal of Aging Research. 2018;2018:1-10. Epub 2018/12/05. doi: 10.1155/2018/1467025. PubMed PMID: 132650858. Language: English. Entry Date: 20181030. Revision Date: 20181030. Publication Type: Article. Journal Subset: Biomedical; PubMed Central PMCID: PMCPMC6230406.
16. Sen S, Witkowski S, Lagoy A, Islam AM. A Six-Week Home Exercise Program Improves Endothelial Function and CD34(+) Circulating Progenitor Cells in Patients With Pre-Diabetes. Journal of Endocrinology and Metabolism. 2015;5(1-2):163-71. doi: 10.14740/jem273w. PubMed PMID: WOS:000360177700002.
17. Black DS, Cole SW, Irwin MR, Breen E, St Cyr NM, Nazarian N, et al. Yogic meditation reverses NF-κB and IRF-related transcriptome dynamics in leukocytes of family dementia caregivers in a randomized controlled trial. Psychoneuroendocrinology. 2013;38(3):348-55. Epub 2012/07/17. doi: 10.1016/j.psyneuen.2012.06.011. PubMed PMID: 22795617; PubMed Central PMCID: PMCPMC3494746.
18. Creswell JD, Irwin MR, Burklund LJ, Lieberman MD, Arevalo JM, Ma J, et al. Mindfulness-Based Stress Reduction training reduces loneliness and pro-inflammatory gene expression in older adults: a small randomized controlled trial. Brain Behav Immun. 2012;26(7):1095-101. Epub 2012/07/24. doi: 10.1016/j.bbi.2012.07.006. PubMed PMID: 22820409; PubMed Central PMCID: PMCPMC3635809.
19. Butcher LR, Thomas A, Backx K, Roberts A, Webb R, Morris K. Low-intensity exercise exerts beneficial effects on plasma lipids via PPARgamma. Medicine & Science in Sports & Exercise. 2008;40(7):1263-70. Epub 2008/06/27. doi: 10.1249/MSS.0b013e31816c091d. PubMed PMID: 105658595. Language: English. Entry Date: 20081003. Revision Date: 20150711. Publication Type: Journal Article.
20. Streese L, Khan AW, Deiseroth A, Hussain S, Suades R, Tiaden A, et al. High-intensity interval training modulates retinal microvascular phenotype and DNA methylation of p66Shc gene: a randomized controlled trial (EXAMIN AGE). Eur Heart J. 2020;41(15):1514-9. Epub 2019/07/20. doi: 10.1093/eurheartj/ehz196. PubMed PMID: 31323685.
21. Rodriguez-Miguelez P, Fernandez-Gonzalo R, Almar M, Mejias Y, Rivas A, de Paz JA, et al. Role of Toll-like receptor 2 and 4 signaling pathways on the inflammatory response to resistance training in elderly subjects. Age. 2014;36(6):9734. Epub 2014/11/28. doi: 10.1007/s11357-014-9734-0. PubMed PMID: WOS:000346770900016; PubMed Central PMCID: PMCPMC4245402.
22. Iyalomhe O, Chen YX, Allard J, Ntekim O, Johnson S, Bond V, et al. A standardized randomized 6-month aerobic exercise-training down-regulated pro-inflammatory genes, but up-regulated anti-inflammatory, neuron survival and axon growth-related genes. Experimental gerontology. 2015;69:159-69. Epub 2015/05/20. doi: 10.1016/j.exger.2015.05.005. PubMed PMID: WOS:000360320200021; PubMed Central PMCID: PMCPMC4553116.

23. Yang X, Lu X, Lombès M, Rha GB, Chi YI, Guerin TM, et al. The G(0)/G(1) switch gene 2 regulates adipose lipolysis through association with adipose triglyceride lipase. Cell metabolism. 2010;11(3):194-205. Epub 2010/03/04. doi: 10.1016/j.cmet.2010.02.003. PubMed PMID: 20197052; PubMed Central PMCID: PMCPMC3658843.
24. Linzmeier R, Michaelson D, Liu L, Ganz T. The structure of neutrophil defensin genes. FEBS letters. 1993;321(2-3):267-73. Epub 1993/04/26. doi: 10.1016/0014-5793(93)80122-b. PubMed PMID: 8477861.
25. Córdova C, Lopes-e-Silva JF, Pires AS, Souza VC, Brito CJ, Moraes CF, et al. Long-Term Resistance Training Is Associated with Reduced Circulating Levels of IL-6, IFN-Gamma and TNF-Alpha in Elderly Women. Neuroimmunomodulation. 2011;18(3):165-70. Epub 2011/02/12. doi: 10.1159/000323396. PubMed PMID: 21311202.
26. Palomo I, Herrera J, Cancino V, Alarcón M, Mujica V, Leiva E, et al. Physical activity reduces circulating TNF-alpha but not pro-thrombotic factors levels in patients with metabolic syndrome. Diabetes & Metabolic Syndrome: Clinical Research & Reviews. 2010;4(4):234-8. doi: https://doi.org/10.1016/j.dsx.2010.05.004.
27. Mosser DM, Zhang X. Interleukin-10: new perspectives on an old cytokine. Immunological reviews. 2008;226:205-18. Epub 2009/01/24. doi: 10.1111/j.1600-065X.2008.00706.x. PubMed PMID: 19161426; PubMed Central PMCID: PMCPMC2724982.
28. Yakeu G, Butcher L, Isa S, Webb R, Roberts AW, Thomas AW, et al. Low-intensity exercise enhances expression of markers of alternative activation in circulating leukocytes: roles of PPARgamma and Th2 cytokines. Atherosclerosis. 2010;212(2):668-73. Epub 2010/08/21. doi: 10.1016/j.atherosclerosis.2010.07.002
10.1016/j.atherosclerosis.2010.07.002. Epub 2010 Jul 16. PubMed PMID: 20723894.
29. Pedersen BK. Anti-inflammatory effects of exercise: role in diabetes and cardiovascular disease. Eur J Clin Invest. 2017;47(8):600-11. Epub 2017/07/20. doi: 10.1111/eci.12781. PubMed PMID: 28722106.
30. Cabral-Santos C, de Lima EA, Fernandes IMD, Pinto RZ, Rosa-Neto JC, Bishop NC, et al. Interleukin-10 responses from acute exercise in healthy subjects: A systematic review. Journal of Cellular Physiology. 2019;234(7):9956-65. Epub 2018/12/12. doi: 10.1002/jcp.27920. PubMed PMID: WOS:000462645700007.

Table 4-1 *Participants, protocol, exercise characteristics, and outcomes of the RCTs included in this review.*

Study	Participants enrolled	Protocol	Exercise intervention	Changes in phenotype	Source of RNA	Methodology for transcripts identification	Transcripts investigated	Regulation after exercise
Low-intensity aerobic exercise								
Butcher et al. (2008) [44]	IG= SED; 17 (9 males, 8 females; 44.94±10.01 years) CG= SED 17 (9 males, 8 females; 46.12±12.2 years) **1^0: -** **2^0: √**	Sedentary apparently healthy participants were randomised to IC or CG (waiting list). Fasting blood was sampled at baseline, after 4 and 8 wk of exercise. Blood was collected 24h before the commencement of the exercise study or 24h after an exercise session. To monitor any possible cardiovascular adaptations to the exercise program, $\dot{V}O_{2max}$ was estimated using a submaximal predictor test (Rockport Fitness Walking Test), which was conducted before and after the exercise program.	Walking 10,000 steps, supervised, during 8 wk, 3 times/wk. Participants selected their on walking speed. Familiarisation: Yes	CG-pre $\dot{V}O_{2max}$: 34.62±5.68 (mL*Kg-1*min^{-1}) CG Delta $\dot{V}O_{2max}$: +1.53±2.63 (mL*Kg-1*min^{-1}) IG-pre $\dot{V}O_{2max}$: 35.49±6.94 (mL*Kg-1*min^{-1}) IG Delta $\dot{V}O_{2max}$: +2.74±4.21 (mL*Kg-1*min^{-1}) $\dot{V}O_{2max}$ was estimated using the Rockport fitness walking test [86].	Buffy coat	RT-PCR	*CD36*, *PPARy*, *LXRa*, *ABCA1* and *ABCG1*	*CD36* and *PPARy* ↑ ($p<0.05$)‡, *LXRa*, *ABCA1* and *ABCG1* ↔ ($p>0.05$)‡ after 4 wk. *CD36*, *PPARy*, *LXRa*, *ABCA1* and *ABCG1* ↑ ($p<0.05$)‡ after 8 wk.
Moderate/high-intensity aerobic exercise								
Thompson et al. (2010) [40]	IG= SED 27 men (54±5 years) CG= SED 27 men (52±4 years) **1^0: -** **2^0: √**	Sedentary male volunteers were recruited from the local community. Participants were randomised to IG or CG (waiting list) using a sealed envelope. Participants in both groups reported to the laboratory at baseline, 4, 12, 24, and 26 wk later, each time following a 12h overnight fast. Before blood sampling, volunteers were asked to refrain from strenuous physical activity for at least 36 h. Participants were also asked whether they had experienced any symptoms of illness in the past 3 days or had taken any medication in the past 48 h. Microarray conducted in six of	24 wk of unsupervised aerobic exercise training, 3 days/wk during the first 2 wk and 4 days/wk for the rest. Duration started as 30min during the first wk and increased 5min every 4 wk. Intensity started as 50% $\dot{V}O_{2max}$ during the first wk and increased in 5% every 6 wk.	CG-pre $\dot{V}O_{2max}$: 35.2±4.7 (mL*Kg-1*min^{-1}) CG-post $\dot{V}O_{2max}$: 34.0±3.8 (mL*Kg-1*min^{-1}) ($p\geq0.02$) IG-pre $\dot{V}O_{2max}$: 34.5±4.2 (mL*Kg-1*min^{-1}) IG-post $\dot{V}O_{2max}$: 37.2±4.0 (mL*Kg-1*min^{-1})($p\leq0.02$)‡ $\dot{V}O_{2max}$ was determined using a progressive incline test to volitional fatigue on a treadmill, consisting of 3-min exercise stages with the gradient increasing by 3% at the end of each stage (Woodway, ELG 70, Weiss, Germany).	PBMC	Microarray Agilent Human Oligo Arrays (catalogue no. G4112F, Agilent Technologies UK)	41,267	53 probes differentially regulated by training in subjects with high baseline IL-6 (FC<2.0 and $p<0.05$) after 24 wk. Of those 53 probes, 31 were no longer significantly differentially expressed and 22 were still differentially expressed after 2 wk of retraining ($p<0.05$)

		the men in the IG with high serum IL-6 at baseline.						
Iyalomhe et al. (2015) [41]	N= SED 10 (3 males, 7 females) IG= SED 5 (distribution unknown; 73±5 years) CG= SED 5 (distribution unknown; 70±9 years) **1^0:** √ **2^0:** -	Prior to baseline test, participants were randomised blindly to IG or CG (active control). The CG underwent a stretch exercise protocol for the duration of the study. At baseline, VO_{2max} and endurance capacity was determined. Blood was collected after 24h fasting, and they refrained from exercise for 72h prior to testing. After 6 months, all tests were repeated using the same methods.	Supervised aerobic exercise training 3 times/wk during 6 months, including treadmill walking or jogging, stair-stepping, elliptical climbing, and an unsupervised 45-60min lower intensity walk on the weekend after the first 4-6 wk of exercise. Volume was Initially 20 min, increased by 5 min/wk until 40min/ wk. Intensity was 50% VO_{2max} during first 5 wk, then increase in 5% VO_{2max} weekly until reaching 70%VO_{2max} Familiarisation: Yes	CG-pre VO_{2max}: 26.48 ($mL*Kg-1*min^{-1}$) CG Delta VO_{2max}: -4.92 ($mL*Kg-1*min^{-1}$) (p=0.372) IG-pre VO_{2max}: 21.39 ($mL*Kg-1*min^{-1}$) IG Delta VO_{2max}: +9.72 ($mL*Kg-1*min^{-1}$) (p=0.018)‡ VO_{2max} and endurance capacity was determined using a modified Bruce protocol.	Buffy coat	Microarray Illumina HumanHT-12 v4 Expression BeadChip	47,000	81 genes differentially expressed in response to aerobic exercise training and not in stretch control. 6 unique, non-overlapping genes differentially expressed in stretch (FC ≥ 2, p<0.01)
Lee at al. (2015) [42]	IG= SED 15 men CG= SED 15 men Students between 20-30 years old. **1^0:** √ **2^0:** -	Participants were randomised to IG or CG (waiting list). Blood samples were available from 15 participants in the exercise-training group and 15 participants in the control group.	12 wk of supervised jogging and/or running programme on a motor-driven treadmill (Quinton, USA). Volume of 5min warm-up, 30 min exercise and 5min cool down, 5 days/wk. Volume was 200min/wk. Intensity of 60-75%HR_{max} Subjects maintained their exercise HR within 5 beats/min of their targeted HR by using a heart rate monitor (POLAR Accurex Plus, Finland). As the fitness level of each subject improved, the running velocity required to maintain the desired	CG-pre VO_2: 46.8±3.2 ($mL*Kg-1*min^{-1}$) CG-post VO_2: 47.8±3.0 ($mL*Kg-1*min^{-1}$) IG-pre VO_2: 45.9±2.10 ($mL*Kg-1*min^{-1}$) IG-post VO_2: 54.5±2.2 ($mL*Kg-1*min^{-1}$) Significant treatment effects post-pre (p<0.001)‡	PBMC	qPCR	*ADIPOR1*, *ADIPOR2*	*ADIPOR1*, *ADIPOR2* ↑ (p<0.001)‡ after 12wk.

			exercise intensity was increased.					
Sen et al. (2015) [45]	N= SED 11 participants with pre-diabetes, recruited from a local primary care physician patient pool and community. IG= SED 5 (distribution unknown; 55±8 SE, years) CG= SED 6 (distribution unknown; 53.57±8 SE, years) Pre-diabetes was defined as per American Diabetes Association (ADA) 2014 Clinical Recommendation guidelines by one of the following: 1) impaired fasting glucose (IFG), defined as fasting glucose 100 - 125 mg/dL; or 2) HbA1C ≥ 5.7-6.4% (39 - 46 mmol/mol). **1⁰:** √ **2⁰:** -	**Pilot study**. Subjects were randomised to IG or CG (waiting list), initially. After the intervention, there was a 4wk washout period. Then, in the second intervention, the IG went to no exercise, and the CG to exercise. Blood was collected from participants at baseline and 6wk after the first intervention, 4 wk after the washout period, and 6wk after the second intervention.	Exercise consisted on prescribing 150min/wk of moderate to vigorous intensity aerobic physical activity (MVPA) spread over at least 3days/wk with no more than two consecutive days without exercise. Participants increased their exercise duration from 70 min/wk in the first wk to 105 min/wk in wk 2 such that they achieved 150 min/wk on wk 3. Familiarisation: Yes	No VO_{2max} test was performed. All their activity was objectively measured by accelerometer (Actigraph model GT3X). Accelerometer data were collected in 60-s epochs and were downloaded every 2 wk to measure min/day spent in MVPA.	$CD34^+$	RT-PCR	*SOD1, SOD2, SOD3, Catalase, Glutathione Peroxidase, p53, p21, BCL2, Caspase-3, eNOS, ET-1, VEGF-A, SDF-1a, IL-6, TNF-a, CD34, VEGFR2* (KDR), *CD31*.	*TNF-a, IL-6, p53* and *p21* ↓ after the exercise phase ($p<0.05$). *SOD1, SOD2, SOD3, Catalase, glutathione peroxidase, Bcl2, caspase-3, eNOS, ET-1, VEGF-A, SDF-1a, CD34, VEGFR2* (KDR) and *CD31* ↔ after exercise ($p>0.05$).
Schenk et al. (2019) [43]	IG= SED 9 women (53.33±0.99 SE, years) CG= SED 7 women (53.57±0.20 SE, years) Participants were chosen to reflect a population with enhanced cancer risk. **1⁰:** √ **2⁰:** -	Venous blood samples were collected before and 1 min after an endurance capacity test. Subsequently, participants were randomised into IG or CG (waiting list). After 4 wk, resting blood samples were collected again and the endurance capacity test was repeated.	4 wk of endurance interval exercise program on a cross trainer 2-3 times/wk. Sessions started with a 3 min warm-up period at low intensity, followed by four bouts of 4 min. Intensity at 70-75% of HR_{max}, resting 1 min between bouts. Exercise intensity was automatically adjusted to maintain HR at the appropriate level.	CG-pre VO_{2peak}: 30.71±2.78 SE ($mL*Kg-1*min^{-1}$) IG-pre VO_{2peak}: 34.67±2.07 SE ($mL*Kg-1*min^{-1}$) IG significantly increased their endurance capacity after 4 wk ($p\leq0.05$)‡ Endurance capacity test was performed on a bicycle ergometer (ergoline GmbH, Bitz, Germany). Spirometry analysis (Cortex Biophysik GmbH, Leipzig, Germany) began with a 1-min rest measurement, followed by a	NK cells	qRT-PCR	*KIR2DS4, KIR3DL1*	*KIR2DS4, KIR3DL1* ↔ ($p>0.05$)‡ after 4 wk.

				3-min warm-up phase at 50 watts of power output and an increase of 25 watts every 2 min until exhaustion (RER > 1). Moreover, HR (Promedia Medizintechnik, Siegen, Germany) and self-perceived exhaustion (Borg scale) were assessed at the beginning of the test and after each intensity interval.				
Streese et al. (2020) [49]	IG= SED 40 (22 males, 18 females; 59±6 yrs) CG= SED 44 (distribution unknown; 58±7 yrs) **1^0: -** **2^0:** √	Participants were randomised into IG or CG (active control). CG attended health education and craft classes twice per week to control for social interaction. Anthropometric measurements and blood sampling was performed in the morning under standardised fasting conditions. Gene expression of $p66^{Shc}$ was assessed in 20 participants randomly selected from each group.	12wk Nordic Walking-based and supervised HIIT 3 times/wk. In the second week, the intensity was increased up to 80-90% HR_{max}. During the following weeks participants performed the following protocol: 10min Warm-up at 60-70% HR_{max} followed by a high-intensity interval consisting of 4x4 min at 80-90% HR_{max} with 3 min active recovery at 60-70% HR_{max} and a cool-down with 10 min at 60-70% HR_{max}. Familiarisation: Yes	CG-pre VO_{2max}: 26.1±5 ($mL*Kg-1*min^{-1}$) CG-post VO_{2max}: 25±4 ($mL*Kg-1*min^{-1}$) (p=0.004) IG-pre VO_{2max}: 26.4±3.8 ($mL*Kg-1*min^{-1}$) IG-post VO_{2max}: 28.7±4.0 ($mL*Kg-1*min^{-1}$)(p<0.001) VO_{2max} and HR_{max} was measured using the Cortex Metalyzer R 3B metabolic test system (Cortex Biophysik GmbH, Leipzig, Germany). Participants wore an Aipermotion 440 accelerometer (Aipermon GmbH, Munich, Germany) on six consecutive days on their left hip. From the five most active days, total steps per day and minutes of walking per day was calculated.	PBMC	RT-PCR	p66Shc	p66Shc ↓ adjusted for age, BMI, systolic and diastolic blood pressure, CV medication, and Delta VO_{2max}, after 12wk (p=0.037)‡
Moderate/high-intensity resistance exercise								
Henagan et al. (2011) [46]	IG= SED 12 women (65±2.6 years) CG= SED 11 women (66.1±3 years) Participants were obese.	Participants were randomised to IG or CG (active control). CG attended health education and craft classes twice per week to control for social interaction. Blood samples were collected before and after the intervention,	12wk of supervised progressive resistance training 3times/wk consisting of 3 sets at their 8-RM of chest press, lat pull-down, shoulder press, seated row, leg abduction,	Strength for each exercise increased significantly in IG (p<0.01)‡. Improvements ranged from 21 to 69%, with no significant changes in IG.	Whole blood	RT-PCR	*MC3R, IL-10, TNF-a*	*MC3R* ↑ (p=0.035), *TNF-α* ↔ (p>0.05) and *IL-10* ↔ (p=0.249) after 12 weeks‡. After stratifying IG into low responders

	1⁰: √ **2⁰: -**	after an overnight fast and after resting in supine position for 20min. The number of participants included in each transcriptomic analysis for each group varies depending on the transcript (MC3R: CG n=10, IG=9; *IL-10*: CG n=9, IG n=8; *TNF-a*: unknown)	leg adduction, leg extension, leg flexion, chest flys, and leg press. Participants performed 8 repetitions in the first two sets and exercised to exhaustion/failure in the third set. When able to complete 12 repetitions in one set, a technician increased the resistance for the exercise to match her new 8RM on the following training day.					(LR: FC<2; n=4) vs high responders (HR: FC≥2; n=5), *MC3R* ↑↑ (p=0.002)‡ in HR and *MC3R* ↔ (p>0.05)‡ in LR.
Rodriguez-Miguelez et al. (2014) [48]	N= SED 26 (7 males, 19 females) IG= SED 16 (distribution unknown; 69.1±1.1) CG= SED 10 (distribution unknown; 70±0.9) **1⁰:** √ **2⁰: -**	Participants were randomised to IG or CG (waiting list). Blood samples were collected 5-6 days before and after the intervention. Samples were collected between 8am and 9am after and overnight fast.	8 wk of resistance exercise, 2 times/wk with at least 48h between sessions. After a 10 min warm-up on a cycle ergometer, then performed three different exercises, e.g., leg press, biceps curl, and peck deck. The number of repetitions per set and load for the three exercises were progressively increased as follows: 3×8, 3×10, and 3×12 at 60%of 1RM during weeks 1, 2, and 3, respectively; 3×8, 3×10, and 3×12 at 70 % of 1RM during weeks 4, 5, and 6, respectively; and 3×8 and 3× 10 at 80 % of 1RM during weeks 7 and 8, respectively.	CG-pre Leg press (1RM: 160.4±13.5, MVIC 96.3±13.1), Biceps curl bench (1RM: 19.0±3.2, MVIC 15.1±2.1), Seated pec deck (1RM 25.7±4.0) CG-post Leg press (1RM 171.3±18.2, MVIC 98.1±15.8), biceps curl bench (1RM: 20.2±4.8, MVIC 16.3±3.3), Seated pec deck (1RM 27.6±5.1) IG-pre Leg press (1RM: 157.0±13.1, MVIC 109.8±12.2), Biceps curl bench (1RM: 19.7±3.1, MVIC 13.2±1.1), Seated pec deck (1RM 24.1±4.3) IG-post Leg press (1RM 198.4±14.3, MVIC 137.4±12.8) (p<0.05)‡, Biceps curl bench (1RM 26.0±3.2, MVIC 19.4±2.0) (p<0.05)‡, Seated pec deck (1RM 31.5±3.0) (p<0.05)‡ Strength test was performed after 10-min warm-up on a cycle ergometer (Tunturi F35, Tunturi®, Turku, Finland). MVIC test was carried out in a 45° incline leg press device (Gervasport,	PBMC	RT-qPCR	*IL-10* and *TNF-a*	*IL-10* ↑ (p<0.05)‡ and *TNF-α*↔ (p>0.05) ‡ after 8 weeks.

				Madrid, Spain) at 110° knee flexion and in a biceps curl bench device (Gervasport) at 90° elbow flexion. Maximal strength was registered by a strain gauge (Globus Ergometer, Globus, Codogne, Italy). After ∼30 min of rest, 1RM test was performed in the same leg press and biceps curl bench and in a seated pec deckmachine (BH Fitness Nevada Pro, BH, Vitoria, Spain). Values are Means (kg) ± SE.				
Macêdo Santiago et al. (2018) [47]	IG= SED 9 women (63±2 years) CG= SED 10 women (63±1 years) **1⁰: -** **2⁰:** √	A pre-test/post-test with a control group was used as the design of the study. Participants were randomised to IG or CG (waiting list). IG performed exercise while CG received no intervention. After 24h, corresponding to 8 weeks, participants were retested and then CG underwent exercise for 8 weeks. Afterwards, participants were tested again. Then, the groups that performed exercise were paired. Blood was collected at 6am after 8-12h fast and 24h after the las day of exercise. Gene expression of *TNF-α* was assessed in 5 participants in IG and 4 in CG.	8 wk of supervised resistance training, with a frequency of 3 times/wk, a volume of approx. 150 min/wk and an intensity of 8-12 MR with 1 min interval between repetitions. The exercises consisted on sitting leg press, sitting supine, knee extension, pulley, lying down knee flexion, low pulley elbow flexion, seated leg press, and pulley elbow extension. The increase in intensity followed two criteria: 1) using the BORG scale. 2) Whenever the participants exceeded the limits of the 8-12 RM zone, an increase corresponding to 15% of the initial load occurred. Familiarisation: Yes	There was a load increase in their respective exercises after 4 and 8 weeks with a significant difference between weeks (p=0.001). Pre-exercise: Seated leg press (20.7±3.8), Elbow flexion (9.0±1.8), Knee extension (9.9±0.5), Supine seated (7.1±0.3), Lying knee flexion (7.9±0.4), Pulley (13.2±0.5), Plantar flexion (20.0±0.7), Elbow extension (8.6±0.6) 4wk post-exercise: Seated leg press (33.6±1.1), Elbow flexion (13.8±0.3), Knee extension (18.4±0.6), Supine seated (13.8±0.4), Lying knee flexion (15.5±2.0), Pulley (21.9±0.4), Plantar flexion (33.38±0.9), Elbow extension (16.42±0.4) 8wk post-exercise: Seated leg (45.48±1.4), Elbow flexion (17.83±0.4), Knee extension (25.90±0.8), Supine seated (17.96±0.7),	Leukocytes	RT-qPCR	*TNF-a*	*TNF-α* ↔ (p=0.007)‡ after 8 weeks.

				Lying knee flexion (17.09±0.5), Pulley (27.03±0.5), Plantar flexion (43.56±1.2), Elbow extension (20.20±0.4) Values are Means (kg) ± SD				
Mind-body exercise								
Creswell et al. (2012) [68]	IG= SED; 20 (3 males, 17 females; 64.35±6 yrs) CG= SED; 20 (5 males; 17 females; 65.16±8 yrs) 64% Caucasian, 12% African American, 10% Latino, 7% Asian American, and 5% Other. **1⁰: -** **2⁰:** √	Participants were randomised to IG or CG (waiting list) using a computerised number generator. Blood was collected at baseline and post-intervention.	8 wk partially supervised MBSR [87] consisting: weekly 120-min group sessions, a day-long retreat in the sixth or seventh wk, and 30-min daily home mindfulness practice.	Intention to treat; Significant treatment condition × time interaction (F(1,35)=7.86, p=.008) CG pre Loneliness (38.40±2.33) CG post Loneliness (40.75±2.30) IG pre Loneliness (42.35±2.23) IG post Loneliness (37.40±2.51)(p=?)‡ In a subsample with complete pre-post data (n=33): IG post (35.65±2.02) lower loneliness vs CG post (42.33±1.73) controlling for baseline loneliness (F(1,30)=6.27, p=0.02, η2=0.17) Loneliness assessed using the composite UCLA-R Loneliness Scale [88]	PBMC	Microarray Human HT-12 BeadChips (Illumina, San Diego CA)	48804	143 genes showing 25% differential change over time between conditions, p value unknown (69 genes relatively down regulated in IG and 74 genes relatively down-regulated in CG; p=?)‡.
Black et al. (2013) [60]	IG= SED; 25 (distribution unknown; 60.5±28.2) CG=SED 20; distribution unknown; 60.6±12.5) Family dementia caregivers. **1⁰: -** **2⁰:** √	Participants were randomised using a computer-generated randomisation table, into IG or CG (active control). CG underwent a RM protocol 12 min/day every day. Blood samples were collected between 10-11 am at baseline and 8 wk later.	8 wk of unsupervised (guided by an audio CD) Kirtan Kriya Meditation (Kundalini Yoga practice). Frequency of 7 days/wk, 12-min each day.	IG significantly lower levels of depressive syntomps and greater improvement in mental health (p>0.05) ‡ (No data available)	PBMC	Microarray Human HT-12 Bead Chips (Illumina, San Diego CA)	48804	68 genes with FC>1.2 (49 down-regulated and 19 up-regulated; p=?)‡

IG=Intervention Group; CG= Control Group; SED= Sedentary; wk= Weeks; h=hours; IL-6= Interleukin-6; $\dot{V}O2max$= maximal oxygen uptake; mL= milliliters; Kg= kilograms; min= minutes; RM= Repetition Maximum; MBSR= Mindfulness-based stress reduction; RER= Respiratory Exchange Ratio; MVIC= Maximum voluntary isometric contraction; PBMC= Peripheral Blood Mononuclear Cell; FC= Fold Change; HR_{max}= Maximum Heart Rate; HR= Heart Rate; $CD34^{+}$= Cluster of Differentiation 34^{+}; NK= Natural Killer; RT-PCR= Real time Polymerase Chain Reaction; qPCR= quantitative Polymerase Chain Reaction; RT-qPCR= Quantitative Reverse Transcription Polymerase Chain Reaction; CD36= Cluster of Differentiation 36; PPARy= peroxisome proliferator-activated receptor gamma; LXRa= Liver X receptor alpha; ABCA1= ATP Binding Cassette Subfamily A Member 1; ABCG1= ATP Binding Cassette Subfamily G Member 1; ADIPOR1= Adiponectin Receptor 1; ADIPOR2= Adiponectin Receptor 2; SOD1= Superoxide Dismutase 1; SOD2= Superoxide Dismutase 2; SOD3= Superoxide Dismutase 3; BCL2= B-Cell Lymphoma 2; eNOS= Endothelial Nitric Oxide Synthase; ET-1= Endothelin 1; VEGF-A= Vascular Endothelial Growth Factor A; SDF-1a= Stromal cell-derived factor 1 alpha; TNF-a= Tumour Necrosis Factor alpha; VEGFR2= Vascular Endothelial Growth Factor Receptor 2; CD31= Cluster of Differentiation 31; KIR2DS4= Killer Cell Immunoglobulin Like Receptor, Two Ig Domains And Short Cytoplasmic Tail 4; KIR3DL1= Killer Cell Immunoglobulin Like Receptor, Three Ig Domains And Long Cytoplasmic Tail 1; p66Shc= SHC Adaptor Protein 1, isoform p66Shc; MC3R= Melanocortin 3 Receptor; IL-10= Interleukin 10; ↑ indicates upregulation of gene expression, ↓ indicates down-regulation of gene expression, and ↔ indicates no changes in gene expression. ‡ indicates that the p-value refers to the comparison of changes in intervention group with changes in control group. √ indicates whether gene expression is the primary (1^0) or secondary (2^0) outcome of the study.

Table 4-2 *List of transcripts examined in at least 2 RCTs. ✓ indicates the transcript was captured and its expression reported; ✗ indicates the transcript was captured but expression not reported.*

	Low-intensity aerobic	Mind-body exercise		Moderate/high-intensity aerobic						Moderate/high-intensity resistance				
	RT-PCR	Microarray				qPCR	qRT-PCR	RT-PCR	RT-qPCR	RT-PCR	RT-qPCR	RT-qPCR	Captured but unavailable	Captured and reported
	Butcher et al. 2008	Creswell et al. 2012	Black et al. 2013	Thompson et al. 2010	Iyalomhe et al. 2015	Lee et al. 2015	Schenk et al. 2019	Sen et al. 2015	Streese et al. 2020	Henagan et al. 2011	Rodriguez-Miguelez et al. 2014	Macêdo Santiago et al. 2018		
CD36	✓	✗	✗	✗	✗								4	1
PPARγ (PPARG)	✓	✗	✗	✗	✗								4	1
LXRa (NR1H3 gene)	✓	✗	✗	✗	✗								4	1
ABCA1	✓	✗	✗	✗	✗								4	1
ABCG1	✓	✗	✗	✗	✗								4	1
AdipoR1		✗	✗	✗	✗	✓							4	1
AdipoR2		✗	✗	✗	✗	✓							4	1
KIR2DS4		✗	✗	✗	✗		✓						4	1
KIR3DL1		✗	✗	✗	✗		✓						4	1
SOD1		✗	✗	✗	✗			✓					4	1
SOD2		✗	✗	✗	✗			✓					4	1
SOD3		✗	✗	✗	✗			✓					4	1
Catalase (CAT)		✗	✗	✗	✗			✓					4	1
Glutathione peroxidase (GPX)		✗	✗	✗	✗			✓					4	1
p53		✗	✗	✗	✗			✓					4	1
p21 (CDKN1A)		✗	✗	✗	✗			✓					4	1
Bcl2		✗	✗	✗	✗			✓					4	1
Caspase-3 (CASP3)		✗	✗	✗	✗			✓					4	1
Enos (NOS3)		✗	✗	✗	✗			✓					4	1
ET-1 (EDN1)		✗	✗	✗	✗			✓					4	1
VEGF-A (VEGFA)		✗	✗	✗	✗			✓					4	1
SDF-1a (CXCL12)		✗	✗	✗	✗			✓					4	1
IL-6		✗	✗	✗	✗			✓					4	1
TNF-a		✗	✗	✗	✗			✓		✓	✓	✓	4	4
CD34		✗	✗	✗	✗			✓					4	1
VEGFR2 (KDR)		✗	✗	✗	✗			✓					4	1
CD31 (PECAM1)		✗	✗	✗	✗			✓					4	1
p66Shc (SHC1)		✗	✗	✗	✗				✓				4	1
MC3R		✗	✗	✗	✗					✓			4	1
IL-10 (IL10)		✗	✗	✗	✗					✓	✓		4	2
CLC		✗	✓	✓	✗								2	2
IL8		✗	✓	✓	✗								2	2
G0S2		✓	✓	✓	✗								1	3
C1orf55		✓	✗	✗	✗								3	1
CD83		✓	✓	✗	✗								2	2
DEFA1		✓	✓	✗	✗								2	2
DEFA1B		✓	✓		✗								1	2
DEFA3		✓	✓	✗	✓								1	3
FOSB		✓	✓	✗	✗								2	2
HBA1		✓	✓	✗	✗								2	2
HBG2		✓	✓		✗								1	2

(exercise[MeSH Terms]) OR resistance train*[Title/Abstract]) OR aerobic train*[Title/Abstract]) OR weight train*[Title/Abstract]) OR interval train*[Title/Abstract]) OR endurance[Title/Abstract]) OR strength[Title/Abstract]) OR athletes[Title/Abstract]) OR weight lift*[Title/Abstract]) OR anaerobic train*[Title/Abstract]) OR walk*[Title/Abstract]) OR jog*[Title/Abstract]) OR swim*[Title/Abstract]) OR marathon[Title/Abstract] **AND** gene espression[Title/Abstract] OR mRNA[Title/Abstract] OR messenger RNA[Title/Abstract] OR lncRNA[Title/Abstract] OR long non coding RNA[Title/Abstract] OR miRNA[Title/Abstract] OR micro RNA[Title/Abstract] OR circRNA[Title/Abstract] OR circular RNA[Title/Abstract] OR transcript*[Title/Abstract] OR ncRNA[Title/Abstract] OR non coding RNA[Title/Abstract] **AND** randomised controlled trial[Title/Abstract] OR controlled trial[Title/Abstract] OR controlled study[Title/Abstract] OR controlled clinical trial[Title/Abstract] OR controlled clinical study[Title/Abstract] OR RCT[Title/Abstract] OR randomi*[Title/Abstract]

Figure 4-1 *Example search string Network Meta-analysis in PubMed.*

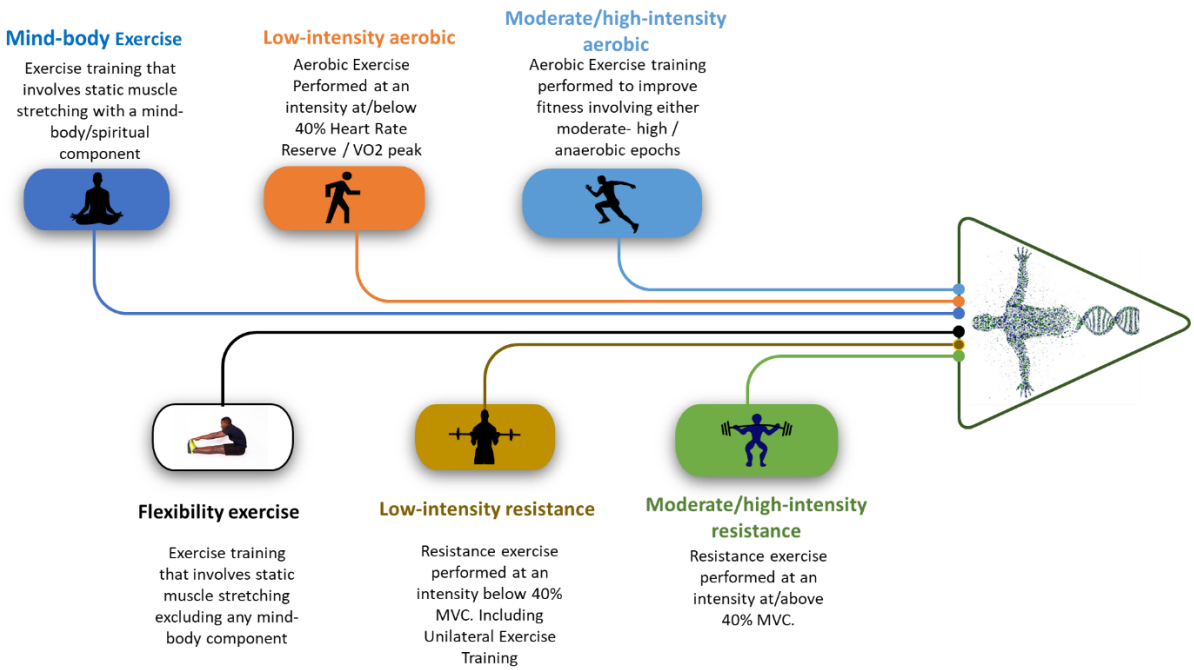

Figure 4-2 *Schematic of exercise types compared within this review. MVC= Maximum voluntary contraction.*

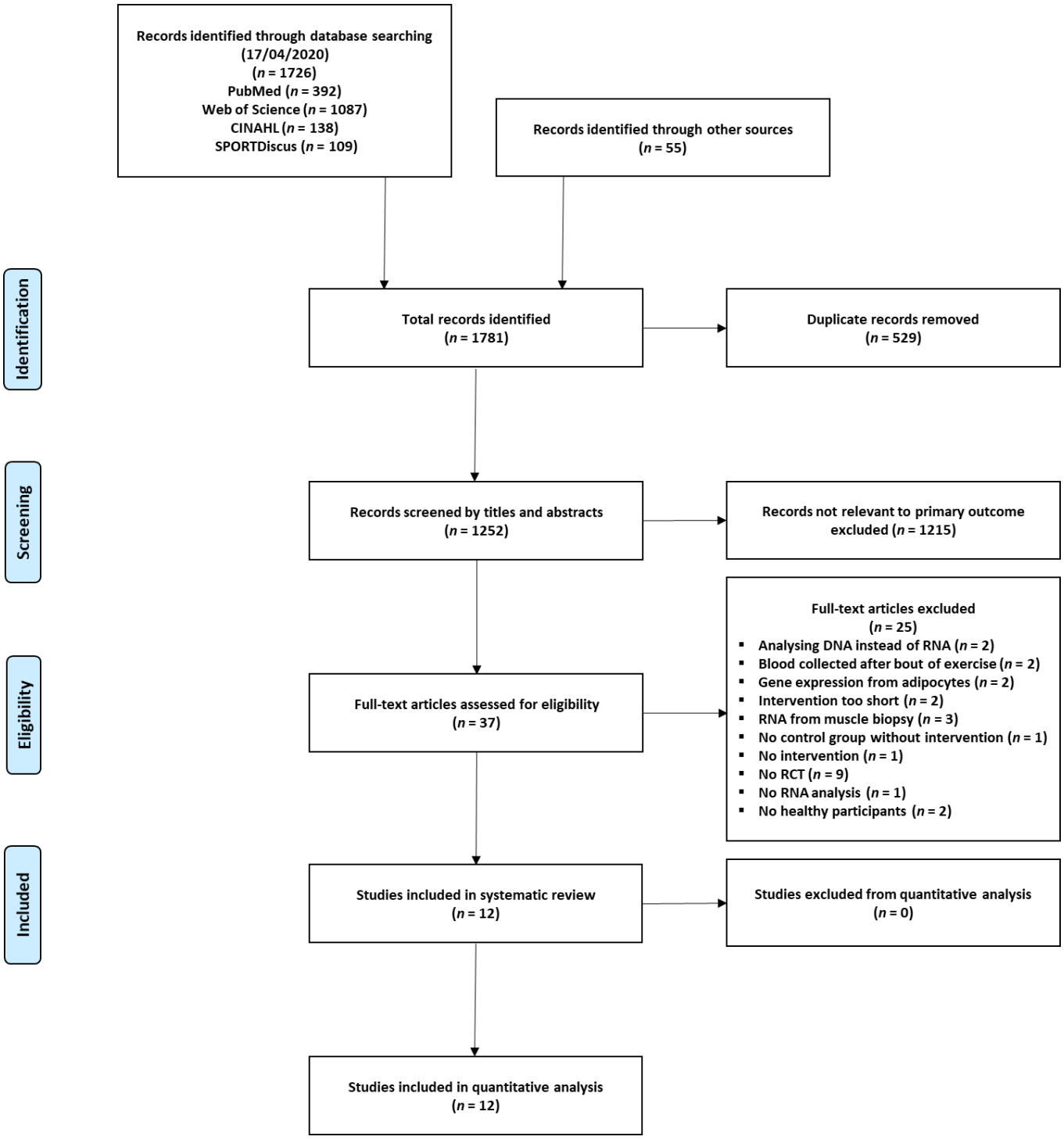

Figure 4-3 *Flowchart of screening process.*

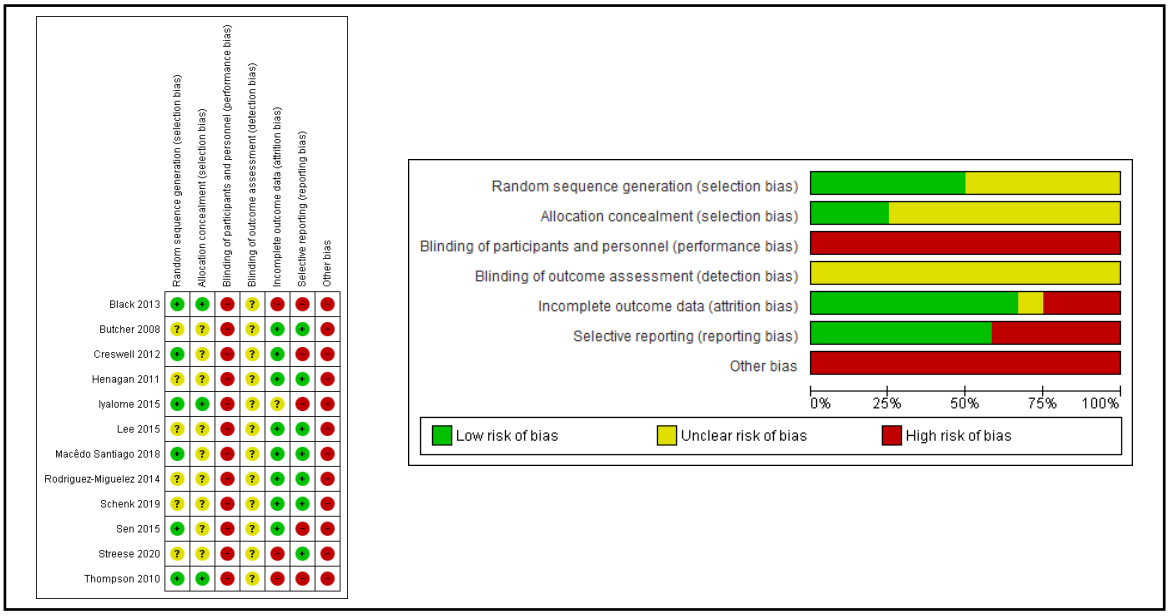

Figure 4-4 *Risk of bias charts of studies included in the review.*

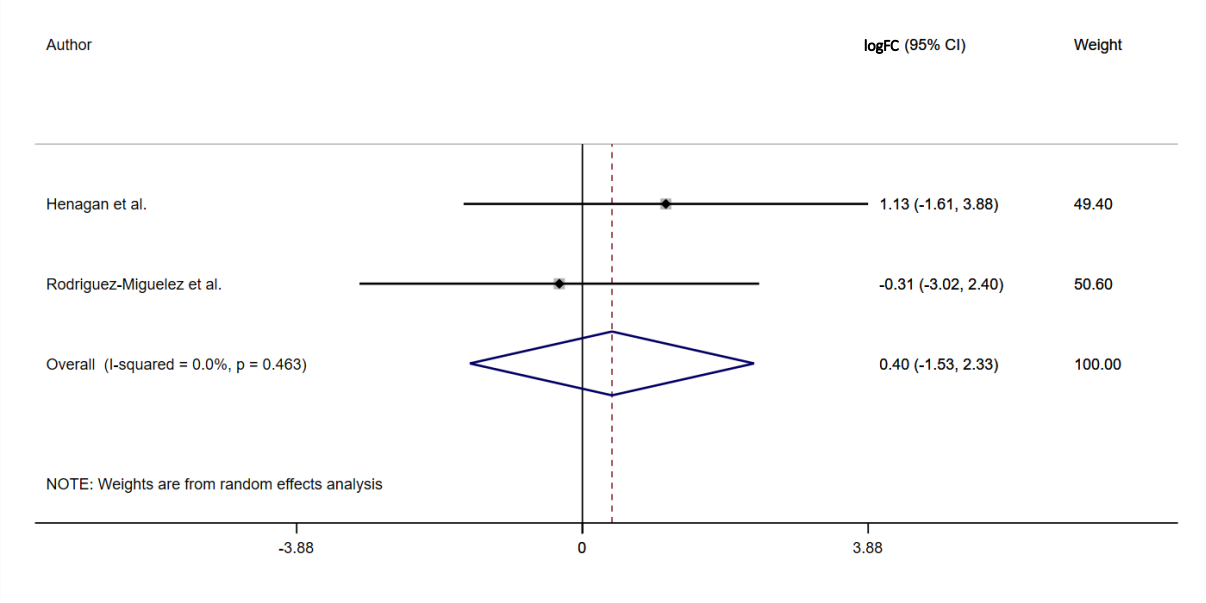

Figure 4-5 *Forest plot of individual and pooled effect size estimates for IL-10 expression after moderate/high-intensity exercise training. 95% CI: 95% confidence interval; logFC: log_2 fold change.*

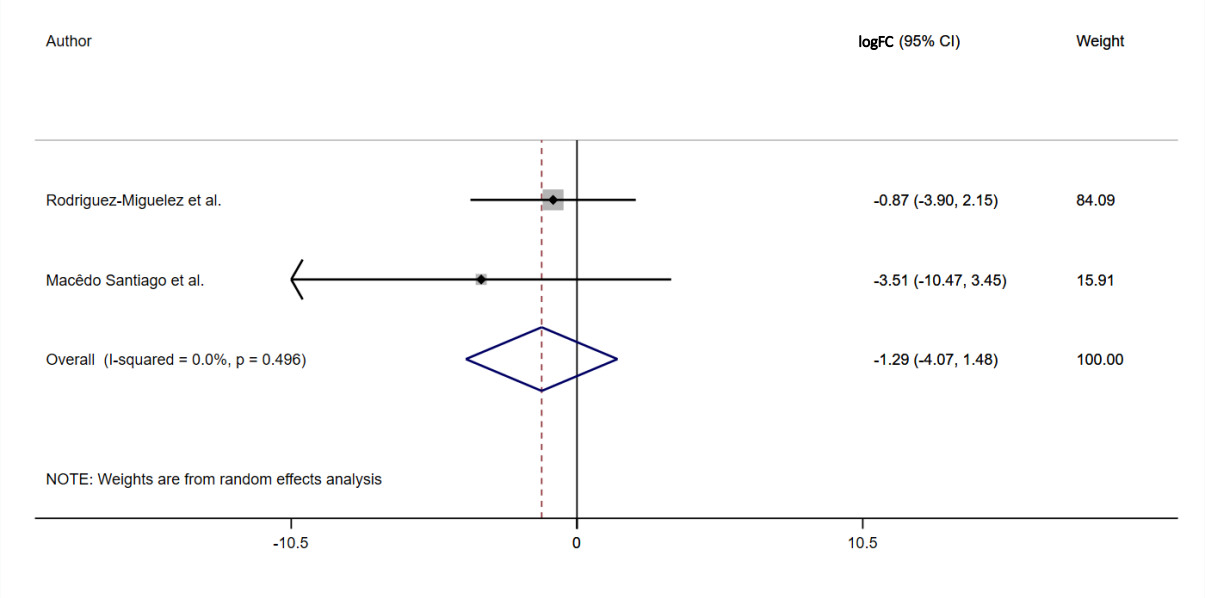

Figure 4-6 *Forest plot of individual and pooled effect size estimates for TNF-α expression after moderate/high-intensity exercise training. 95% CI: 95% confidence interval; logFC: log2 FC.*

5 EXAMINATION OF PERIPHERAL BLOOD TRANSCRIPTOME (PBT) EXPRESSION TO CHARACTERISE TRANSCRIPTOMIC ADAPTATION OF SEDENTARY MALE PARTICIPANTS TO SUPERVISED EXERCISE TRAINING COMPARED WITH ATHLETIC PHENOTYPES: A STROBE COMPLIANT OBSERVATIONAL STUDY.

"The following experimental chapter is presented in accordance with author guidance procedures for the journal ***Biology of Sport***".

https://www.termedia.pl/Journal/Biology_of_Sport-78/Infoe

ISSN: 2083-1862; ISSN: 0860-021X

5.1 ABSTRACT

Background Peripheral blood is becoming an increasingly popular method to examine human genomic response to exercise. However, the body of available data are equivocal.

Aims The present study was to compare phenotypic with transcriptomic characterisation of aerobic and strength athletes with age matched exercise-naïve men both before and after four weeks of mixed exercise training (MET).

Methods Seventy-one (*n*=71) eligible participants (SEDENTARY *n*=31, AEROBIC *n*=20, and STRENGTH *n*=20) were enrolled to a STROBE compliant observational study of divergent exercise phenotypes where differential expression of peripheral blood transcriptome (PBT) expression was analysed using RNA-seq technology.

Results Study compliance was *n*=68/71, where SEDENTARY (*n*=3) were lost to follow-up, resulting in (*n*=68) participants included in final analysis. Physiological characteristics at enrolment were consistent with athletic phenotypes [AEROBIC ($p<0.01$) v STRENGTH v SEDENTARY]; [STRENGTH ($p<0.01$) v AEROBIC v SEDENTARY]. Four weeks of MET successfully induced physiological adaptation in SEDENTARY increasing absolute $\dot{V}O_{2max}$ ($\Delta\dot{V}O_{2max}$ = +239.9 ml.min^{-1}, $p<0.01$), and strength performance: 3 x lifts (1RM) (Δ1RM = +30.3kg, $p<0.01$). Despite this increase, after MET the three groups still presented the same differences than at enrolment ($p<0.01$). Differential expression analysis of peripheral blood transcriptomics at enrolment revealed 426 differentially expressed transcripts in AEROBIC compared with SEDENTARY [407 up-regulated, FC≥2; 19 down-regulated, FC≤0.5; (FDR<0.05)]. Conversely, STRENGTH presented only 14 transcripts differentially expressed compared with SEDENTARY [9 up-regulated, FC≥2; 5 down-regulated, FC≤0.5; (FDR<0.05)]. After four weeks of MET, SEDENTARY presented 2 transcripts up-regulated (FC≥2, FDR<0.05). The differences between groups after MET were reduced. We observed

234 transcripts differentially expressed between AEROBIC and SEDENTARY [231 up-regulated, FC≥2; 3 down-regulated, FC≤0.5; (FDR<0.05)], and 4 differentially expressed in STRENGTH compared with SEDENTARY [2 up-regulated, FC≥2; 2 down-regulated, FC≤0.5; (FDR<0.05)].

Conclusion Despite the identification of characteristic differences in PBT between divergent athletic phenotypes at study enrolment, differences became abrogated between groups following MET in exercise-naïve participants. These data provide cautionary evidence for those wishing to employ PB adaptive transcriptomics to exercise in men.

Keywords: Gene expression, transcriptome, exercise, sedentary, aerobic, strength.

5.2 INTRODUCTION

Peripheral blood is widely used to characterise and diagnose many different pathological conditions, because it is easy to obtain and displays a systemic state of the body as it is a tissue that interacts with many organs and structures within it [1].

Historically, research involving the study of the chronic adaptation to physical exercise has favoured skeletal muscle as the target tissue to examine genomic response to exercise. However, taking into considerations the aforementioned points, peripheral blood has been suggested as a potential alternative to characterise transcriptomic markers of adaptation to exercise [2].

Skeletal muscle adaptations in response to structured exercise regimens are well established [3-11] and many subsequent metabolites may be detected within human systemic circulation. This offers potential for systemic blood downstream route of discovery in the emerging field of exercise transcriptomics. Environmental stimuli such as exercise mode, duration, and intensity, will cause disruption to many tissues depending in the ongoing training history of a given individual [6, 12-14]. Indeed, Peripheral Blood Mononuclear Cells (PBMCs) have been identified as cells of convenience due to inherent reliability during biochemical analytics which coexists within an individual's inflammatory ecosystem and requisite muscle damage which accompanies physical exercise. It is for these reasons that gene expression detected from PBMCs has become the *sine qua non* in the narrow field of peripheral blood exercise transcriptomics [14, 15].

Physiological adaptation to various modes of structured physical exercise is well characterised [3, 16-23]. However, contemporary understanding of the intersection between adaptive transcriptomics and divergent forms of physical exercise, remains to be elucidated. Almost without exception, each human cell contains the full genetic library for that individual, yet, the integration of cellular response to any given stimulus will vary between

individuals. The term ‘gene expression’ is commonly used to characterise this phenomenon, which, more specifically, identifies cellular proteomics which in turn determines phenotypic profile of each human cell.

The current body of literature to examine adaptive PBT response to exercise have chiefly examined an ‘acute’ response to physical exercise [24-33], with relatively fewer studies examining chronic adaptation due to exercise training [34-39]. For instance, Connolly et al. examined the acute response to 30 min of constant moderate-to-high cycle ergometry exercise in *n*=15 healthy men. Using microarray technology to analyse PBMCs gene expression, the authors observed significant changes in 552 genes immediately after the bout of exercise, in 311 genes from end of the exercise bout to 60 min recovery, and in 293 from pre-exercise to recovery. Genes linked to inflammation processes, growth, and repair, were predominantly up-regulated from pre-exercise to immediately after, concluding that PBMCs are able to reflect a response to acute exercise characterised by an activation of genes associated with stress, inflammation, and tissue repair [25]. On the other hand, Iyalomhe and colleagues conducted a standardised randomised 6-month aerobic exercise training in *n*=10 elder males and female participants to study the adaptation to exercise. Microarray analysis of PBT expression indicated that 81 genes were differentially expressed in response to the exercise intervention, showing a characteristic down-regulation of pro-inflammatory genes, and up-regulation of anti-inflammatory genes in peripheral blood in response to chronic aerobic exercise [34]. Conversely, Rodriguez-Miguelez et al. used qPCR to specifically analyse the expression of target genes (*TNF-a*, and *IL-10*) in response to an 8-weeks resistance exercise training program in *n*=16 healthy subjects. After intervention, *TNF-α* did not change its expression, whereas *IL-10* gene expression was up-regulated, supporting the theory that peripheral blood presents an anti-inflammatory transcriptomic response to

physical exercise [35]. Taken together, there is a requirement for further research on chronic adaptation to exercise.

ACSM guidelines recommend physical activity that consists moderate aerobic physical activity for a minimum of 30min 5 times per week, or 20min of vigorous aerobic exercise 3 times per week, which should be complemented with muscular strength exercise twice per week [40]. The combination of aerobic with muscular strength exercise, termed mixed exercise training (MET) is encouraged to achieve health benefits derived from physical exercise. Therefore, this approach will be used in the current study as the exercise training intervention.

Thus, in order to progress our current knowledge relating to adaptive PBT of divergent athletic phenotypes, we conducted a STROBE compliant study of SEDENTARY males compared with either AEROBIC or STRENGHT male athletes. This study tested the hypothesis that; (i) PBT expression discriminates between exercise-naïve sedentary males (SEDENTARY) compared with either AEROBIC or STRENGTH athletic phenotypes. Further, that (ii) 4 weeks of (MET) identifies unique adaptive PBT expression within SEDENTARY compared with either AEROBIC or STRENGTH athletic phenotypes. In order to examine exercise-dependant adaptive PBT, SEDENTARY participants undertook a further four weeks of either strength or aerobic exercise training, with a subsequent minor hypothesis that (iii) 4 weeks of specific exercise (either aerobic or strength) training would identify unique PBT expression in SEDENTARY compared with either AEROBIC or STRENGTH athletic phenotypes.

5.3 METHODS

5.3.1 Participants

Participants (*n*=71) with aged 18-45 years, provided written informed consent to participate in a study of three divergent athletic phenotypes; SEDENTARY (*n*=31), AEROBIC (*n*=20), and RESISTANCE (*n*=20) depending on their ability to perform on a strength test and a $\dot{V}O_{2max}$ test. SEDENTARY (*n*=28) completed 4 weeks of (MET). Sedentary participants were subsequently randomised to four weeks of either strength or aerobic exercise: SEDENTARY STRENGTH (*n*=14) or SEDENTARY AEROBIC (*n*=14). At any given stage, SEDENTARY, SEDENTARY STRENGTH, and SEDENTARY AEROBIC were compared with a biased sample of the highest performing STRENGTH (*n*=10) and AEROBIC (*n*=10*)*. Full details are provided in **Sections 2.2** and **2.3**, respectively.

5.3.2 Study design

We tested a physiological model of systemic transcriptomic adaptation to exercise training in healthy male participants by employing a STROBE compliant observational study [41] of divergent athletic phenotypes and subsequent response to exercise. Full study description is outlined in **Section 2.1.** Briefly, following enrolment to the study, eligible participants attended the exercise physiology laboratory during three subsequent sampling epochs; (i) at enrolment, (ii) following MET, and (iii) following specific exercise in a biased sample of distinct participant phenotypes. All procedures were approved by Federation University Human Research Ethic Committee.

5.3.3 Body composition

Body mass was obtained using a balanced weighing scale, with participants in minimal clothing (Seca, Cardiokinetics, Salford, UK) and height was measured with a

stadiometer (Seca, Cardiokinetics, Salford, UK). Weighing scales were calibrated prior to each “weigh in” with a 5 kg free mass. Procedures are detailed in **Section 2.4.**

5.3.4 Blood collection

Following 15 min seated rest, whole blood was sampled from the non-dominant arm by standard venepuncture into sterile Tempus™ (Life Technologies, Au) vacutainer tubes. Samples were immediately stored at -80°C until subsequent analysis. Detail on the process is provided in **Section 2.5**.

5.3.5 Determination of muscular strength

Muscular strength was assessed using one repetition maximum (1RM) technique following Australian Institute of Sports guidelines [42]. Briefly, participants performed a bench press, a deadlift, and squats exercises, starting with a warm-up and progressively incrementing weight load until reaching 1RM weight. Full description on the protocol is provided in **Section 2.6**.

5.3.6 Determination of maximal oxygen consumption ($\dot{V}O_{2max}$)

Prior to graded exercise testing, metabolic cart (Moxus Modular V̇O2 System, AEI technologies, IL, USA;) was calibrated with medically certified calibration gases (4.05% CO2 and 15.6% O2, 0.3% CO2 and 20.9% O2) and volumes were determined according to the manufacturers guidelines. Maximal oxygen consumption V̇O2max was determined in compliance with ACSM guidelines (Riebe 2018) where participants completed a ramped (beginning at 100 W for SEDENTARY AND 120W for AEROBIC and STRENGTH, and increasing by 20 W.min-1) exercise protocol to voluntary exhaustion using a electromagnetically braked cycle ergometer (Velotron® Pro, Seattle, WA, USA) and concomitant open circuit spirometry to determine maximal oxygen consumption, which is described in detail in **Section 2.6.**

5.3.7 RNA extraction

RNA was extracted from Tempus Blood RNA Tubes (Life Technologies™) MagMAX for Stabilized Blood Tubes RNA Isolation KitTM (Thermo Fisher ScientificTM) following standardised protocol according to manufacturer instructions (Thermo Fisher Scientific). A more detailed explanation of the process can be found in **Section 2.9.**

5.3.8 Library preparation and RNA sequencing

Library preparation and RNA sequencing were conducted following a standardised protocol of TruSeq Stranded Total RNA Sample Preparation Guide (Illumina®) (Illumina 2017) using an Illumina NovaSeq platform (Illumina®) and detailed in **Section 2.9.**

5.3.9 Mixed exercise training (MET)

Participants allocated to SEDENTARY performed 4 weeks of MET consisting of a combination of resistance and aerobic exercise with continuous heart rate monitoring. Participants attended 3 sessions per week, alternating 2 aerobic and 1 resistance sessions one week, with 1 aerobic and 2 resistance the following week, allowing at least 24h between sessions. All exercise sessions were supervised by a qualified personal trainer or Exercise Physiologist (ESSA). More details on the exercise program can be found in **Section 2.8.1.**

5.3.10 Resistance exercise training (RET)

Participants allocated to the SEDENTARY STRENGTH group underwent 4 weeks of RET, 3 times per week, allowing at least 24h between sessions. All exercise sessions were supervised by a qualified personal trainer or Exercise Physiologist (ESSA). Details about this exercise program are outlined in **Section 2.8.2.**

5.3.11 Aerobic exercise training (AET)

Participants allocated to SEDENTARY AEROBIC completed 4 weeks of AET, 3 times per week, allowing at least 24h between sessions. All exercise sessions were supervised

by a qualified personal trainer or Exercise Physiologist (ESSA). More information on this exercise program can be found in **Section 2.8.3.**

5.3.12 RNA sequencing profiling

Following RNA integrity analysis, SEDENTARY (*n*=16*)* RNA samples were available at enrolment, SEDENTARY STRENGTH (*n*=14), SEDENTARY AEROBIC (*n*=14) following MET. Following subsequent specific exercise SEDENTARY STRENGTH (*n*=14*)* and SEDENTARY AEROBIC (*n*=10). For STRENGTH and AEROBIC we selected the samples from the top 10 participants for each group at 2 time points, that demonstrated more consistency in their respective physiological characteristics of interest (Absolute muscular strength for STRENGTH and absolute $\dot{V}O_{2max}$ for AEROBIC). When comparing SEDENTARY, SEDENTARY AEROBIC, and SEDENTARY STRENGTH with the athlete groups (STRENGTH and AEROBIC), average gene expression of the 2 time points for the athlete groups was used. This resulted in 20 RNA samples per athlete group, 10 at each time point, separated 4 weeks. Taking all together, a total of 104 samples were sequenced and included in transcriptomic analysis.

5.3.13 Statistical analysis

Sample power was estimated for an effect size: 0.8 using a single-tailed within-group comparisons with α=0.05 and β=0.95, using minimal expected change in $\dot{V}O_{2max}$ as criterion. This resulting in a required sample of (*n*=17) in each group. Continuous data were analysed using SPSS version 25.0 (SPSS Inc., Chicago, IL, USA). Distribution of normality and homogeneity of variance were tested by analysing residuals. Linear mixed modelling was employed to test continuous secondary outcomes (i.e. training effects) with pairwise comparisons of within and between group simple effects in coalition with Bonferroni correction for multiple comparisons. An alpha value of $p \leq 0.05$ was used to indicate statistical significance. Data are presented as mean ± standard deviation (SD) or confidence

intervals (CI), where appropriate. Data from NG-seq were processed through an RNA-seq expression analysis workflow, which includes alignment, transcript assembly, quantification and normalisation. Differential expression (DE) analysis was applied using EdgeR. This study employed a conservative FC≥2 (up-regulation) and FC≤0.5 (down-regulation) criterion, with FDR<0.05 to identify significantly differentially expressed transcripts for within and between group comparisons. Corresponding description of statistical procedures are located in **Section 2.11**., **Section 2.12**., and **Section 2.13**, respectively.

5.4 RESULTS

A total of *n*=79 healthy male candidates, where screened for eligibility with *n*=71 meeting enrolment criteria. Reasons for exclusion included: *n*=1 having genetic disorder, *n*=4 falling short of performance criteria for enrolment to either AEROBIC or STRENGTH, *n*=1 exceeding criteria for SEDENTARY, and *n*= 2 exceeding age eligibility for enrolment. Thus, *n*=71 eligible participants (SEDENTARY *n*=31, AEROBIC *n*=20, and STRENGTH *n*=20) were enrolled to the study. Study compliance was 95.6% following mixed exercise. Characteristics of eligible participants are shown in Table 4-1. Following MET, *n*=1 participant dropped out of the study, therefore SEDENTARY *n*=29 were randomised into SEDENTARY STRENGTH *n*=15, and SEDENTARY AEROBIC *n*=14. One SEDENTARY STRENGTH stopped attending sessions. SEDENTARY STRENGTH *n*=14, SEDENTARY AEROBIC *n*=14, AEROBIC *n*=20, and STRENGTH *n*=20 completed follow-up 2. Thus, *n*=68 participants were included in the final analysis. Flow diagram of participants through the study, including reasons for withdrawal are shown is depicted in **Figure 5-1**. Participant characteristics at enrolment are outlined in **Table 5-1**.

5.4.1 CRF and Muscular Strength

Full details for physiological characteristics and outcomes throughout the study can be found in **Table 5-2** and **Table 5-3.**

5.4.1.1 Enrolment

Briefly, at enrolment AEROBIC presented with relative $\dot{V}O_{2max}$, and absolute $\dot{V}O_{2max}$ significantly higher than both SEDENTARY and STRENGTH. Absolute $\dot{V}O_{2max}$ was not significantly different between STRENGTH and SEDENTARY. However, STRENGTH had higher relative $\dot{V}O_{2max}$ compared with SEDENTARY. Comparably, STRENGTH had higher absolute strength, and higher relative strength than SEDENTARY and AEROBIC. Furthermore, AEROBIC showed no significant difference in absolute strength with SEDENTARY, but had higher relative strength than that group.

5.4.1.2 Following mixed exercise

Following 4 weeks of mixed exercise training, both relative and absolute $\dot{V}O_{2max}$, and absolute strength were significantly increase in SEDENTARY.

5.4.1.3 Follow-up 1

At follow-up 1, AEROBIC still demonstrated a significantly higher relative $\dot{V}O_{2max}$, and absolute $\dot{V}O_{2max}$ than SEDENTARY, and also higher than STRENGTH. Relative $\dot{V}O_{2max}$ but not absolute $\dot{V}O_{2max}$ was significantly higher in STRENGTH than in SEDENTARY. On the other hand, STRENGTH showed higher absolute and relative muscular strength than SEDENTARY and AEROBIC. Additionally, AEROBIC had higher relative strength that SEDNTARY, although that difference was not significant in the case of absolute strength. When SEDENTARY was randomised into SEDENTARY STRENGTH and SEDENTARY AEROBIC there were no statistically significant differences in muscular strength or $\dot{V}O_{2max}$, both relative and absolute, between these two new groups. Similarly, when SEDENTARY

was split into these new groups, the differences and similarities between SEDENTARY AEROBIC and SEDENTARY STRENGTH, and the athletes groups stated above, remained the same.

5.4.1.4 Following specific exercise.

After 4 weeks of aerobic training, SEDENTARY AEROBIC had a significant increase in absolute and relative $\dot{V}O_{2max}$, but there was no significant change in absolute or relative strength. On the contrary, after 4 weeks of resistance training, SEDENTARY STRENGTH significantly increased their absolute strength but not their relative strength. This group did not significantly change their absolute or relative $\dot{V}O_{2max}$.

5.4.1.5 Follow-up 2

After 4 weeks of specific exercise training, there were no differences in absolute or relative muscular strength and absolute or relative $\dot{V}O_{2max}$ between SEDENTARY STRENGTH and SEDENTARY AEROBIC. AEEROBIC had higher absolute and relative $\dot{V}O_{2max}$ than both SEDENTARY STRENGTH and SEDENTARY AEROBIC. Relative but not absolute $\dot{V}O_{2max}$ was higher in STRENGTH than in SEDENTARY STRENGTH and SEDENTARY AEROBIC. Moreover, STRENGTH showed higher absolute and relative muscular strength than SEDENTARY STRENGHT and SEDENTARY AEROBIC. Interestingly, AEROBIC had higher relative strength than SEDENTARY AEROBIC.

5.4.2 Transcriptome Expression

5.4.2.1 Enrolment

There were 426 differentially expressed transcripts in AEROBIC compared with SEDENTARY at enrolment [407 up-regulated, FC≥2; 19 down-regulated, FC≤0.5; (FDR<0.05)], and a total of 14 differentially expressed transcripts in STRENGTH compared with SEDENTARY at enrolment [9 up-regulated, FC≥2; 5 down-regulated, FC≤0.5;

(FDR<0.05)]. Notably, among those transcripts, 8 were differentially expressed in both AEROBIC and STRENGTH compared with SEDENTARY, 1 down-regulated (*LOC101929887*) and 7 up-regulated (*POLR2M, C9orf16, TXNDC5, LOC100996740, PVRL2, GPR20, RNF17*).

5.4.2.2 Following mixed exercise

After 4 weeks of mixed exercise, there were 2 transcripts up-regulated (FC≥2) and no transcripts down-regulated (FC≤0.5) in SEDENTARY (FDR<0.05).

5.4.2.3 Follow-up 1

Furthermore, at follow-up 1 we found that 234 transcripts were differentially expressed in AEROBIC compared with SEDENTARY [231 up-regulated, FC≥2; 3 down-regulated, FC≤0.5; (FDR<0.05)]. There were 4 transcripts differentially expressed in STRENGTH compared with SEDENTARY [2 up-regulated, FC≥2; 2 down-regulated, FC≤0.5; (FDR<0.05)]. In this case, there were no transcripts differentially expressed in both AEROBIC and STRENGTH at the same time, compared with SEDENTARY.

5.4.2.4 Following specific exercise

There were no differentially expressed transcripts in SEDENTARY STRENGTH after 4 weeks of resistance training (FDR<0.05). In the same way, there were no differentially expressed transcripts in SEDENTARY AEROBIC after 4 weeks of aerobic training (FDR<0.05).

5.4.2.5 Follow-up 2

There were 132 transcripts differentially expressed in AEROBIC compared with SEDENTARY AEROBIC [129 up-regulated, FC≥2; 3 down-regulated, FC≤0.5; (FDR<0.05)]. On the other hand, there were 42 transcripts differentially expressed in STRENGTH compared with SEDENTARY STRENGTH [5 up-regulated, FC≥2; 37 down-regulated, FC≤0.5;

(FDR<0.05)]. A complete list of all the differentially expressed transcripts in every comparison is provided at **Appendices B-I.**

5.5 DISCUSSION

Main findings

The main findings of this study identified 426 unique transcripts between AEROBIC and SEDENTARY participants and 14 unique transcripts between STRENGHT and SEDENTARY phenotypes at enrolment. However, following 4 weeks of successful MET, transcriptomic profile of SEDENTARY participants became abrogated to an extent that 234 unique transcripts were observed between AEROBIC and SEDENTARY and 4 unique transcripts were observed between STRENGTH and SEDENTARY. Following randomisation SEDENTARY participants were separated into distinct cohorts undertaking specific exercise (either STRENGHT or AEROBIC) training, and despite differences in CRF consistent with phenotypic adaptation, there were no differences in transcriptomic profiles. Taken together, these data provide cautionary evidence when employing peripheral blood transcriptomic technologies to characterise adaptive phenotypic response in exercise-naïve participants.

Physiological differences between phenotypes are apparently reflected on the transcriptome expression of peripheral blood at enrolment and are reduced by mixed exercise training.

At enrolment, the presentation of three distinct athletic phenotypes (SEDENTARY, AEROBIC, and STRENGTH) were easily differentiated according to their respective phenotypic group. Similarly, this was hypothetically matched by observed transcriptome expression of peripheral blood. Notably, this established a suitable platform to interrogate the

adaptive peripheral blood transcriptomics of peripheral blood of exercise-naïve participants following 4 weeks of subsequent MET.

Taken together, peripheral blood transcriptomics in the present study identified transcriptomic differences to predominate in AEROBIC (426 transcripts) over STRENGTH (14 transcripts) compared with exercise-naïve SEDENTARY participants. In the absence of comparable literature, the observation of greater abundance of systemic transcripts may be due to (i) molecular processes associated with a strength phenotype may be isolated within skeletal muscle, which would partially explain the relatively lower abundance of circulating transcripts in STRENGTH compared with AEROBIC. (ii) Conversely, the metabolic demands of coordinated propulsion of a person's body mass during aerobic exercise requires the coalition of central factors, namely; O_2 transport from ambient air into pulmonary circulation, arterial blood supply and subsequent translocation to the periphery via systemic circulatory mechanisms. That is to say, PBT may be more available to capturing side-effects of aerobic metabolism than strength exercise as a consequence of a major contribution from systemic circulation during aerobic exercise.

Seven transcripts appear to be characteristic of both AEROBIC and STRENGTH athletes compared with SEDENTARY.

The present investigation identified 7 differentially expressed transcripts to be shared between AEROBIC and STRENGTH, compared with SEDENTARY, at enrolment where 6 were up-regulated; *C9orf16, GPR20, LOC100996740, POLR2M, PVRL2, TXNDC5*; One (a pseudogene with unknown function); *LOC101929887* was down-regulated. *C9orf16* gene (Chromosome 9 Open Reading Frame 16) also known as *BBLN* is a protein coding gene that results on a protein product with the same name, but with no apparent function described until this study. *GPR20* gene codes for G Protein-Coupled Receptor 20 that has been described to constitutively activate G proteins without ligand stimulation and might have a

role in cellular processes such as intracellular cAMP levels and mitogenic signalling [43]. *LOC100996740* has been identified as a lncRNA. Although its function is still unclear, lncRNAs exert a regulatory role at multiple levels, but mainly in RNA transcription. *POLR2M* gene codes for a subunit of a specific form of RNA polymerase II, called Gdown1. This subunit has a crucial role regulating messenger RNA synthesis in eukaryotes by suppressing the transcription process [44]. Adaptation to exercise training is characterised by a tight and controlled regulation of molecular processes leading to a specific phenotype characterised by an aggregate of responses throughout multiple tissues. It is then expected that an important regulatory molecule would be significant when comparing athletes with sedentary participants. *PVRL2* (also known as *NECTIN2*; Nectin Cell Adhesion Molecule 2) codes for a membrane glycoprotein that is one of the plasma membrane component of adherens junctions [45]. It is widely expressed in antigen-presenting cells, with a known role in the regulation of immune system via transcriptomic interaction with T cells [46]. Single bouts of strenuous exercise in an untrained individual may present as an immunological insult whereas regular exercise such as that achieved during a structured exercise program confers a gradual immunoadaptive response leading to enhanced defence against infections and management of autoimmune diseases [17, 47, 48]. The over-expression of this transcript in both STRENGHT and AEROBIC athletes, in our study, may reflect immune benefits from long-term physical exercise. Finally, *TXNDC5* (Thioredoxin Domain Containing 5), this gene encodes a member of the disulfide isomerase (PDI) family of endoplasmic reticulum (ER) proteins that catalyse protein folding and thiol-disulfide interchange reactions [49]. It has been observed that PDIs are expressed under hypoxic conditions and exert a protective against hypoxia-initiated apoptosis. The effect of this gene has not been characterised in peripheral blood, but based on current research it may also work in the same manner that

described above, as high intensity physical exercise typically elicits a hypoxic cellular environment.

Since these transcripts are expressed in both types of athletic phenotypes, independently of the type of exercise these participants practice, they could be characteristics of a more generalised adaptation to exercise training. Metabolic response to exercise has been studied in depth on skeletal muscle [3], and the metabolic processes involved are numerous and paramount for an appropriate adaptation to chronic exercise, especially at early stages. However, metabolic changes occur throughout the body as a consequence of a co-ordinated response between multiple tissues, systemic processes, and anatomical structures [13, 14]. Moreover, both aerobic and resistance exercises share common physiological processes as each require an increase in metabolic rate with concomitant metabolic processes Therefore, it is expected to see some similarities in transcripts overexpressed in both athlete groups when compared with SEDENTARY. Overall, the aforementioned transcripts mainly have a regulatory function or are involved in general cellular processes that are likely to be associated with an early, more generalised athletic adaptation. Similarly, Liu et al. conducted a cross-sectional study employing microarray technology to compare the transcriptome profile of blood leukocytes in young endurance athletes (n=12) compared with non-athlete controls (n=12). The authors found that genes involved in RNA processing (*SNORD14E, SNORD4B, MIR15B, SNHG12, NCRNA00188*), and ribosome biogenesis (*RPL10A, RPL21, RPS27, RPS19, RPLP0, RPL23*) [2]. However, none of the transcripts differentially expressed in their study were differentially expressed between AEROBIC or STRENGTH compared with SEDENTARY in our study.

Additionally, when comparing the transcriptome of AEROBIC with SEDENTARY after mixed exercise, AEROBIC still presents a substantial number of transcripts differentially expressed with SEDENTARY (234), although less than at enrolment. On the

other hand, STRENGH displays fewer transcripts differentially expressed with SEDENTARY than aerobic (4), and reduced the number of differentially expressed transcripts from the same comparison at enrolment, too. Notably, there were no differentially expressed transcripts between both, AEROBIC and STRENGTH, and SEDENTARY, at this stage.

These results could indicate (i) a clear differentiation between three divergent athletic phenotypes; sedentary, aerobic athletes, and strength athletes, that is reflected in the transcriptome of peripheral blood, (ii) that 4 weeks of mixed exercise training has an effect on the transcriptomic profile of the SEDENTARY group, evolving towards closing the gap between a sedentary phenotype and an athletic phenotype, more so in the case of STRENGTH athletes. However, as in the case of physiological characteristics, they are still far from reaching the transcriptome of aerobically fit and strong phenotypes observed in peripheral blood.

Subsequently, SEDENTARY were randomised into SEDENTARY AEROBIC or SEDENTARY STRENGTH, conducting 4 more weeks of aerobic or resistance training, respectively. We observed that sedentary participants engaging on aerobic training kept increasing their CRF yet not reaching that of the AEROBIC athletes. On the other hand, muscular strength did not change in this group, likely because they were not doing resistance training, but still conserving the improvements from the previous stage. Seemingly, sedentary participants engaging on resistance training, further improved muscular strength, however not reaching that of STRENGTH athletes, and conserved the same level of CRF acquired during the previous exercise intervention, most likely because of the same reasons than the other group. However, differences in transcriptome expression between groups showed a different trend than the observed at follow-up 1. AEROBIC and SEDENTARY AEROBIC became

more similar (132 transcripts differentially expressed), whereas STRENGTH and SEDENTARY STRENGTH became more different (42 transcripts differentially expressed).

Four weeks of mixed exercise training appear to have minor impact on the expression of peripheral blood transcripts on sedentary male participants

Four weeks of mixed exercise training had an impact on SEDENTARY participants, significantly improving CRF and muscular strength. Interestingly, despite observing this significant increase in both physiological characteristics, only two transcripts, *RPL13AP5* and *TRNH*, were differentially expressed (up-regulated) in SEDENTARY when criteria for differential expression was set at FC≥2 for up-regulation. These data appear to show that the physiological improvement in CRF and muscular strength that we observe in the SEDENTARY group does not translate in a change as significant in the transcriptome profile of peripheral blood. These results differ from similar studies examining the effect of exercise training on the expression of large transcriptomes of peripheral blood, where several transcripts were found to be differentially expressed after an exercise intervention. Iyalomhe et al. observed 81 genes differentially expressed (FC≥2, $p<0.01$) in a microarray of RNA extracted from buffy coat of sedentary participants after 8 weeks walking routine [34]. In another microarray study of RNA extracted from PBMCs, Thompson et al. found that 24 weeks of aerobic exercise training affected the expression of 53 in sedentary participants with high IL-6 at baseline. Furthermore, another microarray analysis of PBMCs transcriptome, conducted by Dias et al., found 152 transcripts up-regulated, and 59 down-regulated in a sedentary cohort after 18 weeks of running endurance training [50]. These transcripts were found to be mainly related to immune function, cell cycle processes, development, and growth. These differences, however, can be explained by different factors. (i) Intervention factors (type of exercise intervention; duration of intervention) and (ii) Analytics (RNA extracted from PBMCs, or whole blood, or buffy coat…; Microarray vs PCR).

Indeed, this might mean that those physiological changes are driven by transcriptome expression changes in regions of the body other than peripheral blood, more involved in the adaptations to exercise training. Furthermore, we have to take into account that this study uses a restrictive threshold of FC≥2 for up-regulation and FC≤0.5 for down-regulation when identifying differentially expressed transcripts. This allows us for a more confident identification in the results. However, since the physiological adaptation to exercise observed in this study is a mild improvement characterised by an early, novice response, by selecting the aforementioned threshold we might overlook milder variations in transcriptome expression in the SEDENTARY group. Moreover, more significant adaptations to physical activity consolidate after prolonged periods of exercise training, and it is possible that 4 weeks is not enough time to trigger large observable modifications in transcriptome expression in peripheral blood. Therefore, 4 weeks of mixed exercise training did not suffice in triggering a transcriptomic response in peripheral blood able to reach that of athletic phenotypes, in this study.

Four weeks of subsequent aerobic training further improved CRF in SEDENTARY. Four weeks of subsequent resistance training further improved muscular strength in SEDENTARY.

We further investigated whereas 4 weeks of subsequent specific aerobic or resistance training would produce observable changes in the transcriptome expression of SEDENTARY participants. SEDENTARY was randomised into SEDENTARY STRENGTH, conducting 4 weeks of subsequent resistance training, or SEDENTARY AEROBIC, conducting 4 weeks of subsequent aerobic training. As expected, SEDENTARY STRENGTH significantly improved muscular strength, and SEDENTARY AEROBIC significantly improved CRF. However, there was not significant change in the expression of any transcript on any of those groups. It is possible that 4 weeks of specific exercise training produces does not produce a

large variation on the transcriptomic expression profile of peripheral blood, therefore passing undetected in this study.

TRNH appears to be characteristic in peripheral blood of an aerobic athletic phenotype

TRNH, was the sole transcript to be differentially expressed between AEROBIC and SEDENTARY at enrolment and during all subsequent comparisons at all stages (**Fig. 5-2**). Interestingly, TRNH displayed a magnitude of expression which decreased from enrolment (FC=12.5 to FC=5.6) following mixed exercise training. Furthermore, when SEDENTARY were randomised to receive either aerobic or strength training during follow-up 2, sedentary participants receiving aerobic training continued this same trajectory (FC=4.1). Notably, TRNH expression was not different between STRENGHT and SEDENTARY at any measurement point, lending some further support that TRNH may be characteristic of an aerobic athlete phenotype. Indeed, TRNH (or MT-TH; Mitochondrially Encoded TRNA-His (CAU/C)) has known affiliation with the tRNA class. More in depth information for TRNH gene can be found at https://www.ncbi.nlm.nih.gov/gtr/genes/4564/. This gene is located in the mitochondrial DNA and encodes for the transfer RNA in charge of carrying Histidine to the protein synthetic chain on the ribosome ($tRNA^{His}$). In a hybrid cellular model, mitochondria derived from lymphoblastoids carrying a mutation in this gene, presented with a ~70% reduction in the steady levels of $tRNA^{His}$ and showed impaired mitochondrial translation characterised by substantial decreases in mitochondrial ATP levels and membrane potential, leading to increased production of reactive oxygen species (ROS) [51]. Moreover, it has been well described that physical exercise promotes mitochondrial activity and proliferation in muscle [52]. Further support for this tenet can be observed in studies that examine physical activity-induced mitochondrial biogenesis in brain [53, 54], adipose tissue [55, 56], and kidney [54]. Interestingly, Busquets et al. observed that 8 weeks of regular training in professional football players had an effect on PBMCs mitochondria, enhancing antioxidant mitochondria

capabilities to decrease ROS production and mitochondrial biosynthesis [57]. Moreover, Liu et al. 2017 conducted a microarray analysis where they found 71 genes differentially expressed in athletes compared with sedentary participants, which were propose to identify the athletic phenotype from peripheral blood. These genes are mainly encoding ribosomal proteins, and the genes involved in mitochondrial oxidative phosphorylation (OXPHOS) [2]. However, as we could not replicate their findings, with none of the 71 genes identified by Liu and colleagues, the influence of mitochondrial metabolism genes in peripheral blood transcriptomics is conjecture.

Interestingly, other mitochondrially encoded tRNAs genes (*TRNQ, TRNE, TRNF, TRNA*), were significantly expressed in AEROBIC compared with SEDENTARY at enrolment, in the present study. In the same way, the difference in expression for those transcripts between these two phenotypes was reduced after mixed exercise training, and further reduced after specific aerobic training. However, no change of the expression of these transcripts was found in SEDENTARY after mixed exercise. These transcripts have a major role in the synthesis of protein, hence in the metabolism of the cell.

Indeed, it exists evidence of an adaptation of oxidative metabolism in skeletal muscle, driven by modulations in ATP/ADP ratio, $Ca2^{+}$ intracellular levels, and ROS, among others, that elicits mitochondrial biogenesis in skeletal muscle in response to exercise [4], and further evidence proposed that blood cells mimic gene expression alterations related to oxidative metabolism in muscle [58]. Our study also observed the relative over-expression of *CACNA1A* (Calcium Voltage-Gated Channel Subunit Alpha1 A) in AEROBIC compared with sedentary. The protein encoded for this gene is part of the Voltage-dependent calcium channels that plays a role in the entry of calcium ions into excitable cells, regulating different processes such as muscle contraction, hormone or neurotransmitter release, and gene expression. It may be

possible that the over-expression of this gene in the AEROBIC athletes is a reflection of the Ca2+ intracellular levels required for the mitochondrial response to exercise.

Nevertheless, although there are evidences in current literature that mitochondrial responses to exercise can occur within peripheral blood cells, data from this study shows very few transcripts related with these processes. Unfortunately, there is a current lack of comparable research studies to endorse this observation within exercise genomics literature, and whether the well stablished mitochondrial adaptation to aerobic exercise is relevant in peripheral blood, still needs to be elucidated. Therefore, other researchers are encouraged to focus their investigation on mitochondrial metabolism in peripheral blood in response to exercise training. Taken together, these data provide hypothetical support for our observed upregulation of TRNH in peripheral blood, therefore lending plausibility to the involving of the abundance of TRNH to reflect (i) the aerobic athlete phenotype, (ii) adaptation to aerobic training in SEDENTARY.

Strengths and limitations

The present study has some strengths and significant limitations which should be considered to determine the strength of present observations. Although this study successfully compared phenotypes and the exercise-naïve participants improved athletic performance in response to supervised exercise, the present design involved subsequent strength and aerobic exercise and is therefore unable to distinguish the relative contribution of MET intervention on subsequent specific exercise training. Further, it should also be considered that the present study used peripheral whole blood to determine transcriptome expression and it cannot be discounted that individual blood cell subsets such as lymphocytes, neutrophils or monocytes, among others, contributed to varying degrees. In partial mitigation, the present study was not intended to scrutinise different gene expression patterns within whole blood, rather to compare athletic phenotypes with sedentary counterparts before and after exercise training. In

this respect, we encourage that future similar work should extend the present observations by controlling for these factors.

5.6 CONCLUSION

Despite the identification of novel candidate PBT signatures which would appear to distinguish athletic phenotypes at study enrolment, any expected consistency became abrogated following MET in previously exercise-naïve participants. These data provide cautionary evidence to those wishing to employ PBT as a tool to predict adaptive capacity to mixed exercise training in otherwise healthy sedentary men.

5.7 REFERENCES

1. Liew C-C, Ma J, Tang H-C, Zheng R, Dempsey AA. The peripheral blood transcriptome dynamically reflects system wide biology: a potential diagnostic tool. The Journal of Laboratory and Clinical Medicine. 2006;147(3):126-32. doi: 10.1016/j.lab.2005.10.005.
2. Liu D, Wang R, Grant AR, Zhang J, Gordon PM, Wei Y, et al. Immune adaptation to chronic intense exercise training: new microarray evidence. BMC Genomics. 2017;18(1):29. Epub 2017/01/07. doi: 10.1186/s12864-016-3388-5. PubMed PMID: 28056786; PubMed Central PMCID: PMCPMC5216585.
3. Hughes DC, Ellefsen S, Baar K. Adaptations to Endurance and Strength Training. Cold Spring Harbor perspectives in medicine. 2018;8(6):a029769. Epub 2017/05/12. doi: 10.1101/cshperspect.a029769. PubMed PMID: 28490537; PubMed Central PMCID: PMCPMC5983157.
4. Hood DA, Uguccioni G, Vainshtein A, D'Souza D. Mechanisms of exercise-induced mitochondrial biogenesis in skeletal muscle: implications for health and disease. Comprehensive Physiology. 2011;1(3):1119-34. Epub 2011/07/01. doi: 10.1002/cphy.c100074. PubMed PMID: 23733637.
5. Guzzoni V, Ribeiro MBT, Lopes GN, de Cassia Marqueti R, de Andrade RV, Selistre-de-Araujo HS, et al. Effect of Resistance Training on Extracellular Matrix Adaptations in Skeletal Muscle of Older Rats. Frontiers in physiology. 2018;9:374. Epub 2018/04/27. doi: 10.3389/fphys.2018.00374. PubMed PMID: 29695977; PubMed Central PMCID: PMCPMC5904267.
6. Bamman MM, Roberts BM, Adams GR. Molecular Regulation of Exercise-Induced Muscle Fiber Hypertrophy. Cold Spring Harbor perspectives in medicine. 2018;8(6). Epub 2017/05/12. doi: 10.1101/cshperspect.a029751. PubMed PMID: 28490543; PubMed Central PMCID: PMCPMC5983156.
7. Furrer R, Eisele PS, Schmidt A, Beer M, Handschin C. Paracrine cross-talk between skeletal muscle and macrophages in exercise by PGC-1α-controlled BNP. Scientific Reports. 2017;7(1):40789. Epub 2017/01/17. doi: 10.1038/srep40789. PubMed PMID: 28091624; PubMed Central PMCID: PMCPMC5238507.
8. Furrer R, Handschin C. Optimized Engagement of Macrophages and Satellite Cells in the Repair and Regeneration of Exercised Muscle. In: Spiegelman B, editor. Hormones, Metabolism and the Benefits of Exercise. Cham: Springer International Publishing; 2017. p. 57-66.
9. Williams RS, Neufer PD. Regulation of Gene Expression in Skeletal Muscle by Contractile Activity. Comprehensive Physiology. Sumplement 29: Handbook of Physiology1996. p. 1124-50.
10. Wang L, Mascher H, Psilander N, Blomstrand E, Sahlin K. Resistance exercise enhances the molecular signaling of mitochondrial biogenesis induced by endurance exercise in human skeletal muscle. Journal of Applied Physiology. 2011;111(5):1335-44. Epub 2011/08/13. doi: 10.1152/japplphysiol.00086.2011. PubMed PMID: WOS:000297684500017.
11. Pilegaard H, Saltin B, Neufer PD. Exercise induces transient transcriptional activation of the PGC-1alpha gene in human skeletal muscle. The Journal of physiology. 2003;546(Pt 3):851-8. Epub 2003/02/04. doi: 10.1113/jphysiol.2002.034850. PubMed PMID: 12563009; PubMed Central PMCID: PMCPMC2342594.
12. Gjevestad G, Holven K, Ulven S. Effects of Exercise on Gene Expression of Inflammatory Markers in Human Peripheral Blood Cells: A Systematic Review. Current Cardiovascular Risk Reports. 2015;9(7):1-17. doi: 10.1007/s12170-015-0463-4.

13. Pedersen L, Hojman P. Muscle-to-organ cross talk mediated by myokines. Adipocyte. 2012;1(3):164-7. Epub 2013/05/24. doi: 10.4161/adip.20344. PubMed PMID: 23700527; PubMed Central PMCID: PMCPMC3609091.
14. Tidball JG, Villalta SA. Regulatory interactions between muscle and the immune system during muscle regeneration. American journal of physiology Regulatory, integrative and comparative physiology. 2010;298(5):R1173-87. Epub 2010/03/12. doi: 10.1152/ajpregu.00735.2009. PubMed PMID: 20219869; PubMed Central PMCID: PMCPMC2867520.
15. Tidball JG. Inflammatory processes in muscle injury and repair. American journal of physiology Regulatory, integrative and comparative physiology. 2005;288(2):R345-53. Epub 2005/01/08. doi: 10.1152/ajpregu.00454.2004. PubMed PMID: 15637171.
16. Holloszy JO. Biochemical adaptations in muscle. Effects of exercise on mitochondrial oxygen uptake and respiratory enzyme activity in skeletal muscle. The Journal of biological chemistry. 1967;242(9):2278-82. Epub 1967/05/10. PubMed PMID: 4290225.
17. Flynn MG, McFarlin BK, Markofski MM. The Anti-Inflammatory Actions of Exercise Training. Am J Lifestyle Med. 2007;1(3):220-35. Epub 2007/05/01. doi: 10.1177/1559827607300283. PubMed PMID: 25431545; PubMed Central PMCID: PMCPMC4243532.
18. Coyle EF, Coggan AR, Hopper MK, Walters TJ. Determinants of endurance in well-trained cyclists. Journal of applied physiology (Bethesda, Md : 1985). 1988;64(6):2622-30. Epub 1988/06/01. doi: 10.1152/jappl.1988.64.6.2622. PubMed PMID: 3403447.
19. Holloszy JO, Coyle EF. Adaptations of skeletal muscle to endurance exercise and their metabolic consequences. Journal of applied physiology: respiratory, environmental and exercise physiology. 1984;56(4):831-8. Epub 1984/04/01. doi: 10.1152/jappl.1984.56.4.831. PubMed PMID: 6373687.
20. Favier RJ, Constable SH, Chen M, Holloszy JO. Endurance exercise training reduces lactate production. Journal of applied physiology (Bethesda, Md : 1985). 1986;61(3):885-9. Epub 1986/09/01. doi: 10.1152/jappl.1986.61.3.885. PubMed PMID: 3759772.
21. Narici MV, Roi GS, Landoni L, Minetti AE, Cerretelli P. Changes in force, cross-sectional area and neural activation during strength training and detraining of the human quadriceps. European journal of applied physiology and occupational physiology. 1989;59(4):310-9. Epub 1989/01/01. doi: 10.1007/bf02388334. PubMed PMID: 2583179.
22. Pyka G, Lindenberger E, Charette S, Marcus R. Muscle strength and fiber adaptations to a year-long resistance training program in elderly men and women. Journal of gerontology. 1994;49(1):M22-7. Epub 1994/01/01. doi: 10.1093/geronj/49.1.m22. PubMed PMID: 8282977.
23. Häkkinen K, Alén M, Kallinen M, Izquierdo M, Jokelainen K, Lassila H, et al. Muscle CSA, Force Production, and Activation of Leg Extensors during Isometric and Dynamic Actions in Middle-Aged and Elderly Men and Women. Journal of aging and physical activity. 1998;6(3):232-47. doi: 10.1123/japa.6.3.232.
24. Buttner P, Mosig S, Lechtermann A, Funke H, Mooren FC. Exercise affects the gene expression profiles of human white blood cells. Journal of applied physiology (Bethesda, Md : 1985). 2007;102(1):26-36. Epub 2006/09/23. doi: 10.1152/japplphysiol.00066.2006. PubMed PMID: 16990507.
25. Connolly PH, Caiozzo VJ, Zaldivar F, Nemet D, Larson J, Hung SP, et al. Effects of exercise on gene expression in human peripheral blood mononuclear cells. Journal of applied physiology (Bethesda, Md : 1985). 2004;97(4):1461-9. Epub 2004/06/15. doi: 10.1152/japplphysiol.00316.2004. PubMed PMID: 15194674.
26. Kawai T, Morita K, Masuda K, Nishida K, Sekiyama A, Teshima-Kondo S, et al. Physical exercise-associated gene expression signatures in peripheral blood. Clinical journal

of sport medicine : official journal of the Canadian Academy of Sport Medicine. 2007;17(5):375-83. Epub 2007/09/18. doi: 10.1097/JSM.0b013e31814c3e4f. PubMed PMID: 17873550.
27. Lundberg TR, Fernandez-Gonzalo R, Tesch PA, Rullman E, Gustafsson T. Aerobic exercise augments muscle transcriptome profile of resistance exercise. American journal of physiology Regulatory, integrative and comparative physiology. 2016;310(11):R1279-87. Epub 2016/04/22. doi: 10.1152/ajpregu.00035.2016. PubMed PMID: 27101291; PubMed Central PMCID: PMCPMC4935502.
28. Mukherjee K, Edgett BA, Burrows HW, Castro C, Griffin JL, Schwertani AG, et al. Whole blood transcriptomics and urinary metabolomics to define adaptive biochemical pathways of high-intensity exercise in 50-60 year old masters athletes. PloS one. 2014;9(3):e92031. Epub 2014/03/20. doi: 10.1371/journal.pone.0092031. PubMed PMID: 24643011; PubMed Central PMCID: PMCPMC3958411.
29. Carlson LA, Tighe SW, Kenefick RW, Dragon J, Westcott NW, Leclair RJ. Changes in transcriptional output of human peripheral blood mononuclear cells following resistance exercise. European journal of applied physiology. 2011;111(12):2919-29. Epub 03/25. doi: 10.1007/s00421-011-1923-2. PubMed PMID: 21437602; PubMed Central PMCID: PMCPMC4358769.
30. Nakamura S, Kobayashi M, Sugino T, Kajimoto O, Matoba R, Matsubara K. Effect of exercise on gene expression profile in unfractionated peripheral blood leukocytes. Biochemical and biophysical research communications. 2010;391(1):846-51. Epub 2009/12/01. doi: 10.1016/j.bbrc.2009.11.150. PubMed PMID: 19945435.
31. Radom-Aizik S, Zaldivar F, Jr., Leu SY, Cooper DM. A brief bout of exercise alters gene expression and distinct gene pathways in peripheral blood mononuclear cells of early- and late-pubertal females. Journal of applied physiology (Bethesda, Md : 1985). 2009;107(1):168-75. Epub 2009/05/02. doi: 10.1152/japplphysiol.00121.2009. PubMed PMID: 19407257; PubMed Central PMCID: PMCPMC2711785.
32. Slivka DR, Heesch MWS, Dumke CL, Cuddy JS, Hailes WS, Ruby BC. Human Skeletal Muscle mRNA Response to a Single Hypoxic Exercise Bout. Wildern Environ Med. 2014;25(4):462-5. PubMed PMID: WOS:000346895300014.
33. Zieker D, Fehrenbach E, Dietzsch J, Fliegner J, Waidmann M, Nieselt K, et al. cDNA microarray analysis reveals novel candidate genes expressed in human peripheral blood following exhaustive exercise. Physiological genomics. 2005;23(3):287-94. Epub 2005/08/25. doi: 10.1152/physiolgenomics.00096.2005. PubMed PMID: 16118270.
34. Iyalomhe O, Chen YX, Allard J, Ntekim O, Johnson S, Bond V, et al. A standardized randomized 6-month aerobic exercise-training down-regulated pro-inflammatory genes, but up-regulated anti-inflammatory, neuron survival and axon growth-related genes. Experimental gerontology. 2015;69:159-69. Epub 2015/05/20. doi: 10.1016/j.exger.2015.05.005. PubMed PMID: WOS:000360320200021; PubMed Central PMCID: PMCPMC4553116.
35. Rodriguez-Miguelez P, Fernandez-Gonzalo R, Almar M, Mejias Y, Rivas A, de Paz JA, et al. Role of Toll-like receptor 2 and 4 signaling pathways on the inflammatory response to resistance training in elderly subjects. Age. 2014;36(6):9734. Epub 2014/11/28. doi: 10.1007/s11357-014-9734-0. PubMed PMID: WOS:000346770900016; PubMed Central PMCID: PMCPMC4245402.
36. Macêdo Santiago LÂ, Neto LGL, Borges Pereira G, Leite RD, Mostarda CT, de Oliveira Brito Monzani J, et al. Effects of Resistance Training on Immunoinflammatory Response, TNF-Alpha Gene Expression, and Body Composition in Elderly Women. Journal of Aging Research. 2018;2018:1-10. Epub 2018/12/05. doi: 10.1155/2018/1467025. PubMed PMID: 132650858. Language: English. Entry Date: 20181030. Revision Date: 20181030.

Publication Type: Article. Journal Subset: Biomedical; PubMed Central PMCID: PMCPMC6230406.
37. Lee SH, Hong HR, Han TK, Kang HS. Aerobic training increases the expression of adiponectin receptor genes in the peripheral blood mononuclear cells of young men. Biology of sport. 2015;32(3):181-6. Epub 2015/10/02. doi: 10.5604/20831862.1150298. PubMed PMID: 26424919; PubMed Central PMCID: PMCPMC4577554.
38. Streese L, Khan AW, Deiseroth A, Hussain S, Suades R, Tiaden A, et al. High-intensity interval training modulates retinal microvascular phenotype and DNA methylation of p66Shc gene: a randomized controlled trial (EXAMIN AGE). Eur Heart J. 2020;41(15):1514-9. Epub 2019/07/20. doi: 10.1093/eurheartj/ehz196. PubMed PMID: 31323685.
39. Thompson D, Markovitch D, Betts JA, Mazzatti D, Turner J, Tyrrell RM. Time course of changes in inflammatory markers during a 6-mo exercise intervention in sedentary middle-aged men: a randomized-controlled trial. Journal of Applied Physiology. 2010;108(4):769-79. doi: 10.1152/japplphysiol.00822.2009. PubMed PMID: WOS:000276324200003.
40. Riebe D, Ehrman, J. K., Liguori, G., & Magal, M. ACSM's Guidelines for Exercise Testing and Prescription (Tenth edition). American Collegue of Sports Medicine. 2018.
41. von Elm E, Altman DG, Egger M, Pocock SJ, Gøtzsche PC, Vandenbroucke JP. The Strengthening the Reporting of Observational Studies in Epidemiology (STROBE) statement: guidelines for reporting observational studies. J Clin Epidemiol. 2008;61(4):344-9. Epub 2008/03/04. doi: 10.1016/j.jclinepi.2007.11.008. PubMed PMID: 18313558.
42. Tanner RK, Gore CJ. Physiological tests for elite athletes. Champaign, IL : Human Kinetics. 2013.
43. Hase M, Yokomizo T, Shimizu T, Nakamura M. Characterization of an orphan G protein-coupled receptor, GPR20, that constitutively activates Gi proteins. The Journal of biological chemistry. 2008;283(19):12747-55. Epub 2008/03/19. doi: 10.1074/jbc.M709487200. PubMed PMID: 18347022.
44. Wu YM, Chang JW, Wang CH, Lin YC, Wu PL, Huang SH, et al. Regulation of mammalian transcription by Gdown1 through a novel steric crosstalk revealed by cryo-EM. The EMBO journal. 2012;31(17):3575-87. Epub 2012/08/02. doi: 10.1038/emboj.2012.205. PubMed PMID: 22850672; PubMed Central PMCID: PMCPMC3433857.
45. Takahashi K, Nakanishi H, Miyahara M, Mandai K, Satoh K, Satoh A, et al. Nectin/PRR: an immunoglobulin-like cell adhesion molecule recruited to cadherin-based adherens junctions through interaction with Afadin, a PDZ domain-containing protein. The Journal of cell biology. 1999;145(3):539-49. Epub 1999/05/04. doi: 10.1083/jcb.145.3.539. PubMed PMID: 10225955; PubMed Central PMCID: PMCPMC2185068.
46. Zhu Y, Paniccia A, Schulick AC, Chen W, Koenig MR, Byers JT, et al. Identification of CD112R as a novel checkpoint for human T cells. Journal of Experimental Medicine. 2016;213(2):167-76. Epub 2016/01/13. doi: 10.1084/jem.20150785. PubMed PMID: 26755705; PubMed Central PMCID: PMCPMC4749091.
47. Brolinson PG, Elliott D. Exercise and the immune system. Clinics in sports medicine. 2007;26(3):311-9. Epub 2007/09/11. doi: 10.1016/j.csm.2007.04.011. PubMed PMID: 17826186.
48. Gleeson M, Bishop NC, Stensel DJ, Lindley MR, Mastana SS, Nimmo MA. The anti-inflammatory effects of exercise: mechanisms and implications for the prevention and treatment of disease. Nature Reviews Immunology. 2011;11(9):607. Epub 2011/08/06. doi: 10.1038/nri3041. PubMed PMID: 21818123.
49. Knoblach B, Keller BO, Groenendyk J, Aldred S, Zheng J, Lemire BD, et al. ERp19 and ERp46, New Members of the Thioredoxin Family of Endoplasmic Reticulum Proteins *.

Molecular & Cellular Proteomics. 2003;2(10):1104-19. Epub 2003/08/22. doi: 10.1074/mcp.M300053-MCP200. PubMed PMID: 12930873.
50. Dias RG, Silva MS, Duarte NE, Bolani W, Alves CR, Junior JR, et al. PBMCs express a transcriptome signature predictor of oxygen uptake responsiveness to endurance exercise training in men. Physiological genomics. 2015;47(2):13-23. Epub 2014/12/04. doi: 10.1152/physiolgenomics.00072.2014. PubMed PMID: 25465030.
51. Gong S, Peng Y, Jiang P, Wang M, Fan M, Wang X, et al. A deafness-associated tRNAHis mutation alters the mitochondrial function, ROS production and membrane potential. Nucleic acids research. 2014;42(12):8039-48. Epub 2014/06/13. doi: 10.1093/nar/gku466. PubMed PMID: 24920829; PubMed Central PMCID: PMCPMC4081083.
52. Oliveira AN, Hood DA. Exercise is mitochondrial medicine for muscle. Sports Medicine and Health Science. 2019;1(1):11-8. doi: https://doi.org/10.1016/j.smhs.2019.08.008.
53. Steiner JL, Murphy EA, McClellan JL, Carmichael MD, Davis JM. Exercise training increases mitochondrial biogenesis in the brain. Journal of applied physiology (Bethesda, Md : 1985). 2011;111(4):1066-71. Epub 2011/08/06. doi: 10.1152/japplphysiol.00343.2011. PubMed PMID: 21817111.
54. Navarro A, Gomez C, López-Cepero JM, Boveris A. Beneficial effects of moderate exercise on mice aging: survival, behavior, oxidative stress, and mitochondrial electron transfer. American Journal of Physiology-Regulatory, Integrative and Comparative Physiology. 2004;286(3):R505-R11. Epub 2003/11/15. doi: 10.1152/ajpregu.00208.2003. PubMed PMID: 14615275.
55. Laye MJ, Rector RS, Warner SO, Naples SP, Perretta AL, Uptergrove GM, et al. Changes in visceral adipose tissue mitochondrial content with type 2 diabetes and daily voluntary wheel running in OLETF rats. The Journal of physiology. 2009;587(Pt 14):3729-39. Epub 06/02. doi: 10.1113/jphysiol.2009.172601. PubMed PMID: 19491243; PubMed Central PMCID: PMCPMC2742294.
56. Sutherland LN, Bomhof MR, Capozzi LC, Basaraba SA, Wright DC. Exercise and adrenaline increase PGC-1{alpha} mRNA expression in rat adipose tissue. J Physiol. 2009;587(Pt 7):1607-17. Epub 2009/02/18. doi: 10.1113/jphysiol.2008.165464. PubMed PMID: 19221126; PubMed Central PMCID: PMCPMC2678229.
57. Busquets-Cortes C, Capo X, Martorell M, Tur JA, Sureda A, Pons A. Training Enhances Immune Cells Mitochondrial Biosynthesis, Fission, Fusion, and Their Antioxidant Capabilities Synergistically with Dietary Docosahexaenoic Supplementation. Oxidative Medicine and Cellular Longevity. 2016;2016:8950384. Epub 2016/10/05. doi: 10.1155/2016/8950384. PubMed PMID: WOS:000383501600001; PubMed Central PMCID: PMCPMC5028859.
58. Zeibig J, Karlic H, Lohninger A, Damsgaard R, Smekal G. Do blood cells mimic gene expression profile alterations known to occur in muscular adaptation to endurance training? European journal of applied physiology. 2005;95(1):96-104. Epub 2005/04/09. doi: 10.1007/s00421-005-1334-3. PubMed PMID: 15815935.

Table 5-1 *Participants characteristics at enrolment. a – significant compared with STRENGTH (p<0.05), b – significant compared with AEROBIC (p<0.05).*

	SEDENTARY (*n* = 28)	**STRENGTH (*n* = 20)**	**AEROBIC (*n* = 20)**
Age (years)	35.5±7.65[a]	26.2±5.73	31.25±9.86
Height (cm)	181±8[a]	175±7[b]	181±7
Body Mass (Kg)	94.9±17.7[a,b]	79.7±10	72 ±7
BMI (kg/m^2)	28.72±4.9[b]	25.97±2.57[b]	21.83±1.8
$\dot{V}O_{2max}$ (mL.Kg-1.min-1)	32.4±4.85[a,b]	42.73±6.2[b]	59±6.1
Absolute $\dot{V}O_{2max}$ (mL.min-1)	3053.1±577.52[b]	3378.79±473.65[b]	4226.43±401.94
Relative maximum strength (1RM/mass)	2.73±0.58[a,b]	5.67±0.58[b]	3.71±0.58
Absolute maximum strength (1RM)	250.86±58.76[a]	438.97 ±62.65[b]	267.5±44.59

Cm= Centimetres, Kg= Kilograms. BMI= Body Mass Index, m^2= square metres, $\dot{V}O_{2max}$= maximal oxygen consumption, mL= millilitres, min= minutes, 1RM= One-repetition maximum. Values are Means ± SD. a – significant compared with STRENGTH (p<0.05), b – significant compared with AEROBIC (p<0.05).

Table 5-2 *Physiological measurements after 4 weeks of MET for SEDENTARY and the same period for STRENGTH and AEROBIC.*

	SEDENTARY (n = 28)			STRENGTH (n = 20)			AEROBIC (n = 20)		
	Enrolment	**Follow-up 1**	***p value***	**Enrolment**	**Follow-up 1**	***p value***	**Enrolment**	**Follow-up 1**	***p value***
Absolute $\dot{V}O_{2max}$ ($mL \cdot min^{-1}$)	**3053.09 ±577.52[b]**	**3293 ±570.67[b]**	**<0.001**	3378.79 ±473.65[b]	3535.55 ±501.12[b]	0.088	**4226.43 ±401.94**	**4411.22 ±483.04**	**0.031**
$\dot{V}O_{2max}$ ($mL \cdot Kg^{-1} \cdot min^{-1}$)	**32.45±4.85[a,b]**	**35.11±4.75[a,b]**	**0.002**	42.73±6.2[b]	44.78±6.37[b]	0.073	59±6.1	59.8±7.23	1
Squats (Kg)	**76.25±24.46[a]**	**91.5±25.3[a]**	**<0.001**	155.24±29.49[b]	156.1±27.07[b]	1	86.50±17.85	83±16.54	0.66
Deadlift (Kg)	**106.21±26.74[a]**	**117.36±25.6[a]**	**<0.001**	170.95±26.81[b]	171±27.46[b]	1	109±17.14	107.25±15.45	1
Bench press (Kg)	**68.39±15.64[a]**	**72.28±17.3[a]**	**0.004**	110.21±16.2[b]	110.88±16.15 [b]	1	72±15.25	74±15.13	0.479
Absolute strength (1RM;Kg)	**250.86±58.76[a]**	**281.14±60.45[a]**	**<0.001**	438.97 ±62.65[b]	437.98±59.53[b]	1	267.5±44.59	264.25±38.77	1
Relative strength (1RM/body mass; Kg)	**2.73±0.58[a,b]**	**3.07±0.63[a,b]**	**<0.001**	5.67±0.58[b]	5.65±0.51[b]	1	3.71±0.58	3.69±0.58	1
Body mass (kg)	94.91±17.78[a,b]	94.66±17.24[a,b]	1	79.03±10.01	79.61±9.93	1	**73.58±7.31**	**74.17±7.21**	**<0.001**
% Lean body mass	77.77±6.15[a,b]	77.02±6.1[a,b]	0.518	87.40±4.19	86.93±4.03	1	88.55±3.64	88.97±4.15	1
RER_{max}	**1.20±0.09**	**1.16±0.06**	**0.038**	1.22±0.09	1.18±0.05	0.064	1.20±0.09	1.18±0.07	1
HR_{max}	176.64±17.41	174.57±14.24	1	184.15±13.05	184.6±9.21	1	178.43±18.24	178.1±16.53	1
Age predicted HR_{max}	184.5±7.65[a]	184.46±7.71[a]	1	193.8±5.72	193.75±5.75	1	188.75±9.86	188.6±10.02	0.248
RPE	**8.04±1.45[b]**	**8.29±1.41[a,b]**	**<0.001**	8.45±1.01	8.5±1.05	1	9.13±0.78	9.05±0.86	1
Diastolic Blood Pressure (mmHg)	**83.07±7.38[a,b]**	**77.39±9.27[a,b]**	**<0.001**	67.03±7.22	65.6±6.39 [b]	1	73.6±9.43	75.75±10.72	0.629
Systolic Blood Pressure (mmHg)	130.89±9.95[a]	128.96±8.91[a]	0.640	121.55±8.1	118.25±8.45[b]	0.218	125.88±11.54	128.45±12.95	0.482
Mean arterial blood pressure	**186.3±14.17[a,b]**	**180.59±14.11[a]**	**0.032**	166.26±12.15	162.01±11.31[b]	0.319	174.97±16.74	178.98±18.04	0.382

$\dot{V}O_{2max}$= maximal oxygen consumption, mL= millilitres, min= minutes, Kg= Kilograms, 1RM= One repetition maximum, RER= Respiratory Exchange Ratio, HR= Heart Rate, RPE= Rate of Perceived Exertion, mmHg= millimetres of mercury. Values are means ±SD. a – significant compared with STRENGTH (p<0.05), b – significant compared with AEROBIC (p<0.05).

Table 5-3 *Physiological measurements after 4 weeks of AET for SEDENTARY AEROBIC and RET for SEDENTARY STRENGTH, and the same period for STRENGTH and AEROBIC;*

	SEDENTARY STRENGTH (n = 14)			**SEDENTARY AEROBIC (n = 14)**			**STRENGTH (n = 20)**			**AEROBIC (n = 20)**		
	Follow-up 1	**Follow-up 2**	***p value***	**Follow-up 1**	**Follow-up 2**	***p value***	**Follow-up 1**	**Follow-up 2**	***p value***	**Follow-up 1**	**Follow-up 2**	***p value***
Absolute $\dot{V}O2_{max}$ ($mL \cdot min^{-1}$)	3323.82±614.89[b]	3413.82±703.82[b]	1	**3189.40±1005.16[b]**	**3536.87±658.61[b]**	**<0.001**	3535.55 ±501.12[b]	3587.62±541.8[b]	1	4411.22 ±483.04	4373.69±446.05	1
$\dot{V}O_{2max}$ ($mL \cdot Kg^{-1} \cdot min^{-1}$)	36.74±6.06[a,b]	35.89±5.81[a,b]	1	**34.28±5.14[a,b]**	**38.54±6.36[a,b]**	**<0.001**	44.78±6.37[b]	44.92±5.41[b]	1	59.8±7.05	59.52±6.1	1
Squats (Kg)	**96.06±20.30[a]**	**111.07±18.31[a]**	**<0.001**	86.07±31.26[a]	92.68±32.17[a]	0.169	156.1±27.07[b]	156.75±28.16[b]	1	83±16.54	91.75±16.53	0.008
Deadlift (Kg)	120.07±27.40[a]	128.57±30.03[a]	0.184	111.79±28.27[a]	117.68±20.95[a]	0.122	171±27.46[b]	173±26.92[b]	1	107.25±15.45	111.5±15.58	0.299
Bench press (Kg)	69.31±14.6[a]	74.11±15.65[a]	0.139	73.93±16.42[a]	71.25±20.30[a]	0.489	110.88±16.15[b]	110.5±16.48[b]	1	74±15.13	74.13±14.5	1
Absolute strength (1RM;Kg)	**285.44±57.42[a]**	**313.75±58.59[a]**	**<0.001**	271.79±96.5[a]	281.61±64.51[a]	0.245	437.98±59.53[b]	440.25±60.72[a]	1	**264.25±37.79**	**277.38±40.21**	**0.018**
Relative strength (1RM/body mass; Kg)	3.25±0.7[a]	3.38±0.75[a]	0.052	2.96±1.07[a,b]	3.09±0.54[a,b]	1	5.65±0.51[b]	5.66±0.55[b]	1	3.69±0.57	3.87±0.54	0.177
Body mass (kg)	92.31±20.78[a,b]	96.04±18.82[a,b]	1	93.55±16.49[a,b]	92.58±15.6[a,b]	0.221	79.61±9.93	80.19±9.92	0.434	74.17±7.21	73.77±6.63	0.940
% Lean body mass	78.05±7.36[a,b]	76.72±6.52[a,b]	1	76.79±7.1[a,b]	77.26±4.52[a,b]	1	86.93±4.03	87.31±4.65	1	88.97±4.15	87.96±4.12	0.355
RER_{max}	1.16±0.07	1.17±0.09	1	1.18±0.08	1.16±0.05	0.988	1.18±0.05	1.19±0.06	1	1.18±0.07	1.15±0.05	0.165
HR_{max}	177.13±12.62	173.21±13.06	1	173.43±9.37	174±16.95	1	184.6±9.21	184.70±8.72	1	178.1±16.53	178.05±15.55	1
Age predicted HR_{max}	187.13±6.84[a]	186.79±6.17[a]	1	182.07±9.3[a]	182±8.57[a]	0.914	193.75±5.75	193.8±5.73	1	188.6±9.77	188.45±9.64	0.249
RPE	**8.25±1.73[a,b,c]**	**8.36±1.45**	**<0.001**	8.29±1.75	8.86±1.46	0.510	8.5±1.05	9±0.94	0.381	9.05±0.86	9.26±0.78	1
Diastolic Blood Pressure (mmHg)	76±6.12[a]	77.86±11.47[a]	1	78.64±10.03[a]	80.14±7.12[a]	1	65.6±6.39[b]	65.95±5.99	1	75.75±10.72	73.1±10.5	0.366
Systolic Blood Pressure (mmHg)	126.63±8.33	127.07±13.47	1	131.14±10.05[a]	129.14±10.18	1	118.25±8.45	118.95±7.04	1	128.45±12.95	125.3±12.65	0.266
Mean arterial blood pressure	177.32±11.8[a]	179±20.95[a]	1	183.6±16.11[a]	182.60±14.17[a]	1	162.01±11.31[b]	162.94±9.91	1	178.98±18.04	174.06±18.52	0.191

$\dot{V}O_{2max}$= maximal oxygen consumption, mL= millilitres, min= minutes, Kg= Kilograms, 1RM= One repetition maximum, RER= Respiratory Exchange Ratio, HR= Heart Rate, RPE= Rate of Perceived Exertion, mmHg= millimetres of mercury. Values are means ± SD. a – significant compared with STRENGTH (p<0.05), b – significant compared with AEROBIC (p<0.05), c – significant compared with SEDENTARY AEROBIC (p<0.05).

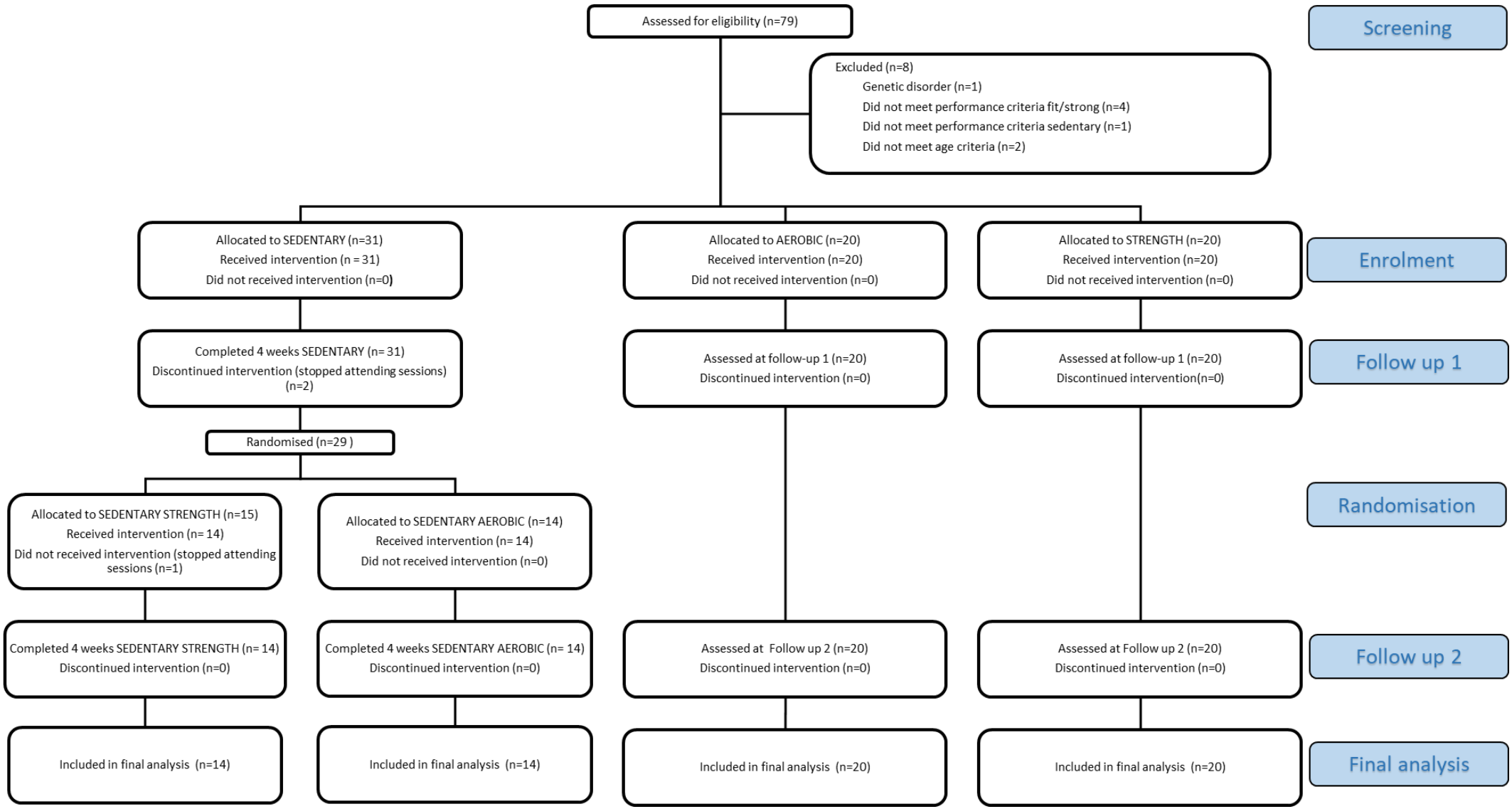

Figure 5-1 *Flow of Participants through the study.*

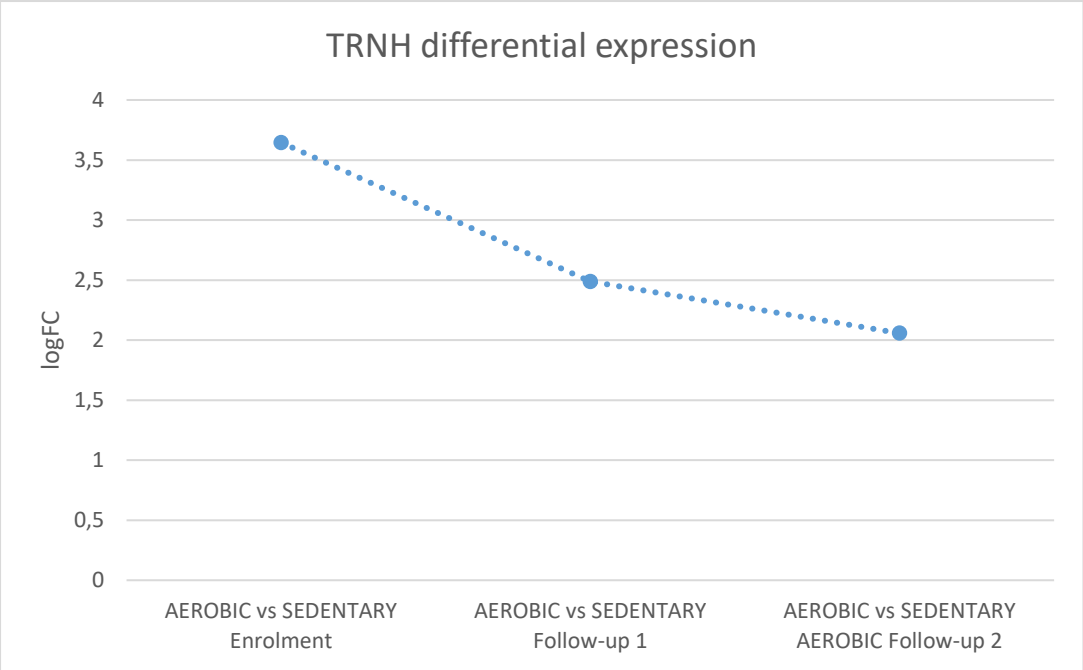

Figure 5-2 *TRNH expression in AEROBIC compared with sedentary participants throughout the study.*

6 PERIPHERAL BLOOD CIRCRNA MAY DIFFERENTIATE ATHLETIC PHENOTYPE BUT DOES NOT CHARACTERISE ADAPTATION TO MIXED EXERCISE TRAINING IN SEDENTARY PHENOTYPE: A STROBE COMPLIANT OBSERVATIONAL STUDY.

"The following experimental chapter is presented in accordance with author guidance procedures for the journal ***European Journal of Applied Physiology***".

https://www.springer.com/journal/421

ISNN: 14396319, ISNN: 14396327

6.1 ABSTRACT

Introduction: This study compared peripheral blood circular RNA (circRNA) expression in divergent exercise phenotypes and examined circRNA expression following 4 weeks of mixed exercise training (MET) in sedentary males, compared with aerobic and strength athletic phenotypes. **Methods:** Male participants (*n*=71*)* consisting: exercise-naïve (*n*=31), aerobic (*n*=20), and strength (*n*=20) phenotypes were enrolled to a STROBE compliant study which examined peripheral blood circRNA both at enrolment and following MET. Linear mixed modelling was employed to test continuous secondary outcomes (i.e. training effects), with Bonferroni correction for multiple comparisons and criterion alpha. $p \leq 0.05$ employed for statistical significance. CircRNAs were identified using CircRNA Identifier (CIRI) tool and differential-expression analysis was performed using the DESeq-*R* package by employing negative binomial modelling techniques with adjusted *p*-values to control false-discovery rate (FDR). An FDR< 0.05 was employed to identify statistical significance for circRNA expression, and $\log^2$ (fold-change) ≥2 and ≤0.5 was employed to indicate up-regulation and down-regulation, respectively. **Results:** Compared with SEDENTARY, AEROBIC presented with *n*=2558 unique differentially expressed circRNAs [n=21 up-regulated, FC≥2; *n*=2537 down-regulated, FC≤0.5; (FDR<0.05)] at enrolment to the study. Compared with SEDENTARY, STRENGTH presented with *n*=619 unique differentially expressed circRNAs [*n*=1 up-regulated, FC≥2; *n*=618 down-regulated, FC≤0.5; (FDR<0.05)]. Following MET, *n*=1 circRNA was differentially expressed [chr19__18537601__18538436___FKBP8, (FC≥2; FDR<0.05)] in SEDENTARY. **Conclusion:** The present study identified a potential associative role for peripheral blood circRNA to identify strength and aerobic athletic phenotypes compared with exercise-naïve counterparts but did not identify any causative role for circRNA to predict adaptation to four weeks of MET in previously exercise-naïve male participants.

6.2 INTRODUCTION

With the advent of 20th Century advances in RNA sequencing (RNA-seq) technologies in coalition with large data bioinformatics, the dynamic expression patterns and relative abundance of non-coding RNA (ncRNA), formerly known as 'Junk DNA' received greater appreciation. Circular RNAs (circRNA) are a novel class of endogenous non-coding RNAs that are gaining greater consideration for playing a central role in human gene expression and signalling pathways. They were first detected several decades ago in viroids and viruses [128, 129], but they had not been reported in mammals until much later [130-132]. Interestingly, non-coding RNAs have been described to regulate gene expression post-transcriptionally. Absolute functions of circRNA remain to be fully established, yet conventional theory identifies their role as 'sponges' for miRNA (micro RNA), capturing complementary miRNA molecules and therefore reducing the effect of the latter [11, 133].

Due to their unique circular covalently bonded structure, circRNAs are structurally stable within tissue access sites and are gaining greater consideration as potential biomarkers of significance in human disease and health. CircRNA is a constituent non-coding RNA characterized with 3′- and 5′-ends covalently linked in a closed-loop structure [134], allowing greater resistance to exonucleases and considered more stable than traditional linear RNA, such as long non-coding RNA (lncRNA) and micro RNA (miRNA) [135]. Another attribute of circRNA relates to their potential to compensate for low organ specificity as a consequence of tissue-specific expression more so than traditional biomarkers. Similarly, circRNAs remain relatively stable within cytoplasm, and exonic circular RNAs have prolonged half-life ($t_{1/2}$) > 48h compared with their linear RNA counterparts ($t_{1/2}$ ~10h) [136]. There is substantive evidence to pursue the capacity for circRNAs as tangible biomarkers of disease, candidate targets for treatment, and personalised medicine.

Allied with clinical genomics, considerable interest exists in the field of sports performance and therapeutic exercise prescription. There is existing aspiration that continuous development within the field of genomics may someday allow comprehensive understanding of genomic factors (e.g., DNA sequence variants) which underlie divergent phenotypic response to exercise training and similarly allow prediction of an individual's capacity for sports performance. The previous three decades of sports medicine research have identified a known variability in exercise adaptation and a body of existing data which indicates comparable variability between and within cohorts of disease and health.

To date, there have been scarce empirical data relating to exercise adaptation and its effect on circRNA expression in human biological tissues. Recent circRNA data from a mouse model of aerobic exercise and ageing conducted by Guo et al. identified circBBS9 to be present at lower levels in ageing mice, but increased following aerobic exercise. These authors further reported that circBBS9 was central to important miRNA-mRNA metabolic gene networks [137]. Recent specific target circRNA expression work of Meinecke and colleagues in a human acute exercise model of marathon runners identified levels of circRNA MBOAT2 to be reduced 24hrs following the completion of a marathon. These authors conclude by offering circRNA MBOAT2 to be a promising biomarker of exercise status in humans [138]. Although this remains to be confirmed, circRNA research does offer plausible lines of enquiry and biomarker potential. However, many fundamental and systematic questions need to be addressed before such claims are realised.

With these aspects in mind, the present study set out to (i) compare peripheral blood circRNA expression profile between sedentary, and aerobically fit in addition to physically strong athletic male phenotypes, and to further (ii) summarise peripheral blood circRNA expression response to four weeks of supervised mixed exercise training in sedentary males compared with aerobic and strength athletes. We hypothesised that peripheral blood circRNA

expression would discriminate between SEDENTARY, AEROBIC and STRENGHT phenotypes. We further hypothesised that peripheral blood circRNA would be different in SEDENTARY undergoing four weeks of mixed exercise training, compared with AEROBIC and SEDENTARY athletes.

6.3 METHODS

6.3.1 Participants

Participants consisted of male volunteers (*n*=71*)* aged 18 - 45 years who provided written informed consent to participate in the study which was approved by Federation University, Australia research ethics committee. Prior to formal enrolment to the study, phenotype characterisation was confirmed according to predefined criteria, resulting in three distinct arms consistent with SEDENTARY (*n*=31), AEROBIC (*n*=20), and STRENGTH (*n*=20) phenotypes. Full details of participant characterisation are detailed in Table 5.1. A detailed list of measurements taken in the study is depicted in **Section 2.1**. A complete explanation on the screening and recruitment of participants can be found in **Section 2.2** and **Section 2.3.**

6.3.2 Study design

To compare expression of circRNA in peripheral blood of divergent exercise phenotypes and to summarise peripheral blood circRNA expression to exercise, we conducted a STROBE compliant observational study [112] with two distinct observational points, (i) comparing phenotype and circRNA expression between SEDENTARY, AEROBIC, and STRENGHT groups at study enrolment and (ii) comparing phenotype and circRNA expression adaptation to four weeks of supervised mixed exercise training in SEDENTARY, compared with positive control groups consisting AEROBIC and STRENGHT athletes.

6.3.3 Body composition

Body mass was obtained using a balanced weighing scale, with participants in minimal clothing (Seca, Cardiokinetics, Salford, UK) and height was measured with a stadiometer (Seca, Cardiokinetics, Salford, UK). Weighing scales were calibrated prior to each "weigh in" with a 5 kg free mass. Procedures are detailed in **Section 2.4**.

6.3.4 Blood collection

Following 15 min seated rest, whole blood was sampled from the non-dominant arm by standard venepuncture into sterile Tempus™ (Life Technologies, Au) vacutainer tubes. Samples were immediately stored at -80°C until subsequent analysis. Detail on the process is provided in **Section 2.5.**

6.3.5 Determination of muscular strength

Muscular strength was assessed using one repetition maximum (1RM) technique following Australian Institute of Sports guidelines [36]. Briefly, participants performed a bench press, a deadlift, and squats exercises, starting with a warm-up and progressively incrementing weight load until reaching 1RM weight. Full description on the protocol is provided in **Section 2.6**.

6.3.6 Determination of maximal oxygen consumption ($\dot{V}O_{2max}$)

Prior to graded exercise testing, metabolic cart (Moxus Modular $\dot{V}O_2$ System, AEI technologies, IL, USA;) was calibrated with medically certified calibration gases (4.05% CO_2 and 15.6% O_2, 0.3% CO_2 and 20.9% O_2) and volumes were determined according to the manufacturers guidelines. Maximal oxygen consumption $\dot{V}O_{2max}$ was determined in compliance with ACSM guidelines [111] where participants completed a ramped (beginning at 100 W for SEDENTARY AND 120W for AEROBIC and STRENGTH, and increasing by 20 W.min^{-1}) exercise protocol to voluntary exhaustion using a electromagnetically braked

cycle ergometer (Velotron® Pro, Seattle, WA, USA) and concomitant open circuit spirometry to determine maximal oxygen consumption, which is described in detail in **Section 2.6**.

6.3.7 RNA extraction

RNA was extracted from Tempus Blood RNA Tubes (Life Technologies™) using MagMAX for Stabilized Blood Tubes RNA Isolation Kit™ (Thermo Fisher Scientific™) following standardised protocol according to manufacturer instructions [37]. A more detailed explanation of the process can be found in **Section 2.9**.

6.3.8 Library preparation and RNA sequencing

Library preparation and RNA sequencing were conducted following a standardised protocol of TruSeq Stranded Total RNA Sample Preparation Guide (Illumina®) [38] using an Illumina NovaSeq platform (Illumina®) and detailed in **Section 2.9**.

6.3.9 Mixed exercise training (MET)

Participants allocated to SEDENTARY performed 4 weeks of MET consisting of a combination of resistance and aerobic exercise with continuous heart rate monitoring. Participants attended 3 sessions per week, alternating 2 aerobic and 1 resistance sessions one week, with 1 aerobic and 2 resistance the following week. All exercise sessions were supervised by a qualified personal trainer or Exercise Physiologist (ESSA). More details on the exercise program can be found in **Section 2.8.1**.

6.3.10 CircRNA microarray expression profiling

Following RNA integrity analysis, complete cohort assays for SEDENTARY (n=16) RNA samples were available at enrolment, and SEDENTARY STRENGTH (n=14) and SEDENTARY AEROBIC (n=14) following MET. Following subsequent specific exercise SEDENTARY STRENGTH (n=14) and SEDENTARY AEROBIC (n=10). For STRENGTH

and AEROBIC we selected the samples from the top 10 participants for each group at 2 time points, that demonstrated more consistency in their respective physiological characteristics of interest (Absolute muscular strength for STRENGTH and absolute $\dot{V}O_{2max}$ for AEROBIC). When comparing SEDENTARY, SEDENTARY AEROBIC, and SEDENTARY STRENGTH with the athlete groups (STRENGTH and AEROBIC), average gene expression of the 2 time points for the athlete groups was used. This resulted in 20 RNA samples per athlete group, 10 at each time point, separated 4 weeks. Taking all together, a total of 104 samples were sequenced and included in transcriptomic analysis.

6.3.11 Statistical analysis

Sample power was estimated for an effect size: 0.8 using a single-tailed within-group comparisons with α=0.05 and β=0.95, using minimal expected change in $\dot{V}O_{2max}$ as criterion. This resulting in a required sample of (n=17) in each group. Continuous data were analysed using SPSS version 25.0 (SPSS Inc., Chicago, IL, USA). Distribution of normality and homogeneity of variance were tested by analysing residuals. Linear mixed modelling was employed to test continuous secondary outcomes (i.e. training effects) with pairwise comparisons of within and between group simple effects in coalition with Bonferroni correction for multiple comparisons. An alpha value of $p \leq 0.05$ was used to indicate statistical significance. Data are presented as mean ± standard deviation (SD) or confidence intervals (CI), where appropriate. CircRNAs were predicted based on the number of junction reads identified using the CircRNA Identifier (CIRI) tool [139]. Differential-expression analysis of two conditions/groups was performed using the DESeq R package, employing negative binomial modelling techniques, where subsequent P-values were adjusted employing the Benjamini–Hochberg approach for controlling the false-discovery rate (FDR). CircRNAs with a FDR< 0.05 were deemed to be significantly differentially expressed, and a log2 (fold-change) >2 : < 0.5 was set to determine up-regulation and down-regulation,

respectively. Corresponding description of statistical procedures are located in **Section 2.11**., **Section 2.12**., and **Section 2.14**, respectively.

6.4 RESULTS

Healthy sedentary males (*n*= 79) were assessed for eligibility. Participants (*n*= 8) were excluded for reasons of; genetic disorder (*n*=1), not meeting athletic performance criteria for respective AEROBIC or STRENGTH groups (*n*= 4), not meeting the eligibility criteria for SEDENTARY (*n*= 1), and not meeting the age inclusion criteria (*n*= 2*)*. Finally, (*n*= 71) participants were enrolled in the study and allocated to one of three arms; SEDENTARY (*n*=31), AEROBIC (*n*= 20), and STRENGTH (*n*= 20). Study compliance was (*n*= 68/71). SEDENTARY (*n*= 31) completed 4 weeks of mixed exercise training. AEROBIC (*n*= 20) and STRENGTH (*n*= 20) completed both enrolment and follow-up assessment epochs. Diagram depicting flow of participants through the study is found in **Figure 6-1**.

6.4.1 Athletic Phenotype Characterisation

AEROBIC demonstrated significantly higher $\dot{V}O_{2max}$ compared with SEDENTARY and STRENGTH at both at study enrolment and during follow-up. Similarly, STRENGHT demonstrated significantly higher relative strength compared with SEDENTARY and AEROBIC at enrolment and during follow-up. Notably, relative strength was comparable between AEROBIC and SEDENTARY at enrolment to the study. Compared with athletic phenotypes, SEDENTARY achieved significant improvements in both relative strength and $\dot{V}O_{2max}$ following 4 weeks MET. Participant characteristics at enrolment and during follow-up, including statistical comparisons is found in **Table 6-2**.

6.4.2 Athletic circRNA Expression Profile Characterisation

Compared with SEDENTARY, AEROBIC presented with *n*= 2558 unique differentially expressed circRNAs [*n*= 21 up-regulated, FC≥2; *n*= 2537 down-regulated, FC≤0.5; (FDR<0.05)] at enrolment to the study. Compared with SEDENTARY, STRENGTH presented with *n*=619 unique differentially expressed circRNAs [*n*= 1 up-regulated, FC≥2; *n*= 618 down-regulated, FC≤0.5; (FDR<0.05)] at enrolment to the study.

Compared with athletic phenotypes, *n*= 1 circRNA was differentially expressed [chr19__18537601__18538436___FKBP8, (FC≥2; FDR<0.05)] in SEDENTARY following MET. Compared with SEDENTARY, AEROBIC presented with *n*= 3349 differentially expressed circRNAs [*n*= 9 up-regulated, FC≥2; *n*= 3340 down-regulated, FC≤0.5; (FDR<0.05)] at follow-up. Compared with SEDENTARY, STRENGTH presented with *n*= 1355 unique differentially expressed circRNAs [*n*= 0 up-regulated, FC≥2; *n*= 1355 down-regulated, FC≤0.5; (FDR<0.05)] at follow-up. Summary of differentially expressed circRNA at enrolment and during follow-up are found in **Appendices J-N.**

6.5 DISCUSSION

At enrolment to the study, aerobic athletes presented with *n*= 2558 (*n*= 21 upregulated) and strength athletes presenting with *n*= 619 (*n*= 1 upregulated) differentially expressed circRNAs compared with sedentary participants. Following four weeks of subsequent MET, a single circRNA became differentially expressed in sedentary participants (*n*= 1 upregulated), with a concomitant *n*= 3349 (*n*= 9 upregulated) and *n*= 1355 (*n*= 0 upregulated) differentially expressed circRNAs compared with aerobic and strength phenotypes, respectively. These data provide preliminary evidence that circRNAs may differentiate athletic male phenotypes, yet conversely, that four weeks of MET falls short of substantiative characterisation of

exercise-circRNA adaptation amongst exercise-naïve, compared with divergent athletic counterparts.

During the past two decades, what once termed “junk DNA”, has seen a gradual acceptance that non-protein coding RNAs are integral components of gene regulatory networks in a broad range of biological processes [2, 3, 140]. Despite a lack of comparative studies in exercise-circRNA research, it is possible to borrow from the broader non-coding RNA literature, which identifies varying circRNA yield in human tissues and cell types, including systemic blood. For instance, circRNAs are evolutionarily conserved, and highly abundant and in human brain tissue [135, 141] and it has been shown it is also similarly abundant in peripheral blood as confirmed in this study.

Unlike linear RNAs, circRNAs have a uniquely circular covalently bonded structure which offers a high degree of tolerance to exonucleases. Furthermore, circRNAs demonstrate greater conservation and relative abundance compared with linear non-coding RNA [135], and it is for these reasons that circRNAs may offer value as candidate biomarkers to identify individualised exercise response. Indeed, the broad rationale underlying the emerging interest in genomic factors (e.g., DNA sequence variants) important for the responses of various phenotypes to exercise, is that we may one day be able to ‘personalise’ exercise prescription at the individual level to optimise the adaptive response to tailored exercise prescription. In coalition with these factors, the relative ease of access to peripheral blood, continues to support ongoing rationale to investigate cirRNAs as an avenue to support exercise genomics. Here, we identified athletic (aerobically fit and physically strong vs exercise-naïve) male phenotypes to present with an independent pool of differentially expressed circRNAs in peripheral blood of divergent athletic cohorts, as observed in gene expression studies of other biological tissues. A four-fold yield of differentially expressed circRNAs was found in AEROBIC vs SEDENTARY (n= 2558) compared with STRENGTH vs SEDENTARY,

which may indicate greater regulation of circRNA-related gene expression networks as a consequence of aerobic metabolism compared with resistance exercise. Conversely, the presence of *n*= 619 differentially expressed circRNAs in strength athletes compared with sedentary participants is hypothetically supported by work in human and animal models that report high-yield enrichment of circRNAs in neuronal tissues and have been suggested as playing important roles in synaptic activity and neuronal function [142], and may be consistent with neuromuscular activity during resistance exercise. However, the lack of adaptive role of circRNA from short term mixed exercise training should not be understated due to the exercise-naïve cohort accumulating a mere single differentially expressed circRNA following MET. It should be further noted that the present study identified a preponderance for differentially expressed cirRNAs to be downregulated in both aerobic (~99.2%) and strength (~99.8%) phenotypes amongst a substantial yield of differentially expressed peripheral blood circRNAs compared with their sedentary counterparts. Whilst this phenomenon does not confirm a lack of regulatory importance, and indeed, may signify activation of negative feedback loop mechanisms, it is prudent to learn from our "junk DNA' scientific predecessors which precludes speculation on circRNA regulatory mechanisms in the absence of a sound knowledgebase.

In the present study, chr19__18537601__18538436___FKBP8 was the single circRNA to reach differential expression following MET in sedentary participants, and although worthy of note, is likely confounded by the Diaconis & Mosteller Law of Truly Large numbers [143], when employing a conservative statistical approach. In short, this circRNA falls within the sequence network of the *FKBP8* gene and interacts with 3 different micro RNAs (*hsa-miR-127-5p, hsa-miR-122-5p, hsa-miR-17-3p*) and may be found using circAtlas 2.0 (http://circatlas.biols.ac.cn/). However, this finding does offer some important considerations. Firstly, it is possible that 4 weeks of MET was an insufficient threshold to

initiate circRNA adaptive biological processes amongst the sedentary cohort, albeit phenotypic adaptation towards aerobic fitness and muscular strength was achieved in this same group. Second, employing a minimum of ≥2; ≤0.5 fold-change criterion to determine direction of circRNA expression may have been overly conservative. However, the same conservative threshold achieved high yield differentially expressed circRNA in comparison with athletic phenotypes. Thirdly, it must be considered that differentially expressed circRNAs identified between phenotypes at enrolment to the study may be a consequence of chance alone and these findings bear no substantive relevance in circRNA differentiation at a phenotypic nor adaptive level. If true, this is more than semantics as the great majority of exercise genomics research employ either cross-sectional design or observe acute exercise phenomenon (ie. before and after a single bout of exercise). Finally, observed outcomes could be a consequence of poor methodological design and execution. However, this study enrolled divergent exercise phenotypes, enrolled *n*=71 participants (*n*=31 sedentary), to a STROBE compliant observational study which maintained high compliance during supervised exercise sessions, and where sedentary participants achieved significant improvements to athletic performance, used well established laboratory techniques for physiological measurement of performance, used dual timepoint comparison of each study arm, employed default high-stringency mode merged counts matrix for each back-spliced junction location and sample in CIRI (Ver 2.0.6) [139] and gold-standard throughput bioinformatic analysis. Importantly, methodological procedures were identical at enrolment and follow-up, precluding methodological aspects as the dominant factor towards sedentary achieving a single differentially expressed circRNA following MET. Although it is likely that a combination of these factors each played their respective part, we encourage that future research be considerate in compliance with the Bradford-Hill criteria for cause-and-effect relationships

before proposing causal inference when interpreting study findings in similar genomics research.

6.6 CONCLUSION

The main findings from this study identify a potential role for systemic circRNAs to determine phenotype in well trained athletes compared with exercise-naïve counterparts. However, four weeks of mixed exercise training abrogated this hypothesis. Progress in this field will only be achieved by the coalition of revisiting first-principles, improving experimental research design and compliance with best practice guidelines.

6.7 REFERENCES

1. Heilig R, Eckenberg R, Petit J, Fonknechten N, Silva C, Cattolico L, et al. International Human Genome Sequencing Consortium. Nature 431, 931-945. Nature. 2004;431(7011):931-45. Epub 2004/10/22. doi: 10.1038/nature03001. PubMed PMID: 15496913.
2. Cabili MN, Trapnell C, Goff L, Koziol M, Tazon-Vega B, Regev A, et al. Integrative annotation of human large intergenic noncoding RNAs reveals global properties and specific subclasses. Genes & development. 2011;25(18):1915-27. Epub 2011/09/06. doi: 10.1101/gad.17446611. PubMed PMID: 21890647; PubMed Central PMCID: PMCPMC3185964.
3. Derrien T, Johnson R, Bussotti G, Tanzer A, Djebali S, Tilgner H, et al. The GENCODE v7 catalog of human long noncoding RNAs: analysis of their gene structure, evolution, and expression. Genome research. 2012;22(9):1775-89. Epub 2012/09/08. doi: 10.1101/gr.132159.111. PubMed PMID: 22955988; PubMed Central PMCID: PMCPMC3431493.
4. Bartel DP. MicroRNAs: genomics, biogenesis, mechanism, and function. Cell. 2004;116(2):281-97. Epub 2004/01/28. PubMed PMID: 14744438.
5. Sood P, Krek A, Zavolan M, Macino G, Rajewsky N. Cell-type-specific signatures of microRNAs on target mRNA expression. Proceedings of the National Academy of Sciences of the United States of America. 2006;103(8):2746-51. Epub 2006/02/16. doi: 10.1073/pnas.0511045103. PubMed PMID: 16477010; PubMed Central PMCID: PMCPMC1413820.
6. Tijsen AJ, Creemers EE, Moerland PD, de Windt LJ, van der Wal AC, Kok WE, et al. MiR423-5p as a circulating biomarker for heart failure. Circulation research. 2010;106(6):1035-9. Epub 2010/02/27. doi: 10.1161/circresaha.110.218297. PubMed PMID: 20185794.
7. Fichtlscherer S, De Rosa S, Fox H, Schwietz T, Fischer A, Liebetrau C, et al. Circulating microRNAs in patients with coronary artery disease. Circulation research. 2010;107(5):677-84. Epub 2010/07/03. doi: 10.1161/circresaha.109.215566. PubMed PMID: 20595655.
8. Long G, Wang F, Duan Q, Chen F, Yang S, Gong W, et al. Human circulating microRNA-1 and microRNA-126 as potential novel indicators for acute myocardial infarction. International journal of biological sciences. 2012;8(6):811-8. Epub 2012/06/22. doi: 10.7150/ijbs.4439. PubMed PMID: 22719221; PubMed Central PMCID: PMCPMC3372885.
9. Niu ZY, Sun SY, Li GX. The polymorphism at the miRNA binding site of GOLGA(7) is associated with the Non-Hodgkin's lymphoma cancer risk. Int J Clin Exp Pathol. 2017;10(3):3735-8. PubMed PMID: WOS:000399083300149.
10. Li Z, Niu YJ. Association between lncRNA H19 (rs217727, rs2735971 and rs3024270) polymorphisms and the risk of bladder cancer in Chinese population. Minerva Urologica E Nefrologica. 2019;71(2):161-7. Epub 2018/03/30. doi: 10.23736/s0393-2249.18.03004-7. PubMed PMID: WOS:000469464100008.
11. Memczak S, Jens M, Elefsinioti A, Torti F, Krueger J, Rybak A, et al. Circular RNAs are a large class of animal RNAs with regulatory potency. Nature. 2013;495(7441):333-8. Epub 2013/03/01. doi: 10.1038/nature11928. PubMed PMID: 23446348.
12. Booth FW, Roberts CK, Laye MJ. Lack of exercise is a major cause of chronic diseases. Comprehensive Physiology. 2012;2(2):1143-211. Epub 2012/04/01. doi: 10.1002/cphy.c110025. PubMed PMID: 23798298; PubMed Central PMCID: PMCPMC4241367.

13. Lear SA, Hu W, Rangarajan S, Gasevic D, Leong D, Iqbal R, et al. The effect of physical activity on mortality and cardiovascular disease in 130 000 people from 17 high-income, middle-income, and low-income countries: the PURE study. Lancet (London, England). 2017;390(10113):2643-54. Epub 2017/09/26. doi: 10.1016/s0140-6736(17)31634-3. PubMed PMID: 28943267.
14. Thompson PD, Eijsvogels TH. New physical activity guidelines: A call to activity for clinicians and patients. Jama. 2018. Epub 2018/11/13. doi: 10.1001/jama.2018.16070. PubMed PMID: 30418469.
15. Blair SN, Kampert JB, Kohl HW, 3rd, Barlow CE, Macera CA, Paffenbarger RS, Jr., et al. Influences of cardiorespiratory fitness and other precursors on cardiovascular disease and all-cause mortality in men and women. Jama. 1996;276(3):205-10. Epub 1996/07/17. PubMed PMID: 8667564.
16. Blair SN, Kohl HW, 3rd, Paffenbarger RS, Jr., Clark DG, Cooper KH, Gibbons LW. Physical fitness and all-cause mortality. A prospective study of healthy men and women. Jama. 1989;262(17):2395-401. Epub 1989/11/03. PubMed PMID: 2795824.
17. Gulati M, Black HR, Shaw LJ, Arnsdorf MF, Merz CN, Lauer MS, et al. The prognostic value of a nomogram for exercise capacity in women. The New England journal of medicine. 2005;353(5):468-75. Epub 2005/08/05. doi: 10.1056/NEJMoa044154. PubMed PMID: 16079370.
18. Kokkinos P, Myers J, Kokkinos JP, Pittaras A, Narayan P, Manolis A, et al. Exercise capacity and mortality in black and white men. Circulation. 2008;117(5):614-22. Epub 2008/01/24. doi: 10.1161/circulationaha.107.734764. PubMed PMID: 18212278.
19. Mora S, Redberg RF, Cui Y, Whiteman MK, Flaws JA, Sharrett AR, et al. Ability of exercise testing to predict cardiovascular and all-cause death in asymptomatic women: a 20-year follow-up of the lipid research clinics prevalence study. Jama. 2003;290(12):1600-7. Epub 2003/09/25. doi: 10.1001/jama.290.12.1600. PubMed PMID: 14506119.
20. Braith RW, Stewart KJ. Resistance exercise training: its role in the prevention of cardiovascular disease. Circulation. 2006;113(22):2642-50. Epub 2006/06/07. doi: 10.1161/CIRCULATIONAHA.105.584060. PubMed PMID: 16754812.
21. Egan B, Zierath J. Exercise Metabolism and the Molecular Regulation of Skeletal Muscle Adaptation. Cell metabolism. 2013;17(2):162-84. Epub 2013/02/12. doi: 10.1016/j.cmet.2012.12.012. PubMed PMID: 23395166.
22. Hughes DC, Ellefsen S, Baar K. Adaptations to Endurance and Strength Training. Cold Spring Harbor perspectives in medicine. 2018;8(6):a029769. Epub 2017/05/12. doi: 10.1101/cshperspect.a029769. PubMed PMID: 28490537; PubMed Central PMCID: PMCPMC5983157.
23. Laine S, Högel H, Ishizu T, Toivanen J, Yli-Karjanmaa M, Grönroos TJ, et al. Effects of Different Exercise Training Protocols on Gene Expression of Rac1 and PAK1 in Healthy Rat Fast- and Slow-Type Muscles. Frontiers in physiology. 2020;11(1448):584661. Epub 2020/12/18. doi: 10.3389/fphys.2020.584661. PubMed PMID: 33329033; PubMed Central PMCID: PMCPMC7711069.
24. Pillon NJ, Gabriel BM, Dollet L, Smith JAB, Sardón Puig L, Botella J, et al. Transcriptomic profiling of skeletal muscle adaptations to exercise and inactivity. Nature communications. 2020;11(1):470. Epub 2020/01/26. doi: 10.1038/s41467-019-13869-w. PubMed PMID: 31980607; PubMed Central PMCID: PMCPMC6981202.
25. Olioso D, Dauriz M, Bacchi E, Negri C, Santi L, Bonora E, et al. Effects of Aerobic and Resistance Training on Circulating Micro-RNA Expression Profile in Subjects With Type 2 Diabetes. J Clin Endocrinol Metab. 2019;104(4):1119-30. Epub 2018/11/18. doi: 10.1210/jc.2018-01820. PubMed PMID: WOS:000469813500017.

26. O'Neill DS, Zheng D, Anderson WK, Dohm GL, Houmard JA. Effect of endurance exercise on myosin heavy chain gene regulation in human skeletal muscle. The American journal of physiology. 1999;276(2):R414-9. Epub 1999/02/10. doi: 10.1152/ajpregu.1999.276.2.R414. PubMed PMID: 9950919.
27. Wadley GD, Tunstall RJ, Sanigorski A, Collier GR, Hargreaves M, Cameron-Smith D. Differential effects of exercise on insulin-signaling gene expression in human skeletal muscle. Journal of applied physiology (Bethesda, Md : 1985). 2001;90(2):436-40. Epub 2001/02/13. doi: 10.1152/jappl.2001.90.2.436. PubMed PMID: 11160039.
28. Welle S, Bhatt K, Thornton CA. Stimulation of myofibrillar synthesis by exercise is mediated by more efficient translation of mRNA. Journal of applied physiology (Bethesda, Md : 1985). 1999;86(4):1220-5. Epub 1999/04/08. doi: 10.1152/jappl.1999.86.4.1220. PubMed PMID: 10194206.
29. Bamman MM, Roberts BM, Adams GR. Molecular Regulation of Exercise-Induced Muscle Fiber Hypertrophy. Cold Spring Harbor perspectives in medicine. 2018;8(6). Epub 2017/05/12. doi: 10.1101/cshperspect.a029751. PubMed PMID: 28490543; PubMed Central PMCID: PMCPMC5983156.
30. Williams RS, Neufer PD. Regulation of Gene Expression in Skeletal Muscle by Contractile Activity. Comprehensive Physiology. Sumplement 29: Handbook of Physiology1996. p. 1124-50.
31. Damas F, Ugrinowitsch C, Libardi CA, Jannig PR, Hector AJ, McGlory C, et al. Resistance training in young men induces muscle transcriptome-wide changes associated with muscle structure and metabolism refining the response to exercise-induced stress. European journal of applied physiology. 2018. Epub 2018/09/10. doi: 10.1007/s00421-018-3984-y. PubMed PMID: 30196447.
32. Timmons JA, Knudsen S, Rankinen T, Koch LG, Sarzynski M, Jensen T, et al. Using molecular classification to predict gains in maximal aerobic capacity following endurance exercise training in humans. Journal of applied physiology (Bethesda, Md : 1985). 2010;108(6):1487-96. Epub 2010/02/06. doi: 10.1152/japplphysiol.01295.2009. PubMed PMID: 20133430; PubMed Central PMCID: PMCPMC2886694.
33. Liew C-C, Ma J, Tang H-C, Zheng R, Dempsey AA. The peripheral blood transcriptome dynamically reflects system wide biology: a potential diagnostic tool. The Journal of Laboratory and Clinical Medicine. 2006;147(3):126-32. doi: 10.1016/j.lab.2005.10.005.
34. Zeibig J, Karlic H, Lohninger A, Damsgaard R, Smekal G. Do blood cells mimic gene expression profile alterations known to occur in muscular adaptation to endurance training? European journal of applied physiology. 2005;95(1):96-104. Epub 2005/04/09. doi: 10.1007/s00421-005-1334-3. PubMed PMID: 15815935.
35. Broadbent J, Sampson D, Sabapathy S, Haseler LJ, Wagner KH, Bulmer AC, et al. Gene networks in skeletal muscle following endurance exercise are coexpressed in blood neutrophils and linked with blood inflammation markers. Journal of applied physiology (Bethesda, Md : 1985). 2017;122(4):752-66. Epub 2017/01/21. doi: 10.1152/japplphysiol.00114.2016. PubMed PMID: 28104750.
36. Tanner RK, Gore CJ. Physiological tests for elite athletes. Champaign, IL : Human Kinetics. 2013.
37. Thermo Fisher Scientific. MagMAX for Stabilized Blood Tubes RNA Isolation Kit. Available from: https://bit.ly/3jIv8V4.
38. Illumina. TruSeq Stranded Total RNA Reference Guide Document # 1000000040499 v00 2017. Available from: https://bit.ly/3w6ZjYV.
39. Kodama S, Saito K, Tanaka S, Maki M, Yachi Y, Asumi M, et al. Cardiorespiratory fitness as a quantitative predictor of all-cause mortality and cardiovascular events in healthy

men and women: a meta-analysis. Jama. 2009;301(19):2024-35. Epub 2009/05/21. doi: 10.1001/jama.2009.681. PubMed PMID: 19454641.
40. Thompson D, Markovitch D, Betts JA, Mazzatti D, Turner J, Tyrrell RM. Time course of changes in inflammatory markers during a 6-mo exercise intervention in sedentary middle-aged men: a randomized-controlled trial. Journal of Applied Physiology. 2010;108(4):769-79. doi: 10.1152/japplphysiol.00822.2009. PubMed PMID: WOS:000276324200003.
41. Iyalomhe O, Chen YX, Allard J, Ntekim O, Johnson S, Bond V, et al. A standardized randomized 6-month aerobic exercise-training down-regulated pro-inflammatory genes, but up-regulated anti-inflammatory, neuron survival and axon growth-related genes. Experimental gerontology. 2015;69:159-69. Epub 2015/05/20. doi: 10.1016/j.exger.2015.05.005. PubMed PMID: WOS:000360320200021; PubMed Central PMCID: PMCPMC4553116.
42. Lee SH, Hong HR, Han TK, Kang HS. Aerobic training increases the expression of adiponectin receptor genes in the peripheral blood mononuclear cells of young men. Biology of sport. 2015;32(3):181-6. Epub 2015/10/02. doi: 10.5604/20831862.1150298. PubMed PMID: 26424919; PubMed Central PMCID: PMCPMC4577554.
43. Schenk A, Pulverer W, Koliamitra C, Bauer CJ, Ilic S, Heer R, et al. Acute Exercise Increases the Expression of KIR2DS4 by Promoter Demethylation in NK Cells. International journal of sports medicine. 2019;40(1):62-70. Epub 2018/12/07. doi: 10.1055/a-0741-7001. PubMed PMID: WOS:000454222500009.
44. Butcher LR, Thomas A, Backx K, Roberts A, Webb R, Morris K. Low-intensity exercise exerts beneficial effects on plasma lipids via PPARgamma. Medicine & Science in Sports & Exercise. 2008;40(7):1263-70. Epub 2008/06/27. doi: 10.1249/MSS.0b013e31816c091d. PubMed PMID: 105658595. Language: English. Entry Date: 20081003. Revision Date: 20150711. Publication Type: Journal Article.
45. Sen S, Witkowski S, Lagoy A, Islam AM. A Six-Week Home Exercise Program Improves Endothelial Function and CD34(+) Circulating Progenitor Cells in Patients With Pre-Diabetes. Journal of Endocrinology and Metabolism. 2015;5(1-2):163-71. doi: 10.14740/jem273w. PubMed PMID: WOS:000360177700002.
46. Henagan TM, Phillips MD, Cheek DJ, Kirk KM, Barbee JJ, Stewart LK. The melanocortin 3 receptor: a novel mediator of exercise-induced inflammation reduction in postmenopausal women? J Aging Res. 2011;2011:512593. Epub 2011/01/22. doi: 10.4061/2011/512593. PubMed PMID: 21253483; PubMed Central PMCID: PMCPMC3022199.
47. Macêdo Santiago LÂ, Neto LGL, Borges Pereira G, Leite RD, Mostarda CT, de Oliveira Brito Monzani J, et al. Effects of Resistance Training on Immunoinflammatory Response, TNF-Alpha Gene Expression, and Body Composition in Elderly Women. Journal of Aging Research. 2018;2018:1-10. Epub 2018/12/05. doi: 10.1155/2018/1467025. PubMed PMID: 132650858. Language: English. Entry Date: 20181030. Revision Date: 20181030. Publication Type: Article. Journal Subset: Biomedical; PubMed Central PMCID: PMCPMC6230406.
48. Rodriguez-Miguelez P, Fernandez-Gonzalo R, Almar M, Mejias Y, Rivas A, de Paz JA, et al. Role of Toll-like receptor 2 and 4 signaling pathways on the inflammatory response to resistance training in elderly subjects. Age. 2014;36(6):9734. Epub 2014/11/28. doi: 10.1007/s11357-014-9734-0. PubMed PMID: WOS:000346770900016; PubMed Central PMCID: PMCPMC4245402.
49. Streese L, Khan AW, Deiseroth A, Hussain S, Suades R, Tiaden A, et al. High-intensity interval training modulates retinal microvascular phenotype and DNA methylation of p66Shc gene: a randomized controlled trial (EXAMIN AGE). Eur Heart J.

2020;41(15):1514-9. Epub 2019/07/20. doi: 10.1093/eurheartj/ehz196. PubMed PMID: 31323685.
50. O'Neill DS, Zheng D, Anderson WK, Dohm GL, Houmard JA. Effect of endurance exercise on myosin heavy chain gene regulation in human skeletal muscle. American Journal of Physiology-Regulatory, Integrative and Comparative Physiology. 1999;276(2):R414-R9. doi: 10.1152/ajpregu.1999.276.2.R414. PubMed PMID: 9950919.
51. Malm C, Nyberg P, Engstrom M, Sjodin B, Lenkei R, Ekblom B, et al. Immunological changes in human skeletal muscle and blood after eccentric exercise and multiple biopsies. The Journal of physiology. 2000;529 Pt 1(Pt 1):243-62. Epub 2000/11/18. doi: 10.1111/j.1469-7793.2000.00243.x. PubMed PMID: 11080266; PubMed Central PMCID: PMCPMC2270185.
52. Gjevestad G, Holven K, Ulven S. Effects of Exercise on Gene Expression of Inflammatory Markers in Human Peripheral Blood Cells: A Systematic Review. Current Cardiovascular Risk Reports. 2015;9(7):1-17. doi: 10.1007/s12170-015-0463-4.
53. Amar D, Lindholm ME, Norrbom J, Wheeler MT, Rivas MA, Ashley EA. Differential response trajectories to acute exercise in blood and muscle. bioRxiv. 2019:863100. doi: 10.1101/863100.
54. Moher D, Liberati A, Tetzlaff J, Altman DG, The PG. Preferred Reporting Items for Systematic Reviews and Meta-Analyses: The PRISMA Statement. PLOS Medicine. 2009;6(7):e1000097. doi: 10.1371/journal.pmed.1000097.
55. Higgins JPT, Altman DG, Gøtzsche PC, Jüni P, Moher D, Oxman AD, et al. The Cochrane Collaboration's tool for assessing risk of bias in randomised trials. BMJ. 2011;343:d5928. Epub 2011/10/20. doi: 10.1136/bmj.d5928. PubMed PMID: 22008217; PubMed Central PMCID: PMCPMC3196245.
56. Valentine JC, Pigott TD, Rothstein HR. How Many Studies Do You Need?: A Primer on Statistical Power for Meta-Analysis. Journal of Educational and Behavioral Statistics. 2010;35(2):215-47. doi: 10.3102/1076998609346961.
57. Chanock SJ, Manolio T, Boehnke M, Boerwinkle E, Hunter DJ, Thomas G, et al. Replicating genotype–phenotype associations. Nature. 2007;447(7145):655-60. Epub 2007/06/08. doi: 10.1038/447655a. PubMed PMID: 17554299.
58. Curtis Fennell KP, Ellen L Glickman. Effects of Supervised Training Compared to Unsupervised Training on Physical Activity, Muscular Endurance, and Cardiovascular Parameters. MOJ Orthop Rheumatol. 2016;5(4). doi: 10.15406/mojor.2016.05.00184.
59. Lacroix A, Kressig RW, Muehlbauer T, Gschwind YJ, Pfenninger B, Bruegger O, et al. Effects of a Supervised versus an Unsupervised Combined Balance and Strength Training Program on Balance and Muscle Power in Healthy Older Adults: A Randomized Controlled Trial. Gerontology. 2016;62(3):275-88. Epub 2015/12/10. doi: 10.1159/000442087. PubMed PMID: 26645282.
60. Black DS, Cole SW, Irwin MR, Breen E, St Cyr NM, Nazarian N, et al. Yogic meditation reverses NF-κB and IRF-related transcriptome dynamics in leukocytes of family dementia caregivers in a randomized controlled trial. Psychoneuroendocrinology. 2013;38(3):348-55. Epub 2012/07/17. doi: 10.1016/j.psyneuen.2012.06.011. PubMed PMID: 22795617; PubMed Central PMCID: PMCPMC3494746.
61. Hecksteden A, Faude O, Meyer T, Donath L. How to Construct, Conduct and Analyze an Exercise Training Study? Frontiers in physiology. 2018;9:1007-. Epub 2018/08/25. doi: 10.3389/fphys.2018.01007. PubMed PMID: 30140237; PubMed Central PMCID: PMCPMC6094975.
62. Schulz KF, Altman DG, Moher D. CONSORT 2010 Statement: Updated Guidelines for Reporting Parallel Group Randomized Trials. Ann Intern Med. 2010;152(11):726-32.

Epub 2010/03/26. doi: 10.7326/0003-4819-152-11-201006010-00232. PubMed PMID: 20335313.
63. Skubic V, Hilgendorf J. Anticipatory, exercise, and recovery heart rates of girls as affected by four running events. Journal of Applied Physiology. 1964;19(5):853-6. Epub 1964/09/01. doi: 10.1152/jappl.1964.19.5.853. PubMed PMID: 14207732.
64. Connolly PH, Caiozzo VJ, Zaldivar F, Nemet D, Larson J, Hung SP, et al. Effects of exercise on gene expression in human peripheral blood mononuclear cells. Journal of applied physiology (Bethesda, Md : 1985). 2004;97(4):1461-9. Epub 2004/06/15. doi: 10.1152/japplphysiol.00316.2004. PubMed PMID: 15194674.
65. Carlson LA, Tighe SW, Kenefick RW, Dragon J, Westcott NW, Leclair RJ. Changes in transcriptional output of human peripheral blood mononuclear cells following resistance exercise. European journal of applied physiology. 2011;111(12):2919-29. Epub 03/25. doi: 10.1007/s00421-011-1923-2. PubMed PMID: 21437602; PubMed Central PMCID: PMCPMC4358769.
66. Buttner P, Mosig S, Lechtermann A, Funke H, Mooren FC. Exercise affects the gene expression profiles of human white blood cells. Journal of applied physiology (Bethesda, Md : 1985). 2007;102(1):26-36. Epub 2006/09/23. doi: 10.1152/japplphysiol.00066.2006. PubMed PMID: 16990507.
67. Kawai T, Morita K, Masuda K, Nishida K, Sekiyama A, Teshima-Kondo S, et al. Physical exercise-associated gene expression signatures in peripheral blood. Clinical journal of sport medicine : official journal of the Canadian Academy of Sport Medicine. 2007;17(5):375-83. Epub 2007/09/18. doi: 10.1097/JSM.0b013e31814c3e4f. PubMed PMID: 17873550.
68. Creswell JD, Irwin MR, Burklund LJ, Lieberman MD, Arevalo JM, Ma J, et al. Mindfulness-Based Stress Reduction training reduces loneliness and pro-inflammatory gene expression in older adults: a small randomized controlled trial. Brain Behav Immun. 2012;26(7):1095-101. Epub 2012/07/24. doi: 10.1016/j.bbi.2012.07.006. PubMed PMID: 22820409; PubMed Central PMCID: PMCPMC3635809.
69. Whitney AR, Diehn M, Popper SJ, Alizadeh AA, Boldrick JC, Relman DA, et al. Individuality and variation in gene expression patterns in human blood. Proceedings of the National Academy of Sciences of the United States of America. 2003;100(4):1896-901. Epub 2003/02/13. doi: 10.1073/pnas.252784499. PubMed PMID: 12578971; PubMed Central PMCID: PMCPMC149930.
70. Liu D, Wang R, Grant AR, Zhang J, Gordon PM, Wei Y, et al. Immune adaptation to chronic intense exercise training: new microarray evidence. BMC Genomics. 2017;18(1):29. Epub 2017/01/07. doi: 10.1186/s12864-016-3388-5. PubMed PMID: 28056786; PubMed Central PMCID: PMCPMC5216585.
71. Bower JE, Irwin MR. Mind–body therapies and control of inflammatory biology: A descriptive review. Brain, Behavior, and Immunity. 2016;51:1-11. Epub 2015/06/28. doi: 10.1016/j.bbi.2015.06.012. PubMed PMID: 26116436; PubMed Central PMCID: PMCPMC4679419.
72. Buric I, Farias M, Jong J, Mee C, Brazil IA. What Is the Molecular Signature of Mind-Body Interventions? A Systematic Review of Gene Expression Changes Induced by Meditation and Related Practices. Frontiers in Immunology. 2017;8:670. Epub 2017/07/04. doi: 10.3389/fimmu.2017.00670. PubMed PMID: WOS:000403397000001; PubMed Central PMCID: PMCPMC5472657.
73. Mavridis D, Giannatsi M, Cipriani A, Salanti G. A primer on network meta-analysis with emphasis on mental health. Evidence-based mental health. 2015;18(2):40-6. Epub 2015/04/25. doi: 10.1136/eb-2015-102088. PubMed PMID: 25908686.

74. Schneider CA, Rasband WS, Eliceiri KW. NIH Image to ImageJ: 25 years of image analysis. Nature Methods. 2012;9(7):671-5. Epub 2012/08/30. doi: 10.1038/nmeth.2089. PubMed PMID: 22930834; PubMed Central PMCID: PMCPMC5554542.
75. Yang X, Lu X, Lombès M, Rha GB, Chi YI, Guerin TM, et al. The G(0)/G(1) switch gene 2 regulates adipose lipolysis through association with adipose triglyceride lipase. Cell metabolism. 2010;11(3):194-205. Epub 2010/03/04. doi: 10.1016/j.cmet.2010.02.003. PubMed PMID: 20197052; PubMed Central PMCID: PMCPMC3658843.
76. Linzmeier R, Michaelson D, Liu L, Ganz T. The structure of neutrophil defensin genes. FEBS letters. 1993;321(2-3):267-73. Epub 1993/04/26. doi: 10.1016/0014-5793(93)80122-b. PubMed PMID: 8477861.
77. Córdova C, Lopes-e-Silva JF, Pires AS, Souza VC, Brito CJ, Moraes CF, et al. Long-Term Resistance Training Is Associated with Reduced Circulating Levels of IL-6, IFN-Gamma and TNF-Alpha in Elderly Women. Neuroimmunomodulation. 2011;18(3):165-70. Epub 2011/02/12. doi: 10.1159/000323396. PubMed PMID: 21311202.
78. Palomo I, Herrera J, Cancino V, Alarcón M, Mujica V, Leiva E, et al. Physical activity reduces circulating TNF-alpha but not pro-thrombotic factors levels in patients with metabolic syndrome. Diabetes & Metabolic Syndrome: Clinical Research & Reviews. 2010;4(4):234-8. doi: https://doi.org/10.1016/j.dsx.2010.05.004.
79. Mosser DM, Zhang X. Interleukin-10: new perspectives on an old cytokine. Immunological reviews. 2008;226:205-18. Epub 2009/01/24. doi: 10.1111/j.1600-065X.2008.00706.x. PubMed PMID: 19161426; PubMed Central PMCID: PMCPMC2724982.
80. Yakeu G, Butcher L, Isa S, Webb R, Roberts AW, Thomas AW, et al. Low-intensity exercise enhances expression of markers of alternative activation in circulating leukocytes: roles of PPARgamma and Th2 cytokines. Atherosclerosis. 2010;212(2):668-73. Epub 2010/08/21. doi: 10.1016/j.atherosclerosis.2010.07.002

10.1016/j.atherosclerosis.2010.07.002. Epub 2010 Jul 16. PubMed PMID: 20723894.
81. Pedersen BK. Anti-inflammatory effects of exercise: role in diabetes and cardiovascular disease. Eur J Clin Invest. 2017;47(8):600-11. Epub 2017/07/20. doi: 10.1111/eci.12781. PubMed PMID: 28722106.
82. Cabral-Santos C, de Lima EA, Fernandes IMD, Pinto RZ, Rosa-Neto JC, Bishop NC, et al. Interleukin-10 responses from acute exercise in healthy subjects: A systematic review. Journal of Cellular Physiology. 2019;234(7):9956-65. Epub 2018/12/12. doi: 10.1002/jcp.27920. PubMed PMID: WOS:000462645700007.
83. Moura AMD, Lamego MK, Paes F, Rocha NBF, Simoes-Silva V, Rocha SA, et al. Comparison Among Aerobic Exercise and Other Types of Interventions to Treat Depression: A Systematic Review. Cns & Neurological Disorders-Drug Targets. 2015;14(9):1171-83. Epub 2015/11/12. doi: 10.2174/1871527315666151111120714. PubMed PMID: WOS:000365807400010.
84. Gallo-Villegas J, Aristizabal JC, Estrada M, Valbuena LH, Narvaez-Sanchez R, Osorio J, et al. Efficacy of high-intensity, low-volume interval training compared to continuous aerobic training on insulin resistance, skeletal muscle structure and function in adults with metabolic syndrome: study protocol for a randomized controlled clinical trial (Intraining-MET). Trials. 2018;19(1):1-. Epub 2018/02/28. doi: 10.1186/s13063-018-2541-7. PubMed PMID: 128200372. Language: English. Entry Date: In Process. Revision Date: 20190410. Publication Type: journal article. Journal Subset: Biomedical; PubMed Central PMCID: PMCPMC5828481.
85. Lundberg TR, Fernandez-Gonzalo R, Tesch PA, Rullman E, Gustafsson T. Aerobic exercise augments muscle transcriptome profile of resistance exercise. American journal of

physiology Regulatory, integrative and comparative physiology. 2016;310(11):R1279-87. Epub 2016/04/22. doi: 10.1152/ajpregu.00035.2016. PubMed PMID: 27101291; PubMed Central PMCID: PMCPMC4935502.
86. Kline GM, Porcari JP, Hintermeister R, Freedson PS, Ward A, McCarron RF, et al. Estimation of VO2max from a one-mile track walk, gender, age, and body weight. Medicine and science in sports and exercise. 1987;19(3):253-9. Epub 1987/06/01. PubMed PMID: 3600239.
87. Goldin PR, Gross JJ. Effects of mindfulness-based stress reduction (MBSR) on emotion regulation in social anxiety disorder. Emotion. 2010;10(1):83-91. doi: 10.1037/a0018441. PubMed PMID: 20141305.
88. Russell D, Peplau LA, Cutrona CE. The revised UCLA Loneliness Scale: concurrent and discriminant validity evidence. Journal of personality and social psychology. 1980;39(3):472-80. Epub 1980/09/01. doi: 10.1037//0022-3514.39.3.472. PubMed PMID: 7431205.
89. Hood DA, Uguccioni G, Vainshtein A, D'Souza D. Mechanisms of exercise-induced mitochondrial biogenesis in skeletal muscle: implications for health and disease. Comprehensive Physiology. 2011;1(3):1119-34. Epub 2011/07/01. doi: 10.1002/cphy.c100074. PubMed PMID: 23733637.
90. Guzzoni V, Ribeiro MBT, Lopes GN, de Cassia Marqueti R, de Andrade RV, Selistre-de-Araujo HS, et al. Effect of Resistance Training on Extracellular Matrix Adaptations in Skeletal Muscle of Older Rats. Frontiers in physiology. 2018;9:374. Epub 2018/04/27. doi: 10.3389/fphys.2018.00374. PubMed PMID: 29695977; PubMed Central PMCID: PMCPMC5904267.
91. Furrer R, Eisele PS, Schmidt A, Beer M, Handschin C. Paracrine cross-talk between skeletal muscle and macrophages in exercise by PGC-1α-controlled BNP. Scientific Reports. 2017;7(1):40789. Epub 2017/01/17. doi: 10.1038/srep40789. PubMed PMID: 28091624; PubMed Central PMCID: PMCPMC5238507.
92. Furrer R, Handschin C. Optimized Engagement of Macrophages and Satellite Cells in the Repair and Regeneration of Exercised Muscle. In: Spiegelman B, editor. Hormones, Metabolism and the Benefits of Exercise. Cham: Springer International Publishing; 2017. p. 57-66.
93. Wang L, Mascher H, Psilander N, Blomstrand E, Sahlin K. Resistance exercise enhances the molecular signaling of mitochondrial biogenesis induced by endurance exercise in human skeletal muscle. Journal of Applied Physiology. 2011;111(5):1335-44. Epub 2011/08/13. doi: 10.1152/japplphysiol.00086.2011. PubMed PMID: WOS:000297684500017.
94. Pilegaard H, Saltin B, Neufer PD. Exercise induces transient transcriptional activation of the PGC-1alpha gene in human skeletal muscle. The Journal of physiology. 2003;546(Pt 3):851-8. Epub 2003/02/04. doi: 10.1113/jphysiol.2002.034850. PubMed PMID: 12563009; PubMed Central PMCID: PMCPMC2342594.
95. Pedersen L, Hojman P. Muscle-to-organ cross talk mediated by myokines. Adipocyte. 2012;1(3):164-7. Epub 2013/05/24. doi: 10.4161/adip.20344. PubMed PMID: 23700527; PubMed Central PMCID: PMCPMC3609091.
96. Tidball JG, Villalta SA. Regulatory interactions between muscle and the immune system during muscle regeneration. American journal of physiology Regulatory, integrative and comparative physiology. 2010;298(5):R1173-87. Epub 2010/03/12. doi: 10.1152/ajpregu.00735.2009. PubMed PMID: 20219869; PubMed Central PMCID: PMCPMC2867520.

97. Tidball JG. Inflammatory processes in muscle injury and repair. American journal of physiology Regulatory, integrative and comparative physiology. 2005;288(2):R345-53. Epub 2005/01/08. doi: 10.1152/ajpregu.00454.2004. PubMed PMID: 15637171.
98. Holloszy JO. Biochemical adaptations in muscle. Effects of exercise on mitochondrial oxygen uptake and respiratory enzyme activity in skeletal muscle. The Journal of biological chemistry. 1967;242(9):2278-82. Epub 1967/05/10. PubMed PMID: 4290225.
99. Flynn MG, McFarlin BK, Markofski MM. The Anti-Inflammatory Actions of Exercise Training. Am J Lifestyle Med. 2007;1(3):220-35. Epub 2007/05/01. doi: 10.1177/1559827607300283. PubMed PMID: 25431545; PubMed Central PMCID: PMCPMC4243532.
100. Coyle EF, Coggan AR, Hopper MK, Walters TJ. Determinants of endurance in well-trained cyclists. Journal of applied physiology (Bethesda, Md : 1985). 1988;64(6):2622-30. Epub 1988/06/01. doi: 10.1152/jappl.1988.64.6.2622. PubMed PMID: 3403447.
101. Holloszy JO, Coyle EF. Adaptations of skeletal muscle to endurance exercise and their metabolic consequences. Journal of applied physiology: respiratory, environmental and exercise physiology. 1984;56(4):831-8. Epub 1984/04/01. doi: 10.1152/jappl.1984.56.4.831. PubMed PMID: 6373687.
102. Favier RJ, Constable SH, Chen M, Holloszy JO. Endurance exercise training reduces lactate production. Journal of applied physiology (Bethesda, Md : 1985). 1986;61(3):885-9. Epub 1986/09/01. doi: 10.1152/jappl.1986.61.3.885. PubMed PMID: 3759772.
103. Narici MV, Roi GS, Landoni L, Minetti AE, Cerretelli P. Changes in force, cross-sectional area and neural activation during strength training and detraining of the human quadriceps. European journal of applied physiology and occupational physiology. 1989;59(4):310-9. Epub 1989/01/01. doi: 10.1007/bf02388334. PubMed PMID: 2583179.
104. Pyka G, Lindenberger E, Charette S, Marcus R. Muscle strength and fiber adaptations to a year-long resistance training program in elderly men and women. Journal of gerontology. 1994;49(1):M22-7. Epub 1994/01/01. doi: 10.1093/geronj/49.1.m22. PubMed PMID: 8282977.
105. Häkkinen K, Alén M, Kallinen M, Izquierdo M, Jokelainen K, Lassila H, et al. Muscle CSA, Force Production, and Activation of Leg Extensors during Isometric and Dynamic Actions in Middle-Aged and Elderly Men and Women. Journal of aging and physical activity. 1998;6(3):232-47. doi: 10.1123/japa.6.3.232.
106. Mukherjee K, Edgett BA, Burrows HW, Castro C, Griffin JL, Schwertani AG, et al. Whole blood transcriptomics and urinary metabolomics to define adaptive biochemical pathways of high-intensity exercise in 50-60 year old masters athletes. PloS one. 2014;9(3):e92031. Epub 2014/03/20. doi: 10.1371/journal.pone.0092031. PubMed PMID: 24643011; PubMed Central PMCID: PMCPMC3958411.
107. Nakamura S, Kobayashi M, Sugino T, Kajimoto O, Matoba R, Matsubara K. Effect of exercise on gene expression profile in unfractionated peripheral blood leukocytes. Biochemical and biophysical research communications. 2010;391(1):846-51. Epub 2009/12/01. doi: 10.1016/j.bbrc.2009.11.150. PubMed PMID: 19945435.
108. Radom-Aizik S, Zaldivar F, Jr., Leu SY, Cooper DM. A brief bout of exercise alters gene expression and distinct gene pathways in peripheral blood mononuclear cells of early- and late-pubertal females. Journal of applied physiology (Bethesda, Md : 1985). 2009;107(1):168-75. Epub 2009/05/02. doi: 10.1152/japplphysiol.00121.2009. PubMed PMID: 19407257; PubMed Central PMCID: PMCPMC2711785.
109. Slivka DR, Heesch MWS, Dumke CL, Cuddy JS, Hailes WS, Ruby BC. Human Skeletal Muscle mRNA Response to a Single Hypoxic Exercise Bout. Wildern Environ Med. 2014;25(4):462-5. PubMed PMID: WOS:000346895300014.

110. Zieker D, Fehrenbach E, Dietzsch J, Fliegner J, Waidmann M, Nieselt K, et al. cDNA microarray analysis reveals novel candidate genes expressed in human peripheral blood following exhaustive exercise. Physiological genomics. 2005;23(3):287-94. Epub 2005/08/25. doi: 10.1152/physiolgenomics.00096.2005. PubMed PMID: 16118270.
111. Riebe D, Ehrman, J. K., Liguori, G., & Magal, M. ACSM's Guidelines for Exercise Testing and Prescription (Tenth edition). American Collegue of Sports Medicine. 2018.
112. von Elm E, Altman DG, Egger M, Pocock SJ, Gøtzsche PC, Vandenbroucke JP. The Strengthening the Reporting of Observational Studies in Epidemiology (STROBE) statement: guidelines for reporting observational studies. J Clin Epidemiol. 2008;61(4):344-9. Epub 2008/03/04. doi: 10.1016/j.jclinepi.2007.11.008. PubMed PMID: 18313558.
113. Hase M, Yokomizo T, Shimizu T, Nakamura M. Characterization of an orphan G protein-coupled receptor, GPR20, that constitutively activates Gi proteins. The Journal of biological chemistry. 2008;283(19):12747-55. Epub 2008/03/19. doi: 10.1074/jbc.M709487200. PubMed PMID: 18347022.
114. Wu YM, Chang JW, Wang CH, Lin YC, Wu PL, Huang SH, et al. Regulation of mammalian transcription by Gdown1 through a novel steric crosstalk revealed by cryo-EM. The EMBO journal. 2012;31(17):3575-87. Epub 2012/08/02. doi: 10.1038/emboj.2012.205. PubMed PMID: 22850672; PubMed Central PMCID: PMCPMC3433857.
115. Takahashi K, Nakanishi H, Miyahara M, Mandai K, Satoh K, Satoh A, et al. Nectin/PRR: an immunoglobulin-like cell adhesion molecule recruited to cadherin-based adherens junctions through interaction with Afadin, a PDZ domain-containing protein. The Journal of cell biology. 1999;145(3):539-49. Epub 1999/05/04. doi: 10.1083/jcb.145.3.539. PubMed PMID: 10225955; PubMed Central PMCID: PMCPMC2185068.
116. Zhu Y, Paniccia A, Schulick AC, Chen W, Koenig MR, Byers JT, et al. Identification of CD112R as a novel checkpoint for human T cells. Journal of Experimental Medicine. 2016;213(2):167-76. Epub 2016/01/13. doi: 10.1084/jem.20150785. PubMed PMID: 26755705; PubMed Central PMCID: PMCPMC4749091.
117. Brolinson PG, Elliott D. Exercise and the immune system. Clinics in sports medicine. 2007;26(3):311-9. Epub 2007/09/11. doi: 10.1016/j.csm.2007.04.011. PubMed PMID: 17826186.
118. Gleeson M, Bishop NC, Stensel DJ, Lindley MR, Mastana SS, Nimmo MA. The anti-inflammatory effects of exercise: mechanisms and implications for the prevention and treatment of disease. Nature Reviews Immunology. 2011;11(9):607. Epub 2011/08/06. doi: 10.1038/nri3041. PubMed PMID: 21818123.
119. Knoblach B, Keller BO, Groenendyk J, Aldred S, Zheng J, Lemire BD, et al. ERp19 and ERp46, New Members of the Thioredoxin Family of Endoplasmic Reticulum Proteins *. Molecular & Cellular Proteomics. 2003;2(10):1104-19. Epub 2003/08/22. doi: 10.1074/mcp.M300053-MCP200. PubMed PMID: 12930873.
120. Dias RG, Silva MS, Duarte NE, Bolani W, Alves CR, Junior JR, et al. PBMCs express a transcriptome signature predictor of oxygen uptake responsiveness to endurance exercise training in men. Physiological genomics. 2015;47(2):13-23. Epub 2014/12/04. doi: 10.1152/physiolgenomics.00072.2014. PubMed PMID: 25465030.
121. Gong S, Peng Y, Jiang P, Wang M, Fan M, Wang X, et al. A deafness-associated tRNAHis mutation alters the mitochondrial function, ROS production and membrane potential. Nucleic acids research. 2014;42(12):8039-48. Epub 2014/06/13. doi: 10.1093/nar/gku466. PubMed PMID: 24920829; PubMed Central PMCID: PMCPMC4081083.
122. Oliveira AN, Hood DA. Exercise is mitochondrial medicine for muscle. Sports Medicine and Health Science. 2019;1(1):11-8. doi: https://doi.org/10.1016/j.smhs.2019.08.008.

123. Steiner JL, Murphy EA, McClellan JL, Carmichael MD, Davis JM. Exercise training increases mitochondrial biogenesis in the brain. Journal of applied physiology (Bethesda, Md : 1985). 2011;111(4):1066-71. Epub 2011/08/06. doi: 10.1152/japplphysiol.00343.2011. PubMed PMID: 21817111.
124. Navarro A, Gomez C, López-Cepero JM, Boveris A. Beneficial effects of moderate exercise on mice aging: survival, behavior, oxidative stress, and mitochondrial electron transfer. American Journal of Physiology-Regulatory, Integrative and Comparative Physiology. 2004;286(3):R505-R11. Epub 2003/11/15. doi: 10.1152/ajpregu.00208.2003. PubMed PMID: 14615275.
125. Laye MJ, Rector RS, Warner SO, Naples SP, Perretta AL, Uptergrove GM, et al. Changes in visceral adipose tissue mitochondrial content with type 2 diabetes and daily voluntary wheel running in OLETF rats. The Journal of physiology. 2009;587(Pt 14):3729-39. Epub 06/02. doi: 10.1113/jphysiol.2009.172601. PubMed PMID: 19491243; PubMed Central PMCID: PMCPMC2742294.
126. Sutherland LN, Bomhof MR, Capozzi LC, Basaraba SA, Wright DC. Exercise and adrenaline increase PGC-1{alpha} mRNA expression in rat adipose tissue. J Physiol. 2009;587(Pt 7):1607-17. Epub 2009/02/18. doi: 10.1113/jphysiol.2008.165464. PubMed PMID: 19221126; PubMed Central PMCID: PMCPMC2678229.
127. Busquets-Cortes C, Capo X, Martorell M, Tur JA, Sureda A, Pons A. Training Enhances Immune Cells Mitochondrial Biosynthesis, Fission, Fusion, and Their Antioxidant Capabilities Synergistically with Dietary Docosahexaenoic Supplementation. Oxidative Medicine and Cellular Longevity. 2016;2016:8950384. Epub 2016/10/05. doi: 10.1155/2016/8950384. PubMed PMID: WOS:000383501600001; PubMed Central PMCID: PMCPMC5028859.
128. Sanger HL, Klotz G, Riesner D, Gross HJ, Kleinschmidt AK. Viroids are single-stranded covalently closed circular RNA molecules existing as highly base-paired rod-like structures. Proceedings of the National Academy of Sciences of the United States of America. 1976;73(11):3852-6. Epub 1976/11/01. doi: 10.1073/pnas.73.11.3852. PubMed PMID: 1069269; PubMed Central PMCID: PMCPMC431239.
129. Kos A, Dijkema R, Arnberg AC, van der Meide PH, Schellekens H. The hepatitis delta (delta) virus possesses a circular RNA. Nature. 1986;323(6088):558-60. Epub 1986/10/09. doi: 10.1038/323558a0. PubMed PMID: 2429192.
130. Cocquerelle C, Mascrez B, Hétuin D, Bailleul B. Mis-splicing yields circular RNA molecules. FASEB journal : official publication of the Federation of American Societies for Experimental Biology. 1993;7(1):155-60. Epub 1993/01/01. doi: 10.1096/fasebj.7.1.7678559. PubMed PMID: 7678559.
131. Nigro JM, Cho KR, Fearon ER, Kern SE, Ruppert JM, Oliner JD, et al. Scrambled exons. Cell. 1991;64(3):607-13. Epub 1991/02/08. doi: 10.1016/0092-8674(91)90244-s. PubMed PMID: 1991322.
132. Zaphiropoulos PG. Circular RNAs from transcripts of the rat cytochrome P450 2C24 gene: correlation with exon skipping. Proceedings of the National Academy of Sciences of the United States of America. 1996;93(13):6536-41. Epub 1996/06/25. doi: 10.1073/pnas.93.13.6536. PubMed PMID: 8692851; PubMed Central PMCID: PMCPMC39059.
133. Hansen TB, Jensen TI, Clausen BH, Bramsen JB, Finsen B, Damgaard CK, et al. Natural RNA circles function as efficient microRNA sponges. Nature. 2013;495(7441):384-8. Epub 2013/03/01. doi: 10.1038/nature11993. PubMed PMID: 23446346.
134. Mahmoudi E, Cairns MJ. Circular RNAs are temporospatially regulated throughout development and ageing in the rat. Scientific Reports. 2019;9(1):2564. Epub 2019/02/24. doi:

10.1038/s41598-019-38860-9. PubMed PMID: 30796328; PubMed Central PMCID: PMCPMC6385508.
135. Memczak S, Papavasileiou P, Peters O, Rajewsky N. Identification and Characterization of Circular RNAs As a New Class of Putative Biomarkers in Human Blood. PloS one. 2015;10(10):e0141214. Epub 2015/10/21. doi: 10.1371/journal.pone.0141214. PubMed PMID: 26485708; PubMed Central PMCID: PMCPMC4617279 covering the use of blood circular RNAs as biomarkers in neurological diseases. This did not alter the authors' adherence to PLOS ONE policies on sharing data and materials.
136. Jeck WR, Sharpless NE. Detecting and characterizing circular RNAs. Nature biotechnology. 2014;32(5):453-61. Epub 2014/05/09. doi: 10.1038/nbt.2890. PubMed PMID: 24811520; PubMed Central PMCID: PMCPMC4121655.
137. Guo M, Qiu J, Shen F, Wang S, Yu J, Zuo H, et al. Comprehensive analysis of circular RNA profiles in skeletal muscles of aging mice and after aerobic exercise intervention. Aging (Albany NY). 2020;12(6):5071-90. Epub 03/17. doi: 10.18632/aging.102932. PubMed PMID: 32182212; PubMed Central PMCID: PMCPMC7138574.
138. Meinecke A, Mitzka S, Just A, Cushman S, Stojanović SD, Xiao K, et al. Cardiac endurance training alters plasma profiles of circular RNA MBOAT2. Am J Physiol-Heart Circul Physiol. 2020;319(1):H13-H21. Epub 2020/05/16. doi: 10.1152/ajpheart.00067.2020. PubMed PMID: 32412780.
139. Gao Y, Wang J, Zhao F. CIRI: an efficient and unbiased algorithm for de novo circular RNA identification. Genome Biology. 2015;16(1):4. Epub 2015/01/15. doi: 10.1186/s13059-014-0571-3. PubMed PMID: 25583365; PubMed Central PMCID: PMCPMC4316645.
140. Beermann J, Piccoli MT, Viereck J, Thum T. Non-coding RNAs in Development and Disease: Background, Mechanisms, and Therapeutic Approaches. Physiological reviews. 2016;96(4):1297-325. Epub 2016/08/19. doi: 10.1152/physrev.00041.2015. PubMed PMID: 27535639.
141. Vea A, Llorente-Cortes V, de Gonzalo-Calvo D. Circular RNAs in Blood. Advances in experimental medicine and biology. 2018;1087:119-30. Epub 2018/09/28. doi: 10.1007/978-981-13-1426-1_10. PubMed PMID: 30259362.
142. Gao Y, Zhao F. Computational Strategies for Exploring Circular RNAs. Trends in Genetics. 2018;34(5):389-400. Epub 2018/01/18. doi: 10.1016/j.tig.2017.12.016. PubMed PMID: 29338875.
143. Diaconis P, Mosteller F. Methods for Studying Coincidences. Journal of the American Statistical Association. 1989;84(408):853-61. doi: 10.1080/01621459.1989.10478847.

TABLES AND FIGURES

Table 6-1 *Participants characteristics at enrolment.*

	SEDENTARY (n = 28)	STRENGTH (n = 20)	AEROBIC (n = 20)
Age (years)	35.5±7.65[a]	26.2±5.73	31.25±9.86
Height (cm)	181±8[a]	175±7[b]	181±7
Body Mass (Kg)	94.9±17.7[a,b]	79.74±10	72 ±7
BMI (kg/m^2)	28.72±4.9[b]	25.97±2.57[b]	21.83±1.8
$\dot{V}$O2max (mL.Kg-1.min-1)	32.45±4.85[a,b]	42.73±6.2[b]	59±6.1
Absolute $\dot{V}$O2max (mL.min-1)	3053.09±577.52[b]	3378.79±473.65[b]	4226.43±401.94
Relative strength (1RM/mass)	2.73±0.58[a,b]	5.67±0.58[b]	3.71±0.58
Absolute strength (1RM)	250.86±58.76[a]	438.97 ±62.65[b]	267.5±44.59

cm= centimetres, Kg= Kilograms, m^2= square metres, mL= millilitres, min= minutes, RM= One Repetition Maximum. Values are means ± SD. a – significant compared with STRENGTH (p<0.05), b – significant compared with AEROBIC (p<0.05).

Table 6-2 *Physiological measurements after 4 weeks of MET for SEDENTARY and the same period for normal training in STRENGTH and AEROBIC.*

	SEDENTARY (n = 28)			**STRENGTH (n = 20)**			**AEROBIC (n = 20)**		
	Enrolment	**Follow-up 1**	***p value***	**Enrolment**	**Follow-up 1**	***p value***	**Enrolment**	**Follow-up 1**	***p value***
Absolute $\dot{V}O_{2max}$ ($mL \cdot min^{-1}$)	**3053.09 ±577.52[b]**	**3293 ±570.67[b]**	**<0.001**	3378.79 ±473.65[b]	3535.55 ±501.12[b]	0.088	**4226.43 ±401.94**	**4411.22 ±483.04**	**0.031**
$\dot{V}O_{2max}$ ($mL \cdot Kg^{-1} \cdot min^{-1}$)	**32.45±4.85[a,b]**	**35.11±4.75[a,b]**	**0.002**	42.73±6.2[b]	44.78±6.37[b]	0.073	59±6.1	59.8±7.23	1
Squats (Kg)	**76.25±24.46[a]**	**91.5±25.3[a]**	**<0.001**	155.24±29.49[b]	156.1±27.07[b]	1	86.50±17.85	83±16.54	0.66
Deadlift (Kg)	**106.21±26.74[a]**	**117.36±25.6[a]**	**<0.001**	170.95±26.81[b]	171±27.46[b]	1	109±17.14	107.25±15.45	1
Bench press (Kg)	**68.39±15.64[a]**	**72.28±17.3[a]**	**0.004**	110.21±16.2[b]	110.88±16.15[b]	1	72±15.25	74±15.13	0.479
Absolute strength (1RM;Kg)	**250.86±58.76[a]**	**281.14±60.45[a]**	**<0.001**	438.97 ±62.65[b]	437.98±59.53[b]	1	267.5±44.59	264.25±38.77	1
Relative strength (1RM/body mass; Kg)	**2.73±0.58[a,b]**	**3.07±0.63[a,b]**	**<0.001**	5.67±0.58[b]	5.65±0.51[b]	1	3.71±0.58	3.69±0.58	1
Body mass (kg)	94.91±17.78[a,b]	94.66±17.24[a,b]	1	79.03±10.01	79.61±9.93	1	**73.58±7.31**	**74.17±7.21**	**<0.001**
% Lean body mass	77.77±6.15[a,b]	77.02±6.1[a,b]	0.518	87.40±4.19	86.93±4.03	1	88.55±3.64	88.97±4.15	1
RER_{max}	**1.20±0.09**	**1.16±0.06**	**0.038**	1.22±0.09	1.18±0.05	0.064	1.20±0.09	1.18±0.07	1
HR_{max}	176.64±17.41	174.57±14.24	1	184.15±13.05	184.6±9.21	1	178.43±18.24	178.1±16.53	1
Age predicted HR_{max}	184.5±7.65[a]	184.46±7.71[a]	1	193.8±5.72	193.75±5.75	1	188.75±9.86	188.6±10.02	0.248
RPE	**8.04±1.45[b]**	**8.29±1.41[a,b]**	**<0.001**	8.45±1.01	8.5±1.05	1	9.13±0.78	9.05±0.86	1
Diastolic Blood Pressure (mmHg)	**83.07±7.38[a,b]**	**77.39±9.27[a,b]**	**<0.001**	67.03±7.22	65.6±6.39[b]	1	73.6±9.43	75.75±10.72	0.629
Systolic Blood Pressure (mmHg)	130.89±9.95[a]	128.96±8.91[a]	0.640	121.55±8.1	118.25±8.45[b]	0.218	125.88±11.54	128.45±12.95	0.482
Mean arterial blood pressure	**186.3±14.17[a,b]**	**180.59±14.11[a]**	**0.032**	166.26±12.15	162.01±11.31[b]	0.319	174.97±16.74	178.98±18.04	0.382

mL= millilitres, min= minutes, Kg= Kilograms, 1RM= One repetition maximum, RER= Respiratory Exchange Ratio, HR= Heart Rate, RPE= Rate of Perceived Exertion, mmHg= millimetres of mercury. Values are means ± SD. a – significant compared with STRENGTH (p<0.05), b – significant compared with AEROBIC (p<0.05)

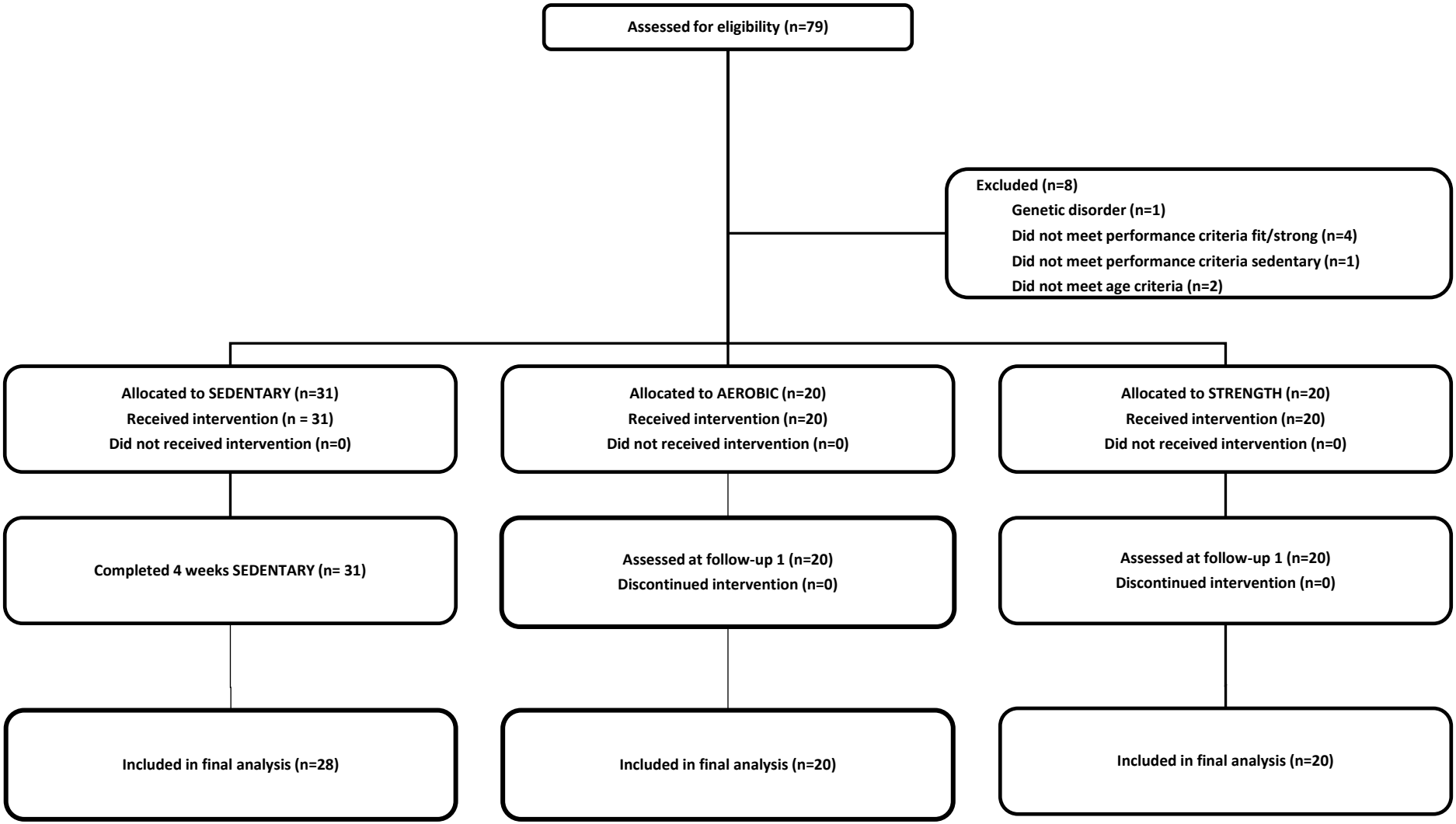

Figure 6-1 *Flow of participants through the study.*

7 REALISATION OF AIMS AND HYPOTHESES

Hypothesis 1

(H_0): Peripheral blood is not a valid source for identifying the effect of physical exercise training on transcriptomic markers of apparently healthy males in (RCTs).

(H_1): Peripheral blood can be considered a valid source for identifying the effect of physical exercise training on transcriptomic markers of apparently healthy males in (RCTs).

Systematic review revealed profound heterogeneity in different aspects of RCTs (Randomised Controlled Trials) that led to a lack of studies available for meta-analysis (n=2), highlighting the current limitations using PBT (Peripheral Blood Transcriptome) expression analysis to interrogate adaptation to exercise training. This, in turn, did not allowed for the identification of peripheral blood transcripts affected by exercise training. Therefore, due to lack of information regarding transcripts expression, and inconsistency in data reporting in RCTs examined in this review, the null hypothesis (H_0) was accepted. Furthermore, in a spirit of good scientific practice, this thesis aimed to provide a set of recommendations for study design, methodological, and data reporting aspects for researchers willing to conduct RCTs to study PBT in adaptation to exercise training.

Hypothesis 2

(H_0): Peripheral blood is not a valid source for identification of differential effects of divergent physical exercise training on transcriptomic markers of apparently healthy exercise-naïve participants in Randomised Controlled Trials (RCTs).

(H_1): Peripheral blood can be considered valid source for identification of differential effects of divergent physical exercise training on transcriptomic markers of apparently healthy exercise-naïve participants in Randomised Controlled Trials (RCTs).

Incomplete reporting of data among the RCTs included in Chapter 3 precluded head-to-head comparison and network meta-analysis of different exercise modalities and their relative effect on PBT expression. However, it was possible to conduct meta-analysis investigating *IL-10* and *TNF-α* expression among 2 studies each. Although results were drawn from this analysis, it was not substantive enough to support the use of PBT to characterise distinct transcriptomic profiles of response to different exercise modalities. Therefore, the null hypothesis (H_0) was accepted.

Hypothesis 3a

(H_0): Peripheral Blood Transcriptome (PBT) expression would not discriminate between exercise-naïve sedentary males (SEDENTARY) compared with either AEROBIC or STRENGTH athletic phenotypes.

(H_1): Peripheral Blood Transcriptome (PBT) expression could discriminate between exercise-naïve sedentary males (SEDENTARY) compared with either AEROBIC or STRENGTH athletic phenotypes.

A comparison of PBT expression between SEDENTARY, AEROBIC athletes, and STRENGTH athletes, at baselines, revealed a large number of differentially expressed transcripts between these groups. It appears that PBT expression analysis has some capacity to distinguish the physiological differences between athletic phenotypes. Additionally, it seems to be more useful to identify transcriptomic differences between SEDENTARY and AEROBIC [407 up-regulated, FC≥2; 19 down-regulated, FC≤0.5; (FDR<0.05)] than between SEDENTARY and STRENGTH [9 up-regulated, FC≥2; 5 down-regulated, FC≤0.5; (FDR<0.05)]. Therefore, the null hypothesis (H_0) is rejected, and the alternative hypothesis is accepted (H_1). However, these results do not suffice to corroborate whether these differences are a result of the athletic training state of each group.

Hypothesis 3b

(H_0): 4 weeks of Mixed Exercise Training (MET) would not identify unique adaptive Peripheral Blood Transcriptome (PBT) expression changes within SEDENTARY compared with either AEROBIC or STRENGTH athletic phenotypes.

(H_1): 4 weeks of Mixed Exercise Training (MET) will identify unique adaptive Peripheral Blood Transcriptome (PBT) expression changes within SEDENTARY compared with either AEROBIC or STRENGTH athletic phenotypes.

In order to further inquire the causality of physical exercise adaptation on the observed differences in PBT between SEDENTARY, AEROBIC, and STRENGTH phenotypes, SEDENTARY participants conducted 4 weeks of MET. Comparison of PBT expression data before and after the intervention showed 2 transcripts were differentially expressed in SEDENTARY [(up-regulated, FC≥2; (FDR<0.05)]. These results support that analysis of PBT expression falls short of any meaningful capacity to identify the adaptation of exercise-naïve men to exercise training. Therefore, the null hypothesis (H_0) was accepted.

Hypothesis 4a

(H_0): Peripheral blood circRNA expression would not discriminate between SEDENTARY, AEROBIC and STRENGHT phenotypes.

(H_1): Peripheral blood circRNA expression will discriminate between SEDENTARY, AEROBIC and STRENGHT phenotypes.

Analysis of peripheral blood circRNA expression revealed significant differences between SEDENTARY and AEROBIC phenotypes [*n*= 21 up-regulated, FC≥2; *n*= 2537 down-regulated, FC≤0.5; (FDR<0.05)] and between SEDENTARY and STRENGTH phenotypes [*n*= 1 up-regulated, FC≥2; *n*= 618 down-regulated, FC≤0.5; (FDR<0.05)]. Based

on these results, the null hypothesis (H_0) was rejected and the alternative hypothesis (H_1) was accepted. However, these differences might be due to additional factors and not just the divergent exercise training state of the participants within each group.

Hypothesis 4b

(H_0): Peripheral blood circRNA expression would not be different in SEDENTARY undergoing four weeks of Mixed Exercise Training (MET), compared with AEROBIC and STRENGTH athletes.

(H_1): Peripheral blood circRNA expression will change in SEDENTARY undergoing four weeks of Mixed Exercise Training (MET), compared with AEROBIC and STRENGTH athletes.

Following MET, a single circRNA was differentially expressed in SEDENTARY [chr19__18537601__18538436___FKBP8, (FC≥2; FDR<0.05)]. These results indicate that circRNA expression on peripheral blood is not affected by exercise training in sedentary participants. Therefore, the null hypothesis (H_0) was accepted.

Appendix A - Data Extraction Form

Author(s):

_____

Year: _____ Country: _____

Publication Status: ❑ Published

❑ Unpublished

Treatment Group			Control Group		
$M_{age}(SD)$	$M_{body\ mass}(SD)$	$M_{BMI}(SD)$	$M_{age}(SD)$	$M_{body\ mass}(SD)$	$M_{BMI}(SD)$

Number of participants included in study: ❑ Intervention: _____

❑ Control: _____

❑ Total: _____

Number of participants included in transcriptomic analysis:

❑ Intervention: _____

❑ Control: _____

❑ Total: _____

Source of Participants:

_____

Cluster RCT Design: ❑ No

❑ Yes: _____ (Number of Clusters)

Method of measuring performance:

_____

_____

Control Type: ❑ Waiting list
❑ Active control: _____

Length of Exercise Intervention: _____ (Total number of days)

Type of Exercise: ❑ Aerobic
❑ Resistance

Intensity of Exercise: ❑ Low ❑ Moderate/high

HRmax / VO2max / 1RM

Frequency of Exercise (Sessions/per week): _____

Volume of Exercise (Minutes/week): _____

Supervised exercise: ❑ Yes
❑ No
❑ Partially

Retention to the study (%): ❑ Control
❑ Exercise
❑ Total

Methodological characteristics

Intention-to-Treat Analysis:

- ❑ No
- ❑ Yes: _____

Type of statistical analysis:

_____

_____

Inclusion Criteria:

_____

_____

Type of blood collection:

_____

Time for blood collection:

_____

Source of RNA from peripheral blood:

- ❑ PBMC
- ❑ Buffy coat
- ❑ Specific cell subtype: _____

Methodology of RNA extraction: _____

Methodology for transcript identification:

- ❑ PCR
- ❑ Microarray
- ❑ Next-generation sequencing

Phenotype data

Control group pre- : _____

Control group post- : _____

Intervention group pre- : _____

Intervention group pre- : _____

Outcome Data

Transcripts investigated:

_____

Regulation after intervention:

❑ Up-regulated: _____

_____

❑ Down-regulated: _____

_____

❑ No change: _____

_____

Risk of Bias Assessment

Random Sequence Generation (Selection Bias): ❑ Low ❑ Unspecified ❑ High

---

Allocation Concealment (Selection Bias): ❑ Low ❑ Unspecified ❑ High

---

Blinding of Outcome Assessment (Detection Bias): ❑ Low ❑ Unspecified ❑ High

---

Incomplete Outcome Data (Attrition Bias): ❑ Low ❑ Unspecified ❑ High

---

Selective Reporting (Reporting Bias): ❑ Low ❑ Unspecified ❑ High

---

Other Bias: ❑ Low ❑ Unspecified ❑ High

Appendix B

List of up-regulated transcripts in AEROBIC *compared with* SEDENTARY *at enrolment* (FDR<0.05).

Transcript	FC	logFC	FDR
TRNQ	42.0424	5.393772	9.49E-18
TRNE	29.5384	4.884521	9.49E-18
TRNH	12.5149	3.64557	3.82E-08
KIF26A	10.7163	3.421735	1.85E-07
DLGAP2	10.0466	3.328633	4.78E-05
TRNF	9.5443	3.254641	1.77E-08
NTRK2	8.5289	3.092363	6.64E-08
LOC101059944	8.0459	3.008248	4.56E-06
CLUL1	7.4786	2.90277	0.00741
CACNA1A	7.1922	2.846432	8.45E-09
SHANK1	6.8319	2.77228	1.49E-06
MUC19	5.9080	2.56267	3.07E-08
LOC400655	5.9012	2.561019	0.011305
TRNA	5.6392	2.495489	1.36E-08
ROR2	5.4811	2.45447	3.18E-06
TMEM191B	5.1959	2.377377	0.000961
MYO3A	5.1191	2.355883	0.000759
C9orf172	5.1146	2.354628	1E-05
LINC00202-2	5.1008	2.350727	0.002042
COL27A1	5.0753	2.343497	1.77E-06
GABRB2	5.0275	2.329844	0.0003
TMEM132B	4.8969	2.291867	2.44E-07
PPL	4.6826	2.227324	1.32E-05
DNAH2	4.6304	2.21113	3.65E-06
TXNDC5	4.6190	2.207574	3.77E-06
PVRL2	4.5342	2.180858	0.000524
B4GALNT4	4.5171	2.175383	4.52E-06
GRIA3	4.5154	2.174853	0.005965
PCSK4	4.4468	2.152781	4.18E-07
FER1L4	4.4355	2.14911	5.74E-06
AMN	4.4344	2.148725	1.48E-06
CDH4	4.4251	2.145718	8.22E-05
SPTBN4	4.4193	2.143818	1.86E-06
LOC729466	4.3970	2.136504	0.046892
A4GALT	4.3949	2.135845	0.021767
GATA6	4.3637	2.125546	0.000134
RYR2	4.3417	2.118254	5.19E-05
PNMA2	4.3208	2.111303	0.015001
CEP170B	4.2390	2.083715	0.000207
CHD5	4.2234	2.078407	2.72E-06
NAT8L	4.2108	2.074102	1.66E-05

RTN4R	4.1693	2.059799	0.000101
SLC22A31	4.1548	2.054778	0.001929
TRNY	4.1382	2.048994	4.06E-08
CITED4	4.1102	2.039199	2.06E-06
COL5A1	4.0090	2.003246	2.99E-07
GLI3	4.0088	2.003178	0.000163
GSTA7P	3.9988	1.999565	0.01528
RELN	3.9141	1.968675	6.14E-05
ADAT3	3.8878	1.958948	3.04E-05
SEMA6A	3.8798	1.955996	8.22E-05
PTPRN	3.8723	1.953194	0.000201
ANKRD18B	3.8404	1.941272	0.000628
LOC642249	3.8262	1.935917	0.048277
ZNF469	3.7740	1.916112	2.16E-07
DOCK6	3.7649	1.912619	6.5E-06
CACNA1C	3.7545	1.908631	4.97E-07
TICAM2	3.7518	1.907589	8.07E-07
OBSL1	3.7376	1.902124	1.66E-05
BAIAP2L2	3.7260	1.897621	4.56E-06
SCT	3.7230	1.89645	4.92E-05
SHD	3.7014	1.888071	0.000632
LAMA5	3.6963	1.886091	4.67E-06
SUSD5	3.6865	1.882264	0.005586
MYO15A	3.6663	1.874314	4.16E-08
TRNN	3.6561	1.87029	0.00025
TRNP	3.6389	1.86349	2.82E-07
COBL	3.6008	1.848301	0.000142
MYO5B	3.5984	1.847347	0.001287
EPHA2	3.5915	1.844567	3.64E-06
SPRED3	3.5810	1.840377	6.57E-06
PCDH8	3.5784	1.839328	0.04993
LOC728763	3.5692	1.835606	3.43E-06
KCNQ3	3.5645	1.833699	0.000309
OR1J2	3.5618	1.832604	0.020188
TRNL2	3.5480	1.827024	9.03E-07
MYRFL	3.5444	1.825524	0.020531
PTPRU	3.5366	1.822365	0.002008
FERMT1	3.5158	1.813861	0.005111
CDO1	3.4963	1.805823	0.016991
PI15	3.4919	1.804012	0.047352
FAM132A	3.4911	1.803667	0.00018
PLA2R1	3.4661	1.793295	0.049766
SPTBN2	3.4471	1.785401	2.57E-06
TAS1R3	3.3732	1.754138	4.92E-05
LOC102724583	3.3601	1.748516	0.022494
DOK7	3.3433	1.741268	1.44E-05

RP11-844P9.2	3.3299	1.7355	7.52E-05
JAG2	3.3274	1.734401	2.68E-05
ASIC1	3.3156	1.729268	0.000271
PPP1R13L	3.2862	1.716437	1.75E-06
TRND	3.2850	1.715872	2.05E-06
LOC100996433	3.2802	1.713763	0.001965
GDA	3.2794	1.713442	0.042288
MUC16	3.2581	1.704042	0.000845
ETV2	3.2397	1.695841	0.000633
POLR2M	3.2378	1.695016	3.13E-06
NCAM2	3.2102	1.68265	0.003659
AMH	3.2081	1.68172	0.000143
DCHS2	3.1957	1.676125	0.000943
C1orf173	3.1916	1.674264	9.54E-05
LOC102724594	3.1902	1.673661	0.035847
GPR20	3.1845	1.671068	0.004922
SSPO	3.1835	1.67063	4.75E-08
TMEM121	3.1812	1.669592	0.002609
SCARF2	3.1631	1.661358	4.75E-08
TENM4	3.1608	1.660296	0.047489
FLJ39080	3.1594	1.659662	0.040402
MTHFS	3.1589	1.659406	0.000143
RP5-1142A6.2	3.1529	1.656668	1E-05
LDLRAD2	3.1341	1.648069	6.45E-05
REEP1	3.1207	1.641849	0.021954
GUCY2D	3.1060	1.635078	7.58E-06
SPEG	3.0782	1.622096	3.83E-05
BEGAIN	3.0748	1.620475	0.010677
MYOM2	3.0734	1.619822	0.026192
PKDCC	3.0603	1.613678	0.004813
SPIRE2	3.0464	1.607098	0.001862
TPGS1	3.0393	1.60373	3.93E-06
PTPRD	3.0382	1.603199	8.09E-05
PCDH17	3.0274	1.598063	0.001685
BAHCC1	3.0205	1.594791	9.85E-08
GRID1	3.0180	1.593609	0.008048
RORB	3.0153	1.592285	0.006456
BAI1	2.9958	1.582929	1.08E-06
TRNS1	2.9924	1.581311	5.81E-06
PAPPA2	2.9739	1.572379	0.000167
OTX1	2.9674	1.569181	9.92E-06
TUBB4A	2.9628	1.566952	0.000628
LOC100506734	2.9502	1.560826	0.001227
GDF7	2.9490	1.560241	0.008462
LOC100996740	2.9463	1.558894	0.000172
DNAH17	2.9448	1.558174	0.001109

VASH2	2.9404	1.556025	0.000102
MMP23B	2.9333	1.552535	0.000996
RHBDL1	2.9308	1.551271	6.64E-06
SORBS2	2.9219	1.546893	0.002218
MEX3A	2.9203	1.546124	0.000692
SRGAP1	2.9144	1.543205	7.44E-07
SPATC1L	2.8966	1.53436	0.000827
PROX1	2.8891	1.53064	0.001553
LOC100505727	2.8746	1.52338	0.038984
RGL3	2.8714	1.521742	0.000484
SCN2B	2.8645	1.518303	0.019898
PAX8	2.8547	1.513347	0.001901
SCRT2	2.8508	1.511367	0.001698
PIGR	2.8448	1.508308	0.019305
BEND6	2.8357	1.503729	0.000108
COL23A1	2.8308	1.501212	0.000309
LOC102723959	2.8158	1.49353	0.003429
LOC441124	2.8109	1.491027	0.002799
DLGAP3	2.8079	1.489515	0.000148
PPP1R14A	2.8057	1.488341	0.000335
CPNE7	2.8041	1.48755	0.000501
MYT1L	2.8026	1.486788	0.01107
SHISA7	2.7961	1.483414	0.003861
PPDPF	2.7930	1.481821	3.63E-06
DNAH11	2.7888	1.47964	6.25E-06
CDH24	2.7690	1.469347	8.59E-06
C2orf81	2.7680	1.46883	0.000105
SCUBE3	2.7652	1.467384	0.005585
ZNF628	2.7643	1.466914	5.34E-07
ATP2A1	2.7582	1.463713	0.000248
TRPM4	2.7535	1.461253	4.22E-05
PLEKHA4	2.7483	1.458541	6.47E-05
CACNA1H	2.7436	1.456054	2.65E-05
FOXD2	2.7422	1.455337	0.000143
PRR22	2.7337	1.450837	0.000486
EXOC3L1	2.7333	1.450641	0.001901
KIF7	2.7287	1.448202	0.000126
MPP4	2.7264	1.447	4.76E-05
RDH14	2.7260	1.446776	0.005455
ZNF296	2.7215	1.444396	2.84E-05
MATN1	2.7198	1.443476	0.003302
PKMYT1	2.7184	1.44275	0.000559
DRP2	2.7184	1.442749	0.002156
PAK6	2.7035	1.434834	0.001572
DCST1	2.6975	1.431649	0.000264
LINGO3	2.6949	1.430251	4.01E-05

ASIC3	2.6782	1.421256	0.001541
IQSEC3	2.6462	1.403937	0.035216
HIC1	2.6460	1.403817	2.31E-05
SCN2A	2.6447	1.403113	0.001568
HSD11B1L	2.6437	1.402584	4.11E-05
CLIC6	2.6424	1.401853	0.002894
LOC102723913	2.6419	1.40156	0.008267
GRID2IP	2.6372	1.399024	4.76E-05
LOC101928038	2.6292	1.394611	0.007634
CHST13	2.6229	1.391164	0.00079
CD248	2.6068	1.382272	0.002838
LEP	2.6037	1.380569	7.58E-05
ZFPM1	2.6034	1.380407	8.07E-07
TRNI	2.5942	1.375301	9.94E-06
SMOC1	2.5747	1.364376	0.000437
FRA10AC1	2.5728	1.363333	0.000279
SEMA6B	2.5674	1.360303	0.001261
DSG3	2.5672	1.360176	0.003345
PABPN1	2.5634	1.358083	1.49E-07
ADM2	2.5571	1.35453	0.005876
TRNK	2.5537	1.35259	4.45E-06
RP3-510O8.4	2.5398	1.344713	0.001584
SLC44A4	2.5375	1.343397	0.028798
CCDC85B	2.5326	1.340609	6.49E-07
MEG3	2.5319	1.340231	0.028045
KCNA5	2.5165	1.331392	0.000512
ETV1	2.5126	1.329181	0.01681
MMP17	2.5091	1.327172	1.9E-05
TRHDE-AS1	2.5057	1.325232	0.016942
JUP	2.5037	1.324048	0.002696
PNMAL2	2.5035	1.323926	0.034028
GPR161	2.5031	1.323723	0.000104
CA12	2.5022	1.323181	0.025031
KIAA1549	2.4985	1.321085	0.000558
SLITRK5	2.4951	1.319112	0.001807
REEP6	2.4862	1.313952	0.001597
BCAM	2.4720	1.30566	0.005926
KIAA1462	2.4697	1.304317	0.001943
GPER1	2.4696	1.30428	0.003394
DLGAP1	2.4613	1.29941	0.003839
DCST2	2.4577	1.297283	0.000178
ADAMTSL5	2.4564	1.296559	0.000391
ZNF579	2.4560	1.296326	3.78E-06
RUNX1T1	2.4524	1.294211	0.032399
ALOX15B	2.4415	1.287766	0.000295
KRTAP5-AS1	2.4397	1.286707	0.005792

LRRC24	2.4374	1.285356	4.22E-05
ZNF358	2.4373	1.285261	0.000103
C20orf24	2.4339	1.283257	5.98E-08
DAAM2	2.4203	1.275182	0.007187
CDT1	2.4192	1.274502	0.002111
BDNF	2.4186	1.274164	0.013275
HCN2	2.4174	1.273428	0.000264
TIMP3	2.4170	1.273226	0.022216
LRFN1	2.4143	1.271616	3.82E-08
C5orf64	2.4122	1.270373	0.01682
EVA1B	2.4090	1.26846	1.66E-05
SLC7A5P1	2.4067	1.267039	8.64E-05
BEST3	2.3936	1.259207	0.026368
DAZL	2.3888	1.25627	0.020825
TEX101	2.3880	1.255796	0.01887
PLXNB3	2.3864	1.254845	0.015957
SLC26A1	2.3841	1.253456	0.000322
ANK2	2.3827	1.252616	0.019524
C1orf127	2.3775	1.249472	0.000593
PABPN1L	2.3741	1.247356	0.001857
C17orf72	2.3728	1.246594	0.005051
NUTM2B	2.3698	1.24478	0.000524
BMP2	2.3691	1.244347	0.01302
C12orf61	2.3655	1.242138	5.4E-05
ESPN	2.3604	1.23903	0.015522
ZNF837	2.3525	1.23417	0.000104
BAI3	2.3517	1.233706	0.029406
PAK4	2.3487	1.231866	0.000161
COL6A1	2.3416	1.227509	0.021884
BRSK1	2.3413	1.227312	2.87E-05
PTCHD2	2.3357	1.223873	0.024787
TRIM74	2.3336	1.222543	0.000582
NUDT3	2.3328	1.222075	4.33E-07
TPBG	2.3272	1.218577	0.002013
KNDC1	2.3270	1.218442	0.005279
SHC3	2.3261	1.217895	2.8E-05
TSKS	2.3211	1.21481	0.016399
SLC16A11	2.3211	1.214809	0.004244
LIMCH1	2.3202	1.214275	0.000228
FLJ45079	2.3192	1.213607	0.003618
SOX2-OT	2.3106	1.208291	0.000266
WASH5P	2.3102	1.208039	0.027833
KCNK7	2.3057	1.205225	0.00079
LOC339862	2.3046	1.204545	0.039322
SERINC2	2.2990	1.201003	0.001101
OLFML2A	2.2980	1.200375	0.000326

AGRN	2.2971	1.199795	0.00032
GPX3	2.2892	1.194844	0.010751
TIE1	2.2882	1.194194	0.000162
KCNN3	2.2869	1.193416	0.000547
COL11A2	2.2868	1.193355	8.22E-05
CFD	2.2862	1.192961	0.002351
NAT14	2.2847	1.191985	1.9E-05
IFITM3	2.2816	1.190056	0.032823
ROR1	2.2801	1.189121	0.008163
DGKI	2.2722	1.184072	0.008213
WNT11	2.2673	1.180962	0.001581
TSPEAR	2.2580	1.175031	0.002778
LRP3	2.2573	1.174576	1.47E-05
CLCN1	2.2571	1.174458	0.038034
KCNG1	2.2559	1.173721	0.009915
RIMKLA	2.2551	1.173203	0.005036
ADORA1	2.2546	1.172885	0.018146
HOXA-AS2	2.2537	1.172312	0.00237
LRFN4	2.2529	1.171752	9.21E-06
SKOR1	2.2439	1.166027	0.00079
ST18	2.2387	1.162639	0.007375
SOCS1	2.2379	1.162142	0.001809
RAPGEF3	2.2378	1.162072	0.016644
GPRIN1	2.2370	1.161597	0.001387
LRFN3	2.2315	1.157992	0.002545
LRRC3	2.2294	1.156681	0.000375
ARHGAP23	2.2214	1.151438	0.000378
CHPF	2.2188	1.149768	1.9E-05
PDZD3	2.2166	1.148327	0.003776
KIAA1161	2.2130	1.146005	0.000326
RGPD1	2.2124	1.145623	0.005051
PI4KAP1	2.2116	1.145118	0.012529
RAB43	2.2009	1.138066	1.9E-05
ZNF503	2.1973	1.135745	0.000434
FSCN1	2.1971	1.135586	0.000293
LOC100131532	2.1961	1.134954	0.009328
MDK	2.1899	1.130862	0.000309
RP11-983P16.4	2.1898	1.130786	0.001227
ANKRD13B	2.1873	1.129154	0.008843
CUX2	2.1833	1.126543	0.000264
HSPG2	2.1770	1.122363	0.000168
SIGLEC15	2.1766	1.122091	5.68E-05
PCOLCE	2.1713	1.118526	0.002448
TENC1	2.1711	1.118432	0.011873
PLIN1	2.1659	1.114944	0.002664
ESPL1	2.1633	1.113224	0.000115

CLEC2L	2.1633	1.113216	0.013917
MICALL2	2.1612	1.111808	0.000192
KIAA1199	2.1594	1.110657	0.014777
RBM20	2.1576	1.109455	0.004896
CCDC114	2.1531	1.106422	0.001861
SLC22A20	2.1526	1.106075	0.001036
ARHGEF4	2.1522	1.10583	0.001348
GPR98	2.1498	1.104228	1.06E-05
HSD17B1	2.1474	1.102589	0.000611
ROCK1P1	2.1473	1.1025	0.006473
LOC101929937	2.1451	1.101012	0.002549
TEN1-CDK3	2.1450	1.100978	0.003825
IGSF10	2.1446	1.100712	0.034279
NTN5	2.1384	1.09653	0.002527
ISL2	2.1336	1.093279	0.000872
EIF4EBP3	2.1321	1.092307	0.002684
SYNPO	2.1277	1.089293	0.007143
GPRC5B	2.1268	1.088696	0.007597
MTSS1L	2.1258	1.087977	9.92E-05
RUNDC3B	2.1216	1.08514	0.035554
CLEC4G	2.1197	1.08389	0.004568
ARHGEF33	2.1173	1.08224	0.001258
PTPN3	2.1165	1.08171	0.01352
KANK3	2.1158	1.081194	0.000656
HSF2BP	2.1113	1.078142	0.000524
CGN	2.1073	1.075412	0.000369
CORO2B	2.1061	1.074585	0.016248
LOC101929017	2.1012	1.071231	0.000848
MSANTD1	2.1007	1.070851	4.15E-05
MPP3	2.0996	1.070144	0.000445
FOXJ1	2.0983	1.069255	0.006583
KIAA1456	2.0963	1.067878	0.014902
KIAA1875	2.0933	1.065774	3.98E-06
KLHL26	2.0878	1.061986	0.000291
LOC102723586	2.0876	1.061832	0.018968
CCDC154	2.0852	1.0602	6.85E-06
WDR96	2.0850	1.060026	0.003826
UBALD1	2.0832	1.058835	4.71E-06
ZNF865	2.0829	1.058616	3.98E-06
KIAA1045	2.0811	1.057329	0.005518
CHST8	2.0810	1.057246	0.035539
RET	2.0809	1.057204	0.00435
SMTN	2.0803	1.056763	3.36E-05
ATP1B2	2.0794	1.056188	0.000628
JAZF1-AS1	2.0761	1.053865	0.001622
SLC39A4	2.0747	1.052898	0.000171

PRRT4	2.0738	1.052254	0.012017
C9orf96	2.0651	1.046184	0.00399
FFAR4	2.0643	1.045632	0.005338
MROH6	2.0641	1.04554	0.000543
FERMT2	2.0620	1.044035	0.004764
TDRD1	2.0619	1.043961	0.007106
PACSIN1	2.0616	1.043749	0.004317
FAM9C	2.0598	1.042474	0.012203
KCNK10	2.0544	1.038746	0.001206
REXO1	2.0530	1.037736	1.76E-06
NUMBL	2.0518	1.036872	7.54E-06
SYCE1L	2.0510	1.036355	8.64E-05
LOC101929129	2.0504	1.035939	0.043686
MYRF	2.0503	1.035804	0.012944
SCARA5	2.0496	1.035352	0.013007
NCKAP5	2.0495	1.035254	0.028793
LOC101060060	2.0493	1.035112	0.039691
MYBPH	2.0478	1.034108	0.013095
ANKRD20A9P	2.0435	1.031054	0.009395
IER5L	2.0422	1.030093	8.4E-05
SAPCD2	2.0400	1.02855	0.025548
NDUFS7	2.0386	1.027583	5.74E-06
EPS8L1	2.0362	1.025894	0.000978
LOC102724601	2.0347	1.024791	0.014145
TANC1	2.0331	1.023653	5.16E-06
CLEC18B	2.0330	1.023644	0.029985
FAM221B	2.0328	1.023442	0.018954
KCNS1	2.0323	1.023145	0.02059
TRNT	2.0315	1.022562	0.000222
CCDC113	2.0313	1.022433	0.008666
CHDH	2.0306	1.021938	0.001639
CLDN9	2.0301	1.021586	0.032863
NLGN1	2.0276	1.019778	0.011717
IGSF22	2.0269	1.01927	0.001378
PEX11G	2.0267	1.019155	0.023145
SEC1P	2.0266	1.019032	0.010195
C9orf16	2.0246	1.017602	3.24E-05
ARPP21	2.0231	1.016575	0.035979
CFB	2.0119	1.008536	0.034611
YJEFN3	2.0092	1.00664	1.17E-05
LOC100509370	2.0071	1.005141	0.009133
TOMM20L	2.0057	1.004131	0.002147
BAAT	2.0034	1.002463	0.008568
TPTE2	2.0013	1.000947	0.010051

List of down-regulated transcripts in AEROBIC *compared with* SEDENTARY *at enrolment* (FDR<0.05).

Transcript	**FC**	**logFC**	**FDR**
LOC102724828	0.0964	-3.37556	0.030204
MMP8	0.3250	-1.62154	0.013861
OLR1	0.3539	-1.49843	0.009501
CTGLF12P	0.3690	-1.43836	0.035847
LOC102724455	0.3712	-1.4296	0.044008
CTSG	0.3776	-1.40508	0.047343
LTF	0.3856	-1.37497	0.036421
SNORD3B-2	0.4009	-1.31879	0.010673
ABCA13	0.4028	-1.31193	0.024929
SNORA54	0.4304	-1.21626	3.3E-05
LOC101929887	0.4452	-1.16758	0.016053
RNY3	0.4600	-1.12036	0.005888
SNORD94	0.4608	-1.11785	2.2E-05
SNORD3B-1	0.4738	-1.0776	0.038343
CAMP	0.4751	-1.07376	0.025101
SNORA63	0.4759	-1.07122	0.000266
SNORA34	0.4822	-1.05224	2.36E-05
HP	0.4887	-1.033	0.026138
LOC101927454	0.4982	-1.00514	0.000123

Appendix C

List of up-regulated transcripts in STRENGTH *compared with* SEDENTARY *at enrolment* (FDR<0.05).

Transcript	FC	logFC	FDR
RNF17	11.43665	3.515592	0.007227
ANKRD24	3.233444	1.693072	0.001093
GPR20	3.144775	1.652957	0.031096
PVRL2	3.03133	1.599951	0.047933
LOC100996740	2.841358	1.50658	0.003626
TXNDC5	2.526116	1.336921	0.041964
FAM167A	2.147055	1.102359	0.026963
C9orf16	2.084176	1.059477	0.000363
POLR2M	2.083111	1.058739	0.025086

List of up-regulated transcripts in STRENGTH *compared with* SEDENTARY *at enrolment* (FDR<0.05).

Transcript	FC	logFC	FDR
CD177	0.2139	-2.225	0.013734
LOC101060569	0.3591	-1.47734	0.011179
LOC101929887	0.3879	-1.36617	0.027671
TMEM200B	0.4113	-1.28168	0.04118
MIR4642	0.4948	-1.01495	0.016687

Appendix D

List of up-regulated transcripts in AEROBIC and STRENGTH *compared with* SEDENTARY *at enrolment* (FDR<0.05).

	AEROBIC			STRENGTH		
Transcript	**FC**	**logFC**	**FDR**	**FC**	**logFC**	**FDR**
ANKRD24	1.92981	0.948459	0.032945	3.233444	1.693072	0.001093
C9orf16	2.02455	1.017602	3.24E-05	2.084176	1.059477	0.000363
GPR20	3.184503	1.671068	0.004922	3.144775	1.652957	0.031096
LOC100996740	2.94628	1.558894	0.000172	2.841358	1.50658	0.003626
POLR2M	3.237806	1.695016	3.13E-06	2.083111	1.058739	0.025086
PVRL2	4.534233	2.180858	0.000524	3.03133	1.599951	0.047933
TXNDC5	4.618979	2.207574	3.77E-06	2.526116	1.336921	0.041964

List of up-regulated transcripts in AEROBIC and STRENGTH *compared with* SEDENTARY *at enrolment* (FDR<0.05).

	AEROBIC			STRENGTH		
Transcript	**FC**	**logFC**	**FDR**	**FC**	**logFC**	**FDR**
LOC101929887	0.445167	-1.16758	0.016053	0.3879	-1.36617	0.027671

Appendix E

List of up-regulated transcripts in SEDENTARY *after 4 weeks of mixed exercise training* (FDR<0.05).

Gene	FC	logFC	FDR
RPL13AP5	2.46787	1.303266	0.005418
TRNH	2.446772	1.29088	0.001173

Appendix F

List of up-regulated transcripts in AEROBIC *compared with* SEDENTARY *at follow-up 1* (FDR<0.05).

Transcript	FC	logFC	FDR
TRNQ	29.1088	4.863384	1.18E-18
TRNE	24.24553	4.599647	4.25E-19
DLGAP2	9.23315	3.206823	0.000105
LOC101059944	7.428011	2.892976	5.86E-06
FERMT1	6.388106	2.675388	0.000513
TRNF	6.150205	2.620635	4.71E-07
NTRK2	5.870342	2.553445	1.05E-06
SHANK1	5.622045	2.491095	5.5E-06
TRNH	5.608989	2.487741	2.16E-05
KIF26A	5.196841	2.377635	2.42E-05
MUC19	4.993419	2.320028	6.91E-08
TMEM132B	4.989135	2.31879	1.19E-07
TRNA	4.702134	2.233316	5.64E-08
LOC400655	4.64601	2.215992	0.041686
LOC642249	4.469281	2.160043	0.048801
ANKRD18B	4.322646	2.111915	0.000165
SCUBE3	4.294699	2.102557	0.00047
C9orf172	4.286	2.099632	4.23E-05
RYR2	4.272646	2.09513	0.000107
PI15	4.251671	2.08803	0.048083
GATA6	4.239923	2.084038	0.000276
NAT8L	4.17957	2.063355	2.56E-05
SLC12A1	4.167137	2.059057	0.047993
LOC101927697	4.130559	2.046337	0.017353
SPTBN4	4.095708	2.034113	4.11E-06
GLI3	4.082176	2.029338	0.000208
FLJ39080	4.073448	2.02625	0.031112
MYOM2	4.023802	2.008559	0.009264
GABRB2	3.95823	1.984855	0.002551
CDH4	3.882623	1.957032	0.000429
CACNA1A	3.789652	1.922065	4.45E-06
TRNY	3.721938	1.896054	7.75E-08
TMEM191B	3.696772	1.886266	0.008381
SPRED3	3.641492	1.86453	6.51E-06
SUSD5	3.635339	1.86209	0.012135
COL27A1	3.634222	1.861647	5.4E-05
PVRL2	3.626571	1.858606	0.004113
RELN	3.601879	1.84875	0.000165
OBSL1	3.556992	1.830658	4.05E-05
SEMA6A	3.531301	1.8202	0.00034
DNAH2	3.520464	1.815765	6.76E-05
CDO1	3.507124	1.810288	0.024339

C1orf173	3.460971	1.791177	5.4E-05
NCAM2	3.441542	1.783055	0.00468
SORBS2	3.420646	1.774269	0.00123
SCRT2	3.329704	1.735394	0.001177
TRNP	3.224449	1.689053	1.79E-06
ROR2	3.204603	1.680145	0.000536
CDH6	3.181227	1.669583	0.02506
DCHS2	3.170064	1.664512	0.002128
MUC16	3.169118	1.664081	0.00247
PCDH17	3.156668	1.658402	0.00252
PAPPA2	3.121305	1.642149	0.000181
TRNN	3.120401	1.641732	0.002421
CA12	3.099509	1.63204	0.016246
SLC22A31	3.087213	1.626305	0.018322
B4GALNT4	3.064974	1.615875	0.00028
DNAH11	3.04888	1.60828	1.39E-06
MYT1L	3.046114	1.60697	0.014559
DAAM2	3.042515	1.605264	0.00123
PROX1	3.041595	1.604828	0.00247
KCNQ3	3.027333	1.598047	0.00258
COL5A1	3.022963	1.595963	1.23E-05
DOCK6	3.013186	1.59129	0.000107
CHD5	2.982038	1.576299	0.000165
MYO15A	2.973341	1.572085	6.84E-07
FER1L4	2.965671	1.568358	0.000486
CACNA1C	2.953332	1.562344	1.67E-05
PCSK4	2.944482	1.558014	5.4E-05
KIF7	2.93153	1.551654	7.08E-05
PTPRD	2.930998	1.551392	0.0002
FRA10AC1	2.922034	1.546973	3.63E-05
COBL	2.869061	1.520578	0.002444
DCST1	2.867626	1.519857	0.000227
MOV10L1	2.829697	1.500648	0.00756
SCN2B	2.806152	1.488593	0.045119
PPL	2.803837	1.487402	0.002342
CLIC6	2.80199	1.486452	0.003972
PNMAL2	2.760805	1.465089	0.036949
BDNF	2.757877	1.463558	0.01108
JAG2	2.722459	1.44491	0.000406
TIMP3	2.718952	1.443051	0.022021
SPEG	2.684994	1.424919	0.000366
TRNL2	2.684418	1.42461	9.55E-05
MEX3A	2.671486	1.417642	0.003413
SPTBN2	2.669207	1.416411	0.000102
C5orf64	2.65741	1.410021	0.016689
DRP2	2.626356	1.393062	0.005659

TRNS1	2.624978	1.392305	8.39E-05
RGL3	2.613935	1.386224	0.002506
CPNE7	2.608444	1.383189	0.001852
ETV1	2.60828	1.383099	0.026756
C9orf96	2.563032	1.357851	0.000625
ASIC1	2.553998	1.352758	0.005119
DGKI	2.548766	1.349799	0.006374
FAM132A	2.532742	1.3407	0.004838
RP11-983P16.4	2.528737	1.338417	0.000373
ADAT3	2.517501	1.331992	0.00375
ST18	2.515441	1.330811	0.004838
KIAA1549	2.512708	1.329243	0.00112
PAK6	2.508107	1.326599	0.005263
FOXD2	2.502618	1.323438	0.000663
PTPRU	2.500919	1.322459	0.033365
KCNN3	2.495706	1.319448	0.00034
GUCY2D	2.493397	1.318113	0.000236
RORB	2.488815	1.315459	0.035434
RTN4R	2.481852	1.311417	0.00992
SOX2-OT	2.475279	1.307591	0.000181
DCST2	2.473037	1.306284	0.000277
SPATC1L	2.472874	1.306189	0.006338
ANK2	2.472298	1.305853	0.029413
AMN	2.467189	1.302868	0.001337
TRND	2.464751	1.301442	0.000309
DOK7	2.461805	1.299716	0.001001
RAPGEF3	2.455031	1.295741	0.016051
SCARA5	2.446676	1.290823	0.00459
GPR161	2.445197	1.289951	0.00028
PKMYT1	2.439076	1.286335	0.003705
ZNF469	2.438074	1.285742	0.000166
MATN1	2.422582	1.276545	0.016689
SHC3	2.422466	1.276477	2.37E-05
MPP4	2.421464	1.27588	0.000438
SLC26A1	2.408155	1.267928	0.000505
CEP170B	2.407119	1.267307	0.024339
SPIRE2	2.402934	1.264797	0.019391
BEND6	2.401334	1.263836	0.001516
RUNDC3B	2.396788	1.261102	0.029413
EPS8L1	2.377304	1.249327	0.00015
BAHCC1	2.370481	1.24518	1.09E-05
AREG	2.368044	1.243696	0.045343
SRGAP1	2.367832	1.243567	3.3E-05
DLGAP1	2.366706	1.242881	0.010775
COL23A1	2.359675	1.238588	0.004113
EPHX4	2.357739	1.237404	0.046468

LOC728763	2.354542	1.235447	0.000935
PTPN3	2.347749	1.231278	0.012631
RGPD1	2.345978	1.230189	0.005659
TMEM121	2.335851	1.223948	0.032221
DNAH17	2.330608	1.220706	0.013862
GRID2IP	2.329644	1.220109	0.000429
RP11-214C8.2	2.326293	1.218033	0.002421
TIE1	2.324271	1.216778	0.000181
ZNF503	2.322162	1.215468	0.000316
ARPP21	2.322122	1.215444	0.024147
SCT	2.31927	1.213671	0.00886
ETV2	2.311618	1.208903	0.016051
DLGAP3	2.291657	1.196391	0.002956
WDR96	2.287545	1.1938	0.002915
ANKRD13B	2.284922	1.192145	0.011913
SLITRK5	2.283355	1.191155	0.008777
PKDCC	2.283033	1.190952	0.048438
TAS1R3	2.282714	1.19075	0.005086
STARD4-AS1	2.276615	1.18689	0.000185
CABLES1	2.266132	1.180232	7.08E-05
C12orf61	2.254201	1.172616	0.00018
GPR137C	2.254014	1.172497	0.000523
RP11-401P9.5	2.252813	1.171727	0.016689
KIR2DL1	2.244061	1.166112	0.007423
ANKRD20A9P	2.243509	1.165757	0.006755
RP11-844P9.2	2.240762	1.163989	0.007046
PAQR5	2.238332	1.162424	0.011781
LAMA5	2.226488	1.15477	0.004505
MMP23B	2.226048	1.154485	0.016111
LDLRAD2	2.216554	1.148319	0.005202
EPHA2	2.211487	1.145017	0.002713
LOC102723913	2.208799	1.143262	0.049442
COL13A1	2.205314	1.140984	0.004838
TPBG	2.202723	1.139288	0.006963
PDZD3	2.201057	1.138196	0.00793
TRNI	2.190977	1.131575	0.00034
FAM221B	2.184406	1.127241	0.01947
PRRT4	2.184041	1.127	0.014427
SHD	2.178257	1.123174	0.046736
GML	2.172008	1.11903	0.006029
LINGO3	2.165053	1.114402	0.001516
BAIAP2L2	2.16125	1.111866	0.004121
SKOR1	2.161146	1.111797	0.002677
TRPM4	2.160977	1.111684	0.002421
SYT1	2.157021	1.10904	0.015123
TSKS	2.156846	1.108923	0.045119

NUTM2B	2.153264	1.106525	0.003705
GPR98	2.140286	1.097804	1.67E-05
LOC102724273	2.137463	1.095899	0.002235
TDRD1	2.13669	1.095377	0.009782
ADAMTSL5	2.133522	1.093237	0.004316
LEP	2.129349	1.090412	0.002421
PLEKHA4	2.128711	1.08998	0.003485
RDH14	2.12683	1.088705	0.048798
BTNL9	2.122333	1.085651	0.030513
SCARF2	2.120828	1.084628	8.39E-05
TXNDC5	2.115338	1.080888	0.013358
SSPO	2.11449	1.08031	0.00015
GPRIN1	2.103923	1.073082	0.006397
NLGN1	2.100091	1.070452	0.016403
CHDH	2.100054	1.070426	0.00243
ALOX15B	2.097504	1.068673	0.004034
KIR2DL4	2.095163	1.067062	0.014219
ABCB11	2.095048	1.066983	0.024115
LIMCH1	2.089638	1.063253	0.002421
MOCS1	2.088131	1.062212	0.046709
PPP1R13L	2.086562	1.061128	0.001852
LOC100506734	2.085336	1.06028	0.03296
CGN	2.08359	1.059071	0.000957
ZNF296	2.08358	1.059065	0.002128
DMKN	2.08287	1.058573	0.006755
VIPR2	2.081723	1.057778	0.006489
GPER1	2.079656	1.056345	0.026829
PTPRB	2.078337	1.05543	0.017353
GSDMC	2.076694	1.054289	0.009888
BCAM	2.072275	1.051215	0.040703
RAI14	2.071694	1.050811	0.022734
FERMT2	2.059516	1.042305	0.009928
HIC1	2.056741	1.04036	0.001852
KBTBD12	2.050763	1.036161	0.017065
LRFN3	2.046423	1.033104	0.012762
OTX1	2.046082	1.032864	0.003485
VASH2	2.044014	1.031405	0.013918
SPTLC3	2.04373	1.031205	0.000572
KIAA1456	2.037008	1.026451	0.036012
KCNK10	2.03479	1.02488	0.003291
LIM2	2.03267	1.023376	0.028122
NAV2	2.026307	1.018853	0.004075
ARSJ	2.023812	1.017075	0.01507
C17orf72	2.023075	1.01655	0.037575
RBM20	2.022929	1.016446	0.018541
ROBO1	2.019079	1.013698	0.026829

CASC8	2.014665	1.01054	0.039688
RP5-1142A6.2	2.011161	1.008028	0.005057
KANK3	2.00986	1.007095	0.002568
CPNE4	2.005698	1.004104	0.01414
BAI1	2.002087	1.001505	0.001337

List of down-regulated transcripts in AEROBIC *compared with* SEDENTARY *at follow-up 1* (FDR<0.05).

Transcript	**FC**	**logFC**	**FDR**
MIR4732	0.463109	-1.110576198	0.037943
CXCL5	0.477419	-1.066672659	0.023785
SNORA54	0.495253	-1.013763385	0.001059

Appendix G

List of up-regulated transcripts in STRENGTH *compared with* SEDENTARY *at follow-up 1* (FDR<0.05).

Transcript	FC	logFC	FDR
RNF17	7.054148	2.81847177	0.035108
ANKRD24	2.889523	1.530831201	0.006688

List of down-regulated transcripts in STRENGTH *compared with* SEDENTARY *at follow-up 1* (FDR<0.05).

Transcript	FC	logFC	FDR
CASC20	0.017424	-5.842794213	0.045957
HOXA-AS2	0.429391	-1.219634615	0.046

Appendix H

List of up-regulated transcripts in AEROBIC *compared with* SEDENTARY AEROBIC *at follow-up 2* (FDR<0.05).

Transcript	FC	logFC	FDR
TRNQ	24.43655	4.610969	9.31E-09
TRNE	17.30973	4.113512	9.31E-09
DLGAP2	10.52231	3.39538	0.033895
SHANK1	6.935528	2.794006	0.008834
LOC101059944	6.795702	2.764623	0.015056
ANKRD18B	6.627986	2.728571	0.005668
NTRK2	5.83971	2.545897	0.011925
TMEM191B	5.374438	2.426114	0.037551
ASIC1	5.000771	2.32215	0.009365
TMEM132B	4.847834	2.27734	0.009365
ROR2	4.845877	2.276758	0.01438
TRNF	4.784081	2.258242	0.011925
SHD	4.448148	2.153205	0.02161
C5orf64	4.328194	2.113765	0.026868
RELN	4.294859	2.102611	0.01318
SCT	4.264476	2.092368	0.009365
TRNH	4.16309	2.057655	0.041411
DNAH2	3.99259	1.997325	0.011925
KIF26A	3.894306	1.961366	0.036066
SPTBN4	3.779433	1.91817	0.01318
SEMA6B	3.763716	1.912158	0.009365
RUNDC3B	3.653442	1.869256	0.036635
C9orf172	3.641181	1.864407	0.018272
NAT8L	3.630943	1.860344	0.026325
GUCY2D	3.6054	1.850159	0.007113
ARPP21	3.510637	1.811733	0.028702
BMP2	3.407583	1.768749	0.04625
MUC19	3.3893	1.760987	0.017378
COBL	3.363908	1.750138	0.041342
MOV10L1	3.333341	1.736969	0.042456
PCSK4	3.318873	1.730693	0.009365
CACNA1C	3.313553	1.728379	0.009365
ANKRD13B	3.274905	1.711453	0.022234
FRA10AC1	3.268538	1.708646	0.003435
CD248	3.262259	1.705871	0.02151
NYNRIN	3.175941	1.667184	0.023631
SPEG	3.125341	1.644014	0.015997
COL23A1	3.097913	1.631297	0.017217
PTPRD	3.096017	1.630414	0.021148
COL5A1	3.058308	1.612734	0.009365
PRRT4	3.050461	1.609027	0.024912

SPTBN2	3.047179	1.607474	0.009365
KCNK10	3.031269	1.599922	0.007113
MOCS1	3.012805	1.591107	0.037551
PPL	3.003947	1.586859	0.043836
CACNA1A	2.993688	1.581924	0.0315
FER1L4	2.984986	1.577724	0.034011
KIF7	2.973209	1.572021	0.015336
C1orf173	2.956442	1.563862	0.028702
TRNY	2.951677	1.561535	0.010175
FAM221B	2.946362	1.558935	0.0315
OBSL1	2.945658	1.55859	0.033994
EPHA2	2.944541	1.558043	0.014597
JAG2	2.942174	1.556883	0.019294
PAPPA2	2.917512	1.544739	0.035611
RP11-844P9.2	2.916214	1.544096	0.02228
CPNE7	2.860024	1.516027	0.028692
ALOX15B	2.821402	1.496412	0.015373
TIE1	2.813419	1.492325	0.007113
SPATC1L	2.762303	1.465872	0.047255
SCARA5	2.741613	1.455025	0.042456
ADAT3	2.736206	1.452177	0.039422
TRNA	2.736101	1.452122	0.030392
AMN	2.734732	1.451399	0.021729
CHD5	2.726871	1.447247	0.03458
LEP	2.720599	1.443924	0.01318
RGPD1	2.688487	1.426795	0.037551
TRNP	2.587533	1.371577	0.019912
SPAG17	2.578002	1.366253	0.044179
BEND6	2.577865	1.366177	0.0315
FOXD2	2.569023	1.36122	0.027777
PIP5KL1	2.56339	1.358053	0.01318
MYO15A	2.55775	1.354875	0.013148
SPRED3	2.549716	1.350336	0.042161
TRNS1	2.516095	1.331186	0.02161
ADAMTSL5	2.508242	1.326676	0.028702
SMOC1	2.497815	1.320666	0.042456
SKOR1	2.472236	1.305817	0.028692
A2M	2.459938	1.298622	0.018942
CAND2	2.429995	1.280954	0.037551
ARHGEF39	2.405887	1.266569	0.0315
CHRM3	2.395598	1.260386	0.01318
C18orf61	2.395574	1.260371	0.037637
ATP2A1	2.393921	1.259376	0.049186
PPP1R13L	2.382823	1.252672	0.018272
HSD11B1L	2.348685	1.231853	0.023631
NUTM2B	2.320736	1.214583	0.046288

SSPO	2.30677	1.205874	0.011427
PPM1J	2.305017	1.204777	0.011925
SHC3	2.301752	1.202732	0.015997
EPS8L1	2.288972	1.1947	0.020927
ARHGEF25	2.275702	1.186312	0.032571
ZNF579	2.264267	1.179044	0.009365
JAZF1-AS1	2.258582	1.175417	0.0315
LIMCH1	2.249973	1.169908	0.038219
EFNA1	2.249844	1.169825	0.044729
CBX2	2.245445	1.167002	0.028942
CABLES1	2.241639	1.164554	0.015997
MDK	2.230195	1.15717	0.020065
GRID2IP	2.222353	1.152088	0.034584
SIGLEC15	2.215414	1.147576	0.01318
STARD4-AS1	2.214873	1.147224	0.02151
ZNF469	2.209597	1.143783	0.0315
PITPNM3	2.207295	1.14228	0.017817
SPTSSB	2.197966	1.136169	0.024309
PCOLCE-AS1	2.193375	1.133152	0.02161
M1AP	2.193105	1.132975	0.009365
TRPM4	2.192328	1.132464	0.043836
LOC728763	2.18857	1.129988	0.045977
CUX2	2.184189	1.127097	0.024295
RHBDL1	2.176972	1.122323	0.02063
MTSS1L	2.17479	1.120876	0.01581
ELOVL3	2.173823	1.120235	0.024792
ALDH7A1	2.155827	1.108242	0.028942
SLC4A3	2.155602	1.108091	0.020065
SCARF2	2.131326	1.091751	0.015568
RNF112	2.125509	1.087809	0.0315
DNAH11	2.115847	1.081235	0.034011
ZNF462	2.108524	1.076234	0.035839
ZBTB8A	2.106314	1.07472	0.024576
AGRN	2.089248	1.062984	0.045977
LMTK3	2.082036	1.057995	0.0315
FCGBP	2.07796	1.055168	0.044086
BAHCC1	2.056581	1.040248	0.02063
WFS1	2.036153	1.025846	0.017378
RASA4	2.035621	1.025469	0.044729
HSPG2	2.011807	1.008492	0.03458
IER5L	2.002854	1.002057	0.017378
SPTLC3	2.001095	1.00079	0.028686

List of down-regulated transcripts in AEROBIC *compared with* SEDENTARY AEROBIC *at follow-up 2* (FDR<0.05).

Transcript	**FC**	**logFC**	**FDR**
GLYATL2	0.063484	-3.977469739	0.033895
FUT10	0.448807	-1.155834137	0.022978
FLJ25917	0.458303	-1.12562568	0.0315

Appendix I

List of up-regulated transcripts in STRENGTH *compared with* SEDENTARY STRENGTH *at follow-up 2* (FDR<0.05).

Transcript	FC	logFC	FDR
RNF17	63.74663	5.994277173	0.001123
TREML4	13.26302	3.729336965	0.036647
FAM154B	3.081135	1.623462028	0.038914
ANKRD24	2.667957	1.415735279	0.007274
FAM167A	2.074398	1.052692922	0.042506

List of down-regulated transcripts in STRENGTH *compared with* SEDENTARY STRENGTH *at follow-up 2* (FDR<0.05).

Transcript	FC	logFC	FDR
CASC20	0.016545	-5.917439814	0.019197
LOC101928702	0.035877	-4.800788012	0.04985
CLUL1	0.114473	-3.12692307	0.015619
FAP	0.174569	-2.518127782	0.006961
TIMP3	0.182446	-2.454457205	0.031291
ALMS1P	0.19715	-2.342633105	0.001303
RSAD2	0.20142	-2.311721259	0.001208
IFI44L	0.240654	-2.054966272	0.005136
CD177	0.268447	-1.897292999	0.037838
NPRL3	0.27202	-1.878217442	0.014191
ANKRD22	0.273251	-1.871703828	0.004744
LAMP3	0.302947	-1.722865011	0.006519
GBP1P1	0.306101	-1.707919037	0.024948
IFIT1	0.311336	-1.683456808	0.012827
OAS3	0.337514	-1.566980353	0.005846
HERC5	0.347251	-1.525948481	0.008537
SERPING1	0.354789	-1.494965275	0.021674
HOXA-AS2	0.35479	-1.494962544	0.004766
GBP6	0.383128	-1.384101304	0.020408
IFI44	0.38394	-1.381045591	0.012665
ABCB11	0.388663	-1.363407827	0.031399
ISG15	0.390192	-1.357743294	0.012247
DIAPH3	0.39787	-1.329631161	0.020221
CXCL10	0.406053	-1.300259061	0.044477
MX1	0.411112	-1.282395157	0.021206
LOC644090	0.419988	-1.251578751	0.041442
SIGLEC1	0.423694	-1.238903992	0.02689
IFI6	0.42935	-1.219772899	0.026879
IFIT3	0.431066	-1.214020021	0.018396
ATF3	0.434244	-1.203421958	0.024049
HGNC:38231	0.434588	-1.202280242	0.014345

TRIM6	0.436071	-1.197365717	0.02168
CD274	0.443507	-1.172970379	0.026605
CMPK2	0.446216	-1.164186007	0.002689
FAM153B	0.463041	-1.110786653	0.031977
RSPH9	0.468953	-1.092485055	0.008726
USP18	0.475442	-1.072660196	0.02829

Appendix J

List of up-regulated circRNA in AEROBIC *compared with* SEDENTARY *at enrolment* (FDR<0.05).

Gene	FC	logFC	FDR
chr16__85633914__85634132___GSE1	8.659233	3.114239	3.17E-07
chr1__235196031__235214026___ARID4B	6.713555	2.747077	0.013658
chr10__93676653__93700106___FRA10AC1	6.49995	2.700429	0.001097
chr1__10403071__10408140___PGD	5.459575	2.448789	0.044815
chr1__47280241__47300152___STIL	5.092494	2.348372	0.040092
chr21__36359955__36364259___MORC3	5.038347	2.33295	0.043
chr16__8801799__8806407___PMM2	5.002557	2.322666	0.035431
chr2__169603642__169614724___PPIG	4.916796	2.297719	0.036015
chr18__79728907__79736521___CTDP1	3.684186	1.881346	0.01563
chr16__11020193__11126146___CLEC16A	3.209628	1.682406	0.010517
chr17__697418__699380___VPS53	3.079956	1.62291	0.047229
chr19__18537601__18538433___FKBP8	2.959355	1.565283	0.027479
chr9__33932562__33933628___UBAP2	2.9096	1.540821	0.005208
chr1__205268950__205269884___TMCC2	2.724764	1.446131	0.027941
chr8__130079902__130092143___ASAP1	2.634908	1.397753	0.021117
chr19__47264603__47264946___CCDC9	2.507031	1.32598	0.005676
chr19__18537601__18538436___FKBP8	2.222633	1.15227	0.02933
chr2__201350711__201351451___ALS2CR12	2.165422	1.114648	0.02666
chr19__8473664__8474244___HNRNPM	2.162022	1.112381	0.049385

List of down-regulated circRNA in AEROBIC *compared with* SEDENTARY *at enrolment* (FDR<0.05).

Gene	FC	logFC	FDR
chr2__88786470__88805408___ANKRD36BP2	0.007957	-6.97351	0.009687
chr1__149964222__149965878___OTUD7B	0.023652	-5.40188	0.000127
chr9__137790848__137818138___EHMT1	0.024479	-5.35228	7.72E-05
chr11__16097609__16234671___SOX6	0.026175	-5.25568	0.028643
chr6__42828493__42830172___GLTSCR1L	0.026214	-5.25354	0.000178
chr10__101461981__101479457___BTRC	0.028004	-5.15824	0.000155
chr10__72715111__72715902___MCU	0.029726	-5.07212	0.000468
chr4__42001616__42078325___SLC30A9	0.030142	-5.0521	0.000908
chr8__129903312__129912515___FAM49B	0.030362	-5.04157	0.040814
chr1__207647317__207753921___NA	0.032892	-4.92614	0.001097
chr10__103091564__103094455___NT5C2	0.03309	-4.91748	0.000685
chr17__50990450__50998617___SPAG9	0.033492	-4.90002	0.000468
chr22__29813430__29825780___ASCC2	0.033921	-4.88168	0.001283
chr14__24218059__24218431___NEDD8-MDP1NEDD8	0.034181	-4.87066	0.001097
chr8__38943789__38946221___PLEKHA2	0.034191	-4.87022	0.001283
chr4__105446383__105456745___PPA2	0.035307	-4.82391	0.000993
chr1__229525936__229549434___ABCB10	0.035564	-4.81345	0.001283
chr10__86443275__86446449___WAPAL	0.035634	-4.81059	0.001404
chr15__42827928__42840433___TTBK2	0.035648	-4.81004	0.001283

chr10__49493117__49506012___ERCC6	0.036134	-4.79049	0.00173
chr3__52411029__52423351___PHF7	0.036405	-4.77974	0.001283
chr15__28751488__28754897___WHAMMP2	0.036621	-4.77119	0.001404
chr1__29053104__29097935___EPB41	0.036648	-4.77011	0.001576
chr1__155725382__155726019___DAP3	0.036865	-4.76162	0.00173
chr13__59692717__59697771___DIAPH3	0.036881	-4.76098	0.001642
chr4__53383773__53428183___FIP1L1	0.037039	-4.7548	0.001576
chr14__30923210__30926885___STRN3	0.037169	-4.74976	0.001858
chr1__205719527__205729621___NUCKS1	0.037187	-4.74905	0.001404
chr5__58988493__58993465___PDE4D	0.038345	-4.7048	0.001598
chr17__61776401__61784424___BRIP1	0.039406	-4.66543	0.002389
chr1__246621429__246634587___CNST	0.039454	-4.66368	0.002021
chr5__179705679__179716294___CANX	0.039482	-4.66267	0.002389
chr8__99481599__99521010___VPS13B	0.039604	-4.65822	0.002055
chr5__40764514__40771863___PRKAA1	0.039622	-4.65754	0.002355
chr2__135748267__135780385___UBXN4	0.040007	-4.6436	0.002736
chr14__65561337__65629606___FUT8	0.04035	-4.63127	0.002389
chr11__62827155__62827631___STX5	0.040354	-4.63114	0.00214
chr12__112219386__112228811___HECTD4	0.040529	-4.62491	0.002389
chr3__20136942__20140364___KAT2B	0.041633	-4.58611	0.002846
chr10__1084403__1096246___WDR37	0.04174	-4.58242	0.003234
chr10__49908455__49935142___PARG	0.042146	-4.56847	0.003931
chr9__36597222__36607673___MELK	0.042625	-4.55215	0.003663
chr2__44484877__44505730___CAMKMT	0.043148	-4.53456	0.033966
chr8__94506500__94512089___KIAA1429	0.04357	-4.52053	0.003826
chr12__123160781__123203375___MPHOSPH9	0.043681	-4.51686	0.003826
chr1__10095461__10105744___UBE4B	0.043836	-4.51175	0.003931
chr10__45533110__45590574___MARCH8	0.04396	-4.50768	0.00333
chr14__103405076__103405267___MARK3	0.043962	-4.5076	0.003826
chr17__60265412__60301704___USP32	0.044255	-4.498	0.003931
chr9__89455888__89479825___SEMA4D	0.04427	-4.49752	0.003931
chr13__113585774__113640375___TFDP1	0.044617	-4.48625	0.003932
chr1__93903765__93904588___GCLM	0.044808	-4.48009	0.004054
chr1__231370562__231374099___EGLN1	0.044834	-4.47925	0.003931
chr10__118691265__118695230___CACUL1	0.044853	-4.47866	0.004054
chr1__185174372__185182057___SWT1	0.045	-4.47394	0.003931
chr17__45081644__45086652___NMT1	0.045074	-4.47155	0.004054
chr10__73692043__73713332___NA	0.045122	-4.47003	0.0043
chr18__50918110__50932360___ME2	0.045422	-4.46045	0.0043
chr4__169580842__169599197___NEK1	0.045436	-4.46003	0.0043
chr15__42264090__42268032___TMEM87A	0.045925	-4.44457	0.0043
chr8__21974670__21985691___XPO7	0.046839	-4.41616	0.004388
chr10__96852645__96858416___LCOR	0.046996	-4.41131	0.004892
chr18__2732265__2762236___SMCHD1	0.047005	-4.41103	0.004892
chr16__17355099__17358050___XYLT1	0.047179	-4.40571	0.005009
chr1__179990507__180006567___CEP350	0.04724	-4.40384	0.004892

chr3__183650296__183651276___KLHL24	0.047287	-4.4024	0.0049
chr1__113093206__113094755___LRIG2	0.047597	-4.39299	0.005009
chr4__139695197__139704196___MGST2	0.047889	-4.38417	0.004884
chr6__136276028__136276508___BCLAF1	0.048102	-4.37775	0.00503
chr2__24137909__24147086___FAM228B	0.048336	-4.37075	0.00503
chr1__113848540__113855049___PTPN22	0.048357	-4.37012	0.00503
chr5__132579317__132589837___RAD50	0.048408	-4.36862	0.00503
chr15__64112573__64118854___SNX1	0.048753	-4.35835	0.00503
chrX__118394055__118407026___WDR44	0.048758	-4.35823	0.00503
chr1__243293091__243344331___SDCCAG8	0.048769	-4.35788	0.00503
chr18__70121556__70128546___RTTN	0.048794	-4.35716	0.00503
chr19__11648358__11650417___NA	0.048887	-4.35441	0.005224
chr15__63734724__63756748___HERC1	0.048957	-4.35233	0.00503
chr17__67910877__67944372___BPTF	0.049131	-4.34723	0.00503
chr16__53498391__53500329___AKTIP	0.049357	-4.34061	0.005208
chr2__8877030__8958642___MBOAT2	0.049585	-4.33396	0.005346
chr14__70584817__70597777___MED6	0.049614	-4.33312	0.00503
chr1__13715541__13749487___PRDM2	0.049707	-4.3304	0.00533
chr17__62011178__62063222___MED13	0.0498	-4.32771	0.005222
chr14__73355626__73366981___NUMB	0.049897	-4.3249	0.00551
chr14__71413948__71414680___LOC102724024	0.050128	-4.31823	0.00551
chr2__20254863__20256170___PUM2	0.050138	-4.31795	0.005346
chr12__50981639__51010766___SLC11A2	0.050147	-4.31771	0.00503
chr5__138006990__138021197___FAM13B	0.050695	-4.302	0.00551
chr3__119947268__120093593___GSK3B	0.050837	-4.29797	0.005208
chr6__87215903__87233527___ZNF292	0.050845	-4.29775	0.005526
chr5__50399232__50411383___EMB	0.050905	-4.29604	0.005676
chr3__43303098__43303792___SNRK	0.051159	-4.28886	0.005569
chr1__44002313__44002985___SLC6A9	0.051286	-4.2853	0.005676
chr7__50319048__50391863___IKZF1	0.051459	-4.28044	0.005676
chr13__50044651__50045232___DLEU2	0.05146	-4.2804	0.005676
chr5__108348399__108367953___FBXL17	0.05149	-4.27957	0.005676
chr17__60198260__60214774___USP32	0.051607	-4.27628	0.005676
chrX__20193487__20195145___RPS6KA3	0.051711	-4.27338	0.005676
chr7__131375424__131411383___MKLN1	0.051868	-4.269	0.005725
chr10__67954595__68014186___HERC4	0.051904	-4.26801	0.005685
chr11__35196746__35204640___CD44	0.051938	-4.26706	0.005676
chr10__119580471__119580846___TIAL1	0.051948	-4.2668	0.005676
chr17__60265412__60288682___USP32	0.052232	-4.25892	0.005676
chr17__49316826__49322508___ZNF652	0.052506	-4.25136	0.005725
chr17__78004170__78009697___TNRC6C	0.052625	-4.24811	0.005822
chr5__43122039__43174494___ZNF131	0.052638	-4.24774	0.005725
chr20__17956933__17961326___SNX5	0.052674	-4.24675	0.005676
chr12__32607957__32611283___FGD4	0.052696	-4.24617	0.005645
chr1__227112312__227119937___CDC42BPA	0.052835	-4.24235	0.005676
chr11__16318446__16341252___SOX6	0.052883	-4.24105	0.005725

chr15__69421647__69423329___KIF23	0.053149	-4.23381	0.005792
chr15__50637422__50639548___TRPM7	0.053233	-4.23154	0.005676
chr15__49625113__49634794___DTWD1	0.053255	-4.23093	0.005854
chr6__98899268__98927822___FBXL4	0.053542	-4.2232	0.006053
chr17__5350451__5363016___RABEP1	0.053596	-4.22174	0.006
chr5__154790325__154792796___LARP1	0.05363	-4.22081	0.005685
chr1__77916055__77918273___NEXN	0.053656	-4.22011	0.006
chr10__13127745__13133581___OPTN	0.053788	-4.21657	0.006159
chr1__229539456__229542371___ABCB10	0.053814	-4.21587	0.005676
chr17__29482197__29498521___TAOK1	0.053952	-4.21217	0.006159
chr6__98875415__98934879___FBXL4	0.053954	-4.21213	0.006
chr5__65528452__65552549___CENPK	0.053959	-4.212	0.006159
chr6__20781145__20955585___CDKAL1	0.05397	-4.21171	0.006159
chr17__39423327__39432016___MED1	0.054188	-4.20587	0.006182
chr13__32436361__32480637___N4BP2L2	0.054251	-4.2042	0.005822
chr12__46239679__46254936___SLC38A1	0.054296	-4.20301	0.006318
chr5__109817273__109830980___MAN2A1	0.054418	-4.19976	0.006309
chr13__72728926__72731387___BORA	0.054418	-4.19978	0.006182
chr19__47089967__47094608___ZC3H4	0.05443	-4.19944	0.006318
chr1__100906852__100921841___SLC30A7	0.054521	-4.19705	0.006309
chr20__44503815__44514040___SERINC3	0.054624	-4.19432	0.006352
chr17__35063576__35066466___RFFLRAD51L3-RFFL	0.054669	-4.19313	0.006375
chr5__60748267__60767903___NA	0.05492	-4.18651	0.005822
chr22__38495796__38501280___DDX17	0.055476	-4.172	0.006352
chr14__45008913__45032376___FAM179B	0.055556	-4.16993	0.006375
chr11__111836165__111857737___ALG9	0.055644	-4.16763	0.006375
chr17__68209654__68210465___AMZ2	0.055759	-4.16465	0.006647
chr20__44479985__44480444___TTPAL	0.055843	-4.16249	0.006647
chr9__105484381__105539351___FSD1L	0.056005	-4.15829	0.006647
chr14__60267215__60277091___PPM1A	0.056052	-4.1571	0.006808
chr2__226838073__226924163___RHBDD1	0.056098	-4.15592	0.006647
chr17__76738282__76742048___MFSD11	0.056222	-4.15271	0.006783
chr11__76513386__76516312___C11orf30	0.056301	-4.15069	0.006739
chr15__68086306__68164804___PIAS1	0.05634	-4.14969	0.006994
chr17__61972727__61983114___MED13	0.05636	-4.14919	0.006752
chr2__71401956__71418639___ZNF638	0.056386	-4.14852	0.006647
chr8__130214556__130236994___ASAP1	0.056478	-4.14616	0.006783
chr4__103163137__103181456___CENPE	0.056698	-4.14056	0.006879
chr3__20174249__20178347___SGOL1	0.056784	-4.13837	0.006752
chr12__68715627__68727389___NUP107	0.05701	-4.13264	0.006389
chr15__63553715__63574403___USP3	0.057064	-4.13127	0.00691
chr2__180982018__180991871___UBE2E3	0.057153	-4.12902	0.006783
chr11__77722688__77725699___RSF1	0.057162	-4.12879	0.007321
chr6__18159883__18166378___KDM1B	0.057324	-4.12472	0.006868
chr17__40406384__40413625___TOP2A	0.05741	-4.12255	0.007304
chr12__49097566__49098105___LMBR1L	0.057552	-4.11899	0.007321

chr5__157294783__157296774___CYFIP2	0.057598	-4.11783	0.007321
chr8__99442401__99521010___VPS13B	0.057613	-4.11745	0.007325
chr15__87355549__87422836___NA	0.057669	-4.11606	0.010601
chr6__13579451__13600949___SIRT5	0.057704	-4.11517	0.006932
chr11__17959470__18008076___SERGEF	0.057767	-4.11361	0.006487
chr14__55315300__55316355___FBXO34	0.057774	-4.11343	0.007314
chr16__14552021__14555709___PARN	0.057852	-4.1115	0.007321
chr19__45854175__45854507___SYMPK	0.058109	-4.10509	0.007325
chr6__135192324__135200415___MYB	0.058146	-4.10417	0.007589
chr6__131145285__131200489___AKAP7	0.058146	-4.10418	0.00735
chr6__82957312__83044659___UBE3D	0.058189	-4.10311	0.007512
chr4__42551198__42556040___ATP8A1	0.058293	-4.10053	0.007512
chr7__130116445__130129576___KLHDC10	0.058455	-4.09652	0.007321
chr17__58694931__58709990___RAD51C	0.058511	-4.09514	0.007512
chr5__168568646__168568998___PANK3	0.058662	-4.09142	0.007512
chr19__53805280__53814988___NLRP12	0.058683	-4.09091	0.007512
chr9__132286423__132311856___SETX	0.058692	-4.0907	0.007459
chr2__169905114__169914146___UBR3	0.058713	-4.09017	0.007581
chr9__120518427__120539164___CDK5RAP2	0.058749	-4.08928	0.007512
chr18__76862186__76865026___ZNF236	0.058761	-4.08899	0.007215
chr11__16283756__16341252___SOX6	0.0588	-4.08803	0.007581
chr5__108341927__108348530___FBXL17	0.058819	-4.08756	0.007714
chr1__201852104__201858994___IPO9	0.058894	-4.08573	0.007661
chr13__21381434__21401685___ZDHHC20	0.05892	-4.0851	0.007512
chr14__45227663__45242518___MIS18BP1	0.059007	-4.08296	0.007589
chr10__68753852__68791341___CCAR1	0.059107	-4.08052	0.005822
chr2__29121374__29181697___CLIP4	0.059316	-4.07544	0.007714
chr7__139053451__139054095___ZC3HAV1	0.059345	-4.07473	0.007714
chr13__99539446__99552326___TM9SF2	0.059426	-4.07277	0.007714
chr17__40396283__40399131___TOP2A	0.059436	-4.07251	0.007714
chr10__63190894__63194375___JMJD1C	0.059474	-4.07159	0.007589
chr4__55403236__55417985___TMEM165	0.059477	-4.07152	0.007325
chr1__193130174__193152444___CDC73	0.059484	-4.07136	0.007589
chr13__77243059__77243951___MYCBP2	0.059543	-4.06993	0.007926
chr13__25307806__25325068___NUPL1	0.05975	-4.06492	0.007512
chr13__28197185__28220378___PAN3	0.059816	-4.06334	0.007926
chr15__98707562__98708107___IGF1R	0.059942	-4.06028	0.007926
chr11__16183886__16270068___SOX6	0.059978	-4.05941	0.007861
chr8__38114192__38135766___ASH2L	0.06	-4.05889	0.007926
chr6__99526064__99531790___TSTD3	0.060187	-4.0544	0.007926
chr14__21371874__21373430___SUPT16H	0.060206	-4.05396	0.007926
chr3__50108070__50108304___RBM5	0.060256	-4.05275	0.007542
chr1__29035826__29072791___EPB41	0.060317	-4.05129	0.007926
chr5__138006990__138011945___FAM13B	0.060472	-4.04759	0.007714
chr9__7040470__7049200___KDM4C	0.060535	-4.04607	0.007589
chr6__90206569__90271941___BACH2	0.060541	-4.04594	0.007926

chr2__15424315__15511350___NBAS	0.060556	-4.04559	0.007926
chr15__74926766__74929232___COX5A	0.060661	-4.04308	0.007688
chr5__77034418__77036720___AGGF1	0.060677	-4.04271	0.007926
chr18__26315229__26335231___TAF4B	0.060842	-4.03879	0.008048
chr6__85517756__85530275___SNX14	0.060927	-4.03678	0.007926
chr13__95157161__95188542___ABCC4	0.061026	-4.03442	0.007926
chr16__67744288__67759732___RANBP10	0.061046	-4.03395	0.007926
chr7__74705164__74718941___GTF2I	0.061186	-4.03066	0.007926
chr10__27526828__27533994___RAB18	0.061303	-4.02791	0.008059
chr19__21447650__21463843___NA	0.061399	-4.02564	0.007926
chr14__31113104__31133675___HECTD1	0.061475	-4.02385	0.008152
chr2__27382126__27387158___PPM1G	0.061617	-4.02052	0.007926
chr4__128992167__129082373___SCLT1	0.06164	-4.02	0.008212
chr4__48833401__48857365___OCIAD1	0.061714	-4.01825	0.008212
chr2__70160625__70181997___C2orf42	0.061733	-4.01781	0.008212
chr4__128957026__129003876___SCLT1	0.061804	-4.01616	0.008348
chr15__49916934__49934182___ATP8B4	0.061808	-4.01605	0.008152
chr17__35362739__35363826___SLFN11	0.061856	-4.01494	0.008437
chr16__75603085__75622464___ADAT1	0.061998	-4.01163	0.008111
chr20__44978443__45001353___STK4	0.062002	-4.01154	0.007926
chr1__235219793__235240451___ARID4B	0.062035	-4.01077	0.008348
chr20__35858302__35869551___PHF20	0.062102	-4.00921	0.008348
chr2__108839185__108856970___CCDC138	0.062147	-4.00817	0.007926
chr11__46776255__46788773___CKAP5	0.062232	-4.00619	0.007926
chr1__223798215__223800047___TP53BP2	0.062278	-4.00513	0.008348
chr11__85981745__86007583___PICALM	0.062315	-4.00427	0.007926
chr7__7234303__7238922___C1GALT1	0.06234	-4.00369	0.007714
chr3__196065443__196075360___TFRC	0.062354	-4.00338	0.008348
chr5__168557423__168568998___PANK3	0.062362	-4.0032	0.008348
chr13__19730239__19759418___PSPC1	0.062457	-4.00099	0.008348
chr1__246627356__246628267___CNST	0.062502	-3.99996	0.007926
chr18__9522160__9522509___RALBP1	0.062644	-3.99669	0.008536
chr10__63184608__63194375___JMJD1C	0.062652	-3.9965	0.008348
chr15__56666395__56682477___ZNF280D	0.062736	-3.99455	0.00805
chr17__20053579__20057817___SPECC1	0.062912	-3.99053	0.008111
chr11__16097609__16111926___SOX6	0.06308	-3.98667	0.008536
chr22__29978442__29998857___MTMR3	0.063194	-3.98406	0.008348
chr19__2185855__2194577___DOT1L	0.063407	-3.97921	0.008536
chr11__34086064__34090678___CAPRIN1	0.063419	-3.97894	0.008777
chrX__14843660__14869043___FANCB	0.063431	-3.97867	0.008777
chr22__21788257__21807846___MAPK1	0.063518	-3.97668	0.00892
chr10__96907265__96907747___LCOR	0.063537	-3.97625	0.00851
chr17__60271350__60288682___USP32	0.063581	-3.97526	0.008536
chr17__16137311__16153395___NCOR1	0.06359	-3.97507	0.008536
chr20__25632158__25634170___NA	0.063596	-3.97491	0.008827
chr22__32479133__32493281___FBXO7	0.063702	-3.97253	0.008619

chr15__101701086__101714963___TARSL2	0.063909	-3.96783	0.008905
chr14__52470037__52491005___TXNDC16	0.063967	-3.96652	0.007714
chr20__37056146__37062270___RBL1	0.064055	-3.96454	0.008997
chr4__78842385__78865720___BMP2K	0.064061	-3.96441	0.008536
chr5__75685207__75702810___POC5	0.064149	-3.96243	0.008212
chr5__151452343__151479489___SLC36A1	0.064238	-3.96043	0.008905
chr6__42663278__42666245___UBR2	0.064282	-3.95943	0.008424
chr3__49962576__49975392___RBM6	0.064331	-3.95834	0.008921
chr12__20616230__20635056___PDE3A	0.064334	-3.95827	0.008921
chr5__115532961__115542901___FEM1C	0.064364	-3.95759	0.008348
chr14__73089049__73089455___RBM25	0.064516	-3.9542	0.007926
chr14__72981789__72993357___ZFYVE1	0.064581	-3.95274	0.008997
chr3__25642322__25645455___TOP2B	0.064748	-3.94902	0.008827
chr5__154865442__154867792___CNOT8	0.064806	-3.94773	0.008731
chr1__236803428__236863554___MTR	0.064862	-3.94648	0.009061
chrX__65821624__65822042___NA	0.064902	-3.9456	0.009258
chrX__123696021__123697751___THOC2	0.065049	-3.94232	0.008212
chr10__27158549__27165539___MASTL	0.065049	-3.94232	0.008997
chr6__111654024__111655556___NA	0.065063	-3.94202	0.009288
chr2__32377588__32406557___BIRC6	0.065377	-3.93507	0.00932
chr2__128183675__128187614___UGGT1	0.065388	-3.93483	0.00928
chr20__5565017__5570239___GPCPD1	0.065396	-3.93466	0.009288
chr18__69873144__69947532___CD226	0.065436	-3.93377	0.009288
chr15__44633505__44657263___SPG11	0.065438	-3.93374	0.009358
chr6__99558497__99561681___CCNC	0.06563	-3.92949	0.00959
chr10__68459104__68465812___DNA2	0.065654	-3.92896	0.009358
chr1__207723618__207724708___NA	0.06575	-3.92687	0.009415
chr1__147293629__147294517___CHD1L	0.065763	-3.92658	0.008997
chr17__27304780__27309272___WSB1	0.065769	-3.92644	0.008731
chr6__89846562__89855544___CASP8AP2	0.065778	-3.92624	0.009358
chr16__70219912__70222480___LOC100506060	0.065806	-3.92565	0.009578
chr9__37768076__37770739___TRMT10B	0.065832	-3.92508	0.009358
chr3__170136419__170136665___PHC3	0.065868	-3.92428	0.009415
chr17__82905936__82911789___TBCD	0.065951	-3.92246	0.009415
chr17__50970707__50987237___SPAG9	0.066019	-3.92098	0.008997
chr1__51402435__51448135___EPS15	0.066067	-3.91993	0.009415
chr2__74156418__74172752___MOB1A	0.06609	-3.91941	0.009415
chr6__154773989__154778045___SCAF8	0.066157	-3.91797	0.009415
chr20__35863013__35871829___PHF20	0.06624	-3.91616	0.009578
chr15__63712775__63734849___HERC1	0.066245	-3.91604	0.009578
chr2__86740927__86773435___RMND5A	0.066367	-3.9134	0.009578
chr8__67118248__67137603___CSPP1	0.066377	-3.91317	0.00959
chr21__33765875__33767828___ITSN1	0.066382	-3.91307	0.009583
chr9__17309058__17366717___CNTLN	0.066387	-3.91295	0.00959
chr1__235438769__235442911___TBCE	0.066535	-3.90975	0.009415
chr15__49011731__49017628___SECISBP2L	0.066651	-3.90722	0.009358

chr16__69160356__69167185___CIRH1A	0.066678	-3.90664	0.008779
chr4__155696756__155722192___GUCY1A3	0.066691	-3.90636	0.009738
chr14__31144111__31172122___HECTD1	0.066705	-3.90606	0.007325
chr8__140830472__140864399___PTK2	0.066997	-3.89976	0.009687
chr7__8003908__8071131___GLCCI1	0.067129	-3.89693	0.008348
chr18__21791374__21804014___MIB1	0.067292	-3.89343	0.00959
chr12__62349221__62384302___USP15	0.067293	-3.8934	0.009061
chr7__27785163__27794446___TAX1BP1	0.067319	-3.89284	0.009738
chr1__160836195__160839049___CD244	0.067352	-3.89213	0.009674
chr14__34597550__34609742___SNX6	0.067463	-3.88976	0.009578
chr16__89895038__89900794___TCF25	0.067469	-3.88964	0.009687
chr2__30476577__30479911___LCLAT1	0.067498	-3.88902	0.009687
chr4__2952275__2956811___NOP14	0.067577	-3.88732	0.008822
chr3__141970073__141995141___TFDP2	0.067625	-3.8863	0.009687
chr15__65667449__65697383___DENND4A	0.06777	-3.88321	0.010052
chr12__100097365__100103951___UHRF1BP1L	0.067836	-3.8818	0.009415
chr15__22278818__22282869___REREP3	0.068002	-3.87829	0.009415
chr1__172092824__172131288___DNM3	0.068071	-3.87682	0.009862
chr8__37862737__37877551___RAB11FIP1	0.0682	-3.87408	0.008997
chr17__43095846__43104956___BRCA1	0.068223	-3.8736	0.010098
chr2__8243565__8287558___LINC00299	0.068248	-3.87307	0.009759
chr2__135748267__135761911___UBXN4	0.068336	-3.8712	0.009854
chr15__90439332__90443478___IQGAP1	0.068354	-3.87083	0.010069
chr10__117243971__117253457___SLC18A2	0.068502	-3.86771	0.010125
chr8__70123884__70124865___NCOA2	0.068677	-3.86403	0.010134
chr2__55206270__55218600___CLHC1	0.068727	-3.86297	0.010265
chr13__40749138__40759106___MRPS31	0.068889	-3.85957	0.010245
chr1__168231514__168243069___NA	0.068903	-3.85928	0.009
chr2__210104104__210154611___KANSL1L	0.068913	-3.85908	0.010265
chr1__45602255__45606591___NASP	0.068935	-3.85861	0.010069
chr9__83669185__83686155___UBQLN1	0.069207	-3.85293	0.010134
chr22__40273425__40280143___TNRC6B	0.06928	-3.85142	0.010069
chr9__85822880__85849543___NA	0.069283	-3.85135	0.010265
chr3__172761610__172784803___ECT2	0.0694	-3.84892	0.010265
chr17__20204333__20247319___SPECC1	0.069407	-3.84878	0.009578
chr3__197081051__197085756___DLG1	0.069573	-3.84534	0.010438
chr4__6994184__7014557___TBC1D14	0.06966	-3.84353	0.00959
chr1__100123210__100125942___SASS6	0.069704	-3.84261	0.010438
chr19__23358430__23362739___ZNF91	0.069706	-3.84256	0.010069
chr21__37087247__37108446___TTC3	0.069708	-3.84253	0.010069
chr1__91501654__91520279___CDC7	0.069804	-3.84054	0.010069
chr9__37126312__37247130___ZCCHC7	0.069843	-3.83975	0.010464
chr1__70292388__70324957___ANKRD13C	0.06986	-3.83939	0.009862
chr17__47142229__47143982___CDC27	0.069935	-3.83784	0.010601
chr1__1825397__1879902___GNB1	0.069941	-3.83773	0.00851
chr7__156966270__156967092___NOM1	0.069951	-3.83751	0.010434

chr10__119038238__119042772___EIF3A	0.069998	-3.83654	0.010438
chr2__190899117__190924593___GLS	0.070025	-3.83598	0.009791
chr18__77095368__77097474___MBP	0.070052	-3.83543	0.010941
chr17__61982198__61995365___MED13	0.07007	-3.83506	0.010265
chr4__139393591__139404490___NA	0.070099	-3.83446	0.010069
chr10__32021022__32021287___KIF5B	0.0701	-3.83444	0.010498
chr1__171523221__171537473___PRRC2C	0.070108	-3.83428	0.010464
chr20__44978443__45025130___STK4	0.070109	-3.83426	0.010602
chr20__50902017__50904001___ADNP	0.070189	-3.83261	0.010245
chr6__63646527__63680161___PHF3	0.070232	-3.83172	0.010738
chr8__140879471__140890769___PTK2	0.07024	-3.83155	0.010069
chr16__67610824__67616878___CTCF	0.070285	-3.83064	0.009862
chr12__122515105__122522299___RSRC2	0.0703	-3.83032	0.009578
chr1__93210802__93239896___CCDC18	0.070335	-3.82961	0.010786
chr1__179341028__179343635___SOAT1	0.070374	-3.8288	0.009533
chrX__107088436__107088839___RBM41	0.07041	-3.82808	0.010601
chr2__121757240__121763084___TSN	0.070453	-3.8272	0.010265
chr1__20747544__20773610___HP1BP3	0.070465	-3.82695	0.010791
chr2__201022059__201024039___FAM126B	0.070471	-3.82682	0.010791
chr10__30313891__30349277___MTPAP	0.070566	-3.82488	0.009358
chr11__85981129__85981988___PICALM	0.070575	-3.8247	0.010542
chr6__130022227__130071127___L3MBTL3	0.070655	-3.82307	0.010069
chr4__88061906__88068061___PKD2	0.070715	-3.82184	0.010733
chr5__36953618__36986301___NIPBL	0.07081	-3.81991	0.010554
chr14__57229734__57247712___EXOC5	0.07088	-3.81848	0.001576
chr2__233263130__233265143___ATG16L1	0.070935	-3.81737	0.010811
chr13__49168613__49175541___FNDC3A	0.07097	-3.81664	0.010811
chr14__54984723__55002185___WDHD1	0.07098	-3.81645	0.010811
chr13__30227412__30241086___KATNAL1	0.07104	-3.81522	0.011011
chr7__8059053__8060248___GLCCI1	0.07105	-3.81502	0.010811
chr8__17205655__17210480___ZDHHC2	0.071114	-3.81373	0.010854
chr21__15799757__15833548___USP25	0.07112	-3.8136	0.010854
chr17__3705098__3705645___NA	0.071187	-3.81224	0.010854
chr14__103448919__103462461___MARK3	0.071466	-3.8066	0.009687
chr22__28694032__28719485___CHEK2	0.071528	-3.80534	0.009801
chr14__73147795__73198129___PSEN1	0.071558	-3.80474	0.010854
chr8__11808794__11838573___FDFT1	0.071601	-3.80388	0.001701
chr8__47407861__47440542___SPIDR	0.071728	-3.80132	0.00959
chr3__17586353__17625224___TBC1D5	0.071731	-3.80126	0.010811
chr12__56741435__56744123___PRIM1	0.071789	-3.80009	0.010464
chr17__47370437__47414919___EFCAB13	0.071917	-3.79752	0.010265
chr11__110136663__110137414___ZC3H12C	0.071935	-3.79717	0.009854
chrX__134413488__134417302___PHF6	0.071991	-3.79604	0.010394
chr3__44814911__44828300___KIF15	0.072021	-3.79543	0.011283
chr1__227254064__227260784___CDC42BPA	0.072029	-3.79528	0.011283
chr4__145823422__145849561___ZNF827	0.072061	-3.79465	0.010554

chr10__32543300__32567891___CCDC7	0.072149	-3.79287	0.010134
chr15__68086306__68146700___PIAS1	0.072389	-3.78808	0.011473
chr16__47428804__47459175___ITFG1	0.072423	-3.78741	0.011244
chr16__68093356__68126610___NFATC3	0.072431	-3.78724	0.010528
chr3__196053418__196069568___TFRC	0.072474	-3.78639	0.010245
chr2__26123518__26124047___RAB10	0.072503	-3.78581	0.011688
chr12__100313422__100326754___SCYL2	0.072551	-3.78486	0.011283
chr18__46118181__46128837___NA	0.072633	-3.78322	0.000685
chr19__47084345__47094608___ZC3H4	0.072687	-3.78216	0.010854
chr16__16124789__16125911___ABCC1	0.072696	-3.78198	0.011409
chr15__41371527__41380203___NUSAP1	0.072766	-3.78059	0.010069
chr11__119076897__119077647___VPS11	0.072792	-3.78008	0.011343
chr1__113952766__113968648___HIPK1	0.072801	-3.77989	0.009862
chr15__67630888__67664645___MAP2K5	0.07285	-3.77893	0.010934
chr12__411747__438554___CCDC77	0.072915	-3.77763	0.009854
chr6__145888020__145894977___SHPRH	0.072937	-3.77721	0.011297
chr1__28987448__29011907___EPB41	0.072961	-3.77672	0.011424
chr1__207545308__207717691___NA	0.073008	-3.77579	0.010069
chr7__131375424__131429145___MKLN1	0.073012	-3.77572	0.011473
chr8__100137565__100138450___FBXO43	0.073037	-3.77523	0.011244
chr9__96509673__96565483___CDC14B	0.073081	-3.77436	0.010854
chr12__124419957__124437996___NCOR2	0.07314	-3.7732	0.01196
chr12__71656885__71660427___ZFC3H1	0.07318	-3.77241	0.011473
chr10__73154256__73156655___ECD	0.073213	-3.77176	0.011244
chr7__26684736__26739964___SKAP2	0.073216	-3.77169	0.010854
chr12__119767087__119776842___CIT	0.073224	-3.77154	0.011471
chr17__27301788__27309272___WSB1	0.073294	-3.77017	0.010791
chr3__44801450__44811043___KIF15	0.073338	-3.76929	0.009061
chr18__9182382__9216900___ANKRD12	0.073368	-3.76871	0.01182
chr17__76738282__76776541___MFSD11	0.073409	-3.7679	0.011473
chr7__77581427__77583650___PTPN12	0.073495	-3.7662	0.01161
chr8__73673107__73709162___STAU2	0.073504	-3.76603	0.011163
chrX__19683823__19706984___SH3KBP1	0.073519	-3.76574	0.011496
chr2__37199704__37206248___NA	0.073542	-3.76529	0.009862
chr4__39910244__39925933___PDS5A	0.073566	-3.76482	0.011297
chr1__39804878__39808198___NA	0.073633	-3.76351	0.011409
chrX__139814878__139826823___ATP11C	0.073643	-3.76331	0.011244
chr15__42827928__42878684___TTBK2	0.073729	-3.76163	0.011163
chr17__62536170__62565137___TLK2	0.073784	-3.76055	0.011011
chr11__76513386__76523291___C11orf30	0.073844	-3.75938	0.011473
chr14__60258964__60277091___PPM1A	0.073866	-3.75894	0.011163
chr6__41052265__41055999___NA	0.074077	-3.75484	0.008997
chr14__67398007__67402868___PLEK2	0.074088	-3.75461	0.010962
chr1__92320599__92345914___RPAP2	0.074256	-3.75134	0.011424
chr12__124419957__124449867___NCOR2	0.074265	-3.75117	0.011686
chr14__91797785__91813825___TC2N	0.074275	-3.75098	0.011936

chr6__131160059__131199573___AKAP7	0.074284	-3.7508	0.011936
chr15__67344063__67359885___IQCH	0.074315	-3.75019	0.011627
chr13__72728926__72735005___BORA	0.074432	-3.74793	0.011409
chr3__195320701__195345317___ACAP2	0.074496	-3.7467	0.011686
chr2__135602500__135622732___R3HDM1	0.074558	-3.7455	0.011424
chr2__181458268__181485992___ITGA4	0.074595	-3.74478	0.011936
chr10__102362475__102363798___GBF1	0.074596	-3.74475	0.009209
chr18__50918110__50924212___ME2	0.074664	-3.74344	0.012149
chr15__68141946__68146700___PIAS1	0.074691	-3.74292	0.010811
chr16__27434347__27437687___IL21R	0.074976	-3.73744	0.010967
chr9__17388162__17416189___CNTLN	0.075037	-3.73625	0.011908
chr17__47402132__47440502___EFCAB13	0.075104	-3.73497	0.012097
chr7__77581427__77592256___PTPN12	0.075289	-3.73142	0.012149
chr15__42950262__42966286___UBR1	0.075305	-3.7311	0.012004
chr1__42828289__42830298___ERMAP	0.07535	-3.73024	0.012149
chr14__103448919__103480490___MARK3	0.075481	-3.72775	0.012164
chr17__44299410__44304207___NA	0.075506	-3.72727	0.011244
chr2__53714384__53716743___ASB3GPR75-ASB3	0.075508	-3.72724	0.011283
chr12__116237468__116237705___MED13L	0.075621	-3.72506	0.012327
chr19__14743420__14743784___EMR2	0.075658	-3.72436	0.010601
chr12__75282251__75326527___CAPS2	0.0757	-3.72357	0.011473
chr16__58528475__58534395___CNOT1	0.075778	-3.72208	0.012485
chr7__130116445__130122202___KLHDC10	0.075901	-3.71975	0.011496
chr14__54981540__55002185___WDHD1	0.075936	-3.71907	0.012097
chr9__121088296__121115200___CNTRL	0.075944	-3.71893	0.010854
chr11__28211062__28233585___METTL15	0.076005	-3.71776	0.012188
chr1__213071006__213117410___RPS6KC1	0.076028	-3.71733	0.012489
chr14__39401176__39412725___FBXO33	0.076048	-3.71694	0.010791
chr5__157241646__157244478___ITK	0.076096	-3.71604	0.012149
chr14__60115719__60125823___PCNXL4	0.07613	-3.7154	0.012149
chr5__113001084__113001674___DCP2	0.07617	-3.71464	0.012251
chr1__155395459__155404350___ASH1L	0.076211	-3.71386	0.011686
chr20__46393093__46394503___ELMO2	0.076252	-3.71308	0.012327
chr22__31602212__31602785___SFI1	0.076258	-3.71296	0.012211
chrX__17029526__17103779___REPS2	0.076378	-3.7107	0.012149
chr15__51887589__51902036___TMOD3	0.076414	-3.71002	0.012542
chr22__40953555__40967884___RBX1	0.076477	-3.70882	0.01232
chr16__3850297__3854850___CREBBP	0.076579	-3.7069	0.012489
chr9__97369922__97371706___CCDC180LOC100499484-C9ORF174	0.076677	-3.70506	0.010941
chr20__5565017__5604440___GPCPD1	0.07668	-3.705	0.011936
chr6__84155298__84186623___KIAA1009	0.076688	-3.70485	0.012188
chr12__100282943__100329319___SCYL2	0.076734	-3.70399	0.011163
chr17__64341634__64352463___PECAM1	0.076769	-3.70333	0.012149
chr8__99556450__99661491___VPS13B	0.076808	-3.70261	0.011936
chr6__158605267__158608750___TMEM181	0.077037	-3.6983	0.012149

chr18__26032399__26057742___SS18	0.077071	-3.69766	0.012285
chr17__16186554__16194639___NCOR1	0.077091	-3.6973	0.011099
chr18__22968806__22984990___RBBP8	0.077093	-3.69725	0.012211
chr10__86497201__86500743___WAPAL	0.077137	-3.69642	0.011473
chr3__123271522__123272563___SEC22A	0.077154	-3.69611	0.012889
chr17__62011002__62063222___MED13	0.077212	-3.69503	0.012884
chr1__46565041__46572167___MKNK1	0.077397	-3.69158	0.012978
chr3__17010905__17014911___PLCL2	0.077404	-3.69145	0.011663
chr16__53439016__53454842___RBL2	0.077499	-3.68967	0.012843
chr2__73572262__73573498___ALMS1	0.077691	-3.68612	0.010967
chr10__31355144__31461237___ZEB1	0.077739	-3.68522	0.012619
chr15__63223042__63249705___RAB8B	0.077935	-3.68159	0.013381
chr12__111525192__111552977___ATXN2	0.077976	-3.68083	0.012327
chr18__57559145__57580199___FECH	0.077977	-3.68081	0.012877
chr1__1495485__1529331___NA	0.078003	-3.68033	0.013239
chr9__96364464__96368305___SLC35D2	0.078078	-3.67894	0.011686
chr14__72693076__72731934___DPF3	0.078093	-3.67866	0.012513
chr3__100294845__100296275___TBC1D23	0.078141	-3.67777	0.012149
chr1__180003174__180024582___CEP350	0.078211	-3.67648	0.011686
chr1__185174372__185204863___SWT1	0.078214	-3.67642	0.011473
chr13__49976333__50045232___NA	0.078364	-3.67366	0.012722
chr2__101288973__101295181___RNF149	0.078378	-3.67341	0.012872
chr1__15916128__15922349___SPEN	0.078397	-3.67305	0.0105
chr14__55380573__55382191___ATG14	0.078413	-3.67276	0.013381
chr9__34306252__34311371___KIF24	0.07843	-3.67246	0.010811
chr4__4457191__4471706___STX18	0.078444	-3.67219	0.013906
chr13__19824920__19851957___ZMYM5	0.078513	-3.67092	0.012531
chr9__15486006__15490124___PSIP1	0.078676	-3.66793	0.012149
chr20__2955609__2965202___PTPRA	0.078681	-3.66785	0.011163
chr6__53505392__53509250___GCLC	0.078727	-3.667	0.013381
chr5__169747396__169761625___DOCK2	0.078768	-3.66625	0.012211
chr15__63674342__63675093___HERC1	0.078797	-3.66572	0.012999
chr16__67036639__67082308___CBFB	0.078931	-3.66327	0.013284
chr1__29115699__29117989___EPB41	0.079006	-3.6619	0.010854
chr11__16183886__16247560___SOX6	0.079041	-3.66126	0.011667
chr14__101882161__101912473___PPP2R5C	0.079244	-3.65755	0.013495
chr12__108619325__108620848___NA	0.079253	-3.65739	0.012327
chr5__126804776__126832801___LMNB1	0.07931	-3.65635	0.013203
chr8__55950459__55953984___LYN	0.079337	-3.65587	0.013658
chr4__15612266__15644708___FBXL5	0.079344	-3.65573	0.012188
chr15__98819862__98824242___IGF1R	0.079389	-3.65491	0.013288
chr20__47224317__47236516___ZMYND8	0.079523	-3.65248	0.013685
chr4__122927634__122979386___SPATA5	0.079546	-3.65206	0.011936
chr5__79619612__79623355___PAPD4	0.079566	-3.6517	0.012889
chr17__20204333__20232414___SPECC1	0.079732	-3.6487	0.012629
chr1__211783229__211793190___LPGAT1	0.079795	-3.64756	0.012327

chr13__50027207__50044768___DLEU2	0.079798	-3.6475	0.012097
chr10__110578628__110593223___SMC3	0.079857	-3.64644	0.011886
chr15__50002153__50047464___ATP8B4	0.079893	-3.64578	0.013381
chr10__5773842__5811956___GDI2	0.079924	-3.64523	0.012164
chr14__35013346__35019074___SRP54	0.079929	-3.64513	0.013182
chr13__32770654__32771693___PDS5B	0.080026	-3.64339	0.011988
chr2__61178981__61187029___AHSA2	0.080031	-3.64331	0.013148
chr1__234418084__234427766___TARBP1	0.080033	-3.64326	0.013145
chr16__46674314__46677398___VPS35	0.080042	-3.6431	0.012629
chr2__32439508__32443588___BIRC6	0.080127	-3.64157	0.012097
chr15__85684741__85710645___AKAP13	0.080231	-3.6397	0.014115
chr15__62589687__62657898___TLN2	0.080242	-3.63949	0.013854
chr8__130159864__130187285___ASAP1	0.08033	-3.63792	0.014454
chr14__34593045__34609742___SNX6	0.080337	-3.63779	0.014185
chr9__97994631__98018489___NA	0.080587	-3.63331	0.01433
chr8__47279862__47294030___SPIDR	0.080591	-3.63324	0.011409
chr4__128936655__128992237___SCLT1	0.08066	-3.632	0.013182
chr22__27894555__27914347___PITPNB	0.080792	-3.62964	0.013948
chr13__72835243__72854155___PIBF1	0.080825	-3.62905	0.014181
chrX__110020352__110023040___TMEM164	0.080825	-3.62906	0.014427
chr15__89268399__89293063___FANCI	0.080836	-3.62885	0.013618
chr2__218476840__218479715___USP37	0.080981	-3.62627	0.013936
chr14__58467735__58470723___KIAA0586	0.081068	-3.62472	0.012188
chr16__58576463__58583182___CNOT1	0.081165	-3.62299	0.013381
chrX__132278008__132283032___RAP2C-AS1	0.081219	-3.62205	0.014615
chr6__53505392__53532766___GCLC	0.081225	-3.62192	0.011589
chr17__68401360__68420506___ARSG	0.081398	-3.61886	0.013495
chr3__195333028__195345317___ACAP2	0.081418	-3.61851	0.012619
chr2__23982896__23984831___UBXN2A	0.081489	-3.61724	0.01425
chr1__95116608__95151419___NA	0.081493	-3.61719	0.014616
chr16__29833733__29834066___MVP	0.08177	-3.61228	0.014969
chr4__82827369__82829058___SEC31A	0.08179	-3.61192	0.012097
chr16__47451396__47459175___ITFG1	0.081851	-3.61086	0.015087
chr10__101806045__101807901___MGEA5	0.08189	-3.61017	0.012091
chr1__28683583__28690186___GMEB1	0.081974	-3.60869	0.013685
chr2__186081330__186086370___NA	0.08199	-3.60842	0.014675
chr16__89305206__89317078___ANKRD11	0.081993	-3.60836	0.015126
chr4__102689574__102690957___MANBA	0.08223	-3.6042	0.011589
chr13__41252645__41263484___MTRF1	0.08224	-3.60401	0.014057
chr6__110887505__110893662___AMD1	0.08227	-3.60348	0.014472
chr1__235773842__235787373___LYST	0.082277	-3.60337	0.014472
chr17__81622166__81629805___NPLOC4	0.082279	-3.60333	0.014185
chr19__48231660__48242644___CARD8	0.082303	-3.60291	0.014577
chr19__17162350__17163122___MYO9B	0.082577	-3.59811	0.011496
chr18__13012973__13019206___CEP192	0.082649	-3.59686	0.014288
chr9__93471263__93498886___FAM120A	0.082667	-3.59655	0.013195

chr12__292759__293169___KDM5A	0.082693	-3.59608	0.00503
chr14__103654564__103654825___KLC1	0.082694	-3.59607	0.015126
chr9__83739705__83768970___GKAP1	0.082857	-3.59324	0.015176
chr17__60299334__60301704___USP32	0.082895	-3.59258	0.012999
chr6__131136778__131169273___AKAP7	0.082902	-3.59245	0.013195
chr19__34430576__34438766___UBA2	0.08291	-3.59231	0.013906
chr7__158879684__158918869___WDR60	0.083015	-3.59048	0.013182
chr5__140189064__140194652___CYSTM1	0.083023	-3.59034	0.012629
chr1__155661307__155777820___NA	0.083023	-3.59035	0.014454
chr15__80073266__80131293___ZFAND6	0.083042	-3.59002	0.014602
chr16__11875761__11876175___GSPT1	0.083124	-3.58859	0.013288
chr2__214780560__214792445___BARD1	0.083132	-3.58846	0.012188
chr3__9453739__9464672___SETD5	0.083134	-3.58841	0.012542
chr14__49799475__49814857___NEMF	0.083376	-3.58423	0.014689
chr5__157294783__157304366___CYFIP2	0.083378	-3.5842	0.012961
chr9__406930__418207___DOCK8	0.083385	-3.58408	0.014457
chr15__49011731__49028682___SECISBP2L	0.083494	-3.58218	0.011473
chr3__136417885__136502779___STAG1	0.083495	-3.58216	0.013345
chr12__56671749__56673065___PTGES3	0.083519	-3.58175	0.015653
chr18__47868323__47870564___SMAD2	0.083623	-3.57996	0.015934
chr2__206056198__206063244___INO80D	0.083625	-3.57991	0.013924
chr6__57124734__57154047___ZNF451	0.083692	-3.57876	0.013422
chr11__78101093__78109581___ALG8	0.083703	-3.57859	0.013685
chr12__51240343__51241116___DAZAP2	0.083824	-3.5765	0.015126
chr14__96846095__96876120___VRK1	0.083878	-3.57557	0.015653
chr2__71332830__71348525___ZNF638	0.083948	-3.57436	0.015934
chr2__233263130__233270067___ATG16L1	0.084044	-3.57272	0.015994
chr5__41907736__41912183___C5orf51	0.084138	-3.5711	0.010453
chr7__93334117__93341575___CCDC132	0.084149	-3.57091	0.012889
chr2__238173534__238185287___ILKAP	0.084163	-3.57068	0.015184
chr1__1804419__1806538___GNB1	0.084198	-3.57008	0.002919
chr11__120437308__120445464___ARHGEF12	0.08436	-3.56729	0.011099
chr3__153164766__153209886___NA	0.084454	-3.56569	0.015423
chr5__93958777__94053227___FAM172A	0.084594	-3.5633	0.014454
chr9__15478477__15490124___PSIP1	0.084684	-3.56177	0.01563
chr2__53934605__53949283___PSME4	0.084778	-3.56017	0.014115
chr7__91992885__92014328___AKAP9	0.084782	-3.56009	0.012843
chr9__131436620__131439061___PRRC2B	0.084834	-3.55922	0.013587
chr17__5308694__5346925___RABEP1	0.084848	-3.55898	0.012251
chr20__35655202__35659014___CPNE1	0.085025	-3.55596	0.016209
chr14__50445041__50456594___MAP4K5	0.085028	-3.55592	0.015126
chr9__120831331__120833456___PSMD5	0.08504	-3.55572	0.016003
chr1__93217738__93239896___CCDC18	0.085194	-3.55311	0.012884
chr2__61108317__61118116___KIAA1841	0.085242	-3.55228	0.001995
chr6__42637011__42642481___UBR2	0.085247	-3.5522	0.015317
chr5__94909251__94912976___MCTP1	0.085352	-3.55043	0.012847

chr1__224365879__224371423___CNIH4	0.085566	-3.54681	0.014455
chr4__38089932__38118192___TBC1D1	0.085653	-3.54536	0.010967
chr12__26628033__26655852___ITPR2	0.085717	-3.54427	0.010601
chr2__43397971__43430302___THADA	0.085729	-3.54407	0.016323
chr17__81569016__81572088___NPLOC4	0.08574	-3.54389	0.015962
chr21__39258487__39274472___BRWD1	0.085754	-3.54364	0.013658
chr12__68727351__68735344___NUP107	0.085811	-3.54269	0.015317
chr8__134600436__134610655___ZFAT	0.085847	-3.54209	0.015404
chr21__15762891__15778027___USP25	0.085869	-3.54173	0.016054
chrX__41217220__41223402___USP9X	0.086002	-3.53948	0.015485
chr15__90439332__90440615___IQGAP1	0.086016	-3.53924	0.013854
chr2__55577315__55591695___SMEK2	0.086039	-3.53887	0.015309
chr2__88776501__88779319___ANKRD36BP2	0.086042	-3.53882	0.016611
chr16__71655240__71658815___PHLPP2	0.086043	-3.5388	0.015087
chr20__34727259__34736758___NCOA6	0.086063	-3.53846	0.016289
chr14__45148837__45159280___FANCM	0.086101	-3.53783	0.016048
chr19__52618936__52635153___ZNF83	0.08612	-3.5375	0.016441
chr1__77858938__77864028___FAM73A	0.086149	-3.53703	0.014472
chr6__43348324__43352476___ZNF318	0.086236	-3.53556	0.015485
chr12__71626260__71629037___ZFC3H1	0.086247	-3.53538	0.013288
chr4__128831733__128852268___JADE1	0.086248	-3.53536	0.013566
chr3__37249698__37251484___GOLGA4	0.086257	-3.53521	0.014602
chr1__90005133__90007750___ZNF326	0.086348	-3.53369	0.016448
chr1__180019949__180021009___CEP350	0.086381	-3.53314	0.012489
chr16__89418284__89431326___ANKRD11	0.086475	-3.53158	0.014185
chr1__207757014__207770362___CD46	0.08656	-3.53015	0.013381
chr19__54222943__54280299___NA	0.086579	-3.52984	0.017447
chr8__30680904__30700135___GSR	0.086581	-3.52981	0.015962
chr3__141974048__141995141___TFDP2	0.086599	-3.5295	0.016551
chr9__5021963__5078444___JAK2	0.086697	-3.52787	0.013288
chr1__20741831__20780540___NA	0.086825	-3.52575	0.013306
chr2__171448681__171473975___DCAF17	0.08692	-3.52417	0.017429
chr2__152719898__152735126___ARL6IP6	0.087069	-3.5217	0.017269
chr17__30266885__30286902___BLMH	0.08711	-3.52102	0.014615
chr7__158644289__158646563___NCAPG2	0.08728	-3.5182	0.013288
chr9__122877471__122897576___RC3H2	0.087439	-3.51557	0.01637
chr1__207697503__207717691___CR1L	0.087449	-3.51541	0.016003
chr2__202952559__202955758___CARF	0.087483	-3.51485	0.017321
chr3__12604136__12606299___RAF1	0.087562	-3.51355	0.015913
chr17__20110427__20205912___SPECC1	0.087564	-3.51352	0.015126
chr20__5176648__5178956___CDS2	0.087608	-3.51279	0.016209
chr5__96985080__97015095___LNPEP	0.087613	-3.51272	0.016159
chr18__24070751__24071023___TTC39C	0.087673	-3.51173	0.014457
chr21__15777904__15833548___USP25	0.087739	-3.51063	0.016432
chr2__218529956__218562813___USP37	0.087755	-3.51037	0.017026
chrX__119930016__119932216___NKAP	0.087781	-3.50995	0.017526

chr10__118685983__118707587___CACUL1	0.087792	-3.50977	0.012935
chr14__73282359__73297285___NUMB	0.087911	-3.5078	0.014288
chr8__132610166__132625454___LRRC6	0.087946	-3.50724	0.017803
chr1__27838699__27843330___PPP1R8	0.087973	-3.50679	0.014258
chr20__35651264__35659014___RBM12	0.087976	-3.50675	0.01637
chr12__82386803__82403130___METTL25	0.087988	-3.50656	0.016129
chr14__92082300__92088817___ATXN3	0.088025	-3.50594	0.017211
chr18__47865059__47930446___SMAD2	0.08809	-3.50488	0.016611
chr3__19975601__19976169___RAB5A	0.088119	-3.50441	0.017429
chr1__161778244__161802272___ATF6	0.088146	-3.50397	0.016748
chr12__111865250__111871180___MAPKAPK5	0.088168	-3.5036	0.017177
chr1__45600385__45602365___NASP	0.088253	-3.50221	0.016159
chr7__77396982__77406105___GSAP	0.088272	-3.5019	0.013381
chr2__175970764__175994280___KIAA1715	0.08829	-3.50161	0.015126
chr1__28613247__28622165___TAF12	0.088355	-3.50055	0.016849
chr1__222715145__222725555___BROX	0.08854	-3.49753	0.014454
chr2__128097429__128129179___UGGT1	0.088624	-3.49616	0.015485
chr10__42816599__42817494___BMS1	0.088636	-3.49597	0.016141
chrX__124021367__124022671___STAG2	0.08864	-3.4959	0.01715
chr5__69355649__69355953___AK6	0.088701	-3.49491	0.016091
chr9__85596362__85646418___AGTPBP1	0.088756	-3.49401	0.017684
chr2__23857415__23895970___ATAD2B	0.088793	-3.49341	0.016323
chr5__179580947__179594963___RUFY1	0.088837	-3.4927	0.016468
chr4__150798081__150831976___LRBA	0.088862	-3.49229	0.017314
chr4__48842636__48857365___OCIAD1	0.088953	-3.49081	0.014185
chr7__48410520__48412583___ABCA13	0.088978	-3.49041	0.017649
chr8__17985447__18011366___PCM1	0.089042	-3.48937	0.016003
chr10__28119651__28131691___MPP7	0.08909	-3.48859	0.01349
chr3__136398749__136423044___STAG1	0.089102	-3.48839	0.015218
chr6__37279304__37291357___TBC1D22B	0.089201	-3.48679	0.016448
chr3__142669390__142671122___PLS1	0.089232	-3.4863	0.018326
chr19__24126254__24128180___ZNF254	0.089352	-3.48436	0.015126
chr3__56745205__56745462___ARHGEF3	0.089361	-3.48421	0.015029
chr13__113233177__113244514___CUL4A	0.089383	-3.48386	0.015317
chr16__72349046__72391215___NA	0.089384	-3.48383	0.016432
chr6__149379411__149409824___TAB2	0.089389	-3.48375	0.01841
chr2__201381124__201420706___TRAK2	0.089422	-3.48323	0.017684
chr5__112985835__113010807___DCP2	0.089425	-3.48318	0.017309
chr8__31141430__31150455___WRN	0.089448	-3.4828	0.015833
chr22__31258291__31260077___LIMK2	0.089696	-3.47881	0.01925
chr16__75391380__75395209___CFDP1	0.0897	-3.47875	0.01816
chr7__6028615__6029032___EIF2AK1	0.089706	-3.47865	0.013381
chr13__98482265__98519473___STK24	0.089742	-3.47808	0.01351
chr13__60439688__60494575___TDRD3	0.089743	-3.47806	0.01563
chr6__130022227__130104575___L3MBTL3	0.089764	-3.47772	0.016003
chr2__74165218__74172752___MOB1A	0.0898	-3.47714	0.015317

chr17__31940286__31976614___SUZ12	0.089807	-3.47702	0.017587
chr9__125301983__125302826___GAPVD1	0.089846	-3.4764	0.017067
chr5__69306817__69314043___CCDC125	0.089852	-3.4763	0.01854
chr16__11684165__11688445___TXNDC11	0.089989	-3.47411	0.015934
chr4__128292934__128483487___NA	0.090025	-3.47353	0.01854
chr18__36142281__36160015___ELP2	0.09003	-3.47345	0.017269
chr10__74838683__74843478___KAT6B	0.090069	-3.47283	0.017803
chrX__2392354__2425304___DHRSX	0.090094	-3.47243	0.015178
chr4__177339707__177353728___NEIL3	0.090098	-3.47236	0.014924
chr5__133006759__133022906___ZCCHC10	0.090221	-3.47039	0.016003
chr3__136472413__136477412___STAG1	0.090222	-3.47038	0.017803
chr2__64569092__64573068___AFTPH	0.090291	-3.46927	0.01735
chr7__139279318__139284574___UBN2	0.090335	-3.46857	0.017269
chr8__21974670__22004030___XPO7	0.090495	-3.46602	0.012327
chr1__233177802__233208689___PCNXL2	0.090519	-3.46564	0.01715
chr9__3484974__3490345___RFX3	0.090538	-3.46533	0.012889
chr11__3735382__3739060___NUP98	0.090561	-3.46497	0.014615
chr10__68911068__68914204___DDX50	0.090667	-3.46327	0.014454
chr6__154808070__154824378___SCAF8	0.090692	-3.46289	0.018521
chr9__86305192__86319670___ZCCHC6	0.090712	-3.46257	0.013956
chr16__70532479__70544533___SF3B3	0.090787	-3.46137	0.013306
chr15__34862867__34870922___AQR	0.090788	-3.46135	0.015934
chr19__5641594__5641950___SAFB	0.090923	-3.4592	0.016003
chr6__36083031__36096066___MAPK14	0.090973	-3.45842	0.018469
chr15__40389506__40393593___KNSTRN	0.091181	-3.45512	0.017865
chr4__127930683__127938838___MFSD8	0.091213	-3.45462	0.017269
chr10__15816835__15843272___FAM188A	0.091259	-3.4539	0.017674
chr10__84380098__84477664___CCSER2	0.091266	-3.45378	0.015126
chr17__75651186__75666620___RECQL5	0.091321	-3.45291	0.017849
chr12__68828771__68839801___MDM2	0.091326	-3.45283	0.016209
chr1__21002713__21089213___EIF4G3	0.09133	-3.45277	0.013906
chr9__120550792__120568388___CDK5RAP2	0.091362	-3.45227	0.017587
chr12__70278132__70319364___CNOT2	0.091439	-3.45105	0.015833
chr11__46769963__46788773___CKAP5	0.091613	-3.4483	0.013685
chr3__160430599__160431825___SMC4	0.091663	-3.44752	0.016003
chr2__128113084__128129179___UGGT1	0.091691	-3.44707	0.018836
chr20__37044086__37047190___RBL1	0.091879	-3.44411	0.018521
chr9__111384522__111385442___KIAA0368	0.091893	-3.44389	0.01854
chr2__224495832__224514772___CUL3	0.091999	-3.44224	0.016323
chr9__96522506__96565483___CDC14B	0.092043	-3.44154	0.002021
chr2__62707164__62874532___EHBP1	0.0921	-3.44066	0.014426
chr7__92213195__92214777___KRIT1	0.092129	-3.4402	0.01637
chr16__48256610__48277479___LONP2	0.092139	-3.44004	0.01854
chr5__36984676__36995804___NIPBL	0.092276	-3.4379	0.014457
chr8__123359577__123380677___ATAD2	0.092283	-3.43779	0.016923
chr16__68053564__68054617___DUS2	0.092305	-3.43745	0.019338

chr2__32414769__32416163___BIRC6	0.092317	-3.43726	0.013936
chr3__155887432__155925366___GMPS	0.092426	-3.43555	0.015833
chr3__160404328__160416415___SMC4	0.092621	-3.43252	0.017803
chr7__129657343__129690546___NRF1	0.092623	-3.43249	0.018036
chr17__61965006__61968258___MED13	0.09265	-3.43206	0.016151
chr15__50303966__50309798___GABPB1	0.092685	-3.43152	0.014454
chr8__116856166__116863259___RAD21	0.09272	-3.43098	0.01925
chr1__92605307__92625934___EVI5	0.092739	-3.43068	0.01637
chr14__45226743__45242518___MIS18BP1	0.09281	-3.42958	0.017526
chr5__176350613__176355749___KIAA1191	0.092824	-3.42936	0.019701
chr11__17330902__17337534___NUCB2	0.092898	-3.42821	0.01563
chr12__97492461__97561047___NA	0.093035	-3.42608	0.019196
chr1__185181946__185190642___SWT1	0.093081	-3.42537	0.018214
chr1__179335506__179343635___SOAT1	0.093145	-3.42438	0.016915
chr22__21769195__21805945___MAPK1	0.093178	-3.42387	0.019338
chr1__11073934__11076948___EXOSC10	0.093256	-3.42266	0.015675
chr8__17924713__17937379___PCM1	0.093362	-3.42102	0.019338
chr6__63646527__63685911___PHF3	0.093371	-3.42088	0.018469
chr12__827042__830160___WNK1	0.093497	-3.41894	0.015653
chr5__115275216__115284908___CCDC112	0.093523	-3.41853	0.020294
chr11__16046514__16111926___SOX6	0.093636	-3.4168	0.014472
chr10__12081472__12091684___DHTKD1	0.093756	-3.41495	0.01925
chr15__42528262__42529819___SNAP23	0.093819	-3.41397	0.018799
chr5__73051349__73052507___FCHO2	0.093833	-3.41376	0.01925
chr6__75666712__75678927___SENP6	0.093839	-3.41367	0.01816
chr18__58165788__58333892___NEDD4L	0.093843	-3.41361	0.016273
chr3__100267100__100281847___TBC1D23	0.093944	-3.41205	0.01637
chr14__55378279__55380389___ATG14	0.093987	-3.41139	0.018028
chr6__100798713__100848707___ASCC3	0.093991	-3.41134	0.014457
chr14__70166639__70168484___SLC8A3	0.09401	-3.41104	0.018333
chr1__31907661__31919658___PTP4A2	0.094017	-3.41093	0.018843
chr7__7209427__7243750___C1GALT1	0.094032	-3.41071	0.019356
chr5__95736889__95755761___RHOBTB3	0.094094	-3.40976	0.020702
chr8__28713457__28718207___EXTL3	0.09412	-3.40936	0.016014
chr2__197078703__197090032___ANKRD44	0.094139	-3.40907	0.017849
chr11__6608601__6611452___NA	0.094195	-3.4082	0.018697
chr12__123313620__123323831___SBNO1	0.094238	-3.40755	0.020294
chr10__6097048__6115311___RBM17	0.094445	-3.40438	0.020294
chr21__37108392__37147603___TTC3	0.094454	-3.40424	0.019881
chr2__201129729__201149835___CFLAR	0.094486	-3.40376	0.01925
chr17__82720272__82720841___FN3KRP	0.094558	-3.40266	0.017706
chr20__21340721__21346550___XRN2	0.094565	-3.40256	0.018295
chr19__52383849__52385742___ZNF880	0.094588	-3.4022	0.017649
chr14__99257471__99257836___BCL11B	0.094596	-3.40207	0.015934
chr13__77243059__77264002___MYCBP2	0.09461	-3.40187	0.017684
chr6__36158648__36158941___LOC102723648	0.094663	-3.40106	0.014904

chr20__34477772__34481206___ITCH	0.094703	-3.40045	0.017649
chr7__131387120__131429145___MKLN1	0.094711	-3.40032	0.020452
chr2__119962616__119967972___PTPN4	0.094878	-3.39778	0.020874
chr10__16752539__16754989___RSU1	0.094943	-3.39679	0.019687
chr12__123313620__123315660___SBNO1	0.094956	-3.3966	0.018092
chr7__2213212__2222754___MAD1L1	0.095041	-3.39531	0.018389
chr2__197418896__197420227___SF3B1	0.095056	-3.39508	0.02099
chr19__53407698__53410425___ZNF765	0.095085	-3.39464	0.013288
chr9__137728349__137762820___EHMT1	0.095105	-3.39434	0.020717
chr10__84438512__84477664___CCSER2	0.095122	-3.39407	0.005736
chr19__4896671__4898085___ARRDC5	0.095136	-3.39386	0.01925
chr14__96833467__96945382___NA	0.095136	-3.39387	0.015126
chr11__94445810__94447438___MRE11A	0.095207	-3.39278	0.019362
chr12__14665859__14672314___GUCY2C	0.095218	-3.39262	0.015833
chr2__96359045__96367373___NCAPH	0.095242	-3.39226	0.01998
chr19__8337795__8339167___KANK3	0.095272	-3.39181	0.016151
chr8__58565019__58572314___SDCBP	0.095359	-3.39049	0.015475
chr2__232832857__232833093___GIGYF2	0.095373	-3.39028	0.018843
chr10__121790169__121870038___ATE1	0.095431	-3.3894	0.016849
chr7__80672770__80674147___CD36	0.095462	-3.38894	0.013854
chr1__229450525__229465519___NUP133	0.095474	-3.38875	0.019732
chr6__131216412__131219808___AKAP7	0.095567	-3.38734	0.016209
chr5__50399859__50411383___EMB	0.095621	-3.38653	0.01845
chr2__23857415__23869761___ATAD2B	0.095777	-3.38418	0.017803
chr12__2873977__2874525___FOXM1	0.095824	-3.38347	0.020232
chr1__154170400__154176248___TPM3	0.095867	-3.38282	0.020033
chr7__105142008__105146658___SRPK2	0.095938	-3.38176	0.01841
chr7__93259550__93297243___CCDC132	0.095963	-3.38137	0.018371
chr7__148766561__148767749___CUL1	0.096005	-3.38074	0.018538
chr11__65435053__65437657___NA	0.096022	-3.3805	0.00503
chr15__34890215__34904505___AQR	0.096074	-3.37972	0.021117
chr12__82369387__82434724___METTL25	0.096117	-3.37907	0.020592
chr10__92616737__92630364___KIF11	0.096145	-3.37864	0.015934
chr9__20923660__20933103___FOCAD	0.096155	-3.3785	0.020729
chr2__43578513__43590954___THADA	0.09616	-3.37841	0.015184
chr5__10415488__10417404___MARCH6	0.096268	-3.3768	0.019338
chr7__154967816__154998784___PAXIP1	0.09641	-3.37467	0.017309
chr11__108267171__108267342___ATM	0.096429	-3.37439	0.020076
chr1__220001138__220007338___EPRS	0.096436	-3.37429	0.019196
chr12__355158__363097___KDM5A	0.096465	-3.37385	0.01841
chr9__112250929__112262599___PTBP3	0.096671	-3.37077	0.017803
chr9__137728349__137744090___EHMT1	0.096695	-3.37041	0.022374
chr18__13408993__13438384___LDLRAD4	0.096697	-3.37038	0.02023
chr2__37037855__37041292___HEATR5B	0.096737	-3.36979	0.017535
chr12__121416159__121417911___RNF34	0.096743	-3.36969	0.021908
chr2__158620990__158621421___PKP4	0.096794	-3.36894	0.021161

chr12__42317340__42324104___ZCRB1	0.096814	-3.36864	0.005208
chr1__174969277__174976182___RABGAP1L	0.096874	-3.36775	0.014629
chr8__26410909__26411069___BNIP3L	0.096907	-3.36726	0.01854
chr7__129873855__129880971___UBE2H	0.097054	-3.36506	0.021055
chr9__85596362__85646435___AGTPBP1	0.097089	-3.36455	0.015833
chr10__110881233__110887886___PDCD4	0.097101	-3.36438	0.007512
chr6__130052859__130057497___L3MBTL3	0.097129	-3.36396	0.020108
chr6__14131520__14135909___CD83	0.097183	-3.36315	0.01925
chr14__32117143__32152528___ARHGAP5	0.097238	-3.36233	0.020203
chr6__28271854__28272787___ZSCAN26	0.097285	-3.36164	0.01925
chr6__159682474__159685033___SOD2	0.097291	-3.36155	0.016151
chr7__23604086__23611553___CCDC126	0.097306	-3.36133	0.019316
chr17__27301788__27303635___WSB1	0.097437	-3.35939	0.005725
chr10__7276892__7285954___SFMBT2	0.097465	-3.35898	0.015653
chr11__16183886__16318653___SOX6	0.097475	-3.35883	0.022497
chr13__49196877__49198574___FNDC3A	0.0975	-3.35846	0.020702
chr12__122601536__122624688___KNTC1	0.097562	-3.35754	0.021107
chr3__146189799__146222092___NA	0.097573	-3.35737	0.019298
chr20__47294666__47298872___ZMYND8	0.097587	-3.35717	0.021251
chr2__108751264__108751994___RANBP2	0.097736	-3.35496	0.018469
chr2__174378923__174387779___CIR1	0.097758	-3.35465	0.02099
chr2__32377588__32380290___BIRC6	0.097808	-3.35391	0.021583
chr6__130022227__130120958___L3MBTL3	0.097876	-3.3529	0.018816
chr7__40078005__40078851___CDK13	0.097928	-3.35213	0.01925
chr2__160329680__160331910___RBMS1	0.097979	-3.35138	0.021014
chr17__47402135__47414919___EFCAB13	0.098012	-3.3509	0.021479
chr7__131338841__131341388___MKLN1	0.098082	-3.34987	0.021251
chr12__50430495__50454417___LARP4	0.098088	-3.34977	0.018816
chr1__95134782__95136731___TMEM56TMEM56-RWDD3	0.098219	-3.34785	0.015716
chr13__52429236__52434882___VPS36	0.098302	-3.34663	0.015934
chr4__83416731__83448961___HELQ	0.098459	-3.34433	0.016003
chr15__51896419__51902036___TMOD3	0.098509	-3.34359	0.016943
chr4__103140814__103141104___CENPE	0.098528	-3.34333	0.022012
chr4__76130656__76136412___NUP54	0.098568	-3.34274	0.02293
chr15__42558198__42563857___HAUS2	0.098649	-3.34155	0.021889
chr14__92810254__92816421___GOLGA5	0.098654	-3.34149	0.019106
chr4__36290373__36316486___DTHD1	0.098667	-3.34129	0.01638
chr2__32478635__32493667___BIRC6	0.098667	-3.34129	0.02157
chr16__68174374__68191775___NFATC3	0.098784	-3.33957	0.022645
chr1__203847184__203847687___ZC3H11A	0.098874	-3.33827	0.021583
chr8__123129066__123142456___TBC1D31	0.09892	-3.3376	0.014021
chr6__144451370__144459354___UTRN	0.098934	-3.33739	0.017269
chr4__89822246__89836789___SNCA	0.098988	-3.33661	0.021446
chr1__185174372__185276668___SWT1	0.099031	-3.33598	0.015449
chr9__135850137__135866536___CAMSAP1	0.099037	-3.3359	0.02272
chr18__37066890__37067545___KIAA1328	0.09904	-3.33584	0.01925

chr20__495719__508660___CSNK2A1	0.099098	-3.335	0.019158
chr4__53383773__53396061___FIP1L1	0.099112	-3.33479	0.016209
chr12__56168060__56170208___SMARCC2	0.099225	-3.33315	0.020957
chr8__94851553__94866191___INTS8	0.099249	-3.3328	0.021216
chr3__196058284__196072152___TFRC	0.099258	-3.33268	0.022566
chr10__7243558__7285954___SFMBT2	0.0993	-3.33206	0.005676
chr13__19851355__19852190___ZMYM5	0.099315	-3.33185	0.021117
chr4__107682015__107701285___PAPSS1	0.099479	-3.32947	0.007926
chr15__63558106__63559970___USP3	0.099489	-3.32932	0.017865
chr3__37108637__37121691___LRRFIP2	0.099558	-3.32832	0.01816
chr1__235213769__235240451___ARID4B	0.099578	-3.32803	0.0188
chr1__15529088__15548428___DNAJC16	0.099606	-3.32762	0.020033
chrX__71367499__71460803___TAF1	0.099731	-3.32582	0.021128
chr10__124706636__124706887___FAM53B	0.099768	-3.32528	0.017865
chr18__70047971__70065922___RTTN	0.099934	-3.32289	0.017177
chr13__37044078__37051583___SUPT20H	0.100095	-3.32056	0.021117
chr15__52605133__52611777___FAM214A	0.100424	-3.31582	0.020702
chr7__107281300__107298346___COG5	0.100427	-3.31579	0.01809
chr13__40826506__40872160___TPTE2P5	0.100449	-3.31547	0.020033
chr2__15415546__15511350___NBAS	0.100483	-3.31497	0.014454
chr5__133000132__133006920___ZCCHC10	0.100496	-3.31478	0.018699
chr12__30725966__30751133___CAPRIN2	0.100538	-3.31419	0.018371
chr15__65731642__65761438___DENND4A	0.1006	-3.3133	0.020702
chr19__17772457__17772741___FCHO1	0.100602	-3.31327	0.01854
chr8__96834973__96880005___CPQ	0.100611	-3.31314	0.021255
chr8__85341599__85342825___CA1	0.10068	-3.31215	0.018521
chr4__1900626__1904378___WHSC1	0.100697	-3.31191	0.021152
chr3__138228918__138235114___ARMC8	0.100712	-3.31169	0.023237
chr10__124816576__124831463___FAM175B	0.100725	-3.31151	0.016679
chr22__21788257__21805945___MAPK1	0.100735	-3.31136	0.01998
chr1__35747907__35753936___CLSPN	0.100769	-3.31087	0.023414
chr12__28225795__28391411___CCDC91	0.10081	-3.31029	0.021285
chr12__26621123__26632059___ITPR2	0.100836	-3.30992	0.019302
chr3__37053855__37055165___LRRFIP2	0.101048	-3.30689	0.022795
chr3__195519018__195524896___PPP1R2	0.101086	-3.30635	0.020108
chr6__16274415__16290621___GMPR	0.101089	-3.30631	0.022958
chr5__10415488__10426522___MARCH6	0.101102	-3.30612	0.021117
chr1__174304986__174371072___RABGAP1L	0.101117	-3.3059	0.016323
chr1__70181086__70187338___LRRC40	0.101259	-3.30388	0.021098
chr17__47402132__47404633___EFCAB13	0.101318	-3.30303	0.020108
chr5__102257115__102270806___SLCO4C1	0.101367	-3.30233	0.021839
chr7__77626705__77627675___PTPN12	0.101373	-3.30225	0.018816
chr20__44987132__44995257___STK4	0.101387	-3.30205	0.020761
chr8__21974670__21995599___XPO7	0.10141	-3.30172	0.02023
chr13__79312485__79319691___RBM26	0.101429	-3.30145	0.020784
chr1__34992234__35015162___ZMYM6	0.101459	-3.30103	0.023307

chr4__139116649__139168042___ELF2	0.10149	-3.30059	0.023604
chr17__62010462__62063222___MED13	0.101572	-3.29943	0.021839
chr2__20307978__20333063___PUM2	0.101622	-3.29871	0.023773
chr9__121167489__121175224___CNTRL	0.101623	-3.2987	0.01816
chr1__207715312__207738571___NA	0.101669	-3.29805	0.021041
chr2__128097429__128121298___UGGT1	0.101676	-3.29795	0.020232
chr15__44615363__44629388___SPG11	0.101731	-3.29716	0.02272
chr18__57554260__57580199___FECH	0.101851	-3.29547	0.02176
chr22__28780948__28783645___CCDC117	0.102126	-3.29158	0.018425
chr1__245858496__245929937___SMYD3	0.102188	-3.2907	0.02099
chr7__87439667__87440402___ABCB4	0.102262	-3.28966	0.008348
chr4__139067684__139073567___ELF2	0.102335	-3.28863	0.024391
chr8__102833056__102834747___AZIN1	0.102369	-3.28815	0.015754
chr15__40170062__40170681___BUB1B	0.102381	-3.28799	0.023718
chr11__8435494__8464822___STK33	0.102426	-3.28735	0.018521
chr12__70342107__70346324___CNOT2	0.102437	-3.28719	0.020767
chr6__149572285__149591790___NA	0.102585	-3.2851	0.01637
chr20__36607715__36609730___TGIF2-C20orf24C20orf24	0.102603	-3.28485	0.024627
chr12__813642__813814___WNK1	0.102658	-3.28408	0.024519
chr3__42125420__42125614___TRAK1	0.102693	-3.28359	0.021096
chr9__131150324__131164144___NUP214	0.102705	-3.28342	0.01998
chr5__146483540__146503539___TCERG1	0.102753	-3.28275	0.020081
chr13__24484653__24503777___PARP4	0.102757	-3.28268	0.024162
chr17__37437738__37444768___TADA2A	0.102902	-3.28066	0.023745
chr8__119762415__119791459___TAF2	0.102927	-3.28031	0.01925
chr11__108327645__108335961___ATM	0.102928	-3.2803	0.02099
chr22__30494150__30495971___SEC14L4	0.10295	-3.27999	0.022872
chr9__34234216__34242108___UBAP1	0.102972	-3.27968	0.01792
chr16__72523332__72555326___LOC102723844	0.102981	-3.27954	0.02157
chr10__68381232__68394136___RUFY2	0.103023	-3.27896	0.021098
chr17__49311312__49312845___ZNF652	0.103109	-3.27776	0.007926
chr15__63718574__63756748___HERC1	0.10318	-3.27676	0.01894
chr11__108104190__108106295___CUL5	0.103205	-3.27641	0.020118
chr14__92142164__92155323___CPSF2	0.103206	-3.2764	0.021117
chr16__14599904__14609123___PARN	0.103253	-3.27575	0.021743
chr13__32078834__32117473___FRY	0.103267	-3.27555	0.019886
chr2__203289765__203292326___CYP20A1	0.103328	-3.27469	0.021098
chr7__152249876__152250966___KMT2C	0.103339	-3.27455	0.021903
chr18__22990937__23001729___RBBP8	0.103365	-3.27418	0.023942
chr11__2969803__2972279___NAP1L4	0.103587	-3.27108	0.023414
chr3__71693875__71699708___EIF4E3	0.103603	-3.27087	0.019147
chr16__68121987__68158068___NFATC3	0.103641	-3.27033	0.023191
chr12__100282943__100317925___SCYL2	0.103665	-3.26999	0.021515
chr8__96879798__96902096___CPQ	0.103762	-3.26865	0.022276
chr4__174297966__174316290___CEP44	0.103788	-3.26829	0.020717
chr1__50738863__50752523___FAF1	0.103817	-3.26789	0.025637

chr12__128945326__128957643___GLT1D1	0.103833	-3.26766	0.02389
chr3__25628847__25645455___TOP2B	0.103834	-3.26764	0.020717
chr9__128750616__128755659___ZER1	0.10387	-3.26715	0.024104
chr4__139137630__139168042___ELF2	0.103879	-3.26703	0.008609
chr6__75659262__75666941___SENP6	0.103897	-3.26677	0.021117
chr5__177191884__177204292___NSD1	0.1039	-3.26674	0.024613
chr10__110875966__110890670___PDCD4	0.103904	-3.26668	0.018836
chr2__23816637__23823569___ATAD2B	0.103913	-3.26655	0.021041
chr11__108329021__108332037___ATM	0.103913	-3.26655	0.025067
chr1__235172618__235196115___ARID4B	0.103943	-3.26613	0.01854
chr13__20596150__20597119___IFT88	0.104113	-3.26378	0.025067
chr2__8958497__8974435___MBOAT2	0.104148	-3.26329	0.020221
chr20__44503815__44512994___SERINC3	0.104149	-3.26327	0.024583
chr14__101901719__101909690___PPP2R5C	0.104199	-3.26259	0.02106
chr13__77205256__77212160___MYCBP2	0.104235	-3.26208	0.022811
chr10__5765987__5811956___GDI2	0.10425	-3.26189	0.018697
chr7__107140847__107153251___PRKAR2B	0.104269	-3.26162	0.021255
chr15__22667898__22681605___WHAMMP3	0.104269	-3.26162	0.020015
chr17__1354211__1362008___YWHAE	0.104295	-3.26125	0.021903
chr6__152236107__152239706___SYNE1	0.104444	-3.2592	0.021176
chr3__136443287__136477412___STAG1	0.104482	-3.25867	0.023807
chr14__74778447__74778683___YLPM1	0.104538	-3.2579	0.022245
chr15__72544820__72572165___ARIH1	0.104538	-3.2579	0.020874
chr13__19741565__19782791___PSPC1	0.104591	-3.25717	0.022012
chr11__96209454__96210334___MAML2	0.104711	-3.25552	0.021182
chr2__200949554__200958133___ORC2	0.104717	-3.25544	0.022497
chr9__4823548__4849550___RCL1	0.104736	-3.25517	0.019886
chr17__61987007__61995365___MED13	0.104748	-3.255	0.021128
chr17__30855143__30869646___ATAD5	0.104761	-3.25482	0.021522
chr1__163336751__163349080___NUF2	0.104763	-3.2548	0.022818
chr2__26364302__26383347___EPT1	0.104797	-3.25433	0.022964
chr3__154295284__154306295___DHX36	0.1048	-3.25429	0.024243
chr2__157284282__157312023___NA	0.104805	-3.25422	0.021789
chr5__112204375__112209982___EPB41L4A	0.104822	-3.25399	0.025419
chr12__70219393__70225390___LOC101928062	0.104979	-3.25182	0.021551
chr4__42503450__42543986___ATP8A1	0.105112	-3.24999	0.024032
chr18__56758865__56781656___WDR7	0.105132	-3.24973	0.021964
chr22__40848294__40849895___ST13	0.105171	-3.24919	0.021583
chr11__128758115__128782023___FLI1	0.10519	-3.24893	0.025945
chr14__39151746__39158402___TRAPPC6B	0.105191	-3.24892	0.02176
chr2__151441905__151443709___RIF1	0.10524	-3.24825	0.019316
chr3__132473145__132478140___DNAJC13	0.105292	-3.24754	0.02526
chr15__75854386__75873568___UBE2Q2	0.105305	-3.24735	0.004892
chr2__151438684__151461289___RIF1	0.105431	-3.24563	0.01998
chr3__71690010__71728623___EIF4E3	0.105588	-3.24348	0.022413
chr1__156158070__156158824___SEMA4A	0.105604	-3.24327	0.01998

chrX__110067347__110109146___TMEM164	0.105617	-3.24309	0.006101
chr20__5559940__5570239___GPCPD1	0.105648	-3.24266	0.022872
chr12__112216292__112228811___HECTD4	0.105753	-3.24123	0.020952
chr6__13578772__13584225___SIRT5	0.10581	-3.24046	0.019338
chr16__4817598__4823907___GLYR1	0.10583	-3.24018	0.005676
chr20__3963875__3974400___RNF24	0.105883	-3.23946	0.019886
chrX__3817545__3818500___LOC389906	0.10594	-3.23868	0.023666
chr5__139318908__139319501___MATR3	0.105951	-3.23853	0.022437
chr15__76728595__76733384___SCAPER	0.10604	-3.23731	0.023807
chr14__52455324__52491005___TXNDC16	0.106107	-3.23641	0.017865
chr6__97267882__97273062___MMS22L	0.106125	-3.23616	0.024286
chr1__47368469__47373107___CMPK1	0.106131	-3.23609	0.025544
chr17__60679453__60709325___BCAS3	0.106179	-3.23543	0.020033
chr3__123931308__123931756___CCDC14	0.106299	-3.23381	0.024391
chrY__12709388__12722187___USP9Y	0.106336	-3.23329	0.020874
chr1__19172864__19175033___UBR4	0.106346	-3.23316	0.025637
chr17__67151046__67185145___HELZ	0.106482	-3.23132	0.025742
chr12__50435488__50441643___LARP4	0.106502	-3.23104	0.020969
chr8__21991868__22004030___XPO7	0.106519	-3.23082	0.005792
chr1__197539964__197583253___DENND1B	0.106554	-3.23034	0.020341
chr3__125453810__125460860___SNX4	0.106572	-3.2301	0.01932
chr17__67866464__67875744___BPTF	0.106582	-3.22997	0.024945
chr3__56663541__56673725___FAM208A	0.106609	-3.2296	0.025419
chr2__171046174__171061156___TLK1	0.106621	-3.22944	0.017865
chr12__32619698__32633689___FGD4	0.106626	-3.22937	0.022276
chr13__19709542__19782791___PSPC1	0.106765	-3.22748	0.022503
chr1__158667858__158686537___SPTA1	0.106774	-3.22737	0.023807
chr4__177339694__177353728___NEIL3	0.106848	-3.22637	0.020455
chr1__158677690__158683496___SPTA1	0.106859	-3.22623	0.023953
chr8__99467414__99481802___VPS13B	0.106899	-3.22568	0.020294
chr14__73282359__73287314___NUMB	0.10692	-3.22539	0.02156
chrX__14850505__14865580___FANCB	0.106939	-3.22515	0.020952
chr18__56610993__56638505___TXNL1	0.107014	-3.22412	0.025798
chr1__174442889__174455838___RABGAP1L	0.107192	-3.22173	0.02456
chr16__11020193__11047342___CLEC16A	0.107226	-3.22127	0.0236
chr12__112203636__112219489___HECTD4	0.107275	-3.22062	0.020108
chr15__63712775__63718897___HERC1	0.107328	-3.2199	0.022497
chr9__122865349__122897576___RC3H2	0.107358	-3.2195	0.022225
chr2__33128432__33222151___LTBP1	0.107426	-3.21858	0.02058
chr1__212863725__212870168___FLVCR1	0.107431	-3.21852	0.024525
chr15__68211263__68218650___CLN6	0.107509	-3.21747	0.025274
chr2__24026799__24033257___NA	0.107524	-3.21728	0.00211
chr10__128104661__128119319___MKI67	0.107532	-3.21716	0.026371
chr3__16271659__16272321___OXNAD1	0.107583	-3.21648	0.024391
chr5__142131808__142144676___NDFIP1	0.107604	-3.21619	0.023312
chr17__59737453__59765138___VMP1	0.107692	-3.21501	0.020761

chr16__19616114__19626223___C16orf62	0.10771	-3.21477	0.009415
chr15__63727647__63749791___HERC1	0.10772	-3.21464	0.021095
chr2__24270671__24271941___ITSN2	0.107769	-3.21399	0.028522
chr13__100257595__100273346___PCCA	0.107793	-3.21367	0.021561
chr8__53970392__54010492___TCEA1	0.10788	-3.2125	0.027168
chr4__78859584__78878891___BMP2K	0.107933	-3.21179	0.008542
chr2__33523879__33534400___RASGRP3	0.107952	-3.21154	0.02463
chr2__69358329__69363670___GFPT1	0.107961	-3.21142	0.026259
chr9__122989297__122990213___RABGAP1	0.107996	-3.21094	0.025637
chr4__128936655__128952840___SCLT1	0.107999	-3.21092	0.02156
chr22__41158412__41173784___EP300	0.108035	-3.21043	0.02099
chr10__68765888__68773099___CCAR1	0.108147	-3.20894	0.026226
chr4__42022838__42039053___SLC30A9	0.108162	-3.20873	0.020081
chr10__102157019__102158214___NOLC1	0.108178	-3.20853	0.005702
chr2__23884765__23895970___ATAD2B	0.108188	-3.20838	0.022497
chr15__44626331__44629388___SPG11	0.108195	-3.2083	0.027126
chr10__68786136__68791341___CCAR1	0.108231	-3.20782	0.025742
chr4__48534545__48542121___FRYL	0.108261	-3.20741	0.025742
chr2__88801099__88805408___ANKRD36BP2	0.108302	-3.20687	0.021583
chr12__22055149__22065287___CMAS	0.108323	-3.2066	0.025849
chr11__35201082__35204640___CD44	0.108382	-3.2058	0.021128
chr4__51860543__51891851___DCUN1D4	0.108414	-3.20538	0.025798
chr11__58584856__58614343___ZFP91ZFP91-CNTF	0.108509	-3.20412	0.026575
chr8__38347497__38348143___WHSC1L1	0.10855	-3.20357	0.025457
chr5__134535858__134552209___JADE2	0.108751	-3.2009	0.026944
chr8__103404776__103407784___SLC25A32	0.108753	-3.20087	0.021117
chr14__60267215__60268435___PPM1A	0.108757	-3.20082	0.024733
chr17__5346790__5368468___RABEP1	0.108764	-3.20073	0.025637
chr13__32432789__32444126___N4BP2L2	0.10878	-3.20051	0.021161
chr10__22539971__22609717___PIP4K2A	0.108812	-3.2001	0.025411
chr5__71495250__71504751___BDP1	0.108836	-3.19977	0.001146
chr18__21020151__21044186___ROCK1	0.108905	-3.19886	0.022962
chr20__49067190__49070297___CSE1L	0.108943	-3.19836	0.024519
chr7__139237005__139259370___UBN2	0.108944	-3.19834	0.025604
chr7__848418__849603___SUN1	0.108947	-3.1983	0.019881
chr10__60787224__60787470___CDK1	0.109021	-3.19732	0.023822
chr8__25483399__25484210___CDCA2	0.109042	-3.19704	0.022468
chr17__67166478__67195470___HELZ	0.10908	-3.19654	0.025531
chr12__98677425__98686873___APAF1	0.109134	-3.19583	0.024243
chr7__77571078__77600806___PTPN12	0.109172	-3.19532	0.027539
chr5__145764931__145796547___PRELID2	0.109276	-3.19396	0.023329
chr22__32478981__32487828___FBXO7	0.109356	-3.19289	0.025487
chr1__159010003__159032691___IFI16	0.109423	-3.19201	0.027457
chr16__18841565__18850467___SMG1	0.109426	-3.19197	0.021967
chr22__31282294__31283288___PIK3IP1	0.109464	-3.19147	0.02099
chr10__131940031__131945459___PPP2R2D	0.109481	-3.19125	0.025799

chr4__145110968__145121391___ABCE1	0.109531	-3.19059	0.023807
chr22__29813430__29822464___ASCC2	0.109534	-3.19055	0.022872
chr4__39904040__39925933___PDS5A	0.109552	-3.19031	0.024903
chr2__23823258__23828939___ATAD2B	0.109559	-3.19022	0.026457
chr1__236850344__236853088___MTR	0.109607	-3.18959	0.026713
chr1__174275833__174305127___RABGAP1L	0.109657	-3.18893	0.023604
chr17__68429996__68433575___WIPI1	0.109716	-3.18815	0.025444
chr11__34063052__34063363___CAPRIN1	0.109823	-3.18674	0.026503
chr5__157803650__157817547___CLINT1	0.109887	-3.1859	0.01816
chr20__47282102__47294779___ZMYND8	0.10993	-3.18534	0.01569
chr6__42810306__42830172___GLTSCR1L	0.10996	-3.18495	0.026718
chr11__74374415__74378658___PGM2L1	0.109965	-3.18489	0.026752
chr8__21970144__21987857___XPO7	0.109969	-3.18483	0.01984
chr7__139371387__139409654___LUC7L2	0.110039	-3.18391	0.024823
chr18__45928869__45952643___EPG5	0.110067	-3.18355	0.01637
chr2__218546919__218560883___USP37	0.110072	-3.18348	0.026845
chr11__74118228__74133557___C2CD3	0.110073	-3.18347	0.028161
chr20__47623911__47628023___NCOA3	0.11014	-3.18259	0.025742
chr3__152298258__152300367___MBNL1	0.110146	-3.18251	0.02099
chr4__1696202__1700070___SLBP	0.110266	-3.18094	0.025418
chr1__35381259__35390098___ZMYM4	0.110358	-3.17973	0.027352
chr1__21715389__21721166___USP48	0.110518	-3.17765	0.027539
chr12__102148230__102182627___PARPBP	0.110558	-3.17712	0.02526
chr5__137942875__137943216___FAM13B	0.11062	-3.17631	0.028149
chr3__108661877__108677598___DZIP3	0.110632	-3.17616	0.022476
chr20__41076171__41101353___TOP1	0.110762	-3.17446	0.02099
chr13__28266715__28288122___PAN3	0.110811	-3.17383	0.026534
chr6__18215007__18217885___KDM1B	0.110867	-3.17309	0.02779
chr12__2868563__2868754___FOXM1	0.110887	-3.17283	0.021095
chr5__137985257__138011945___FAM13B	0.110889	-3.17282	0.018389
chr7__139269394__139279360___UBN2	0.110944	-3.1721	0.024894
chr13__41316846__41331369___NAA16	0.110947	-3.17206	0.02679
chr14__35126735__35127611___KIAA0391	0.11097	-3.17176	0.027539
chr4__106164392__106248306___TBCK	0.111049	-3.17073	0.023718
chr3__56615890__56618212___CCDC66	0.11105	-3.17071	0.025713
chr2__33300451__33301644___LTBP1	0.111099	-3.17008	0.026323
chr12__112229698__112231715___HECTD4	0.111143	-3.16951	0.021786
chr14__31141858__31172122___HECTD1	0.111221	-3.16849	0.010343
chr1__117378660__117420649___MAN1A2	0.111238	-3.16828	0.027215
chr11__34947506__34970286___PDHX	0.111251	-3.16811	0.02156
chr12__120554718__120563943___RNF10	0.111315	-3.16728	0.024688
chr20__35734186__35738621___RBM39	0.111347	-3.16686	0.020619
chr15__74923648__74926887___COX5A	0.111443	-3.16563	0.025531
chrY__13399938__13403888___UTY	0.111453	-3.16549	0.026567
chr12__92851111__92853025___EEA1	0.111457	-3.16544	0.027352
chr10__101793913__101795480___MGEA5	0.111484	-3.16509	0.007926

chr22__16637040__16638740___TPTEP1	0.111493	-3.16497	0.0286
chr4__84904343__84905271___WDFY3	0.111501	-3.16486	0.020081
chr5__172117481__172156788___STK10	0.111523	-3.16458	0.027423
chr14__34758704__34762223___BAZ1A	0.111534	-3.16444	0.009923
chr4__183683975__183693147___TRAPPC11	0.111551	-3.16422	0.025487
chr17__43063333__43067695___BRCA1	0.111649	-3.16295	0.028308
chr3__52678500__52682233___PBRM1	0.11166	-3.16281	0.029088
chr16__75600220__75622464___ADAT1	0.111665	-3.16275	0.010438
chr21__46349012__46367139___PCNT	0.111767	-3.16144	0.022795
chr1__84865385__84866138___LPAR3	0.111825	-3.16068	0.024291
chr7__93259550__93311272___CCDC132	0.111872	-3.16008	0.02312
chr1__93217722__93232593___CCDC18	0.111897	-3.15975	0.02156
chr17__3814322__3818572___C17orf85	0.111903	-3.15968	0.025927
chr12__95287664__95296258___VEZT	0.111975	-3.15875	0.027352
chr9__98004964__98012472___ANP32B	0.112032	-3.15802	0.021117
chr2__201392909__201420706___TRAK2	0.112174	-3.15618	0.026816
chr4__109449417__109463644___SEC24B	0.112219	-3.15561	0.023312
chr3__52411029__52414587___PHF7	0.112295	-3.15463	0.022872
chr3__179764002__179765848___USP13	0.112359	-3.15381	0.024243
chr8__528895__531576___TDRP	0.112485	-3.1522	0.025418
chr6__84155298__84175347___KIAA1009	0.112568	-3.15113	0.017657
chr3__37315420__37321886___GOLGA4	0.112595	-3.15078	0.026713
chr4__186706563__186709845___FAT1	0.112654	-3.15003	0.005744
chr10__31461037__31461783___ZEB1	0.112758	-3.1487	0.023423
chr3__132434538__132450847___DNAJC13	0.11278	-3.14841	0.02156
chr6__129599216__129618852___ARHGAP18	0.11281	-3.14803	0.0236
chr4__98574362__98574905___TSPAN5	0.113004	-3.14555	0.02779
chr12__6510279__6510532___SCARNA10	0.113026	-3.14527	0.020033
chr5__96985080__97028612___LNPEP	0.113101	-3.14431	0.006752
chr17__8518631__8535931___MYH10	0.113162	-3.14354	0.020952
chr17__50964511__50964872___SPAG9	0.113303	-3.14174	0.026282
chr17__56844019__56845809___DGKE	0.113307	-3.14169	0.026567
chr10__119526032__119527424___RGS10	0.113326	-3.14144	0.029158
chrX__3822073__3826729___LOC389906	0.113386	-3.14069	0.023807
chr17__21004202__21004990___USP22	0.113411	-3.14037	0.027806
chr16__75411825__75412754___CFDP1	0.113417	-3.1403	0.023942
chr4__53998206__54014119___NA	0.113441	-3.13998	0.02002
chrX__68513327__68522917___YIPF6	0.113446	-3.13993	0.023649
chr11__130126700__130135715___APLP2	0.113449	-3.13989	0.025637
chrX__71368054__71387461___TAF1	0.113491	-3.13935	0.02842
chr2__45546732__45553730___SRBD1	0.113498	-3.13927	0.026713
chr12__40302789__40304134___LRRK2	0.113537	-3.13877	0.029088
chr5__131395563__131408207___NA	0.113556	-3.13853	0.02677
chr1__1719328__1722831___CDK11A	0.113635	-3.13752	0.022763
chr14__52730459__52771183___STYX	0.113663	-3.13717	0.028457
chr3__12599691__12604289___RAF1	0.11369	-3.13683	0.026713

chr5__79613011__79645192___PAPD4	0.113753	-3.13602	0.028609
chr2__208642225__208656989___LOC101927960	0.113764	-3.13589	0.023518
chr7__5641154__5641376___RNF216	0.113778	-3.1357	0.00503
chr7__140834609__140834872___BRAF	0.113797	-3.13547	0.02272
chr17__67947726__67948306___BPTF	0.113813	-3.13526	0.024214
chr4__48851806__48857365___OCIAD1	0.113869	-3.13455	0.02058
chr16__84758716__84768358___USP10	0.113871	-3.13452	0.017447
chr3__20099862__20152579___KAT2B	0.113888	-3.13432	0.028484
chr15__65700544__65738875___DENND4A	0.113978	-3.13318	0.023072
chr13__32753332__32760720___PDS5B	0.114031	-3.13251	0.010811
chr2__26254247__26263479___HADHB	0.114034	-3.13246	0.022603
chr18__47829474__47896809___NA	0.114103	-3.13159	0.024219
chr2__33257284__33263392___LTBP1	0.114263	-3.12957	0.026302
chr18__9182382__9195698___ANKRD12	0.114287	-3.12927	0.039177
chr5__79645123__79682061___PAPD4	0.114305	-3.12904	0.025067
chr9__33953285__33973237___UBAP2	0.114372	-3.1282	0.023718
chrX__129920457__129921587___UTP14A	0.114377	-3.12813	0.025862
chr20__49074785__49092127___CSE1L	0.114483	-3.1268	0.025995
chr7__80646652__80666489___CD36	0.114493	-3.12667	0.023237
chr1__21089138__21111383___EIF4G3	0.114512	-3.12643	0.026457
chr8__140585091__140605914___AGO2	0.114578	-3.1256	0.025862
chr1__227145489__227317246___CDC42BPA	0.114634	-3.1249	0.027878
chr1__62816575__62821209___ATG4C	0.114661	-3.12455	0.025457
chr19__43925325__43930000___ZNF45	0.114741	-3.12355	0.028314
chr2__100006632__100008932___AFF3	0.114805	-3.12275	0.029816
chr4__128291800__128303035___NA	0.114888	-3.1217	0.026226
chr17__32173831__32201056___RHOT1	0.114917	-3.12134	0.024243
chr6__4854525__4892379___CDYL	0.114927	-3.12121	0.026564
chr5__154790325__154795319___LARP1	0.114965	-3.12074	0.027671
chr6__35857261__35891013___SRPK1	0.115157	-3.11833	0.024903
chr15__49632159__49634794___DTWD1	0.115171	-3.11815	0.02693
chr9__27044742__27062110___IFT74	0.115195	-3.11786	0.023023
chr9__125298890__125302826___GAPVD1	0.115249	-3.11717	0.02542
chr18__116842__118504___ROCK1P1	0.11537	-3.11567	0.024669
chr10__21668917__21670704___MLLT10	0.115399	-3.1153	0.031256
chr3__141963812__141993585___TFDP2	0.115476	-3.11434	0.025419
chr4__39841948__39845880___PDS5A	0.115526	-3.11371	0.026752
chr8__99142974__99275254___VPS13B	0.115545	-3.11347	0.02469
chr14__91465480__91469112___SMEK1	0.115642	-3.11227	0.024104
chr16__74923926__74951543___WDR59	0.115731	-3.11115	0.022413
chr7__152783187__152825122___ACTR3B	0.115743	-3.11101	0.022645
chr1__200569911__200593769___KIF14	0.115781	-3.11053	0.030904
chr13__41937315__41939586___VWA8	0.11584	-3.1098	0.027941
chr2__128172573__128174858___UGGT1	0.115888	-3.10919	0.026953
chr15__49235851__49239367___GALK2	0.115891	-3.10915	0.027215
chr2__32514990__32518946___BIRC6	0.115948	-3.10845	0.029221

chr12__128926359__128927154___GLT1D1	0.116037	-3.10734	0.02593
chr5__109817273__109855334___MAN2A1	0.116057	-3.10709	0.022872
chr7__102366018__102407498___LOC100630923	0.11608	-3.10681	0.024613
chr17__27303367__27311616___WSB1	0.116096	-3.10662	0.030901
chr14__49789146__49831361___NEMF	0.116111	-3.10642	0.024669
chr20__50096483__50098981___UBE2V1	0.116261	-3.10456	0.02807
chr17__60190563__60214774___USP32	0.116311	-3.10394	0.029875
chr8__98526742__98596169___STK3	0.116358	-3.10336	0.025229
chr17__20187958__20205912___SPECC1	0.116387	-3.103	0.027539
chr3__27411642__27452498___SLC4A7	0.116389	-3.10298	0.022497
chr8__123370903__123380677___ATAD2	0.116443	-3.1023	0.029875
chr12__3821873__3863957___PARP11	0.116535	-3.10117	0.030626
chr10__68355353__68404844___RUFY2	0.116551	-3.10097	0.029731
chr7__142942434__142943883___KEL	0.116569	-3.10075	0.030157
chr15__82823100__82826846___WHAMM	0.116788	-3.09803	0.03321
chr12__122568261__122574380___KNTC1	0.116788	-3.09804	0.025093
chr20__35842573__35871829___PHF20	0.116895	-3.09671	0.022276
chr16__47463899__47589102___PHKB	0.116909	-3.09655	0.025067
chr14__50442732__50445194___MAP4K5	0.11694	-3.09616	0.024918
chr20__47262288__47276905___ZMYND8	0.117109	-3.09408	0.02677
chr12__829309__829944___WNK1	0.117128	-3.09385	0.02693
chr7__38010921__38013581___NA	0.117162	-3.09342	0.005526
chr10__6613631__6613987___NA	0.117177	-3.09323	0.023308
chr10__1080011__1086357___WDR37	0.117193	-3.09304	0.023329
chr17__60252381__60288682___USP32	0.117236	-3.09252	0.024894
chr3__183987770__184014447___ABCC5	0.117267	-3.09213	0.025483
chr1__179986169__179992221___CEP350	0.117421	-3.09024	0.025637
chr8__130152736__130188183___ASAP1	0.117474	-3.08959	0.025419
chr6__13632370__13641307___RANBP9	0.117483	-3.08948	0.024243
chr1__174219248__174394145___RABGAP1L	0.117545	-3.08871	0.029151
chr2__201008973__201011472___FAM126B	0.117564	-3.08848	0.024903
chr6__53498607__53532766___GCLC	0.117595	-3.0881	0.028627
chr17__67891844__67903918___BPTF	0.11761	-3.08792	0.026567
chr2__61492035__61495613___XPO1	0.117623	-3.08776	0.030871
chr9__112268049__112276013___PTBP3	0.117655	-3.08737	0.031651
chr15__74805718__74806064___NA	0.117678	-3.08709	0.025945
chr15__65706091__65756472___DENND4A	0.117693	-3.0869	0.026031
chr16__1632212__1641187___CRAMP1L	0.117741	-3.08631	0.025927
chr3__152414941__152459345___MBNL1	0.117766	-3.086	0.027045
chr15__34243974__34245867___SLC12A6	0.117862	-3.08483	0.024894
chr9__36372496__36376127___RNF38	0.117965	-3.08357	0.030008
chr7__139398599__139412580___C7orf55-LUC7L2LUC7L2	0.118046	-3.08257	0.029816
chr18__26052624__26087577___SS18	0.118055	-3.08247	0.023807
chr2__26364302__26373629___EPT1	0.118138	-3.08146	0.010786
chr14__75707018__75720703___TTLL5	0.118188	-3.08084	0.027475
chr9__5021963__5081861___JAK2	0.118204	-3.08065	0.028303

chr13__45988787__46020557___ZC3H13	0.118253	-3.08005	0.024391
chr3__17214207__17238419___TBC1D5	0.118264	-3.07992	0.027126
chr9__19423862__19424841___ACER2	0.118272	-3.07982	0.024903
chr9__68876677__68940790___PIP5K1B	0.118274	-3.0798	0.028206
chr18__39207685__39208789___LINC00669	0.118358	-3.07877	0.023807
chr3__155893518__155937881___NA	0.118386	-3.07842	0.021967
chr1__100049909__100069685___HIAT1	0.118533	-3.07664	0.027423
chr1__20744744__20749882___HP1BP3	0.118587	-3.07598	0.02731
chr16__57164001__57178852___FAM192A	0.118604	-3.07578	0.027412
chr7__87884979__87888059___DBF4	0.118614	-3.07566	0.028167
chr3__196055080__196077122___TFRC	0.118614	-3.07566	0.029985
chr19__9652953__9653878___ZNF562	0.118617	-3.07562	0.028894
chr20__49072286__49072697___CSE1L	0.118624	-3.07553	0.021117
chr1__207655190__207686940___CR1L	0.11866	-3.0751	0.029398
chr3__180947865__180951468___FXR1	0.118703	-3.07458	0.027942
chr19__8473664__8483211___HNRNPM	0.118712	-3.07446	0.030608
chr7__112286873__112296311___ZNF277	0.118713	-3.07445	0.030141
chr8__55785719__55796152___TGS1	0.118732	-3.07421	0.026321
chr21__34102835__34103519___SLC5A3	0.118804	-3.07334	0.029731
chr3__37383226__37386370___NA	0.118806	-3.07332	0.02456
chr8__130134296__130180880___ASAP1	0.118836	-3.07295	0.03236
chr1__61111371__61277585___NFIA	0.118845	-3.07284	0.021414
chr7__80662973__80674147___CD36	0.118848	-3.07281	0.026401
chr3__148446266__148586237___NA	0.118855	-3.07272	0.025485
chr5__73006445__73006780___FCHO2	0.11886	-3.07267	0.025229
chr1__243293091__243330692___SDCCAG8	0.118968	-3.07136	0.012149
chr9__19060088__19096769___HAUS6	0.118971	-3.07132	0.026708
chr6__136669283__136698682___MAP3K5	0.118977	-3.07125	0.029231
chr1__233198939__233218184___PCNXL2	0.119004	-3.07092	0.030187
chr16__19535940__19537587___CCP110	0.119017	-3.07076	0.026752
chr15__63529014__63563008___USP3	0.119032	-3.07058	0.024685
chr9__96336717__96352109___SLC35D2	0.119034	-3.07056	0.0288
chr16__72308056__72391215___NA	0.119061	-3.07023	0.025998
chr14__50423121__50429260___MAP4K5	0.119149	-3.06916	0.025477
chr6__149521060__149541586___PPIL4	0.119196	-3.0686	0.029398
chr18__2718158__2752552___SMCHD1	0.119284	-3.06752	0.023237
chr18__77077285__77080793___MBP	0.119412	-3.06598	0.022012
chr4__169507037__169508852___NEK1	0.119469	-3.06529	0.02938
chr16__14606484__14617650___PARN	0.119479	-3.06517	0.030626
chr9__120408347__120409316___CDK5RAP2	0.119484	-3.06511	0.024291
chr1__153889678__153898982___GATAD2B	0.119514	-3.06474	0.021128
chr9__95978061__95979866___LOC101928170	0.119572	-3.06405	0.029875
chr10__118685983__118730410___CACUL1	0.119647	-3.06314	0.025861
chr2__53866085__53887467___PSME4	0.119688	-3.06265	0.024015
chr1__26462669__26463433___DHDDS	0.119844	-3.06077	0.034558
chr11__28211062__28212331___METTL15	0.119906	-3.06003	0.023942

chr4__76996425__77030970___SEPT11	0.119939	-3.05963	0.027539
chr9__33351560__33354892___NFX1	0.119952	-3.05947	0.026567
chr1__35381259__35381758___ZMYM4	0.119987	-3.05904	0.025067
chr18__58341038__58343103___NEDD4L	0.120045	-3.05835	0.023743
chr17__77402059__77402703___SEPT9	0.120112	-3.05755	0.023807
chr5__163473179__163475672___HMMR	0.120212	-3.05635	0.025637
chr12__30713785__30753559___CAPRIN2	0.120236	-3.05605	0.02732
chr7__131437785__131445903___MKLN1	0.120249	-3.0559	0.025357
chr9__3668263__3674648___RP11-509J21.1	0.12026	-3.05577	0.026314
chr2__58058352__58060201___VRK2	0.120285	-3.05547	0.033728
chr1__77631835__77641655___ZZZ3	0.120302	-3.05527	0.02725
chr1__235677091__235697272___LYST	0.120327	-3.05496	0.031067
chr16__8903268__8917156___USP7	0.120365	-3.05451	0.026671
chr18__22936754__22975219___RBBP8	0.120374	-3.0544	0.024613
chr4__78826037__78859687___BMP2K	0.120431	-3.05372	0.026845
chr1__156744163__156745373___HDGF	0.120489	-3.05303	0.021479
chr2__134253095__134270550___MGAT5	0.120491	-3.053	0.032793
chr12__50435488__50454417___LARP4	0.120541	-3.0524	0.024243
chr4__109659011__109660365___CCDC109B	0.12072	-3.05026	0.032598
chr10__124774675__124790338___METTL10	0.120734	-3.05009	0.022958
chr2__171965338__171966949___HAT1	0.120736	-3.05007	0.025544
chr17__29451455__29522519___TAOK1	0.120759	-3.04979	0.024243
chr1__169477155__169477757___SLC19A2	0.120817	-3.04911	0.025776
chr1__47272076__47300152___STIL	0.120935	-3.0477	0.028128
chr1__15909321__15916279___SPEN	0.120951	-3.0475	0.03024
chr11__48063236__48066680___PTPRJ	0.120967	-3.04731	0.022497
chr21__36338779__36345031___MORC3	0.121005	-3.04686	0.034693
chr5__131255095__131256192___NA	0.121008	-3.04683	0.031788
chr10__86446242__86473973___WAPAL	0.121008	-3.04683	0.024243
chr1__38441190__38442939___NA	0.121016	-3.04673	0.022497
chr12__89655679__89656107___ATP2B1	0.121029	-3.04658	0.03405
chr6__99476143__99510230___USP45	0.121166	-3.04494	0.029838
chr12__95494056__95496098___METAP2	0.121259	-3.04384	0.008473
chr8__100709133__100713181___PABPC1	0.121269	-3.04372	0.030883
chr7__24623666__24641868___MPP6	0.121299	-3.04336	0.026321
chr15__63696124__63749791___HERC1	0.121354	-3.04271	0.035353
chr2__75687827__75702423___GCFC2	0.121378	-3.04242	0.0288
chr9__19093171__19096769___HAUS6	0.121422	-3.0419	0.006271
chr15__68086306__68153695___PIAS1	0.121499	-3.04098	0.026321
chr11__77374328__77392541___PAK1	0.121531	-3.0406	0.023807
chr15__56142778__56243287___RFX7	0.121587	-3.03994	0.037037
chr15__63660973__63675093___HERC1	0.121589	-3.03992	0.02677
chr6__592469__619543___EXOC2	0.121621	-3.03954	0.029398
chr14__61721509__61741188___HIF1A	0.121666	-3.039	0.028371
chr2__119920069__119967972___PTPN4	0.121708	-3.03851	0.030871
chr14__35099252__35108236___PPP2R3C	0.121847	-3.03686	0.026953

chr11__94445810__94461036___MRE11A	0.121849	-3.03684	0.029158
chr4__2689506__2690970___FAM193A	0.121888	-3.03638	0.025485
chr13__95105046__95188542___ABCC4	0.121979	-3.03529	0.027347
chr20__62281790__62291793___OSBPL2	0.121987	-3.0352	0.034436
chr7__112895569__112915447___C7orf60	0.121999	-3.03506	0.027063
chr15__34003032__34023497___AVENCHRM5	0.122035	-3.03463	0.024519
chr20__35801491__35871829___PHF20	0.122109	-3.03376	0.028732
chr1__185160833__185222036___SWT1	0.12212	-3.03362	0.029386
chr7__91941095__92023009___AKAP9	0.122157	-3.03319	0.026713
chr9__133042087__133043926___GTF3C5	0.122164	-3.03311	0.03236
chr7__11061791__11111467___PHF14	0.122167	-3.03308	0.023072
chrX__155506898__155545277___TMLHE	0.122198	-3.03271	0.025125
chr1__86124845__86146183___COL24A1	0.122227	-3.03237	0.00945
chr11__47166268__47168251___ARFGAP2	0.122283	-3.03171	0.030626
chr1__21002713__21050994___EIF4G3	0.1223	-3.0315	0.02965
chr17__20204333__20306082___SPECC1	0.122324	-3.03122	0.021551
chr10__48890579__48901863___WDFY4	0.122327	-3.03118	0.030668
chr9__125298890__125312612___GAPVD1	0.122364	-3.03075	0.024652
chr4__98574457__98578081___TSPAN5	0.12238	-3.03056	0.034625
chr3__56730666__56731299___ARHGEF3	0.122431	-3.02996	0.024838
chr1__197084354__197092010___ASPM	0.122459	-3.02963	0.031307
chr3__47097955__47101555___SETD2	0.122567	-3.02836	0.012188
chr14__49820343__49834449___NEMF	0.122579	-3.02822	0.031307
chr16__71669275__71681905___PHLPP2	0.12258	-3.0282	0.030322
chrX__148651328__148662768___AFF2	0.122581	-3.02819	0.030556
chr12__1739068__1754514___ADIPOR2	0.122589	-3.0281	0.028506
chr2__113916884__113942359___ACTR3	0.122618	-3.02776	0.026919
chr8__94491578__94491909___KIAA1429	0.122642	-3.02748	0.035457
chr11__68544838__68564432___PPP6R3	0.122776	-3.02589	0.027063
chr3__20111596__20127549___KAT2B	0.122814	-3.02545	0.035286
chr12__123194386__123203375___MPHOSPH9	0.122866	-3.02484	0.033981
chr16__23621362__23623130___PALB2	0.122962	-3.02372	0.025849
chr19__48918726__48919286___NUCB1	0.122988	-3.02341	0.029059
chr1__11989165__11992690___MFN2	0.12301	-3.02315	0.025487
chr3__119912704__120093593___GSK3B	0.123053	-3.02264	0.027878
chr2__202206737__202220106___SUMO1	0.123137	-3.02167	0.032588
chr10__100937402__100944128___FAM178A	0.12318	-3.02116	0.030772
chr2__152132114__152150229___STAM2	0.123282	-3.01997	0.024801
chr13__50927407__50934999___RNASEH2B	0.12338	-3.01882	0.014185
chr16__19706592__19711440___KNOP1	0.123534	-3.01702	0.028894
chr17__39297127__39303639___FBXL20	0.123587	-3.0164	0.033568
chr10__92613040__92621473___KIF11	0.123658	-3.01557	0.029309
chr12__64409962__64420521___XPOT	0.123658	-3.01558	0.027352
chr17__63792412__63800617___DDX42	0.123753	-3.01447	0.030248
chr16__53231419__53243016___CHD9	0.12377	-3.01427	0.024613
chr3__57583898__57584464___ARF4	0.123802	-3.01389	0.034164

chr5__60642812__60647533___DEPDC1B	0.123814	-3.01376	0.028899
chr18__61814607__61816598___RNF152	0.12382	-3.01369	0.026254
chr11__68554145__68596218___PPP6R3	0.123844	-3.0134	0.030443
chr1__1649499__1657498___CDK11B	0.1239	-3.01275	0.025056
chr3__183736718__183762279___YEATS2	0.123965	-3.012	0.033945
chr11__77675036__77691238___RSF1	0.12397	-3.01194	0.025637
chr2__24665162__24665915___NCOA1	0.124001	-3.01158	0.030899
chr22__31455852__31463133___EIF4ENIF1	0.124019	-3.01137	0.027461
chr11__33286413__33306009___HIPK3	0.124072	-3.01075	0.034037
chr1__6806983__6825210___CAMTA1	0.124079	-3.01067	0.009
chr1__39434414__39439500___MACF1	0.124083	-3.01062	0.030186
chr18__62138243__62163656___PIGN	0.124212	-3.00912	0.033414
chr16__24775604__24777358___TNRC6A	0.124219	-3.00904	0.026226
chr1__86715724__86735179___SH3GLB1	0.124272	-3.00843	0.010134
chr3__183775915__183777700___YEATS2	0.124313	-3.00795	0.024154
chr1__95143891__95191681___TMEM56	0.124407	-3.00687	0.028578
chr9__121375231__121378100___LOC102723324	0.124578	-3.00488	0.032655
chr7__6580555__6585260___ZDHHC4	0.124582	-3.00483	0.031408
chr14__73147795__73148094___PSEN1	0.124641	-3.00415	0.013345
chr17__29517453__29534300___TAOK1	0.124675	-3.00376	0.031405
chr14__96833467__96837817___VRK1	0.124714	-3.00331	0.027917
chr5__55340010__55358698___SKIV2L2	0.124728	-3.00314	0.025604
chr6__69697563__69701953___LMBRD1	0.12478	-3.00254	0.010601
chr1__10404161__10408140___PGD	0.124786	-3.00247	0.031621
chr11__120476661__120477526___ARHGEF12	0.124929	-3.00082	0.027363
chr12__53381659__53411435___SP1	0.125103	-2.99881	0.027539
chr1__185123857__185151935___TRMT1L	0.125238	-2.99725	0.026401
chr4__143989877__144001283___NA	0.125277	-2.9968	0.029838
chr15__41069570__41087682___INO80	0.125294	-2.99661	0.02526
chr11__124954724__125005212___CCDC15	0.12536	-2.99586	0.035191
chr3__43699502__43702008___ABHD5	0.125414	-2.99523	0.029491
chr10__68465667__68470163___DNA2	0.12542	-2.99516	0.028781
chr7__158631644__158646563___NCAPG2	0.125595	-2.99315	0.031883
chr7__116110708__116112038___NA	0.125617	-2.99289	0.038819
chr8__55941855__55969793___LYN	0.125617	-2.9929	0.031788
chr2__175080660__175151158___ATF2	0.125633	-2.99271	0.030921
chr3__33409236__33425741___UBP1	0.125698	-2.99197	0.031244
chr13__113306485__113310867___LAMP1	0.125795	-2.99085	0.033945
chr2__232815637__232819985___GIGYF2	0.125822	-2.99054	0.030626
chr2__37139631__37141701___EIF2AK2	0.125871	-2.98999	0.023807
chrX__75098942__75114834___ABCB7	0.12594	-2.98919	0.029655
chr18__6237964__6312056___L3MBTL4	0.125991	-2.98861	0.033771
chr9__112250929__112276013___PTBP3	0.126121	-2.98712	0.033032
chr3__38221578__38230430___OXSR1	0.12618	-2.98644	0.032366
chr14__30633947__30639864___SCFD1	0.126195	-2.98627	0.027224
chr1__51402435__51465326___EPS15	0.126241	-2.98574	0.033414

chr14__31121422__31156886___HECTD1	0.126271	-2.98541	0.0255
chr18__54877567__54884436___RAB27B	0.126302	-2.98505	0.035388
chr9__77337255__77345142___VPS13A	0.126308	-2.98498	0.030746
chr7__105073619__105102194___KMT2E	0.12632	-2.98484	0.025742
chr5__179709873__179719781___CANX	0.126351	-2.98449	0.027215
chr19__10173090__10182077___DNMT1	0.126353	-2.98447	0.034429
chr1__204558641__204570746___MDM4	0.126415	-2.98376	0.028161
chr9__36669310__36674937___MELK	0.126429	-2.9836	0.027539
chr16__89878461__89883310___TCF25	0.12645	-2.98336	0.026259
chr12__123194386__123210162___MPHOSPH9	0.126523	-2.98253	0.026549
chr16__27211146__27215008___KDM8	0.126537	-2.98237	0.030871
chr1__158652467__158654748___SPTA1	0.126586	-2.98181	0.025464
chr1__243316755__243330692___SDCCAG8	0.126732	-2.98014	0.027457
chr13__60509763__60535233___TDRD3	0.126825	-2.97909	0.027539
chr11__46795594__46821268___CKAP5	0.126959	-2.97757	0.035021
chr14__34586230__34609742___SNX6	0.127107	-2.97589	0.034963
chr22__25663630__25674528___ADRBK2	0.127218	-2.97463	0.031576
chr10__72708283__72741845___MCU	0.127247	-2.9743	0.025742
chr14__88416711__88433212___SPATA7	0.127289	-2.97382	0.031374
chr2__201420417__201420706___TRAK2	0.127296	-2.97374	0.025705
chr3__108669681__108677598___DZIP3	0.127549	-2.97087	0.031408
chr6__24687405__24687693___ACOT13	0.127873	-2.96721	0.028161
chr10__104008177__104010908___SLK	0.12806	-2.96511	0.038032
chr3__132681914__132692818___NPHP3-ACAD11	0.128079	-2.96489	0.030832
chr17__12095575__12113360___MAP2K4	0.128118	-2.96445	0.034816
chr15__64203082__64204949___CSNK1G1	0.128121	-2.96442	0.029816
chr8__85472029__85473468___CA2	0.128191	-2.96363	0.037855
chr9__40994633__41011730___LOC100132352	0.128236	-2.96313	0.034816
chr1__29060422__29115803___EPB41	0.128294	-2.96248	0.030871
chr19__37199400__37207254___ZNF585B	0.128387	-2.96143	0.026953
chr2__23819747__23834078___ATAD2B	0.128403	-2.96124	0.037199
chr10__50519831__50523704___SGMS1	0.128416	-2.96111	0.03307
chr11__68784815__68796933___CPT1A	0.128514	-2.96001	0.038819
chr10__119160915__119161081___SFXN4	0.128552	-2.95958	0.038224
chr6__136558800__136567874___MAP3K5	0.128599	-2.95905	0.040256
chr7__77778338__77780774___NA	0.128607	-2.95895	0.012149
chr10__48401612__48404981___MAPK8	0.128681	-2.95813	0.031405
chrY__13355003__13369349___UTY	0.128692	-2.958	0.030871
chr9__33504538__33509336___SUGT1P1	0.128707	-2.95784	0.039188
chr7__139083780__139089759___ZC3HAV1	0.128771	-2.95712	0.029398
chr9__6984166__7011879___KDM4C	0.128786	-2.95695	0.027647
chr15__92885515__92892072___LOC100507217	0.128867	-2.95605	0.010811
chr17__61972727__61985090___MED13	0.12889	-2.95579	0.037675
chr7__74239938__74246763___RFC2	0.128976	-2.95482	0.035431
chr1__42825623__42840296___ERMAP	0.128999	-2.95457	0.028442
chr9__33941649__33963791___UBAP2	0.129001	-2.95454	0.010791

chr11__601574__603436___PHRF1	0.129004	-2.95451	0.033414
chr19__48230438__48241063___CARD8	0.129061	-2.95388	0.03761
chrX__150814862__150816078___CD99L2	0.129073	-2.95374	0.038819
chr12__117049019__117056886___TESC	0.129308	-2.95111	0.040986
chr1__207697503__207708263___CR1L	0.129324	-2.95093	0.040665
chr7__158869855__158891333___WDR60	0.129408	-2.95	0.033382
chr2__223998115__224001922___SERPINE2	0.129459	-2.94943	0.035191
chr2__68513080__68545312___APLF	0.129513	-2.94883	0.028609
chr3__69187770__69189952___FRMD4B	0.129624	-2.94759	0.03236
chr17__35820024__35820437___TAF15	0.129705	-2.94669	0.03562
chr17__43377913__43380107___LINC00910	0.129737	-2.94634	0.03237
chr17__44154556__44155411___C17orf53	0.129895	-2.94458	0.035431
chr19__3623688__3624162___CACTIN	0.129916	-2.94435	0.035191
chr22__32479133__32485209___FBXO7	0.129971	-2.94374	0.036455
chr12__94169153__94227235___PLXNC1	0.129986	-2.94357	0.027504
chr1__150343309__150344547___PRPF3	0.13002	-2.94319	0.036125
chr12__28255581__28362515___CCDC91	0.130062	-2.94273	0.035071
chr11__121045674__121073040___TBCEL	0.130161	-2.94163	0.030139
chr1__15638307__15649823___DDI2	0.13022	-2.94098	0.036207
chr2__61112518__61118116___KIAA1841	0.13024	-2.94076	0.031176
chr3__20095364__20152365___KAT2B	0.130296	-2.94014	0.015218
chr1__108882580__108929975___GPSM2	0.130434	-2.93861	0.011244
chr10__15833630__15843272___FAM188A	0.130454	-2.93839	0.011473
chr3__44828214__44840456___KIF15	0.1305	-2.93788	0.013658
chr10__22541804__22542047___PIP4K2A	0.130525	-2.9376	0.031968
chr19__15268905__15273133___BRD4	0.130574	-2.93706	0.033966
chr1__185180391__185190642___SWT1	0.130591	-2.93687	0.007926
chr15__63529014__63574403___USP3	0.130691	-2.93577	0.029363
chr5__79290121__79306461___JMY	0.130768	-2.93492	0.031283
chr17__47122444__47151918___CDC27	0.130825	-2.93429	0.032578
chr14__60256824__60260010___PPM1A	0.130861	-2.93389	0.036475
chr17__76767386__76776541___MFSD11	0.130913	-2.93332	0.031986
chr20__47310056__47312035___ZMYND8	0.130947	-2.93294	0.027539
chr18__69895701__69947433___CD226	0.131025	-2.93208	0.034429
chr1__150230571__150231926___ANP32E	0.131072	-2.93157	0.002021
chr12__112266912__112279386___HECTD4	0.131116	-2.93109	0.02779
chr1__20840856__20865262___EIF4G3	0.131139	-2.93083	0.013381
chr2__10791795__10793202___PDIA6	0.131203	-2.93013	0.035421
chr12__111658736__111681835___BRAP	0.131205	-2.9301	0.036366
chr2__32377588__32395593___BIRC6	0.131206	-2.9301	0.030734
chr3__47169169__47174263___KIF9-AS1	0.131232	-2.92981	0.032406
chr20__21326490__21330539___XRN2	0.131247	-2.92964	0.031845
chr12__71918451__71921454___TBC1D15	0.131313	-2.92892	0.029737
chr2__99429840__99435941___REV1	0.131317	-2.92887	0.035431
chr10__96544076__96578320___TM9SF3	0.131424	-2.9277	0.036065
chr19__32899857__32901412___CEP89	0.131426	-2.92768	0.02927

chr2__30525587__30568176___LCLAT1	0.131444	-2.92748	0.016209
chr11__125597059__125608289___STT3A	0.131541	-2.92642	0.031408
chr16__74938150__74951543___WDR59	0.131675	-2.92494	0.029875
chr6__152628265__152628554___SYNE1	0.131704	-2.92463	0.036236
chr18__37160200__37173081___KIAA1328	0.131829	-2.92326	0.038819
chr22__40830840__40848369___ST13	0.131862	-2.9229	0.028403
chr7__104161072__104188381___ORC5	0.131893	-2.92256	0.027412
chr15__56700933__56701238___ZNF280D	0.131898	-2.9225	0.042607
chr16__11875761__11898035___GSPT1	0.131902	-2.92247	0.038326
chr2__171117739__171132092___TLK1	0.132013	-2.92125	0.03197
chr16__11886471__11887750___GSPT1	0.132047	-2.92087	0.016003
chr1__235780865__235782087___LYST	0.132104	-2.92026	0.044149
chr19__45277923__45278615___MARK4	0.132207	-2.91913	0.017526
chr7__139398599__139407350___C7orf55-LUC7L2LUC7L2	0.132233	-2.91884	0.038266
chr3__141512163__141540609___RASA2	0.132249	-2.91867	0.040521
chr6__144537582__144557311___UTRN	0.132262	-2.91853	0.031405
chr6__42650284__42658824___UBR2	0.132275	-2.91838	0.029875
chr19__11830617__11947307___NA	0.132375	-2.91729	0.034429
chr11__76447070__76448680___C11orf30	0.132378	-2.91727	0.028343
chr6__149572285__149580723___GINM1	0.132444	-2.91655	0.028506
chr2__55644637__55646486___PNPT1	0.132462	-2.91635	0.029647
chr1__174219125__174305127___RABGAP1L	0.132473	-2.91622	0.030775
chr9__121375215__121378100___LOC102723324	0.132528	-2.91563	0.034816
chr1__112555868__112616895___ST7L	0.132677	-2.91401	0.033633
chr12__76059798__76060279___NAP1L1	0.132689	-2.91388	0.035648
chr2__182952405__182953331___NCKAP1	0.132747	-2.91325	0.035648
chr12__128799259__128815070___SLC15A4	0.132793	-2.91275	0.026619
chr13__21400373__21413772___ZDHHC20	0.1328	-2.91267	0.035386
chr13__28174272__28220378___PAN3	0.132801	-2.91267	0.013422
chr1__20757166__20776750___HP1BP3	0.132815	-2.91251	0.042299
chr8__108228267__108241913___EIF3E	0.132817	-2.91249	0.032225
chr18__23519680__23520313___C18orf8NPC1	0.132898	-2.91161	0.035444
chr15__92978234__92992998___CHD2	0.133021	-2.91027	0.031854
chr1__77206640__77212347___PIGK	0.133044	-2.91002	0.043554
chr7__16258390__16301466___ISPD	0.133059	-2.90986	0.033966
chr1__243645893__243843282___AKT3	0.133075	-2.90969	0.035286
chr18__56624288__56626457___TXNL1	0.133121	-2.90919	0.029875
chr17__32017972__32035639___NA	0.133135	-2.90904	0.035353
chr4__343782__344430___ZNF141	0.133253	-2.90776	0.033959
chr5__132699171__132711057___KIF3A	0.133286	-2.9074	0.030141
chr4__177351380__177360677___NEIL3	0.133315	-2.90709	0.01132
chr20__50940865__50942126___DPM1	0.133374	-2.90645	0.030322
chr14__39177841__39179462___PNN	0.133393	-2.90624	0.039629
chr9__5787061__5831028___ERMP1	0.133443	-2.9057	0.042064
chr12__22055149__22062434___CMAS	0.133522	-2.90485	0.030608
chr10__80468547__80469881___TSPAN14	0.133585	-2.90417	0.027539

chr17__30856955__30879487___ATAD5	0.133738	-2.90252	0.03236
chr3__15766234__15814309___ANKRD28	0.133793	-2.90193	0.036236
chr15__63723182__63749791___HERC1	0.133831	-2.90152	0.031256
chr4__128957026__128999794___SCLT1	0.13392	-2.90056	0.028314
chr15__63732924__63756748___HERC1	0.134298	-2.89649	0.030602
chr14__21263667__21268668___HNRNPC	0.13453	-2.894	0.034313
chrX__65075474__65113813___NA	0.134545	-2.89384	0.008059
chr6__85536792__85542043___SNX14	0.13481	-2.891	0.041858
chr13__19824920__19835689___ZMYM5	0.134823	-2.89086	0.028686
chr17__45475100__45478147___PLEKHM1	0.134838	-2.8907	0.036765
chr11__108046270__108055441___CUL5	0.134839	-2.89069	0.03132
chr17__47402132__47429961___EFCAB13	0.134891	-2.89014	0.036028
chr13__74406315__74406780___LOC101927121	0.134894	-2.8901	0.035889
chr2__33565246__33568187___NA	0.134969	-2.8893	0.039258
chr15__34250298__34251057___SLC12A6	0.134975	-2.88924	0.033981
chr12__70278132__70311017___CNOT2	0.134988	-2.8891	0.032065
chr17__28921688__28927063___PHF12	0.13501	-2.88887	0.037981
chr16__12199601__12278036___SNX29	0.13508	-2.88811	0.037952
chr5__97013648__97028612___LNPEP	0.135105	-2.88784	0.044182
chr5__14741827__14751239___ANKH	0.135107	-2.88782	0.031883
chr7__77083887__77098951___NA	0.135133	-2.88754	0.042623
chr8__55782748__55787060___TGS1	0.135256	-2.88623	0.030921
chr9__86033282__86046572___GOLM1	0.13528	-2.88598	0.033489
chr12__122601536__122622607___KNTC1	0.135453	-2.88414	0.029088
chr11__3768581__3771928___NUP98	0.135496	-2.88367	0.033885
chr3__47675475__47678311___SMARCC1	0.135629	-2.88226	0.035286
chr18__79096476__79207012___ATP9B	0.13567	-2.88183	0.018528
chr17__40408492__40416512___TOP2A	0.135696	-2.88155	0.045129
chr14__63998914__64022863___SYNE2	0.135729	-2.8812	0.00338
chr1__28027789__28058094___EYA3	0.135863	-2.87977	0.017849
chr1__1755374__1756343___NADK	0.135958	-2.87877	0.041398
chr17__50740306__50744813___LUC7L3	0.136035	-2.87795	0.036613
chr2__128170288__128173939___UGGT1	0.136082	-2.87745	0.039836
chr4__98404477__98421394___RAP1GDS1	0.136177	-2.87644	0.033285
chr17__59910562__59936541___RPS6KB1	0.136274	-2.87542	0.03914
chr13__95161189__95194937___ABCC4	0.136345	-2.87467	0.040092
chr3__160277306__160282613___IFT80	0.136359	-2.87452	0.03203
chr12__50988382__51010766___SLC11A2	0.13638	-2.87429	0.039188
chr1__95143891__95230994___TMEM56-RWDD3	0.136409	-2.87399	0.046123
chr12__112319225__112319742___HECTD4	0.136512	-2.8729	0.005685
chr15__44569398__44570658___SPG11	0.136524	-2.87278	0.044648
chr9__85618983__85712566___AGTPBP1	0.136561	-2.87239	0.039461
chr6__109656756__109675756___AK9	0.136567	-2.87232	0.037875
chr1__95140673__95173889___TMEM56TMEM56-RWDD3	0.136609	-2.87187	0.016369
chr1__185181946__185231708___SWT1	0.13663	-2.87166	0.030832
chr14__54408745__54411706___CDKN3	0.1368	-2.86986	0.036269

chr6__149342685__149370099___TAB2	0.136851	-2.86933	0.030626
chr10__91951403__91966757___BTAF1	0.136986	-2.8679	0.008348
chr21__36338779__36356724___MORC3	0.137042	-2.86731	0.019196
chr20__47236326__47249439___ZMYND8	0.137116	-2.86653	0.034412
chr6__53498607__53514497___GCLC	0.137278	-2.86483	0.030626
chrX__77988242__77989958___ATP7A	0.13728	-2.86481	0.031493
chr1__180052970__180065272___CEP350	0.13729	-2.86471	0.036065
chr5__151473673__151479489___SLC36A1	0.137408	-2.86346	0.047297
chr16__46668930__46676692___VPS35	0.137429	-2.86325	0.033957
chr4__117575655__117575857___NA	0.137436	-2.86317	0.045129
chr17__79077430__79077864___ENGASE	0.137437	-2.86316	0.037672
chr10__31373018__31461237___ZEB1	0.137491	-2.86259	0.013854
chr20__447889__448074___TBC1D20	0.137502	-2.86248	0.034374
chr17__8551185__8551981___MYH10	0.137533	-2.86215	0.040624
chr5__5441112__5444326___KIAA0947	0.137578	-2.86168	0.042819
chr18__62539681__62556297___ZCCHC2	0.137592	-2.86153	0.038804
chr1__172131175__172182896___DNM3	0.137594	-2.86151	0.047303
chr4__83439863__83446086___HELQ	0.137603	-2.86141	0.035388
chrX__11055936__11110981___MID1-2	0.137636	-2.86107	0.03321
chr2__26364302__26375148___EPT1	0.137672	-2.86069	0.044325
chr9__89418056__89475550___SEMA4D	0.137715	-2.86024	0.031457
chr4__145064572__145081750___ANAPC10	0.137861	-2.85872	0.045475
chr1__8541214__8624380___RERE	0.137862	-2.8587	0.027539
chr3__37383226__37399659___NA	0.137946	-2.85782	0.034241
chr8__60572046__60591969___RAB2A	0.137985	-2.85742	0.046949
chr18__69895701__69896045___CD226	0.13803	-2.85695	0.039027
chr14__58306022__58330169___ARID4A	0.13804	-2.85684	0.037508
chr5__176943335__176969706___UIMC1	0.138094	-2.85628	0.034811
chr10__86443275__86460496___WAPAL	0.138119	-2.85602	0.036328
chr1__93869090__93875783___NA	0.138122	-2.85599	0.040556
chr17__32171043__32175362___RHOT1	0.138189	-2.85529	0.044257
chr5__95748333__95763620___RHOBTB3	0.138206	-2.8551	0.019366
chr2__152657889__152659009___PRPF40A	0.138336	-2.85376	0.035431
chr4__1900626__1951203___WHSC1	0.138364	-2.85346	0.029647
chr20__5557945__5570239___GPCPD1	0.138444	-2.85262	0.036668
chr15__50637422__50648885___TRPM7	0.13847	-2.85235	0.035804
chr10__31373018__31502509___ZEB1	0.138475	-2.8523	0.039367
chr3__141970073__141993585___TFDP2	0.138598	-2.85102	0.033308
chr1__75728401__75750546___ACADM	0.138665	-2.85032	0.045148
chr2__15394227__15396475___NBAS	0.138675	-2.85022	0.031651
chr2__106830066__106834146___ST6GAL2	0.138684	-2.85012	0.014455
chr18__2700539__2729409___SMCHD1	0.138719	-2.84976	0.044648
chr2__55577315__55588956___SMEK2	0.138737	-2.84957	0.041016
chr1__155767425__155777820___GON4L	0.138748	-2.84946	0.036015
chr9__111440372__111451555___KIAA0368	0.138917	-2.8477	0.031326
chr3__44840355__44841238___KIF15	0.138942	-2.84745	0.038266

chr10__119049801__119051321___EIF3A	0.138994	-2.84691	0.04412
chr11__68564303__68576043___PPP6R3	0.139067	-2.84615	0.03264
chr2__61115979__61121276___KIAA1841	0.139075	-2.84607	0.03558
chr9__83665030__83678599___UBQLN1	0.139106	-2.84575	0.042729
chr3__172773903__172784803___ECT2	0.139118	-2.84562	0.030921
chr11__12138390__12162419___MICAL2	0.139151	-2.84528	0.030964
chr17__5399552__5416682___NUP88	0.139179	-2.84499	0.041624
chr10__45590524__45592060___MARCH8	0.139201	-2.84475	0.036525
chr11__31452718__31488241___IMMP1L	0.139408	-2.84261	0.035889
chr1__93544107__93560915___NA	0.139444	-2.84224	0.039629
chr1__145974825__145975436___POLR3GL	0.139518	-2.84148	0.043631
chr21__15762891__15805258___USP25	0.139552	-2.84112	0.040256
chr12__27046158__27066226___NA	0.139578	-2.84086	0.036005
chr14__80862757__80906081___CEP128	0.139645	-2.84017	0.033945
chrX__68511849__68513405___YIPF6	0.139816	-2.8384	0.036058
chr7__103182378__103184127___DPY19L2P2	0.139835	-2.8382	0.03197
chr3__56571181__56594028___CCDC66	0.139994	-2.83656	0.030008
chr22__40277077__40285770___TNRC6B	0.140018	-2.83632	0.012211
chr1__185180391__185222036___SWT1	0.140048	-2.836	0.036236
chr17__39298990__39301075___FBXL20	0.140116	-2.83531	0.048641
chr7__48466956__48489344___ABCA13	0.140241	-2.83402	0.03914
chr6__18249651__18263996___DEK	0.140282	-2.8336	0.045768
chr15__92885515__92901299___NA	0.140384	-2.83255	0.044963
chr11__120465237__120467308___ARHGEF12	0.140458	-2.83179	0.009
chr1__88740988__88805671___PKN2	0.140465	-2.83171	0.031307
chr2__20297553__20327378___PUM2	0.140526	-2.83109	0.037242
chr11__16465701__16589400___NA	0.140531	-2.83103	0.036015
chr10__179994__221356___ZMYND11	0.140589	-2.83045	0.042555
chr14__96852831__96860735___VRK1	0.140716	-2.82915	0.045632
chr5__69115237__69128132___SLC30A5	0.140756	-2.82873	0.043972
chr10__16695023__16782084___RSU1	0.140825	-2.82803	0.028112
chr15__49235851__49283718___GALK2	0.140827	-2.828	0.04037
chr3__138694786__138699095___PIK3CB	0.140841	-2.82786	0.02058
chr1__25300946__25301686___RHD	0.140855	-2.82772	0.047124
chr17__77176198__77176681___SEC14L1	0.140876	-2.8275	0.003736
chr11__68189570__68190152___SUV420H1	0.140911	-2.82714	0.044077
chr1__180084018__180087717___CEP350	0.140949	-2.82676	0.036765
chr17__28163543__28185265___NLK	0.14096	-2.82664	0.039188
chr1__179901302__179908673___TOR1AIP1	0.140988	-2.82636	0.043972
chr17__29676820__29703062___SSH2	0.141213	-2.82406	0.038076
chr9__85692689__85723868___AGTPBP1	0.141281	-2.82336	0.040372
chr9__121190554__121193419___RAB14	0.141406	-2.82208	0.035645
chr9__77247259__77283650___VPS13A	0.141467	-2.82147	0.016611
chr6__89749223__89750532___MDN1	0.141593	-2.82018	0.03307
chr1__155921375__155925843___KIAA0907	0.141613	-2.81998	0.036269
chr7__2229984__2230764___MAD1L1	0.141624	-2.81986	0.041708

chr3__142355401__142376594___XRN1	0.14165	-2.8196	0.039082
chr1__26268483__26272071___CEP85	0.14169	-2.81919	0.041322
chr12__112203636__112226758___HECTD4	0.14173	-2.81878	0.008731
chr17__5361208__5373454___RABEP1	0.141749	-2.81859	0.031098
chr7__35781209__35794022___AC007551.3	0.141869	-2.81736	0.040928
chr8__99502836__99521010___VPS13B	0.141919	-2.81686	0.03867
chr4__48833401__48850082___OCIAD1	0.141921	-2.81684	0.033414
chr11__3735191__3753408___NUP98	0.141971	-2.81633	0.039629
chr1__51840226__51855388___NRD1	0.142035	-2.81568	0.039668
chr10__87864454__87936905___PTEN	0.142067	-2.81536	0.039836
chr2__62859169__62874532___EHBP1	0.142069	-2.81534	0.033633
chr10__97229147__97266125___ARHGAP19ARHGAP19-SLIT1	0.142209	-2.81392	0.035431
chr16__11721577__11736233___TXNDC11	0.142258	-2.81342	0.035286
chr12__98527886__98537572___TMPO	0.142368	-2.81231	0.035286
chr20__58999343__58999809___CTSZ	0.142377	-2.81222	0.049954
chr9__132400035__132402828___TTF1	0.142399	-2.81199	0.04412
chr9__5050686__5055788___JAK2	0.142511	-2.81085	0.045049
chr3__148446266__148619264___NA	0.142555	-2.81041	0.03321
chr3__121467519__121468431___POLQ	0.142658	-2.80936	0.045092
chr11__107416209__107433749___CWF19L2	0.142658	-2.80937	0.034035
chr11__46776255__46778599___CKAP5	0.142728	-2.80866	0.037855
chr22__29282390__29287134___EWSR1	0.14275	-2.80844	0.043529
chr9__111433233__111444494___KIAA0368	0.142779	-2.80814	0.038705
chr1__246631894__246634587___CNST	0.143009	-2.80582	0.037001
chr18__50895809__50908196___ME2	0.143121	-2.80469	0.047695
chr12__130791674__130801488___STX2	0.143174	-2.80415	0.034593
chr4__184661774__184678394___PRIMPOL	0.143176	-2.80414	0.037087
chr22__45178238__45181367___NUP50	0.143276	-2.80313	0.036455
chr3__119905755__120093593___GSK3B	0.143474	-2.80114	0.001576
chr15__44648866__44652266___SPG11	0.143502	-2.80086	0.034811
chr2__230269532__230287966___SP140	0.14351	-2.80078	0.043804
chr7__105005318__105009209___NA	0.143635	-2.79952	0.041399
chr14__88607243__88610940___ZC3H14	0.143656	-2.79931	0.037982
chr12__62313992__62355475___USP15	0.143848	-2.79739	0.042623
chr20__46063360__46079453___NCOA5	0.143893	-2.79693	0.036765
chr4__25151960__25159107___SEPSECS	0.14392	-2.79666	0.021117
chr22__41154995__41173784___EP300	0.143983	-2.79603	0.04015
chr15__66513988__66540210___ZWILCH	0.14401	-2.79576	0.043018
chr16__3780732__3782926___CREBBP	0.144353	-2.79232	0.040256
chr4__48642277__48646017___FRYL	0.144361	-2.79225	0.041535
chr22__28695710__28699937___CHEK2	0.144386	-2.792	0.021415
chr2__189728660__189744788___ANKAR	0.144443	-2.79143	0.014891
chr13__52460899__52474084___CKAP2	0.144476	-2.7911	0.044687
chr6__24456498__24467274___GPLD1	0.144477	-2.79109	0.03903
chr8__26338890__26354633___PPP2R2A	0.144528	-2.79058	0.015173
chr21__33340999__33345360___IFNAR1	0.144539	-2.79047	0.013854

chr3__38183003__38236961___OXSR1	0.144746	-2.7884	0.035358
chr12__65181741__65184482___LEMD3	0.144788	-2.78798	0.04292
chr8__140789474__140890769___PTK2	0.144864	-2.78723	0.039187
chr16__1724557__1729578___MAPK8IP3	0.144937	-2.7865	0.044687
chr18__79096476__79176907___ATP9B	0.14495	-2.78637	0.006599
chr8__123084162__123097441___TBC1D31	0.144969	-2.78618	0.041548
chr11__16183886__16283918___SOX6	0.144972	-2.78615	0.044891
chr10__11594631__11601980___USP6NL	0.144988	-2.786	0.037735
chr8__47927194__47930787___PRKDC	0.144999	-2.78588	0.037508
chr16__71656571__71679535___PHLPP2	0.145001	-2.78586	0.017526
chr11__108192118__108197420___NPAT	0.14515	-2.78438	0.039632
chr17__5410703__5414134___NUP88	0.145205	-2.78384	0.048261
chr5__171964198__171997051___FBXW11	0.145252	-2.78337	0.044787
chr14__88754512__88766867___EML5	0.145302	-2.78287	0.043177
chr2__168063500__168075231___STK39	0.145408	-2.78182	0.041164
chr14__102714423__102721377___RCOR1	0.145443	-2.78147	0.042623
chr17__32755492__32780784___MYO1D	0.145492	-2.78099	0.036924
chr20__34031522__34033318___RALY	0.145513	-2.78078	0.012489
chr12__49460770__49490731___SPATS2	0.145523	-2.78068	0.047647
chr10__7769216__7780307___KIN	0.14557	-2.78021	0.043728
chr5__39201826__39202987___FYB	0.145574	-2.78017	0.015948
chr12__62194933__62207250___NA	0.145671	-2.77921	0.042629
chr1__236803428__236829268___MTR	0.145752	-2.77841	0.043745
chr1__222725450__222730177___BROX	0.14581	-2.77784	0.043566
chr1__28987431__28997574___EPB41	0.145811	-2.77782	0.043135
chr9__77337255__77344281___VPS13A	0.145917	-2.77678	0.035506
chr9__85575315__85596449___AGTPBP1	0.145932	-2.77663	0.008997
chr11__34931404__34978182___PDHX	0.145982	-2.77614	0.036455
chr3__56660731__56661017___FAM208A	0.146001	-2.77595	0.045095
chrX__48939910__48940907___OTUD5	0.146026	-2.7757	0.038819
chr5__138006990__138019146___FAM13B	0.146063	-2.77533	0.03883
chrX__68192919__68201710___OPHN1	0.146085	-2.77512	0.04412
chr20__48941199__48953790___ARFGEF2	0.146115	-2.77482	0.005853
chr13__41811225__41833531___VWA8	0.146124	-2.77473	0.049385
chr1__201854595__201858994___IPO9	0.14627	-2.7733	0.044849
chr5__139614586__139623461___UBE2D2	0.146523	-2.7708	0.033945
chr12__100591736__100601753___GAS2L3	0.146606	-2.76998	0.037981
chr9__100340257__100349372___TEX10	0.146694	-2.76912	0.036023
chr3__152414941__152432920___MBNL1	0.14679	-2.76817	0.00959
chr17__73203000__73203793___COG1	0.146818	-2.7679	0.035191
chr5__50399107__50428227___EMB	0.146825	-2.76783	0.02293
chr1__1649499__1655484___CDK11B	0.14689	-2.76719	0.017803
chr7__151470571__151498180___RHEB	0.146935	-2.76675	0.017649
chr12__122594276__122622607___KNTC1	0.147011	-2.76601	0.021491
chr14__50425907__50429260___MAP4K5	0.147063	-2.7655	0.037013
chr12__110485078__110487943___FAM216A	0.147068	-2.76545	0.018445

chr12__28412863__28484165___CCDC91	0.147354	-2.76265	0.039677
chr22__41808875__41810291___CCDC134	0.147484	-2.76137	0.038392
chr14__31116236__31121505___HECTD1	0.147665	-2.7596	0.040256
chr2__9350808__9358889___ASAP2	0.147791	-2.75837	0.022276
chr10__32451592__32481782___CCDC7	0.14796	-2.75672	0.009862
chrX__10063445__10094281___WWC3	0.147995	-2.75638	0.04049
chr4__78844928__78865720___BMP2K	0.148018	-2.75615	0.048049
chr17__50982524__50985778___SPAG9	0.148022	-2.75611	0.033945
chr5__77053965__77055596___AGGF1	0.148052	-2.75582	0.04659
chr1__179131311__179133374___ABL2	0.148063	-2.75572	0.040071
chr17__47129393__47158303___CDC27	0.148104	-2.75532	0.039831
chr2__227491547__227536993___AGFG1	0.14812	-2.75516	0.046231
chr13__32770121__32773324___PDS5B	0.148212	-2.75426	0.04292
chr15__56700933__56707306___ZNF280D	0.14828	-2.7536	0.038819
chr1__70184785__70187338___LRRC40	0.148301	-2.7534	0.039367
chr20__1452493__1458274___NSFL1C	0.148464	-2.75181	0.008059
chr9__27044742__27062119___IFT74	0.148468	-2.75178	0.040641
chr14__50446079__50456594___MAP4K5	0.148545	-2.75103	0.038819
chr12__26982773__26983596___TM7SF3	0.148579	-2.7507	0.044815
chr12__116205053__116237705___MED13L	0.148663	-2.74989	0.017803
chr15__63661753__63669698___HERC1	0.148717	-2.74936	0.016003
chr14__50145170__50150230___SOS2	0.148722	-2.74931	0.048227
chr14__103428387__103492034___MARK3	0.148725	-2.74928	0.041231
chr10__68025546__68044558___HERC4	0.148758	-2.74896	0.035286
chr5__134199086__134206131___PPP2CA	0.14879	-2.74865	0.044983
chr10__86460399__86461287___WAPAL	0.148864	-2.74793	0.023718
chr14__60266538__60277365___PPM1A	0.148944	-2.74716	0.047151
chr22__41135813__41141222___EP300	0.149077	-2.74587	0.047177
chr1__243695591__243843282___AKT3	0.149089	-2.74576	0.038804
chr2__37101923__37104132___NA	0.149098	-2.74566	0.044787
chr1__163343733__163349080___NUF2	0.149169	-2.74498	0.049954
chr17__43099775__43104956___BRCA1	0.149181	-2.74486	0.038328
chr5__109755329__109774965___MAN2A1	0.149247	-2.74423	0.038804
chr2__224557659__224558241___CUL3	0.149291	-2.7438	0.041475
chr20__18297985__18306393___ZNF133	0.149548	-2.74132	0.023191
chr6__35874233__35891013___SRPK1	0.149582	-2.74099	0.039927
chr11__108185232__108189330___NPAT	0.149659	-2.74025	0.045662
chrX__13744415__13751368___OFD1	0.149711	-2.73975	0.037442
chr1__37582223__37587495___GNL2	0.149871	-2.73821	0.024519
chr1__243545510__243573048___AKT3	0.149906	-2.73787	0.015126
chr1__61137588__61140329___NFIA	0.150047	-2.73651	0.037492
chr9__125213370__125220700___RABEPK	0.150119	-2.73582	0.036015
chr5__55269413__55281515___DHX29	0.150172	-2.73531	0.043554
chr3__155910692__155922302___GMPS	0.150202	-2.73503	0.049414
chr1__77713200__77715868___USP33	0.150219	-2.73486	0.046147
chr16__15732485__15734462___MYH11	0.150228	-2.73477	0.044648

chr6__133980082__133982880___TBPL1	0.150328	-2.73381	0.035265
chr13__46020449__46042275___ZC3H13	0.150452	-2.73263	0.044815
chr20__47235924__47236516___ZMYND8	0.150879	-2.72853	0.044399
chr12__69365633__69370975___YEATS4	0.150889	-2.72844	0.040945
chr17__42727662__42730918___EZH1	0.150909	-2.72825	0.048007
chr19__58294098__58295581___ZNF8	0.15097	-2.72767	0.039927
chr7__77765495__77778814___RSBN1L	0.150988	-2.72749	0.043661
chr5__138159555__138166108___BRD8	0.151043	-2.72696	0.03914
chr14__50159431__50161609___SOS2	0.151052	-2.72688	0.023822
chr7__125329682__125347207___RP11-3B12.2	0.151133	-2.72611	0.048021
chr2__172568741__172596023___PDK1	0.151137	-2.72608	0.043135
chr6__154199668__154223243___IPCEF1	0.151383	-2.72372	0.047297
chr5__179617989__179618323___HNRNPH1	0.15144	-2.72319	0.042692
chr1__25458391__25485795___TMEM57	0.151751	-2.72023	0.040372
chr1__25340474__25351693___TMEM50A	0.151813	-2.71963	0.024894
chr5__112754873__112801383___APC	0.151827	-2.7195	0.046165
chr9__135866456__135883078___CAMSAP1	0.152025	-2.71762	0.047836
chr17__49311312__49312042___ZNF652	0.152039	-2.71749	0.003826
chr11__117238601__117246948___RNF214	0.152055	-2.71734	0.044787
chr20__41097220__41101353___TOP1	0.152075	-2.71715	0.02099
chr10__21730900__21735235___MLLT10	0.152152	-2.71642	0.048227
chr9__19360244__19361963___DENND4C	0.152322	-2.71481	0.047162
chr1__247157000__247159813___ZNF124	0.152395	-2.71411	0.045683
chr17__61889786__61891689___INTS2	0.152419	-2.71388	0.045092
chr10__4830675__4842504___AKR1E2	0.152765	-2.71061	0.026254
chr14__92809300__92816421___GOLGA5	0.152872	-2.7096	0.047695
chr17__18582658__18595181___CCDC144B	0.152906	-2.70928	0.042645
chr2__207567463__207577655___CREB1	0.153071	-2.70773	0.044787
chr2__61370321__61370579___USP34	0.15318	-2.7067	0.040182
chr4__1699564__1700070___SLBP	0.153215	-2.70637	0.047158
chr13__45979813__46020557___ZC3H13	0.153301	-2.70556	0.043501
chr9__2181571__2192802___SMARCA2	0.153394	-2.70469	0.045768
chr17__46119968__46169605___KANSL1	0.153424	-2.7044	0.049666
chr7__37013299__37033412___ELMO1	0.153478	-2.7039	0.043631
chr14__103428387__103457212___MARK3	0.153491	-2.70377	0.012629
chr12__130795995__130801488___STX2	0.153683	-2.70197	0.010069
chr9__123757703__123769563___DENND1A	0.153684	-2.70196	0.021251
chr20__58895612__58905480___GNAS	0.153747	-2.70137	0.012097
chr8__99384208__99521010___VPS13B	0.153865	-2.70027	0.049385
chr12__51116315__51118772___TFCP2	0.153902	-2.69992	0.041708
chr20__19580000__19585544___SLC24A3	0.153905	-2.69988	0.045092
chr3__130967145__130969396___ATP2C1	0.153943	-2.69953	0.046123
chr2__48346201__48362707___FOXN2	0.154086	-2.6982	0.025742
chr6__161165577__161166417___AGPAT4	0.154092	-2.69814	0.026644
chr10__27117576__27121448___YME1L1	0.154094	-2.69811	0.046152
chr14__49663315__49665163___POLE2	0.154252	-2.69664	0.049058

chr9__123089758__123099549___RABGAP1	0.154365	-2.69558	0.047587
chr6__159784666__159785496___TCP1	0.154646	-2.69296	0.04512
chr7__80664406__80674147___CD36	0.154679	-2.69265	0.04659
chrX__150638943__150649901___MTM1	0.154955	-2.69008	0.045768
chr10__35501501__35530243___CCNY	0.154977	-2.68988	0.01854
chr5__94654630__94663908___ANKRD32	0.155097	-2.68876	0.043314
chr3__142403674__142414291___XRN1	0.155108	-2.68866	0.012149
chr4__56019353__56019555___CEP135	0.155115	-2.68859	0.044399
chr4__25256543__25263849___PI4K2B	0.155181	-2.68797	0.041475
chr8__52673845__52684013___RB1CC1	0.155315	-2.68673	0.042181
chr5__43292474__43297166___HMGCS1	0.155318	-2.6867	0.047957
chr4__82428018__82428446___HNRNPDL	0.155973	-2.68063	0.020607
chr4__73118688__73125312___ANKRD17	0.155973	-2.68063	0.013911
chr2__197276198__197277037___ANKRD44ANKRD44-IT1	0.155987	-2.6805	0.047326
chr3__155897927__155916192___GMPS	0.156172	-2.67879	0.026671
chr3__149074215__149076047___HLTF	0.156172	-2.67879	0.009
chr9__100498765__100550160___MSANTD3-TMEFF1TMEFF1	0.156205	-2.67849	0.048485
chr6__89862126__89869082___CASP8AP2	0.156224	-2.67832	0.046233
chr16__89758577__89767237___FANCA	0.156439	-2.67633	0.042922
chr2__9344532__9350895___ASAP2	0.156512	-2.67565	0.044849
chr8__85138035__85138475___LRRCC1	0.156513	-2.67564	0.015423
chr7__155672867__155707068___RBM33	0.156647	-2.67442	0.047124
chr9__96458379__96484633___HABP4	0.156774	-2.67324	0.046968
chr14__49813988__49831361___NEMF	0.156792	-2.67307	0.007926
chr1__108782422__108794907___STXBP3	0.156895	-2.67213	0.049937
chr1__25225002__25228235___SYF2	0.156962	-2.67152	0.008348
chr1__70274720__70315566___ANKRD13C	0.157113	-2.67013	0.045129
chr14__103571623__103571820___APOPT1	0.157217	-2.66917	0.048918
chr15__50300789__50314670___GABPB1	0.157225	-2.6691	0.044554
chr12__28255581__28452654___CCDC91	0.157257	-2.6688	0.045266
chr2__181474960__181511775___ITGA4	0.157278	-2.66861	0.045518
chr6__130022227__130094367___L3MBTL3	0.15734	-2.66804	0.038819
chr17__30792440__30793672___CRLF3	0.157471	-2.66684	0.049338
chr8__60794986__60808272___CHD7	0.157614	-2.66553	0.049666
chr7__21440958__21445594___SP4	0.157752	-2.66427	0.027539
chr7__6416627__6416921___DAGLB	0.157824	-2.66361	0.049007
chr1__200569911__200615609___KIF14	0.157859	-2.66329	0.042064
chr16__53442800__53490301___RBL2	0.157877	-2.66313	0.04706
chr15__41707728__41713496___MGA	0.157901	-2.6629	0.013495
chr1__92605307__92636336___EVI5	0.157906	-2.66286	0.018458
chr4__128936655__129039096___SCLT1	0.157912	-2.66281	0.044815
chrX__118654602__118654961___DOCK11	0.15825	-2.65972	0.027487
chr12__430664__438554___CCDC77	0.158416	-2.65821	0.022659
chr21__32737254__32759269___PAXBP1	0.158644	-2.65614	0.045768
chr1__108796234__108798237___STXBP3	0.158686	-2.65575	0.044635
chr5__112766326__112801383___APC	0.158748	-2.65519	0.008437

chr19__19465340__19474118___GATAD2A	0.158758	-2.6551	0.027477
chr4__76995781__77020670___SEPT11	0.158861	-2.65416	0.04187
chr12__56169776__56170208___SMARCC2	0.158997	-2.65293	0.018807
chr7__105040839__105091314___KMT2E	0.159155	-2.65149	0.046792
chr2__8788647__8803127___KIDINS220	0.159219	-2.65092	0.04659
chr6__10702369__10704844___PAK1IP1	0.159491	-2.64846	0.045683
chr6__119361291__119363332___NA	0.159621	-2.64728	0.044507
chrX__123686548__123712908___THOC2	0.159634	-2.64716	0.044257
chr1__32378215__32378839___BSDC1	0.159873	-2.645	0.048356
chr2__159729009__159748903___MARCH7	0.159905	-2.64471	0.04037
chr19__10166598__10173905___DNMT1	0.160049	-2.64341	0.023606
chr9__68917548__68923386___PIP5K1B	0.160222	-2.64185	0.040779
chr19__10166598__10173174___DNMT1	0.16026	-2.64151	0.047326
chr6__79015082__79043003___PHIP	0.160424	-2.64004	0.045683
chr19__11867306__11903965___NA	0.160518	-2.63919	0.045113
chr18__79710346__79718016___CTDP1	0.160532	-2.63907	0.046852
chr10__7367649__7381949___SFMBT2	0.160553	-2.63888	0.027896
chr1__247138716__247159813___ZNF124	0.160639	-2.63811	0.028411
chr4__128888679__128946152___SCLT1	0.160732	-2.63727	0.044353
chr3__196067518__196075360___TFRC	0.160952	-2.6353	0.046161
chr7__50376533__50382707___IKZF1	0.161095	-2.63401	0.044787
chr12__68715627__68725796___NUP107	0.161244	-2.63268	0.024519
chr5__133064980__133076898___HSPA4	0.16125	-2.63263	0.046262
chr8__31087776__31091898___WRN	0.161305	-2.63213	0.044648
chr13__48373405__48381443___RB1	0.16135	-2.63174	0.029264
chr1__197084354__197100914___ASPM	0.161397	-2.63131	0.045438
chr10__68025546__68044563___HERC4	0.161514	-2.63027	0.009288
chr5__66012049__66054951___ERBB2IP	0.161795	-2.62776	0.015126
chr10__89714955__89726521___KIF20B	0.161906	-2.62677	0.044787
chr18__57566447__57567876___FECH	0.162175	-2.62438	0.047326
chr8__38107021__38119363___ASH2L	0.16224	-2.6238	0.015962
chr6__24416397__24418578___MRS2	0.162512	-2.62138	0.049686
chr12__11121010__11147135___PRH1-PRR4	0.162588	-2.62071	0.017941
chr19__34208929__34221738___LSM14A	0.162745	-2.61932	0.042003
chr2__15461201__15478321___NBAS	0.162787	-2.61894	0.044325
chr13__77081427__77087633___MYCBP2	0.16287	-2.6182	0.021117
chr3__114693528__114717527___LOC102723469	0.162993	-2.61712	0.02938
chr5__138198199__138202155___CDC23	0.162993	-2.61712	0.049311
chr11__120420753__120477526___ARHGEF12	0.163027	-2.61682	0.0105
chr20__50902017__50928825___ADNP	0.163228	-2.61504	0.043662
chr6__110743008__110746201___CDK19	0.163342	-2.61403	0.019186
chr2__9448198__9459618___CPSF3	0.163364	-2.61384	0.048356
chr1__211260108__211304140___RCOR3	0.163788	-2.6101	0.049065
chr9__77214311__77227485___VPS13A	0.164015	-2.6081	0.042064
chr12__62294179__62355475___USP15	0.16425	-2.60604	0.030608
chr18__45988702__45992202___PSTPIP2	0.164367	-2.605	0.022186

chr4__42001616__42023384___SLC30A9	0.164656	-2.60247	0.031038
chr18__51046920__51067187___SMAD4	0.164958	-2.59982	0.033157
chr1__214613714__214622281___CENPF	0.164974	-2.59969	0.022437
chr7__44700141__44702529___OGDH	0.165092	-2.59866	0.045632
chr2__200569663__200575461___SGOL2	0.165411	-2.59587	0.025995
chr17__81667729__81670453___CCDC137	0.165484	-2.59524	0.046123
chr15__75854386__75883424___UBE2Q2	0.165554	-2.59462	0.018621
chr9__86346299__86346480___ZCCHC6	0.165662	-2.59369	0.024814
chr2__61501996__61533903___XPO1	0.165726	-2.59313	0.031326
chr4__88649840__88658491___HERC3	0.165783	-2.59263	0.049822
chr14__50437476__50440441___MAP4K5	0.165884	-2.59176	0.025998
chr2__20278583__20327378___PUM2	0.165944	-2.59123	0.015931
chr10__101624745__101676436___FBXW4	0.165968	-2.59102	0.022659
chr2__30459552__30533314___LCLAT1	0.166009	-2.59067	0.026314
chr1__13715541__13742157___PRDM2	0.166274	-2.58836	0.012097
chr8__91008743__91024366___TMEM55A	0.166305	-2.5881	0.012646
chr8__106702906__106707145___OXR1	0.166639	-2.5852	0.049954
chr5__54094176__54098085___ARL15	0.16671	-2.58459	0.015653
chr18__24366892__24377535___OSBPL1A	0.16672	-2.5845	0.026913
chr1__27749068__27755330___FAM76A	0.166944	-2.58257	0.045662
chr6__90556500__90571807___MAP3K7	0.167109	-2.58113	0.048106
chr20__49135833__49154071___STAU1	0.16766	-2.57639	0.047647
chr1__203703652__203722689___ATP2B4	0.167701	-2.57603	0.03236
chr8__99641811__99661491___VPS13B	0.168086	-2.57273	0.031411
chr4__75790150__75790797___USO1	0.168176	-2.57196	0.019881
chr9__68818461__68894638___PIP5K1B	0.168208	-2.57168	0.048441
chr5__87331348__87341321___RASA1	0.168322	-2.5707	0.02389
chr11__74775146__74789699___RNF169	0.168468	-2.56946	0.031946
chr1__25340474__25343073___TMEM50A	0.16856	-2.56866	0.021117
chr6__136561533__136562615___MAP3K5	0.16861	-2.56823	0.047624
chr15__85113873__85121014___PDE8A	0.168815	-2.56649	0.025927
chr15__41069570__41074565___INO80	0.168873	-2.56599	0.033575
chr14__37110827__37138520___SLC25A21	0.169004	-2.56487	0.03363
chr17__48848064__48849377___CALCOCO2	0.169092	-2.56412	0.020761
chrX__41218372__41223402___USP9X	0.169181	-2.56336	0.03197
chr2__15415546__15478289___NBAS	0.169731	-2.55868	0.049711
chr3__37323588__37329093___GOLGA4	0.16974	-2.5586	0.048918
chr9__137811461__137818138___EHMT1	0.169829	-2.55785	0.033414
chr20__41512846__41533570___CHD6	0.169935	-2.55694	0.01841
chr1__88741043__88786213___PKN2	0.17002	-2.55623	0.048154
chr12__118400659__118403517___SUDS3	0.170211	-2.5546	0.049788
chr21__33340999__33343676___IFNAR1	0.170593	-2.55137	0.025485
chr17__20253505__20306082___SPECC1	0.170598	-2.55133	0.035286
chr22__21805825__21807846___MAPK1	0.17098	-2.5481	0.02099
chr1__114421436__114433733___TRIM33	0.171158	-2.5466	0.028838
chr3__121647319__121657352___HCLS1	0.171169	-2.5465	0.013711

chr11__16264698__16286213___SOX6	0.17159	-2.54296	0.022276
chr4__102722871__102726683___MANBA	0.171927	-2.54013	0.029088
chr14__49795791__49833496___NEMF	0.172351	-2.53658	0.049338
chr15__94440176__94470442___MCTP2	0.172504	-2.5353	0.026226
chr20__32366384__32371874___ASXL1	0.172517	-2.53519	0.034623
chr19__18175040__18175697___IFI30	0.172722	-2.53348	0.024388
chr22__38552666__38568289___DMC1	0.172881	-2.53215	0.021251
chr4__119596523__119607297___PDE5A	0.172949	-2.53158	0.012149
chr3__146121112__146124229___PLOD2	0.172981	-2.53132	0.013148
chr6__42659656__42679832___UBR2	0.173045	-2.53078	0.024903
chr17__61946020__62063222___MED13	0.173092	-2.53039	0.030045
chr7__117099762__117138532___ST7	0.173151	-2.5299	0.049451
chr4__128936655__129093148___SCLT1	0.173351	-2.52823	0.029731
chr3__155906160__155916192___GMPS	0.17352	-2.52683	0.030045
chr16__11846501__11847806___RSL1D1	0.173577	-2.52635	0.007926
chr2__113913172__113942359___ACTR3	0.173601	-2.52615	0.02023
chr14__52711101__52711524___PSMC6	0.173838	-2.52419	0.006389
chr7__105078846__105091314___KMT2E	0.174522	-2.51852	0.02099
chr2__181493325__181511775___ITGA4	0.174633	-2.51761	0.026226
chr1__158842134__158844122___MNDA	0.17482	-2.51606	0.026302
chr1__214647078__214663780___CENPF	0.175222	-2.51275	0.030481
chr4__39300021__39303151___RFC1	0.175424	-2.51108	0.02965
chr11__108235670__108249102___ATM	0.175482	-2.51061	0.030364
chr3__56639986__56673725___FAM208A	0.175604	-2.5096	0.034816
chr15__49996677__50018976___ATP8B4	0.175876	-2.50737	0.0315
chr7__64521064__64544432___ZNF680	0.176068	-2.50579	0.025742
chr14__31127785__31172122___HECTD1	0.176227	-2.50449	0.005257
chr17__68450728__68452992___WIPI1	0.176649	-2.50105	0.019196
chr10__50343492__50344345___SGMS1	0.176709	-2.50055	0.038596
chr3__185687057__185689627___IGF2BP2	0.176776	-2.5	0.021014
chr2__24643966__24683128___NCOA1	0.177041	-2.49784	0.031038
chr20__50127975__50130947___TMEM189TMEM189-UBE2V1	0.177127	-2.49715	0.036464
chr6__42662184__42666245___UBR2	0.177458	-2.49445	0.005676
chr11__85976623__85981228___PICALM	0.177513	-2.49401	0.037787
chr7__112286873__112287074___ZNF277	0.177765	-2.49196	0.027215
chr1__27874146__27874663___THEMIS2	0.178259	-2.48795	0.037617
chr19__48149763__48150210___LIG1	0.178846	-2.48321	0.011283
chr1__29035826__29109437___EPB41	0.1789	-2.48277	0.013639
chr4__82930943__82984876___LIN54	0.179155	-2.48072	0.024613
chr7__35890668__35898383___SEPT7	0.179314	-2.47944	0.026282
chr12__50995629__51005436___SLC11A2	0.179637	-2.47684	0.033032
chr3__17009674__17068065___PLCL2	0.17964	-2.47682	0.018509
chr11__12204250__12216319___MICAL2	0.179806	-2.47548	0.025201
chr17__41981855__41982401___DNAJC7	0.180059	-2.47346	0.039082
chr5__177209636__177212195___NSD1	0.180198	-2.47235	0.038224

chr22__31454144__31463133___EIF4ENIF1	0.180472	-2.47016	0.038809
chr11__68548067__68576043___PPP6R3	0.180714	-2.46822	0.020767
chr14__92088730__92096838___ATXN3	0.180746	-2.46797	0.033981
chr12__30728648__30735206___CAPRIN2	0.181038	-2.46564	0.020284
chr16__4466153__4469465___NMRAL1	0.18133	-2.46331	0.024393
chr13__27075191__27116596___USP12	0.181497	-2.46198	0.032984
chr12__120557282__120560886___RNF10	0.181738	-2.46007	0.029648
chr1__93544107__93549426___FNBP1L	0.182244	-2.45605	0.043021
chr9__36351115__36353331___RNF38	0.18237	-2.45506	0.04255
chr9__4726083__4727924___AK3LOC102723969	0.182841	-2.45134	0.03316
chr11__68569748__68583129___PPP6R3	0.183188	-2.4486	0.040489
chr11__17988597__18008076___SERGEF	0.183478	-2.44632	0.029875
chr8__43069555__43072307___FNTA	0.183627	-2.44515	0.017803
chr2__151789752__151791908___LOC101929356	0.183777	-2.44397	0.02496
chr7__100019231__100024307___ZKSCAN1	0.184425	-2.43889	0.044648
chr15__55951376__55966546___NEDD4	0.184545	-2.43795	0.043
chr18__9182382__9239556___ANKRD12	0.185117	-2.43349	0.020746
chr3__196064309__196068130___TFRC	0.185175	-2.43304	0.036768
chr21__36344579__36364259___MORC3	0.185659	-2.42927	0.044399
chrX__155277134__155299145___CLIC2	0.185765	-2.42845	0.031968
chr17__29648144__29650800___SSH2	0.18596	-2.42694	0.044257
chr14__49650265__49655843___POLE2	0.186006	-2.42658	0.020952
chr4__39837856__39845880___PDS5A	0.186241	-2.42476	0.030481
chr5__94628811__94651845___ANKRD32	0.186568	-2.42223	0.044687
chr2__39336920__39337581___MAP4K3	0.186842	-2.42011	0.020952
chr12__25209799__25227412___KRAS	0.187114	-2.41801	0.045149
chr11__68544838__68558679___PPP6R3	0.187332	-2.41633	0.018816
chr1__155676548__155680456___YY1AP1	0.187813	-2.41263	0.026226
chr2__128097429__128123246___UGGT1	0.187815	-2.41261	0.045546
chr8__103040798__103042407___ATP6V1C1	0.187919	-2.41182	0.037805
chr2__210003438__210004118___RPE	0.188198	-2.40968	0.032842
chr14__45217019__45218432___MIS18BP1	0.189166	-2.40228	0.029165
chr17__29451455__29451680___TAOK1	0.189174	-2.40222	0.010265
chr13__21155693__21159987___SKA3	0.189189	-2.4021	0.039027
chr13__48360017__48381443___RB1	0.190515	-2.39202	0.045943
chr10__45639751__45663842___ZFAND4	0.190901	-2.38911	0.046949
chr15__92996957__93014909___CHD2	0.191288	-2.38618	0.030045
chr16__31120186__31120514___KAT8	0.191372	-2.38554	0.040521
chr5__62347130__62350120___KIF2A	0.191672	-2.38329	0.006182
chr18__62221037__62244876___KIAA1468	0.192602	-2.37631	0.045266
chr14__60282684__60283537___PPM1A	0.192619	-2.37618	0.014712
chr11__119271735__119274953___CBL	0.192735	-2.37531	0.013711
chr1__75728401__75734871___ACADM	0.192745	-2.37523	0.039188
chr4__106116203__106309998___TBCK	0.192778	-2.37499	0.027539
chr1__32279671__32280210___LCK	0.193261	-2.37138	0.040779
chr2__171448681__171469030___DCAF17	0.193297	-2.37111	0.014689

chr10__133398435__133399619___MTG1	0.1934	-2.37034	0.04292
chr12__89466770__89497342___POC1B	0.193647	-2.3685	0.031335
chr11__120446403__120469388___ARHGEF12	0.194275	-2.36383	0.028729
chr5__50750151__50763242___PARP8	0.1944	-2.3629	0.020952
chr6__131136778__131219808___AKAP7	0.194915	-2.35908	0.036125
chr1__229539456__229549584___ABCB10	0.194981	-2.35859	0.010464
chr9__5064883__5081861___JAK2	0.19517	-2.35719	0.020033
chr1__185166572__185231708___SWT1	0.195392	-2.35556	0.037882
chr20__17969801__17970130___MGME1	0.195552	-2.35438	0.037982
chr7__16216066__16259012___ISPD	0.195557	-2.35434	0.043775
chr10__110951608__110985765___SHOC2	0.195716	-2.35317	0.025418
chr10__43154897__43160595___CSGALNACT2	0.19612	-2.35019	0.033432
chr21__36364093__36372531___MORC3	0.196308	-2.34881	0.02058
chr10__32543300__32571893___CCDC7	0.196961	-2.34402	0.038328
chr2__128113084__128145967___UGGT1	0.197216	-2.34215	0.020957
chr6__135039573__135042126___HBS1L	0.197384	-2.34092	0.03307
chr1__229530199__229549434___ABCB10	0.197607	-2.33929	0.010811
chr11__16183886__16199254___SOX6	0.197864	-2.33742	0.045446
chr15__65702305__65732818___DENND4A	0.198059	-2.336	0.038804
chr2__159729009__159752571___MARCH7	0.198316	-2.33413	0.026314
chr3__115071219__115073056___ZBTB20	0.198394	-2.33356	0.027412
chr17__32200956__32203973___RHOT1	0.19873	-2.33112	0.035388
chr3__123933673__123949132___CCDC14	0.198825	-2.33043	0.033945
chr1__36358239__36362656___STK40	0.198933	-2.32965	0.039836
chr14__73071627__73077536___RBM25	0.199001	-2.32915	0.026457
chr3__136398749__136502779___STAG1	0.199148	-2.32809	0.046161
chr11__46541945__46548500___AMBRA1	0.199427	-2.32607	0.040521
chr11__16183886__16318529___SOX6	0.199865	-2.3229	0.046123
chr2__36883932__36886826___STRN	0.199937	-2.32238	0.048106
chr9__26984257__27011968___IFT74	0.200312	-2.31968	0.035506
chr5__143037196__143057747___ARHGAP26	0.200453	-2.31866	0.049058
chr20__49639678__49640665___B4GALT5	0.200668	-2.31712	0.032635
chr14__65430216__65455718___FUT8	0.200852	-2.31579	0.026259
chr16__68157869__68191775___NFATC3	0.200994	-2.31478	0.035648
chr1__154225084__154241565___UBAP2L	0.201146	-2.31368	0.04747
chr6__110431171__110457017___SLC22A16	0.201567	-2.31067	0.031405
chr5__94868333__94912976___MCTP1	0.202034	-2.30733	0.031576
chr16__67036639__67082339___CBFB	0.202244	-2.30583	0.021251
chr20__44972078__44987296___STK4	0.202502	-2.30399	0.042064
chr1__25446762__25454382___TMEM57	0.202561	-2.30357	0.036071
chr1__51394381__51448135___EPS15	0.20299	-2.30052	0.01748
chr3__37063742__37083806___LRRFIP2	0.203227	-2.29883	0.014183
chr18__63280887__63281214___BCL2	0.203656	-2.2958	0.021117
chr15__34250298__34255392___SLC12A6	0.203918	-2.29394	0.021449
chr14__55648025__55648870___KTN1	0.203934	-2.29382	0.01925
chr4__48581420__48605833___FRYL	0.204043	-2.29306	0.043631

chr10__11597631__11601467___USP6NL	0.204161	-2.29222	0.043143
chr1__155670320__155784089___NA	0.204599	-2.28913	0.029618
chr6__149759328__149773169___PCMT1	0.204625	-2.28894	0.044257
chr15__50583089__50586488___TRPM7	0.204818	-2.28759	0.028739
chr19__51573210__51588078___ZNF175	0.204854	-2.28733	0.04412
chr10__69359897__69369624___HK1	0.204934	-2.28677	0.037541
chr11__17988597__18010139___SERGEF	0.205237	-2.28464	0.03558
chr3__9388087__9390497___NA	0.20528	-2.28434	0.038481
chr14__74802556__74821137___YLPM1	0.205295	-2.28423	0.044257
chr1__231795242__231818517___TSNAX-DISC1DISC1	0.205419	-2.28336	0.011988
chr5__74834426__74841679___FAM169A	0.205657	-2.28169	0.022497
chr13__28174272__28197346___PAN3	0.205718	-2.28126	0.034363
chr17__58703196__58720812___RAD51C	0.206641	-2.2748	0.036789
chr11__108330214__108335961___ATM	0.206858	-2.27328	0.044325
chr1__224189577__224190319___DEGS1	0.207432	-2.26929	0.037508
chr11__74078115__74078717___C2CD3	0.207569	-2.26834	0.045129
chr7__142349370__142507430___NA	0.208278	-2.26342	0.018816
chr18__21765772__21804014___MIB1	0.208468	-2.2621	0.023517
chr1__233198939__233236980___PCNXL2	0.208468	-2.2621	0.048029
chr17__27301788__27304911___WSB1	0.208612	-2.26111	0.008536
chr19__48913011__48913564___NUCB1	0.209262	-2.25662	0.041322
chr19__18342859__18343415___PGPEP1	0.209518	-2.25485	0.03321
chr19__9614021__9618179___ZNF561	0.20958	-2.25443	0.02058
chr3__195959012__195960086___NA	0.210024	-2.25138	0.023666
chr12__123345258__123345570___SBNO1	0.211238	-2.24306	0.017587
chr1__198232553__198279061___NEK7	0.211274	-2.24282	0.047452
chr14__103428387__103480490___MARK3	0.211485	-2.24138	0.048227
chr15__82813103__82826846___WHAMM	0.211606	-2.24055	0.023807
chr2__230255452__230287966___SP140	0.211881	-2.23867	0.01735
chr4__129039041__129093148___SCLT1	0.212523	-2.23431	0.021097
chr3__20072395__20148487___KAT2B	0.212664	-2.23335	0.03013
chr18__62556203__62565096___ZCCHC2	0.212717	-2.23299	0.038328
chr1__174272414__174394145___RABGAP1L	0.213016	-2.23096	0.044018
chr10__31373018__31387266___ZEB1	0.213533	-2.22747	0.025742
chr12__28225795__28307749___CCDC91	0.213952	-2.22464	0.014181
chr9__77794463__77797648___GNAQ	0.214006	-2.22428	0.013854
chr9__33953285__33989126___UBAP2	0.214757	-2.21922	0.043875
chr10__92606265__92621473___KIF11	0.215174	-2.21642	0.024568
chr3__183205876__183207823___MCF2L2	0.215316	-2.21547	0.023807
chr10__68337199__68341851___HNRNPH3	0.216993	-2.20428	0.03398
chr5__40852174__40854096___CARD6	0.217104	-2.20354	0.018333
chr3__28263291__28298350___CMC1	0.217104	-2.20354	0.042158
chr20__2964272__2975241___PTPRA	0.217204	-2.20288	0.009061
chr15__51893815__51902036___TMOD3	0.21726	-2.2025	0.025418
chrX__78009102__78021079___ATP7A	0.217353	-2.20189	0.041322
chr11__46750274__46753497___CKAP5	0.217952	-2.19792	0.026282

chr4__109468361__109473186___SEC24B	0.218047	-2.19729	0.023178
chr19__10637644__10638315___SLC44A2	0.218377	-2.1951	0.031335
chr6__47283938__47286595___TNFRSF21	0.218523	-2.19414	0.041016
chr15__40628070__40641027___CASC5	0.218531	-2.19409	0.042181
chr2__181458196__181498777___ITGA4	0.218576	-2.19379	0.024243
chr11__35198121__35210054___CD44	0.218777	-2.19246	0.034735
chr5__143399656__143400852___NR3C1	0.219219	-2.18955	0.048115
chr9__68727596__68728934___PIP5K1B	0.219739	-2.18613	0.027352
chr6__35888024__35891013___SRPK1	0.219961	-2.18468	0.030045
chr2__135748267__135776351___UBXN4	0.220906	-2.1785	0.04412
chr6__100798713__100805880___ASCC3	0.220939	-2.17828	0.030008
chr7__106092949__106099282___SYPL1	0.221246	-2.17628	0.044307
chr5__154865192__154872651___CNOT8	0.221386	-2.17536	0.023532
chr18__54277703__54287411___POLI	0.221594	-2.17401	0.045322
chr15__50569887__50575919___TRPM7	0.222451	-2.16844	0.036796
chr1__1716346__1722831___CDK11A	0.222716	-2.16673	0.030626
chr14__103448919__103457212___MARK3	0.222978	-2.16502	0.008348
chr2__175939552__175964533___KIAA1715	0.223742	-2.16009	0.045833
chr8__119758073__119791459___TAF2	0.223808	-2.15967	0.046165
chr17__76558374__76558600___SNHG16	0.224022	-2.15829	0.043661
chr13__77217840__77243951___MYCBP2	0.224305	-2.15647	0.01563
chr3__41224021__41227352___CTNNB1	0.224355	-2.15615	0.045053
chr1__155771067__155773210___GON4L	0.22472	-2.1538	0.0454
chr6__78965703__78985428___PHIP	0.225255	-2.15037	0.034735
chr4__1900626__1918623___WHSC1	0.225273	-2.15026	0.046068
chr1__77154449__77169395___PIGK	0.225414	-2.14935	0.049306
chr3__152938209__152944616___NA	0.225454	-2.14909	0.028314
chr15__57231152__57234107___TCF12	0.225881	-2.14637	0.01256
chr8__23109545__23111311___TNFRSF10C	0.226704	-2.14112	0.016369
chr22__41808875__41813822___CCDC134	0.227059	-2.13886	0.04887
chr17__47154672__47172064___CDC27	0.2272	-2.13797	0.025544
chr13__95161189__95207925___ABCC4	0.227484	-2.13617	0.020221
chr9__33351560__33352719___NFX1	0.228375	-2.13052	0.036317
chr2__196139620__196163427___STK17B	0.228377	-2.13051	0.041398
chr20__50902017__50918781___ADNP	0.229979	-2.12043	0.044503
chr6__34646601__34646798___C6orf106	0.23027	-2.1186	0.035775
chr11__93747297__93757465___C11orf54	0.230788	-2.11536	0.028308
chr12__42128046__42129851___GXYLT1	0.230943	-2.11439	0.025544
chr15__65669779__65670188___DENND4A	0.231331	-2.11197	0.046182
chr17__47370437__47395977___EFCAB13	0.231473	-2.11109	0.020953
chr16__89978810__89981923___AFG3L1P	0.231497	-2.11093	0.027539
chr17__27303367__27310174___WSB1	0.231538	-2.11068	0.02099
chr17__35624397__35627726___AP2B1	0.231765	-2.10927	0.032445
chr13__48239226__48261321___ITM2B	0.231766	-2.10926	0.019356
chr7__135577796__135593192___NUP205	0.232568	-2.10427	0.043135
chr18__9524594__9530941___RALBP1	0.23272	-2.10333	0.035932

chr9__5920544__5923309___KIAA2026	0.232809	-2.10278	0.013685
chr11__17878208__18008076___SERGEF	0.232966	-2.10181	0.046931
chr14__103451918__103462461___MARK3	0.233696	-2.09729	0.027539
chr1__95143891__95178938___TMEM56TMEM56-RWDD3	0.234746	-2.09083	0.037628
chr15__63746918__63755325___HERC1	0.235855	-2.08403	0.036236
chr19__36089038__36089306___WDR62	0.235995	-2.08317	0.01854
chr5__109713520__109755456___MAN2A1	0.236485	-2.08018	0.040986
chr5__160093101__160094065___PWWP2A	0.238865	-2.06573	0.042804
chr19__34450265__34464131___UBA2	0.239631	-2.06111	0.038852
chr15__92978234__92985673___CHD2	0.239712	-2.06062	0.004884
chr17__20017987__20205912___SPECC1	0.240083	-2.0584	0.009358
chr21__36247517__36251284___DOPEY2	0.240924	-2.05335	0.015272
chr8__61618978__61644632___ASPH	0.240994	-2.05293	0.048798
chr3__57841299__57849816___SLMAP	0.241846	-2.04784	0.01925
chr2__32174063__32184338___SLC30A6	0.243915	-2.03555	0.044399
chr6__75702645__75711416___SENP6	0.243959	-2.03529	0.047036
chr9__19086734__19089559___HAUS6	0.244624	-2.03136	0.020588
chr2__44201186__44209327___PPM1B	0.245015	-2.02906	0.036613
chr10__11481770__11485911___USP6NL	0.24526	-2.02761	0.020761
chr15__42794644__42840433___TTBK2	0.245563	-2.02584	0.040986
chr17__63760914__63766194___CCDC47	0.245653	-2.02531	0.00333
chr10__113898110__113908523___NHLRC2	0.245662	-2.02525	0.038328
chr14__60266538__60268435___PPM1A	0.246013	-2.02319	0.022964
chr10__93681480__93694937___FRA10AC1	0.246915	-2.01791	0.048356
chr18__24064140__24069271___TTC39C	0.246996	-2.01744	0.044878
chr10__13663453__13670528___FRMD4A	0.247775	-2.0129	0.010069
chr11__46754888__46760784___CKAP5	0.248029	-2.01142	0.040015
chr9__109057191__109064567___TMEM245	0.248338	-2.00962	0.038763
chr8__30101898__30106843___LEPROTL1	0.248468	-2.00887	0.046923
chr4__48593930__48605833___FRYL	0.248532	-2.0085	0.013924
chrX__1288519__1288888___CSF2RA	0.24874	-2.00729	0.021117
chr20__5557945__5584322___GPCPD1	0.248817	-2.00684	0.03914
chr15__62033441__62044255___VPS13C	0.249777	-2.00128	0.011471
chr10__45618140__45639963___ZFAND4	0.250973	-1.9944	0.029054
chrY__13335563__13336335___UTY	0.251143	-1.99342	0.033248
chr1__35381259__35389082___ZMYM4	0.251184	-1.99318	0.02593
chr4__153580826__153589007___KIAA0922	0.25138	-1.99206	0.014454
chr12__69592059__69593613___CCT2	0.252204	-1.98734	0.029018
chr20__33619517__33623296___CBFA2T2	0.252543	-1.9854	0.006911
chr20__21365421__21368590___XRN2	0.252601	-1.98507	0.025357
chr16__19616114__19647882___C16orf62	0.252891	-1.98341	0.010601
chr5__66046353__66054951___ERBB2IP	0.252996	-1.98282	0.045784
chrY__19587210__19590772___TXLNG2P	0.25414	-1.9763	0.023807
chr10__68393138__68404844___RUFY2	0.254264	-1.9756	0.048541
chrX__132382178__132392334___MBNL3	0.254649	-1.97342	0.025637
chr3__50060956__50062108___RBM6	0.255567	-1.96823	0.021041

chr5__94888879__94912976___MCTP1	0.255762	-1.96713	0.048834
chr18__79126267__79193263___ATP9B	0.255788	-1.96698	0.036259
chr16__67744288__67772086___RANBP10	0.255863	-1.96655	0.041717
chr4__159186642__159314768___RAPGEF2	0.256568	-1.96258	0.030481
chr1__193069034__193070619___TROVE2	0.256725	-1.9617	0.033605
chr11__83161327__83184908___PCF11	0.257851	-1.95539	0.042605
chr10__11979057__12014184___UPF2	0.257858	-1.95535	0.027539
chr4__38826685__38829537___TLR6	0.260535	-1.94045	0.026401
chr5__79618647__79623489___PAPD4	0.260859	-1.93866	0.049058
chr22__40273425__40285770___TNRC6B	0.261093	-1.93736	0.030746
chr14__30628209__30638247___SCFD1	0.261183	-1.93687	0.048441
chr4__15625252__15644708___FBXL5	0.261564	-1.93476	0.019366
chr1__21701498__21703618___USP48	0.262196	-1.93128	0.035286
chr10__11601345__11601980___USP6NL	0.262386	-1.93024	0.019775
chr3__138221926__138229010___ARMC8	0.262605	-1.92903	0.040779
chr2__229858772__229859574___TRIP12	0.263626	-1.92344	0.045632
chr20__2947982__2975241___PTPRA	0.263685	-1.92311	0.009975
chr18__69895701__69947532___CD226	0.264139	-1.92063	0.027774
chr9__97994631__98005153___ANP32B	0.264607	-1.91808	0.015126
chr3__196361844__196362687___UBXN7	0.264899	-1.91648	0.038328
chr15__63213989__63214386___RAB8B	0.265097	-1.91541	0.023237
chr22__41137653__41141222___EP300	0.266304	-1.90886	0.029894
chr2__206127797__206130242___NDUFS1	0.266787	-1.90624	0.019458
chr3__196058284__196077122___TFRC	0.267548	-1.90213	0.008111
chr10__110881233__110890670___PDCD4	0.26816	-1.89883	0.036893
chr4__153602152__153604430___KIAA0922	0.268331	-1.89792	0.020874
chr17__61776401__61808757___BRIP1	0.268344	-1.89784	0.025742
chr20__31782249__31797515___TPX2	0.26928	-1.89282	0.010786
chr5__126603570__126604183___PHAX	0.269799	-1.89004	0.041708
chr8__41661834__41663742___ANK1	0.270477	-1.88642	0.03438
chr15__49235851__49292537___GALK2	0.271494	-1.88101	0.04576
chr5__112792446__112801383___APC	0.27256	-1.87536	0.027539
chr4__1900626__1939778___WHSC1	0.272635	-1.87496	0.037108
chr11__120447874__120469388___ARHGEF12	0.273828	-1.86866	0.02272
chr13__114041000__114073837___RASA3	0.276157	-1.85644	0.022205
chr9__5954016__5988545___KIAA2026	0.277161	-1.8512	0.026249
chr11__108158920__108162180___NPAT	0.27761	-1.84887	0.041475
chr3__71710412__71728623___EIF4E3	0.277638	-1.84873	0.026321
chr17__48848064__48856187___CALCOCO2	0.278745	-1.84298	0.029088
chr15__50002153__50018976___ATP8B4	0.278868	-1.84235	0.016849
chr9__125268936__125273649___GAPVD1	0.278874	-1.84232	0.028314
chr10__45939361__45962994___LOC728407	0.280319	-1.83486	0.049479
chr3__20119598__20140364___KAT2B	0.28112	-1.83074	0.036617
chr9__4823548__4833228___RCL1	0.281326	-1.82969	0.021251
chr15__90217439__90221765___SEMA4B	0.281639	-1.82808	0.020328
chr18__79126267__79207012___ATP9B	0.2828	-1.82215	0.031038

chr17__18865469__18877870___PRPSAP2	0.283752	-1.8173	0.044868
chr17__62010550__62063301___MED13	0.284355	-1.81424	0.009738
chr17__67910877__67924589___BPTF	0.285208	-1.80991	0.049841
chr19__17162988__17168064___MYO9B	0.288467	-1.79352	0.043691
chr14__102193463__102197847___WDR20	0.288924	-1.79124	0.04659
chr6__43055545__43056445___MRPL2	0.289558	-1.78807	0.029618
chr12__116096669__116119779___MED13L	0.290859	-1.78161	0.014544
chr5__115540885__115542901___FEM1C	0.292694	-1.77253	0.027539
chr11__77672042__77693611___RSF1	0.293422	-1.76895	0.016672
chr12__48074324__48074793___SENP1	0.293852	-1.76684	0.038392
chr17__43521369__43522226___DHX8	0.294518	-1.76357	0.037927
chr2__8943187__8982144___MBOAT2	0.294808	-1.76215	0.031651
chr15__58621471__58643978___ADAM10	0.295518	-1.75868	0.028732
chr19__47094389__47110956___ZC3H4	0.295767	-1.75747	0.041177
chr12__122594276__122624688___KNTC1	0.298311	-1.74511	0.038804
chr9__99959917__99960155___STX17	0.298798	-1.74276	0.028308
chr8__140818277__140890769___PTK2	0.30053	-1.73442	0.027412
chr1__182803698__182825820___NPL	0.301016	-1.73209	0.02542
chr2__230461262__230474447___SP100	0.301163	-1.73138	0.020806
chr1__53818971__53832591___NDC1	0.302598	-1.72452	0.043631
chr22__32478981__32485209___FBXO7	0.303992	-1.7179	0.020294
chr19__29971193__30012531___URI1	0.304746	-1.71432	0.041535
chr1__168019545__168045227___DCAF6	0.307258	-1.70248	0.020874
chr10__101521639__101538371___BTRC	0.307548	-1.70112	0.009738
chr6__17661653__17675770___NUP153	0.307684	-1.70048	0.042003
chr3__142355401__142371328___XRN1	0.309464	-1.69216	0.041322
chr8__85134847__85141517___LRRCC1	0.309591	-1.69157	0.025429
chr15__72518067__72561549___ARIH1	0.309882	-1.69021	0.030348
chr7__149018992__149021147___PDIA4	0.310261	-1.68845	0.036028
chr1__185166572__185175113___SWT1	0.310742	-1.68621	0.037037
chr14__34575756__34609742___SNX6	0.311117	-1.68447	0.040489
chr20__62139075__62140944___PSMA7	0.311127	-1.68443	0.02156
chr1__35413972__35415714___ZMYM4	0.311881	-1.68093	0.024294
chr11__77693507__77702495___RSF1	0.311911	-1.68079	0.02272
chr8__47969798__47971468___MCM4	0.312302	-1.67899	0.010256
chr17__51201592__51203228___MBTD1	0.312676	-1.67726	0.027324
chr3__37273536__37302332___GOLGA4	0.3127	-1.67715	0.007861
chr7__93252653__93259632___CCDC132	0.313288	-1.67444	0.01854
chr12__46229153__46254936___SLC38A1	0.313592	-1.67304	0.009674
chrX__53399589__53403893___SMC1A	0.315237	-1.66549	0.027878
chr4__88131061__88140014___ABCG2	0.315269	-1.66535	0.039677
chr3__32716225__32717237___CNOT10	0.315742	-1.66318	0.006389
chr1__28987448__29018442___EPB41	0.316364	-1.66034	0.037651
chr1__151024611__151027327___PRUNE	0.317137	-1.65682	0.034409
chr1__153811731__153813452___GATAD2B	0.318012	-1.65285	0.01563
chr15__76274412__76295737___ETFA	0.319578	-1.64576	0.008437

chr14__49607400__49608121___LRR1	0.319966	-1.64401	0.012149
chr12__120557282__120557682___RNF10	0.320094	-1.64343	0.015126
chr13__99539446__99543995___TM9SF2	0.323035	-1.63024	0.021128
chr2__8882511__8958642___MBOAT2	0.324554	-1.62347	0.031283
chr12__112306064__112319742___HECTD4	0.326493	-1.61488	0.021161
chr1__203707009__203708104___ATP2B4	0.327296	-1.61133	0.030646
chr6__158573420__158625754___TMEM181	0.331216	-1.59416	0.024903
chr5__14741827__14758598___ANKH	0.33124	-1.59405	0.043065
chr11__16183886__16217474___SOX6	0.331835	-1.59146	0.044648
chr10__84371014__84373815___CCSER2	0.332917	-1.58677	0.008536
chr14__91792367__91802421___TC2N	0.336226	-1.5725	0.038819
chr20__45000392__45001353___STK4	0.337368	-1.5676	0.00928
chr16__30499074__30499489___ITGAL	0.339004	-1.56062	0.019826
chr7__93252653__93311272___CCDC132	0.341423	-1.55037	0.040645
chr16__70258980__70262524___AARS	0.34191	-1.54831	0.021014
chr7__139073856__139089759___ZC3HAV1	0.344097	-1.53911	0.045768
chr10__112460524__112464657___VTI1A	0.344173	-1.53879	0.031457
chr3__120002046__120093593___GSK3B	0.347783	-1.52374	0.007926
chr1__90937485__90982370___ZNF644	0.349225	-1.51777	0.013145
chr19__34208929__34215661___LSM14A	0.350814	-1.51122	0.031482
chr2__189805652__189818180___PMS1	0.352777	-1.50317	0.040372
chr6__36902221__36902434___C6orf89	0.352895	-1.50269	0.047124
chr1__155675010__155784089___NA	0.353116	-1.50179	0.037855
chr9__96458379__96471094___HABP4	0.354219	-1.49729	0.016003
chr17__62010550__62063222___MED13	0.354629	-1.49562	0.044815
chr1__244408712__244417752___ADSS	0.357299	-1.48479	0.027539
chr13__21161790__21168399___SKA3	0.35741	-1.48435	0.021127
chr10__72708283__72715902___MCU	0.358791	-1.47878	0.048908
chr14__45235814__45237721___MIS18BP1	0.35977	-1.47485	0.020232
chr16__1625973__1632365___CRAMP1L	0.362427	-1.46424	0.029111
chr1__158678401__158685347___SPTA1	0.362587	-1.4636	0.040928
chr11__128768118__128782023___FLI1	0.36369	-1.45922	0.041603
chr16__28166508__28169909___XPO6	0.365243	-1.45307	0.023661
chr10__124038515__124046724___CHST15	0.367657	-1.44357	0.030871
chr10__31908172__31910563___ARHGAP12	0.368573	-1.43998	0.036424
chr22__32478981__32493281___FBXO7	0.369005	-1.43829	0.030008
chr1__50738863__50744775___FAF1	0.369974	-1.4345	0.040256
chr1__207677389__207678297___CR1L	0.370429	-1.43273	0.047478
chr6__149765691__149773169___PCMT1	0.371463	-1.42871	0.031333
chr1__86715724__86724405___SH3GLB1	0.371883	-1.42708	0.049058
chr17__48848064__48851628___CALCOCO2	0.374118	-1.41844	0.04412
chr1__151088190__151118139___GABPB2	0.378508	-1.4016	0.029838
chr11__121045674__121053732___TBCEL	0.378881	-1.40018	0.03399
chr9__128471308__128473741___ODF2	0.379156	-1.39914	0.035506
chr3__47635190__47636136___SMARCC1	0.379191	-1.399	0.028314
chr4__6923373__6924111___TBC1D14	0.380243	-1.39501	0.04037

chr11__85981129__85982003___PICALM	0.380439	-1.39426	0.011473
chr10__101956597__101957732___C10orf76	0.382732	-1.38559	0.041122
chr16__53155926__53157541___CHD9	0.384494	-1.37897	0.018326
chr1__31910038__31911826___PTP4A2	0.385593	-1.37485	0.044687
chr7__140776912__140787584___BRAF	0.386168	-1.3727	0.045632
chr6__98899268__98934879___FBXL4	0.390307	-1.35732	0.026314
chr5__66021322__66054951___ERBB2IP	0.391565	-1.35267	0.012149
chr2__61223060__61281242___USP34	0.393166	-1.34679	0.037069
chr12__64648537__64649552___RASSF3	0.393231	-1.34655	0.030921
chr13__75560753__75569507___UCHL3	0.396781	-1.33358	0.035153
chr10__114843741__114848737___FAM160B1	0.398457	-1.3275	0.030871
chr3__47067070__47098081___SETD2	0.39993	-1.32218	0.045546
chr15__63532647__63537156___USP3	0.403078	-1.31087	0.044811
chr21__36356620__36364259___MORC3	0.404013	-1.30753	0.034174
chr2__208345111__208348023___PIKFYVE	0.404455	-1.30595	0.044413
chr3__52412811__52414587___PHF7	0.404726	-1.30498	0.046161
chr7__140355668__140358785___SLC37A3	0.410632	-1.28408	0.017326
chr12__53719739__53722183___CALCOCO1	0.413219	-1.27502	0.03476
chr6__116689320__116705160___KPNA5	0.413661	-1.27348	0.042566
chr13__41318806__41336756___NAA16	0.41991	-1.25185	0.039629
chr8__99431537__99585517___VPS13B	0.423108	-1.2409	0.04659
chr16__66730112__66732505___DYNC1LI2	0.429413	-1.21956	0.029875
chr19__45263113__45263367___MARK4	0.430416	-1.2162	0.035191
chr5__78089393__78129307___AP3B1	0.431091	-1.21394	0.040986
chr20__5557945__5604440___GPCPD1	0.431381	-1.21297	0.045446
chr3__16286342__16303592___OXNAD1	0.438679	-1.18876	0.040212
chr2__33134793__33222151___LTBP1	0.439419	-1.18633	0.042181
chr12__88148288__88176319___TMTC3	0.440895	-1.18149	0.04037
chr12__112207874__112219489___HECTD4	0.443065	-1.17441	0.039677
chr8__100259107__100288267___RNF19A	0.448329	-1.15737	0.024905
chr19__21405129__21405856___ZNF493	0.449931	-1.15222	0.033966
chr13__41466823__41468838___RGCC	0.456708	-1.13066	0.02463
chr8__41692648__41693201___ANK1	0.461318	-1.11617	0.049666
chr9__3647338__3651867___NA	0.466104	-1.10128	0.037087
chr9__77337255__77371149___VPS13A	0.486154	-1.04052	0.032932
chr18__21765772__21819646___MIB1	0.492644	-1.02138	0.040665

Appendix K

List of up-regulated circRNA in STRENGTH *compared with* SEDENTARY *at enrolment* (FDR<0.05).

Gene	FC	logFC	FDR
chr16__85633914__85634132___GSE1	2.916551	1.544263	0.02845

List of down-regulated circRNA in STRENGTH *compared with* SEDENTARY *at enrolment* (FDR<0.05).

Gene	FC	logFC	FDR
chr7__140454603__140472011___MKRN1	0.009571	-6.70709	0.034318
chr1__158654811__158654951___SPTA1	0.016242	-5.94416	0.033595
chr12__10420364__10435410___NA	0.021805	-5.51919	0.045716
chr10__68355353__68386128___RUFY2	0.03459	-4.85351	0.014516
chr11__2969803__2979237___NAP1L4	0.03591	-4.79946	0.045099
chr2__108451028__108475850___GCC2	0.039393	-4.66591	0.019501
chr5__55272087__55281515___DHX29	0.040566	-4.6236	0.019501
chr1__47287551__47304996___STIL	0.043044	-4.53804	0.019501
chr10__110124017__110132400___ADD3	0.043146	-4.53462	0.019501
chr15__50569887__50575919___TRPM7	0.043857	-4.51104	0.019501
chr10__114162637__114163329___C10orf118	0.045183	-4.46807	0.022213
chr20__41061394__41081240___TOP1	0.047908	-4.38359	0.023039
chr17__50385118__50388132___LRRC59	0.048488	-4.36623	0.023039
chr21__33340999__33343676___IFNAR1	0.048896	-4.35415	0.023039
chr9__85959793__85996577___NAA35	0.049457	-4.33768	0.023039
chr11__9286455__9295387___TMEM41B	0.049607	-4.33331	0.023039
chr6__87215903__87233527___ZNF292	0.050845	-4.29775	0.023039
chrX__78009102__78021079___ATP7A	0.051136	-4.28951	0.023039
chrX__20193487__20195145___RPS6KA3	0.051711	-4.27338	0.023039
chrX__155277134__155299145___CLIC2	0.053244	-4.23123	0.023039
chr4__150467673__150491035___LRBA	0.054301	-4.20289	0.023039
chr15__65702305__65732818___DENND4A	0.054316	-4.20249	0.023039
chr2__151416561__151428922___RIF1	0.054412	-4.19992	0.023039
chr1__20765377__20776750___HP1BP3	0.055197	-4.17926	0.023039
chr17__3705081__3705645___NA	0.055276	-4.17719	0.023039
chr21__42994848__42995343___PKNOX1	0.055613	-4.16843	0.023039
chr11__17988597__18010139___SERGEF	0.055749	-4.16491	0.023039
chr1__187303466__187313449___NA	0.055762	-4.16458	0.023039
chr10__11929865__11948508___UPF2	0.056421	-4.14761	0.023039
chr17__32200956__32203973___RHOT1	0.05696	-4.1339	0.023039
chr17__39564760__39566892___CDK12	0.057087	-4.13068	0.023039
chr16__8910745__8919139___USP7	0.05726	-4.12632	0.023039
chr1__198232553__198279061___NEK7	0.057389	-4.12309	0.023039
chr6__13579451__13600949___SIRT5	0.057704	-4.11517	0.023039
chrX__77829031__77830895___MAGT1	0.057757	-4.11385	0.023039
chr17__43104122__43104956___BRCA1	0.057945	-4.10918	0.023039
chr14__74022916__74046130___CCDC176	0.058111	-4.10504	0.023039

chr8__103040798__103042407___ATP6V1C1	0.058189	-4.10312	0.023039
chr11__16283756__16341252___SOX6	0.0588	-4.08803	0.023039
chr5__108341927__108348530___FBXL17	0.058819	-4.08756	0.023039
chr13__21381434__21401685___ZDHHC20	0.05892	-4.0851	0.023039
chr14__45227663__45242518___MIS18BP1	0.059007	-4.08296	0.023039
chr10__68753852__68791341___CCAR1	0.059107	-4.08052	0.023039
chr1__222650292__222654793___MIA3	0.059197	-4.07833	0.023039
chr10__63190894__63194375___JMJD1C	0.059474	-4.07159	0.023039
chr4__55403236__55417985___TMEM165	0.059477	-4.07152	0.023039
chr6__30021667__30035983___ZNRD1-AS1	0.059504	-4.07087	0.023039
chr1__75728401__75734871___ACADM	0.060168	-4.05486	0.023039
chr9__5066678__5090911___JAK2	0.060247	-4.05297	0.023364
chr3__50108070__50108304___RBM5	0.060256	-4.05275	0.023039
chr3__196885151__196886694___SENP5	0.060369	-4.05004	0.023039
chr15__74926766__74929232___COX5A	0.060661	-4.04308	0.023039
chr5__142885298__142913293___ARHGAP26	0.060876	-4.03797	0.023364
chr2__27382126__27387158___PPM1G	0.061617	-4.02052	0.023039
chr2__44174762__44180397___PPM1B	0.061636	-4.02009	0.024516
chr4__128957026__129003876___SCLT1	0.061804	-4.01616	0.02508
chr2__61501996__61533903___XPO1	0.061914	-4.0136	0.024516
chr2__108839185__108856970___CCDC138	0.062147	-4.00817	0.023039
chr17__61015751__61040892___BCAS3	0.062174	-4.00754	0.023039
chr11__85981745__86007583___PICALM	0.062315	-4.00427	0.023039
chr10__96907265__96907747___LCOR	0.063537	-3.97625	0.02508
chr14__52470037__52491005___TXNDC16	0.063967	-3.96652	0.023039
chr4__78842385__78865720___BMP2K	0.064061	-3.96441	0.02508
chr8__26360169__26363890___PPP2R2A	0.064175	-3.96184	0.02508
chr5__154865442__154867792___CNOT8	0.064806	-3.94773	0.026105
chr17__27304780__27309272___WSB1	0.065769	-3.92644	0.026105
chr6__89846562__89855544___CASP8AP2	0.065778	-3.92624	0.02845
chr13__72778187__72778380___DIS3	0.066115	-3.91888	0.028551
chr15__32633933__32636408___ARHGAP11A	0.066316	-3.91451	0.023039
chr9__3630938__3633465___NA	0.066321	-3.9144	0.028188
chr1__95143891__95161149___TMEM56TMEM56-RWDD3	0.06642	-3.91223	0.02845
chr1__171524821__171537473___PRRC2C	0.066516	-3.91016	0.027336
chr3__196019880__196020735___LOC102723457	0.066986	-3.89999	0.02845
chr16__53222644__53229100___CHD9	0.067067	-3.89826	0.028188
chr14__30929201__30936624___STRN3	0.067308	-3.89307	0.028551
chr10__45639751__45663842___ZFAND4	0.067622	-3.88637	0.028551
chr10__68393138__68396881___RUFY2	0.06772	-3.88428	0.029238
chr1__243316755__243426558___SDCCAG8	0.067972	-3.87892	0.02845
chr6__138907495__138914761___REPS1	0.068098	-3.87625	0.02845
chr2__8243565__8287558___LINC00299	0.068248	-3.87307	0.029238
chr10__27526828__27538028___RAB18	0.06826	-3.87283	0.028694
chrX__101101058__101148161___CENPI	0.068483	-3.86811	0.029768

chr10__117243971__117253457___SLC18A2	0.068502	-3.86771	0.029768
chr2__210104104__210154611___KANSL1L	0.068913	-3.85908	0.029768
chr1__1825397__1879902___GNB1	0.069941	-3.83773	0.02508
chr13__49993793__50044768___DLEU2	0.07005	-3.83547	0.030133
chr8__140879471__140890769___PTK2	0.07024	-3.83155	0.029768
chr12__122515105__122522299___RSRC2	0.0703	-3.83032	0.028551
chr10__17704431__17714678___STAM	0.070329	-3.82973	0.02845
chr20__5559940__5565078___GPCPD1	0.070338	-3.82956	0.029768
chr1__35003968__35015162___ZMYM6	0.070343	-3.82944	0.030972
chr19__5653115__5657347___SAFB	0.071464	-3.80664	0.030972
chr22__28694032__28719485___CHEK2	0.071528	-3.80534	0.029238
chr19__53148681__53153793___ZNF347	0.071594	-3.80402	0.030972
chrX__134413488__134417302___PHF6	0.071991	-3.79604	0.030002
chr4__145823422__145849561___ZNF827	0.072061	-3.79465	0.030401
chr10__5773842__5786050___GDI2	0.072099	-3.79387	0.030401
chr3__167720062__167725473___PDCD10	0.072387	-3.78812	0.031189
chr8__23566108__23568378___SLC25A37	0.072463	-3.78662	0.031393
chr3__196053418__196069568___TFRC	0.072474	-3.78639	0.029768
chr12__110018345__110033957___ANKRD13A	0.072582	-3.78424	0.030447
chr3__112563385__112573956___SLC35A5	0.072617	-3.78354	0.031393
chr10__13659323__13675044___FRMD4A	0.072625	-3.78339	0.031393
chr12__14434337__14438267___ATF7IP	0.072667	-3.78255	0.029768
chr6__147205971__147239270___STXBP5	0.072967	-3.77661	0.029768
chr1__207545308__207717691___NA	0.073008	-3.77579	0.029768
chr3__44801450__44811043___KIF15	0.073338	-3.76929	0.027977
chr12__49990684__49992655___RACGAP1	0.073446	-3.76718	0.031393
chr7__6187050__6190531___CYTH3	0.073501	-3.76609	0.031393
chr15__42827928__42878684___TTBK2	0.073729	-3.76163	0.031189
chr15__42988819__43025429___UBR1	0.073771	-3.7608	0.031393
chr17__62536170__62565137___TLK2	0.073784	-3.76055	0.031147
chr18__54271360__54287411___POLI	0.073823	-3.75978	0.03102
chr1__92693802__92704744___EVI5	0.074007	-3.75619	0.031417
chr6__41052265__41055999___NA	0.074077	-3.75484	0.027734
chr14__67398007__67402868___PLEK2	0.074088	-3.75461	0.03102
chr4__169477124__169508852___NEK1	0.074475	-3.7471	0.031393
chr3__138681967__138684803___PIK3CB	0.074507	-3.74648	0.031805
chr10__27134831__27136385___YME1L1	0.075353	-3.73019	0.031805
chrX__11367771__11370505___ARHGAP6	0.075397	-3.72934	0.031805
chr9__120439399__120448126___CDK5RAP2	0.075408	-3.72914	0.03102
chr6__42676056__42684871___UBR2	0.075633	-3.72484	0.029768
chr9__112438431__112441770___HSDL2	0.075777	-3.7221	0.032604
chr14__60256824__60268435___PPM1A	0.07583	-3.72108	0.032366
chr11__28211062__28233585___METTL15	0.076005	-3.71776	0.032539
chr4__169463243__169556095___NEK1	0.076651	-3.70555	0.029768
chr20__5565017__5604440___GPCPD1	0.07668	-3.705	0.031805
chr15__90217439__90219891___SEMA4B	0.076725	-3.70416	0.033348

chr8__99556450__99661491___VPS13B	0.076808	-3.70261	0.031805
chr18__22968806__22984990___RBBP8	0.077093	-3.69725	0.032539
chr10__86497201__86500743___WAPAL	0.077137	-3.69642	0.031393
chr4__143433491__143440382___GAB1	0.077191	-3.69542	0.033348
chr22__20933779__20934244___CRKL	0.077351	-3.69245	0.033348
chr18__51046920__51049324___SMAD4	0.077607	-3.68766	0.031393
chrX__77589834__77600564___ATRX	0.077626	-3.68733	0.031393
chr10__69155812__69158211___VPS26A	0.077871	-3.68277	0.032539
chr9__96364464__96368305___SLC35D2	0.078078	-3.67894	0.031393
chr14__72693076__72731934___DPF3	0.078093	-3.67866	0.033348
chr1__180003174__180024582___CEP350	0.078211	-3.67648	0.031393
chr14__55380573__55382191___ATG14	0.078413	-3.67276	0.033556
chr9__34306252__34311371___KIF24	0.07843	-3.67246	0.030972
chr4__4457191__4471706___STX18	0.078444	-3.67219	0.033595
chr13__19824920__19851957___ZMYM5	0.078513	-3.67092	0.033348
chr11__93696320__93702919___KIAA1731	0.078535	-3.67052	0.03336
chr5__10213491__10224061___NA	0.078684	-3.66779	0.030401
chr20__4195282__4204704___NA	0.078808	-3.66551	0.033595
chr1__29115699__29117989___EPB41	0.079006	-3.6619	0.03102
chr11__16183886__16247560___SOX6	0.079041	-3.66126	0.031393
chr5__126804776__126832801___LMNB1	0.07931	-3.65635	0.03336
chr20__47224317__47236516___ZMYND8	0.079523	-3.65248	0.033595
chr3__138621407__138629156___FAIM	0.079584	-3.65137	0.03336
chr10__5773842__5811956___GDI2	0.079924	-3.64523	0.032539
chrX__17103718__17106052___REPS2	0.080004	-3.64379	0.033205
chr1__234418084__234427766___TARBP1	0.080033	-3.64326	0.03336
chr10__45624583__45627105___ZFAND4	0.080255	-3.63926	0.033595
chr8__47279862__47294030___SPIDR	0.080591	-3.63324	0.031393
chr4__128936655__128992237___SCLT1	0.08066	-3.632	0.03336
chr3__148582857__148592265___NA	0.080685	-3.63156	0.03336
chr6__57124734__57150862___ZNF451	0.080834	-3.62889	0.031393
chr16__67685457__67685802___GFOD2	0.080919	-3.62737	0.033595
chr6__36524341__36525642___STK38	0.080998	-3.62598	0.033595
chr14__58467735__58470723___KIAA0586	0.081068	-3.62472	0.032539
chr8__140347757__140360193___TRAPPC9	0.081466	-3.61766	0.033595
chr2__108752998__108755259___RANBP2	0.081702	-3.61349	0.029768
chr21__15777904__15842540___USP25	0.081811	-3.61155	0.03336
chrY__19041370__19045288___NA	0.081894	-3.61009	0.033595
chr1__28683583__28690186___GMEB1	0.081974	-3.60869	0.033595
chr17__2665372__2670331___PAFAH1B1	0.08199	-3.60841	0.033595
chr6__136694140__136720589___MAP3K5	0.08211	-3.6063	0.034276
chr16__75412535__75414695___CFDP1	0.082136	-3.60585	0.033595
chr4__102689574__102690957___MANBA	0.08223	-3.6042	0.031393
chr7__157382246__157385611___DNAJB6	0.082279	-3.60334	0.033348
chr4__20704466__20727397___PACRGL	0.082438	-3.60054	0.034318
chr1__158681527__158685347___SPTA1	0.082535	-3.59885	0.033348

chr19__17162350__17163122___MYO9B	0.082577	-3.59811	0.031393
chr9__125341177__125342299___GAPVD1	0.082581	-3.59805	0.033348
chr10__87864454__87961118___PTEN	0.082595	-3.5978	0.034276
chr18__13012973__13019206___CEP192	0.082649	-3.59686	0.033595
chr1__224393828__224404570___WDR26	0.082685	-3.59624	0.034318
chr21__36341399__36345031___MORC3	0.08269	-3.59615	0.034318
chr8__85336945__85338449___CA1	0.082751	-3.59508	0.034318
chr17__60299334__60301704___USP32	0.082895	-3.59258	0.03336
chr19__34430576__34438766___UBA2	0.08291	-3.59231	0.033595
chr15__80073266__80131293___ZFAND6	0.083042	-3.59002	0.033595
chr9__83739705__83799240___GKAP1	0.083228	-3.58679	0.031393
chr8__85109595__85126837___LRRCC1	0.083355	-3.58459	0.033595
chr8__132777796__132798860___PHF20L1	0.083441	-3.58311	0.030447
chr15__49011731__49028682___SECISBP2L	0.083494	-3.58218	0.031393
chr1__28987431__29097935___EPB41	0.083494	-3.58219	0.033595
chr3__136417885__136502779___STAG1	0.083495	-3.58216	0.033373
chr3__143985543__143989832___C3orf58	0.083525	-3.58165	0.032539
chr12__96909752__96912817___NEDD1	0.083558	-3.58107	0.03336
chr2__206056198__206063244___INO80D	0.083625	-3.57991	0.033595
chr17__48133535__48137337___SKAP1	0.083942	-3.57447	0.033595
chrX__10860043__10883281___MID1-2	0.084008	-3.57333	0.034318
chr5__41907736__41912183___C5orf51	0.084138	-3.5711	0.030124
chr7__93334117__93341575___CCDC132	0.084149	-3.57091	0.033348
chr2__23867835__23875904___ATAD2B	0.084301	-3.5683	0.034318
chr11__120437308__120445464___ARHGEF12	0.08436	-3.56729	0.031147
chr3__69039551__69044595___TMF1	0.084371	-3.56711	0.033595
chr11__67180079__67181892___KDM2A	0.084566	-3.56378	0.034318
chr14__58457759__58487166___KIAA0586	0.084585	-3.56345	0.033595
chr8__100264034__100300651___RNF19A	0.084732	-3.56095	0.034318
chr7__91992885__92014328___AKAP9	0.084782	-3.56009	0.033348
chr19__51133313__51134407___SIGLEC9	0.08484	-3.55911	0.033595
chr1__93217738__93239896___CCDC18	0.085194	-3.55311	0.033348
chr6__42637011__42642481___UBR2	0.085247	-3.5522	0.034318
chr16__72171197__72174070___NA	0.085402	-3.54959	0.033595
chr7__48466953__48489344___ABCA13	0.085635	-3.54565	0.035049
chr4__38089932__38118192___TBC1D1	0.085653	-3.54536	0.03102
chr12__26628033__26655852___ITPR2	0.085717	-3.54427	0.030401
chr15__90439332__90440615___IQGAP1	0.086016	-3.53924	0.033595
chr19__52618936__52635153___ZNF83	0.08612	-3.5375	0.035049
chr12__71626260__71629037___ZFC3H1	0.086247	-3.53538	0.03336
chr4__128831733__128852268___JADE1	0.086248	-3.53536	0.033595
chr1__182822115__182859117___NA	0.086677	-3.5282	0.033595
chr11__128758115__128772985___FLI1	0.086694	-3.52792	0.033595
chr9__5021963__5078444___JAK2	0.086697	-3.52787	0.03336
chr9__4892405__4966194___NA	0.086796	-3.52623	0.035809
chr1__20741831__20780540___NA	0.086825	-3.52575	0.03336

chr4__109513747__109520484___SEC24B	0.086897	-3.52455	0.035049
chr7__105040839__105081797___KMT2E	0.086982	-3.52314	0.035049
chr8__123325893__123336532___ATAD2	0.087108	-3.52104	0.035049
chr2__218529956__218562813___USP37	0.087755	-3.51037	0.035895
chr17__12081356__12113360___MAP2K4	0.087897	-3.50804	0.035049
chr20__35651264__35659014___RBM12	0.087976	-3.50675	0.035049
chr3__121726913__121730973___GOLGB1	0.08798	-3.50669	0.034318
chr6__109140421__109150239___CEP57L1	0.088484	-3.49843	0.033595
chr1__222715145__222725555___BROX	0.08854	-3.49753	0.033595
chr12__56738434__56744123___PRIM1	0.088567	-3.49708	0.033595
chr1__174969277__174988838___RABGAP1L	0.088609	-3.4964	0.035049
chr1__243270105__243308177___SDCCAG8	0.088652	-3.49571	0.034318
chr15__63690541__63694894___HERC1	0.088806	-3.4932	0.036577
chr7__73462922__73466401___BAZ1B	0.088819	-3.49298	0.035918
chr7__77292952__77294938___CCDC146	0.088917	-3.4914	0.033348
chr5__146263491__146271058___RBM27	0.088925	-3.49126	0.037464
chr4__48842636__48857365___OCIAD1	0.088953	-3.49081	0.033595
chr7__48410520__48412583___ABCA13	0.088978	-3.49041	0.036577
chr7__93303460__93334197___CCDC132	0.088985	-3.49029	0.035049
chr11__58610298__58611738___ZFP91ZFP91-CNTF	0.089189	-3.48699	0.034318
chr17__61776401__61781005___BRIP1	0.089211	-3.48663	0.035049
chr4__152411303__152482673___FBXW7	0.089278	-3.48555	0.035049
chr5__131504626__131510491___RAPGEF6	0.089287	-3.48541	0.035049
chr3__56745205__56745462___ARHGEF3	0.089361	-3.48421	0.034318
chr21__39224408__39232498___BRWD1	0.089365	-3.48415	0.033595
chr16__72349046__72391215___NA	0.089384	-3.48383	0.035049
chr2__200920222__200937966___ORC2	0.089487	-3.48218	0.034318
chr7__6028615__6029032___EIF2AK1	0.089706	-3.47865	0.033556
chr4__169585349__169599197___NEK1	0.089941	-3.47488	0.036715
chr12__19274516__19274983___PLEKHA5	0.090027	-3.4735	0.033348
chr15__65690415__65761438___DENND4A	0.090442	-3.46687	0.037464
chr9__3484974__3490345___RFX3	0.090538	-3.46533	0.033348
chr10__68911068__68914204___DDX50	0.090667	-3.46327	0.033595
chr9__86305192__86319670___ZCCHC6	0.090712	-3.46257	0.033595
chr17__48112031__48112660___SNX11	0.090806	-3.46106	0.037108
chr1__21002713__21089213___EIF4G3	0.09133	-3.45277	0.033595
chr9__120550792__120568388___CDK5RAP2	0.091362	-3.45227	0.036577
chr12__70278132__70319364___CNOT2	0.091439	-3.45105	0.034318
chr5__77463095__77464809___WDR41	0.091598	-3.44854	0.035049
chr11__46769963__46788773___CKAP5	0.091613	-3.4483	0.033595
chr15__42558198__42566706___HAUS2	0.091617	-3.44824	0.033595
chr2__120285874__120289757___RALB	0.091666	-3.44747	0.037786
chr3__25635936__25645470___TOP2B	0.091744	-3.44624	0.035809
chr2__224495832__224514772___CUL3	0.091999	-3.44224	0.035049
chr5__36984676__36995804___NIPBL	0.092276	-3.4379	0.033595
chr2__32414769__32416163___BIRC6	0.092317	-3.43726	0.033595

chr3__155887432__155925366___GMPS	0.092426	-3.43555	0.034318
chr17__61965006__61968258___MED13	0.09265	-3.43206	0.035049
chr15__50303966__50309798___GABPB1	0.092685	-3.43152	0.033595
chr14__45226743__45242518___MIS18BP1	0.09281	-3.42958	0.036577
chrX__101101058__101161569___CENPI	0.09284	-3.42911	0.036206
chr8__27748077__27748598___CCDC25	0.09304	-3.42601	0.036702
chr19__4354949__4355173___MPND	0.093093	-3.42518	0.037672
chr3__17372075__17384015___TBC1D5	0.093112	-3.42489	0.037672
chr1__179335506__179343635___SOAT1	0.093145	-3.42438	0.035809
chr6__63646527__63685911___PHF3	0.093371	-3.42088	0.037469
chr12__827042__830160___WNK1	0.093497	-3.41894	0.034318
chr19__54594665__54631306___NA	0.093534	-3.41836	0.042959
chr11__16046514__16111926___SOX6	0.093636	-3.4168	0.033595
chr15__42528262__42529819___SNAP23	0.093819	-3.41397	0.03789
chr5__73051349__73052507___FCHO2	0.093833	-3.41376	0.039241
chr3__100267100__100281847___TBC1D23	0.093944	-3.41205	0.035049
chr6__119188405__119204882___MAN1A1	0.093986	-3.4114	0.036577
chr14__55378279__55380389___ATG14	0.093987	-3.41139	0.037127
chr14__50145170__50158646___SOS2	0.094021	-3.41087	0.034318
chr8__99134632__99275254___VPS13B	0.094295	-3.40668	0.035918
chr1__29096155__29097935___EPB41	0.094299	-3.40661	0.037464
chr11__116759074__116765446___BUD13	0.094462	-3.40412	0.037464
chr19__52383849__52385742___ZNF880	0.094588	-3.4022	0.036577
chr17__20204333__20227620___SPECC1	0.094628	-3.40159	0.039435
chr8__99096312__99136752___VPS13B	0.094772	-3.3994	0.037672
chr1__169798857__169807929___C1orf112	0.095116	-3.39416	0.035165
chr14__96833467__96945382___NA	0.095136	-3.39387	0.034318
chrX__80288906__80310233___CHMP1B2P	0.095208	-3.39278	0.038829
chr12__14665859__14672314___GUCY2C	0.095218	-3.39262	0.034318
chr19__8337795__8339167___KANK3	0.095272	-3.39181	0.035049
chr8__58565019__58572314___SDCBP	0.095359	-3.39049	0.034318
chr6__63691737__63703671___PHF3	0.095441	-3.38925	0.037464
chr1__229450525__229465519___NUP133	0.095474	-3.38875	0.040392
chr14__35050784__35053451___FAM177A1	0.09558	-3.38715	0.037464
chr5__50399859__50411383___EMB	0.095621	-3.38653	0.037464
chr7__152220523__152238826___KMT2C	0.095788	-3.38401	0.042128
chr9__36597222__36633200___MELK	0.095833	-3.38334	0.034318
chr7__148766561__148767749___CUL1	0.096005	-3.38074	0.037672
chr4__9641071__9641450___NA	0.096015	-3.38059	0.042128
chr11__47499453__47500932___CELF1	0.09608	-3.37961	0.035049
chr10__92616737__92630364___KIF11	0.096145	-3.37864	0.034516
chr7__154967816__154998784___PAXIP1	0.09641	-3.37467	0.036261
chr10__68383798__68394451___RUFY2	0.096444	-3.37417	0.041189
chr11__9420411__9425262___IPO7	0.096651	-3.37107	0.035049
chr2__158620990__158621421___PKP4	0.096794	-3.36894	0.04279
chr1__174969277__174976182___RABGAP1L	0.096874	-3.36775	0.033595

chr8__26410909__26411069___BNIP3L	0.096907	-3.36726	0.037672
chr4__169585349__169602678___NEK1	0.097082	-3.36465	0.038565
chr6__159682474__159685033___SOD2	0.097291	-3.36155	0.035049
chr2__148048359__148054449___MBD5	0.09735	-3.36067	0.034318
chr8__85138035__85138475___LRRCC1	0.097401	-3.35991	0.02508
chr10__7276892__7285954___SFMBT2	0.097465	-3.35898	0.034318
chr12__122601536__122624688___KNTC1	0.097562	-3.35754	0.042537
chr2__174378923__174387779___CIR1	0.097758	-3.35465	0.042273
chr1__182822115__182843434___NA	0.097862	-3.3531	0.037464
chr8__42925557__42943445___HOOK3	0.098075	-3.34997	0.035843
chr13__49990860__50045232___DLEU2	0.09817	-3.34858	0.034609
chr1__95134782__95136731___TMEM56TMEM56-RWDD3	0.098219	-3.34785	0.034318
chr15__51896419__51902036___TMOD3	0.098509	-3.34359	0.035809
chr13__77018600__77021861___FBXL3	0.09853	-3.34329	0.042537
chr5__177041126__177064601___ZNF346	0.098567	-3.34275	0.036539
chr1__212020122__212021212___INTS7	0.098699	-3.34082	0.036702
chr8__123129066__123142456___TBC1D31	0.09892	-3.3376	0.033595
chr6__144451370__144459354___UTRN	0.098934	-3.33739	0.036206
chr4__89822246__89836789___SNCA	0.098988	-3.33661	0.042959
chr1__185174372__185276668___SWT1	0.099031	-3.33598	0.034318
chr18__37066890__37067545___KIAA1328	0.09904	-3.33584	0.039241
chr9__20360742__20365744___MLLT3	0.099084	-3.3352	0.042273
chr3__37108637__37121691___LRRFIP2	0.099558	-3.32832	0.037294
chrX__71367499__71460803___TAF1	0.099731	-3.32582	0.042709
chr18__70047971__70065922___RTTN	0.099934	-3.32289	0.035972
chr1__229518841__229549434___ABCB10	0.099997	-3.32197	0.042537
chr12__75312848__75326527___CAPS2	0.100036	-3.32141	0.044597
chr2__61496879__61526521___XPO1	0.100056	-3.32112	0.036702
chr8__143640579__143641432___ZNF623	0.100141	-3.3199	0.036702
chr15__67231814__67236820___AAGAB	0.100298	-3.31764	0.035809
chr13__40826506__40872160___TPTE2P5	0.100449	-3.31547	0.040474
chr2__15415546__15511350___NBAS	0.100483	-3.31497	0.033595
chr21__33559230__33559775___SON	0.100493	-3.31483	0.045716
chr5__66012049__66028343___ERBB2IP	0.100582	-3.31356	0.042959
chr8__96834973__96880005___CPQ	0.100611	-3.31314	0.042959
chr10__124816576__124831463___FAM175B	0.100725	-3.31151	0.035577
chr1__53806425__53832591___NDC1	0.10074	-3.3113	0.037672
chr1__47289435__47300152___STIL	0.100745	-3.31123	0.036577
chr12__26621123__26632059___ITPR2	0.100836	-3.30992	0.039241
chr1__61111371__61188399___NFIA	0.100919	-3.30873	0.042128
chr11__108169744__108173851___NPAT	0.101019	-3.3073	0.037054
chr1__174304986__174371072___RABGAP1L	0.101117	-3.3059	0.035049
chr5__97101759__97183669___NA	0.101226	-3.30435	0.035809
chr20__44987132__44995257___STK4	0.101387	-3.30205	0.042128
chr12__88096888__88107098___CEP290	0.101443	-3.30126	0.042128

chr9__121167489__121175224___CNTRL	0.101623	-3.2987	0.037294
chr1__65364635__65389627___DNAJC6	0.102066	-3.29243	0.042273
chr8__102833056__102834747___AZIN1	0.102369	-3.28815	0.034318
chr2__60887508__60901083___REL	0.102414	-3.28751	0.037672
chr18__20968772__20980004___ROCK1	0.102417	-3.28747	0.036839
chr12__102164438__102182627___PARPBP	0.102427	-3.28733	0.04488
chr12__70342107__70346324___CNOT2	0.102437	-3.28719	0.042128
chr6__149572285__149591790___NA	0.102585	-3.2851	0.035049
chr8__99013760__99064287___VPS13B	0.10272	-3.28321	0.043015
chr13__24484653__24503777___PARP4	0.102757	-3.28268	0.046104
chr1__86372431__86384801___ODF2L	0.103092	-3.278	0.045716
chr11__108104190__108106295___CUL5	0.103205	-3.27641	0.040688
chr14__92142164__92155323___CPSF2	0.103206	-3.2764	0.042537
chr5__32390275__32397338___ZFR	0.103234	-3.276	0.044297
chr6__53514204__53532766___GCLC	0.103448	-3.27302	0.044825
chr9__79704783__79709699___TLE4	0.103636	-3.2704	0.042222
chr4__174297966__174316290___CEP44	0.103788	-3.26829	0.042128
chr12__69409884__69410727___NA	0.103854	-3.26737	0.042128
chr1__235172618__235196115___ARID4B	0.103943	-3.26613	0.037672
chrX__77656560__77664778___ATRX	0.103964	-3.26585	0.042709
chr2__190655977__190673152___NAB1	0.10401	-3.26521	0.040474
chr10__68771206__68771445___CCAR1	0.104029	-3.26495	0.042359
chr1__207526753__207701618___NA	0.104172	-3.26296	0.045716
chr6__119188405__119248354___MAN1A1	0.104186	-3.26277	0.042121
chr10__5765987__5811956___GDI2	0.10425	-3.26189	0.037693
chr15__22667898__22681605___WHAMMP3	0.104269	-3.26162	0.040474
chr2__200949554__200958133___ORC2	0.104717	-3.25544	0.044597
chr9__4823548__4849550___RCL1	0.104736	-3.25517	0.040474
chr17__30855143__30869646___ATAD5	0.104761	-3.25482	0.042959
chr2__26364302__26383347___EPT1	0.104797	-3.25433	0.045099
chr4__103174736__103181456___CENPE	0.104832	-3.25384	0.043975
chr2__148761782__148765146___EPC2	0.104849	-3.25362	0.023039
chr15__89871475__89889140___C15orf38-AP3S2AP3S2	0.104968	-3.25198	0.042959
chr12__70219393__70225390___LOC101928062	0.104979	-3.25182	0.042959
chr22__40848294__40849895___ST13	0.105171	-3.24919	0.043098
chr14__39151746__39158402___TRAPPC6B	0.105191	-3.24892	0.043375
chr2__151441905__151443709___RIF1	0.10524	-3.24825	0.039241
chr2__151438684__151461289___RIF1	0.105431	-3.24563	0.040474
chr5__41794003__41807438___OXCT1	0.105447	-3.24541	0.042959
chr1__113837590__113838620___PTPN22	0.105619	-3.24306	0.040912
chr20__5559940__5570239___GPCPD1	0.105648	-3.24266	0.04488
chr20__3963875__3974400___RNF24	0.105883	-3.23946	0.040474
chr6__97267882__97273062___MMS22L	0.106125	-3.23616	0.04618
chr15__50912078__50930971___AP4E1	0.106135	-3.23603	0.047176
chrY__12709388__12722187___USP9Y	0.106336	-3.23329	0.042222

chr9__83677727__83683066___UBQLN1	0.106375	-3.23277	0.040474
chr12__50435488__50441643___LARP4	0.106502	-3.23104	0.042273
chr21__39209995__39215362___BRWD1	0.106521	-3.23079	0.047173
chr3__125453810__125460860___SNX4	0.106572	-3.2301	0.039241
chr2__171046174__171061156___TLK1	0.106621	-3.22944	0.036839
chr12__32619698__32633689___FGD4	0.106626	-3.22937	0.044349
chr9__121460104__121463328___GGTA1P	0.106719	-3.22812	0.04488
chr6__149525143__149535738___PPIL4	0.106753	-3.22766	0.04488
chr2__110649234__110661841___BUB1	0.106763	-3.22752	0.047188
chr1__158667858__158686537___SPTA1	0.106774	-3.22737	0.045716
chr1__158677690__158683496___SPTA1	0.106859	-3.22623	0.045716
chr15__56391243__56394834___TEX9	0.106877	-3.22598	0.044597
chr8__99467414__99481802___VPS13B	0.106899	-3.22568	0.041225
chr11__118768223__118786518___DDX6	0.107304	-3.22023	0.03803
chr2__33128432__33222151___LTBP1	0.107426	-3.21858	0.04196
chrX__119629318__119629508___SEPT6	0.107477	-3.2179	0.042709
chr15__68211263__68218650___CLN6	0.107509	-3.21747	0.04734
chrX__1770497__1771629___NA	0.107698	-3.21494	0.045716
chr15__63727647__63749791___HERC1	0.10772	-3.21464	0.042537
chr5__64800248__64804386___CWC27	0.107884	-3.21245	0.047763
chr2__33523879__33534400___RASGRP3	0.107952	-3.21154	0.046951
chr4__128936655__128952840___SCLT1	0.107999	-3.21092	0.042959
chr4__42022838__42039053___SLC30A9	0.108162	-3.20873	0.040474
chr2__23884765__23895970___ATAD2B	0.108188	-3.20838	0.044597
chr8__103404776__103407784___SLC25A32	0.108753	-3.20087	0.042537
chr14__60267215__60268435___PPM1A	0.108757	-3.20082	0.047073
chr7__848418__849603___SUN1	0.108947	-3.1983	0.040474
chr10__60787224__60787470___CDK1	0.109021	-3.19732	0.045716
chr12__98677425__98686873___APAF1	0.109134	-3.19583	0.046104
chr1__93183360__93221936___CCDC18	0.109135	-3.19582	0.042959
chr5__145764931__145796547___PRELID2	0.109276	-3.19396	0.045461
chr17__19939713__19968461___AKAP10	0.109338	-3.19313	0.042959
chr8__92916929__92929574___TRIQK	0.109378	-3.19261	0.047306
chr16__18841565__18850467___SMG1	0.109426	-3.19197	0.043897
chr22__29813430__29822464___ASCC2	0.109534	-3.19055	0.04488
chr10__32565296__32584304___CCDC7	0.1097	-3.18837	0.045293
chr17__68429996__68433575___WIPI1	0.109716	-3.18815	0.047684
chr5__157803650__157817547___CLINT1	0.109887	-3.1859	0.037294
chr20__47282102__47294779___ZMYND8	0.10993	-3.18534	0.034318
chr1__224404430__224413335___WDR26	0.10995	-3.18508	0.043971
chr8__21970144__21987857___XPO7	0.109969	-3.18483	0.040459
chr7__139371387__139409654___LUC7L2	0.110039	-3.18391	0.047173
chr18__45928869__45952643___EPG5	0.110067	-3.18355	0.035049
chr11__74775146__74810330___RNF169	0.110167	-3.18224	0.045716
chr15__43809755__43817448___MFAP1	0.110327	-3.18015	0.042537
chr20__41076171__41101353___TOP1	0.110762	-3.17446	0.042273

chr4__128936655__128946152___SCLT1	0.110838	-3.17348	0.049037
chr5__137985257__138011945___FAM13B	0.110889	-3.17282	0.037464
chr4__106164392__106248306___TBCK	0.111049	-3.17073	0.045716
chr11__34947506__34970286___PDHX	0.111251	-3.16811	0.042959
chr5__123346605__123382889___CEP120	0.111271	-3.16785	0.042273
chr8__21991868__22004030___XPO7	0.111293	-3.16756	0.023039
chr20__35734186__35738621___RBM39	0.111347	-3.16686	0.042128
chr4__84904343__84905271___WDFY3	0.111501	-3.16486	0.040474
chr4__183683975__183693147___TRAPPC11	0.111551	-3.16422	0.047684
chr1__84865385__84866138___LPAR3	0.111825	-3.16068	0.04618
chr6__109641518__109672167___AK9	0.111831	-3.16061	0.039995
chr7__93259550__93311272___CCDC132	0.111872	-3.16008	0.045099
chr2__37032629__37041292___HEATR5B	0.111904	-3.15967	0.045167
chr4__48351500__48383784___SLAIN2	0.112187	-3.15602	0.042128
chr10__30313891__30322442___MTPAP	0.112218	-3.15563	0.04948
chr3__52411029__52414587___PHF7	0.112295	-3.15463	0.04488
chr3__47622207__47678311___SMARCC1	0.112378	-3.15357	0.043786
chr6__84155298__84175347___KIAA1009	0.112568	-3.15113	0.036577
chr8__130134296__130169067___ASAP1	0.112719	-3.1492	0.045863
chr10__31461037__31461783___ZEB1	0.112758	-3.1487	0.045538
chr3__132434538__132450847___DNAJC13	0.11278	-3.14841	0.042959
chr20__62256057__62260125___OSBPL2	0.112864	-3.14734	0.04488
chr17__30843913__30844916___ATAD5	0.112903	-3.14685	0.02508
chr12__6510279__6510532___SCARNA10	0.113026	-3.14527	0.040474
chr17__8518631__8535931___MYH10	0.113162	-3.14354	0.042222
chr10__31461037__31502509___ZEB1	0.113336	-3.14132	0.044597
chr16__75411825__75412754___CFDP1	0.113417	-3.1403	0.045716
chr4__53998206__54014119___NA	0.113441	-3.13998	0.040474
chr17__37619768__37621520___DDX52	0.113693	-3.13679	0.047173
chr16__84758716__84768358___USP10	0.113871	-3.13452	0.036539
chr15__65700544__65738875___DENND4A	0.113978	-3.13318	0.045099
chr2__26254247__26263479___HADHB	0.114034	-3.13246	0.044618
chr4__56017648__56019555___CEP135	0.114206	-3.13029	0.032366
chr5__79645123__79682061___PAPD4	0.114305	-3.12904	0.047188
chr2__86159536__86162079___IMMT	0.114651	-3.12468	0.045538
chr16__15615830__15621911___KIAA0430	0.114683	-3.12427	0.045099
chr20__35655202__35658982___CPNE1	0.114865	-3.12199	0.044449
chr17__32173831__32201056___RHOT1	0.114917	-3.12134	0.046104
chr9__27044742__27062110___IFT74	0.115195	-3.11786	0.045099
chr9__125298890__125302826___GAPVD1	0.115249	-3.11717	0.047684
chr2__229840822__229859574___TRIP12	0.115324	-3.11623	0.045716
chr18__116842__118504___ROCK1P1	0.11537	-3.11567	0.046951
chr16__68810197__68813495___CDH1	0.115435	-3.11485	0.047763
chr3__141963812__141993585___TFDP2	0.115476	-3.11434	0.047684
chr8__99142974__99275254___VPS13B	0.115545	-3.11347	0.046951
chr1__20757166__20771073___HP1BP3	0.115608	-3.11268	0.045716

chr2__61092464__61118116___KIAA1841	0.115701	-3.11152	0.044825
chr20__35655157__35659014___RBM12	0.115875	-3.10935	0.047282
chr14__49789146__49831361___NEMF	0.116111	-3.10642	0.046951
chr6__149517042__149541586___PPIL4	0.116169	-3.10571	0.046951
chr3__27411642__27452498___SLC4A7	0.116389	-3.10298	0.044597
chr3__32703868__32708820___CNOT10	0.116766	-3.09831	0.043987
chr20__35842573__35871829___PHF20	0.116895	-3.09671	0.044349
chr16__47463899__47589102___PHKB	0.116909	-3.09655	0.047188
chr14__50442732__50445194___MAP4K5	0.11694	-3.09616	0.047188
chr10__6613631__6613987___NA	0.117177	-3.09323	0.045293
chr5__176969601__176982623___UIMC1	0.11728	-3.09198	0.047271
chr8__130152736__130188183___ASAP1	0.117474	-3.08959	0.047684
chr3__14443624__14447816___SLC6A6	0.117483	-3.08947	0.047188
chr6__13632370__13641307___RANBP9	0.117483	-3.08948	0.046104
chr2__201008973__201011472___FAM126B	0.117564	-3.08848	0.047176
chr10__89745899__89754673___KIF20B	0.117925	-3.08406	0.045716
chr18__26052624__26087577___SS18	0.118055	-3.08247	0.045716
chr12__26911178__26917733___ASUN	0.118095	-3.08199	0.023039
chr7__27785163__27796219___TAX1BP1	0.11819	-3.08083	0.047684
chr4__143524367__143528714___SMARCA5	0.118244	-3.08017	0.046449
chr13__45988787__46020557___ZC3H13	0.118253	-3.08005	0.046449
chr9__19423862__19424841___ACER2	0.118272	-3.07982	0.047179
chr18__39207685__39208789___LINC00669	0.118358	-3.07877	0.045716
chr3__155893518__155937881___NA	0.118386	-3.07842	0.043897
chr20__49072286__49072697___CSE1L	0.118624	-3.07553	0.042537
chr1__168038371__168045203___DCAF6	0.118642	-3.07532	0.045863
chr10__12081472__12094271___DHTKD1	0.118674	-3.07492	0.033595
chr1__61111371__61277585___NFIA	0.118845	-3.07284	0.042959
chr5__73006445__73006780___FCHO2	0.11886	-3.07267	0.047282
chr14__50423121__50429260___MAP4K5	0.119149	-3.06916	0.047684
chr18__2718158__2752552___SMCHD1	0.119284	-3.06752	0.045167
chr17__8443927__8460160___NDEL1	0.119449	-3.06554	0.049037
chr9__120408347__120409316___CDK5RAP2	0.119484	-3.06511	0.04618
chr1__153889678__153898982___GATAD2B	0.119514	-3.06474	0.042673
chr10__118685983__118730410___CACUL1	0.119647	-3.06314	0.048671
chr9__162432__172172___CBWD1	0.119728	-3.06217	0.047835
chr19__11441240__11442515___PRKCSH	0.119827	-3.06097	0.047176
chr11__28211062__28212331___METTL15	0.119906	-3.06003	0.045716
chr18__58341038__58343103___NEDD4L	0.120045	-3.05835	0.045716
chr17__77402059__77402703___SEPT9	0.120112	-3.05755	0.045716
chr5__163473179__163475672___HMMR	0.120212	-3.05635	0.047835
chr7__131437785__131445903___MKLN1	0.120249	-3.0559	0.047347
chr1__156744163__156745373___HDGF	0.120489	-3.05303	0.042959
chr12__50435488__50454417___LARP4	0.120541	-3.0524	0.046104
chr2__171965338__171966949___HAT1	0.120736	-3.05007	0.047763
chr1__12578718__12579412___DHRS3	0.120785	-3.04948	0.04825

chr11__48063236__48066680___PTPRJ	0.120967	-3.04731	0.044597
chr1__38441190__38442939___NA	0.121016	-3.04673	0.044597
chr14__30605505__30612379___G2E3	0.121166	-3.04495	0.046951
chr12__64409962__64448297___XPOT	0.121355	-3.04269	0.046951
chr11__77374328__77392541___PAK1	0.121531	-3.0406	0.045716
chr3__37286014__37302332___GOLGA4	0.121778	-3.03767	0.034318
chr1__51836131__51855388___NRD1	0.121841	-3.03693	0.033595
chr4__2689506__2690970___FAM193A	0.121888	-3.03638	0.047684
chr7__11061791__11111467___PHF14	0.122167	-3.03308	0.045099
chr17__20204333__20306082___SPECC1	0.122324	-3.03122	0.042959
chr9__125298890__125312612___GAPVD1	0.122364	-3.03075	0.046951
chr1__113093206__113094755___LRIG2	0.122737	-3.02636	0.034318
chr1__11989165__11992690___MFN2	0.12301	-3.02315	0.047684
chr14__52455324__52470680___TXNDC16	0.123154	-3.02147	0.034318
chr1__93221609__93239896___CCDC18	0.123191	-3.02103	0.034318
chr10__45939361__45962994___LOC728407	0.123225	-3.02063	0.029768
chr9__123757703__123769563___DENND1A	0.123294	-3.01982	0.034318
chr1__1649499__1657498___CDK11B	0.1239	-3.01275	0.047188
chr11__77675036__77691238___RSF1	0.12397	-3.01194	0.047869
chr16__24775604__24777358___TNRC6A	0.124219	-3.00904	0.04948
chr3__183775915__183777700___YEATS2	0.124313	-3.00795	0.045884
chr15__41069570__41087682___INO80	0.125294	-2.99661	0.047282
chr14__55350381__55355222___NA	0.125757	-2.99128	0.047188
chr2__37139631__37141701___EIF2AK2	0.125871	-2.98999	0.045716
chr14__31121422__31156886___HECTD1	0.126271	-2.98541	0.047684
chr1__158652467__158654748___SPTA1	0.126586	-2.98181	0.047684
chr1__155771067__155777820___GON4L	0.127109	-2.97586	0.035049
chr10__72708283__72741845___MCU	0.127247	-2.9743	0.048137
chr2__201420417__201420706___TRAK2	0.127296	-2.97374	0.048037
chr11__77353536__77374365___PAK1	0.127518	-2.97122	0.036332
chr12__110013125__110029635___ANKRD13A	0.129292	-2.95129	0.035049
chr1__44002313__44002985___SLC6A9	0.131805	-2.92353	0.037672
chr5__95748333__95763620___RHOBTB3	0.132696	-2.91381	0.038361
chr1__113833111__113855049___PTPN22	0.134174	-2.89783	0.039241
chr1__185124944__185151935___TRMT1L	0.137051	-2.86722	0.042222
chr16__47633899__47635022___PHKB	0.138048	-2.85675	0.042273
chr10__50433476__50598823___SGMS1	0.138247	-2.85468	0.042273
chr2__210003438__210004118___RPE	0.138631	-2.85068	0.042186
chr17__59910562__59926582___RPS6KB1	0.138746	-2.84948	0.034318
chr5__168566013__168566266___PANK3	0.141288	-2.82329	0.044349
chr1__243293091__243344331___SDCCAG8	0.144785	-2.78802	0.040474
chr3__69027900__69028295___TMF1	0.14508	-2.78508	0.045716
chr2__99103967__99117759___TSGA10	0.146834	-2.76774	0.045716
chr8__52683549__52686967___RB1CC1	0.147287	-2.76329	0.037464
chr3__179413412__179426242___GNB4	0.147337	-2.76281	0.036702
chr17__60265412__60301704___USP32	0.147867	-2.75763	0.037464

chr19__53805280__53814988___NLRP12	0.150816	-2.72914	0.04948
chr5__168559032__168566266___PANK3	0.151235	-2.72514	0.039241
chr7__93271220__93311272___CCDC132	0.151237	-2.72511	0.036539
chr1__8614561__8656441___RERE	0.151621	-2.72146	0.04488
chr15__42264090__42268032___TMEM87A	0.153446	-2.70419	0.040688
chr15__44328685__44380976___CASC4	0.153965	-2.69933	0.045167
chr14__103405076__103405267___MARK3	0.155042	-2.68927	0.042128
chr20__35847350__35863400___PHF20	0.158799	-2.65472	0.047684
chr10__43154897__43160595___CSGALNACT2	0.160961	-2.63522	0.045716
chr19__11648358__11650417___NA	0.163341	-2.61404	0.047188
chr3__172247533__172285984___FNDC3B	0.163416	-2.61338	0.027977
chr13__113585774__113640375___TFDP1	0.167055	-2.58161	0.044825
chr20__2947982__2975241___PTPRA	0.168006	-2.57341	0.019501
chr11__16264698__16286210___SOX6	0.1728	-2.53283	0.043375
chr11__12204250__12216319___MICAL2	0.178777	-2.48376	0.047176
chr1__225406664__225415332___LBR	0.180316	-2.4714	0.036702
chr8__17195523__17221975___ZDHHC2	0.181918	-2.45864	0.032539
chr17__61776401__61784424___BRIP1	0.182976	-2.45027	0.046845
chr17__58458768__58480267___HSF5	0.185012	-2.43431	0.044618
chr1__207647317__207753921___NA	0.185054	-2.43398	0.03743
chr1__93894614__93897898___GCLM	0.186893	-2.41972	0.04488
chr11__9283371__9299629___TMEM41B	0.189788	-2.39754	0.046951
chr14__30923210__30926885___STRN3	0.195136	-2.35745	0.046951
chr7__93252653__93297243___CCDC132	0.206909	-2.27293	0.048932
chr5__50750151__50763242___PARP8	0.211359	-2.24223	0.047282
chr1__197084354__197100526___ASPM	0.218512	-2.19421	0.044707
chrX__77599411__77600564___ATRX	0.252912	-1.9833	0.045293
chr2__171337453__171339554___METTL8	0.287764	-1.79704	0.045716
chr3__56669700__56673725___FAM208A	0.299434	-1.73969	0.03336
chr16__81024715__81026638___CENPN	0.340167	-1.55569	0.048945
chr2__171540808__171541793___CYBRD1	0.357143	-1.48542	0.042959
chrX__77971621__78003236___ATP7A	0.374812	-1.41576	0.045661

Appendix L

List of up-regulated transcripts in SEDENTARY *after 4 weeks of mixed exercise training* (FDR<0.05).

Gene	FC	logFC	FDR
chr19__18537601__18538436___FKBP8	2.427067	1.279214	0.041681

Appendix M

List of up-regulated circRNA in AEROBIC *compared with* SEDENTARY *at follow-up 1* (FDR<0.05).

Gene	FC	logFC	FDR
chr10__93676653__93700106___FRA10AC1	4.807432	2.265266	0.001522
chr11__14830698__14861366___PDE3B	4.260046	2.090869	0.020652
chr16__85633914__85634132___GSE1	3.84753	1.943933	0.000387
chr1__235196031__235214026___ARID4B	3.299774	1.722367	0.042811
chr17__697418__699380___VPS53	2.935597	1.553654	0.029934
chr8__130079902__130092143___ASAP1	2.790455	1.4805	0.007651
chr15__58912563__58919972___SLTM	2.505763	1.32525	0.036593
chr9__33932562__33933628___UBAP2	2.379548	1.250688	0.006929
chr19__47264603__47264946___CCDC9	2.12266	1.085873	0.007335

List of down-regulated circRNA in AEROBIC *compared with* SEDENTARY *at follow-up 1* (FDR<0.05).

Gene	FC	logFC	FDR
chr2__88786470__88805408___ANKRD36BP2	0.013597	-6.20056	0.011691
chr8__129903312__129912515___FAM49B	0.019063	-5.71311	0.014835
chr9__137790848__137818138___EHMT1	0.026044	-5.26289	7.44E-05
chr10__103091564__103094455___NT5C2	0.026776	-5.22292	9.13E-05
chr11__16097609__16234671___SOX6	0.027438	-5.18766	0.021582
chr10__101461981__101479457___BTRC	0.027559	-5.18131	7.44E-05
chr17__50990450__50998617___SPAG9	0.028375	-5.13923	7.44E-05
chr3__52411029__52423351___PHF7	0.029711	-5.07288	0.000283
chr10__72715111__72715902___MCU	0.031151	-5.00457	0.0003
chr14__70584817__70597777___MED6	0.031265	-4.99932	0.00044
chr15__42827928__42840433___TTBK2	0.031747	-4.97724	0.000402
chr4__105446383__105456745___PPA2	0.031784	-4.97553	0.000283
chr6__42828493__42830172___GLTSCR1L	0.032444	-4.9459	0.000327
chr2__44484877__44505730___CAMKMT	0.032681	-4.93539	0.014124
chr12__32607957__32611283___FGD4	0.032881	-4.92659	0.000509
chr1__229539456__229542371___ABCB10	0.032957	-4.92326	0.000495
chr17__60271350__60288682___USP32	0.033111	-4.91656	0.000697
chr1__149964222__149965878___OTUD7B	0.034247	-4.86788	0.00044
chr5__58988493__58993465___PDE4D	0.034273	-4.86679	0.000525
chrX__124021367__124022671___STAG2	0.034485	-4.85789	0.00075
chr14__24218059__24218431___NEDD8-MDP1NEDD8	0.034521	-4.85639	0.000525
chr12__50981639__51010766___SLC11A2	0.034926	-4.83956	0.000726
chr19__21447650__21463843___NA	0.03502	-4.83569	0.000751
chr17__20053579__20057817___SPECC1	0.035746	-4.80607	0.000751
chr15__50637422__50639548___TRPM7	0.036031	-4.79462	0.000751
chr12__68715627__68727389___NUP107	0.036054	-4.79368	0.000751
chr13__25307806__25325068___NUPL1	0.03613	-4.79064	0.000751
chr17__60265412__60288682___USP32	0.036166	-4.78922	0.000859
chr1__246621429__246634587___CNST	0.036657	-4.76975	0.000789

chr1__205719527__205729621___NUCKS1	0.036675	-4.76906	0.000726
chr12__56671749__56673065___PTGES3	0.036817	-4.76349	0.000859
chr17__67910877__67944372___BPTF	0.037028	-4.75523	0.000859
chr14__55380573__55382191___ATG14	0.037706	-4.72906	0.00113
chr5__154790325__154792796___LARP1	0.038592	-4.69555	0.001018
chr3__141970073__141995141___TFDP2	0.038727	-4.69052	0.001281
chr1__229525936__229549434___ABCB10	0.039222	-4.67218	0.000881
chr6__149379411__149409824___TAB2	0.039421	-4.66488	0.001348
chr18__2732265__2762236___SMCHD1	0.0395	-4.662	0.001348
chr13__95157161__95188542___ABCC4	0.039808	-4.65081	0.001393
chr14__45008913__45032376___FAM179B	0.039845	-4.64946	0.001348
chr12__2873977__2874525___FOXM1	0.039862	-4.64886	0.001348
chr22__27894555__27914347___PITPNB	0.040149	-4.6385	0.001431
chr20__37056146__37062270___RBL1	0.040336	-4.63178	0.001431
chr8__99481599__99521010___VPS13B	0.040463	-4.62724	0.00134
chr16__14552021__14555709___PARN	0.040638	-4.62101	0.001431
chr1__231370562__231374099___EGLN1	0.041227	-4.60026	0.001455
chr11__62827155__62827631___STX5	0.041633	-4.58612	0.001348
chr15__63553715__63574403___USP3	0.041665	-4.58502	0.001522
chr4__128292934__128483487___NA	0.041701	-4.58377	0.001532
chr10__45533110__45590574___MARCH8	0.041749	-4.5821	0.001348
chr4__128957026__129003876___SCLT1	0.04175	-4.58209	0.001537
chr5__43122039__43174494___ZNF131	0.041905	-4.57672	0.001512
chr2__20254863__20256170___PUM2	0.042049	-4.57179	0.001537
chr2__24137909__24147086___FAM228B	0.042059	-4.57144	0.001522
chr14__65561337__65629606___FUT8	0.042204	-4.56646	0.001512
chr14__103405076__103405267___MARK3	0.042372	-4.56076	0.001462
chr13__59692717__59697771___DIAPH3	0.042376	-4.56062	0.001431
chr1__29053104__29097935___EPB41	0.042685	-4.55012	0.001512
chr4__139695197__139704196___MGST2	0.042721	-4.54891	0.001529
chr10__73692043__73713332___NA	0.042826	-4.54538	0.001625
chr16__68174374__68191775___NFATC3	0.042849	-4.5446	0.001625
chr2__226838073__226924163___RHBDD1	0.043066	-4.53732	0.001643
chr3__138228918__138235114___ARMC8	0.043127	-4.53527	0.001532
chr1__201852104__201858994___IPO9	0.043164	-4.53402	0.001673
chr1__13715541__13749487___PRDM2	0.043209	-4.53252	0.00165
chr6__85517756__85530275___SNX14	0.043782	-4.5135	0.00169
chr11__16318446__16341252___SOX6	0.043875	-4.51047	0.001673
chr5__40764514__40771863___PRKAA1	0.043968	-4.50739	0.001639
chr3__170136419__170136665___PHC3	0.044046	-4.50486	0.001697
chr2__201022059__201024039___FAM126B	0.044143	-4.50166	0.00188
chr15__28751488__28754897___WHAMMP2	0.044209	-4.49952	0.001512
chr16__67744288__67759732___RANBP10	0.044225	-4.49899	0.001796
chr20__35655202__35659014___CPNE1	0.04452	-4.4894	0.001877
chr18__26315229__26335231___TAF4B	0.044604	-4.48668	0.001909
chr10__118691265__118695230___CACUL1	0.044614	-4.48637	0.001889

chr5__113001084__113001674___DCP2	0.044635	-4.4857	0.001796
chr8__132610166__132625454___LRRC6	0.044684	-4.48409	0.001971
chr13__28197185__28220378___PAN3	0.044989	-4.47428	0.001958
chr8__130214556__130236994___ASAP1	0.045011	-4.47358	0.001944
chr3__142669390__142671122___PLS1	0.045377	-4.46191	0.001944
chr17__61972727__61983114___MED13	0.045389	-4.46152	0.002005
chrX__132278008__132283032___RAP2C-AS1	0.045823	-4.44777	0.00205
chr13__113585774__113640375___TFDP1	0.046067	-4.44012	0.002036
chr22__32479133__32493281___FBXO7	0.046206	-4.43578	0.00205
chr12__112219386__112228811___HECTD4	0.04632	-4.43222	0.001987
chr1__213071006__213117410___RPS6KC1	0.046489	-4.42698	0.002203
chr20__44503815__44514040___SERINC3	0.046554	-4.42496	0.002166
chr4__42551198__42556040___ATP8A1	0.046659	-4.4217	0.002133
chr14__34593045__34609742___SNX6	0.046684	-4.42094	0.002228
chr10__86443275__86446449___WAPAL	0.046692	-4.42069	0.001889
chr22__29813430__29825780___ASCC2	0.046756	-4.4187	0.001986
chr11__68784815__68796933___CPT1A	0.046891	-4.41455	0.001944
chr15__101701086__101714963___TARSL2	0.047015	-4.41074	0.002203
chr17__60198260__60214774___USP32	0.047062	-4.4093	0.002203
chr16__75391380__75395209___CFDP1	0.047069	-4.40908	0.002133
chr5__151473673__151479489___SLC36A1	0.047172	-4.40592	0.002203
chr12__49097566__49098105___LMBR1L	0.047193	-4.40527	0.002228
chr20__17956933__17961326___SNX5	0.047381	-4.39955	0.002133
chr16__67036639__67082308___CBFB	0.047383	-4.39949	0.002203
chr1__235219793__235240451___ARID4B	0.047839	-4.38566	0.002486
chr13__19730239__19759418___PSPC1	0.048476	-4.36658	0.002463
chr8__21974670__21985691___XPO7	0.048694	-4.36013	0.002203
chr2__113934279__113942359___ACTR3	0.04881	-4.35668	0.002426
chr4__53383773__53428183___FIP1L1	0.048819	-4.35642	0.002142
chr1__20747544__20773610___HP1BP3	0.048937	-4.35294	0.002628
chr1__113848540__113855049___PTPN22	0.049008	-4.35085	0.002461
chr5__168568646__168568998___PANK3	0.049009	-4.3508	0.002517
chrX__14843660__14869043___FANCB	0.049071	-4.349	0.002628
chr4__42001616__42078325___SLC30A9	0.049142	-4.34691	0.002461
chr17__39423327__39432016___MED1	0.04925	-4.34375	0.002628
chr3__52678500__52682233___PBRM1	0.049441	-4.33815	0.002533
chr6__99558497__99561681___CCNC	0.049573	-4.33431	0.002658
chr20__5565017__5570239___GPCPD1	0.049656	-4.3319	0.002658
chr10__96852645__96858416___LCOR	0.04967	-4.33149	0.002628
chr20__35863013__35871829___PHF20	0.04976	-4.32887	0.00259
chr15__44626331__44629388___SPG11	0.049825	-4.32697	0.002667
chr2__119962616__119967972___PTPN4	0.050057	-4.3203	0.002658
chr14__21371874__21373430___SUPT16H	0.05029	-4.31358	0.002743
chr1__179990507__180006567___CEP350	0.05042	-4.30987	0.002658
chr1__100906852__100921841___SLC30A7	0.050432	-4.30952	0.002743
chr17__76738282__76776541___MFSD11	0.05044	-4.30927	0.002815

chr2__26123518__26124047___RAB10	0.050632	-4.30382	0.002847
chr1__207647317__207753921___NA	0.05069	-4.30216	0.002461
chr15__63734724__63756748___HERC1	0.050883	-4.29666	0.002658
chr1__95143891__95230994___TMEM56-RWDD3	0.050903	-4.29609	0.002658
chr11__35196746__35204640___CD44	0.05107	-4.29137	0.002743
chr18__9182382__9216900___ANKRD12	0.051073	-4.2913	0.002968
chr15__87355549__87422836___NA	0.051079	-4.29112	0.005216
chr5__109817273__109830980___MAN2A1	0.051285	-4.28532	0.003003
chr21__33765875__33767828___ITSN1	0.051443	-4.28089	0.00293
chr12__20616230__20635056___PDE3A	0.051445	-4.28084	0.003003
chr15__63712775__63734849___HERC1	0.051461	-4.28037	0.00293
chr2__32377588__32406557___BIRC6	0.051596	-4.27659	0.003056
chr1__185174372__185182057___SWT1	0.051653	-4.275	0.002815
chr17__58694931__58709990___RAD51C	0.051657	-4.27489	0.00293
chr7__129873855__129880971___UBE2H	0.051763	-4.27193	0.002795
chr3__119947268__120093593___GSK3B	0.051824	-4.27025	0.002658
chr14__54984723__55002185___WDHD1	0.051969	-4.2662	0.003031
chr15__68086306__68146700___PIAS1	0.051969	-4.26621	0.002968
chr11__16183886__16318653___SOX6	0.051976	-4.26602	0.00293
chr2__158620990__158621421___PKP4	0.052034	-4.2644	0.00293
chr1__44002313__44002985___SLC6A9	0.052049	-4.26398	0.002968
chr9__36597222__36607673___MELK	0.052206	-4.25964	0.003031
chr12__116237468__116237705___MED13L	0.052276	-4.25771	0.003056
chr6__131160059__131199573___AKAP7	0.052285	-4.25746	0.003003
chr1__50738863__50752523___FAF1	0.052341	-4.25591	0.003031
chr7__116110708__116112038___NA	0.052341	-4.25592	0.003103
chr11__85981129__85981988___PICALM	0.052473	-4.25228	0.003031
chr2__32377588__32380290___BIRC6	0.052491	-4.2518	0.003031
chr8__99442401__99521010___VPS13B	0.052572	-4.24955	0.003056
chr16__47451396__47459175___ITFG1	0.052609	-4.24855	0.003056
chr15__92900789__92929091___CHD2	0.052636	-4.2478	0.002896
chr1__19172864__19175033___UBR4	0.052642	-4.24763	0.003024
chr22__31602212__31602785___SFI1	0.052795	-4.24346	0.003056
chr4__139116649__139168042___ELF2	0.052842	-4.24216	0.003031
chr14__91797785__91813825___TC2N	0.052858	-4.24174	0.003245
chr9__135850137__135866536___CAMSAP1	0.053091	-4.23538	0.003283
chr13__72728926__72731387___BORA	0.053112	-4.23483	0.003003
chrX__65821624__65822042___NA	0.053244	-4.23123	0.003283
chr14__72981789__72993357___ZFYVE1	0.053247	-4.23117	0.003195
chr3__49962576__49975392___RBM6	0.053271	-4.2305	0.003204
chr1__93903765__93904588___GCLM	0.053357	-4.22818	0.003195
chr4__76130656__76136412___NUP54	0.053555	-4.22284	0.003283
chr3__20136942__20140364___KAT2B	0.05365	-4.22027	0.003245
chr17__78004170__78009697___TNRC6C	0.053677	-4.21955	0.003344
chr15__90439332__90443478___IQGAP1	0.053897	-4.21365	0.00354
chr5__65528452__65552549___CENPK	0.05395	-4.21224	0.003332

chr6__135192324__135200415___MYB	0.054018	-4.21042	0.003283
chr12__123160781__123203375___MPHOSPH9	0.054191	-4.2058	0.003332
chr12__813642__813814___WNK1	0.054198	-4.20561	0.003421
chr2__152719898__152735126___ARL6IP6	0.054267	-4.20378	0.003283
chr4__7006632__7014557___TBC1D14	0.054533	-4.19673	0.003332
chr5__108348399__108367953___FBXL17	0.05462	-4.19442	0.003508
chr14__60267215__60277091___PPM1A	0.054784	-4.1901	0.003564
chr2__218546919__218560883___USP37	0.054816	-4.18926	0.003229
chr2__171448681__171473975___DCAF17	0.054822	-4.18909	0.003619
chr6__18159883__18166378___KDM1B	0.054889	-4.18735	0.003276
chr1__155725382__155726019___DAP3	0.055062	-4.18279	0.00334
chr17__5350451__5363016___RABEP1	0.055104	-4.1817	0.003619
chr18__9522160__9522509___RALBP1	0.05514	-4.18077	0.003606
chrX__107088436__107088839___RBM41	0.055328	-4.17585	0.003772
chr2__74156418__74172752___MOB1A	0.055461	-4.17238	0.003772
chr14__30923210__30926885___STRN3	0.055515	-4.17099	0.003564
chr11__74118228__74133557___C2CD3	0.055524	-4.17075	0.00374
chr1__235780865__235782087___LYST	0.055545	-4.17021	0.0036
chr15__49625113__49634794___DTWD1	0.055671	-4.16692	0.003623
chr12__123313620__123323831___SBNO1	0.055697	-4.16626	0.003713
chr6__111654024__111655556___NA	0.055747	-4.16497	0.003772
chr1__25300946__25301686___RHD	0.056025	-4.1578	0.003245
chr14__88574693__88609803___ZC3H14	0.056129	-4.15511	0.003782
chr13__77243059__77243951___MYCBP2	0.056143	-4.15475	0.003832
chr22__31258291__31260077___LIMK2	0.056351	-4.14941	0.003875
chr8__17205655__17210480___ZDHHC2	0.056362	-4.14912	0.003864
chr2__86740927__86773435___RMND5A	0.056383	-4.14858	0.003734
chr7__77571078__77600806___PTPN12	0.05649	-4.14587	0.003864
chr2__55206270__55218600___CLHC1	0.056619	-4.14256	0.003995
chr4__139067684__139073567___ELF2	0.05663	-4.14229	0.00386
chr10__13127745__13133581___OPTN	0.056636	-4.14214	0.003875
chr7__8059053__8060248___GLCCI1	0.056674	-4.14117	0.003875
chr1__26462669__26463433___DHDDS	0.056751	-4.13922	0.00386
chr8__130159864__130187285___ASAP1	0.056806	-4.1378	0.00386
chr21__15799757__15833548___USP25	0.056924	-4.13481	0.003875
chr2__197418896__197420227___SF3B1	0.056999	-4.13291	0.003864
chr22__40273425__40280143___TNRC6B	0.057076	-4.13098	0.003782
chr15__62589687__62657898___TLN2	0.057097	-4.13045	0.00386
chr8__140830472__140864399___PTK2	0.057183	-4.12826	0.003877
chr1__117378660__117420649___MAN1A2	0.057289	-4.1256	0.003772
chrX__119930016__119932216___NKAP	0.057291	-4.12555	0.003875
chr16__47428804__47459175___ITFG1	0.057337	-4.12439	0.004037
chr5__79613011__79645192___PAPD4	0.057363	-4.12373	0.003772
chr11__28211062__28233585___METTL15	0.057435	-4.12193	0.003916
chr3__123271522__123272563___SEC22A	0.057522	-4.11973	0.003995
chr8__38943789__38946221___PLEKHA2	0.05756	-4.11879	0.00386

chr2__8877030__8958642___MBOAT2	0.057591	-4.118	0.004037
chr4__98574457__98578081___TSPAN5	0.057715	-4.11491	0.003875
chr1__93210802__93239896___CCDC18	0.05779	-4.11304	0.004037
chr20__35858302__35869551___PHF20	0.057824	-4.11219	0.004233
chr4__139393591__139404490___NA	0.057899	-4.11032	0.003864
chr18__70121556__70128546___RTTN	0.057908	-4.11008	0.003995
chr1__95116608__95151419___NA	0.057969	-4.10858	0.004161
chr21__36338779__36345031___MORC3	0.05803	-4.10706	0.004176
chr15__63696124__63749791___HERC1	0.058051	-4.10654	0.004084
chr8__47969798__47975848___MCM4	0.058067	-4.10614	0.003804
chr15__64112573__64118854___SNX1	0.058236	-4.10195	0.004029
chr5__151452343__151479489___SLC36A1	0.058298	-4.10042	0.004305
chr2__233263130__233270067___ATG16L1	0.058327	-4.09969	0.004094
chr4__48534545__48542121___FRYL	0.058499	-4.09544	0.003875
chr1__117622842__117624099___FAM46C	0.058533	-4.09461	0.003864
chr22__16637040__16638740___TPTEP1	0.058541	-4.0944	0.003916
chr22__40953555__40967884___RBX1	0.058589	-4.09324	0.003875
chr6__145888020__145894977___SHPRH	0.058753	-4.0892	0.004397
chr4__169580842__169599197___NEK1	0.059119	-4.08023	0.00454
chr7__131375424__131429145___MKLN1	0.05921	-4.07802	0.004208
chr13__30227412__30241086___KATNAL1	0.059259	-4.07682	0.004582
chr1__223798215__223800047___TP53BP2	0.059279	-4.07633	0.004378
chr14__96846095__96876120___VRK1	0.059351	-4.07459	0.004476
chr13__49976333__50045232___NA	0.05936	-4.07436	0.004084
chr6__82957312__83044659___UBE3D	0.059412	-4.07309	0.004476
chr5__132579317__132589837___RAD50	0.059577	-4.06911	0.00454
chr17__61776401__61784424___BRIP1	0.059695	-4.06625	0.004568
chr5__179705679__179716294___CANX	0.059743	-4.0651	0.004208
chr20__25632158__25634170___NA	0.060037	-4.05799	0.004566
chr9__33504538__33509336___SUGT1P1	0.060096	-4.05659	0.004358
chr20__34477772__34479789___ITCH	0.060185	-4.05446	0.003875
chr2__101288973__101295181___RNF149	0.060307	-4.05154	0.004358
chr12__122601536__122624688___KNTC1	0.060352	-4.05045	0.004523
chr6__16274415__16290621___GMPR	0.060452	-4.04807	0.004397
chr11__120353093__120353753___ARHGEF12	0.060608	-4.04436	0.004566
chr14__45148837__45159280___FANCM	0.060985	-4.0354	0.004863
chr17__45081644__45086652___NMT1	0.060995	-4.03516	0.004447
chr4__150798081__150831976___LRBA	0.061021	-4.03455	0.004523
chr15__65667449__65697383___DENND4A	0.061118	-4.03227	0.004808
chr9__85596362__85646418___AGTPBP1	0.061141	-4.03171	0.004877
chr10__117243971__117253457___SLC18A2	0.061157	-4.03133	0.004877
chr22__21788257__21807846___MAPK1	0.061218	-4.0299	0.00484
chr20__36607715__36609730___TGIF2-C20orf24C20orf24	0.061394	-4.02576	0.004877
chr11__16097609__16111926___SOX6	0.061406	-4.02547	0.004976
chr9__137728349__137744090___EHMT1	0.061438	-4.02473	0.005019

chr1__35747907__35753936___CLSPN	0.061619	-4.02049	0.004738
chr1__51402435__51448135___EPS15	0.061639	-4.02	0.005019
chr5__50399232__50411383___EMB	0.061694	-4.01872	0.005019
chr2__186081330__186086370___NA	0.061725	-4.01801	0.005055
chr19__52618936__52635153___ZNF83	0.061844	-4.01523	0.005
chr10__49908455__49935142___PARG	0.061856	-4.01494	0.005453
chr14__31113104__31133675___HECTD1	0.061892	-4.01411	0.005019
chr20__50902017__50904001___ADNP	0.061897	-4.01398	0.004877
chr17__62011178__62063222___MED13	0.061913	-4.01362	0.005024
chr8__67118248__67137603___CSPP1	0.062096	-4.00936	0.00511
chr1__77206640__77212347___PIGK	0.062238	-4.00607	0.004999
chr6__136276028__136276508___BCLAF1	0.062456	-4.00102	0.00515
chr10__119526032__119527424___RGS10	0.062497	-4.00006	0.005019
chr18__47868323__47870564___SMAD2	0.062504	-3.99991	0.005216
chr2__20307978__20333063___PUM2	0.062515	-3.99964	0.0051
chr10__27158549__27165539___MASTL	0.062522	-3.9995	0.00515
chr15__42558198__42563857___HAUS2	0.062656	-3.9964	0.005019
chr10__73156275__73156655___ECD	0.062665	-3.99619	0.004358
chr4__103163137__103181456___CENPE	0.062668	-3.99612	0.005019
chr1__207526753__207708263___NA	0.062758	-3.99407	0.005019
chr4__145162640__145171720___OTUD4	0.062806	-3.99296	0.00386
chr15__63674342__63675093___HERC1	0.062829	-3.99242	0.005019
chr7__50319048__50391863___IKZF1	0.062837	-3.99224	0.005275
chr3__141974048__141995141___TFDP2	0.063058	-3.98717	0.00511
chr17__40408492__40416512___TOP2A	0.063078	-3.98672	0.00511
chr15__56700933__56701238___ZNF280D	0.06308	-3.98668	0.00511
chr3__44814911__44828300___KIF15	0.063248	-3.98284	0.005171
chr14__101882161__101912473___PPP2R5C	0.063315	-3.98131	0.00515
chr1__100123210__100125942___SASS6	0.063344	-3.98064	0.005362
chr7__48410520__48412583___ABCA13	0.06342	-3.97892	0.00515
chr11__76513386__76516312___C11orf30	0.063478	-3.97759	0.005171
chr16__29833733__29834066___MVP	0.063613	-3.97454	0.005362
chr18__36142281__36160015___ELP2	0.063634	-3.97407	0.005019
chr3__20099862__20152579___KAT2B	0.06364	-3.97393	0.005019
chrX__118394055__118407026___WDR44	0.063691	-3.97277	0.005216
chr9__125301983__125302826___GAPVD1	0.063775	-3.97086	0.005019
chr13__40749138__40759106___MRPS31	0.06393	-3.96736	0.005408
chr1__207563864__207708263___NA	0.06401	-3.96556	0.005019
chr16__70219912__70222480___LOC100506060	0.064013	-3.9655	0.005445
chr9__128750616__128755659___ZER1	0.064134	-3.96277	0.005278
chr13__24294739__24297735___SPATA13	0.064168	-3.962	0.004863
chr18__46118181__46128837___NA	0.064187	-3.96157	0.000156
chr15__68086306__68164804___PIAS1	0.0642	-3.96129	0.005439
chr20__46393093__46394503___ELMO2	0.064228	-3.96066	0.005408
chr20__62281790__62291793___OSBPL2	0.06423	-3.96062	0.00515
chr14__73147795__73198129___PSEN1	0.064302	-3.95899	0.005445

chr1__171523221__171537473___PRRC2C	0.064303	-3.95896	0.005275
chr11__128758115__128782023___FLI1	0.064381	-3.95721	0.005488
chr14__103448919__103480490___MARK3	0.064417	-3.95641	0.005408
chr17__29482197__29498521___TAOK1	0.064453	-3.95562	0.005657
chr2__218529956__218562813___USP37	0.064462	-3.9554	0.005275
chr1__20757166__20776750___HP1BP3	0.06448	-3.95501	0.00538
chr5__115275216__115284908___CCDC112	0.064485	-3.95489	0.005439
chr6__136558800__136567874___MAP3K5	0.064537	-3.95374	0.005216
chr2__61178981__61187029___AHSA2	0.064567	-3.95307	0.005019
chr9__122989297__122990213___RABGAP1	0.064578	-3.95282	0.00511
chr4__4457191__4471706___STX18	0.064598	-3.95238	0.005588
chr19__47089967__47094608___ZC3H4	0.064684	-3.95044	0.005445
chr11__77722688__77725699___RSF1	0.064712	-3.94982	0.005537
chr1__46565041__46572167___MKNK1	0.065036	-3.94262	0.005445
chr10__96907265__96907747___LCOR	0.065047	-3.94237	0.005457
chr2__174378923__174387779___CIR1	0.065065	-3.94198	0.00515
chr4__39910244__39925933___PDS5A	0.065133	-3.94047	0.005439
chr6__99526064__99531790___TSTD3	0.065426	-3.93398	0.005657
chr13__32436361__32480637___N4BP2L2	0.065454	-3.93338	0.005369
chr6__20781145__20955585___CDKAL1	0.065489	-3.93261	0.005657
chr7__131375424__131411383___MKLN1	0.065548	-3.9313	0.00553
chr18__77095368__77097474___MBP	0.065565	-3.93093	0.005488
chr2__210104104__210154611___KANSL1L	0.065619	-3.92975	0.005657
chr22__29978442__29998857___MTMR3	0.065646	-3.92915	0.005439
chr9__89455888__89479825___SEMA4D	0.065692	-3.92814	0.00576
chr5__134535858__134552209___JADE2	0.065809	-3.92557	0.005445
chr20__47294666__47298947___ZMYND8	0.065928	-3.92297	0.005
chr9__120518427__120539164___CDK5RAP2	0.066	-3.92139	0.005657
chr11__34086064__34090678___CAPRIN1	0.066006	-3.92127	0.005744
chr12__46239679__46254936___SLC38A1	0.066039	-3.92053	0.005657
chr15__42827928__42878684___TTBK2	0.06616	-3.91789	0.005445
chr2__23819747__23834078___ATAD2B	0.066162	-3.91786	0.005171
chr13__20596150__20597119___IFT88	0.066241	-3.91613	0.00575
chr6__154808070__154824378___SCAF8	0.066254	-3.91585	0.005657
chr3__100294845__100296275___TBC1D23	0.066256	-3.91581	0.005396
chr10__32471064__32481782___CCDC7	0.066273	-3.91544	0.005019
chr14__71413948__71414680___LOC102724024	0.066421	-3.91222	0.005807
chr7__77581427__77583650___PTPN12	0.066424	-3.91215	0.005871
chr14__102707351__102711013___RCOR1	0.06645	-3.91158	0.005537
chr6__53505392__53509250___GCLC	0.066456	-3.91146	0.005657
chr9__17309058__17366717___CNTLN	0.066497	-3.91056	0.00585
chr17__67166478__67195470___HELZ	0.06651	-3.91027	0.00538
chr3__155914419__155925366___GMPS	0.066523	-3.90999	0.005275
chr9__112268049__112276013___PTBP3	0.0666	-3.90833	0.005657
chr8__94506500__94512089___KIAA1429	0.06661	-3.90812	0.005852
chr15__49916934__49934182___ATP8B4	0.066629	-3.90772	0.005861

chr2__88776501__88779319___ANKRD36BP2	0.066665	-3.90693	0.005852
chr15__34890215__34904505___AQR	0.066682	-3.90657	0.00575
chr10__21668917__21670704___MLLT10	0.066711	-3.90593	0.005573
chr4__78842385__78865720___BMP2K	0.066724	-3.90565	0.005657
chr2__148178700__148342336___MBD5	0.066894	-3.90198	0.005445
chr2__181458268__181485992___ITGA4	0.066894	-3.90198	0.00576
chr2__30476577__30479911___LCLAT1	0.066909	-3.90165	0.005871
chr10__68459104__68465812___DNA2	0.066924	-3.90133	0.005871
chr22__21769195__21805945___MAPK1	0.066934	-3.90112	0.005657
chr17__40396283__40399131___TOP2A	0.066984	-3.90003	0.005941
chrX__110020352__110023040___TMEM164	0.067066	-3.89827	0.00576
chr8__18799295__18804898___PSD3	0.067125	-3.897	0.005488
chr8__116856166__116863259___RAD21	0.067148	-3.89651	0.005657
chr15__42950262__42966286___UBR1	0.067201	-3.89538	0.00576
chr7__142942434__142943883___KEL	0.067282	-3.89364	0.005657
chr12__82369387__82434724___METTL25	0.067341	-3.89237	0.005657
chrX__20193487__20195145___RPS6KA3	0.067348	-3.89223	0.005871
chr1__45602255__45606591___NASP	0.067401	-3.8911	0.00576
chr11__16183886__16270068___SOX6	0.067496	-3.88906	0.00576
chr9__120831331__120833456___PSMD5	0.067564	-3.8876	0.005971
chr3__56663541__56673725___FAM208A	0.067579	-3.88727	0.005692
chr12__56741435__56744123___PRIM1	0.067618	-3.88644	0.005672
chr14__30935163__30936624___STRN3	0.067648	-3.8858	0.005537
chr5__36953618__36986301___NIPBL	0.067692	-3.88487	0.005871
chr17__30484214__30492766___GOSR1	0.067702	-3.88465	0.005484
chr11__124954724__125005212___CCDC15	0.067749	-3.88367	0.005588
chr8__70123884__70124865___NCOA2	0.067766	-3.88328	0.006004
chr3__20111596__20127549___KAT2B	0.067781	-3.88297	0.005657
chr12__3821873__3863957___PARP11	0.067792	-3.88273	0.00564
chr8__55950459__55953984___LYN	0.067806	-3.88244	0.005871
chr6__42810306__42830172___GLTSCR1L	0.067811	-3.88233	0.00575
chr2__61492035__61495613___XPO1	0.06787	-3.88109	0.00576
chr9__105484381__105539351___FSD1L	0.067891	-3.88064	0.005987
chr1__229450525__229465519___NUP133	0.067923	-3.87996	0.005657
chr10__49493117__49506012___ERCC6	0.068027	-3.87775	0.005871
chr15__89268399__89293063___FANCI	0.068029	-3.87772	0.00576
chr3__183650296__183651276___KLHL24	0.068058	-3.8771	0.006152
chr20__34727259__34736758___NCOA6	0.068139	-3.87539	0.005941
chr1__20767584__20780540___HP1BP3	0.068273	-3.87253	0.005019
chr1__172092824__172131288___DNM3	0.068389	-3.8701	0.006133
chr17__60265412__60301704___USP32	0.068473	-3.86832	0.005987
chr5__5441112__5444326___KIAA0947	0.06854	-3.86692	0.005484
chr1__155661307__155777820___NA	0.06862	-3.86522	0.00576
chr14__30935163__31023080___STRN3	0.068653	-3.86453	0.005439
chr17__37437738__37444768___TADA2A	0.068666	-3.86426	0.00582
chr2__69358329__69363670___GFPT1	0.068699	-3.86356	0.005871

chr10__27526828__27533994___RAB18	0.06871	-3.86335	0.006242
chr9__37768076__37770739___TRMT10B	0.068764	-3.8622	0.006253
chr18__50918110__50932360___ME2	0.068772	-3.86203	0.006253
chr1__28987448__29011907___EPB41	0.068817	-3.86108	0.006253
chr6__98875415__98934879___FBXL4	0.068829	-3.86083	0.006179
chr20__44479985__44480444___TTPAL	0.068893	-3.85949	0.006152
chr6__63646527__63680161___PHF3	0.068968	-3.85793	0.005987
chr17__43095846__43104956___BRCA1	0.068979	-3.8577	0.006253
chr1__47368469__47373107___CMPK1	0.069031	-3.8566	0.005942
chr12__22055149__22065287___CMAS	0.069065	-3.85589	0.005941
chr17__16137311__16153395___NCOR1	0.069103	-3.85511	0.005871
chr6__110887505__110893662___AMD1	0.069106	-3.85504	0.006152
chr10__1084403__1096246___WDR37	0.069159	-3.85393	0.006179
chr13__32346827__32355288___BRCA2	0.069165	-3.85382	0.0057
chr17__62011002__62063222___MED13	0.069191	-3.85328	0.00622
chr20__41092472__41112925___TOP1	0.069319	-3.85061	0.005275
chr3__17622648__17733460___TBC1D5	0.06938	-3.84933	0.00575
chr11__108329021__108332037___ATM	0.069405	-3.84881	0.006331
chr1__161778244__161802272___ATF6	0.069419	-3.84852	0.006209
chr6__90206569__90271941___BACH2	0.069438	-3.84813	0.006717
chr3__141970073__141972900___TFDP2	0.069452	-3.84784	0.00575
chr6__89846562__89855544___CASP8AP2	0.069511	-3.84661	0.006253
chr21__37087247__37108446___TTC3	0.069566	-3.84548	0.006152
chr12__40302789__40304134___LRRK2	0.0696	-3.84477	0.006152
chr13__21381434__21401685___ZDHHC20	0.069618	-3.8444	0.006253
chr1__51394381__51421858___EPS15	0.06962	-3.84434	0.006253
chr16__68053564__68054617___DUS2	0.069644	-3.84386	0.006377
chr5__77034418__77036720___AGGF1	0.069664	-3.84344	0.006242
chr2__71332830__71348525___ZNF638	0.069837	-3.83986	0.006253
chr10__73154256__73156655___ECD	0.069869	-3.83921	0.006238
chr4__51860543__51891851___DCUN1D4	0.069949	-3.83755	0.006018
chr9__132400035__132402828___TTF1	0.070043	-3.83561	0.00538
chr18__54877567__54884436___RAB27B	0.070127	-3.83388	0.00594
chr7__77581427__77592256___PTPN12	0.07031	-3.83012	0.006335
chr12__68727351__68735344___NUP107	0.07044	-3.82747	0.00594
chr20__44503815__44512994___SERINC3	0.070447	-3.82731	0.006253
chr11__111836165__111857737___ALG9	0.070462	-3.82701	0.006331
chr1__200569911__200593769___KIF14	0.070473	-3.82678	0.006336
chr11__65435053__65437657___NA	0.070495	-3.82634	0.000606
chr18__50918110__50924212___ME2	0.070504	-3.82614	0.006633
chr3__197081051__197085756___DLG1	0.070512	-3.82599	0.006533
chr13__72835243__72854155___PIBF1	0.070562	-3.82497	0.006616
chr15__68211263__68218650___CLN6	0.070606	-3.82408	0.005961
chr15__56142778__56243287___RFX7	0.070637	-3.82343	0.006253
chr15__63223042__63249705___RAB8B	0.070796	-3.82019	0.006633
chr17__47142229__47143982___CDC27	0.070797	-3.82016	0.006556

chr1__236803428__236863554___MTR	0.070825	-3.81959	0.006723
chr10__74838683__74843478___KAT6B	0.070885	-3.81837	0.006253
chr15__98707562__98708107___IGF1R	0.070922	-3.81762	0.006598
chr19__10173090__10182077___DNMT1	0.070928	-3.81751	0.00582
chr5__112204375__112209982___EPB41L4A	0.070929	-3.81747	0.006633
chr3__196058284__196072152___TFRC	0.070993	-3.81617	0.006377
chr2__96359045__96367373___NCAPH	0.071048	-3.81505	0.006152
chr4__128992167__129082373___SCLT1	0.071077	-3.81448	0.006796
chr15__44569398__44570658___SPG11	0.071081	-3.8144	0.006253
chr2__29121374__29181697___CLIP4	0.071258	-3.8108	0.006633
chr10__68431862__68470163___DNA2	0.071341	-3.80913	0.005987
chr12__121416159__121417911___RNF34	0.071425	-3.80743	0.006717
chr18__69873144__69947532___CD226	0.071606	-3.80377	0.006723
chr5__177191884__177204292___NSD1	0.071656	-3.80277	0.006717
chr14__73355626__73366981___NUMB	0.071657	-3.80276	0.00683
chr15__82823100__82826846___WHAMM	0.071684	-3.80221	0.006723
chr9__97994631__98018489___NA	0.07169	-3.80208	0.006621
chr18__13408993__13438384___LDLRAD4	0.07176	-3.80069	0.00638
chr17__43063333__43067695___BRCA1	0.071769	-3.8005	0.006729
chr15__40170062__40170681___BUB1B	0.071899	-3.79788	0.006633
chr9__133042087__133043926___GTF3C5	0.071977	-3.79632	0.006235
chr6__149521060__149541586___PPIL4	0.072008	-3.79569	0.00576
chr6__3283852__3298218___SLC22A23	0.072082	-3.79423	0.005987
chr20__5176648__5178956___CDS2	0.072101	-3.79385	0.006311
chr9__5787061__5831028___ERMP1	0.072234	-3.79117	0.006533
chr16__58528475__58534395___CNOT1	0.072266	-3.79053	0.006796
chr17__40406384__40413625___TOP2A	0.072268	-3.79051	0.006786
chr18__47865059__47930446___SMAD2	0.072302	-3.78983	0.006633
chr2__128113084__128129179___UGGT1	0.072327	-3.78932	0.006717
chr12__117038983__117046838___TESC	0.072372	-3.78843	0.005871
chr10__67954595__68014186___HERC4	0.072377	-3.78833	0.006932
chr16__17355099__17358050___XYLT1	0.072396	-3.78795	0.007141
chr7__73225711__73226051___NCF1B	0.072455	-3.78678	0.005472
chr9__83669185__83686155___UBQLN1	0.072524	-3.78539	0.006748
chr2__203289765__203292326___CYP20A1	0.072649	-3.78291	0.005852
chr2__169905114__169914146___UBR3	0.072656	-3.78278	0.006929
chr5__126804776__126832801___LMNB1	0.072702	-3.78187	0.006723
chr17__75651186__75666620___RECQL5	0.072718	-3.78154	0.006473
chr12__89655679__89656107___ATP2B1	0.072759	-3.78074	0.006723
chr14__39151746__39158402___TRAPPC6B	0.072767	-3.78057	0.00585
chr4__42503450__42543986___ATP8A1	0.07277	-3.78051	0.006533
chr14__92082300__92088817___ATXN3	0.072794	-3.78003	0.006723
chr3__20095364__20152579___KAT2B	0.072801	-3.7799	0.005871
chr1__1755374__1756343___NADK	0.072882	-3.77829	0.006253
chr2__70160625__70181997___C2orf42	0.072908	-3.77777	0.006942
chr3__195320701__195345317___ACAP2	0.072918	-3.77757	0.006773

chr1__92320599__92345914___RPAP2	0.072953	-3.77689	0.006723
chr6__87215903__87233527___ZNF292	0.073092	-3.77415	0.006996
chr10__32021022__32021287___KIF5B	0.073141	-3.77317	0.007019
chr1__28613247__28622165___TAF12	0.073145	-3.77309	0.006723
chr1__46688353__46688544___EFCAB14	0.073148	-3.77303	0.005588
chr2__8243565__8287558___LINC00299	0.073171	-3.77258	0.006796
chr20__23389946__23403072___NAPB	0.073176	-3.77248	0.005871
chr5__95736889__95755761___RHOBTB3	0.073331	-3.76943	0.006929
chr1__158667858__158686537___SPTA1	0.073342	-3.76922	0.006312
chr20__35863013__35869551___PHF20	0.073459	-3.76692	0.00515
chr17__16137311__16165161___NCOR1	0.073544	-3.76525	0.006238
chr2__202206737__202220106___SUMO1	0.073576	-3.76462	0.006335
chr17__31940286__31976614___SUZ12	0.073663	-3.76291	0.006796
chr2__58058352__58060201___VRK2	0.073679	-3.76261	0.006941
chr10__119038238__119042772___EIF3A	0.073689	-3.7624	0.007008
chr14__52730459__52771183___STYX	0.073839	-3.75948	0.006747
chr17__35063576__35066466___RFFLRAD51L3-RFFL	0.073853	-3.7592	0.007183
chr2__202952559__202955758___CARF	0.073862	-3.75903	0.006773
chr10__68786136__68791341___CCAR1	0.073925	-3.7578	0.006796
chr1__234418084__234427766___TARBP1	0.074018	-3.75599	0.006796
chr2__43397971__43430302___THADA	0.074031	-3.75572	0.007141
chr20__47228605__47229806___ZMYND8	0.074068	-3.75501	0.005987
chr1__160836195__160839049___CD244	0.074143	-3.75354	0.007487
chr19__2185855__2194577___DOT1L	0.074143	-3.75355	0.00722
chr6__158605267__158608750___TMEM181	0.074211	-3.75223	0.006796
chr6__53498607__53532766___GCLC	0.074218	-3.75208	0.006485
chr10__131943968__131945459___PPP2R2D	0.074235	-3.75175	0.006796
chr11__34063052__34063363___CAPRIN1	0.074315	-3.75019	0.006556
chr17__64341634__64352463___PECAM1	0.074316	-3.75018	0.007183
chr14__54981540__55002185___WDHD1	0.074406	-3.74843	0.007141
chr11__96209454__96210334___MAML2	0.074409	-3.74838	0.005893
chr17__35820024__35820437___TAF15	0.074442	-3.74773	0.006235
chr9__137728349__137762820___EHMT1	0.07446	-3.74739	0.007153
chr17__21004202__21004990___USP22	0.074532	-3.74599	0.006729
chr2__24270671__24271941___ITSN2	0.074678	-3.74317	0.007499
chr10__31355144__31461237___ZEB1	0.074701	-3.74272	0.007176
chr5__69306817__69314043___CCDC125	0.074716	-3.74243	0.007337
chr7__131338841__131341388___MKLN1	0.074728	-3.74221	0.007183
chr4__88061906__88068061___PKD2	0.074732	-3.74212	0.007324
chr3__37053855__37055165___LRRFIP2	0.074735	-3.74207	0.007282
chr12__124419957__124449867___NCOR2	0.074812	-3.74059	0.007326
chr13__24484653__24503777___PARP4	0.074823	-3.74038	0.007176
chr4__103140814__103141104___CENPE	0.074861	-3.73964	0.007176
chr12__56168060__56170208___SMARCC2	0.074864	-3.73959	0.006723
chrX__139814878__139826823___ATP11C	0.074907	-3.73876	0.007052
chr7__74239938__74246763___RFC2	0.074953	-3.73787	0.006331

chr2__32478635__32493667___BIRC6	0.075022	-3.73654	0.007176
chr12__112269704__112279386___HECTD4	0.075041	-3.73617	0.006941
chr15__67344063__67359885___IQCH	0.075057	-3.73587	0.007269
chr8__96834973__96880005___CPQ	0.07507	-3.73562	0.006796
chr15__69421647__69423329___KIF23	0.075111	-3.73482	0.007272
chr9__20923660__20933103___FOCAD	0.075129	-3.7345	0.007176
chr1__29035826__29072791___EPB41	0.075172	-3.73367	0.007337
chr14__60267215__60268435___PPM1A	0.075202	-3.73308	0.006633
chr15__51887589__51902036___TMOD3	0.075251	-3.73215	0.007225
chr6__53522415__53532766___GCLC	0.075384	-3.7296	0.006877
chr4__109659011__109660365___CCDC109B	0.07541	-3.7291	0.007159
chr8__70583164__70594590___TRAM1	0.075584	-3.72577	0.005795
chrX__10944205__11110981___MID1-2	0.075632	-3.72487	0.005591
chr17__35362739__35363826___SLFN11	0.075642	-3.72466	0.007487
chr15__62453645__62541282___TLN2	0.075723	-3.72312	0.005439
chr9__36372496__36376127___RNF38	0.075733	-3.72293	0.006796
chr20__35651264__35659014___RBM12	0.075742	-3.72276	0.007075
chr19__52383849__52385742___ZNF880	0.075786	-3.72193	0.006533
chr1__207697503__207708263___CR1L	0.075795	-3.72176	0.007529
chr18__57554260__57580199___FECH	0.075873	-3.72026	0.006929
chr17__27303367__27311616___WSB1	0.075883	-3.72009	0.007219
chr20__5565017__5604440___GPCPD1	0.075918	-3.71941	0.006929
chr17__81622166__81629805___NPLOC4	0.07601	-3.71766	0.00722
chr5__176350613__176355749___KIAA1191	0.076019	-3.71749	0.007176
chr5__137942875__137943216___FAM13B	0.076147	-3.71507	0.007413
chr13__72728926__72735005___BORA	0.07616	-3.71483	0.007337
chr20__5559940__5570239___GPCPD1	0.07619	-3.71425	0.006747
chr14__96852831__96860735___VRK1	0.076286	-3.71244	0.007139
chr19__34430576__34438766___UBA2	0.07631	-3.71198	0.007077
chr1__88740988__88741983___PKN2	0.076327	-3.71165	0.007326
chr9__83665030__83678599___UBQLN1	0.076353	-3.71118	0.006717
chr10__91819270__91842391___TNKS2	0.076362	-3.71099	0.006929
chr2__206056198__206063244___INO80D	0.076373	-3.71079	0.006796
chr2__135748267__135761911___UBXN4	0.076391	-3.71045	0.007479
chr2__128170288__128173939___UGGT1	0.076467	-3.70902	0.006616
chr1__236850344__236853088___MTR	0.076471	-3.70895	0.007545
chrY__13399938__13403888___UTY	0.076472	-3.70892	0.007052
chr18__56610993__56638505___TXNL1	0.076503	-3.70834	0.007709
chr1__155395459__155404350___ASH1L	0.076527	-3.70789	0.007225
chr15__80073266__80131293___ZFAND6	0.076557	-3.70731	0.00749
chr2__15424315__15511350___NBAS	0.07658	-3.70689	0.007545
chr9__111384522__111385442___KIAA0368	0.076603	-3.70646	0.007517
chr14__34597550__34609742___SNX6	0.076648	-3.70561	0.00749
chr14__60258964__60277091___PPM1A	0.076719	-3.70427	0.007335
chr18__57559145__57580199___FECH	0.076857	-3.70168	0.007545
chr5__79619612__79623355___PAPD4	0.076865	-3.70154	0.007216

chr14__50445041__50456594___MAP4K5	0.076868	-3.70148	0.00752
chr22__38495796__38501280___DDX17	0.076886	-3.70113	0.007878
chr5__53636856__53658624___NDUFS4	0.076887	-3.70111	0.006253
chr9__40994633__41011730___LOC100132352	0.076914	-3.70062	0.006723
chr9__15478477__15490124___PSIP1	0.076941	-3.70011	0.007545
chr11__119076897__119077647___VPS11	0.07696	-3.69975	0.007779
chr7__27785163__27794446___TAX1BP1	0.076988	-3.69921	0.007827
chr13__50044651__50045232___DLEU2	0.076997	-3.69906	0.007779
chr1__207655190__207686940___CR1L	0.077042	-3.69822	0.006717
chr3__183937901__183953270___ABCC5	0.077104	-3.69705	0.007487
chr7__139053451__139054095___ZC3HAV1	0.077113	-3.69687	0.007709
chr16__11020193__11047342___CLEC16A	0.077125	-3.69666	0.006796
chr15__92924321__92927330___CHD2	0.077147	-3.69624	0.006331
chr21__15762891__15778027___USP25	0.077276	-3.69383	0.007573
chr12__82386803__82403130___METTL25	0.077454	-3.69052	0.007545
chr12__109904085__109907557___TCHP	0.077575	-3.68827	0.006209
chr11__16283756__16341252___SOX6	0.077634	-3.68717	0.007899
chr13__113306485__113310867___LAMP1	0.077669	-3.68651	0.006773
chr3__20174249__20178347___SGOL1	0.077798	-3.68413	0.007779
chr21__37108392__37147603___TTC3	0.077803	-3.68404	0.007749
chr18__21791374__21804014___MIB1	0.077885	-3.68251	0.007833
chr12__111658736__111681835___BRAP	0.077928	-3.68172	0.006717
chr16__75603085__75622464___ADAT1	0.077931	-3.68165	0.007749
chr6__97267882__97273062___MMS22L	0.077933	-3.68161	0.007335
chr4__98574362__98574905___TSPAN5	0.077943	-3.68144	0.00746
chr12__111865250__111871180___MAPKAPK5	0.078046	-3.67952	0.007778
chr16__72349046__72391215___NA	0.078054	-3.67938	0.00746
chr1__28683583__28690186___GMEB1	0.078112	-3.67831	0.007499
chr1__207697503__207717691___CR1L	0.07826	-3.67558	0.007545
chr10__86497201__86500743___WAPAL	0.078315	-3.67457	0.007019
chr17__61972727__61985090___MED13	0.078321	-3.67445	0.007483
chr2__201392909__201420706___TRAK2	0.078423	-3.67257	0.00744
chr2__64569092__64573068___AFTPH	0.078439	-3.67229	0.007545
chr6__18215007__18217885___KDM1B	0.07846	-3.67191	0.007752
chr1__147293629__147294517___CHD1L	0.0785	-3.67116	0.007833
chr2__201381124__201420706___TRAK2	0.078518	-3.67083	0.007719
chr1__70181086__70187338___LRRC40	0.07858	-3.6697	0.007216
chr1__203847184__203847687___ZC3H11A	0.078603	-3.66928	0.007808
chr1__35381259__35390098___ZMYM4	0.078614	-3.66906	0.008022
chr11__2969803__2972279___NAP1L4	0.07863	-3.66877	0.007545
chr2__238173534__238185287___ILKAP	0.078763	-3.66633	0.007878
chr20__47224317__47236516___ZMYND8	0.078766	-3.66628	0.008022
chrX__19683823__19706984___SH3KBP1	0.078804	-3.66559	0.008108
chr7__77083887__77098951___NA	0.078814	-3.6654	0.007454
chr19__4361679__4364120___SH3GL1	0.07888	-3.66419	0.007719
chr12__119850174__119857698___CIT	0.07896	-3.66274	0.007164

chr1__90005133__90007750___ZNF326	0.078965	-3.66265	0.008031
chr2__23982896__23984831___UBXN2A	0.07897	-3.66255	0.008261
chr19__48231660__48242644___CARD8	0.078989	-3.6622	0.007847
chr4__155696756__155722192___GUCY1A3	0.078992	-3.66214	0.008439
chr2__99429840__99435941___REV1	0.079055	-3.66099	0.006796
chr11__77685105__77693611___RSF1	0.079101	-3.66016	0.007515
chr2__26364302__26383347___EPT1	0.079194	-3.65846	0.007479
chr7__152249876__152250966___KMT2C	0.079213	-3.65811	0.007363
chr5__138006990__138021197___FAM13B	0.079282	-3.65686	0.008484
chr13__99539446__99552326___TM9SF2	0.079285	-3.65681	0.008439
chr10__12081472__12091684___DHTKD1	0.079318	-3.6562	0.007826
chr7__7209427__7243750___C1GALT1	0.079338	-3.65585	0.007807
chr20__58999343__58999809___CTSZ	0.079341	-3.65579	0.007948
chr3__180947865__180951468___FXR1	0.07944	-3.65398	0.006792
chr18__79695225__79704917___CTDP1	0.079482	-3.65323	0.006929
chr3__138681967__138699095___PIK3CB	0.079517	-3.6526	0.007267
chr1__227145489__227317246___CDC42BPA	0.079521	-3.65253	0.007529
chr19__45854175__45854507___SYMPK	0.07959	-3.65128	0.008484
chr18__62138243__62163656___PIGN	0.079621	-3.65071	0.007643
chr8__60572046__60591969___RAB2A	0.079633	-3.6505	0.007948
chr16__3850297__3854850___CREBBP	0.079664	-3.64992	0.007966
chr2__128097429__128129179___UGGT1	0.079676	-3.64971	0.007352
chr2__26364302__26375148___EPT1	0.079746	-3.64844	0.007326
chr9__85822880__85849543___NA	0.079808	-3.64732	0.008313
chr6__63646527__63685911___PHF3	0.07981	-3.64729	0.007545
chr6__18249651__18263996___DEK	0.079821	-3.6471	0.007517
chr2__128183675__128187614___UGGT1	0.079848	-3.6466	0.00854
chr10__119160915__119161081___SFXN4	0.079918	-3.64533	0.008261
chr15__68141946__68146700___PIAS1	0.08	-3.64386	0.007515
chr2__24665162__24665915___NCOA1	0.080059	-3.64279	0.006796
chr2__61108317__61118116___KIAA1841	0.080118	-3.64172	0.000743
chr8__94491578__94491909___KIAA1429	0.080187	-3.64049	0.008121
chrX__71367499__71460803___TAF1	0.080198	-3.64029	0.007719
chr1__235677091__235697272___LYST	0.080215	-3.63999	0.007545
chr16__58576463__58583182___CNOT1	0.080299	-3.63848	0.007826
chr17__67866464__67875744___BPTF	0.080341	-3.63771	0.007826
chr22__21788257__21805945___MAPK1	0.080399	-3.63668	0.007228
chr9__17388162__17416189___CNTLN	0.080463	-3.63553	0.008548
chr12__112246901__112252528___HECTD4	0.080623	-3.63267	0.007529
chr3__123931308__123931756___CCDC14	0.08064	-3.63236	0.008031
chr3__132473145__132478140___DNAJC13	0.080712	-3.63107	0.008716
chr12__28225795__28391411___CCDC91	0.080819	-3.62916	0.007888
chr1__207723618__207724708___NA	0.080858	-3.62846	0.008791
chr13__95161189__95194937___ABCC4	0.080947	-3.62688	0.007337
chr4__48833401__48857365___OCIAD1	0.080953	-3.62677	0.008903
chr2__121757240__121763084___TSN	0.080983	-3.62623	0.008277

chr3__196065443__196075360___TFRC	0.081059	-3.62489	0.008793
chr2__53934605__53949283___PSME4	0.081078	-3.62454	0.007826
chr2__218476840__218479715___USP37	0.081132	-3.62358	0.008395
chr1__243293091__243344331___SDCCAG8	0.081166	-3.62298	0.008845
chr1__193130174__193152444___CDC73	0.081183	-3.62268	0.00874
chr15__42264090__42268032___TMEM87A	0.081224	-3.62194	0.00874
chr5__108341927__108348530___FBXL17	0.081254	-3.62142	0.009237
chr1__233198939__233218184___PCNXL2	0.081315	-3.62034	0.007878
chr18__26032399__26057742___SS18	0.081322	-3.62021	0.008548
chr8__38114192__38135766___ASH2L	0.08143	-3.61829	0.008599
chr17__49311312__49312845___ZNF652	0.081449	-3.61797	0.002128
chr5__131255095__131256192___NA	0.081501	-3.61704	0.008206
chr19__11648358__11650417___NA	0.08151	-3.61688	0.008793
chr6__98899268__98927822___FBXL4	0.081561	-3.61598	0.008612
chr17__47402135__47414919___EFCAB13	0.081571	-3.6158	0.008599
chr2__23823258__23828939___ATAD2B	0.081656	-3.6143	0.00819
chr1__93894614__93901669___GCLM	0.081712	-3.61331	0.006792
chr11__46795594__46821268___CKAP5	0.08176	-3.61246	0.007808
chr6__43348324__43352476___ZNF318	0.081806	-3.61165	0.008277
chr1__145974825__145975436___POLR3GL	0.081823	-3.61135	0.007778
chr14__45227663__45242518___MIS18BP1	0.081838	-3.61109	0.008897
chr1__42828289__42830298___ERMAP	0.081867	-3.61057	0.008903
chr2__24026799__24033257___NA	0.081875	-3.61043	0.000283
chr13__21400373__21413772___ZDHHC20	0.082047	-3.60741	0.007335
chr9__20819796__20823115___FOCAD	0.082115	-3.60622	0.007176
chr2__45546732__45553730___SRBD1	0.082117	-3.60617	0.007779
chr5__97013648__97028612___LNPEP	0.082129	-3.60597	0.00861
chr15__92953357__92955512___CHD2	0.082149	-3.60562	0.008439
chr5__69115237__69128132___SLC30A5	0.0822	-3.60471	0.007705
chr1__1495485__1529331___NA	0.082254	-3.60376	0.00938
chr3__136472413__136477412___STAG1	0.082311	-3.60278	0.008484
chr12__49460770__49490731___SPATS2	0.082326	-3.60251	0.007749
chr2__233263130__233265143___ATG16L1	0.082335	-3.60236	0.009446
chr16__68093356__68126610___NFATC3	0.082388	-3.60141	0.008277
chr17__3705098__3705645___NA	0.082443	-3.60045	0.009527
chr17__81569016__81572088___NPLOC4	0.082485	-3.59972	0.008793
chr9__122877471__122897576___RC3H2	0.082499	-3.59948	0.008836
chr4__39841948__39845880___PDS5A	0.082511	-3.59927	0.007749
chr13__41811225__41833531___VWA8	0.082534	-3.59887	0.007749
chr1__212863725__212870168___FLVCR1	0.082541	-3.59874	0.008277
chr19__7382792__7383203___ARHGEF18	0.082623	-3.5973	0.007326
chr10__16752539__16754989___RSU1	0.082628	-3.59722	0.008484
chr7__129657343__129690546___NRF1	0.08264	-3.59702	0.008424
chr7__154975696__154998784___PAXIP1	0.082691	-3.59612	0.006796
chr6__131136778__131169273___AKAP7	0.082699	-3.59599	0.008261
chr1__75728401__75750546___ACADM	0.08294	-3.59179	0.008439

chr3__50108070__50108304___RBM5	0.083008	-3.5906	0.008716
chr5__139318908__139319501___MATR3	0.083013	-3.59051	0.007702
chr18__50895809__50908196___ME2	0.083017	-3.59045	0.008189
chr3__182961226__182964049___DCUN1D1	0.08303	-3.59023	0.008864
chr13__112565111__112569259___TUBGCP3	0.083082	-3.58931	0.00755
chr15__52605133__52611777___FAM214A	0.083098	-3.58905	0.007779
chr6__131145285__131200489___AKAP7	0.083171	-3.58778	0.009284
chr3__11358418__11426926___ATG7	0.083233	-3.58669	0.007487
chr22__41125864__41135906___EP300	0.083271	-3.58605	0.007749
chr7__77109938__77113483___NA	0.083309	-3.58538	0.008793
chr1__15636313__15643650___DDI2	0.083379	-3.58417	0.008677
chr8__53970392__54010492___TCEA1	0.083403	-3.58375	0.008494
chr4__169507037__169508852___NEK1	0.083502	-3.58205	0.007995
chr14__22909483__22913845___RBM23	0.08351	-3.5819	0.00757
chr9__5021963__5081861___JAK2	0.083513	-3.58185	0.007826
chr5__157294783__157296774___CYFIP2	0.083561	-3.58102	0.009629
chr1__88691724__88771879___PKN2	0.083572	-3.58084	0.008279
chr5__133096098__133099652___HSPA4	0.083595	-3.58044	0.007694
chr7__139237005__139259370___UBN2	0.083598	-3.58039	0.008762
chr14__74778447__74778683___YLPM1	0.083702	-3.57859	0.008189
chr14__58410843__58424095___TIMM9	0.083726	-3.57818	0.007233
chr7__139398599__139407350___C7orf55-LUC7L2LUC7L2	0.083733	-3.57806	0.008453
chr8__17924713__17937379___PCM1	0.083758	-3.57763	0.009446
chr22__30494150__30495971___SEC14L4	0.083777	-3.57731	0.009125
chr15__44633505__44657263___SPG11	0.083804	-3.57683	0.009629
chr8__38347497__38348143___WHSC1L1	0.08381	-3.57673	0.0088
chr13__49196877__49198574___FNDC3A	0.083822	-3.57653	0.008857
chr2__95914108__95916171___ANKRD36C	0.083829	-3.57641	0.011991
chr17__68209654__68210465___AMZ2	0.083892	-3.57532	0.009533
chr4__117575655__117575857___NA	0.083962	-3.57412	0.008914
chr3__141512163__141540609___RASA2	0.083977	-3.57386	0.008841
chr12__98677425__98686873___APAF1	0.084173	-3.57051	0.008189
chr5__138006990__138011945___FAM13B	0.084174	-3.57048	0.009284
chr17__27301788__27309272___WSB1	0.084182	-3.57034	0.009284
chr7__6580555__6585260___ZDHHC4	0.084278	-3.5687	0.007888
chr9__37126312__37247130___ZCCHC7	0.084294	-3.56843	0.009608
chrX__44931938__44945523___KDM6A	0.084336	-3.56771	0.008031
chr4__78859584__78878891___BMP2K	0.084379	-3.56698	0.002203
chr1__235773842__235787373___LYST	0.084396	-3.56669	0.009533
chr9__19060088__19096769___HAUS6	0.084409	-3.56646	0.007403
chr4__1900626__1904378___WHSC1	0.084423	-3.56622	0.008762
chr20__44978443__45025130___STK4	0.084429	-3.56612	0.009684
chr3__44828214__44840456___KIF15	0.084468	-3.56546	0.001996
chr3__143019969__143043276___U2SURP	0.084475	-3.56533	0.007808
chr12__119767087__119776842___CIT	0.084527	-3.56444	0.009284

chr1__20744744__20749882___HP1BP3	0.084586	-3.56343	0.007719
chr14__55315300__55316355___FBXO34	0.084602	-3.56316	0.009727
chr11__58584856__58614343___ZFP91ZFP91-CNTF	0.084604	-3.56313	0.009513
chr4__145064572__145081750___ANAPC10	0.084769	-3.56032	0.008914
chr10__68341174__68341851___HNRNPH3	0.084871	-3.55859	0.008439
chr17__50970707__50987237___SPAG9	0.084905	-3.55801	0.008914
chr3__153164766__153209886___NA	0.085001	-3.55637	0.009446
chr15__44615363__44629388___SPG11	0.085043	-3.55566	0.009353
chr22__24302195__24369320___SPECC1L-ADORA2ASPECC1L	0.085223	-3.55261	0.008261
chr10__6097048__6115311___RBM17	0.085224	-3.55259	0.009533
chr10__63184608__63194375___JMJD1C	0.085227	-3.55255	0.009464
chr2__135602500__135622732___R3HDM1	0.085303	-3.55125	0.009527
chr20__21340721__21346550___XRN2	0.085319	-3.55099	0.008439
chr10__31461037__31461783___ZEB1	0.085398	-3.54965	0.007399
chr1__34992234__35015162___ZMYM6	0.085462	-3.54858	0.009284
chr3__56615890__56618212___CCDC66	0.085543	-3.54721	0.008395
chr1__51402435__51465326___EPS15	0.085563	-3.54688	0.008599
chr12__51240343__51241116___DAZAP2	0.085583	-3.54653	0.009608
chr18__22990937__23001729___RBBP8	0.085619	-3.54592	0.00946
chr1__91501654__91520279___CDC7	0.085624	-3.54584	0.00961
chr6__130022227__130071127___L3MBTL3	0.085627	-3.54579	0.0093
chr18__69895701__69896045___CD226	0.085635	-3.54565	0.007808
chr15__74926766__74929232___COX5A	0.085662	-3.54521	0.009284
chr4__122190000__122201126___KIAA1109	0.085688	-3.54476	0.009313
chr3__16271659__16272321___OXNAD1	0.085724	-3.54415	0.008677
chr1__235438769__235442911___TBCE	0.085755	-3.54363	0.010022
chr3__154295284__154306295___DHX36	0.085854	-3.54197	0.009276
chr13__52460896__52465465___CKAP2	0.085861	-3.54185	0.007694
chr1__95140673__95173889___TMEM56TMEM56-RWDD3	0.085909	-3.54104	0.002426
chr2__160329680__160331910___RBMS1	0.085931	-3.54068	0.009436
chr4__88906379__89009078___FAM13A	0.085933	-3.54064	0.009369
chr4__78844928__78865720___BMP2K	0.085986	-3.53975	0.008599
chr3__160404328__160416415___SMC4	0.086007	-3.53941	0.009215
chr7__130116445__130129576___KLHDC10	0.086039	-3.53886	0.009655
chr2__71401956__71418639___ZNF638	0.086053	-3.53863	0.009833
chr9__96522506__96565483___CDC14B	0.086154	-3.53695	0.000751
chr17__67151046__67185145___HELZ	0.086159	-3.53685	0.009944
chr6__130052859__130057497___L3MBTL3	0.086235	-3.53558	0.009312
chr1__1804419__1806538___GNB1	0.086284	-3.53476	0.001462
chr2__207555628__207560372___CREB1	0.086299	-3.53451	0.007487
chr5__50750151__50778650___PARP8	0.086392	-3.53296	0.007545
chr2__119920069__119967972___PTPN4	0.086414	-3.53258	0.008768
chr15__77283883__77286504___PEAK1	0.086648	-3.52869	0.008153
chr11__74374415__74378658___PGM2L1	0.086698	-3.52786	0.009284

chr10__16752539__16817084___RSU1	0.086779	-3.52651	0.009106
chr5__154790325__154795319___LARP1	0.08685	-3.52534	0.008791
chr1__220001138__220007338___EPRS	0.086879	-3.52485	0.008864
chr1__174442889__174455838___RABGAP1L	0.086896	-3.52457	0.009513
chr8__119781053__119791459___TAF2	0.086903	-3.52445	0.00849
chr5__112985835__113010807___DCP2	0.087003	-3.52279	0.00987
chr6__28271854__28272787___ZSCAN26	0.087008	-3.52271	0.008848
chr14__69768138__69769251___SRSF5	0.087014	-3.52262	0.009446
chr1__207715312__207738571___NA	0.087022	-3.52248	0.008903
chr5__96985080__97015095___LNPEP	0.087049	-3.52203	0.009596
chr3__52634602__52644789___PBRM1	0.087066	-3.52175	0.008118
chr13__95034605__95083290___ABCC4	0.087401	-3.5162	0.008816
chr1__39804878__39808198___NA	0.087422	-3.51586	0.009876
chr14__35126735__35127611___KIAA0391	0.087426	-3.5158	0.009533
chr2__44456568__44549728___CAMKMT	0.087435	-3.51565	0.007545
chr6__36083031__36096066___MAPK14	0.087447	-3.51545	0.009669
chr9__95978061__95979866___LOC101928170	0.087537	-3.51396	0.009219
chr6__75659262__75663518___SENP6	0.087635	-3.51235	0.008296
chr1__29064982__29115803___EPB41	0.087662	-3.5119	0.009284
chr17__29648144__29667223___SSH2	0.087666	-3.51184	0.009533
chr4__1912091__1917037___WHSC1	0.087687	-3.51149	0.008031
chr5__115852979__115870128___AP3S1	0.087737	-3.51067	0.008365
chr17__62010550__62052705___MED13	0.087738	-3.51065	0.008261
chr7__105038126__105081797___KMT2E	0.087796	-3.50969	0.008154
chr2__226837548__226867688___RHBDD1	0.087836	-3.50905	0.007545
chr22__29813430__29822464___ASCC2	0.087888	-3.50819	0.008135
chr2__31917926__31943383___MEMO1	0.087917	-3.50771	0.008612
chr9__131150324__131164144___NUP214	0.087922	-3.50763	0.008277
chr5__131395563__131408207___NA	0.087943	-3.50728	0.009031
chr10__119049801__119051321___EIF3A	0.087968	-3.50688	0.009856
chr17__68429996__68433575___WIPI1	0.087969	-3.50686	0.009284
chr2__135748267__135780385___UBXN4	0.088012	-3.50615	0.010688
chr16__48256610__48277479___LONP2	0.088078	-3.50508	0.01006
chr14__58223622__58230480___ACTR10	0.088107	-3.5046	0.009629
chr8__100137565__100138450___FBXO43	0.088192	-3.50321	0.010411
chr11__47750916__47753102___FNBP4	0.088248	-3.5023	0.008791
chr12__123194386__123203375___MPHOSPH9	0.08825	-3.50227	0.010118
chr18__23519680__23520313___C18orf8NPC1	0.088266	-3.50201	0.008261
chr5__10415488__10417404___MARCH6	0.088284	-3.5017	0.00961
chr10__48401612__48404981___MAPK8	0.088287	-3.50166	0.007878
chr22__32479133__32485209___FBXO7	0.088292	-3.50158	0.00961
chr7__103233800__103257724___DPY19L2P2	0.088314	-3.50122	0.007734
chr4__78826037__78859687___BMP2K	0.088367	-3.50035	0.007826
chr21__15777904__15833548___USP25	0.088392	-3.49995	0.010553
chr14__34771511__34774490___BAZ1A	0.088415	-3.49956	0.009312
chr9__34286617__34311371___KIF24	0.088445	-3.49907	0.009833

chr10__68765888__68773099___CCAR1	0.088478	-3.49854	0.010339
chr7__125329682__125347207___RP11-3B12.2	0.088626	-3.49613	0.008323
chr4__6994184__7014557___TBC1D14	0.088626	-3.49613	0.010022
chr3__112534257__112550262___ATG3	0.088773	-3.49373	0.009284
chr18__13012973__13019206___CEP192	0.088827	-3.49286	0.010509
chr18__9182382__9195698___ANKRD12	0.088882	-3.49197	0.016651
chr14__92142164__92155323___CPSF2	0.088889	-3.49185	0.009284
chr8__130134296__130180880___ASAP1	0.08892	-3.49134	0.010234
chr1__6806983__6825210___CAMTA1	0.088971	-3.49053	0.001673
chr4__153473845__153474514___KIAA0922	0.089066	-3.48897	0.008439
chr4__39300021__39303151___RFC1	0.089129	-3.48796	0.002438
chr17__60190563__60214774___USP32	0.089234	-3.48627	0.00983
chr3__195333028__195345317___ACAP2	0.089267	-3.48574	0.00946
chr17__50139263__50141373___PPP1R9B	0.089302	-3.48516	0.008439
chr6__42663278__42666245___UBR2	0.089371	-3.48406	0.010618
chr5__79640851__79682061___PAPD4	0.089376	-3.48397	0.008177
chr1__31907661__31919658___PTP4A2	0.089381	-3.48389	0.010022
chr3__136443287__136477412___STAG1	0.089443	-3.48288	0.010255
chr12__6981595__6983539___LPCAT3	0.089553	-3.48111	0.010403
chr17__20245926__20306082___SPECC1	0.08956	-3.481	0.009284
chr12__70219393__70225390___LOC101928062	0.089563	-3.48096	0.009106
chr2__100006632__100008932___AFF3	0.089671	-3.47922	0.01111
chr9__98018289__98018489___NA	0.089709	-3.47861	0.010325
chr9__96364464__96368305___SLC35D2	0.089747	-3.47799	0.009727
chr6__84155298__84186623___KIAA1009	0.089812	-3.47695	0.010582
chr14__60115719__60125823___PCNXL4	0.089848	-3.47636	0.011003
chr7__148766561__148767749___CUL1	0.08985	-3.47633	0.00961
chr14__30601770__30608069___G2E3	0.089852	-3.4763	0.009446
chr16__53439016__53454842___RBL2	0.089872	-3.47599	0.011213
chr19__9652953__9653878___ZNF562	0.089898	-3.47557	0.009284
chr14__45226743__45242518___MIS18BP1	0.089925	-3.47513	0.009629
chr4__145143365__145146429___OTUD4	0.089948	-3.47477	0.008439
chr18__116842__118504___ROCK1P1	0.089949	-3.47476	0.008344
chr16__89305206__89317078___ANKRD11	0.089962	-3.47454	0.011036
chr12__100313422__100326754___SCYL2	0.089973	-3.47437	0.011068
chr12__117049019__117056886___TESC	0.090018	-3.47365	0.010266
chr6__85536792__85542043___SNX14	0.090073	-3.47277	0.010132
chr3__53874211__53876080___ACTR8	0.090149	-3.47154	0.008439
chr12__1739068__1754514___ADIPOR2	0.09022	-3.47041	0.008715
chr20__37044086__37047190___RBL1	0.09027	-3.4696	0.01067
chr20__5557945__5570239___GPCPD1	0.090303	-3.46909	0.008279
chr1__10095461__10105744___UBE4B	0.090369	-3.46803	0.011317
chr12__109988963__109991760___GIT2	0.09037	-3.46801	0.008677
chr7__92213195__92214777___KRIT1	0.090528	-3.46548	0.009727
chr2__8908621__8997343___MBOAT2	0.090538	-3.46533	0.010381
chr8__42957094__42964474___HOOK3	0.090555	-3.46506	0.007709

chr3__194419339__194419812___ATP13A3	0.09066	-3.46339	0.009437
chr17__50964511__50964872___SPAG9	0.090695	-3.46284	0.009533
chr1__93869090__93875783___NA	0.0907	-3.46275	0.00946
chr5__73051349__73052507___FCHO2	0.090708	-3.46263	0.01111
chr1__154249239__154251653___UBAP2L	0.090772	-3.46162	0.008725
chr16__67610824__67616878___CTCF	0.090817	-3.46089	0.011023
chr2__33565246__33568187___NA	0.090831	-3.46067	0.009629
chr16__4817598__4823907___GLYR1	0.090995	-3.45806	0.001593
chr14__39177841__39179462___PNN	0.091056	-3.45711	0.01
chr3__12604136__12606299___RAF1	0.091125	-3.456	0.010908
chr7__87884979__87888059___DBF4	0.091126	-3.45599	0.00983
chr10__128104661__128119319___MKI67	0.09122	-3.4545	0.010833
chr2__152732531__152735126___ARL6IP6	0.091257	-3.45392	0.009727
chr2__214780560__214781509___BARD1	0.091283	-3.4535	0.008845
chr20__49074785__49092127___CSE1L	0.091302	-3.45321	0.009629
chr13__40826506__40872160___TPTE2P5	0.091308	-3.45311	0.009527
chr10__68355353__68404844___RUFY2	0.091318	-3.45296	0.010403
chr16__69160356__69167185___CIRH1A	0.091388	-3.45184	0.010244
chr17__76738282__76742048___MFSD11	0.091403	-3.45161	0.011608
chr10__63190894__63194375___JMJD1C	0.091408	-3.45154	0.011652
chr22__32478981__32487828___FBXO7	0.091457	-3.45076	0.010567
chr19__23358430__23362739___ZNF91	0.091477	-3.45044	0.0114
chr12__111525192__111552977___ATXN2	0.091495	-3.45016	0.011023
chr17__76007060__76010543___EVPL	0.091511	-3.44991	0.010234
chr14__92810254__92816421___GOLGA5	0.091518	-3.4498	0.00946
chr19__10173871__10179982___DNMT1	0.09152	-3.44978	0.010381
chr22__28694032__28719485___CHEK2	0.091526	-3.44968	0.010132
chr2__26364302__26373629___EPT1	0.091537	-3.44951	0.002916
chr16__14606484__14617650___PARN	0.091553	-3.44924	0.010712
chr3__43303098__43303792___SNRK	0.091565	-3.44906	0.011914
chr1__113093206__113094755___LRIG2	0.091581	-3.44881	0.012203
chr5__138319219__138328529___CDC25C	0.091693	-3.44705	0.009856
chr17__20187958__20205912___SPECC1	0.091736	-3.44637	0.010172
chr4__183683975__183693147___TRAPPC11	0.091753	-3.4461	0.009704
chr3__17372075__17406526___TBC1D5	0.091829	-3.44491	0.009446
chr13__41316846__41331369___NAA16	0.091873	-3.44421	0.011023
chrX__132384663__132406392___MBNL3	0.091875	-3.44418	0.009284
chr21__39224408__39229436___BRWD1	0.091884	-3.44404	0.008439
chr1__174219248__174394145___RABGAP1L	0.091908	-3.44367	0.010158
chr1__15626669__15651895___DDI2	0.09195	-3.44301	0.008893
chr7__2229984__2230764___MAD1L1	0.091958	-3.44288	0.009106
chr3__158646165__158653467___GFM1	0.092	-3.44222	0.007709
chr9__85669485__85692813___AGTPBP1	0.092019	-3.44193	0.010791
chr6__154773989__154778045___SCAF8	0.092033	-3.4417	0.011652
chr22__40552106__40594735___MKL1	0.092233	-3.43858	0.010206
chr2__108839185__108856970___CCDC138	0.092235	-3.43855	0.011032

chr17__68401360__68420506___ARSG	0.092243	-3.43842	0.011257
chr8__91018390__91024366___TMEM55A	0.092264	-3.43809	0.010022
chr17__32171043__32175362___RHOT1	0.092365	-3.43651	0.011055
chr3__17622648__17623913___TBC1D5	0.092368	-3.43646	0.0097
chrX__71368054__71387461___TAF1	0.092499	-3.43442	0.01111
chr6__136669283__136698682___MAP3K5	0.092509	-3.43426	0.010266
chr8__11808794__11838573___FDFT1	0.092542	-3.43374	0.002533
chr13__19851355__19852190___ZMYM5	0.092586	-3.43306	0.011235
chr17__62010462__62063222___MED13	0.092614	-3.43262	0.011231
chr8__123370903__123380677___ATAD2	0.092628	-3.43241	0.01118
chr9__121375231__121378100___LOC102723324	0.092704	-3.43122	0.010465
chr15__85684741__85710645___AKAP13	0.092778	-3.43007	0.01251
chr8__73673107__73709162___STAU2	0.092789	-3.4299	0.01145
chr16__89098591__89102759___ACSF3	0.092807	-3.42962	0.01067
chr3__172761610__172784803___ECT2	0.092828	-3.4293	0.0114
chr9__112250929__112276013___PTBP3	0.092829	-3.42928	0.010175
chr14__49799475__49814857___NEMF	0.09284	-3.42911	0.011341
chr7__74705164__74718941___GTF2I	0.09285	-3.42896	0.012545
chr5__77053965__77055596___AGGF1	0.093047	-3.4259	0.009727
chr12__829309__829944___WNK1	0.093072	-3.42551	0.010022
chr3__37315420__37321886___GOLGA4	0.093075	-3.42546	0.010172
chr5__79290121__79306461___JMY	0.093182	-3.4238	0.008762
chr12__8039819__8040165___FOXJ2	0.093281	-3.42227	0.009312
chr15__40389506__40393593___KNSTRN	0.09335	-3.4212	0.011521
chr16__72523332__72555326___LOC102723844	0.093402	-3.4204	0.010778
chr22__43039780__43046573___TTLL1	0.09341	-3.42028	0.009727
chr2__55558771__55591571___SMEK2	0.093445	-3.41974	0.011003
chr8__85472029__85473468___CA2	0.093514	-3.41868	0.011257
chr11__16183886__16247560___SOX6	0.093548	-3.41815	0.01067
chr15__50459000__50471795___USP8	0.093751	-3.41502	0.009313
chr1__21089138__21111383___EIF4G3	0.093879	-3.41306	0.010583
chr2__55577315__55591695___SMEK2	0.093902	-3.4127	0.011494
chr14__70166639__70168484___SLC8A3	0.093915	-3.4125	0.011692
chr15__49235851__49239367___GALK2	0.094016	-3.41095	0.010499
chr12__108619325__108620848___NA	0.094023	-3.41084	0.011504
chrX__41217220__41223402___USP9X	0.094052	-3.41039	0.011692
chr4__107944970__107947537___CYP2U1	0.094056	-3.41033	0.009488
chr4__2952275__2956811___NOP14	0.094065	-3.4102	0.01111
chr2__33257284__33263392___LTBP1	0.0941	-3.40966	0.010757
chr12__68713865__68714904___NUP107	0.094165	-3.40867	0.007948
chr1__197084354__197092010___ASPM	0.094219	-3.40784	0.010801
chr8__25460240__25469980___CDCA2	0.094255	-3.40728	0.009215
chr2__53714384__53716743___ASB3GPR75-ASB3	0.094304	-3.40654	0.011831
chr17__60252381__60288682___USP32	0.094308	-3.40648	0.009284
chr15__56678664__56682477___ZNF280D	0.094329	-3.40616	0.009589
chr14__55158522__55170787___DLGAP5	0.094422	-3.40473	0.010322

chr12__71626260__71629037___ZFC3H1	0.094434	-3.40455	0.010112
chr7__156966270__156967092___NOM1	0.094437	-3.40451	0.012503
chr13__41252645__41263484___MTRF1	0.094456	-3.40421	0.011956
chr2__32514990__32518946___BIRC6	0.094513	-3.40334	0.011723
chr1__185181946__185190642___SWT1	0.094519	-3.40326	0.011286
chr14__49820343__49834449___NEMF	0.094555	-3.4027	0.010913
chr9__100498765__100550160___MSANTD3-TMEFF1TMEFF1	0.094566	-3.40253	0.009147
chr18__56758865__56781656___WDR7	0.094595	-3.40209	0.010688
chr13__79312485__79319691___RBM26	0.094612	-3.40184	0.010592
chr3__142093061__142126315___TFDP2	0.094619	-3.40172	0.009856
chr3__121467519__121468431___POLQ	0.094692	-3.40062	0.010908
chr8__21966857__21974774___XPO7	0.094697	-3.40054	0.011036
chr11__33286413__33306009___HIPK3	0.094732	-3.4	0.011848
chr1__10007570__10008274___RBP7	0.094744	-3.39982	0.009727
chr7__105038126__105091314___KMT2E	0.094745	-3.3998	0.009736
chr8__528895__531576___TDRP	0.094754	-3.39968	0.01067
chr1__163343733__163349080___NUF2	0.09476	-3.39957	0.010987
chr1__28027789__28038905___EYA3	0.094851	-3.39819	0.008903
chrX__3817545__3818500___LOC389906	0.094861	-3.39804	0.011608
chr2__241407537__241436538___FARP2	0.09494	-3.39684	0.008903
chr9__122865349__122897576___RC3H2	0.095005	-3.39586	0.010266
chr10__48890579__48901863___WDFY4	0.095221	-3.39258	0.011238
chr19__39329000__39333126___GMFG	0.095238	-3.39232	0.011162
chr9__406930__418207___DOCK8	0.095243	-3.39225	0.012186
chr11__85981745__86007583___PICALM	0.095259	-3.39201	0.012186
chr2__37037855__37041292___HEATR5B	0.095276	-3.39175	0.010266
chr17__20204333__20247319___SPECC1	0.095392	-3.38998	0.011669
chr4__3154293__3157199___HTT	0.095491	-3.38849	0.011104
chr10__22539971__22609717___PIP4K2A	0.095623	-3.3865	0.011608
chr20__47276314__47283648___ZMYND8	0.095623	-3.38651	0.009313
chr19__15268905__15273133___BRD4	0.095711	-3.38517	0.010172
chr17__62560016__62565137___TLK2	0.095781	-3.38412	0.009629
chr4__143989877__144001283___NA	0.095886	-3.38253	0.009629
chr14__75707018__75720703___TTLL5	0.095905	-3.38224	0.01084
chr5__172117481__172156788___STK10	0.095905	-3.38225	0.012369
chr1__159010003__159032691___IFI16	0.095948	-3.38161	0.012497
chr14__35013346__35019074___SRP54	0.095963	-3.38138	0.011914
chr5__168557423__168568998___PANK3	0.096047	-3.38012	0.013009
chr14__57229734__57247712___EXOC5	0.096056	-3.37997	0.002658
chr12__100282943__100329319___SCYL2	0.096137	-3.37877	0.011317
chr2__23857415__23895970___ATAD2B	0.096214	-3.3776	0.012235
chr15__75854386__75873568___UBE2Q2	0.096239	-3.37723	0.001512
chr13__41937315__41939586___VWA8	0.096255	-3.37699	0.011317
chr9__120550792__120568388___CDK5RAP2	0.096273	-3.37672	0.011947
chr15__92900789__92955512___CHD2	0.096505	-3.37325	0.00874

chr17__49316826__49322508___ZNF652	0.096516	-3.37309	0.013908
chr1__17341943__17342402___PADI4	0.096524	-3.37296	0.008762
chr14__49663315__49665163___POLE2	0.096562	-3.37239	0.010234
chr4__185247294__185267155___SNX25	0.096599	-3.37184	0.009313
chr12__97492461__97561047___NA	0.096618	-3.37157	0.01295
chr2__134253095__134270550___MGAT5	0.096683	-3.37059	0.01267
chr7__24623666__24641868___MPP6	0.09673	-3.36989	0.009608
chr7__130116445__130122202___KLHDC10	0.096782	-3.36911	0.012885
chr3__38221578__38230430___OXSR1	0.09679	-3.369	0.010764
chr12__124419957__124437996___NCOR2	0.096803	-3.3688	0.01299
chr1__158677690__158683496___SPTA1	0.096829	-3.36842	0.011859
chr1__179901302__179908673___TOR1AIP1	0.096848	-3.36813	0.011257
chr18__6237964__6312056___L3MBTL4	0.096855	-3.36803	0.011512
chr6__14131520__14135909___CD83	0.096922	-3.36703	0.011956
chr15__42528262__42529819___SNAP23	0.096942	-3.36673	0.012235
chr3__196055080__196077122___TFRC	0.096942	-3.36674	0.011956
chr5__179580947__179594963___RUFY1	0.096999	-3.36589	0.012735
chr4__1696202__1700070___SLBP	0.097024	-3.36551	0.011341
chr19__43925325__43930000___ZNF45	0.097032	-3.3654	0.011715
chr1__108782422__108794907___STXBP3	0.097072	-3.36479	0.009629
chr1__227254064__227260784___CDC42BPA	0.097226	-3.36251	0.013803
chr8__99556450__99661491___VPS13B	0.097258	-3.36204	0.012953
chr1__243645893__243843282___AKT3	0.097438	-3.35936	0.011213
chr19__34431861__34464131___UBA2	0.097449	-3.3592	0.010211
chr1__185160833__185184931___SWT1	0.097467	-3.35894	0.010908
chr5__154865442__154867792___CNOT8	0.097497	-3.3585	0.013124
chr3__19975601__19976169___RAB5A	0.097512	-3.35828	0.013932
chr15__63727647__63749791___HERC1	0.097556	-3.35762	0.010266
chr3__174523413__174553757___NAALADL2	0.097588	-3.35715	0.011055
chr13__77243059__77264002___MYCBP2	0.097611	-3.35681	0.01145
chr9__83739705__83768970___GKAP1	0.097625	-3.3566	0.013908
chr6__99476143__99510230___USP45	0.097675	-3.35586	0.011238
chr17__62536170__62565137___TLK2	0.097719	-3.35521	0.01314
chr3__132681914__132692818___NPHP3-ACAD11	0.097746	-3.35482	0.01067
chr14__101901719__101909690___PPP2R5C	0.097772	-3.35444	0.011238
chr8__96879798__96902096___CPQ	0.097826	-3.35364	0.012241
chr4__82427190__82428446___HNRNPDL	0.097845	-3.35335	0.012184
chr17__60299334__60301704___USP32	0.097874	-3.35293	0.011951
chr9__93476256__93498886___FAM120A	0.097894	-3.35264	0.009629
chr7__7234303__7238922___C1GALT1	0.097897	-3.35259	0.012735
chr16__16124789__16125911___ABCC1	0.09803	-3.35064	0.013995
chr16__68121987__68158068___NFATC3	0.098105	-3.34953	0.012875
chr10__84438512__84477664___CCSER2	0.098151	-3.34885	0.003332
chr4__128936655__128992237___SCLT1	0.098163	-3.34867	0.012707
chr10__87506268__87552541___MINPP1	0.098216	-3.3479	0.010602
chr17__30734897__30769064___SUZ12P1	0.098333	-3.34618	0.011512

chrX__150638943__150649901___MTM1	0.098371	-3.34562	0.009488
chr3__152414941__152459345___MBNL1	0.098387	-3.34538	0.011021
chr2__190899117__190924593___GLS	0.098446	-3.34452	0.013441
chr15__98819862__98824242___IGF1R	0.098447	-3.34451	0.013482
chr12__92851111__92853025___EEA1	0.098544	-3.3431	0.01328
chr1__15638307__15649823___DDI2	0.098602	-3.34224	0.012518
chr15__63660973__63675093___HERC1	0.098639	-3.3417	0.010266
chr18__2544195__2547529___METTL4	0.098727	-3.34041	0.010172
chr16__53498391__53500329___AKTIP	0.09877	-3.33978	0.014124
chr17__61965006__61968258___MED13	0.098808	-3.33923	0.011582
chr1__66958059__66959743___MIER1	0.098842	-3.33873	0.012137
chr2__27382126__27387158___PPM1G	0.099044	-3.33579	0.013525
chr9__5050686__5055788___JAK2	0.099099	-3.33498	0.011956
chr1__15909321__15916279___SPEN	0.09912	-3.33468	0.012453
chr21__46643535__46644488___PRMT2	0.099232	-3.33305	0.012953
chr20__47294666__47298872___ZMYND8	0.099238	-3.33296	0.014283
chr19__3623688__3624162___CACTIN	0.099276	-3.33241	0.011982
chr19__10159658__10175618___DNMT1	0.099395	-3.33069	0.01067
chr16__18841565__18850467___SMG1	0.099462	-3.32971	0.011213
chr8__134600436__134610655___ZFAT	0.099509	-3.32902	0.013292
chr8__26410909__26411069___BNIP3L	0.099548	-3.32847	0.011843
chr18__22968806__22984990___RBBP8	0.099558	-3.32832	0.014032
chr10__112527087__112538330___VTI1A	0.099589	-3.32788	0.009833
chr17__61982198__61995365___MED13	0.099649	-3.327	0.014098
chr9__132286423__132311856___SETX	0.099698	-3.3263	0.013914
chr17__20110427__20205912___SPECC1	0.099725	-3.32591	0.012812
chr7__2213212__2222754___MAD1L1	0.099738	-3.32571	0.012735
chr2__201394798__201420706___TRAK2	0.0998	-3.32482	0.010568
chr14__58467735__58470723___KIAA0586	0.09982	-3.32452	0.012259
chr1__245858496__245929937___SMYD3	0.099823	-3.32448	0.012369
chr14__55378279__55380389___ATG14	0.099863	-3.3239	0.013028
chr6__130022227__130104575___L3MBTL3	0.099878	-3.32369	0.01299
chr1__227112312__227119937___CDC42BPA	0.099908	-3.32325	0.013978
chr9__96336717__96352109___SLC35D2	0.099909	-3.32325	0.011848
chr8__17985447__18011366___PCM1	0.099941	-3.32278	0.013622
chr16__1724557__1729578___MAPK8IP3	0.09996	-3.3225	0.011608
chr2__33300451__33301644___LTBP1	0.099975	-3.32229	0.012953
chr11__68544838__68564432___PPP6R3	0.099982	-3.32218	0.0106
chr16__14599904__14609123___PARN	0.100044	-3.32129	0.012518
chr9__121375215__121378100___LOC102723324	0.100068	-3.32095	0.011091
chr3__56660731__56661017___FAM208A	0.100086	-3.32069	0.011697
chr9__77238002__77283650___VPS13A	0.100183	-3.31928	0.011829
chr4__128291800__128303035___NA	0.100214	-3.31885	0.011521
chr10__86443275__86460496___WAPAL	0.100261	-3.31816	0.010987
chr1__172131175__172182896___DNM3	0.100337	-3.31707	0.014365
chr10__15816835__15843272___FAM188A	0.100342	-3.31701	0.013908

chrX__134413488__134417302___PHF6	0.100351	-3.31688	0.013827
chr8__17195523__17215349___ZDHHC2	0.100382	-3.31643	0.01185
chr5__60686962__60687838___DEPDC1B	0.100383	-3.31641	0.017227
chr1__77713200__77715868___USP33	0.100452	-3.31542	0.011502
chr3__47675475__47678311___SMARCC1	0.100461	-3.3153	0.010958
chr1__243270092__243308177___SDCCAG8	0.100511	-3.31458	0.010992
chr2__9350808__9358889___ASAP2	0.100527	-3.31435	0.004808
chr2__128172573__128174858___UGGT1	0.10054	-3.31416	0.011947
chr1__90916640__90941309___ZNF644	0.100574	-3.31367	0.009925
chr2__157284282__157312023___NA	0.10062	-3.31301	0.01243
chr14__63998914__64022863___SYNE2	0.100704	-3.31181	0.000306
chr3__20095364__20152365___KAT2B	0.100754	-3.31109	0.004999
chr1__224365879__224371423___CNIH4	0.100798	-3.31046	0.013124
chr14__92809300__92816421___GOLGA5	0.100852	-3.30969	0.011735
chr10__131940031__131945459___PPP2R2D	0.100863	-3.30953	0.013727
chr8__91008743__91024366___TMEM55A	0.10093	-3.30857	0.001348
chr13__41316846__41320824___NAA16	0.100954	-3.30823	0.01135
chr1__207526753__207717691___NA	0.101008	-3.30746	0.009722
chr9__96509673__96565483___CDC14B	0.101014	-3.30738	0.01434
chr5__157241646__157244478___ITK	0.101073	-3.30653	0.014188
chr8__123084162__123097441___TBC1D31	0.101115	-3.30592	0.010977
chr4__39904040__39925933___PDS5A	0.10121	-3.30457	0.013103
chr1__77916055__77918273___NEXN	0.101318	-3.30304	0.015885
chr3__37249698__37251484___GOLGA4	0.101414	-3.30167	0.012953
chr3__155910692__155922302___GMPS	0.101425	-3.30152	0.01254
chr12__75282251__75326527___CAPS2	0.101454	-3.3011	0.014124
chr9__68876677__68940790___PIP5K1B	0.101497	-3.30049	0.012608
chr12__28255581__28362515___CCDC91	0.1015	-3.30045	0.012608
chr3__17586353__17625224___TBC1D5	0.10151	-3.3003	0.014865
chr3__125451305__125460860___SNX4	0.101513	-3.30026	0.01113
chrX__123696021__123697751___THOC2	0.101566	-3.2995	0.013937
chr2__106830066__106834146___ST6GAL2	0.101573	-3.29941	0.003619
chr5__142131808__142144676___NDFIP1	0.101623	-3.2987	0.012953
chr4__177339707__177353728___NEIL3	0.101641	-3.29844	0.012475
chr12__100097365__100103951___UHRF1BP1L	0.101649	-3.29833	0.01396
chr17__63792412__63800617___DDX42	0.101677	-3.29793	0.012485
chr13__49168613__49175541___FNDC3A	0.101735	-3.29711	0.014865
chr13__37044078__37051583___SUPT20H	0.101736	-3.2971	0.013995
chr14__73089049__73089455___RBM25	0.101738	-3.29707	0.01302
chr11__76513386__76523291___C11orf30	0.101764	-3.29671	0.014836
chr19__34431861__34467014___UBA2	0.101768	-3.29664	0.010973
chr10__87864454__87936905___PTEN	0.101803	-3.29614	0.011213
chr2__201129729__201149835___CFLAR	0.101866	-3.29526	0.014219
chr18__23515856__23516423___C18orf8	0.101902	-3.29474	0.009284
chr4__127930683__127938838___MFSD8	0.101911	-3.29462	0.013856
chr10__101793913__101795480___MGEA5	0.101949	-3.29408	0.003421

chr15__93004617__93009323___CHD2	0.101967	-3.29383	0.011021
chr2__151441905__151443709___RIF1	0.102096	-3.29201	0.011053
chrX__118396970__118398470___WDR44	0.102114	-3.29175	0.011582
chr17__1354211__1362008___YWHAE	0.102179	-3.29083	0.013441
chr3__4410865__4420146___SUMF1	0.102197	-3.29058	0.011623
chr16__75640184__75641723___KARS	0.102376	-3.28806	0.01175
chr17__47370437__47414919___EFCAB13	0.102378	-3.28803	0.014672
chr15__69426070__69438405___KIF23	0.102456	-3.28692	0.011975
chr5__50399859__50411383___EMB	0.102463	-3.28683	0.013944
chr13__32770654__32771693___PDS5B	0.102547	-3.28564	0.013342
chr1__219179147__219211752___LYPLAL1	0.102582	-3.28515	0.01145
chr2__61115979__61121276___KIAA1841	0.1026	-3.2849	0.010974
chr9__26923178__26928408___PLAA	0.102726	-3.28313	0.010266
chr22__29282390__29287134___EWSR1	0.10273	-3.28307	0.012089
chr15__67630888__67664645___MAP2K5	0.102816	-3.28187	0.01523
chr15__65700544__65738875___DENND4A	0.102872	-3.28108	0.011298
chr22__30456402__30457525___SEC14L3	0.102915	-3.28047	0.012186
chrX__68192919__68201710___OPHN1	0.102927	-3.28031	0.012137
chr3__136398749__136477412___STAG1	0.102998	-3.27932	0.012369
chr3__183736718__183762279___YEATS2	0.103102	-3.27786	0.014398
chr15__49632159__49634794___DTWD1	0.103312	-3.27491	0.01354
chr7__131387120__131429145___MKLN1	0.103528	-3.27191	0.015823
chr1__236803428__236829268___MTR	0.103537	-3.27178	0.012118
chr5__133006759__133022906___ZCCHC10	0.103664	-3.27001	0.013944
chrX__129920457__129921587___UTP14A	0.103742	-3.26893	0.013285
chr1__21715389__21721166___USP48	0.103798	-3.26814	0.015691
chr9__77337255__77345142___VPS13A	0.103816	-3.26791	0.01299
chr18__37066890__37067545___KIAA1328	0.103822	-3.26781	0.01348
chr7__93334117__93341575___CCDC132	0.103832	-3.26768	0.013124
chr12__71656885__71660427___ZFC3H1	0.103844	-3.26751	0.016735
chr12__68828771__68839801___MDM2	0.103868	-3.26717	0.013981
chr10__42816599__42817494___BMS1	0.103871	-3.26713	0.014782
chr19__5641594__5641950___SAFB	0.103896	-3.26679	0.01406
chr4__55403236__55417985___TMEM165	0.10396	-3.26591	0.015386
chr1__84865385__84866138___LPAR3	0.10403	-3.26492	0.012875
chr18__62539681__62556297___ZCCHC2	0.104057	-3.26456	0.01302
chr17__56844019__56845809___DGKE	0.104081	-3.26423	0.013995
chr16__21612645__21614318___METTL9	0.104122	-3.26366	0.011253
chr10__5773842__5811956___GDI2	0.104171	-3.26298	0.014845
chr4__42001616__42023384___SLC30A9	0.104192	-3.26268	0.005573
chr16__71655240__71658815___PHLPP2	0.104224	-3.26224	0.014821
chr2__23857415__23869761___ATAD2B	0.104251	-3.26187	0.013839
chr13__19824920__19851957___ZMYM5	0.104258	-3.26177	0.015823
chr7__112286873__112296311___ZNF277	0.104297	-3.26124	0.0141
chr7__16258390__16301466___ISPD	0.104397	-3.25985	0.01247
chr6__42637011__42642481___UBR2	0.104399	-3.25982	0.015251

chr10__100937402__100944128___FAM178A	0.104438	-3.25928	0.01348
chr1__51840226__51855388___NRD1	0.104554	-3.25768	0.011914
chr17__27301788__27303635___WSB1	0.104608	-3.25693	0.003782
chr19__48230438__48241063___CARD8	0.104695	-3.25574	0.01523
chr17__47402132__47429961___EFCAB13	0.104738	-3.25514	0.012525
chr3__60765524__60767098___FHIT	0.104746	-3.25504	0.012622
chr18__76862186__76865026___ZNF236	0.104779	-3.25458	0.016013
chr3__20174249__20175055___SGOL1	0.104783	-3.25453	0.012648
chr6__119301988__119306992___MAN1A1	0.104787	-3.25446	0.010764
chr10__179994__221356___ZMYND11	0.104787	-3.25447	0.013995
chr2__33523879__33534400___RASGRP3	0.10488	-3.25319	0.014817
chr17__5346790__5368468___RABEP1	0.104889	-3.25307	0.015659
chr3__69038564__69042912___TMF1	0.104923	-3.2526	0.013229
chr6__108854225__108858271___ARMC2	0.104936	-3.25242	0.012385
chr5__163473179__163475672___HMMR	0.104957	-3.25212	0.011935
chr9__19093171__19096769___HAUS6	0.104963	-3.25205	0.001922
chr15__92924321__92949076___CHD2	0.104981	-3.25181	0.010515
chr2__171117739__171132092___TLK1	0.105064	-3.25066	0.011317
chr4__48842636__48857365___OCIAD1	0.105116	-3.24995	0.013727
chr17__47402132__47440502___EFCAB13	0.105181	-3.24905	0.015235
chr2__200949554__200958133___ORC2	0.105181	-3.24906	0.014283
chr12__128926359__128927154___GLT1D1	0.105189	-3.24894	0.01359
chr17__27304780__27309272___WSB1	0.105195	-3.24886	0.015498
chr3__146189799__146222092___NA	0.105252	-3.24808	0.014186
chr2__33128432__33222151___LTBP1	0.105313	-3.24724	0.011956
chr7__139279318__139284574___UBN2	0.105327	-3.24705	0.015403
chr10__30313891__30349277___MTPAP	0.105335	-3.24694	0.014186
chr12__68757148__68759239___SLC35E3	0.105419	-3.24579	0.011605
chr14__72693076__72731934___DPF3	0.105457	-3.24527	0.015842
chr12__120554718__120563943___RNF10	0.10546	-3.24524	0.013908
chr17__3814322__3818572___C17orf85	0.105469	-3.2451	0.014358
chr6__4854525__4892379___CDYL	0.105498	-3.24471	0.013443
chr17__67891844__67903918___BPTF	0.105558	-3.2439	0.012608
chr8__94851553__94866191___INTS8	0.105745	-3.24134	0.015806
chr11__120457721__120467308___ARHGEF12	0.105889	-3.23938	0.015559
chr17__31966147__31988497___SUZ12	0.105966	-3.23833	0.014672
chr9__26861066__26887513___CAAP1	0.106068	-3.23694	0.01111
chr5__138006990__138019146___FAM13B	0.106078	-3.23681	0.011238
chr5__119097979__119121139___DMXL1	0.106086	-3.2367	0.01067
chr5__79640851__79657001___PAPD4	0.106124	-3.23617	0.012497
chr5__102257115__102270806___SLCO4C1	0.106195	-3.23521	0.015806
chr4__145110968__145121391___ABCE1	0.106212	-3.23498	0.013995
chr17__39297127__39303639___FBXL20	0.106239	-3.23462	0.014672
chr12__70342107__70346324___CNOT2	0.106331	-3.23337	0.014817
chr19__53805280__53814988___NLRP12	0.106333	-3.23334	0.017321
chr6__33406196__33406875___KIFC1	0.106525	-3.23074	0.012137

chr8__98526742__98596169___STK3	0.106563	-3.23022	0.013167
chr14__103654564__103654825___KLC1	0.106578	-3.23002	0.016422
chr22__41154995__41173784___EP300	0.106611	-3.22957	0.012684
chr12__89459638__89461306___POC1B	0.106666	-3.22883	0.014428
chr16__71669275__71681905___PHLPP2	0.106695	-3.22844	0.014337
chr15__42775135__42840433___TTBK2	0.106806	-3.22694	0.011505
chr5__43675511__43677806___NNT	0.10682	-3.22675	0.010843
chr9__128750616__128751527___ZER1	0.106834	-3.22655	0.014124
chr11__85981745__86031611___PICALM	0.106884	-3.22589	0.012717
chr17__5410703__5414134___NUP88	0.1069	-3.22567	0.014679
chr18__2750043__2750507___SMCHD1	0.106924	-3.22534	0.01243
chr3__12599691__12604289___RAF1	0.10693	-3.22526	0.014438
chr10__5765987__5811956___GDI2	0.106955	-3.22492	0.011831
chr1__155777622__155784089___GON4L	0.107048	-3.22367	0.013124
chr15__52605133__52613857___FAM214A	0.107124	-3.22264	0.011914
chr4__145823422__145849561___ZNF827	0.107128	-3.2226	0.016077
chr9__19423862__19424841___ACER2	0.107147	-3.22234	0.012498
chr7__23604086__23611553___CCDC126	0.107187	-3.2218	0.014835
chr16__11875761__11898035___GSPT1	0.107288	-3.22044	0.015403
chr17__67891847__67894165___BPTF	0.107296	-3.22033	0.01299
chr12__94366714__94376017___CCDC41	0.107299	-3.22029	0.013937
chrX__2392354__2425304___DHRSX	0.107373	-3.21929	0.01406
chr14__96833467__96945382___NA	0.107389	-3.21908	0.01299
chr9__125298890__125302826___GAPVD1	0.107397	-3.21897	0.013707
chr1__155612418__155747896___NA	0.107416	-3.21871	0.014359
chr2__177232392__177234271___NFE2L2	0.107453	-3.21822	0.012596
chr12__102148230__102182627___PARPBP	0.107515	-3.21739	0.01587
chr11__121045674__121047667___TBCEL	0.10755	-3.21692	0.010604
chr1__113952766__113968648___HIPK1	0.107581	-3.2165	0.01512
chr17__59910562__59936541___RPS6KB1	0.107611	-3.2161	0.01512
chr15__65478880__65481615___DPP8	0.107632	-3.21582	0.013345
chrX__17029526__17103779___REPS2	0.107634	-3.2158	0.017392
chr9__85618983__85712566___AGTPBP1	0.107643	-3.21568	0.014438
chr8__21974670__21995599___XPO7	0.107669	-3.21533	0.014186
chr11__72984088__73083740___FCHSD2	0.107675	-3.21524	0.011956
chr4__121811583__121814047___EXOSC9	0.107699	-3.21492	0.013103
chr3__179764002__179765848___USP13	0.107741	-3.21436	0.014124
chr8__55785719__55796152___TGS1	0.107751	-3.21423	0.01316
chr7__128641203__128648982___NA	0.107758	-3.21414	0.011956
chr10__119580471__119580846___TIAL1	0.107811	-3.21343	0.017492
chr4__53145333__53145582___SCFD2	0.10782	-3.2133	0.012453
chr15__49011731__49017628___SECISBP2L	0.107955	-3.2115	0.017287
chr20__49067190__49070297___CSE1L	0.108077	-3.20987	0.015546
chr1__15529088__15548428___DNAJC16	0.108145	-3.20896	0.015433
chr2__182952405__182953331___NCKAP1	0.108183	-3.20845	0.01406
chr13__20058575__20059562___ZMYM2	0.108237	-3.20773	0.016718

chr5__171964198__171997051___FBXW11	0.10827	-3.20729	0.013995
chr13__77744283__77753358___SLAIN1	0.108276	-3.20721	0.013995
chr3__15766234__15814309___ANKRD28	0.108293	-3.20698	0.014244
chr6__42662184__42676873___UBR2	0.108339	-3.20638	0.011213
chrX__68518770__68521497___YIPF6	0.10835	-3.20623	0.014979
chr5__93958777__94053227___FAM172A	0.108419	-3.20531	0.015823
chr6__13632370__13641307___RANBP9	0.108635	-3.20244	0.012713
chr20__50096483__50098981___UBE2V1	0.108719	-3.20133	0.01523
chr1__88786104__88806017___PKN2	0.108759	-3.2008	0.013012
chr8__30680904__30700135___GSR	0.108803	-3.2002	0.017401
chr9__34306252__34311371___KIF24	0.108881	-3.19918	0.013995
chr15__40383228__40392023___KNSTRN	0.108911	-3.19878	0.012397
chr1__235213769__235240451___ARID4B	0.108913	-3.19875	0.014355
chr3__136398749__136423044___STAG1	0.10892	-3.19865	0.015576
chr12__50988382__51010766___SLC11A2	0.108938	-3.19842	0.015205
chr17__30855143__30869646___ATAD5	0.108976	-3.19791	0.014982
chr5__10415488__10426522___MARCH6	0.108989	-3.19774	0.016077
chr13__50027207__50044768___DLEU2	0.109018	-3.19736	0.015314
chr19__21454383__21456588___NA	0.10915	-3.19562	0.014728
chr12__76059798__76060279___NAP1L1	0.10915	-3.19562	0.014555
chr7__35781209__35794022___AC007551.3	0.109164	-3.19543	0.013978
chr2__180982018__180991871___UBE2E3	0.109168	-3.19537	0.017401
chr4__1699564__1700070___SLBP	0.10918	-3.19522	0.013087
chr10__128103215__128119319___MKI67	0.109216	-3.19474	0.015885
chr17__47402132__47404633___EFCAB13	0.109305	-3.19357	0.015659
chr11__34450988__34464235___CAT	0.109352	-3.19295	0.013434
chr2__61112518__61118116___KIAA1841	0.109416	-3.1921	0.013873
chr14__34586230__34609742___SNX6	0.109531	-3.19059	0.016077
chr8__123077111__123128513___TBC1D31	0.109643	-3.18912	0.013109
chr17__35420274__35423068___SLFN12	0.109673	-3.18871	0.013339
chr5__176496486__176500146___FAF2	0.109743	-3.1878	0.015659
chr16__27434347__27437687___IL21R	0.109755	-3.18764	0.017009
chr6__75666712__75678927___SENP6	0.109814	-3.18686	0.01656
chr9__7040470__7049200___KDM4C	0.109908	-3.18563	0.017303
chr8__123359577__123380677___ATAD2	0.110016	-3.18421	0.016077
chr12__70278132__70319364___CNOT2	0.110058	-3.18367	0.015842
chr16__47463899__47589102___PHKB	0.11012	-3.18285	0.013908
chr8__99142974__99275254___VPS13B	0.110125	-3.18278	0.0141
chr2__218474630__218482234___USP37	0.110192	-3.18191	0.014681
chr17__30785919__30796337___CRLF3	0.110203	-3.18176	0.013345
chr12__122568261__122574380___KNTC1	0.110336	-3.18003	0.014244
chr4__106164392__106248306___TBCK	0.110378	-3.17947	0.01587
chr17__20096631__20205912___SPECC1	0.110436	-3.17871	0.014124
chr11__6608601__6611452___NA	0.110473	-3.17823	0.017163
chr6__42573734__42617507___UBR2	0.110496	-3.17794	0.014679
chr16__89895038__89900794___TCF25	0.110518	-3.17765	0.01826

chrX__3822073__3826729___LOC389906	0.110521	-3.1776	0.014124
chr10__92616737__92630364___KIF11	0.110523	-3.17758	0.013981
chr5__122801869__122803613___SNX2	0.110584	-3.17679	0.015485
chr15__56666395__56682477___ZNF280D	0.110615	-3.17638	0.017492
chr14__61721509__61741188___HIF1A	0.110706	-3.1752	0.015306
chr18__47829474__47896809___NA	0.110733	-3.17484	0.014124
chr15__49235851__49283718___GALK2	0.110752	-3.17459	0.015
chr14__35099252__35108236___PPP2R3C	0.110771	-3.17435	0.013859
chr2__232832857__232833093___GIGYF2	0.110831	-3.17356	0.017239
chr17__61987007__61995365___MED13	0.110834	-3.17353	0.015806
chr5__61472681__61473037___ZSWIM6	0.11086	-3.17318	0.013908
chr11__68189570__68190152___SUV420H1	0.110902	-3.17264	0.015576
chr8__60794986__60808272___CHD7	0.110931	-3.17227	0.013441
chr15__85664563__85710645___AKAP13	0.110956	-3.17194	0.013908
chr1__24649971__24651612___SRRM1	0.110988	-3.17153	0.013288
chr11__130126700__130135715___APLP2	0.111046	-3.17077	0.015842
chr7__93259550__93297243___CCDC132	0.111097	-3.17011	0.016024
chr1__158674329__158674675___SPTA1	0.111224	-3.16846	0.011991
chr6__149572285__149580723___GINM1	0.111311	-3.16733	0.011956
chr1__247157000__247159813___ZNF124	0.111341	-3.16695	0.01396
chr11__3723157__3753408___NUP98	0.111539	-3.16438	0.012053
chr7__112895569__112915447___C7orf60	0.111556	-3.16416	0.014124
chr5__75685207__75702810___POC5	0.111609	-3.16348	0.017812
chr5__169747396__169761625___DOCK2	0.111633	-3.16316	0.017678
chr1__201854595__201858994___IPO9	0.111649	-3.16296	0.01523
chr5__69197053__69208359___CENPH	0.111754	-3.1616	0.013995
chr19__54222943__54280299___NA	0.111758	-3.16155	0.01834
chr13__20574380__20592404___IFT88	0.111797	-3.16104	0.013995
chr7__154967816__154998784___PAXIP1	0.111821	-3.16074	0.015546
chr11__70354301__70356254___PPFIA1	0.111948	-3.15909	0.013847
chr15__92885515__92901299___NA	0.111957	-3.15898	0.016715
chr11__47166268__47168251___ARFGAP2	0.111969	-3.15882	0.016508
chr10__7243558__7285954___SFMBT2	0.111987	-3.15859	0.004476
chr4__139137630__139168042___ELF2	0.112009	-3.15831	0.006209
chr4__15612266__15644708___FBXL5	0.112061	-3.15765	0.017954
chr5__71495250__71504751___BDP1	0.112069	-3.15754	0.000606
chr21__15808809__15827203___USP25	0.112071	-3.15752	0.013918
chr16__21962460__21976243___UQCRC2	0.112088	-3.1573	0.017009
chr1__155767425__155777820___GON4L	0.112133	-3.15672	0.014032
chr7__155665175__155678684___RBM33	0.112176	-3.15616	0.015485
chr17__28163543__28185265___NLK	0.112187	-3.15602	0.01523
chr1__185299376__185301185___IVNS1ABP	0.112209	-3.15574	0.01348
chr12__102148230__102205152___NA	0.112217	-3.15563	0.015899
chr15__66513988__66540210___ZWILCH	0.112268	-3.15498	0.01515
chr17__5399552__5416682___NUP88	0.112435	-3.15284	0.016975
chr18__69895701__69947433___CD226	0.112472	-3.15236	0.01609

chr11__601574__603436___PHRF1	0.112525	-3.15169	0.016116
chr16__19616114__19626223___C16orf62	0.112546	-3.15142	0.006253
chr16__72373830__72391215___NA	0.11262	-3.15047	0.012503
chr6__13641199__13644729___RANBP9	0.112706	-3.14936	0.015669
chr6__156829227__156901525___ARID1B	0.112754	-3.14875	0.013684
chr2__68513080__68545312___APLF	0.112805	-3.1481	0.013441
chr6__37279304__37291357___TBC1D22B	0.112868	-3.14729	0.017436
chr2__32439508__32443588___BIRC6	0.112872	-3.14725	0.017392
chr1__198220999__198279061___NEK7	0.112898	-3.14691	0.015659
chr15__65731642__65761438___DENND4A	0.113002	-3.14557	0.017076
chr7__139083780__139089759___ZC3HAV1	0.113007	-3.14552	0.014021
chr2__227491547__227536993___AGFG1	0.113019	-3.14536	0.015659
chr18__21020151__21044186___ROCK1	0.113085	-3.14452	0.016067
chr1__66534246__66643719___SGIP1	0.113086	-3.1445	0.013908
chr1__92605307__92625934___EVI5	0.113098	-3.14435	0.016461
chr16__3780732__3782926___CREBBP	0.113139	-3.14383	0.014778
chr2__88801099__88805408___ANKRD36BP2	0.113142	-3.1438	0.015403
chr20__34477772__34481206___ITCH	0.113155	-3.14363	0.016581
chr19__17772457__17772741___FCHO1	0.11322	-3.1428	0.015465
chr11__94445810__94461036___MRE11A	0.113268	-3.14218	0.015659
chr7__105142008__105146658___SRPK2	0.11327	-3.14217	0.018273
chr1__10404161__10408140___PGD	0.11328	-3.14204	0.017216
chr15__92945821__92956649___CHD2	0.113308	-3.14167	0.012953
chr9__135866456__135883078___CAMSAP1	0.113416	-3.1403	0.015115
chr2__181458196__181535566___ITGA4	0.113587	-3.13813	0.015723
chr22__40277077__40285770___TNRC6B	0.113639	-3.13748	0.004084
chr8__99467414__99481802___VPS13B	0.113744	-3.13614	0.014904
chr15__74805718__74806064___NA	0.11378	-3.13568	0.015659
chr15__51535663__51547408___DMXL2	0.113827	-3.13509	0.015796
chr14__67398007__67402868___PLEK2	0.11384	-3.13492	0.019127
chr10__31373018__31502509___ZEB1	0.113872	-3.13452	0.016693
chr12__69365633__69370975___YEATS4	0.113906	-3.13408	0.013931
chr10__45533110__45534914___MARCH8	0.11395	-3.13353	0.011669
chrX__10063445__10094281___WWC3	0.113974	-3.13323	0.013856
chr17__44154556__44155411___C17orf53	0.114059	-3.13215	0.017062
chr14__52470037__52491005___TXNDC16	0.114118	-3.1314	0.017078
chr4__184661774__184678394___PRIMPOL	0.114131	-3.13124	0.013441
chr17__78092933__78093763___TNRC6C	0.114323	-3.12881	0.012953
chr16__19706592__19711440___KNOP1	0.114336	-3.12865	0.015945
chr13__77205256__77212160___MYCBP2	0.114358	-3.12837	0.01881
chr2__151438684__151461289___RIF1	0.114386	-3.12801	0.015576
chr2__44484877__44492454___CAMKMT	0.114388	-3.12799	0.015314
chr17__32173831__32201056___RHOT1	0.114412	-3.12769	0.01609
chr8__140539320__140541358___AGO2	0.114518	-3.12636	0.014782
chr17__82905936__82911789___TBCD	0.1146	-3.12533	0.020127
chr15__22667898__22681605___WHAMMP3	0.114654	-3.12465	0.016091

chr1__100049909__100069685___HIAT1	0.114679	-3.12433	0.016422
chr8__99502836__99521010___VPS13B	0.114708	-3.12396	0.014782
chr2__224495832__224514772___CUL3	0.114766	-3.12323	0.017678
chr8__99384208__99521010___VPS13B	0.114767	-3.12322	0.016035
chr7__35890668__35898383___SEPT7	0.114896	-3.12159	0.004378
chr7__32869984__32879942___KBTBD2	0.114961	-3.12078	0.012735
chr8__31085166__31096850___WRN	0.114974	-3.12062	0.013109
chr1__154170400__154176248___TPM3	0.115024	-3.12	0.018636
chr8__109409865__109420690___PKHD1L1	0.115046	-3.11972	0.016461
chr11__46776255__46788773___CKAP5	0.11506	-3.11954	0.019233
chr2__15394227__15396475___NBAS	0.115093	-3.11913	0.012707
chr3__25642322__25645455___TOP2B	0.115108	-3.11894	0.020645
chr4__122927634__122979386___SPATA5	0.115122	-3.11877	0.017857
chr20__49849579__49855581___SLC9A8	0.115158	-3.11832	0.013963
chr2__218546919__218562813___USP37	0.115193	-3.11787	0.014937
chr17__49732280__49732720___FAM117A	0.115304	-3.11649	0.017145
chr10__96544076__96559736___TM9SF3	0.115319	-3.1163	0.017287
chr11__46795594__46809874___CKAP5	0.115324	-3.11623	0.014422
chr2__37101923__37104132___NA	0.115369	-3.11567	0.016035
chr10__7769216__7780307___KIN	0.115375	-3.1156	0.016795
chr17__60222409__60226231___USP32	0.115384	-3.11548	0.016735
chr6__13579451__13600949___SIRT5	0.115404	-3.11523	0.019892
chr8__31141430__31150455___WRN	0.115456	-3.11458	0.018096
chr10__124021256__124046724___CHST15	0.115532	-3.11364	0.016103
chr16__16007816__16036603___ABCC1	0.115541	-3.11352	0.014032
chr21__34102835__34103519___SLC5A3	0.115588	-3.11293	0.018318
chr11__31456260__31469797___IMMP1L	0.115686	-3.11172	0.017363
chr11__125597059__125608289___STT3A	0.115734	-3.11111	0.015595
chr16__14580874__14593378___PARN	0.115752	-3.11089	0.019273
chr22__41135813__41141222___EP300	0.115829	-3.10993	0.016715
chr7__107281300__107283732___COG5	0.11585	-3.10968	0.016035
chr2__74165218__74172752___MOB1A	0.115892	-3.10915	0.017231
chr17__16186554__16194639___NCOR1	0.115925	-3.10874	0.018842
chrX__68513327__68522917___YIPF6	0.116011	-3.10767	0.015447
chrX__124022531__124051394___STAG2	0.11615	-3.10594	0.016035
chr1__86715724__86735179___SH3GLB1	0.116182	-3.10554	0.005084
chr12__26982773__26983596___TM7SF3	0.116189	-3.10545	0.015447
chr14__21263667__21268668___HNRNPC	0.116193	-3.1054	0.015842
chr12__122515105__122522299___RSRC2	0.116222	-3.10504	0.018779
chr3__37108637__37121691___LRRFIP2	0.116237	-3.10486	0.016396
chrY__13355003__13369349___UTY	0.116261	-3.10456	0.016202
chr14__73282359__73287314___NUMB	0.116314	-3.10391	0.017287
chr4__146305926__146308459___SLC10A7	0.116376	-3.10313	0.012953
chr8__67095293__67112075___CSPP1	0.116421	-3.10257	0.016396
chr3__196053418__196069568___TFRC	0.116432	-3.10245	0.019188
chr3__25628847__25645455___TOP2B	0.116456	-3.10215	0.017078

chr9__123089758__123099549___RABGAP1	0.116576	-3.10066	0.015485
chr1__45600385__45602365___NASP	0.116609	-3.10025	0.019233
chr9__121088296__121115200___CNTRL	0.116635	-3.09993	0.018976
chr9__85692689__85723868___AGTPBP1	0.116835	-3.09746	0.01677
chr11__16283756__16290180___SOX6	0.116871	-3.09701	0.013282
chr14__52711101__52711524___PSMC6	0.117006	-3.09535	0.000439
chr1__11016844__11018873___TARDBP	0.117068	-3.09459	0.016653
chr14__73147795__73148094___PSEN1	0.117314	-3.09156	0.006877
chr18__216486__224994___THOC1	0.11735	-3.09111	0.01609
chrX__24775197__24843677___POLA1	0.117364	-3.09093	0.015789
chr20__5557945__5586269___GPCPD1	0.117418	-3.09027	0.016405
chr12__62349221__62384302___USP15	0.117624	-3.08774	0.021392
chr20__44987132__44995257___STK4	0.11772	-3.08657	0.018411
chr22__20043355__20048328___TANGO2	0.117728	-3.08648	0.016492
chr2__55558775__55588956___SMEK2	0.117745	-3.08626	0.018391
chr1__95143891__95191681___TMEM56	0.117757	-3.08611	0.016663
chr7__77765495__77778814___RSBN1L	0.117818	-3.08537	0.01523
chr5__73056065__73068779___FCHO2	0.117828	-3.08524	0.018373
chr4__82428018__82428446___HNRNPDL	0.117868	-3.08476	0.005871
chr10__11594631__11601980___USP6NL	0.117875	-3.08466	0.01439
chr8__42459896__42463090___SLC20A2	0.117898	-3.08439	0.013853
chr1__179335506__179343635___SOAT1	0.117921	-3.08411	0.019761
chr5__79645123__79682061___PAPD4	0.117949	-3.08377	0.017657
chr15__63732924__63756748___HERC1	0.117955	-3.08369	0.014835
chr14__103428387__103492034___MARK3	0.117965	-3.08356	0.016054
chr1__168231514__168243069___NA	0.118016	-3.08295	0.019555
chr17__45475100__45478147___PLEKHM1	0.118168	-3.08109	0.017062
chr20__19580000__19585544___SLC24A3	0.118195	-3.08076	0.015312
chr14__32117143__32152528___ARHGAP5	0.118225	-3.08039	0.020711
chr3__141963812__141993585___TFDP2	0.118285	-3.07966	0.01681
chr1__26268483__26272071___CEP85	0.118365	-3.07868	0.016735
chr22__25663630__25674528___ADRBK2	0.118376	-3.07855	0.017898
chr1__35381259__35381758___ZMYM4	0.118408	-3.07816	0.015485
chr3__172760156__172783909___ECT2	0.118442	-3.07775	0.014838
chr11__43403998__43451265___TTC17	0.118443	-3.07774	0.013802
chr14__71413948__71512845___NA	0.118474	-3.07736	0.016735
chr3__47097955__47101555___SETD2	0.118529	-3.07669	0.006796
chr8__140879471__140890769___PTK2	0.118587	-3.07598	0.021663
chr1__62816575__62821209___ATG4C	0.118595	-3.07589	0.017287
chr1__163336751__163349080___NUF2	0.118658	-3.07512	0.019519
chr7__155737530__155745602___RBM33	0.118684	-3.07481	0.018625
chr17__5405057__5416682___NUP88	0.118724	-3.07431	0.016035
chr15__52593578__52600235___FAM214A	0.118807	-3.07331	0.016405
chr1__62441488__62443319___USP1	0.118884	-3.07237	0.013671
chr16__11875761__11876175___GSPT1	0.118896	-3.07223	0.019539
chr6__154199668__154223243___IPCEF1	0.118974	-3.07128	0.017793

chr16__46674314__46677398___VPS35	0.118986	-3.07114	0.020449
chr2__214780560__214792445___BARD1	0.119015	-3.07078	0.018779
chr1__155676548__155680456___YY1AP1	0.119064	-3.0702	0.004029
chr6__41871298__41891875___USP49	0.119068	-3.07015	0.016669
chr7__36399079__36415884___ANLN	0.119072	-3.0701	0.007749
chr1__180019949__180021009___CEP350	0.119092	-3.06985	0.016818
chr11__94445810__94447438___MRE11A	0.119125	-3.06945	0.021196
chr15__65706091__65756472___DENND4A	0.119146	-3.0692	0.016975
chr12__50435488__50441643___LARP4	0.119149	-3.06916	0.017314
chr8__58565019__58572314___SDCBP	0.119162	-3.069	0.016318
chr2__9356047__9368519___ASAP2	0.119239	-3.06807	0.017213
chr17__29517453__29534300___TAOK1	0.119348	-3.06676	0.018922
chr6__24687405__24687693___ACOT13	0.119474	-3.06523	0.015863
chr2__24643966__24683128___NCOA1	0.119589	-3.06384	0.006269
chr2__208642225__208656989___LOC101927960	0.119711	-3.06237	0.017009
chr4__42022838__42039053___SLC30A9	0.119776	-3.06159	0.016305
chr17__8551185__8551981___MYH10	0.119796	-3.06135	0.019273
chr16__74923926__74951543___WDR59	0.119841	-3.0608	0.015849
chr12__411747__438554___CCDC77	0.119842	-3.06079	0.019471
chr13__27075191__27116596___USP12	0.119857	-3.06061	0.006209
chr14__49806021__49832277___NEMF	0.11989	-3.06021	0.01314
chr6__75659262__75666941___SENP6	0.119966	-3.0593	0.01915
chr1__169477155__169477757___SLC19A2	0.119992	-3.05899	0.017145
chr5__134199086__134206131___PPP2CA	0.120014	-3.05873	0.017316
chr2__62707164__62874532___EHBP1	0.120075	-3.05799	0.016928
chr1__108782422__108796726___STXBP3	0.120122	-3.05743	0.017221
chr1__243293091__243330692___SDCCAG8	0.120126	-3.05738	0.00755
chr6__35857261__35891013___SRPK1	0.120141	-3.0572	0.017392
chr11__108327645__108335961___ATM	0.120262	-3.05575	0.019293
chr12__32619698__32633689___FGD4	0.120266	-3.0557	0.01915
chr8__26338890__26354633___PPP2R2A	0.120318	-3.05508	0.005445
chr9__112250929__112262599___PTBP3	0.120319	-3.05507	0.019188
chr15__34152790__34163690___KATNBL1	0.120327	-3.05496	0.016998
chr9__15486006__15490124___PSIP1	0.120348	-3.05472	0.021224
chr3__47686049__47701402___SMARCC1	0.120372	-3.05443	0.015546
chr2__168063500__168075231___STK39	0.120488	-3.05304	0.017208
chr15__63529014__63563008___USP3	0.120533	-3.0525	0.016116
chr17__39297127__39343241___FBXL20	0.120537	-3.05245	0.014845
chr15__49129477__49130816___COPS2	0.12059	-3.05182	0.015447
chr5__146483540__146498686___TCERG1	0.120628	-3.05136	0.016412
chr1__15916128__15922349___SPEN	0.120632	-3.05131	0.017635
chr10__22541804__22542047___PIP4K2A	0.120689	-3.05064	0.016715
chr2__171448681__171453213___DCAF17	0.120782	-3.04953	0.017678
chr1__95134782__95136731___TMEM56TMEM56-RWDD3	0.120797	-3.04934	0.016257
chr2__148051910__148054449___MBD5	0.120798	-3.04933	0.014124

chr10__124942457__124987504___ZRANB1	0.120856	-3.04864	0.013694
chr7__30323642__30326497___ZNRF2	0.120904	-3.04807	0.016461
chr17__29648144__29650800___SSH2	0.120909	-3.048	0.007769
chr1__235172618__235196115___ARID4B	0.12091	-3.048	0.016581
chr14__54408745__54411706___CDKN3	0.120924	-3.04783	0.017062
chr7__104161072__104188381___ORC5	0.120981	-3.04715	0.014332
chr15__56700933__56707306___ZNF280D	0.120989	-3.04706	0.015343
chr4__177339694__177353728___NEIL3	0.120994	-3.047	0.017062
chr2__174378923__174395635___CIR1	0.120997	-3.04695	0.016091
chr17__42727662__42730918___EZH1	0.121015	-3.04675	0.018251
chr2__223998115__224001922___SERPINE2	0.121055	-3.04627	0.019741
chr17__29507896__29510992___TAOK1	0.121076	-3.04601	0.020791
chr4__83416731__83448961___HELQ	0.121079	-3.04598	0.016913
chr7__139269394__139279360___UBN2	0.121081	-3.04595	0.020449
chr3__197115927__197149796___DLG1	0.121081	-3.04596	0.017714
chr17__12095575__12113360___MAP2K4	0.121092	-3.04582	0.020449
chr11__47486750__47500932___CELF1	0.121198	-3.04456	0.015504
chr2__55577315__55588956___SMEK2	0.121279	-3.0436	0.020449
chr1__27838699__27843330___PPP1R8	0.121282	-3.04357	0.01981
chr7__158631644__158646563___NCAPG2	0.121292	-3.04344	0.019188
chr14__58306022__58329604___ARID4A	0.121292	-3.04345	0.017678
chr1__70292388__70324957___ANKRD13C	0.121354	-3.04271	0.021995
chr9__77794463__77931856___GNAQ	0.121428	-3.04182	0.017388
chr14__49789146__49831361___NEMF	0.121442	-3.04166	0.018096
chr11__34947506__34970286___PDHX	0.121478	-3.04123	0.018248
chr12__50430495__50454417___LARP4	0.121707	-3.03852	0.020039
chr4__82827369__82829058___SEC31A	0.12174	-3.03813	0.019367
chr1__62803719__62834852___ATG4C	0.121749	-3.03801	0.014869
chr12__95287664__95296258___VEZT	0.121756	-3.03794	0.021817
chr11__117238601__117246948___RNF214	0.121792	-3.03751	0.016625
chr11__18083535__18089510___SAAL1	0.121854	-3.03678	0.017107
chr1__25340474__25351693___TMEM50A	0.121928	-3.0359	0.008279
chr16__75411825__75412754___CFDP1	0.121935	-3.03581	0.018448
chr5__36984676__36995804___NIPBL	0.121944	-3.03571	0.01776
chr20__47235924__47236516___ZMYND8	0.121954	-3.03559	0.017403
chrY__12709388__12722187___USP9Y	0.121956	-3.03557	0.018625
chr14__50442732__50445194___MAP4K5	0.12196	-3.03552	0.017509
chr19__32615658__32643631___ANKRD27	0.122066	-3.03427	0.020305
chr2__23884765__23895970___ATAD2B	0.122076	-3.03415	0.019539
chr14__34758704__34762223___BAZ1A	0.122091	-3.03397	0.007355
chr18__2700539__2729409___SMCHD1	0.12213	-3.03351	0.021928
chr5__116291517__116303683___NA	0.122164	-3.0331	0.019796
chr14__88754512__88766867___EML5	0.122164	-3.03311	0.018297
chr11__78101093__78109581___ALG8	0.122169	-3.03305	0.021021
chr8__47279862__47294030___SPIDR	0.12227	-3.03186	0.018731
chr8__60533308__60533558___RAB2A	0.122287	-3.03165	0.017185

chr5__94909251__94924021___MCTP1	0.122362	-3.03078	0.008111
chr5__69371035__69374711___RAD17	0.122378	-3.03058	0.018625
chr3__148592184__148619264___NA	0.122426	-3.03002	0.019297
chr8__130152736__130188183___ASAP1	0.122463	-3.02958	0.018731
chr16__89418284__89431326___ANKRD11	0.122491	-3.02925	0.020316
chr1__185160833__185222036___SWT1	0.122513	-3.029	0.019796
chr16__15732485__15734462___MYH11	0.122609	-3.02787	0.01874
chr21__15864268__15877991___USP25	0.122616	-3.02778	0.017062
chr20__47623911__47628023___NCOA3	0.122645	-3.02744	0.022067
chr3__185687057__185689627___IGF2BP2	0.122714	-3.02662	0.004397
chr12__42374956__42398994___PPHLN1	0.122814	-3.02546	0.015151
chr17__30266885__30286902___BLMH	0.122868	-3.02481	0.022048
chr8__140735251__140752316___PTK2	0.122936	-3.02403	0.019188
chr14__31121422__31156886___HECTD1	0.122988	-3.02342	0.014904
chr4__82978883__82984876___LIN54	0.123019	-3.02305	0.019233
chr5__115532961__115542901___FEM1C	0.123022	-3.02302	0.022795
chr7__91941095__92023009___AKAP9	0.123108	-3.02201	0.017965
chr21__33414888__33421685___IFNGR2	0.123284	-3.01994	0.019555
chr21__15762891__15805258___USP25	0.123294	-3.01983	0.020101
chr1__207616575__207620065___CR1	0.123303	-3.01972	0.018581
chr11__108192118__108197420___NPAT	0.123328	-3.01943	0.016735
chr2__24564295__24673463___NCOA1	0.123376	-3.01887	0.015837
chr22__21805850__21819501___MAPK1	0.123398	-3.01861	0.023016
chr1__155921375__155925843___KIAA0907	0.123399	-3.0186	0.01776
chr1__77858938__77864028___FAM73A	0.123461	-3.01787	0.022694
chr13__32078834__32117473___FRY	0.123551	-3.01683	0.019539
chr16__81895807__81908591___PLCG2	0.123601	-3.01624	0.016944
chr9__93471263__93498886___FAM120A	0.123617	-3.01605	0.021995
chr5__34919840__34923234___BRIX1	0.123651	-3.01565	0.015806
chr1__150343309__150344547___PRPF3	0.123779	-3.01416	0.021088
chr8__140585091__140605914___AGO2	0.123895	-3.01281	0.019519
chr19__24126254__24128180___ZNF254	0.123988	-3.01173	0.020813
chr8__21991868__22004030___XPO7	0.124044	-3.01108	0.005408
chr15__34862867__34870922___AQR	0.124065	-3.01083	0.021817
chr9__19360244__19361963___DENND4C	0.124139	-3.00997	0.019174
chr5__94779110__94912976___MCTP1	0.124158	-3.00975	0.021198
chr12__112319225__112319742___HECTD4	0.124168	-3.00964	0.001944
chr16__71658233__71676649___PHLPP2	0.124172	-3.00959	0.015626
chr14__50445041__50448832___MAP4K5	0.124195	-3.00932	0.018298
chr20__44978443__45001353___STK4	0.124225	-3.00897	0.024326
chr19__47084345__47094608___ZC3H4	0.124238	-3.00882	0.023109
chr14__58306022__58330169___ARID4A	0.124246	-3.00873	0.019233
chr6__85528262__85542043___SNX14	0.124264	-3.00852	0.018946
chr12__6730402__6730820___COPS7A	0.124297	-3.00814	0.016814
chr7__131338841__131375493___MKLN1	0.124309	-3.008	0.016425
chr10__27117576__27121448___YME1L1	0.124336	-3.00768	0.018273

chr4__83439863__83448961___HELQ	0.124348	-3.00754	0.016422
chr7__90604218__90623543___CDK14	0.124412	-3.0068	0.020734
chr11__3735191__3753408___NUP98	0.124588	-3.00476	0.018625
chr11__128480191__128490576___ETS1	0.124656	-3.00398	0.019539
chr2__23816637__23823569___ATAD2B	0.124665	-3.00388	0.020903
chr3__130967145__130969396___ATP2C1	0.124801	-3.0023	0.018245
chrX__132382178__132406392___MBNL3	0.124874	-3.00145	0.014865
chr18__35478282__35480563___INO80C	0.124884	-3.00134	0.02006
chr3__134531845__134537268___CEP63	0.124993	-3.00008	0.018731
chr7__155672867__155707068___RBM33	0.125042	-2.99951	0.017332
chr11__85996826__86034941___PICALM	0.125062	-2.99929	0.018661
chr3__9453739__9464672___SETD5	0.125105	-2.99879	0.021719
chr12__65181741__65184482___LEMD3	0.125129	-2.99851	0.019174
chr3__136417885__136502779___STAG1	0.125179	-2.99793	0.022483
chr7__139398599__139412580___C7orf55-LUC7L2LUC7L2	0.125202	-2.99767	0.023036
chr14__88416711__88433212___SPATA7	0.125209	-2.99759	0.019892
chr7__139371387__139409654___LUC7L2	0.125378	-2.99565	0.021868
chr10__68911068__68914204___DDX50	0.125382	-2.9956	0.019233
chr14__88607243__88610940___ZC3H14	0.125422	-2.99514	0.017664
chr9__33953285__33973237___UBAP2	0.125429	-2.99505	0.019539
chr18__216486__224179___THOC1	0.125505	-2.99418	0.01871
chr16__11883015__11887750___GSPT1	0.125579	-2.99333	0.019821
chr5__43292474__43297166___HMGCS1	0.125675	-2.99223	0.018731
chr7__131437785__131445903___MKLN1	0.125708	-2.99185	0.018671
chr17__46119968__46169605___KANSL1	0.125731	-2.99158	0.021021
chr19__10908039__10909207___CARM1	0.1258	-2.99079	0.016735
chr1__1825397__1879902___GNB1	0.125817	-2.9906	0.021179
chr12__100282943__100317925___SCYL2	0.125924	-2.98938	0.022586
chr11__120437308__120447085___ARHGEF12	0.125993	-2.98858	0.018617
chr4__48642277__48646017___FRYL	0.126002	-2.98848	0.018922
chr11__3768581__3771928___NUP98	0.126059	-2.98783	0.018405
chr8__73738284__73739868___STAU2	0.126215	-2.98604	0.017548
chr5__60748267__60767903___NA	0.126236	-2.9858	0.025303
chr21__28986139__28986934___LTN1	0.126237	-2.9858	0.01915
chr18__24070751__24071023___TTC39C	0.126259	-2.98554	0.022701
chr1__243316755__243330692___SDCCAG8	0.126296	-2.98512	0.017831
chr1__207757014__207770362___CD46	0.12635	-2.98451	0.021989
chr1__185180391__185190642___SWT1	0.12641	-2.98382	0.004101
chr5__176943335__176969706___UIMC1	0.126413	-2.98378	0.018354
chr1__21002713__21050994___EIF4G3	0.126484	-2.98297	0.022272
chr1__155395459__155439068___ASH1L	0.126548	-2.98224	0.014753
chr4__177351380__177360677___NEIL3	0.126666	-2.9809	0.00609
chr14__50423121__50435065___MAP4K5	0.126782	-2.97957	0.017621
chr13__60439688__60494575___TDRD3	0.126892	-2.97833	0.02411
chr19__4896671__4898085___ARRDC5	0.126986	-2.97726	0.024193

chr15__50002153__50047464___ATP8B4	0.127071	-2.97629	0.026219
chr1__58533949__58539306___OMA1	0.127126	-2.97567	0.020654
chr17__76767386__76776541___MFSD11	0.127147	-2.97543	0.019856
chr8__108228267__108241913___EIF3E	0.127218	-2.97463	0.019409
chr15__64203082__64204949___CSNK1G1	0.127246	-2.97431	0.019233
chr20__3963875__3974400___RNF24	0.127278	-2.97395	0.019526
chr7__6416627__6416921___DAGLB	0.127356	-2.97306	0.019238
chr12__62313992__62355475___USP15	0.127428	-2.97225	0.020944
chr17__32017972__32035639___NA	0.127449	-2.97201	0.020627
chr7__40092965__40094396___CDK13	0.127451	-2.97199	0.019238
chr10__45639816__45652033___ZFAND4	0.127583	-2.97049	0.016135
chr7__91992885__92014328___AKAP9	0.127604	-2.97026	0.022139
chr15__50637422__50648885___TRPM7	0.127622	-2.97005	0.019416
chr12__128945326__128957643___GLT1D1	0.127634	-2.96991	0.026159
chr9__97369922__97371706___CCDC180LOC100499484-C9ORF174	0.12766	-2.96962	0.02357
chr1__197539964__197583253___DENND1B	0.127664	-2.96958	0.020449
chr14__73282359__73297285___NUMB	0.127694	-2.96924	0.022124
chr6__53505392__53532766___GCLC	0.12771	-2.96906	0.021302
chr6__161165577__161166417___AGPAT4	0.127824	-2.96777	0.009284
chr1__187254973__187329060___NA	0.12783	-2.9677	0.01926
chr2__197078703__197090032___ANKRD44	0.12794	-2.96647	0.022832
chr14__91465480__91469112___SMEK1	0.127979	-2.96603	0.020679
chr2__207567463__207577655___CREB1	0.127986	-2.96594	0.019464
chr16__72308056__72391215___NA	0.12803	-2.96545	0.020292
chr15__43809755__43815074___MFAP1	0.128042	-2.96531	0.020717
chr15__63558106__63559970___USP3	0.128082	-2.96486	0.021253
chr17__41981855__41982401___DNAJC7	0.128096	-2.96471	0.008716
chr21__46349012__46367139___PCNT	0.128102	-2.96464	0.020449
chr2__37199704__37206248___NA	0.128131	-2.96431	0.023389
chr10__31373018__31461237___ZEB1	0.128161	-2.96397	0.006796
chr14__50159431__50161609___SOS2	0.128205	-2.96347	0.009284
chr12__30713785__30753559___CAPRIN2	0.128277	-2.96266	0.021086
chr4__112560733__112585725___C4orf21	0.128297	-2.96244	0.0201
chr14__50423121__50429260___MAP4K5	0.128335	-2.96202	0.020397
chr16__71656571__71679535___PHLPP2	0.128373	-2.96159	0.007517
chr13__97275632__97276409___MBNL2	0.128396	-2.96132	0.019659
chr2__99064939__99104118___TSGA10	0.128407	-2.9612	0.017974
chr6__53269087__53276256___ELOVL5	0.12855	-2.9596	0.024481
chr6__36158648__36158941___LOC102723648	0.128599	-2.95905	0.019238
chrX__123686548__123712908___THOC2	0.128679	-2.95815	0.016916
chr2__160281417__160284868___RBMS1	0.128763	-2.95722	0.019406
chr9__111433233__111444494___KIAA0368	0.128872	-2.95598	0.019539
chr5__60748267__60772093___NA	0.128921	-2.95544	0.02418
chr4__89822246__89836789___SNCA	0.128922	-2.95543	0.028304
chr1__180003174__180024582___CEP350	0.129053	-2.95397	0.024513

chr17__47137152__47138891___CDC27	0.12913	-2.9531	0.017401
chr7__100019231__100024307___ZKSCAN1	0.129146	-2.95292	0.0097
chr16__8903268__8917156___USP7	0.129209	-2.95222	0.020648
chr8__47900373__47930787___PRKDC	0.129251	-2.95175	0.016842
chr1__92605307__92636336___EVI5	0.129308	-2.95112	0.006179
chr13__19741565__19782791___PSPC1	0.129328	-2.95089	0.022818
chr3__47169169__47174263___KIF9-AS1	0.129361	-2.95052	0.020679
chr1__20741831__20780540___NA	0.129386	-2.95025	0.021783
chr15__50912078__50958794___AP4E1	0.129466	-2.94935	0.017678
chr13__95105046__95188542___ABCC4	0.129474	-2.94926	0.021965
chr19__40582351__40583717___SHKBP1	0.129483	-2.94917	0.01874
chr5__140189064__140194652___CYSTM1	0.129522	-2.94874	0.025236
chrY__13355003__13360528___UTY	0.12956	-2.94831	0.009629
chr14__50145170__50150230___SOS2	0.129563	-2.94828	0.023662
chr19__8337795__8339167___KANK3	0.129688	-2.94688	0.021205
chr14__80862757__80906081___CEP128	0.129766	-2.94601	0.019371
chr7__158644289__158646563___NCAPG2	0.129767	-2.94601	0.022145
chr7__26684736__26739964___SKAP2	0.129873	-2.94483	0.026482
chr3__138500110__138532570___CEP70	0.129881	-2.94474	0.017891
chr10__32543300__32567891___CCDC7	0.129886	-2.94468	0.024826
chr10__118685983__118730410___CACUL1	0.129946	-2.94402	0.021254
chr5__60642812__60647533___DEPDC1B	0.129971	-2.94374	0.022503
chr4__168998202__169007756___CBR4	0.129986	-2.94357	0.01874
chr9__27044742__27062119___IFT74	0.130041	-2.94297	0.020006
chr5__154029489__154034967___FAM114A2	0.130045	-2.94291	0.020784
chr5__133000132__133006920___ZCCHC10	0.130104	-2.94227	0.022694
chr7__77778338__77780774___NA	0.13012	-2.94208	0.00754
chr9__68818461__68894638___PIP5K1B	0.130144	-2.94182	0.015369
chr2__151789752__151791908___LOC101929356	0.130145	-2.9418	0.005547
chr3__152298258__152300367___MBNL1	0.130179	-2.94143	0.020137
chr12__112229698__112231715___HECTD4	0.13024	-2.94076	0.020428
chr1__174275833__174305127___RABGAP1L	0.130243	-2.94073	0.022139
chr12__122594276__122622607___KNTC1	0.130277	-2.94034	0.009284
chr2__168074982__168129758___STK39	0.130347	-2.93957	0.021649
chr10__50519831__50523704___SGMS1	0.130394	-2.93905	0.023797
chr1__1649499__1655484___CDK11B	0.130396	-2.93903	0.007545
chr20__47262288__47276905___ZMYND8	0.130593	-2.93685	0.022994
chr7__8003908__8071131___GLCCI1	0.130729	-2.93535	0.025332
chr14__103448919__103462461___MARK3	0.130745	-2.93517	0.027481
chr2__175080660__175151158___ATF2	0.130773	-2.93486	0.022694
chr4__102795426__102826636___UBE2D3	0.130865	-2.93385	0.016425
chr10__92613040__92621473___KIF11	0.130879	-2.93369	0.022515
chr6__149579834__149580723___GINM1	0.130917	-2.93327	0.019233
chr11__35201082__35204640___CD44	0.130922	-2.93322	0.021021
chr8__47407861__47440542___SPIDR	0.131009	-2.93226	0.025293
chr6__131160059__131165217___AKAP7	0.131085	-2.93142	0.024481

chr20__43635926__43642624___IFT52	0.131104	-2.93122	0.019233
chr1__179986169__179992221___CEP350	0.131199	-2.93017	0.021312
chr3__71684572__71728623___EIF4E3	0.131224	-2.9299	0.018822
chr3__155890668__155925366___GMPS	0.131268	-2.92941	0.019188
chr10__28535562__28611922___WAC	0.13136	-2.9284	0.01892
chr5__50399107__50428227___EMB	0.131385	-2.92812	0.010158
chr19__17162350__17163122___MYO9B	0.131403	-2.92793	0.022866
chr10__110875966__110890670___PDCD4	0.131423	-2.92771	0.021391
chr14__34754827__34762223___BAZ1A	0.131459	-2.92731	0.019852
chr15__34250298__34251057___SLC12A6	0.131469	-2.9272	0.020685
chrX__120237455__120240355___NKAPP1	0.131497	-2.9269	0.017793
chr12__100591736__100601753___GAS2L3	0.131513	-2.92672	0.019835
chr1__31911696__31919658___PTP4A2	0.131676	-2.92494	0.021635
chr1__29115699__29117989___EPB41	0.131708	-2.92458	0.024118
chr12__112203636__112219489___HECTD4	0.131714	-2.92452	0.021198
chr7__80662973__80674147___CD36	0.131757	-2.92405	0.022818
chr15__92978234__92992998___CHD2	0.131784	-2.92375	0.021021
chr1__50705786__50752523___FAF1	0.131805	-2.92352	0.018625
chr4__128936655__128952840___SCLT1	0.131858	-2.92294	0.022843
chr1__93544107__93560915___NA	0.131895	-2.92254	0.022701
chr8__85473324__85480805___CA2	0.131912	-2.92236	0.020685
chr16__24775604__24777358___TNRC6A	0.131924	-2.92222	0.020236
chr6__149533458__149541586___PPIL4	0.131968	-2.92174	0.018488
chr2__108751264__108751994___RANBP2	0.131989	-2.92151	0.025902
chr17__44299410__44304207___NA	0.13224	-2.91877	0.027255
chr9__89418056__89475550___SEMA4D	0.132242	-2.91875	0.018842
chr4__2689506__2690970___FAM193A	0.132256	-2.9186	0.020428
chr3__119912704__120093593___GSK3B	0.132396	-2.91707	0.021698
chr1__92320683__92324375___RPAP2	0.132591	-2.91495	0.018872
chr20__48941199__48953790___ARFGEF2	0.132612	-2.91471	0.001971
chr10__68381232__68394136___RUFY2	0.132655	-2.91425	0.023665
chr16__58558473__58560362___CNOT1	0.132767	-2.91303	0.020397
chr16__12199601__12278036___SNX29	0.132814	-2.91252	0.024185
chr4__88949326__88953934___FAM13A	0.132944	-2.91111	0.018857
chr2__61235845__61281242___USP34	0.13305	-2.90996	0.01769
chr4__1900626__1951203___WHSC1	0.13306	-2.90985	0.016715
chr17__82720272__82720841___FN3KRP	0.13309	-2.90953	0.026752
chr10__14825479__14828272___CDNF	0.133309	-2.90716	0.021349
chr20__59743107__59755364___PHACTR3	0.133355	-2.90666	0.020428
chr9__131436620__131439061___PRRC2B	0.133374	-2.90645	0.026742
chr1__229530199__229549434___ABCB10	0.133426	-2.90589	0.001431
chr2__108489838__108497109___GCC2	0.133511	-2.90497	0.019214
chr1__27412572__27428933___WASF2	0.133527	-2.9048	0.018617
chr16__11886471__11887750___GSPT1	0.133633	-2.90365	0.010115
chr1__15643522__15651895___DDI2	0.133633	-2.90365	0.018245
chr2__144424796__144425538___ZEB2	0.133644	-2.90354	0.019921

chr17__73203000__73203793___COG1	0.133784	-2.90202	0.018499
chr1__222715145__222725555___BROX	0.13387	-2.9011	0.02557
chr2__73572262__73573498___ALMS1	0.133886	-2.90093	0.026228
chr8__38321072__38348143___WHSC1L1	0.133989	-2.89981	0.019367
chr5__41762111__41807438___OXCT1	0.134083	-2.89881	0.022139
chr1__28027789__28058094___EYA3	0.134181	-2.89774	0.010087
chr4__15711807__15718993___BST1	0.134197	-2.89758	0.018842
chr9__36669310__36674937___MELK	0.134242	-2.8971	0.021325
chr7__131429033__131478677___MKLN1	0.134332	-2.89613	0.024693
chr15__63672496__63675117___HERC1	0.134522	-2.89409	0.019188
chr9__137811461__137818138___EHMT1	0.134535	-2.89395	0.010234
chr13__28266715__28288122___PAN3	0.13458	-2.89346	0.02995
chr13__74406315__74406780___LOC101927121	0.13465	-2.89271	0.023223
chr5__66012049__66054951___ERBB2IP	0.134682	-2.89237	0.005439
chr9__121190554__121193419___RAB14	0.134774	-2.89138	0.020544
chr9__120408347__120409316___CDK5RAP2	0.134853	-2.89054	0.021203
chr6__129599216__129618852___ARHGAP18	0.134886	-2.89019	0.024481
chr2__119932424__119952129___PTPN4	0.135022	-2.88874	0.022079
chr8__100709133__100713181___PABPC1	0.135062	-2.8883	0.027191
chr15__99276576__99287951___LRRC28	0.13507	-2.88822	0.019741
chr17__28921688__28927063___PHF12	0.135079	-2.88812	0.024982
chr14__49650265__49655843___POLE2	0.135187	-2.88697	0.004999
chr6__134986066__134993875___HBS1L	0.13523	-2.88652	0.01926
chr13__113233177__113244514___CUL4A	0.135288	-2.88589	0.028003
chr7__105005318__105009209___NA	0.135315	-2.88561	0.024693
chr3__17214207__17238419___TBC1D5	0.135318	-2.88557	0.027131
chr12__123313620__123315660___SBNO1	0.135398	-2.88472	0.026306
chr9__121167489__121175224___CNTRL	0.135426	-2.88442	0.023151
chr14__50425907__50429260___MAP4K5	0.135464	-2.88402	0.020862
chr2__26254247__26263479___HADHB	0.135538	-2.88323	0.023837
chr6__20758595__20781265___CDKAL1	0.135579	-2.88279	0.020679
chr12__116205053__116237705___MED13L	0.13572	-2.8813	0.008022
chr14__103448919__103468186___MARK3	0.135746	-2.88102	0.020428
chr10__110578628__110593223___SMC3	0.135864	-2.87977	0.029332
chr10__102362475__102365599___GBF1	0.135936	-2.879	0.019852
chr5__145764931__145796547___PRELID2	0.136026	-2.87804	0.024881
chr17__29676820__29703062___SSH2	0.136029	-2.87801	0.024073
chr7__87439667__87440402___ABCB4	0.136043	-2.87786	0.01067
chr4__153583190__153598732___KIAA0922	0.136046	-2.87783	0.021144
chr3__182947238__182961356___DCUN1D1	0.136058	-2.87771	0.026605
chr6__98875415__98905670___FBXL4	0.136078	-2.8775	0.020903
chr2__144464166__144486308___ZEB2	0.13608	-2.87747	0.0201
chr6__152628265__152628554___SYNE1	0.136103	-2.87722	0.027191
chr12__64409962__64420521___XPOT	0.13618	-2.87641	0.022793
chr10__5783324__5800705___GDI2	0.136181	-2.8764	0.022498
chr20__21326490__21330539___XRN2	0.136186	-2.87635	0.02357

chr1__185123857__185151935___TRMT1L	0.136197	-2.87623	0.021663
chr15__63529014__63574403___USP3	0.13631	-2.87503	0.022288
chr12__28412863__28484165___CCDC91	0.136409	-2.87399	0.022503
chr17__48848064__48849377___CALCOCO2	0.136507	-2.87295	0.006152
chr12__47666980__47670345___RPAP3	0.136556	-2.87243	0.022823
chr6__53498607__53514497___GCLC	0.136622	-2.87174	0.020449
chr1__61109778__61163075___NFIA	0.136649	-2.87146	0.010942
chr2__241242460__241249980___HDLBP	0.136655	-2.87139	0.019403
chr4__76996425__77030970___SEPT11	0.136676	-2.87117	0.026524
chr9__86305192__86319670___ZCCHC6	0.136681	-2.87111	0.024693
chr11__77353536__77359017___PAK1	0.136826	-2.86959	0.01926
chr4__119596523__119607297___PDE5A	0.136829	-2.86955	0.003283
chr11__17959470__18008076___SERGEF	0.136874	-2.86908	0.02966
chr20__58895612__58905480___GNAS	0.136876	-2.86906	0.00511
chr2__152657889__152659009___PRPF40A	0.136911	-2.86869	0.022832
chr4__48586621__48605833___FRYL	0.136962	-2.86815	0.022503
chr8__132746942__132757294___TMEM71	0.136993	-2.86783	0.023674
chrX__65075474__65113813___NA	0.137051	-2.86721	0.005275
chr6__119361291__119363332___NA	0.137067	-2.86705	0.020449
chr9__93013852__93018215___FGD3	0.13708	-2.86691	0.018922
chr13__52460899__52474084___CKAP2	0.137097	-2.86673	0.026883
chr10__4830675__4842504___AKR1E2	0.137098	-2.86672	0.010522
chr1__93217738__93239896___CCDC18	0.137199	-2.86566	0.026228
chr16__23621362__23623130___PALB2	0.13722	-2.86543	0.022401
chr4__104518577__104523319___AC004053.1	0.137327	-2.86431	0.026605
chr9__3668263__3674648___RP11-509J21.1	0.137342	-2.86416	0.024154
chrX__150699195__150718700___MTMR1	0.137389	-2.86366	0.022139
chr11__31452718__31488241___IMMP1L	0.137602	-2.86142	0.023027
chr1__92605307__92639237___EVI5	0.137643	-2.861	0.02527
chr12__95494056__95496098___METAP2	0.137749	-2.85988	0.006929
chr19__10166598__10173174___DNMT1	0.137797	-2.85939	0.020903
chr2__32377588__32395593___BIRC6	0.13781	-2.85925	0.024046
chr18__2718158__2752552___SMCHD1	0.137847	-2.85886	0.02228
chr4__1892166__1904378___WHSC1	0.137936	-2.85792	0.01915
chr5__55269413__55281515___DHX29	0.137944	-2.85785	0.024863
chr11__83224855__83248087___ANKRD42	0.137992	-2.85734	0.020202
chr2__23782869__23823569___ATAD2B	0.138128	-2.85592	0.020903
chr21__33340999__33345360___IFNAR1	0.138133	-2.85587	0.007498
chr8__55941855__55969793___LYN	0.138236	-2.85479	0.028658
chr6__24416397__24418578___MRS2	0.138274	-2.8544	0.022701
chr4__107682015__107701285___PAPSS1	0.138277	-2.85436	0.011836
chr8__97661072__97691188___MTDH	0.138296	-2.85417	0.011941
chr17__20204333__20232414___SPECC1	0.138398	-2.85311	0.028839
chr12__42317340__42324104___ZCRB1	0.138422	-2.85286	0.007843
chr19__18175040__18175697___IFI30	0.138523	-2.85181	0.007948
chr1__47272076__47300152___STIL	0.138525	-2.85179	0.028304

chr16__11846501__11847806___RSL1D1	0.13862	-2.85079	0.001796
chr17__59737453__59765138___VMP1	0.138757	-2.84937	0.024519
chr8__60584208__60591969___RAB2A	0.138765	-2.84928	0.022231
chr12__112216292__112228811___HECTD4	0.138831	-2.8486	0.026554
chr17__49311312__49312042___ZNF652	0.138835	-2.84856	0.00113
chr14__103428387__103457212___MARK3	0.138837	-2.84854	0.005871
chr6__24456498__24467274___GPLD1	0.138856	-2.84834	0.023036
chr1__185214507__185232945___SWT1	0.138902	-2.84786	0.02391
chr3__125453810__125460860___SNX4	0.139039	-2.84644	0.025145
chr1__93210850__93234884___CCDC18	0.139115	-2.84565	0.02397
chr1__61109778__61119827___NFIALOC102724281	0.139155	-2.84523	0.022832
chr17__43377913__43380107___LINC00910	0.139165	-2.84513	0.024982
chr10__121790169__121870038___ATE1	0.139272	-2.84402	0.028424
chr12__101908186__101914232___DRAM1	0.139473	-2.84195	0.025192
chr6__42650284__42658824___UBR2	0.139532	-2.84133	0.022832
chr1__26716114__26716720___ARID1A	0.139595	-2.84068	0.024118
chr3__108661877__108677598___DZIP3	0.13961	-2.84052	0.026228
chr8__120693692__120693908___SNTB1	0.139728	-2.83931	0.022832
chr9__96320998__96324169___SLC35D2	0.139829	-2.83826	0.022822
chr8__37862737__37877551___RAB11FIP1	0.139885	-2.83769	0.031202
chr16__57164001__57178852___FAM192A	0.139919	-2.83733	0.030165
chr17__50740306__50744813___LUC7L3	0.139927	-2.83726	0.027527
chr2__48328561__48359147___FOXN2	0.139979	-2.83672	0.022405
chr7__103182378__103184127___DPY19L2P2	0.139996	-2.83655	0.022008
chr10__102157019__102158214___NOLC1	0.140021	-2.83628	0.006723
chr7__36423817__36424742___ANLN	0.140114	-2.83533	0.011831
chr7__848418__849603___SUN1	0.140167	-2.83478	0.024481
chr19__1090908__1091907___POLR2E	0.140255	-2.83387	0.023438
chr20__47236326__47249439___ZMYND8	0.14027	-2.83372	0.023848
chr15__99671323__99675458___MEF2A	0.140297	-2.83344	0.022832
chr16__19535940__19537587___CCP110	0.140334	-2.83306	0.026228
chr5__112754873__112801383___APC	0.140375	-2.83264	0.025437
chr3__69187770__69189952___FRMD4B	0.140463	-2.83174	0.026228
chr15__22278818__22282869___REREP3	0.140635	-2.82998	0.034383
chr2__9344532__9350895___ASAP2	0.140716	-2.82914	0.022823
chr2__171117739__171153527___TLK1	0.140959	-2.82666	0.024513
chr2__39286852__39288280___MAP4K3	0.140988	-2.82636	0.026228
chr15__99256032__99300532___LRRC28	0.14099	-2.82634	0.021904
chr18__39207685__39208789___LINC00669	0.140997	-2.82627	0.024444
chr11__11873800__11880380___USP47	0.141023	-2.826	0.024572
chr15__85113873__85121014___PDE8A	0.141039	-2.82584	0.009312
chr7__93259550__93311272___CCDC132	0.141101	-2.8252	0.027481
chr2__43578513__43590954___THADA	0.14116	-2.82459	0.026219
chr8__25483399__25484210___CDCA2	0.141188	-2.82431	0.027248
chr14__59521574__59543454___CCDC175	0.141297	-2.8232	0.028555
chr6__158580940__158589782___TMEM181	0.141335	-2.82281	0.022771

chr6__35874233__35891013___SRPK1	0.141434	-2.8218	0.023905
chr3__152414941__152432920___MBNL1	0.141446	-2.82168	0.005099
chr1__1649499__1657498___CDK11B	0.14159	-2.82021	0.022435
chr3__160430599__160431825___SMC4	0.141685	-2.81925	0.031013
chrX__150814862__150816078___CD99L2	0.14181	-2.81797	0.032886
chr6__100798713__100848707___ASCC3	0.14182	-2.81787	0.026102
chr14__31141858__31172122___HECTD1	0.141825	-2.81782	0.012186
chr15__44606025__44613536___SPG11	0.141829	-2.81778	0.022379
chr20__13559008__13587370___TASP1	0.141857	-2.8175	0.030069
chr1__226266213__226301205___LIN9	0.14187	-2.81736	0.021519
chr10__86458989__86461287___WAPAL	0.141881	-2.81724	0.02706
chr14__39401176__39412725___FBXO33	0.141924	-2.81681	0.031799
chr17__20253505__20306082___SPECC1	0.141996	-2.81608	0.011608
chr2__127999741__128000454___SAP130	0.14202	-2.81584	0.024118
chr4__98404477__98421394___RAP1GDS1	0.142169	-2.81432	0.026502
chr17__7945728__7945986___CNTROB	0.14222	-2.8138	0.020654
chr3__141974048__141978682___TFDP2	0.142221	-2.8138	0.022401
chr10__74969660__74989112___KAT6B	0.142258	-2.81342	0.022818
chr12__827042__830160___WNK1	0.142317	-2.81282	0.029149
chr9__109033307__109064567___TMEM245	0.142361	-2.81238	0.02767
chr12__28255581__28452654___CCDC91	0.142521	-2.81076	0.022139
chr7__40078005__40078851___CDK13	0.142606	-2.8099	0.03205
chr7__30563731__30574881___LOC401320	0.142689	-2.80905	0.023901
chr4__25256543__25263849___PI4K2B	0.142769	-2.80824	0.022498
chr20__18543019__18554390___SEC23B	0.142912	-2.8068	0.012497
chr16__74938150__74951543___WDR59	0.143029	-2.80562	0.025407
chr2__230269532__230287966___SP140	0.143035	-2.80556	0.029551
chr7__80646652__80666489___CD36	0.143068	-2.80522	0.026228
chr7__139137847__139148377___TTC26	0.143099	-2.80491	0.023833
chr10__6613631__6613987___NA	0.143157	-2.80433	0.025482
chr3__27411642__27452498___SLC4A7	0.143159	-2.80431	0.026228
chr3__57583898__57584464___ARF4	0.143195	-2.80394	0.034526
chr17__43063333__43074521___BRCA1	0.143308	-2.80281	0.022231
chr9__85575315__85646435___AGTPBP1	0.143394	-2.80195	0.022498
chr12__70329423__70332846___CNOT2	0.143412	-2.80176	0.022822
chr16__27211146__27215008___KDM8	0.143498	-2.8009	0.027884
chr5__138198199__138202155___CDC23	0.143512	-2.80075	0.024684
chr1__185174372__185204863___SWT1	0.143518	-2.8007	0.034679
chr17__60679453__60709325___BCAS3	0.14357	-2.80017	0.02846
chr7__102366018__102407498___LOC100630923	0.143613	-2.79974	0.027103
chr2__44430281__44505730___CAMKMT	0.143669	-2.79918	0.024775
chr11__108329021__108335961___ATM	0.143679	-2.79908	0.028768
chr11__85976623__85981228___PICALM	0.143846	-2.7974	0.013068
chr18__58165788__58333892___NEDD4L	0.143881	-2.79705	0.031406
chr3__196053418__196071498___TFRC	0.143901	-2.79685	0.025236
chr1__225987896__225993002___SDE2	0.144003	-2.79583	0.023241

chr12__76827360__76827979___ZDHHC17	0.144034	-2.79552	0.023539
chr19__45277923__45278615___MARK4	0.14405	-2.79536	0.013564
chr4__128936655__128972397___SCLT1	0.144125	-2.79461	0.011036
chr11__3735382__3739060___NUP98	0.144152	-2.79433	0.030902
chr11__16046514__16111926___SOX6	0.144235	-2.79351	0.027134
chr12__65182631__65218619___LEMD3	0.144289	-2.79297	0.022832
chr2__175970764__175994280___KIAA1715	0.144297	-2.79289	0.032886
chr7__151470571__151498180___RHEB	0.144329	-2.79257	0.009856
chr12__122601536__122622607___KNTC1	0.144594	-2.78992	0.022525
chr6__127812883__127813931___THEMIS	0.144623	-2.78963	0.02454
chr1__204558641__204570746___MDM4	0.144626	-2.7896	0.027705
chr14__61740505__61744813___HIF1A	0.144799	-2.78787	0.026005
chr4__129036278__129082373___SCLT1	0.144824	-2.78763	0.025096
chr11__108267171__108267342___ATM	0.144835	-2.78752	0.034878
chr12__130795995__130808704___STX2	0.14488	-2.78707	0.026882
chr1__207545308__207717691___NA	0.145182	-2.78406	0.032886
chr15__43400044__43401850___TUBGCP4	0.145188	-2.78401	0.009078
chr7__48466956__48489344___ABCA13	0.145192	-2.78397	0.030379
chr13__46020449__46042275___ZC3H13	0.145211	-2.78377	0.02727
chr19__34451981__34467014___UBA2	0.145309	-2.7828	0.029045
chr14__60256824__60260010___PPM1A	0.145333	-2.78257	0.031713
chr10__97229147__97266125___ARHGAP19ARHGAP19-SLIT1	0.145406	-2.78184	0.024479
chr22__28780948__28783645___CCDC117	0.145412	-2.78178	0.028119
chr12__355158__363097___KDM5A	0.145438	-2.78152	0.032685
chr14__80743075__80761613___CEP128	0.145459	-2.78132	0.022288
chr17__61889786__61891689___INTS2	0.145627	-2.77965	0.028917
chr14__102714423__102721377___RCOR1	0.145643	-2.77949	0.02995
chr3__41224021__41227352___CTNNB1	0.145669	-2.77923	0.007181
chrX__11055936__11110981___MID1-2	0.145713	-2.7788	0.027431
chr7__112286873__112287074___ZNF277	0.145727	-2.77866	0.009312
chr1__185180391__185222036___SWT1	0.145736	-2.77857	0.028058
chr8__47927194__47930787___PRKDC	0.14578	-2.77813	0.026208
chr16__11894954__11898035___GSPT1	0.145908	-2.77687	0.030949
chr11__16177809__16186955___SOX6	0.145929	-2.77666	0.022503
chr14__30633947__30639864___SCFD1	0.145965	-2.77631	0.026146
chr12__112266912__112279386___HECTD4	0.146073	-2.77524	0.024756
chr8__99641811__99661491___VPS13B	0.146169	-2.77429	0.013584
chr18__69873144__69947433___CD226	0.146193	-2.77406	0.025381
chr2__223894234__223895630___WDFY1	0.146249	-2.7735	0.032631
chr3__42125420__42125614___TRAK1	0.146279	-2.77321	0.033368
chr9__123440360__123457897___DENND1A	0.146496	-2.77107	0.010764
chr6__79513212__79519085___LCA5	0.146504	-2.77099	0.013908
chr1__155670320__155784089___NA	0.146569	-2.77035	0.006633
chr14__31136531__31156886___HECTD1	0.146589	-2.77015	0.026804
chr15__41371527__41380203___NUSAP1	0.146714	-2.76892	0.034008

chr1__51748369__51765981___OSBPL9	0.146742	-2.76865	0.024653
chr8__140789474__140890769___PTK2	0.146759	-2.76848	0.029175
chr15__68086306__68153695___PIAS1	0.1468	-2.76808	0.028029
chr10__16484337__16486617___PTER	0.146812	-2.76796	0.011669
chr11__28211062__28212331___METTL15	0.146919	-2.7669	0.026975
chr20__34031522__34033318___RALY	0.146984	-2.76627	0.007499
chr4__36290373__36316486___DTHD1	0.146988	-2.76623	0.02953
chr1__39434414__39439500___MACF1	0.146993	-2.76618	0.032358
chr3__108669681__108677598___DZIP3	0.147019	-2.76592	0.031727
chr1__1817837__1839238___GNB1	0.147027	-2.76585	0.009669
chr22__40273425__40301333___TNRC6B	0.147072	-2.76541	0.027311
chr7__77396982__77406105___GSAP	0.147092	-2.76521	0.032445
chr4__169424553__169537911___NEK1	0.147183	-2.76432	0.025879
chr3__63898399__63952483___ATXN7	0.147295	-2.76322	0.028424
chr15__75854386__75883424___UBE2Q2	0.14733	-2.76287	0.008118
chr6__42659656__42679832___UBR2	0.147403	-2.76216	0.009353
chr1__236803428__236816543___MTR	0.147421	-2.76199	0.014186
chr11__17122188__17145942___PIK3C2A	0.147456	-2.76164	0.027418
chr16__75600220__75622464___ADAT1	0.147528	-2.76094	0.013482
chr1__150230571__150231926___ANP32E	0.147537	-2.76085	0.001857
chr1__179341028__179343635___SOAT1	0.147577	-2.76046	0.03656
chr1__247138716__247159813___ZNF124	0.147788	-2.7584	0.014817
chr15__43043215__43056442___UBR1	0.147836	-2.75793	0.0282
chr4__174297966__174316290___CEP44	0.147965	-2.75667	0.033481
chr8__17956604__17964768___PCM1	0.148205	-2.75434	0.022818
chr17__31976521__31983104___SUZ12	0.148223	-2.75415	0.025234
chr4__67728540__67732345___NA	0.148409	-2.75235	0.030789
chr12__26621123__26632059___ITPR2	0.148555	-2.75093	0.031757
chr1__108882580__108929975___GPSM2	0.148598	-2.75051	0.00946
chr3__52411029__52414587___PHF7	0.148626	-2.75024	0.030949
chr12__30720811__30724451___CAPRIN2	0.148627	-2.75023	0.02757
chr22__28695710__28699937___CHEK2	0.148628	-2.75022	0.014848
chr1__233177802__233208689___PCNXL2	0.148631	-2.75019	0.039067
chr1__25225002__25228235___SYF2	0.148874	-2.74784	0.00386
chr8__123359221__123380677___ATAD2	0.148887	-2.74771	0.024481
chr3__195519018__195524896___PPP1R2	0.148964	-2.74696	0.033227
chr11__107416209__107433749___CWF19L2	0.149129	-2.74537	0.026409
chr11__68564303__68576043___PPP6R3	0.149249	-2.74421	0.027028
chr12__56169776__56170208___SMARCC2	0.149373	-2.74301	0.009608
chr15__63723182__63749791___HERC1	0.149482	-2.74195	0.028921
chr2__55644637__55646486___PNPT1	0.149537	-2.74142	0.027418
chr17__30856955__30879487___ATAD5	0.14958	-2.74101	0.027924
chr5__176289654__176290955___SIMC1	0.149642	-2.74041	0.031727
chr17__30449553__30451846___CPD	0.149689	-2.73996	0.028424
chr4__70942823__70944710___MOB1B	0.149749	-2.73938	0.039287
chr18__21778103__21779685___MIB1	0.149804	-2.73885	0.026986

chr2__10791795__10793202___PDIA6	0.149831	-2.7386	0.034742
chr1__108154983__108185954___SLC25A24	0.149905	-2.73788	0.022991
chr21__15860622__15877991___USP25	0.149961	-2.73734	0.024982
chr5__145587325__145670827___NA	0.150006	-2.73691	0.027431
chr1__211260108__211304140___RCOR3	0.150032	-2.73666	0.027759
chr12__118400659__118403517___SUDS3	0.150063	-2.73636	0.024481
chr6__14284195__14292214___NA	0.150071	-2.73628	0.030188
chr2__210431725__210476412___LANCL1	0.150082	-2.73618	0.027705
chr2__75687827__75702423___GCFC2	0.150251	-2.73456	0.03386
chrX__68511849__68513405___YIPF6	0.150413	-2.733	0.031017
chr2__9318524__9335179___ASAP2	0.15046	-2.73255	0.029725
chr11__46769963__46788773___CKAP5	0.150519	-2.73199	0.030265
chr17__81667729__81670453___CCDC137	0.150526	-2.73192	0.023481
chr14__99257471__99257836___BCL11B	0.150555	-2.73163	0.032681
chr6__135039573__135042126___HBS1L	0.150656	-2.73067	0.008775
chr4__102689574__102690957___MANBA	0.15066	-2.73063	0.032278
chr9__123757703__123769563___DENND1A	0.150724	-2.73002	0.012485
chr9__6984166__7011879___KDM4C	0.150731	-2.72995	0.027576
chr13__46213002__46246625___LRRC63	0.150889	-2.72844	0.029699
chr14__96833467__96837817___VRK1	0.151041	-2.72699	0.031684
chr17__77176198__77176681___SEC14L1	0.151186	-2.72561	0.002299
chr2__240005210__240022340___NDUFA10	0.151243	-2.72506	0.030073
chr3__33409236__33425741___UBP1	0.151337	-2.72416	0.033391
chr12__123194386__123210162___MPHOSPH9	0.151418	-2.72339	0.027249
chr5__133064980__133076898___HSPA4	0.151501	-2.7226	0.029213
chr5__96985080__97028612___LNPEP	0.151506	-2.72256	0.008914
chr3__188406112__188524787___LPP	0.15158	-2.72185	0.027431
chr20__47249287__47262428___ZMYND8	0.151613	-2.72153	0.026579
chr11__61364476__61367998___TMEM138	0.151695	-2.72075	0.024132
chr4__343782__344430___ZNF141	0.151714	-2.72058	0.031524
chr3__71690010__71728623___EIF4E3	0.151828	-2.71949	0.036446
chr3__196055080__196060247___TFRC	0.151981	-2.71804	0.03025
chr22__26476993__26479355___HPS4	0.152023	-2.71764	0.030393
chr15__50300789__50314670___GABPB1	0.152035	-2.71752	0.028304
chr12__827042__862270___WNK1	0.152048	-2.71741	0.025733
chr9__86346299__86346480___ZCCHC6	0.15216	-2.71634	0.012184
chr1__174219125__174305127___RABGAP1L	0.152189	-2.71607	0.029441
chr9__85575315__85596449___AGTPBP1	0.152212	-2.71584	0.005876
chr1__243545510__243573048___AKT3	0.152222	-2.71575	0.009353
chr3__56588862__56594028___CCDC66	0.152274	-2.71526	0.027015
chr5__112985835__113013536___DCP2	0.152303	-2.71498	0.026312
chr21__36344579__36364259___MORC3	0.152362	-2.71442	0.015562
chr8__119762415__119791459___TAF2	0.152389	-2.71417	0.033365
chr3__20161109__20178347___SGOL1	0.152447	-2.71362	0.028304
chr11__68554145__68596218___PPP6R3	0.1525	-2.71312	0.035193
chr12__120557282__120560886___RNF10	0.152582	-2.71234	0.010845

chr12__27046158__27066226___NA	0.152597	-2.7122	0.031406
chr1__93217722__93232593___CCDC18	0.152777	-2.7105	0.030426
chr12__25079244__25090197___LRMP	0.15279	-2.71038	0.03481
chr5__94654630__94663908___ANKRD32	0.152814	-2.71015	0.028871
chr10__21730900__21735235___MLLT10	0.152895	-2.70939	0.033391
chr7__8003908__8024814___GLCCI1	0.152908	-2.70926	0.031005
chr11__121045674__121073040___TBCEL	0.152964	-2.70873	0.031013
chr9__5021963__5078444___JAK2	0.152986	-2.70853	0.036642
chr5__94909251__94912976___MCTP1	0.153051	-2.70792	0.037333
chr10__32451592__32481782___CCDC7	0.153081	-2.70763	0.006253
chr17__39684597__39686019___PGAP3	0.153141	-2.70707	0.011438
chr6__157592988__157595723___ZDHHC14	0.153158	-2.7069	0.026228
chr15__34003032__34023497___AVENCHRM5	0.153237	-2.70616	0.029653
chr13__41761128__41833531___VWA8	0.153323	-2.70535	0.029902
chr10__104008177__104010908___SLK	0.153362	-2.70499	0.042145
chr18__77077285__77080793___MBP	0.15344	-2.70425	0.026186
chr15__76728595__76733384___SCAPER	0.153465	-2.70402	0.041182
chr20__2955609__2965202___PTPRA	0.153517	-2.70353	0.038138
chr2__99078659__99117759___TSGA10	0.153573	-2.703	0.024481
chr11__110136663__110137414___ZC3H12C	0.153745	-2.70139	0.038307
chr5__54094176__54098085___ARL15	0.153764	-2.70121	0.007335
chr2__128097429__128121298___UGGT1	0.153791	-2.70096	0.03606
chr16__70532479__70544533___SF3B3	0.153819	-2.7007	0.033208
chr12__122515105__122521428___RSRC2	0.153832	-2.70057	0.029318
chr1__61103769__61159155___NFIA	0.153833	-2.70056	0.032764
chr2__201149003__201154407___CFLARCFLAR-AS1	0.153903	-2.6999	0.028465
chr3__71693875__71699708___EIF4E3	0.153918	-2.69976	0.033481
chr14__96520055__96565214___PAPOLA	0.153937	-2.69958	0.031555
chrX__148651328__148662768___AFF2	0.153954	-2.69943	0.037898
chr3__183987770__184014447___ABCC5	0.154057	-2.69847	0.033738
chr2__15603192__15607313___DDX1	0.154383	-2.69542	0.027663
chr6__131136775__131219808___AKAP7	0.154413	-2.69514	0.011521
chr12__101714090__101720254___CHPT1	0.154422	-2.69505	0.017078
chr1__84179177__84197824___PRKACB	0.154422	-2.69505	0.031727
chr10__110881233__110887886___PDCD4	0.154565	-2.69372	0.01549
chr16__46668930__46676692___VPS35	0.154569	-2.69367	0.031449
chr14__31127785__31172122___HECTD1	0.154592	-2.69346	0.001462
chr12__22055149__22062434___CMAS	0.154614	-2.69325	0.03052
chr5__73006445__73006780___FCHO2	0.154782	-2.69169	0.034367
chr18__61814607__61816598___RNF152	0.154875	-2.69082	0.031089
chr2__181493325__181511775___ITGA4	0.154899	-2.6906	0.011003
chr5__143037196__143057747___ARHGAP26	0.1549	-2.69059	0.01396
chr17__58703196__58720812___RAD51C	0.154977	-2.68987	0.008762
chr8__31087776__31091898___WRN	0.155282	-2.68704	0.028254
chr20__38551071__38554076___RALGAPB	0.15537	-2.68622	0.026397
chr11__16014942__16111923___SOX6	0.155487	-2.68513	0.030069

chr15__74923648__74926887___COX5A	0.155621	-2.68389	0.039875
chr11__120476661__120477526___ARHGEF12	0.155692	-2.68324	0.032377
chr2__55362308__55419140___CCDC88A	0.155707	-2.6831	0.032219
chr19__11830617__11947307___NA	0.155783	-2.68239	0.034367
chr14__90978306__91001159___RPS6KA5	0.155848	-2.68179	0.033122
chr12__70278132__70311017___CNOT2	0.155932	-2.68101	0.034557
chr5__14741827__14751239___ANKH	0.156112	-2.67935	0.030903
chr7__80664406__80674147___CD36	0.156124	-2.67924	0.032624
chr22__41158412__41173784___EP300	0.156184	-2.67868	0.033738
chr4__88649840__88658491___HERC3	0.1562	-2.67853	0.029194
chr1__185174372__185276668___SWT1	0.156379	-2.67688	0.031555
chr2__208809452__208845226___NA	0.156398	-2.67671	0.032996
chr5__62347130__62350120___KIF2A	0.156685	-2.67406	0.001348
chr2__15415546__15511350___NBAS	0.156744	-2.67352	0.026086
chr17__43099775__43104956___BRCA1	0.156757	-2.6734	0.030991
chr10__101806045__101807901___MGEA5	0.156818	-2.67284	0.038419
chr18__26052624__26087577___SS18	0.15685	-2.67254	0.033173
chr2__171965338__171966949___HAT1	0.156861	-2.67244	0.034764
chr6__42662184__42666245___UBR2	0.156947	-2.67165	0.001529
chr10__68025546__68044563___HERC4	0.157087	-2.67037	0.00515
chr10__27138767__27145590___YME1L1	0.157134	-2.66993	0.012118
chr14__37110827__37138520___SLC25A21	0.157167	-2.66963	0.017321
chr17__30792440__30793672___CRLF3	0.157243	-2.66894	0.034127
chr1__92563642__92639237___EVI5	0.157248	-2.66889	0.035193
chr7__102399548__102404683___PRKRIP1LOC100630923	0.157381	-2.66766	0.026606
chr4__38089932__38118192___TBC1D1	0.157402	-2.66747	0.031377
chr2__48346201__48362707___FOXN2	0.15741	-2.6674	0.017678
chr10__86460399__86461287___WAPAL	0.157507	-2.66651	0.017363
chr1__42825623__42840296___ERMAP	0.157547	-2.66615	0.033122
chr1__172555869__172589926___SUCO	0.157552	-2.6661	0.029476
chr7__107281300__107298346___COG5	0.157646	-2.66524	0.038671
chr22__17900842__17906886___MICAL3	0.157757	-2.66422	0.030368
chr13__19824920__19835689___ZMYM5	0.157776	-2.66405	0.029626
chr11__68569748__68574224___PPP6R3	0.157905	-2.66287	0.034961
chr21__32737254__32759269___PAXBP1	0.158019	-2.66183	0.031138
chr10__60787224__60787470___CDK1	0.158033	-2.6617	0.039918
chr4__128936655__129039096___SCLT1	0.158075	-2.66132	0.032064
chr18__79126267__79193263___ATP9B	0.158161	-2.66054	0.004808
chr11__111836165__111853736___ALG9	0.158183	-2.66034	0.031773
chr9__4823548__4849550___RCL1	0.158224	-2.65996	0.036104
chr18__79710346__79718016___CTDP1	0.158227	-2.65994	0.032064
chrX__13744415__13751368___OFD1	0.158231	-2.65989	0.029778
chr11__120465237__120467308___ARHGEF12	0.15843	-2.65808	0.007545
chr1__93544107__93549426___FNBP1L	0.158441	-2.65798	0.017664
chr3__185675296__185689627___IGF2BP2	0.158472	-2.6577	0.030702
chr2__232815637__232819985___GIGYF2	0.15865	-2.65608	0.03778

chr15__72544820__72572165___ARIH1	0.158665	-2.65595	0.038354
chr7__158879684__158918869___WDR60	0.158699	-2.65564	0.04256
chr1__224411427__224419615___WDR26	0.158701	-2.65562	0.01819
chr6__159682474__159685033___SOD2	0.159095	-2.65204	0.036154
chr11__16183886__16283918___SOX6	0.159314	-2.65006	0.037788
chr6__152236107__152239706___SYNE1	0.159335	-2.64987	0.039828
chr12__53381659__53411435___SP1	0.159364	-2.6496	0.034742
chr5__904148__908461___TRIP13	0.159505	-2.64833	0.018096
chr17__79077430__79077864___ENGASE	0.15955	-2.64792	0.03948
chr10__124706636__124706887___FAM53B	0.159584	-2.64761	0.038466
chr14__103571623__103571820___APOPT1	0.159647	-2.64704	0.035628
chr17__47129393__47158303___CDC27	0.159941	-2.64439	0.034878
chr3__141970073__141993585___TFDP2	0.160005	-2.64381	0.032219
chr2__189728660__189744788___ANKAR	0.160005	-2.64381	0.012235
chr12__50435488__50454417___LARP4	0.160039	-2.64351	0.032271
chr9__122280443__122291840___MRRF	0.160068	-2.64325	0.029711
chr18__37066890__37084232___KIAA1328	0.160184	-2.6422	0.012771
chr15__41069570__41087682___INO80	0.160333	-2.64085	0.033122
chr8__9743464__9748212___TNKS	0.160401	-2.64025	0.031555
chr2__30459552__30533314___LCLAT1	0.160434	-2.63995	0.015546
chr4__56019353__56019555___CEP135	0.160445	-2.63985	0.033391
chr5__132699171__132711057___KIF3A	0.160491	-2.63944	0.03292
chr11__69667895__69673321___ORAOV1	0.160558	-2.63884	0.03673
chr1__222725450__222730177___BROX	0.160575	-2.63868	0.039067
chr7__5641154__5641376___RNF216	0.160584	-2.6386	0.007545
chr18__58341038__58343103___NEDD4L	0.160588	-2.63856	0.034698
chr1__246631894__246634587___CNST	0.160609	-2.63838	0.034127
chr2__222613811__222624775___FARSB	0.160774	-2.63689	0.030193
chr13__32432789__32444126___N4BP2L2	0.160955	-2.63527	0.038466
chr20__495719__508660___CSNK2A1	0.160958	-2.63524	0.04256
chr11__120437308__120445464___ARHGEF12	0.160997	-2.6349	0.03606
chr9__122877471__122883379___RC3H2	0.161012	-2.63476	0.029633
chr6__79015082__79043003___PHIP	0.161014	-2.63474	0.031666
chr3__155887432__155925366___GMPS	0.161127	-2.63373	0.042509
chr12__26628033__26655852___ITPR2	0.161198	-2.63309	0.032815
chr11__108185232__108189330___NPAT	0.161202	-2.63306	0.039918
chr22__21805825__21807846___MAPK1	0.161252	-2.63261	0.010402
chr1__51394381__51448135___EPS15	0.161258	-2.63255	0.005019
chr8__94530963__94538346___KIAA1429	0.161259	-2.63255	0.03206
chr3__132434538__132450847___DNAJC13	0.161278	-2.63238	0.036082
chr15__40386405__40392023___KNSTRN	0.16134	-2.63182	0.036845
chr16__1632212__1641187___CRAMP1L	0.161517	-2.63025	0.040356
chr10__68959806__68962157___DDX21	0.161631	-2.62922	0.015846
chr16__48258618__48277479___LONP2	0.161648	-2.62907	0.034526
chr5__112766326__112801383___APC	0.161774	-2.62795	0.005472
chr7__140834609__140834872___BRAF	0.16196	-2.62629	0.03481

chr12__62194933__62207250___NA	0.161978	-2.62613	0.040353
chr4__186706563__186709845___FAT1	0.161999	-2.62594	0.009527
chr13__32753332__32760720___PDS5B	0.162242	-2.62379	0.019154
chr1__13715541__13742157___PRDM2	0.162416	-2.62223	0.006729
chr19__34327421__34330347___KIAA0355	0.162436	-2.62206	0.006932
chr4__109468361__109473186___SEC24B	0.162459	-2.62186	0.005445
chr1__70184785__70187338___LRRC40	0.162474	-2.62172	0.034742
chr10__118685983__118707587___CACUL1	0.162485	-2.62162	0.039419
chr3__125277726__125331238___ZNF148	0.162652	-2.62014	0.031854
chr13__98482265__98519473___STK24	0.162741	-2.61935	0.038306
chr1__35003968__35015162___ZMYM6	0.162831	-2.61855	0.016035
chr13__28174272__28220378___PAN3	0.162841	-2.61846	0.015933
chr3__37058790__37096660___LRRFIP2	0.162887	-2.61806	0.032354
chr7__38789801__38796864___VPS41	0.162895	-2.61798	0.035387
chr2__152132114__152150229___STAM2	0.162914	-2.61782	0.032988
chr22__41125864__41130003___EP300	0.16299	-2.61715	0.031017
chr1__211353239__211354467___TRAF5	0.163033	-2.61677	0.036347
chr12__813642__862270___WNK1	0.163133	-2.61588	0.034969
chr4__128831733__128852268___JADE1	0.163232	-2.61501	0.042897
chr6__109475399__109476930___ZBTB24	0.163314	-2.61428	0.040886
chr6__149342685__149370099___TAB2	0.16335	-2.61396	0.033538
chr3__123955843__123956795___CCDC14	0.163383	-2.61367	0.035545
chr6__144451370__144459354___UTRN	0.163552	-2.61218	0.03964
chr15__63661753__63669698___HERC1	0.163632	-2.61147	0.013483
chr10__72475100__72508269___MICU1	0.163697	-2.6109	0.019353
chr3__44801450__44811043___KIF15	0.163713	-2.61076	0.043019
chr15__30967920__30976955___MTMR10	0.163751	-2.61042	0.029219
chr2__53693884__53750941___ASB3GPR75-ASB3	0.163835	-2.60968	0.019273
chr8__123361539__123372686___ATAD2	0.163841	-2.60964	0.039109
chr16__30993130__30997059___STX1B	0.163922	-2.60892	0.017175
chr3__20072395__20148487___KAT2B	0.164022	-2.60804	0.007808
chr3__136452033__136502779___STAG1	0.164073	-2.60759	0.035505
chr15__92885515__92892072___LOC100507217	0.164148	-2.60693	0.01396
chr3__17010905__17014911___PLCL2	0.164151	-2.60691	0.048726
chr1__28476112__28480604___PHACTR4	0.164211	-2.60638	0.036845
chr4__75790150__75790797___USO1	0.164326	-2.60536	0.011298
chr10__32291163__32293194___EPC1	0.164367	-2.60501	0.016425
chr20__34634615__34637985___PIGU	0.164406	-2.60466	0.035549
chr18__22936754__22975219___RBBP8	0.164432	-2.60444	0.038144
chr10__91994535__92008275___BTAF1	0.164439	-2.60438	0.01915
chr6__149342685__149379518___TAB2	0.164534	-2.60354	0.020428
chr11__77374328__77392541___PAK1	0.164711	-2.60199	0.036035
chr6__159784666__159785496___TCP1	0.164712	-2.60198	0.037646
chr18__57566447__57567876___FECH	0.164722	-2.6019	0.034698
chr15__92953357__92967513___CHD2	0.16474	-2.60174	0.032178
chr10__133398435__133399619___MTG1	0.164781	-2.60138	0.017062

chr1__179131311__179133374___ABL2	0.164908	-2.60027	0.037691
chr17__61743013__61793729___BRIP1	0.164927	-2.6001	0.035642
chr9__131643239__131650949___RAPGEF1	0.165014	-2.59934	0.03615
chr4__48602020__48609823___FRYL	0.165168	-2.598	0.039008
chr1__182872337__182880608___DHX9	0.165229	-2.59746	0.037212
chr7__140127442__140133656___KDM7A	0.165254	-2.59724	0.014279
chrX__155506898__155545277___TMLHE	0.165319	-2.59668	0.035412
chr13__51382029__51389444___INTS6	0.165394	-2.59602	0.031985
chr11__108104190__108106295___CUL5	0.165476	-2.59531	0.044918
chr5__143295460__143314168___NR3C1	0.165595	-2.59427	0.031377
chr9__85596362__85646435___AGTPBP1	0.165657	-2.59373	0.038144
chr2__230357805__230371651___SP140L	0.165779	-2.59267	0.035387
chr10__28119651__28131691___MPP7	0.165834	-2.59219	0.043024
chr1__193028085__193029657___UCHL5	0.165938	-2.59129	0.016913
chr3__9388087__9390497___NA	0.166057	-2.59025	0.012622
chr9__124922724__124923223___GOLGA1	0.166117	-2.58973	0.036006
chr3__56571181__56594028___CCDC66	0.166216	-2.58887	0.030319
chr14__50437476__50440441___MAP4K5	0.166267	-2.58842	0.017062
chr9__5064883__5081861___JAK2	0.166286	-2.58826	0.007326
chr5__146483540__146503539___TCERG1	0.166315	-2.58801	0.04545
chr9__100340257__100349372___TEX10	0.166338	-2.58781	0.03469
chr12__98527886__98537572___TMPO	0.166463	-2.58673	0.037691
chr1__211783229__211793190___LPGAT1	0.166473	-2.58664	0.047742
chr4__84896911__84932363___WDFY3	0.166485	-2.58654	0.017213
chr16__15667286__15677949___NDE1	0.166508	-2.58634	0.013694
chr5__55259848__55272175___DHX29	0.166512	-2.5863	0.033992
chr8__102833056__102834747___AZIN1	0.166515	-2.58628	0.035628
chr10__96544076__96578320___TM9SF3	0.166539	-2.58606	0.046567
chr1__156744163__156745373___HDGF	0.166542	-2.58605	0.032009
chr7__158869855__158891333___WDR60	0.166563	-2.58586	0.045901
chr1__11989165__11992690___MFN2	0.166614	-2.58542	0.038165
chr12__4500138__4525583___C12orf4	0.166689	-2.58477	0.040693
chr16__11684165__11688445___TXNDC11	0.1667	-2.58467	0.048706
chr4__87046166__87047674___AFF1	0.166999	-2.58209	0.020685
chr1__185181946__185231708___SWT1	0.167014	-2.58196	0.035628
chr21__36338779__36356724___MORC3	0.167027	-2.58184	0.020903
chr21__39202325__39212707___BRWD1	0.16721	-2.58027	0.033365
chr18__37160200__37173081___KIAA1328	0.167352	-2.57904	0.048387
chr22__41808875__41810291___CCDC134	0.167465	-2.57807	0.037156
chr12__110485078__110487943___FAM216A	0.167472	-2.578	0.017198
chr6__109656756__109675756___AK9	0.16782	-2.57501	0.047242
chr2__44549555__44558013___CAMKMT	0.167924	-2.57412	0.021177
chr1__200559330__200560880___KIF14	0.167944	-2.57395	0.04256
chr17__68450728__68452992___WIPI1	0.168114	-2.57248	0.009669
chr8__103404776__103407784___SLC25A32	0.168124	-2.5724	0.042491
chr20__2964272__2988474___PTPRA	0.168134	-2.57232	0.034051

chr2__175097444__175121540___ATF2	0.168433	-2.56975	0.021442
chr12__292759__293169___KDM5A	0.168604	-2.56829	0.020579
chr20__35801491__35871829___PHF20	0.168632	-2.56805	0.04708
chr13__45979813__45989097___ZC3H13	0.168769	-2.56688	0.042038
chr10__69359897__69369624___HK1	0.168825	-2.5664	0.012608
chr14__31116236__31121505___HECTD1	0.168836	-2.5663	0.040389
chr20__49639678__49640665___B4GALT5	0.168933	-2.56548	0.01243
chr14__49813988__49831361___NEMF	0.168947	-2.56535	0.00576
chr15__65715478__65717996___DENND4A	0.169066	-2.56434	0.033873
chr2__32414769__32416163___BIRC6	0.169333	-2.56206	0.041945
chr13__50927407__50934999___RNASEH2B	0.169361	-2.56183	0.02177
chr12__100282943__100335906___SCYL2	0.169379	-2.56168	0.034742
chr17__8518631__8535931___MYH10	0.169448	-2.56108	0.038649
chr15__44606025__44610985___SPG11	0.169806	-2.55804	0.022689
chr3__155897927__155916192___GMPS	0.169813	-2.55798	0.022832
chr3__56730666__56731299___ARHGEF3	0.169815	-2.55796	0.039654
chr9__15457960__15460313___SNAPC3	0.170086	-2.55567	0.021989
chr9__77247259__77283650___VPS13A	0.170119	-2.55539	0.018096
chr6__144537582__144557311___UTRN	0.170144	-2.55517	0.04256
chr12__2868563__2868754___FOXM1	0.170339	-2.55352	0.040356
chr22__38537592__38568286___DMC1	0.17061	-2.55122	0.016275
chr13__45979813__46020557___ZC3H13	0.170611	-2.55122	0.040427
chr11__35198121__35210054___CD44	0.170688	-2.55057	0.009527
chr17__18582658__18595181___CCDC144B	0.170724	-2.55026	0.041764
chr2__38577920__38581560___HNRNPLL	0.171009	-2.54785	0.021989
chr1__86124845__86146183___COL24A1	0.171085	-2.54722	0.015806
chr1__174969277__174976182___RABGAP1L	0.171087	-2.5472	0.042368
chrX__14850505__14865580___FANCB	0.171126	-2.54687	0.048342
chr10__68025546__68044558___HERC4	0.171175	-2.54646	0.034989
chr9__2181571__2192802___SMARCA2	0.17123	-2.54599	0.04101
chr15__52593578__52601165___FAM214A	0.171255	-2.54578	0.018822
chr13__60509763__60535233___TDRD3	0.171375	-2.54478	0.041912
chr3__20170724__20178347___SGOL1	0.171404	-2.54453	0.040115
chr4__109506331__109539667___SEC24B	0.171438	-2.54424	0.023145
chr13__19838700__19838985___ZMYM5	0.17145	-2.54414	0.039918
chr3__196361844__196362687___UBXN7	0.17166	-2.54237	0.005573
chr10__68363590__68404844___RUFY2	0.171769	-2.54146	0.041119
chr17__59935193__59936541___RPS6KB1	0.172076	-2.53888	0.022016
chr4__189855886__189864786___NA	0.172081	-2.53884	0.033042
chr14__50640750__50645014___SAV1	0.172102	-2.53866	0.016091
chrX__75098942__75114834___ABCB7	0.172102	-2.53867	0.046516
chr13__25307806__25327512___NUPL1	0.172242	-2.53749	0.047803
chr2__112299849__112321865___ZC3H6	0.172355	-2.53654	0.019526
chr20__1452493__1458274___NSFL1C	0.17244	-2.53583	0.007326
chr2__128097429__128123246___UGGT1	0.172567	-2.53477	0.022515
chr14__50446079__50456594___MAP4K5	0.172675	-2.53387	0.041377

chr7__152783187__152825122___ACTR3B	0.172806	-2.53277	0.042509
chr10__68465667__68470163___DNA2	0.172812	-2.53273	0.045875
chr12__430664__438554___CCDC77	0.172897	-2.53202	0.018731
chrX__101101058__101148161___CENPI	0.172962	-2.53147	0.020648
chr18__24366892__24377535___OSBPL1A	0.173098	-2.53034	0.019233
chrX__77988242__77989958___ATP7A	0.173487	-2.5271	0.04303
chr16__18815175__18819654___SMG1	0.173507	-2.52694	0.037334
chr12__30725966__30751133___CAPRIN2	0.173573	-2.52638	0.04788
chr5__69194647__69208359___CENPH	0.173608	-2.5261	0.044231
chr7__105040839__105091314___KMT2E	0.173918	-2.52352	0.042993
chr3__100267100__100281847___TBC1D23	0.174143	-2.52165	0.049513
chr15__49011731__49028682___SECISBP2L	0.174203	-2.52116	0.048225
chr7__37013299__37033412___ELMO1	0.174269	-2.52062	0.042342
chr9__137790848__137800984___EHMT1	0.174279	-2.52053	0.04545
chr16__11721577__11736233___TXNDC11	0.17448	-2.51887	0.041993
chr3__56572337__56594028___CCDC66	0.174515	-2.51858	0.020021
chr19__10637644__10638315___SLC44A2	0.174632	-2.51761	0.009284
chr12__89626454__89630645___ATP2B1	0.174679	-2.51722	0.038875
chr4__39837856__39845880___PDS5A	0.174722	-2.51687	0.016091
chr5__54084765__54094975___ARL15	0.174763	-2.51653	0.041126
chr1__29060422__29115803___EPB41	0.174792	-2.51629	0.047073
chr11__108169744__108177090___NPAT	0.174793	-2.51628	0.020449
chrY__20582590__20589575___EIF1AY	0.175151	-2.51333	0.041289
chr11__35204512__35208206___CD44	0.175158	-2.51327	0.01135
chr11__46816198__46821248___CKAP5	0.17523	-2.51268	0.04788
chr1__70274720__70315566___ANKRD13C	0.17535	-2.51169	0.043019
chr1__1719328__1722831___CDK11A	0.175464	-2.51076	0.047391
chr7__103321932__103327754___DNAJC2	0.175481	-2.51062	0.049522
chr2__181474960__181511775___ITGA4	0.175617	-2.50949	0.042668
chr18__26389845__26394481___NA	0.175742	-2.50847	0.022743
chr2__128113084__128145967___UGGT1	0.175772	-2.50823	0.008439
chr16__11894954__11896782___GSPT1	0.175989	-2.50644	0.040357
chr11__16183886__16199254___SOX6	0.176513	-2.50216	0.020449
chr15__40208637__40210210___BUB1B	0.176934	-2.49872	0.044706
chr21__39215237__39225197___BRWD1	0.177254	-2.49611	0.043019
chr5__41907736__41912183___C5orf51	0.177514	-2.49399	0.043037
chr12__11121010__11147135___PRH1-PRR4	0.177621	-2.49312	0.014745
chr2__120278618__120280907___RALB	0.177651	-2.49289	0.044488
chr4__143840807__143848527___NA	0.177663	-2.49279	0.049325
chr5__103190842__103201675___PPIP5K2	0.177832	-2.49141	0.041397
chr7__64521064__64544432___ZNF680	0.177856	-2.49121	0.016542
chr2__30525587__30568176___LCLAT1	0.177878	-2.49104	0.025849
chr9__77794463__77797648___GNAQ	0.177943	-2.49051	0.004582
chr17__32755492__32780784___MYO1D	0.177945	-2.4905	0.045012
chr9__33351560__33352719___NFX1	0.178017	-2.48991	0.010022
chr18__45988702__45992202___PSTPIP2	0.178199	-2.48844	0.017806

chr3__37289235__37302332___GOLGA4	0.178239	-2.48812	0.047982
chr1__45616626__45617591___NASP	0.17848	-2.48617	0.048208
chr18__56624288__56626457___TXNL1	0.178617	-2.48506	0.046364
chr2__60786947__60792289___PAPOLG	0.178651	-2.48479	0.04303
chr4__53383773__53396061___FIP1L1	0.178683	-2.48452	0.048729
chr19__29817137__29817541___CCNE1	0.178829	-2.48334	0.020922
chr19__19465340__19474118___GATAD2A	0.178907	-2.48272	0.026752
chr2__113916884__113942359___ACTR3	0.178917	-2.48264	0.047242
chr5__95748333__95763620___RHOBTB3	0.179003	-2.48195	0.026975
chr8__99134632__99156743___VPS13B	0.179219	-2.4802	0.007749
chr5__55340010__55358698___SKIV2L2	0.179412	-2.47865	0.046989
chr8__31120243__31167230___WRN	0.179472	-2.47817	0.015574
chr2__213310059__213364145___SPAG16	0.179573	-2.47736	0.045577
chr10__91951403__91966757___BTAF1	0.179591	-2.47721	0.010992
chr20__2947982__2975241___PTPRA	0.179632	-2.47688	0.000859
chr4__2875896__2884666___ADD1	0.179634	-2.47687	0.043254
chr2__232747615__232761436___GIGYF2	0.179669	-2.47659	0.026387
chr12__92832512__92842581___EEA1	0.179681	-2.47649	0.043278
chr6__90556500__90571807___MAP3K7	0.179722	-2.47616	0.041182
chr7__26195847__26196658___HNRNPA2B1	0.179729	-2.47611	0.047898
chr14__69768138__69768674___SRSF5	0.179774	-2.47574	0.021254
chr5__94628811__94651845___ANKRD32	0.179976	-2.47413	0.027555
chr9__27044742__27062110___IFT74	0.180028	-2.47371	0.049015
chr20__35842573__35871829___PHF20	0.180139	-2.47282	0.047696
chr2__11278442__11287736___ROCK2	0.180179	-2.4725	0.048092
chr14__92088730__92096838___ATXN3	0.180182	-2.47247	0.022054
chr6__110887505__110890356___AMD1	0.180227	-2.47211	0.046603
chr4__48833401__48850082___OCIAD1	0.180269	-2.47178	0.043512
chr1__174219501__174220436___RABGAP1L	0.180432	-2.47047	0.049681
chr6__37929959__37939219___ZFAND3	0.180488	-2.47002	0.013827
chr5__77046347__77055596___AGGF1	0.18055	-2.46953	0.044823
chrX__110067347__110109146___TMEM164	0.180668	-2.46859	0.017231
chr14__31380467__31387375___HEATR5A	0.180673	-2.46855	0.048658
chr7__24620052__24680520___MPP6	0.181066	-2.46541	0.019416
chr3__149074215__149076047___HLTF	0.181078	-2.46532	0.008172
chr9__125298890__125312612___GAPVD1	0.18114	-2.46482	0.046398
chr9__68727596__68728934___PIP5K1B	0.181251	-2.46394	0.00882
chr16__11875761__11887750___GSPT1	0.181374	-2.46296	0.019188
chr20__49068715__49070297___CSE1L	0.181436	-2.46247	0.01866
chr6__53523255__53532766___GCLC	0.18155	-2.46156	0.049062
chr3__142318592__142318903___XRN1	0.181664	-2.46065	0.025852
chr14__103487379__103487707___MARK3	0.181695	-2.46041	0.020486
chr5__146263491__146271058___RBM27	0.181872	-2.459	0.019539
chr1__229521592__229549434___ABCB10	0.181953	-2.45836	0.014904
chr9__33935839__33941862___UBAP2	0.181956	-2.45834	0.021847
chr8__55782748__55787060___TGS1	0.182099	-2.4572	0.047499

chr3__138694786__138699095___PIK3CB	0.182113	-2.4571	0.030426
chr14__52455324__52491005___TXNDC16	0.182122	-2.45702	0.048033
chr3__119905755__120093593___GSK3B	0.182233	-2.45614	0.002628
chr11__77675036__77691238___RSF1	0.18226	-2.45593	0.046989
chr20__49151582__49179244___STAU1	0.182326	-2.45541	0.042988
chr6__57193842__57207713___RAB23	0.182372	-2.45505	0.046204
chr3__196064309__196068130___TFRC	0.182422	-2.45465	0.023833
chr2__226837722__226914351___RHBDD1	0.182517	-2.4539	0.040709
chr3__150571958__150581746___EIF2A	0.182531	-2.45379	0.012235
chr1__88691724__88786213___PKN2	0.182632	-2.45299	0.019519
chr16__4466153__4469465___NMRAL1	0.182696	-2.45249	0.016116
chr8__123134114__123144855___TBC1D31	0.182706	-2.4524	0.029084
chr16__15664736__15696860___NDE1	0.182763	-2.45195	0.043019
chr6__87545616__87564232___RARS2	0.182868	-2.45113	0.046408
chr2__159729009__159752571___MARCH7	0.18289	-2.45095	0.012932
chr18__62830035__62860601___PHLPP1	0.183182	-2.44865	0.042368
chr19__10168330__10175618___DNMT1	0.18324	-2.44819	0.02966
chr12__48063710__48101516___SENP1	0.183523	-2.44597	0.020293
chr14__52470037__52544371___TXNDC16	0.183663	-2.44487	0.024248
chr2__169537227__169544835___FASTKD1	0.183663	-2.44487	0.013482
chr19__7163032__7163199___INSR	0.183774	-2.444	0.043024
chr3__195336932__195345317___ACAP2	0.183827	-2.44358	0.021179
chr17__59257122__59275970___GDPD1	0.183922	-2.44283	0.045081
chr1__197084354__197100914___ASPM	0.184145	-2.44108	0.046089
chr6__116692055__116726622___KPNA5	0.184227	-2.44044	0.029643
chr2__175939552__175964533___KIAA1715	0.184387	-2.43919	0.014904
chr9__77337255__77344281___VPS13A	0.184468	-2.43856	0.048706
chr17__43067608__43074521___BRCA1	0.18452	-2.43815	0.028099
chr7__7055395__7091828___NA	0.184589	-2.43761	0.017227
chr14__49825867__49829426___NEMF	0.184634	-2.43726	0.020654
chr15__41069570__41074565___INO80	0.184706	-2.4367	0.031096
chr4__82878730__82880922___SEC31A	0.184942	-2.43485	0.04788
chr18__62556203__62565096___ZCCHC2	0.185142	-2.4333	0.015658
chr15__94440176__94470442___MCTP2	0.185371	-2.43151	0.021234
chr15__82813103__82826846___WHAMM	0.185483	-2.43064	0.009488
chr22__42817142__42826999___ARFGAP3	0.185644	-2.42939	0.024972
chr3__141959674__142005544___TFDP2	0.185649	-2.42935	0.024818
chr4__73118688__73125312___ANKRD17	0.185784	-2.4283	0.014865
chr11__46754888__46760784___CKAP5	0.185896	-2.42743	0.009284
chr17__61034666__61040892___BCAS3	0.185995	-2.42667	0.048033
chr6__133975050__133987168___TBPL1	0.186031	-2.42638	0.028917
chr15__90217439__90219891___SEMA4B	0.186087	-2.42595	0.025069
chr2__39336920__39337581___MAP4K3	0.186289	-2.42439	0.012646
chr17__19939713__19958571___AKAP10	0.186301	-2.42429	0.0248
chr5__138159555__138166108___BRD8	0.186376	-2.42371	0.048346
chr5__71544357__71553320___BDP1	0.186453	-2.42311	0.048658

chr2__201381124__201393046___TRAK2	0.186474	-2.42296	0.041224
chr3__155906160__155916192___GMPS	0.186572	-2.4222	0.024982
chr7__50376533__50382707___IKZF1	0.186723	-2.42103	0.047205
chr11__108330214__108335961___ATM	0.186847	-2.42007	0.020685
chr13__48373405__48381443___RB1	0.187031	-2.41865	0.032988
chr20__47290187__47298872___ZMYND8	0.187086	-2.41823	0.043877
chr17__61743013__61780401___BRIP1	0.187176	-2.41754	0.020903
chr5__87331348__87341321___RASA1	0.187427	-2.4156	0.021273
chr7__26190993__26197866___HNRNPA2B1	0.187471	-2.41526	0.047369
chr3__146121112__146124229___PLOD2	0.187574	-2.41447	0.010255
chr11__17309572__17312120___NUCB2	0.187596	-2.4143	0.031491
chr18__8624938__8635622___RAB12	0.187642	-2.41395	0.032667
chr5__139614586__139623461___UBE2D2	0.187649	-2.41389	0.046989
chr4__82870325__82881940___SEC31A	0.187653	-2.41386	0.049522
chr12__68715627__68725796___NUP107	0.187766	-2.413	0.026103
chr2__190900564__190910321___GLS	0.187811	-2.41265	0.043434
chr4__102722871__102726683___MANBA	0.187886	-2.41207	0.026186
chr16__71656571__71664099___PHLPP2	0.187986	-2.4113	0.046845
chr1__224189577__224190319___DEGS1	0.187996	-2.41123	0.018096
chr22__38552666__38568289___DMC1	0.188263	-2.40918	0.01874
chr9__77922161__77999328___GNAQ	0.188283	-2.40903	0.045469
chr1__154225084__154241565___UBAP2L	0.188347	-2.40854	0.026159
chr13__28174272__28197346___PAN3	0.188366	-2.40839	0.016505
chr14__35014744__35019074___SRP54	0.188503	-2.40734	0.013932
chr17__16101250__16101757___NCOR1	0.188712	-2.40574	0.048008
chr22__42817142__42822409___ARFGAP3	0.18883	-2.40484	0.022139
chr16__50786855__50793664___CYLD	0.188842	-2.40475	0.022035
chr1__231795242__231818517___TSNAX-DISC1DISC1	0.188928	-2.40409	0.005437
chr2__32174063__32184338___SLC30A6	0.188936	-2.40403	0.011956
chr12__26621123__26655852___ITPR2	0.189271	-2.40148	0.021663
chr4__51860543__51899378___DCUN1D4	0.189863	-2.39697	0.027702
chr15__65671792__65701890___DENND4A	0.189926	-2.39649	0.032667
chr12__69592059__69593613___CCT2	0.19024	-2.39411	0.006717
chr6__42632552__42637194___UBR2	0.190253	-2.39401	0.022503
chr3__28263291__28298350___CMC1	0.190261	-2.39395	0.01776
chr3__142403674__142414291___XRN1	0.190309	-2.39359	0.014865
chr3__123933673__123949132___CCDC14	0.19033	-2.39343	0.019539
chr11__121583458__121595772___SORL1	0.190385	-2.39301	0.045768
chr3__47686049__47693300___SMARCC1	0.190581	-2.39152	0.04954
chr21__29305204__29329693___BACH1	0.190597	-2.3914	0.006941
chr12__112203636__112226758___HECTD4	0.190751	-2.39024	0.012953
chr5__79618647__79623489___PAPD4	0.191052	-2.38797	0.009727
chr3__143985543__143997584___NA	0.19162	-2.38368	0.04984
chr2__15415546__15478289___NBAS	0.191955	-2.38116	0.049325
chr17__81270525__81271024___SLC38A10	0.191964	-2.38109	0.033074
chr20__50902017__50918781___ADNP	0.192141	-2.37976	0.016103

chr6__130022227__130094367___L3MBTL3	0.192291	-2.37864	0.047182
chr8__97686668__97689103___MTDH	0.192356	-2.37815	0.024046
chr5__36950999__36962274___NIPBL	0.192448	-2.37746	0.010843
chr1__229539456__229549584___ABCB10	0.192544	-2.37674	0.005871
chr17__42000482__42003557___DNAJC7	0.192551	-2.37669	0.009629
chr4__20702141__20727397___PACRGL	0.192766	-2.37508	0.049621
chr6__47595861__47612536___CD2AP	0.192969	-2.37356	0.032764
chr16__67036639__67082339___CBFB	0.193041	-2.37302	0.01145
chr2__24643966__24673463___NCOA1	0.193137	-2.37231	0.018638
chr2__159729009__159748903___MARCH7	0.193259	-2.37139	0.049325
chr13__27069090__27116596___USP12	0.193336	-2.37082	0.033947
chr16__11875761__11894987___GSPT1	0.193547	-2.36925	0.01634
chr20__49135833__49154071___STAU1	0.193559	-2.36915	0.048706
chr3__143982408__143985846___C3orf58	0.193634	-2.36859	0.035628
chr20__2964272__2975241___PTPRA	0.193653	-2.36846	0.003276
chr1__77736056__77741748___USP33	0.194124	-2.36495	0.030426
chr6__15246156__15246584___JARID2	0.194171	-2.3646	0.034524
chrX__118654602__118654961___DOCK11	0.194366	-2.36315	0.035509
chr10__863743__864270___LARP4B	0.194742	-2.36036	0.035395
chr20__17969801__17970130___MGME1	0.194815	-2.35982	0.02487
chr6__136694140__136720589___MAP3K5	0.195251	-2.3566	0.029412
chr11__72887470__72889945___FCHSD2	0.195423	-2.35533	0.032631
chr13__21155693__21159987___SKA3	0.195474	-2.35495	0.029226
chr3__121647319__121657352___HCLS1	0.195772	-2.35275	0.013458
chr10__15833630__15843272___FAM188A	0.196321	-2.34871	0.025879
chr10__67988663__68014186___HERC4	0.196614	-2.34656	0.011512
chr2__174472965__174481987___GPR155	0.196682	-2.34606	0.02706
chr20__37055553__37065473___RBL1	0.196852	-2.34482	0.029772
chr5__154865192__154872651___CNOT8	0.196859	-2.34476	0.009488
chr2__201386218__201389880___TRAK2	0.197558	-2.33965	0.035549
chr2__55558775__55573777___SMEK2	0.19762	-2.3392	0.038337
chr14__103448919__103457212___MARK3	0.197971	-2.33664	0.002851
chrX__78003073__78009263___ATP7A	0.197972	-2.33663	0.030813
chr15__49027365__49037769___SECISBP2L	0.198034	-2.33618	0.013908
chr11__3744509__3753408___NUP98	0.198064	-2.33596	0.025879
chr8__61618978__61644632___ASPH	0.198067	-2.33594	0.015771
chr3__71710412__71728623___EIF4E3	0.198178	-2.33513	0.004935
chr1__213117317__213129889___RPS6KC1	0.198281	-2.33438	0.0097
chr4__82930943__82984876___LIN54	0.198316	-2.33413	0.022503
chr3__115071219__115073056___ZBTB20	0.198759	-2.33091	0.018312
chr11__3768581__3773739___NUP98	0.199135	-2.32818	0.022503
chr13__48239226__48261321___ITM2B	0.199143	-2.32812	0.006748
chr1__1716346__1722831___CDK11A	0.199153	-2.32805	0.013482
chrX__24723155__24743329___POLA1	0.199234	-2.32747	0.0335
chr14__55146446__55148473___NA	0.199636	-2.32456	0.032061
chr6__136694140__136698682___MAP3K5	0.199718	-2.32397	0.01874

chr4__82821037__82829058___SEC31A	0.199836	-2.32311	0.027685
chr1__61111371__61152356___NFIA	0.199965	-2.32218	0.039654
chr12__82369387__82456820___METTL25	0.200098	-2.32122	0.027259
chr2__24135119__24161613___FAM228B	0.200165	-2.32073	0.033225
chr1__70173465__70189273___LRRC40	0.200187	-2.32058	0.020449
chr10__11597631__11601467___USP6NL	0.20027	-2.31998	0.026228
chr9__83665030__83677961___UBQLN1	0.200273	-2.31996	0.027588
chr3__149822518__149921227___RNF13	0.200847	-2.31583	0.040356
chr12__48071667__48096427___SENP1	0.201949	-2.30793	0.036383
chr3__160366043__160384646___IFT80	0.202091	-2.30693	0.027556
chr3__160356013__160377540___IFT80	0.202295	-2.30546	0.03481
chr16__66608309__66610003___CMTM3	0.203196	-2.29906	0.008599
chr6__149676260__149680457___LATS1	0.203362	-2.29788	0.017954
chr4__106116203__106309998___TBCK	0.20371	-2.29541	0.02255
chr9__17330632__17416189___CNTLN	0.203747	-2.29515	0.035509
chr3__128795360__128813471___RAB7A	0.203793	-2.29482	0.013584
chr6__169759838__169768171___ERMARD	0.203978	-2.29351	0.042057
chr1__158842134__158844122___MNDA	0.204294	-2.29128	0.028172
chr10__45533110__45533289___MARCH8	0.204296	-2.29126	0.016396
chr20__49072286__49091022___CSE1L	0.204411	-2.29045	0.040511
chr18__79096476__79176907___ATP9B	0.204571	-2.28933	0.0114
chr17__47137152__47151918___CDC27	0.204806	-2.28767	0.043831
chr5__94888879__94912976___MCTP1	0.204866	-2.28725	0.014782
chr1__32279671__32280210___LCK	0.20499	-2.28637	0.035387
chr22__36341370__36349255___MYH9	0.205331	-2.28398	0.031351
chr2__152132114__152135603___STAM2	0.205427	-2.2833	0.036417
chr7__74235532__74246763___RFC2	0.205509	-2.28273	0.019558
chr2__233256102__233265143___ATG16L1	0.205694	-2.28143	0.019555
chr17__43521369__43522226___DHX8	0.206288	-2.27727	0.006533
chr3__25751098__25778688___NGLY1	0.206922	-2.27284	0.032591
chr2__171448681__171469030___DCAF17	0.20707	-2.27181	0.010339
chr15__55951376__55966546___NEDD4	0.207081	-2.27173	0.045094
chr18__79096476__79207012___ATP9B	0.207163	-2.27116	0.047154
chr1__11124498__11133197___MTOR	0.207168	-2.27113	0.043759
chr12__102148230__102150371___PARPBP	0.207277	-2.27037	0.036971
chr6__131136778__131219808___AKAP7	0.207399	-2.26952	0.030193
chr9__112262435__112276013___PTBP3	0.207727	-2.26724	0.042986
chr3__56639986__56673725___FAM208A	0.207857	-2.26634	0.040886
chr1__214613714__214622281___CENPF	0.208176	-2.26412	0.031377
chr3__56623644__56628614___FAM208A	0.208228	-2.26376	0.040427
chr13__77081427__77087633___MYCBP2	0.208252	-2.2636	0.031406
chr8__22474954__22475624___PPP3CC	0.208478	-2.26203	0.037605
chr20__32366384__32371874___ASXL1	0.208542	-2.26159	0.044256
chr19__10166598__10173905___DNMT1	0.208729	-2.26029	0.037298
chr1__180824753__180825344___XPR1	0.208916	-2.25901	0.030492
chr12__29293300__29297200___FAR2	0.209084	-2.25784	0.047154

chr22__41125864__41131633___EP300	0.209112	-2.25765	0.015447
chr21__33340999__33343676___IFNAR1	0.209315	-2.25625	0.033391
chr19__51573210__51588078___ZNF175	0.209713	-2.25351	0.031799
chr14__30628209__30643405___SCFD1	0.209856	-2.25253	0.038036
chr6__145864388__145894977___SHPRH	0.209981	-2.25167	0.044262
chr13__95157161__95170628___ABCC4	0.210033	-2.25131	0.032317
chr20__21365421__21368590___XRN2	0.2101	-2.25085	0.007902
chr20__41512846__41533570___CHD6	0.210202	-2.25015	0.02371
chr15__67600685__67664645___MAP2K5	0.210294	-2.24952	0.038466
chr22__32478981__32485209___FBXO7	0.210485	-2.24821	0.002426
chr10__35501501__35530243___CCNY	0.210846	-2.24574	0.033122
chr12__110018345__110025823___ANKRD13A	0.211072	-2.24419	0.022401
chr15__62033441__62044255___VPS13C	0.211122	-2.24385	0.003804
chr6__149616007__149623283___KATNA1	0.211167	-2.24354	0.040875
chr16__11841695__11842000___RSL1D1	0.211943	-2.23825	0.043859
chr5__66043077__66054951___ERBB2IP	0.2121	-2.23718	0.03507
chr15__49129477__49139653___COPS2	0.212141	-2.2369	0.020449
chr7__105066727__105091314___KMT2E	0.212243	-2.23621	0.022498
chr1__111147642__111184280___CEPT1	0.212286	-2.23592	0.033749
chr4__121833231__121839696___BBS7	0.212359	-2.23542	0.026636
chr4__78845016__78878891___BMP2K	0.212489	-2.23454	0.04545
chr12__26711173__26725765___ITPR2	0.21292	-2.23161	0.041224
chr2__36883932__36886826___STRN	0.21303	-2.23087	0.040285
chr5__87372118__87374916___RASA1	0.213551	-2.22735	0.02291
chr3__49324702__49325845___USP4	0.213853	-2.22531	0.041645
chr5__73056065__73070950___FCHO2	0.213981	-2.22445	0.031138
chr11__83206058__83236509___ANKRD42	0.214289	-2.22237	0.035446
chr9__33941649__33963791___UBAP2	0.214438	-2.22137	0.033391
chr17__82884145__82903478___TBCD	0.214839	-2.21867	0.035587
chr11__120420753__120477526___ARHGEF12	0.214858	-2.21855	0.015644
chr3__136417885__136423044___STAG1	0.214993	-2.21764	0.01892
chr10__68761007__68766079___CCAR1	0.215128	-2.21674	0.048268
chr11__46750274__46753497___CKAP5	0.215145	-2.21662	0.015854
chr3__138209817__138245183___ARMC8	0.215305	-2.21555	0.02146
chr7__80656592__80674147___CD36	0.215349	-2.21525	0.03055
chr21__36364093__36372531___MORC3	0.215437	-2.21466	0.017476
chr19__8465324__8474244___HNRNPM	0.215501	-2.21423	0.035413
chr5__168488602__168495436___RARS	0.215545	-2.21394	0.014608
chr15__89871475__89889140___C15orf38-AP3S2AP3S2	0.215567	-2.21379	0.042491
chr7__38010921__38013581___NA	0.215773	-2.21242	0.0201
chr17__29451455__29451680___TAOK1	0.216055	-2.21053	0.009237
chr6__110431171__110457017___SLC22A16	0.216749	-2.2059	0.027131
chr3__196069455__196075360___TFRC	0.21694	-2.20463	0.036624
chr18__21765772__21804014___MIB1	0.217033	-2.20401	0.017635
chr9__77339516__77351446___VPS13A	0.217273	-2.20242	0.049928
chrY__13335563__13336335___UTY	0.217279	-2.20238	0.012608

chr9__36657241__36674937___MELK	0.21732	-2.20211	0.028003
chr12__112446276__112456063___PTPN11	0.217326	-2.20207	0.035642
chr13__98474821__98519473___STK24	0.217488	-2.20099	0.014124
chr1__155354473__155357749___ASH1L	0.218404	-2.19493	0.029318
chr7__16216066__16259012___ISPD	0.218527	-2.19411	0.044317
chr9__120487294__120491477___CDK5RAP2	0.218977	-2.19115	0.04796
chr15__44328685__44380976___CASC4	0.219485	-2.18781	0.019416
chr12__28225795__28307749___CCDC91	0.219682	-2.18651	0.009446
chr1__185166572__185175113___SWT1	0.219934	-2.18486	0.00622
chr3__57841299__57849816___SLMAP	0.219934	-2.18486	0.007749
chr3__152938209__152944616___NA	0.220254	-2.18276	0.016422
chrX__13744415__13755242___OFD1	0.220452	-2.18147	0.040353
chr11__65430769__65444059___NA	0.220628	-2.18032	0.029194
chr11__57491224__57491862___SLC43A1	0.220768	-2.17939	0.00515
chr15__50583089__50586488___TRPM7	0.220797	-2.17921	0.024241
chr15__65665199__65706224___DENND4A	0.220872	-2.17872	0.048287
chr2__85043564__85049648___KCMF1	0.220927	-2.17836	0.03052
chr11__16283756__16288096___SOX6	0.221114	-2.17713	0.01067
chr9__37842089__37861235___DCAF10	0.22136	-2.17553	0.039764
chr19__48149763__48150210___LIG1	0.22138	-2.1754	0.013484
chrX__77520788__77523401___ATRX	0.221409	-2.17521	0.040595
chr15__44560249__44563225___NA	0.221562	-2.17422	0.040357
chr9__6980925__6990524___KDM4C	0.221789	-2.17274	0.010063
chr7__135577796__135593192___NUP205	0.221834	-2.17245	0.024241
chr9__17187084__17236588___CNTLN	0.221898	-2.17203	0.031013
chr15__62020479__62047814___VPS13C	0.221942	-2.17174	0.039109
chr6__110746126__110785609___CDK19	0.222066	-2.17094	0.028304
chr4__102714438__102736435___MANBA	0.222206	-2.17003	0.042491
chr15__52584745__52593736___FAM214A	0.222585	-2.16757	0.042756
chr18__54277703__54287411___POLI	0.22267	-2.16702	0.03185
chr12__42128046__42129851___GXYLT1	0.22287	-2.16573	0.013805
chr8__38247713__38253718___DDHD2	0.223217	-2.16348	0.028099
chr12__50427762__50461347___LARP4	0.223637	-2.16077	0.02737
chr12__110018345__110033957___ANKRD13A	0.223968	-2.15864	0.039799
chr4__1900626__1918623___WHSC1	0.224684	-2.15403	0.03256
chr19__5653115__5657347___SAFB	0.224826	-2.15312	0.044185
chr7__92457552__92492286___NA	0.224842	-2.15302	0.023468
chr5__109713520__109755456___MAN2A1	0.225281	-2.1502	0.023386
chr2__61300951__61301454___USP34	0.225331	-2.14988	0.029084
chr15__76283757__76295737___ETFA	0.225735	-2.1473	0.031899
chr5__94868333__94912976___MCTP1	0.225951	-2.14592	0.032274
chr18__9182382__9239556___ANKRD12	0.226352	-2.14336	0.025773
chr14__60256824__60268435___PPM1A	0.226848	-2.1402	0.042846
chr3__183205876__183207823___MCF2L2	0.227058	-2.13887	0.017776
chr17__32027769__32035639___LRRC37B	0.227246	-2.13767	0.045757
chr2__113913172__113942359___ACTR3	0.227519	-2.13594	0.033391

chr10__114157554__114163329___C10orf118	0.22752	-2.13594	0.024982
chr7__6022787__6024801___EIF2AK1	0.227793	-2.13421	0.048342
chr4__48832620__48860812___OCIAD1	0.227839	-2.13391	0.044845
chr13__27069111__27116596___USP12	0.228218	-2.13152	0.016651
chr6__69697563__69701953___LMBRD1	0.228238	-2.13139	0.047519
chr1__222724092__222725569___BROX	0.228247	-2.13133	0.017208
chr5__168559032__168568998___PANK3	0.228382	-2.13048	0.026115
chr1__28038839__28042650___EYA3	0.228554	-2.12939	0.01523
chr13__77217840__77243951___MYCBP2	0.228597	-2.12912	0.010172
chr1__63411926__63429126___ALG6	0.22889	-2.12727	0.041549
chr15__57231152__57234107___TCF12	0.228924	-2.12706	0.007749
chr10__87864454__87961118___PTEN	0.228975	-2.12674	0.03766
chr3__167704842__167725473___PDCD10	0.229035	-2.12636	0.041764
chr19__18342859__18343415___PGPEP1	0.229103	-2.12593	0.029179
chr20__37065424__37067297___RBL1	0.229235	-2.1251	0.022515
chr10__49932100__49934163___PARG	0.22938	-2.12419	0.044852
chr8__18013964__18025658___PCM1	0.229468	-2.12364	0.034972
chr6__20781145__20797742___CDKAL1	0.229847	-2.12126	0.020457
chr5__160089506__160094065___PWWP2A	0.229867	-2.12113	0.021663
chrX__155277134__155299145___CLIC2	0.230048	-2.11999	0.047428
chr5__55272087__55281515___DHX29	0.230068	-2.11987	0.019555
chr17__20253505__20260294___SPECC1	0.230148	-2.11936	0.029281
chrX__1288519__1288888___CSF2RA	0.230261	-2.11866	0.009856
chr14__74802556__74821137___YLPM1	0.230637	-2.11631	0.047077
chr3__195688533__195689438___NA	0.230854	-2.11495	0.022401
chr20__18543019__18551175___SEC23B	0.230892	-2.11471	0.044648
chr3__50054335__50058562___RBM6	0.231071	-2.11359	0.039875
chr12__102153869__102205152___NA	0.231078	-2.11355	0.023341
chr22__28699838__28725367___CHEK2	0.231758	-2.10931	0.035476
chr1__95143891__95178938___TMEM56TMEM56-RWDD3	0.232112	-2.10711	0.023697
chr22__29970976__29979052___MTMR3	0.232146	-2.1069	0.035943
chr15__28995753__29014280___APBA2	0.232261	-2.10618	0.033391
chr17__18865469__18877870___PRPSAP2	0.232422	-2.10518	0.013482
chr15__40628070__40641027___CASC5	0.232436	-2.10509	0.035387
chr10__48325897__48410168___MAPK8	0.232503	-2.10468	0.036347
chr2__68138742__68141795___WDR92	0.232522	-2.10456	0.049342
chrX__53403598__53403893___SMC1A	0.232575	-2.10423	0.041591
chr2__135748267__135776351___UBXN4	0.232679	-2.10359	0.037793
chr4__129039041__129093148___SCLT1	0.232784	-2.10294	0.018245
chr12__50780140__50796009___ATF1	0.232983	-2.1017	0.013936
chr11__68544838__68558679___PPP6R3	0.233327	-2.09957	0.024248
chr9__5920544__5923309___KIAA2026	0.233335	-2.09952	0.008283
chr15__66532247__66537263___ZWILCH	0.233369	-2.09932	0.04694
chr15__51893815__51902036___TMOD3	0.23364	-2.09764	0.021995
chr1__61186428__61188399___NFIA	0.233721	-2.09714	0.031874

chr2__68490190__68567387___APLF	0.23385	-2.09635	0.029412
chr3__152414941__152447773___MBNL1	0.234117	-2.0947	0.04097
chr14__60282684__60283537___PPM1A	0.234629	-2.09154	0.017022
chr10__110951608__110985765___SHOC2	0.23522	-2.08792	0.030971
chr14__72993143__72993357___ZFYVE1	0.235837	-2.08414	0.0178
chr12__65181757__65184482___LEMD3	0.236211	-2.08185	0.033028
chr12__22478313__22484888___C2CD5	0.236751	-2.07856	0.0248
chr10__114830852__114848737___FAM160B1	0.236765	-2.07847	0.021989
chr2__32439508__32453942___BIRC6	0.236839	-2.07802	0.029412
chr15__34250298__34255392___SLC12A6	0.237122	-2.0763	0.022231
chr5__134781133__134785586___DDX46	0.237491	-2.07406	0.040336
chr9__97994631__98005153___ANP32B	0.237764	-2.0724	0.005871
chr3__160401915__160416415___SMC4	0.237849	-2.07188	0.040395
chr10__68786136__68789915___CCAR1	0.237883	-2.07168	0.036462
chr14__45217019__45218432___MIS18BP1	0.237935	-2.07136	0.04601
chr1__193020307__193029657___UCHL5	0.237945	-2.0713	0.026905
chr2__96359045__96360710___NCAPH	0.238121	-2.07024	0.01118
chr2__71526220__71539239___DYSF	0.238342	-2.06889	0.026752
chr17__47156913__47172064___CDC27	0.238474	-2.0681	0.022079
chr19__8554477__8555796___MYO1F	0.238682	-2.06684	0.038402
chr3__138221926__138229010___ARMC8	0.23876	-2.06637	0.01892
chr16__89978810__89981923___AFG3L1P	0.238765	-2.06634	0.020944
chr19__54596189__54632760___NA	0.239184	-2.0638	0.022365
chr7__139055205__139061138___ZC3HAV1	0.239229	-2.06354	0.033654
chr20__5557945__5584322___GPCPD1	0.239261	-2.06334	0.021582
chr1__29035826__29109437___EPB41	0.239839	-2.05986	0.022991
chr2__175113994__175121540___ATF2	0.239879	-2.05962	0.04679
chr2__127989564__127989866___SAP130	0.240341	-2.05685	0.029699
chr3__196058284__196077122___TFRC	0.240637	-2.05507	0.002569
chr1__25340474__25343073___TMEM50A	0.240919	-2.05338	0.047866
chr3__182963881__182965753___DCUN1D1	0.241019	-2.05278	0.024118
chr14__24116917__24121517___DCAF11	0.241052	-2.05258	0.026963
chr8__31141430__31157530___WRN	0.241197	-2.05171	0.030511
chr6__35888024__35891013___SRPK1	0.241381	-2.05061	0.028432
chr2__210153495__210154611___KANSL1L	0.241446	-2.05023	0.014014
chr11__77683710__77685159___RSF1	0.241549	-2.04961	0.027139
chr9__109057191__109064567___TMEM245	0.242048	-2.04663	0.023481
chr7__105481052__105495253___PUS7	0.24221	-2.04567	0.022231
chr22__28699838__28734727___CHEK2	0.242283	-2.04524	0.02201
chr2__27677295__27677924___SLC4A1AP	0.242989	-2.04104	0.030688
chr11__119271735__119274953___CBL	0.243266	-2.03939	0.018731
chr10__92606265__92621473___KIF11	0.243308	-2.03914	0.025095
chr4__153580826__153589007___KIAA0922	0.243543	-2.03775	0.00749
chr6__133982568__133984671___TBPL1	0.243893	-2.03568	0.039542
chr19__36089038__36089306___WDR62	0.244186	-2.03395	0.013084
chr18__21765772__21791557___MIB1	0.24442	-2.03257	0.032064

chr1__1806475__1839238___GNB1	0.244556	-2.03176	0.031465
chr5__73015626__73037215___FCHO2	0.244989	-2.02921	0.04485
chr3__37063742__37083806___LRRFIP2	0.245049	-2.02886	0.017145
chr20__48951323__48953790___ARFGEF2	0.245387	-2.02687	0.042643
chr3__153164766__153247531___NA	0.245403	-2.02678	0.031387
chr4__169602008__169602678___NEK1	0.245622	-2.02549	0.010764
chr6__78965703__78985428___PHIP	0.245877	-2.02399	0.033257
chr9__271627__289581___DOCK8	0.245896	-2.02388	0.04606
chr8__86368939__86381629___WWP1	0.246177	-2.02223	0.046382
chr5__66012049__66014725___ERBB2IP	0.24632	-2.02139	0.026849
chr3__112563385__112573956___SLC35A5	0.246883	-2.0181	0.036829
chr10__11601345__11601980___USP6NL	0.247408	-2.01503	0.009515
chr18__44701175__44701832___SETBP1	0.248028	-2.01143	0.042668
chr4__169561480__169562196___NEK1	0.248438	-2.00904	0.048016
chr15__63659736__63664594___HERC1	0.24865	-2.00781	0.029081
chr6__34646601__34646798___C6orf106	0.248657	-2.00777	0.032274
chr1__35381259__35389082___ZMYM4	0.2491	-2.0052	0.016396
chr11__16014942__16101330___SOX6	0.249104	-2.00518	0.038337
chr17__67910877__67924589___BPTF	0.249174	-2.00478	0.019297
chr10__45939361__45962994___LOC728407	0.249543	-2.00264	0.018731
chr11__108158920__108170043___NPAT	0.249919	-2.00047	0.043465
chr5__36136309__36143406___LMBRD2	0.250018	-1.9999	0.034742
chr2__44174762__44180397___PPM1B	0.250025	-1.99985	0.0282
chr8__31058372__31068327___WRN	0.250039	-1.99978	0.046773
chr11__46780194__46780485___CKAP5	0.25006	-1.99965	0.039764
chr8__17969577__17972687___PCM1	0.250076	-1.99956	0.048008
chrX__154788027__154790022___MPP1	0.250323	-1.99814	0.02513
chr14__60266538__60268435___PPM1A	0.250454	-1.99739	0.015546
chr2__88776501__88792494___ANKRD36BP2	0.250951	-1.99452	0.02287
chr21__36247517__36251284___DOPEY2	0.251382	-1.99205	0.010987
chr1__182803698__182825820___NPL	0.251737	-1.99001	0.007545
chr17__67920015__67924589___BPTF	0.251773	-1.9898	0.034383
chr14__58219694__58223856___ACTR10	0.252107	-1.98789	0.034417
chr11__65435053__65444063___NA	0.252656	-1.98475	0.026306
chr1__61109778__61112343___NFIALOC102724281	0.252656	-1.98476	0.018872
chr11__77683710__77691238___RSF1	0.252747	-1.98424	0.028232
chr2__68386502__68394176___PLEK	0.252836	-1.98373	0.029412
chr18__63280887__63281214___BCL2	0.253064	-1.98242	0.031215
chr2__20278583__20327378___PUM2	0.253298	-1.98109	0.04545
chr15__50300789__50309798___GABPB1	0.253408	-1.98047	0.01587
chr14__73071627__73077536___RBM25	0.253585	-1.97946	0.043037
chr14__55648025__55648870___KTN1	0.25374	-1.97858	0.024118
chr18__24064140__24069271___TTC39C	0.253818	-1.97813	0.035642
chr12__66209456__66217235___IRAK3	0.254939	-1.97178	0.014531
chr2__240552914__240555055___ANKMY1	0.255217	-1.9702	0.012419
chr8__38107021__38119363___ASH2L	0.255299	-1.96974	0.048512

chr15__90217439__90221765___SEMA4B	0.25586	-1.96657	0.008283
chr11__83161327__83184908___PCF11	0.255956	-1.96603	0.027924
chr4__48593930__48605833___FRYL	0.256771	-1.96145	0.009284
chr10__31373018__31387266___ZEB1	0.256958	-1.96039	0.03307
chr3__20119598__20140364___KAT2B	0.256994	-1.96019	0.015314
chr19__47094389__47094608___ZC3H4	0.258032	-1.95438	0.046133
chr15__22681176__22681605___WHAMMP3	0.258058	-1.95423	0.038144
chr6__20546346__20548705___CDKAL1	0.258469	-1.95194	0.0277
chr14__103451918__103462461___MARK3	0.258533	-1.95158	0.02537
chr1__93305388__93325895___NA	0.259546	-1.94594	0.035379
chr1__6531968__6533441___NOL9	0.260532	-1.94047	0.033703
chr11__85981745__85982003___PICALM	0.26074	-1.93932	0.026403
chr1__92605307__92607727___EVI5	0.260771	-1.93914	0.04485
chr19__9614021__9618179___ZNF561	0.261231	-1.9366	0.03038
chr9__99959917__99960155___STX17	0.261297	-1.93624	0.010266
chr5__112792446__112801383___APC	0.261354	-1.93592	0.014782
chr21__15860622__15870147___USP25	0.261562	-1.93477	0.047783
chr18__51054781__51067187___SMAD4	0.262086	-1.93189	0.038337
chr12__66203711__66217235___IRAK3	0.262141	-1.93159	0.029045
chr4__15625252__15644708___FBXL5	0.263367	-1.92485	0.011914
chr10__11979057__12014184___UPF2	0.263536	-1.92393	0.019367
chr1__185184243__185231708___SWT1	0.264599	-1.91812	0.027509
chr10__113898110__113908523___NHLRC2	0.264612	-1.91805	0.033481
chr4__1900626__1939778___WHSC1	0.264619	-1.91801	0.022832
chr10__101797980__101813606___MGEA5	0.264721	-1.91746	0.043947
chr1__50738863__50744775___FAF1	0.264815	-1.91694	0.005871
chr6__75702645__75711416___SENP6	0.264986	-1.91601	0.043459
chr4__48163702__48176186___TEC	0.265018	-1.91584	0.027189
chr2__8882511__8958642___MBOAT2	0.265062	-1.9156	0.008341
chr12__110016388__110025823___ANKRD13A	0.265082	-1.91549	0.036081
chr15__63746918__63755325___HERC1	0.265348	-1.91404	0.037789
chr17__47156913__47158303___CDC27	0.266077	-1.91008	0.023027
chr3__50060956__50062108___RBM6	0.266115	-1.90988	0.01512
chr20__44972078__44995257___STK4	0.266653	-1.90697	0.025281
chr2__128159514__128164825___UGGT1	0.267251	-1.90373	0.046089
chr1__93212101__93217869___CCDC18	0.268174	-1.89876	0.044496
chr10__68393138__68396881___RUFY2	0.268371	-1.8977	0.039097
chr2__120073178__120078581___EPB41L5	0.268964	-1.89451	0.024009
chr17__27301788__27304911___WSB1	0.269526	-1.8915	0.01302
chr17__35624397__35627726___AP2B1	0.269649	-1.89084	0.038373
chr5__141581915__141583615___DIAPH1	0.269818	-1.88994	0.039828
chr7__44674411__44675268___OGDH	0.270181	-1.888	0.036966
chr12__130795995__130801488___STX2	0.271111	-1.88304	0.044496
chr21__37374234__37375117___DYRK1A	0.271139	-1.88289	0.039542
chr5__74834426__74841679___FAM169A	0.272405	-1.87618	0.042491
chr4__88938088__88991150___FAM13A	0.272613	-1.87508	0.021534

chr7__66808886__66810847___RABGEF1	0.272756	-1.87432	0.02737
chr18__12370849__12371691___AFG3L2	0.272936	-1.87336	0.04672
chr4__78859584__78872798___BMP2K	0.273978	-1.86787	0.042543
chr15__50300789__50304133___GABPB1	0.274577	-1.86472	0.016795
chr18__9524594__9530941___RALBP1	0.274901	-1.86302	0.046989
chr8__123344884__123348273___ATAD2	0.275074	-1.86211	0.020679
chr8__123253322__123256171___ZHX1	0.275492	-1.85992	0.04303
chr8__30101898__30106843___LEPROTL1	0.275576	-1.85948	0.048706
chr13__40559509__40560860___FOXO1	0.275623	-1.85923	0.037978
chr7__107580759__107613432___BCAP29	0.276303	-1.85568	0.02612
chr8__106679210__106684359___OXR1	0.276528	-1.8545	0.042875
chr9__125268936__125273649___GAPVD1	0.277012	-1.85198	0.017298
chr16__67744288__67772086___RANBP10	0.277242	-1.85078	0.038687
chr18__69895701__69947532___CD226	0.277254	-1.85072	0.022832
chr6__36601708__36603173___SRSF3	0.278289	-1.84534	0.042897
chr2__200942685__200958133___ORC2	0.278782	-1.84279	0.031412
chr10__15140987__15141557___NMT2	0.27974	-1.83784	0.047483
chr15__63746918__63747858___HERC1	0.280027	-1.83636	0.036851
chr15__92978234__92985673___CHD2	0.280031	-1.83634	0.004877
chr22__40273425__40285770___TNRC6B	0.280465	-1.83411	0.026569
chr2__241407537__241413421___FARP2	0.280527	-1.83379	0.008864
chr17__20017987__20205912___SPECC1	0.281998	-1.82625	0.009833
chr11__76985643__76998821___ACER3	0.282305	-1.82467	0.01915
chr15__50631417__50663046___TRPM7	0.282581	-1.82327	0.040162
chr5__62347130__62355254___KIF2A	0.282818	-1.82205	0.019406
chr4__159186642__159314768___RAPGEF2	0.28333	-1.81945	0.030553
chr17__12081356__12095694___MAP2K4	0.283471	-1.81872	0.024481
chr1__207677389__207678297___CR1L	0.283515	-1.8185	0.008903
chr7__2363632__2364529___EIF3B	0.284325	-1.81439	0.016282
chr1__53818971__53832591___NDC1	0.284763	-1.81217	0.022035
chr15__50002153__50018976___ATP8B4	0.286159	-1.80511	0.011582
chr10__11481770__11485911___USP6NL	0.286621	-1.80278	0.024982
chr16__47497399__47610920___PHKB	0.287114	-1.80031	0.022743
chr14__21401957__21403663___CHD8	0.287452	-1.79861	0.04402
chr17__63760914__63766194___CCDC47	0.287537	-1.79818	0.0036
chr1__35413972__35415714___ZMYM4	0.288107	-1.79533	0.010266
chr20__62139075__62140944___PSMA7	0.288296	-1.79438	0.009629
chr14__103571623__103574170___APOPT1	0.288613	-1.79279	0.024782
chr3__15411245__15415942___METTL6	0.289057	-1.79057	0.041173
chr2__8943187__8982144___MBOAT2	0.289172	-1.79	0.019526
chr17__61982198__61983114___MED13	0.289613	-1.7878	0.022822
chr2__168129541__168140758___STK39	0.289759	-1.78707	0.02391
chr17__68433468__68452992___WIPI1	0.289869	-1.78653	0.036421
chr1__161791408__161792327___ATF6	0.29004	-1.78568	0.024745
chr6__34606555__34606904___C6orf106	0.290127	-1.78524	0.018872
chr8__17268258__17286427___VPS37A	0.290438	-1.7837	0.025381

chr14__102040236__102040673___DYNC1H1	0.290636	-1.78272	0.008979
chr13__42963255__42970670___EPSTI1	0.291171	-1.78006	0.046584
chr5__115540885__115542901___FEM1C	0.291592	-1.77798	0.017544
chrX__155298785__155299145___CLIC2	0.29173	-1.7773	0.025461
chr1__21701498__21703618___USP48	0.292206	-1.77494	0.038334
chr13__50027363__50044768___DLEU2	0.292301	-1.77447	0.012545
chr10__45618140__45639963___ZFAND4	0.292722	-1.7724	0.036503
chr6__41871564__41891875___USP49	0.292785	-1.77208	0.026272
chr4__38826685__38829537___TLR6	0.29301	-1.77098	0.02872
chr16__19616114__19616808___C16orf62	0.293632	-1.76792	0.023481
chr5__138810038__138827718___CTNNA1	0.294468	-1.76382	0.049263
chr6__131199461__131219808___AKAP7	0.294502	-1.76365	0.024481
chr13__99539446__99543995___TM9SF2	0.294552	-1.76341	0.008485
chr17__61776401__61808757___BRIP1	0.295029	-1.76107	0.025208
chr19__17162988__17168064___MYO9B	0.295166	-1.7604	0.032064
chr12__14828517__14829462___NA	0.295574	-1.75841	0.044974
chr5__112775629__112801383___APC	0.295783	-1.75739	0.01892
chr5__79613011__79649190___PAPD4	0.296063	-1.75602	0.017812
chr13__95161189__95207925___ABCC4	0.296266	-1.75504	0.035636
chr9__5944871__5954095___KIAA2026	0.296687	-1.75299	0.029211
chr9__33941649__33956146___UBAP2	0.297174	-1.75062	0.049571
chr13__49993793__50045232___DLEU2	0.297424	-1.74941	0.037646
chr1__193069034__193070619___TROVE2	0.297951	-1.74685	0.041491
chr18__79126267__79207012___ATP9B	0.298281	-1.74525	0.026228
chr4__48556978__48557712___FRYL	0.298524	-1.74408	0.044845
chr1__15659837__15661159___NA	0.298783	-1.74283	0.02537
chr17__62010550__62063301___MED13	0.298929	-1.74213	0.006929
chr22__41137653__41141222___EP300	0.299036	-1.74161	0.030949
chr6__37282882__37317206___TBC1D22B	0.299857	-1.73765	0.008439
chr2__230461262__230474447___SP100	0.299969	-1.73711	0.012239
chr20__25413790__25425327___GINS1	0.300008	-1.73693	0.024743
chr11__108158920__108162180___NPAT	0.300134	-1.73632	0.037274
chr9__4823548__4833228___RCL1	0.300188	-1.73606	0.016928
chr16__58599236__58599511___CNOT1	0.300244	-1.73579	0.049896
chrX__53399589__53403893___SMC1A	0.300731	-1.73345	0.014835
chr10__32291163__32293737___EPC1	0.301484	-1.72985	0.04788
chr17__51201592__51203228___MBTD1	0.301871	-1.728	0.014821
chr10__31355144__31387266___ZEB1	0.302738	-1.72386	0.048171
chr12__122594276__122624688___KNTC1	0.3033	-1.72118	0.028143
chr2__20739971__20740205___C2orf43	0.303553	-1.71998	0.009274
chr11__9286455__9299701___TMEM41B	0.30523	-1.71203	0.042509
chr1__229525936__229542371___ABCB10	0.305733	-1.70966	0.011164
chr11__35196746__35210181___CD44	0.306018	-1.70831	0.04383
chr1__47287551__47295848___STIL	0.306503	-1.70603	0.004716
chr11__28228871__28233585___METTL15	0.307694	-1.70043	0.046197
chr4__55964274__56008382___CEP135	0.308692	-1.69576	0.049525

chr17__32171043__32183272___RHOT1	0.30925	-1.69316	0.027739
chr2__201389300__201399493___TRAK2	0.309501	-1.69199	0.028768
chr1__21001199__21002808___EIF4G3	0.309531	-1.69184	0.020679
chr15__72518067__72561549___ARIH1	0.309618	-1.69144	0.020679
chr4__98574457__98580407___TSPAN5	0.309721	-1.69096	0.045013
chr12__50094437__50096972___SMARCD1	0.31029	-1.68831	0.025872
chr1__168019545__168045227___DCAF6	0.310443	-1.6876	0.013283
chr14__49607400__49608121___LRR1	0.310551	-1.6871	0.006533
chr10__110881233__110890670___PDCD4	0.31068	-1.6865	0.047187
chr12__11121010__11129363___PRH1-PRR4	0.310694	-1.68643	0.022515
chr17__27303367__27310174___WSB1	0.310883	-1.68556	0.044648
chr1__93210802__93226449___CCDC18	0.310913	-1.68542	0.028555
chr3__100281742__100283811___TBC1D23	0.311135	-1.68439	0.04101
chr20__47262288__47290274___ZMYND8	0.311231	-1.68394	0.046173
chr17__29648144__29672129___SSH2	0.311251	-1.68385	0.025992
chr8__23109545__23111311___TNFRSF10C	0.311787	-1.68137	0.038687
chr15__58621471__58643978___ADAM10	0.312095	-1.67994	0.024684
chr8__140818277__140890769___PTK2	0.313014	-1.6757	0.021391
chr6__149765691__149773169___PCMT1	0.314052	-1.67092	0.008845
chr3__32716225__32717237___CNOT10	0.314851	-1.66726	0.003229
chr10__101956597__101957732___C10orf76	0.314974	-1.6667	0.010234
chr1__246627356__246631924___CNST	0.315022	-1.66648	0.045469
chr14__103428387__103462461___MARK3	0.31614	-1.66136	0.045766
chr11__9494646__9501270___ZNF143	0.316278	-1.66073	0.028859
chr11__16183886__16217474___SOX6	0.316679	-1.65891	0.023803
chr8__119783381__119791459___TAF2	0.316969	-1.65758	0.040184
chr4__153602152__153604430___KIAA0922	0.31763	-1.65458	0.025461
chr1__95143891__95152602___TMEM56TMEM56-RWDD3	0.317994	-1.65293	0.04435
chr20__50902017__50904849___ADNP	0.319065	-1.64808	0.037646
chr13__41068561__41071573___WBP4	0.319356	-1.64676	0.046133
chr13__19705662__19709599___PSPC1	0.319489	-1.64616	0.030426
chr5__140651714__140653144___IK	0.319784	-1.64483	0.046778
chr1__172555869__172591071___SUCO	0.320566	-1.6413	0.033578
chr16__70258980__70262524___AARS	0.32117	-1.63859	0.009215
chr20__31782249__31797515___TPX2	0.321174	-1.63857	0.01299
chr13__114041000__114073837___RASA3	0.321886	-1.63538	0.026228
chr12__120557282__120557682___RNF10	0.322371	-1.63321	0.00854
chr3__120002046__120093593___GSK3B	0.322606	-1.63216	0.002628
chr20__33619517__33623296___CBFA2T2	0.324443	-1.62396	0.010974
chr7__105285009__105297533___SRPK2	0.325601	-1.61882	0.042038
chr2__208345111__208348023___PIKFYVE	0.325642	-1.61864	0.009727
chr6__79654495__79673799___SH3BGRL2	0.325695	-1.61841	0.049151
chr21__15864268__15870147___USP25	0.326469	-1.61498	0.04009
chr15__40196545__40202694___BUB1B	0.326509	-1.6148	0.046989
chr2__61495455__61499894___XPO1	0.326856	-1.61327	0.017022

chr7__105481052__105506273___PUS7	0.32717	-1.61189	0.032907
chr1__207655190__207683957___CR1L	0.327589	-1.61004	0.047447
chr12__110018345__110030758___ANKRD13A	0.32763	-1.60986	0.04303
chr14__58286640__58291707___FLJ31306	0.327822	-1.60902	0.03841
chr1__28987448__29018442___EPB41	0.327908	-1.60864	0.029503
chr14__30633947__30643405___SCFD1	0.328133	-1.60765	0.009846
chr7__140776912__140787584___BRAF	0.32874	-1.60498	0.013791
chr11__86249471__86252240___EED	0.32875	-1.60494	0.019835
chr5__80767933__80792844___MSH3	0.328928	-1.60416	0.040396
chr16__10419581__10473989___ATF7IP2	0.329207	-1.60293	0.019233
chr17__31155983__31169997___NF1	0.331332	-1.59365	0.020077
chr15__89312904__89314707___FANCI	0.332831	-1.58714	0.046989
chr6__57141302__57148693___ZNF451	0.332836	-1.58712	0.047077
chr11__117159934__117163892___PAFAH1B2	0.33328	-1.58519	0.030193
chr1__153811731__153813452___GATAD2B	0.333757	-1.58313	0.011723
chr3__138209817__138229010___ARMC8	0.334046	-1.58188	0.021783
chr18__9931810__9950568___VAPA	0.334278	-1.58088	0.032685
chr3__185931577__185932846___TRA2B	0.335065	-1.57749	0.041119
chr6__99439769__99465136___USP45	0.335622	-1.57509	0.013963
chr3__182940359__182965753___NA	0.336665	-1.57062	0.021144
chr18__20986950__20992937___ROCK1	0.337405	-1.56745	0.042668
chr2__151440027__151443709___RIF1	0.337574	-1.56672	0.040339
chr15__76274412__76295737___ETFA	0.337924	-1.56523	0.006411
chr7__148828740__148847305___EZH2	0.338371	-1.56332	0.015843
chr8__47969798__47971468___MCM4	0.338882	-1.56115	0.008296
chr9__132296887__132300803___SETX	0.338941	-1.5609	0.038306
chr15__77133005__77133750___PEAK1	0.339026	-1.56053	0.027468
chr15__80073266__80098578___ZFAND6	0.339993	-1.55642	0.025972
chr10__13663453__13670528___FRMD4A	0.340448	-1.55449	0.022795
chr21__36333646__36349408___MORC3	0.341493	-1.55007	0.034698
chr15__40650301__40652105___CASC5	0.342262	-1.54683	0.036082
chr6__43055545__43056445___MRPL2	0.342338	-1.54651	0.041591
chr6__17661653__17675770___NUP153	0.342569	-1.54553	0.04788
chr14__58215205__58223856___ACTR10	0.344369	-1.53797	0.031773
chr3__37273536__37302332___GOLGA4	0.345015	-1.53527	0.006796
chr8__17195523__17220921___ZDHHC2	0.345242	-1.53432	0.035642
chr4__98574457__98575203___TSPAN5	0.34539	-1.5337	0.04788
chr14__45235814__45237721___MIS18BP1	0.346427	-1.52938	0.010266
chr5__65451475__65473952___ADAMTS6	0.346538	-1.52892	0.035142
chr4__87084120__87090070___AFF1	0.346871	-1.52753	0.049342
chr1__155675010__155784089___NA	0.347131	-1.52645	0.022452
chr21__36356620__36364259___MORC3	0.347196	-1.52618	0.009284
chr3__56623644__56673725___FAM208A	0.34743	-1.52521	0.033286
chr7__131387120__131388972___MKLN1	0.347464	-1.52507	0.042811
chr9__85822880__85829606___LOC389765	0.347576	-1.5246	0.037688
chr17__30856955__30869646___ATAD5	0.350384	-1.51299	0.02391

chr4__158825916__158835476___FNIP2	0.350437	-1.51277	0.022832
chr1__200589217__200592240___KIF14	0.351303	-1.50921	0.030282
chr12__112306064__112313147___HECTD4	0.352326	-1.50502	0.029814
chr1__230663141__230664587___COG2	0.352452	-1.5045	0.048542
chr10__114843741__114848737___FAM160B1	0.352652	-1.50368	0.010411
chr8__85134847__85141517___LRRCC1	0.353188	-1.50149	0.031377
chr3__142347234__142376594___XRN1	0.353499	-1.50022	0.0477
chr4__147857553__147881932___ARHGAP10	0.354175	-1.49746	0.037793
chr19__10795372__10798572___DNM2	0.355221	-1.49321	0.038672
chr2__15488894__15534641___NBAS	0.355883	-1.49052	0.038116
chr2__189805652__189818180___PMS1	0.356872	-1.48652	0.028871
chr13__45151687__45207505___GTF2F2	0.357438	-1.48423	0.02177
chr11__77672042__77693611___RSF1	0.357733	-1.48305	0.025631
chr17__30837206__30840781___ATAD5	0.357865	-1.48251	0.021995
chr19__37425868__37444964___ZNF569	0.360901	-1.47032	0.031993
chr7__93252653__93311272___CCDC132	0.361163	-1.46928	0.035668
chr12__112306064__112319742___HECTD4	0.361567	-1.46766	0.021847
chr13__19741565__19751467___PSPC1	0.362033	-1.46581	0.04541
chr12__116096669__116119779___MED13L	0.362174	-1.46525	0.024326
chr17__60269450__60288682___USP32	0.362941	-1.46219	0.031671
chr19__34208929__34215661___LSM14A	0.362979	-1.46204	0.024086
chr16__53439016__53447106___RBL2	0.363118	-1.46149	0.045609
chr16__1625973__1632365___CRAMP1L	0.364074	-1.45769	0.019471
chr11__3702463__3702892___NUP98	0.365684	-1.45133	0.048208
chrX__53411995__53412253___SMC1A	0.366046	-1.4499	0.035587
chr6__57052686__57055797___NA	0.366376	-1.4486	0.034091
chr7__27950018__27956804___JAZF1	0.366993	-1.44618	0.026624
chr6__82214227__82214829___IBTK	0.368916	-1.43864	0.044823
chr16__19616114__19647882___C16orf62	0.370035	-1.43427	0.035476
chr10__84371014__84373815___CCSER2	0.370069	-1.43413	0.007948
chr14__78957242__78988141___NRXN3	0.370173	-1.43373	0.015885
chr4__98574477__98574905___TSPAN5	0.370948	-1.43071	0.025208
chr10__112460524__112464657___VTI1A	0.371178	-1.42982	0.030849
chr5__74745678__74750667___GFM2	0.372339	-1.42531	0.017227
chr13__75560753__75569507___UCHL3	0.374138	-1.41836	0.016735
chr10__94350113__94352403___NOC3L	0.375002	-1.41503	0.02715
chr1__90937485__90982370___ZNF644	0.37524	-1.41412	0.011257
chr11__581492__582081___PHRF1	0.375373	-1.4136	0.038671
chr6__17668975__17669546___NUP153	0.375828	-1.41185	0.033365
chr7__8055436__8071131___GLCCI1	0.376761	-1.40828	0.037077
chr3__52412811__52414587___PHF7	0.377106	-1.40696	0.020627
chr13__41318806__41336756___NAA16	0.377126	-1.40688	0.014767
chr7__93252653__93259632___CCDC132	0.377819	-1.40423	0.027781
chr9__96336717__96368305___SLC35D2	0.378535	-1.4015	0.024169
chr9__120467860__120491477___CDK5RAP2	0.379102	-1.39934	0.013829
chr15__63553715__63559970___USP3	0.379338	-1.39844	0.041685

chr11__68583043__68596218___PPP6R3	0.379832	-1.39657	0.038306
chr10__72708283__72715902___MCU	0.380614	-1.3936	0.04545
chr4__70942823__70959040___MOB1B	0.383144	-1.38404	0.036863
chr13__50044651__50075653___DLEU2	0.385174	-1.37642	0.032064
chr17__27303367__27303635___WSB1	0.385211	-1.37628	0.028575
chr20__48690947__48692790___PREX1	0.385639	-1.37468	0.021177
chr16__71745144__71745614___AP1G1	0.38602	-1.37325	0.020208
chr6__36902221__36902434___C6orf89	0.386563	-1.37123	0.048727
chr19__10904951__10909207___CARM1	0.386791	-1.37037	0.047647
chr9__125337018__125337591___GAPVD1	0.387627	-1.36726	0.017812
chr7__140355668__140358785___SLC37A3	0.388683	-1.36333	0.007749
chr6__89751431__89753622___MDN1	0.389559	-1.36009	0.049513
chr11__77693507__77702495___RSF1	0.389796	-1.35921	0.043199
chr10__101521639__101538371___BTRC	0.390957	-1.35492	0.017898
chr4__6923373__6924111___TBC1D14	0.391872	-1.35154	0.033538
chr14__49653990__49655843___POLE2	0.3919	-1.35144	0.036104
chr10__17603560__17604047___PTPLA	0.392788	-1.34818	0.049982
chr2__53897870__53901559___PSME4	0.392824	-1.34804	0.019587
chr1__50705786__50744775___FAF1	0.393104	-1.34702	0.019273
chrY__19739528__19741857___KDM5D	0.394368	-1.34239	0.048351
chr1__70184785__70189273___LRRC40	0.396443	-1.33482	0.039109
chr22__32478981__32493281___FBXO7	0.397444	-1.33118	0.0295
chr12__112075678__112078741___NAA25	0.397856	-1.32968	0.04541
chr20__5557945__5604440___GPCPD1	0.398662	-1.32676	0.019471
chr1__207717464__207724708___NA	0.398854	-1.32607	0.035595
chr17__1636709__1637062___SCARF1	0.399736	-1.32288	0.041477
chr1__13731000__13749487___PRDM2	0.400279	-1.32092	0.015947
chr3__160356013__160381718___IFT80	0.402636	-1.31245	0.047287
chr4__77773081__77776392___CNOT6L	0.402719	-1.31215	0.015691
chr19__5650978__5654456___SAFB	0.402989	-1.31119	0.013937
chr19__2189732__2194577___DOT1L	0.403198	-1.31044	0.02727
chr15__40389506__40392023___KNSTRN	0.403921	-1.30786	0.014186
chr3__155893518__155916192___GMPS	0.403985	-1.30763	0.037165
chr2__8888018__8958642___MBOAT2	0.404131	-1.3071	0.011829
chr11__85981129__85982003___PICALM	0.404352	-1.30632	0.00946
chr8__130118161__130126089___ASAP1	0.404632	-1.30532	0.018821
chr1__151088190__151118139___GABPB2	0.40473	-1.30497	0.028435
chr18__57571392__57580199___FECH	0.406178	-1.29982	0.041791
chr15__72518067__72572165___ARIH1	0.408216	-1.2926	0.046575
chr16__53155926__53157541___CHD9	0.409813	-1.28696	0.015659
chr18__79126267__79214038___ATP9B	0.410002	-1.2863	0.037646
chr6__98899268__98934879___FBXL4	0.410384	-1.28495	0.022936
chr11__121045674__121053732___TBCEL	0.411779	-1.28006	0.036953
chr12__53719739__53722183___CALCOCO1	0.412206	-1.27856	0.021609
chr15__64974602__64983593___SPG21	0.413946	-1.27249	0.03256
chr6__97254557__97269992___MMS22L	0.415391	-1.26746	0.039935

chr20__38531167__38532859___RALGAPB	0.415666	-1.2665	0.047182
chr1__244408712__244417752___ADSS	0.41614	-1.26486	0.044465
chr10__46010223__46013639___NCOA4	0.420056	-1.25135	0.038557
chr6__75659262__75678927___SENP6	0.420251	-1.25068	0.049556
chr12__46229153__46254936___SLC38A1	0.422399	-1.24332	0.026228
chr9__133412299__133412921___REXO4	0.423116	-1.24087	0.033074
chr17__51263274__51268904___UTP18	0.4236	-1.23922	0.026272
chr3__16286342__16303592___OXNAD1	0.424399	-1.23651	0.021847
chr19__45263113__45263367___MARK4	0.42443	-1.2364	0.021609
chr15__63532647__63537156___USP3	0.426811	-1.22833	0.04263
chr11__755879__760253___TALDO1	0.428347	-1.22315	0.014021
chr20__10556231__10560820___SLX4IP	0.428433	-1.22286	0.025222
chr13__21161790__21168399___SKA3	0.429753	-1.21842	0.034698
chr12__94220016__94227235___PLXNC1	0.430651	-1.21541	0.028679
chr20__45000392__45001353___STK4	0.430778	-1.21498	0.019621
chr2__171540808__171541793___CYBRD1	0.431308	-1.21321	0.032215
chr2__61223060__61281242___USP34	0.432572	-1.20899	0.044399
chr11__117152441__117163892___PAFAH1B2	0.433485	-1.20595	0.040951
chr20__5557945__5561530___GPCPD1	0.436643	-1.19547	0.026228
chr6__116689320__116705160___KPNA5	0.43824	-1.19021	0.041338
chr13__21381434__21425678___ZDHHC20	0.439052	-1.18754	0.026228
chr6__89846562__89857199___CASP8AP2	0.439295	-1.18674	0.029616
chr3__129458599__129464781___IFT122	0.439671	-1.1855	0.028424
chr11__65430769__65444063___NA	0.439935	-1.18464	0.01926
chr16__1625973__1641187___CRAMP1L	0.440337	-1.18332	0.029412
chr3__20072395__20152579___KAT2B	0.440513	-1.18274	0.029081
chr11__130109429__130122513___APLP2	0.442337	-1.17678	0.029359
chr17__47402132__47409691___EFCAB13	0.444087	-1.17108	0.027189
chr2__25799385__25845563___ASXL2	0.44419	-1.17075	0.02388
chr9__107300141__107325004___RAD23B	0.444394	-1.17009	0.033513
chr1__66891154__66905375___WDR78	0.446822	-1.16223	0.028507
chr18__46118181__46120060___HAUS1	0.447091	-1.16136	0.035642
chr5__66021322__66054951___ERBB2IP	0.448447	-1.15699	0.016735
chr2__33134793__33222151___LTBP1	0.448821	-1.15579	0.034008
chrX__101041317__101042312___TRMT2B	0.449484	-1.15366	0.040027
chrX__118394055__118404444___WDR44	0.449937	-1.1522	0.049513
chr11__16183886__16341252___SOX6	0.44994	-1.15219	0.03778
chr11__46808031__46809874___CKAP5	0.455237	-1.13531	0.048856
chr7__32620404__32639365___DPY19L1P1	0.456613	-1.13096	0.043351
chr11__86250296__86252240___EED	0.4577	-1.12752	0.016975
chr11__125003867__125005212___CCDC15	0.458107	-1.12624	0.022822
chr8__43059092__43064215___FNTA	0.465955	-1.10174	0.026138
chr11__77683710__77693611___RSF1	0.466676	-1.09951	0.013458
chr12__30710448__30753559___CAPRIN2	0.468282	-1.09455	0.045098
chr14__95140659__95141748___DICER1	0.472401	-1.08192	0.046985
chr3__196062582__196077122___TFRC	0.472922	-1.08033	0.006941

chr8__41692648__41693201___ANK1	0.473859	-1.07747	0.039407
chr13__48253808__48261321___ITM2B	0.474811	-1.07457	0.03988
chr19__1032392__1032696___CNN2	0.476744	-1.06871	0.027303
chr9__77337255__77371149___VPS13A	0.477082	-1.06769	0.018922
chr20__35713019__35725155___RBM39	0.477331	-1.06694	0.011956
chr6__7176655__7189322___RREB1	0.479966	-1.05899	0.037334
chr12__128814775__128815070___SLC15A4	0.482119	-1.05254	0.012508
chr1__213077696__213117410___RPS6KC1	0.484187	-1.04636	0.02357
chr4__48684673__48710698___FRYL	0.491683	-1.0242	0.042668
chr5__112275326__112307490___EPB41L4A	0.496033	-1.01149	0.01892

Appendix N

List of down-regulated circRNA in STRENGTH *compared with* SEDENTARY *at follow-up 1* (FDR<0.05).

Gene	FC	logFC	FDR
chr1__10403071__10408140___PGD	0.087355	-3.51697	0.019681
chr1__108154983__108185954___SLC25A24	0.149905	-2.73788	0.037734
chr1__108782422__108794907___STXBP3	0.097072	-3.36479	0.020246
chr1__108782422__108796726___STXBP3	0.120122	-3.05743	0.030101
chr1__111147642__111153371___CEPT1	0.112058	-3.15768	0.024309
chr1__113091318__113107757___LRIG2	0.133333	-2.90689	0.038055
chr1__113833111__113855049___PTPN22	0.162815	-2.6187	0.034864
chr1__114463104__114477087___TRIM33	0.184023	-2.44204	0.037734
chr1__117396952__117420649___MAN1A2	0.282558	-1.82338	0.048758
chr1__117456085__117466427___MAN1A2	0.136829	-2.86956	0.020442
chr1__12578718__12579412___DHRS3	0.117531	-3.08889	0.027455
chr1__13773078__13782831___PRDM2	0.083871	-3.57568	0.020209
chr1__150817920__150826617___ARNT	0.102391	-3.28784	0.022213
chr1__151658235__151668635___SNX27	0.197546	-2.33974	0.049261
chr1__155395459__155439068___ASH1L	0.126548	-2.98224	0.026509
chr1__155668627__155773210___NA	0.151738	-2.72035	0.048139
chr1__155676548__155680456___YY1AP1	0.274394	-1.86568	0.043515
chr1__155717006__155726019___DAP3	0.319446	-1.64636	0.034915
chr1__155771067__155777820___GON4L	0.14559	-2.78001	0.026601
chr1__155921375__155925843___KIAA0907	0.123399	-3.0186	0.030709
chr1__15626669__15638434___DDI2	0.091437	-3.45108	0.020647
chr1__15638307__15649823___DDI2	0.098602	-3.34224	0.023672
chr1__15643522__15651895___DDI2	0.133633	-2.90365	0.031354
chr1__158654811__158654951___SPTA1	0.022723	-5.4597	0.027658
chr1__158667858__158686537___SPTA1	0.073342	-3.76922	0.018908
chr1__158674329__158674675___SPTA1	0.111224	-3.16846	0.02321
chr1__158674329__158683496___SPTA1	0.114589	-3.12546	0.030008
chr1__158677690__158683496___SPTA1	0.096829	-3.36842	0.023102
chr1__158681527__158685347___SPTA1	0.136626	-2.8717	0.044462
chr1__158683371__158686537___SPTA1	0.098004	-3.35102	0.023672
chr1__161846449__161853323___ATF6	0.207458	-2.26911	0.041706
chr1__164792494__164821626___PBX1	0.130728	-2.93536	0.034864
chr1__1649499__1657498___CDK11B	0.14159	-2.82021	0.036666
chr1__168038371__168045203___DCAF6	0.14877	-2.74885	0.043277
chr1__169323117__169324500___NME7	0.129832	-2.94528	0.034864
chr1__169798857__169807929___C1orf112	0.090215	-3.47049	0.019951
chr1__171524821__171537473___PRRC2C	0.09829	-3.34682	0.02436
chr1__172038319__172055926___DNM3	0.159916	-2.64461	0.020886
chr1__17341943__17342402___PADI4	0.096524	-3.37296	0.019681
chr1__174250570__174278779___RABGAP1L	0.108982	-3.19783	0.028042
chr1__174969277__174988838___RABGAP1L	0.088651	-3.49572	0.020623
chr1__1755374__1756343___NADK	0.187307	-2.41652	0.049921

chr1__179335506__179343635___SOAT1	0.117921	-3.08411	0.033416
chr1__179900126__179914054___TOR1AIP1	0.128229	-2.96321	0.035288
chr1__180003174__180024582___CEP350	0.129053	-2.95397	0.039402
chr1__180824753__180825344___XPR1	0.05988	-4.06178	0.018075
chr1__1825397__1879902___GNB1	0.125817	-2.9906	0.034911
chr1__182822115__182843434___NA	0.100778	-3.31075	0.023666
chr1__182822115__182859117___NA	0.093156	-3.42421	0.020886
chr1__182842545__182843434___DHX9	0.112342	-3.15403	0.027905
chr1__185123857__185151935___TRMT1L	0.136197	-2.87623	0.0354
chr1__185174372__185276668___SWT1	0.156379	-2.67688	0.049921
chr1__185180391__185190642___SWT1	0.234608	-2.09168	0.029366
chr1__185180391__185222036___SWT1	0.145736	-2.77857	0.044696
chr1__185184243__185214655___SWT1	0.270474	-1.88644	0.049194
chr1__185184243__185231708___SWT1	0.258473	-1.95191	0.041935
chr1__187303466__187313449___NA	0.083669	-3.57916	0.019788
chr1__193020307__193029657___UCHL5	0.172001	-2.53951	0.025392
chr1__197084354__197092010___ASPM	0.094219	-3.40784	0.021999
chr1__197084354__197096028___ASPM	0.079353	-3.65558	0.019072
chr1__198220999__198279061___NEK7	0.112898	-3.14691	0.027843
chr1__198232553__198279061___NEK7	0.079205	-3.65827	0.019466
chr1__198277961__198297240___NEK7	0.174918	-2.51525	0.032177
chr1__200565069__200598421___KIF14	0.119265	-3.06775	0.029897
chr1__200569911__200598421___KIF14	0.158388	-2.65846	0.027843
chr1__200580254__200589369___KIF14	0.125825	-2.99051	0.034915
chr1__20741831__20780540___NA	0.129386	-2.95025	0.035569
chr1__20744744__20749882___HP1BP3	0.084586	-3.56343	0.019072
chr1__207526753__207701618___NA	0.066354	-3.91368	0.018075
chr1__207526753__207717691___NA	0.101008	-3.30746	0.020246
chr1__20765377__20776750___HP1BP3	0.058937	-4.08469	0.018075
chr1__207655190__207686940___CR1L	0.077042	-3.69822	0.018908
chr1__20767584__20776750___HP1BP3	0.083857	-3.57592	0.019466
chr1__20767584__20780540___HP1BP3	0.068273	-3.87253	0.018075
chr1__20774636__20776005___HP1BP3	0.139975	-2.83676	0.039936
chr1__20904883__20942330___EIF4G3	0.137956	-2.85772	0.023672
chr1__211260108__211304140___RCOR3	0.150032	-2.73666	0.044233
chr1__219193130__219241308___NA	0.094944	-3.39679	0.020246
chr1__222650292__222654793___MIA3	0.050749	-4.30048	0.014522
chr1__222715145__222725555___BROX	0.13387	-2.9011	0.040902
chr1__222724092__222725569___BROX	0.190752	-2.39023	0.023816
chr1__222724100__222725555___BROX	0.079084	-3.66047	0.019466
chr1__224393828__224404570___WDR26	0.07584	-3.7209	0.019072
chr1__225406664__225415332___LBR	0.18317	-2.44875	0.022546
chr1__226266213__226301205___LIN9	0.14187	-2.81736	0.035288
chr1__227016080__227048010___CDC42BPA	0.112957	-3.14616	0.024402
chr1__229450525__229465519___NUP133	0.067923	-3.87996	0.018075
chr1__229518841__229549434___ABCB10	0.078354	-3.67384	0.019072

chr1__229531636__229549434___ABCB10	0.092057	-3.44132	0.019888
chr1__234418084__234427766___TARBP1	0.074018	-3.75599	0.018908
chr1__235172618__235196115___ARID4B	0.12091	-3.048	0.02909
chr1__235219793__235240451___ARID4B	0.196362	-2.34841	0.037823
chr1__235780865__235782087___LYST	0.143693	-2.79894	0.025999
chr1__243270105__243308177___SDCCAG8	0.11738	-3.09074	0.032065
chr1__243293091__243330692___SDCCAG8	0.212378	-2.23529	0.037904
chr1__243316755__243330692___SDCCAG8	0.126296	-2.98512	0.030831
chr1__243316755__243426558___SDCCAG8	0.116256	-3.10462	0.033888
chr1__243330540__243344331___SDCCAG8	0.167358	-2.57899	0.026106
chr1__25340474__25351693___TMEM50A	0.204477	-2.28999	0.038055
chr1__26716114__26716720___ARID1A	0.139595	-2.84068	0.038892
chr1__27412572__27428933___WASF2	0.133527	-2.9048	0.031508
chr1__27418269__27428933___WASF2	0.098903	-3.33784	0.022172
chr1__28027789__28038905___EYA3	0.094851	-3.39819	0.019788
chr1__28683583__28690186___GMEB1	0.078112	-3.67831	0.019072
chr1__28987431__29097935___EPB41	0.099429	-3.3302	0.02633
chr1__28987448__29018442___EPB41	0.309127	-1.69373	0.041784
chr1__29096155__29097935___EPB41	0.088913	-3.49147	0.020246
chr1__29097807__29109437___EPB41	0.091834	-3.44483	0.020813
chr1__29115699__29117989___EPB41	0.131708	-2.92458	0.038892
chr1__32030298__32031640___KHDRBS1	0.078179	-3.67708	0.019072
chr1__32631827__32634792___ZBTB8OS	0.078386	-3.67326	0.019072
chr1__35003968__35015162___ZMYM6	0.05083	-4.29818	0.014522
chr1__35470863__35479212___KIAA0319L	0.099846	-3.32415	0.022403
chr1__44002313__44002985___SLC6A9	0.133767	-2.90221	0.022626
chr1__45421725__45488604___TESK2	0.134359	-2.89584	0.038055
chr1__45602255__45606591___NASP	0.17322	-2.52932	0.041143
chr1__45604936__45606591___NASP	0.115279	-3.1168	0.029487
chr1__46688353__46688544___EFCAB14	0.073148	-3.77303	0.018075
chr1__47280241__47300152___STIL	0.154386	-2.69539	0.044862
chr1__47287551__47304996___STIL	0.042987	-4.53996	0.009368
chr1__47289435__47300152___STIL	0.124657	-3.00397	0.031491
chr1__50705786__50752523___FAF1	0.131805	-2.92352	0.031515
chr1__51236734__51271473___RNF11	0.200322	-2.31961	0.035288
chr1__51827796__51840514___NRD1	0.126895	-2.9783	0.029163
chr1__51836131__51855388___NRD1	0.159619	-2.6473	0.034332
chr1__51840226__51855388___NRD1	0.104554	-3.25768	0.023102
chr1__55137515__55166603___USP24	0.102127	-3.29156	0.022108
chr1__61111371__61188399___NFIA	0.115819	-3.11006	0.030559
chr1__62441488__62443319___USP1	0.118884	-3.07237	0.024881
chr1__66534246__66643719___SGIP1	0.113086	-3.1445	0.025333
chr1__70292388__70313790___ANKRD13C	0.138429	-2.85278	0.037734
chr1__75728401__75734871___ACADM	0.113385	-3.1407	0.032065
chr1__77206640__77212347___PIGK	0.062238	-4.00607	0.018075
chr1__77713200__77715868___USP33	0.100452	-3.31542	0.022775

chr1__84865385__84866138___LPAR3	0.10403	-3.26492	0.024301
chr1__8624310__8656441___RERE	0.10603	-3.23746	0.026106
chr1__86372431__86384801___ODF2L	0.080047	-3.64301	0.019466
chr1__90937485__90941309___ZNF644	0.166166	-2.5893	0.029199
chr1__92323445__92345914___RPAP2	0.151729	-2.72043	0.043177
chr1__92693802__92704744___EVI5	0.047064	-4.40925	0.012744
chr1__93183360__93221936___CCDC18	0.143432	-2.80156	0.045029
chr1__93217738__93239896___CCDC18	0.137199	-2.86566	0.041935
chr1__93221609__93239896___CCDC18	0.171672	-2.54227	0.041245
chr1__93894614__93897898___GCLM	0.157862	-2.66326	0.019466
chr1__95134782__95136731___TMEM56TMEM56-RWDD3	0.120797	-3.04934	0.028695
chr1__95143891__95161149___TMEM56TMEM56-RWDD3	0.063316	-3.98129	0.018075
chr1__95143891__95230994___TMEM56-RWDD3	0.209349	-2.25602	0.042658
chr10__101797980__101813606___MGEA5	0.188077	-2.41061	0.033512
chr10__102362475__102365599___GBF1	0.135936	-2.879	0.033416
chr10__110124017__110132400___ADD3	0.058488	-4.09572	0.018075
chr10__112527087__112538330___VTI1A	0.099589	-3.32788	0.020246
chr10__114151092__114157680___C10orf118	0.18627	-2.42453	0.045203
chr10__114157554__114163329___C10orf118	0.237981	-2.07108	0.049465
chr10__114162637__114163329___C10orf118	0.063024	-3.98796	0.018075
chr10__11594631__11601980___USP6NL	0.117875	-3.08466	0.025999
chr10__117243971__117253457___SLC18A2	0.061157	-4.03133	0.018075
chr10__118685983__118730410___CACUL1	0.129946	-2.94402	0.034915
chr10__118691265__118707587___CACUL1	0.152151	-2.71642	0.030579
chr10__119073441__119073937___EIF3A	0.123749	-3.01451	0.033512
chr10__11929865__11948508___UPF2	0.089892	-3.47567	0.022229
chr10__12081472__12094271___DHTKD1	0.127322	-2.97345	0.020246
chr10__124696158__124706887___FAM53B	0.181659	-2.4607	0.047441
chr10__124828756__124831463___FAM175B	0.1153	-3.11654	0.025427
chr10__124942457__124987504___ZRANB1	0.120856	-3.04864	0.024932
chr10__13659323__13675044___FRMD4A	0.064261	-3.9599	0.018075
chr10__14848609__14855943___HSPA14	0.108002	-3.21088	0.026509
chr10__16752539__16817084___RSU1	0.086779	-3.52651	0.019951
chr10__17684832__17700279___STAM	0.085616	-3.54597	0.019681
chr10__17704431__17714678___STAM	0.082238	-3.60405	0.019466
chr10__22317884__22319018___COMMD3COMMD3-BMI1	0.353108	-1.50182	0.043109
chr10__22541804__22542047___PIP4K2A	0.120689	-3.05064	0.029199
chr10__27117576__27121448___YME1L1	0.124336	-3.00768	0.031354
chr10__27134831__27136385___YME1L1	0.093092	-3.42519	0.022936
chr10__27526828__27538028___RAB18	0.08806	-3.50537	0.020725
chr10__30313891__30322442___MTPAP	0.082445	-3.60043	0.019466
chr10__31355144__31387266___ZEB1	0.222306	-2.16938	0.035288
chr10__31461037__31461783___ZEB1	0.085398	-3.54965	0.019072
chr10__32037254__32040457___KIF5B	0.11665	-3.09974	0.028302
chr10__32047412__32048551___KIF5B	0.159294	-2.65023	0.045203
chr10__32291163__32293194___EPC1	0.150407	-2.73306	0.025392

chr10__32471064__32481782___CCDC7	0.066273	-3.91544	0.018075
chr10__32565296__32584304___CCDC7	0.105617	-3.24309	0.02436
chr10__45533110__45534914___MARCH8	0.11395	-3.13353	0.023008
chr10__45624583__45627105___ZFAND4	0.067752	-3.88359	0.018075
chr10__45639751__45663842___ZFAND4	0.079665	-3.64991	0.019466
chr10__45639816__45652033___ZFAND4	0.127583	-2.97049	0.028422
chr10__45648294__45663842___ZFAND4	0.081686	-3.61377	0.019681
chr10__45939361__45962994___LOC728407	0.109696	-3.18841	0.018075
chr10__45939361__45965855___LOC728407	0.287744	-1.79714	0.035009
chr10__48401612__48404981___MAPK8	0.088287	-3.50166	0.019466
chr10__50433476__50598823___SGMS1	0.143312	-2.80277	0.025958
chr10__50519831__50523704___SGMS1	0.130394	-2.93905	0.038499
chr10__5765987__5811956___GDI2	0.106955	-3.22492	0.023102
chr10__5773842__5786050___GDI2	0.08273	-3.59545	0.019681
chr10__5773842__5811956___GDI2	0.104171	-3.26298	0.026601
chr10__5785142__5811956___GDI2	0.201427	-2.31167	0.049591
chr10__5794885__5811956___GDI2	0.159996	-2.64389	0.033481
chr10__63190894__63194375___JMJD1C	0.091408	-3.45154	0.023008
chr10__6613631__6613987___NA	0.143157	-2.80433	0.040889
chr10__68337199__68341309___HNRNPH3	0.097596	-3.35703	0.023102
chr10__68355353__68386128___RUFY2	0.034284	-4.86631	0.004247
chr10__68383798__68394451___RUFY2	0.07636	-3.71104	0.019072
chr10__68393138__68396881___RUFY2	0.040874	-4.61269	0.008229
chr10__68442917__68450247___DNA2	0.083817	-3.57661	0.020098
chr10__68736876__68742569___CCAR1	0.100974	-3.30795	0.02556
chr10__68911068__68914204___DDX50	0.125382	-2.9956	0.032177
chr10__68959806__68967203___DDX21	0.132258	-2.91857	0.033416
chr10__69155812__69158211___VPS26A	0.096735	-3.36982	0.024164
chr10__69392125__69395105___HK1	0.096064	-3.37987	0.021999
chr10__73156275__73156655___ECD	0.162641	-2.62024	0.031863
chr10__7769216__7780307___KIN	0.115375	-3.1156	0.029366
chr10__80463088__80468687___TSPAN14	0.102695	-3.28357	0.024487
chr10__86443275__86460496___WAPAL	0.100261	-3.31816	0.022172
chr10__86497201__86500743___WAPAL	0.078315	-3.67457	0.019072
chr10__87508336__87552541___MINPP1	0.128756	-2.95729	0.031515
chr10__87864454__87894109___PTEN	0.080599	-3.6331	0.019466
chr10__87864454__87961118___PTEN	0.055374	-4.17463	0.017322
chr10__87875405__87933251___PTEN	0.26587	-1.9112	0.044462
chr10__884447__903516___LARP4B	0.071343	-3.80908	0.018908
chr10__91939952__91953873___BTAF1	0.119338	-3.06687	0.028404
chr10__91939952__91956657___BTAF1	0.141804	-2.81803	0.043293
chr10__92616737__92630364___KIF11	0.110523	-3.17758	0.025392
chr10__93681480__93687449___FRA10AC1	0.232879	-2.10235	0.048674
chr10__96855010__96907747___LCOR	0.139687	-2.83973	0.033888
chr10__96907265__96907747___LCOR	0.065047	-3.94237	0.018075
chr11__107416209__107433749___CWF19L2	0.149129	-2.74537	0.041991

chr11__108146202__108148858___NA	0.133777	-2.9021	0.038898
chr11__108169744__108173851___NPAT	0.141238	-2.8238	0.041914
chr11__108169744__108177090___NPAT	0.182727	-2.45224	0.037313
chr11__116759074__116765446___BUD13	0.093282	-3.42226	0.022546
chr11__117238601__117246948___RNF214	0.121792	-3.03751	0.02909
chr11__11873800__11880380___USP47	0.141023	-2.826	0.039593
chr11__120440129__120449214___ARHGEF12	0.135611	-2.88245	0.023463
chr11__121045674__121047667___TBCEL	0.10755	-3.21692	0.021612
chr11__121045674__121073040___TBCEL	0.152964	-2.70873	0.049194
chr11__130229829__130261029___ZBTB44	0.074782	-3.74117	0.019072
chr11__16046514__16111926___SOX6	0.144235	-2.79351	0.043177
chr11__16071714__16186955___SOX6	0.014859	-6.0725	0.022213
chr11__16177809__16186955___SOX6	0.145929	-2.77666	0.036863
chr11__16183886__16247560___SOX6	0.093548	-3.41815	0.021835
chr11__16264698__16286210___SOX6	0.174047	-2.52245	0.024437
chr11__16283756__16341252___SOX6	0.077634	-3.68717	0.019466
chr11__17122188__17145942___PIK3C2A	0.147456	-2.76164	0.04362
chr11__17295324__17296211___NUCB2	0.128466	-2.96054	0.034864
chr11__28211062__28212331___METTL15	0.146919	-2.7669	0.043015
chr11__28211062__28233585___METTL15	0.057435	-4.12193	0.018075
chr11__2969803__2979237___NAP1L4	0.029837	-5.06676	0.022213
chr11__31452718__31488241___IMMP1L	0.137602	-2.86142	0.037773
chr11__31456260__31469797___IMMP1L	0.115686	-3.11172	0.030247
chr11__34063052__34063363___CAPRIN1	0.074315	-3.75019	0.018908
chr11__34450988__34464235___CAT	0.109352	-3.19295	0.024437
chr11__34947506__34970286___PDHX	0.121478	-3.04123	0.031354
chr11__35198121__35208206___CD44	0.196588	-2.34675	0.047172
chr11__3723157__3753408___NUP98	0.111539	-3.16438	0.023211
chr11__3735191__3753408___NUP98	0.124588	-3.00476	0.031515
chr11__43326507__43335994___API5	0.195233	-2.35673	0.0387
chr11__43403998__43414776___TTC17	0.097317	-3.36116	0.022146
chr11__46769963__46788773___CKAP5	0.150519	-2.73199	0.048304
chr11__46811007__46821268___CKAP5	0.202338	-2.30516	0.0354
chr11__47486750__47500932___CELF1	0.121198	-3.04456	0.027634
chr11__47495943__47500932___CELF1	0.072939	-3.77716	0.018908
chr11__47499453__47500932___CELF1	0.131066	-2.93164	0.036144
chr11__47750916__47753102___FNBP4	0.088248	-3.5023	0.019681
chr11__58584856__58612328___ZFP91ZFP91-CNTF	0.157419	-2.66732	0.032269
chr11__58609830__58611738___ZFP91ZFP91-CNTF	0.159312	-2.65007	0.049858
chr11__58610298__58611738___ZFP91ZFP91-CNTF	0.122332	-3.03113	0.034864
chr11__61364476__61367998___TMEM138	0.151695	-2.72075	0.038892
chr11__65502321__65505019___MALAT1	0.215475	-2.21441	0.019466
chr11__67180079__67181892___KDM2A	0.096824	-3.3685	0.024309
chr11__68175018__68185928___SUV420H1	0.082327	-3.60249	0.019466
chr11__68544838__68564432___PPP6R3	0.099982	-3.32218	0.021612
chr11__68596097__68603492___PPP6R3	0.187878	-2.41213	0.034864

chr11__68784815__68796933___CPT1A	0.046891	-4.41455	0.011892
chr11__70354301__70356254___PPFIA1	0.111948	-3.15909	0.02524
chr11__74374415__74378658___PGM2L1	0.086698	-3.52786	0.020098
chr11__74775146__74810330___RNF169	0.109168	-3.19538	0.027846
chr11__77353536__77359017___PAK1	0.136826	-2.86959	0.032216
chr11__77353536__77374365___PAK1	0.144853	-2.78734	0.025508
chr11__77624963__77629899___CLNS1A	0.080171	-3.64078	0.019072
chr11__77685105__77693611___RSF1	0.079101	-3.66016	0.019072
chr11__77691159__77693611___RSF1	0.065835	-3.92501	0.018075
chr11__77978996__77991299___INTS4	0.117266	-3.09214	0.024432
chr11__85976623__85981228___PICALM	0.174905	-2.51536	0.032177
chr11__85981745__86007583___PICALM	0.095259	-3.39201	0.023463
chr11__85996826__86014963___PICALM	0.095525	-3.38797	0.021449
chr11__9283371__9299701___TMEM41B	0.075591	-3.72564	0.018908
chr11__9286455__9295387___TMEM41B	0.104706	-3.25558	0.029366
chr11__93696320__93702919___KIAA1731	0.085048	-3.55558	0.020246
chr11__9420411__9425262___IPO7	0.130608	-2.93668	0.03625
chr11__96209454__96210334___MAML2	0.191231	-2.38661	0.048371
chr12__100591736__100601753___GAS2L3	0.131513	-2.92672	0.033416
chr12__102148230__102153976___PARPBP	0.161572	-2.62975	0.034864
chr12__102164438__102182627___PARPBP	0.084839	-3.55913	0.020098
chr12__110018345__110025823___ANKRD13A	0.170581	-2.55147	0.027455
chr12__110018345__110033957___ANKRD13A	0.064194	-3.96141	0.018075
chr12__111482787__111510582___ATXN2	0.108886	-3.19911	0.028715
chr12__111681637__111683307___BRAP	0.079295	-3.65662	0.018908
chr12__112175736__112176702___HECTD4	0.195979	-2.35123	0.036144
chr12__116237468__116237705___MED13L	0.13435	-2.89594	0.023102
chr12__117038983__117046838___TESC	0.186623	-2.4218	0.046657
chr12__118255448__118266759___TAOK3	0.152783	-2.71045	0.023601
chr12__118400659__118403517___SUDS3	0.150063	-2.73636	0.039387
chr12__122515105__122522299___RSRC2	0.116222	-3.10504	0.031586
chr12__122517227__122522299___RSRC2	0.130935	-2.93308	0.021999
chr12__122601536__122622607___KNTC1	0.144594	-2.78992	0.036935
chr12__122601536__122624688___KNTC1	0.060352	-4.05045	0.018075
chr12__123160781__123181210___MPHOSPH9	0.109927	-3.18539	0.024309
chr12__123345258__123348133___SBNO1	0.12377	-3.01427	0.030273
chr12__123679189__123687035___TCTN2	0.084819	-3.55948	0.019072
chr12__130795995__130808704___STX2	0.14488	-2.78707	0.042905
chr12__14434337__14438267___ATF7IP	0.130401	-2.93897	0.041086
chr12__1739068__1754514___ADIPOR2	0.09022	-3.47041	0.019681
chr12__22055149__22062434___CMAS	0.154614	-2.69325	0.048674
chr12__22055149__22065287___CMAS	0.178671	-2.48462	0.045086
chr12__26550247__26655852___ITPR2	0.074815	-3.74052	0.018983
chr12__26621123__26655852___ITPR2	0.139421	-2.84248	0.023894
chr12__26911178__26917733___ASUN	0.148759	-2.74896	0.018793
chr12__26982773__26983596___TM7SF3	0.116189	-3.10545	0.027496

chr12__28255581__28452654___CCDC91	0.142521	-2.81076	0.036144
chr12__30713785__30753559___CAPRIN2	0.128277	-2.96266	0.034864
chr12__32619698__32633689___FGD4	0.120266	-3.0557	0.032106
chr12__42374956__42398994___PPHLN1	0.122814	-3.02546	0.026883
chr12__4517061__4518880___C12orf4	0.132236	-2.91881	0.034864
chr12__45945249__45964188___SCAF11	0.201822	-2.30884	0.049261
chr12__48837281__48837657___DDX23	0.074973	-3.73748	0.019072
chr12__49489465__49490731___SPATS2	0.111902	-3.15969	0.029199
chr12__49990684__49992655___RACGAP1	0.063489	-3.97735	0.018075
chr12__50435488__50441643___LARP4	0.119149	-3.06916	0.030247
chr12__50981639__51010766___SLC11A2	0.2482	-2.01042	0.040514
chr12__56671749__56673065___PTGES3	0.22106	-2.17749	0.033362
chr12__56739294__56746181___PRIM1	0.125751	-2.99136	0.026601
chr12__62500783__62508480___MON2	0.108081	-3.20982	0.027264
chr12__64409962__64420521___XPOT	0.13618	-2.87641	0.037352
chr12__64409962__64448297___XPOT	0.136008	-2.87824	0.034864
chr12__65181741__65184482___LEMD3	0.125129	-2.99851	0.032106
chr12__65182631__65218619___LEMD3	0.144289	-2.79297	0.037563
chr12__6730402__6730820___COPS7A	0.124297	-3.00814	0.029366
chr12__68757148__68759239___SLC35E3	0.105419	-3.24579	0.022932
chr12__69365633__69370975___YEATS4	0.113906	-3.13408	0.025392
chr12__69409884__69410727___NA	0.125317	-2.99634	0.034142
chr12__70219393__70225390___LOC101928062	0.089563	-3.48096	0.019951
chr12__70278132__70319364___CNOT2	0.110058	-3.18367	0.028042
chr12__70342107__70346324___CNOT2	0.106331	-3.23337	0.026576
chr12__71626260__71629037___ZFC3H1	0.094434	-3.40455	0.020725
chr12__75312848__75326527___CAPS2	0.081004	-3.62587	0.019466
chr12__76827360__76827979___ZDHHC17	0.144034	-2.79552	0.038055
chr12__813642__813814___WNK1	0.170599	-2.55132	0.034864
chr12__827042__830160___WNK1	0.142317	-2.81282	0.046319
chr12__827042__862270___WNK1	0.152048	-2.71741	0.041105
chr12__89642158__89656107___ATP2B1	0.10905	-3.19693	0.024432
chr12__89655679__89677816___ATP2B1	0.119092	-3.06985	0.03163
chr12__95294272__95296258___VEZT	0.129574	-2.94816	0.031404
chr12__96909752__96912817___NEDD1	0.124641	-3.00415	0.035288
chr12__98677425__98686873___APAF1	0.084173	-3.57051	0.019466
chr13__113218945__113229519___CUL4A	0.132561	-2.91527	0.036144
chr13__113306485__113310867___LAMP1	0.077669	-3.68651	0.018908
chr13__113520616__113539507___TMCO3	0.091864	-3.44436	0.021835
chr13__113585774__113640375___TFDP1	0.172482	-2.53548	0.028166
chr13__19661698__19668531___MPHOSPH8	0.140905	-2.82721	0.0336
chr13__19824920__19851957___ZMYM5	0.104258	-3.26177	0.028042
chr13__20574380__20592404___IFT88	0.111797	-3.16104	0.025392
chr13__21381434__21401685___ZDHHC20	0.069618	-3.8444	0.018908
chr13__21387508__21425678___ZDHHC20	0.253831	-1.97806	0.037823
chr13__24484653__24503777___PARP4	0.074823	-3.74038	0.019072

chr13__26337567__26353880___CDK8	0.228069	-2.13246	0.031404
chr13__28260447__28280541___PAN3	0.178441	-2.48648	0.038055
chr13__29530538__29536202___SLC7A1	0.091542	-3.44943	0.020246
chr13__32517857__32538684___N4BP2L2	0.113925	-3.13385	0.030247
chr13__32732101__32746100___PDS5B	0.117364	-3.09094	0.028772
chr13__40826506__40872160___TPTE2P5	0.091308	-3.45311	0.020246
chr13__41068561__41071573___WBP4	0.279709	-1.838	0.048821
chr13__41761128__41833531___VWA8	0.153323	-2.70535	0.047726
chr13__41937315__41939586___VWA8	0.096255	-3.37699	0.022491
chr13__46010348__46042275___ZC3H13	0.115819	-3.11006	0.030101
chr13__46020449__46045516___ZC3H13	0.087448	-3.51543	0.020164
chr13__49993793__50044768___DLEU2	0.109268	-3.19406	0.030541
chr13__52433662__52434882___VPS36	0.218641	-2.19337	0.033457
chr13__59911735__59924870___DIAPH3	0.081763	-3.61241	0.019466
chr13__72778187__72778380___DIS3	0.070471	-3.82682	0.018908
chr13__77018600__77021861___FBXL3	0.082899	-3.5925	0.019888
chr13__95105046__95188542___ABCC4	0.129474	-2.94926	0.035962
chr13__95157161__95170628___ABCC4	0.201142	-2.31372	0.049194
chr13__99529467__99541667___TM9SF2	0.113787	-3.1356	0.023102
chr14__103405076__103405267___MARK3	0.149434	-2.74242	0.021612
chr14__103571623__103574170___APOPT1	0.281845	-1.82702	0.040213
chr14__30601770__30608069___G2E3	0.089852	-3.4763	0.020164
chr14__30633947__30639864___SCFD1	0.145965	-2.77631	0.041755
chr14__30929201__30936624___STRN3	0.093151	-3.42429	0.023102
chr14__31121422__31156886___HECTD1	0.122988	-3.02342	0.026625
chr14__31136531__31156886___HECTD1	0.146589	-2.77015	0.042658
chr14__31148721__31150221___HECTD1	0.097909	-3.35242	0.022213
chr14__34529358__34533539___EAPP	0.091539	-3.44947	0.019681
chr14__35050784__35053451___FAM177A1	0.122982	-3.02348	0.034864
chr14__35099252__35108236___PPP2R3C	0.110771	-3.17435	0.02524
chr14__35126735__35127611___KIAA0391	0.087426	-3.5158	0.020246
chr14__39151746__39158402___TRAPPC6B	0.072767	-3.78057	0.018075
chr14__45011975__45027474___FAM179B	0.150551	-2.73167	0.045409
chr14__45226743__45242518___MIS18BP1	0.089925	-3.47513	0.020246
chr14__45226743__45242874___MIS18BP1	0.142748	-2.80846	0.041388
chr14__45227663__45242518___MIS18BP1	0.081838	-3.61109	0.019788
chr14__49607400__49608121___LRR1	0.422611	-1.2426	0.045006
chr14__49663315__49665163___POLE2	0.096562	-3.37239	0.020886
chr14__49789146__49795944___NEMF	0.126824	-2.9791	0.033512
chr14__49789146__49831361___NEMF	0.121442	-3.04166	0.031354
chr14__49795791__49806133___NEMF	0.080071	-3.64257	0.019466
chr14__50138612__50153173___SOS2	0.102705	-3.28343	0.022213
chr14__50145170__50158646___SOS2	0.117951	-3.08374	0.030101
chr14__50423121__50429260___MAP4K5	0.128335	-2.96202	0.033976
chr14__50423121__50435065___MAP4K5	0.126782	-2.97957	0.030541
chr14__50425907__50429260___MAP4K5	0.135464	-2.88402	0.034864

chr14__50442732__50445194___MAP4K5	0.12196	-3.03552	0.030421
chr14__50445041__50448832___MAP4K5	0.124195	-3.00932	0.031354
chr14__52455324__52470680___TXNDC16	0.170297	-2.55388	0.0403
chr14__52455324__52476347___TXNDC16	0.113412	-3.14035	0.031354
chr14__52470037__52491005___TXNDC16	0.114118	-3.1314	0.029897
chr14__52470037__52544371___TXNDC16	0.176935	-2.49871	0.038055
chr14__52506090__52544371___TXNDC16	0.109698	-3.18839	0.02792
chr14__52730459__52771183___STYX	0.073839	-3.75948	0.018908
chr14__54408745__54411706___CDKN3	0.120924	-3.04783	0.029864
chr14__54955561__54957635___WDHD1	0.072907	-3.77781	0.018908
chr14__55158522__55170787___DLGAP5	0.094422	-3.40473	0.020975
chr14__55378279__55380389___ATG14	0.099863	-3.3239	0.024309
chr14__55380573__55382191___ATG14	0.037706	-4.72906	0.006314
chr14__58306022__58330169___ARID4A	0.124246	-3.00873	0.032177
chr14__58457759__58487166___KIAA0586	0.108398	-3.20559	0.028042
chr14__58467735__58470723___KIAA0586	0.09982	-3.32452	0.023529
chr14__60256824__60268435___PPM1A	0.062378	-4.00281	0.018075
chr14__60256824__60277365___PPM1A	0.286221	-1.8048	0.049261
chr14__60267215__60268435___PPM1A	0.075202	-3.73308	0.018908
chr14__60267215__60277091___PPM1A	0.206195	-2.27792	0.048531
chr14__65455621__65458207___FUT8	0.074368	-3.74917	0.018908
chr14__67398007__67402868___PLEK2	0.11384	-3.13492	0.032106
chr14__70584817__70597777___MED6	0.164867	-2.60063	0.019681
chr14__72693076__72731934___DPF3	0.105457	-3.24527	0.028042
chr14__72981789__72993357___ZFYVE1	0.158698	-2.65564	0.028772
chr14__74022916__74046130___CCDC176	0.077902	-3.6822	0.019466
chr14__74713485__74734170___FCF1	0.162399	-2.62238	0.034864
chr14__75707018__75720703___TTLL5	0.095905	-3.38224	0.021999
chr14__78957242__78968346___NRXN3	0.083612	-3.58014	0.019681
chr14__80743075__80761613___CEP128	0.145459	-2.78132	0.036405
chr14__80862757__80906081___CEP128	0.129766	-2.94601	0.032478
chr14__88754512__88766867___EML5	0.122164	-3.03311	0.031354
chr14__92142164__92155323___CPSF2	0.088889	-3.49185	0.020098
chr14__96520055__96565214___PAPOLA	0.153937	-2.69958	0.049921
chr14__96833467__96945382___NA	0.107389	-3.21908	0.024309
chr14__96846095__96856586___VRK1	0.087269	-3.51838	0.019681
chr15__22667898__22681605___WHAMMP3	0.114654	-3.12465	0.028404
chr15__30967920__30976955___MTMR10	0.163751	-2.61042	0.046409
chr15__32633933__32636408___ARHGAP11A	0.139263	-2.84412	0.045562
chr15__34152790__34163690___KATNBL1	0.120327	-3.05496	0.029557
chr15__34250298__34251057___SLC12A6	0.131469	-2.9272	0.034671
chr15__34890215__34897705___AQR	0.173098	-2.53034	0.041935
chr15__42528262__42529819___SNAP23	0.096942	-3.36673	0.023513
chr15__42558198__42566706___HAUS2	0.133769	-2.90219	0.037829
chr15__42775135__42840433___TTBK2	0.106806	-3.22694	0.022775
chr15__42827928__42878684___TTBK2	0.06616	-3.91789	0.018075

chr15__42988819__43025429___UBR1	0.080138	-3.64137	0.019681
chr15__43395107__43401850___TUBGCP4	0.109368	-3.19274	0.024437
chr15__43398038__43401850___TUBGCP4	0.118503	-3.077	0.031515
chr15__43809755__43817448___MFAP1	0.150694	-2.73031	0.049869
chr15__44328685__44380976___CASC4	0.103877	-3.26705	0.018075
chr15__44484224__44486700___CTDSPL2	0.111288	-3.16763	0.025627
chr15__44606025__44613536___SPG11	0.141829	-2.81778	0.036508
chr15__49129477__49139653___COPS2	0.220553	-2.1808	0.039402
chr15__50300789__50314670___GABPB1	0.152035	-2.71752	0.045029
chr15__50449400__50465191___USP8	0.13647	-2.87334	0.037823
chr15__50459000__50471795___USP8	0.093751	-3.41502	0.020098
chr15__50569887__50575919___TRPM7	0.073768	-3.76087	0.019072
chr15__50912078__50930971___AP4E1	0.082041	-3.60751	0.019681
chr15__50912078__50958794___AP4E1	0.129466	-2.94935	0.030579
chr15__56391243__56394834___TEX9	0.089373	-3.48401	0.019788
chr15__58899469__58899709___SLTM	0.15829	-2.65936	0.048674
chr15__63690541__63694894___HERC1	0.074257	-3.75132	0.019072
chr15__63712775__63734849___HERC1	0.132702	-2.91374	0.022475
chr15__63723182__63749791___HERC1	0.149482	-2.74195	0.045971
chr15__63727647__63749791___HERC1	0.097556	-3.35762	0.020886
chr15__63746918__63747858___HERC1	0.209363	-2.25592	0.031515
chr15__63749367__63756748___HERC1	0.493324	-1.01939	0.048852
chr15__63754505__63755003___HERC1	0.134897	-2.89007	0.040213
chr15__64203082__64204949___CSNK1G1	0.127246	-2.97431	0.032177
chr15__65153547__65157910___CLPX	0.117196	-3.09301	0.028542
chr15__65478880__65481615___DPP8	0.107632	-3.21582	0.024437
chr15__65665199__65706224___DENND4A	0.082515	-3.59919	0.019072
chr15__65690415__65761438___DENND4A	0.074083	-3.75472	0.018983
chr15__65700544__65738875___DENND4A	0.102872	-3.28108	0.022475
chr15__65702305__65732818___DENND4A	0.071493	-3.80606	0.018908
chr15__66532247__66537263___ZWILCH	0.164478	-2.60403	0.035288
chr15__68211263__68218650___CLN6	0.070606	-3.82408	0.018607
chr15__69439904__69441079___KIF23	0.138441	-2.85266	0.042905
chr15__71991103__72010447___MYO9A	0.189217	-2.40189	0.0403
chr15__72518067__72544964___ARIH1	0.217535	-2.20068	0.025569
chr15__74926766__74929232___COX5A	0.085662	-3.54521	0.020098
chr15__80073266__80131293___ZFAND6	0.076557	-3.70731	0.019072
chr15__82400633__82408367___UBE2Q2P2UBE2Q2P3	0.191266	-2.38635	0.04183
chr15__89113732__89116521___ABHD2	0.255968	-1.96597	0.0444
chr15__89871475__89889140___C15orf38-AP3S2AP3S2	0.080534	-3.63426	0.019072
chr15__90217439__90219891___SEMA4B	0.059142	-4.07967	0.018075
chr15__90979158__90981981___PRC1	0.155475	-2.68525	0.048945
chr15__92885515__92901299___NA	0.111957	-3.15898	0.029199
chr15__92900789__92929091___CHD2	0.156265	-2.67794	0.026479
chr15__92924321__92927330___CHD2	0.077147	-3.69624	0.018908
chr15__92924321__92949076___CHD2	0.104981	-3.25181	0.021449

chr15__92978234__92992998___CHD2	0.131784	-2.92375	0.034864
chr15__93004617__93009323___CHD2	0.101967	-3.29383	0.022213
chr15__99256032__99300532___LRRC28	0.14099	-2.82634	0.035839
chr15__99276576__99287951___LRRC28	0.13507	-2.88822	0.033324
chr15__99671323__99675458___MEF2A	0.140297	-2.83344	0.037563
chr16__10414574__10440462___ATF7IP2	0.29431	-1.76459	0.038949
chr16__11841695__11847806___RSL1D1	0.190108	-2.39511	0.019788
chr16__11875761__11898035___GSPT1	0.107288	-3.22044	0.027455
chr16__12199601__12278036___SNX29	0.132814	-2.91252	0.038898
chr16__14552021__14593378___PARN	0.09344	-3.41981	0.023008
chr16__14552021__14617650___PARN	0.135665	-2.88188	0.040053
chr16__15615830__15621911___KIAA0430	0.132761	-2.9131	0.036144
chr16__18841565__18850467___SMG1	0.099462	-3.32971	0.022375
chr16__20911183__20915714___LYRM1	0.156863	-2.67243	0.027634
chr16__21612645__21614318___METTL9	0.104122	-3.26366	0.022403
chr16__24750726__24763781___TNRC6A	0.13017	-2.94153	0.030579
chr16__24775604__24777358___TNRC6A	0.131924	-2.92222	0.033763
chr16__28175898__28181031___XPO6	0.063342	-3.98069	0.018075
chr16__3778011__3778817___CREBBP	0.128785	-2.95697	0.018075
chr16__3780732__3782926___CREBBP	0.113139	-3.14383	0.026509
chr16__47428804__47459175___ITFG1	0.19338	-2.37049	0.044862
chr16__47463899__47589102___PHKB	0.11012	-3.18285	0.025284
chr16__47633899__47635022___PHKB	0.15205	-2.71738	0.031354
chr16__48252225__48303305___LONP2	0.228502	-2.12972	0.034915
chr16__53222644__53229100___CHD9	0.111823	-3.16071	0.031515
chr16__67685457__67685802___GFOD2	0.051298	-4.28495	0.014522
chr16__68810197__68813495___CDH1	0.127058	-2.97644	0.034864
chr16__71658233__71676649___PHLPP2	0.124172	-3.00959	0.027771
chr16__72349046__72391215___NA	0.078054	-3.67938	0.019072
chr16__72373830__72391215___NA	0.11262	-3.15047	0.023672
chr16__74923926__74956610___WDR59	0.134741	-2.89174	0.037237
chr16__74938150__74951543___WDR59	0.143029	-2.80562	0.040678
chr16__75362875__75395209___CFDP1	0.067418	-3.89071	0.018075
chr16__75411825__75412754___CFDP1	0.121935	-3.03581	0.031419
chr16__75412535__75414695___CFDP1	0.116372	-3.10318	0.033362
chr16__81024715__81026638___CENPN	0.35127	-1.50935	0.033595
chr16__8903268__8917156___USP7	0.129209	-2.95222	0.034459
chr16__8910745__8919139___USP7	0.052378	-4.2549	0.015563
chr17__12081356__12113360___MAP2K4	0.088778	-3.49366	0.020813
chr17__18865469__18911251___PRPSAP2	0.219529	-2.18752	0.048538
chr17__19939713__19958571___AKAP10	0.150449	-2.73265	0.029199
chr17__20017987__20057817___SPECC1	0.130676	-2.93593	0.032065
chr17__20204333__20227620___SPECC1	0.081634	-3.61469	0.019466
chr17__2665372__2670331___PAFAH1B1	0.08971	-3.47858	0.021999
chr17__27301788__27303635___WSB1	0.268305	-1.89805	0.04667
chr17__27303367__27311616___WSB1	0.075883	-3.72009	0.019072

chr17__27304780__27309272___WSB1	0.105195	-3.24886	0.027634
chr17__29676820__29703062___SSH2	0.136029	-2.87801	0.038849
chr17__30449553__30451846___CPD	0.149689	-2.73996	0.045173
chr17__30843913__30844916___ATAD5	0.136653	-2.87141	0.019466
chr17__30855143__30869646___ATAD5	0.108976	-3.19791	0.026635
chr17__30856955__30879487___ATAD5	0.14958	-2.74101	0.044462
chr17__30856955__30887372___ATAD5	0.167832	-2.57491	0.020246
chr17__30868333__30869646___ATAD5	0.100919	-3.30873	0.024309
chr17__31976521__31983104___SUZ12	0.148223	-2.75415	0.0403
chr17__32017972__32035639___NA	0.127449	-2.97201	0.034442
chr17__32171043__32175362___RHOT1	0.092365	-3.43651	0.022213
chr17__32173831__32194107___RHOT1	0.265276	-1.91444	0.032848
chr17__32173831__32201056___RHOT1	0.114412	-3.12769	0.028404
chr17__32200956__32203973___RHOT1	0.129188	-2.95245	0.037823
chr17__32202770__32203973___RHOT1	0.081767	-3.61235	0.019681
chr17__35820024__35820437___TAF15	0.074442	-3.74773	0.018908
chr17__3705081__3705645___NA	0.083151	-3.58813	0.020164
chr17__37458524__37465541___TADA2A	0.097059	-3.365	0.024437
chr17__37619768__37621520___DDX52	0.120289	-3.05542	0.031354
chr17__39258305__39259296___FBXL20	0.178235	-2.48815	0.033874
chr17__39419717__39427790___MED1	0.120578	-3.05197	0.031515
chr17__39564760__39566892___CDK12	0.080548	-3.63401	0.019681
chr17__40408492__40416512___TOP2A	0.162111	-2.62495	0.034864
chr17__42706007__42708083___EZH1	0.100081	-3.32075	0.022475
chr17__43067608__43074521___BRCA1	0.068935	-3.85862	0.018075
chr17__43099775__43104956___BRCA1	0.156757	-2.6734	0.049194
chr17__43377913__43380107___LINC00910	0.139165	-2.84513	0.040053
chr17__45475100__45478147___PLEKHM1	0.118168	-3.08109	0.029837
chr17__46119968__46169605___KANSL1	0.125731	-2.99158	0.034864
chr17__47129393__47154786___CDC27	0.109707	-3.18828	0.027634
chr17__47137152__47138891___CDC27	0.12913	-2.9531	0.030247
chr17__47402132__47429961___EFCAB13	0.104738	-3.25514	0.023672
chr17__48112031__48113401___SNX11	0.147779	-2.75848	0.027784
chr17__48133535__48137337___SKAP1	0.125488	-2.99438	0.038055
chr17__49311312__49322508___ZNF652	0.151219	-2.72529	0.044862
chr17__50385118__50388132___LRRC59	0.10924	-3.19443	0.031059
chr17__5354359__5368468___RABEP1	0.216126	-2.21006	0.020246
chr17__58458768__58480267___HSF5	0.139224	-2.84452	0.018075
chr17__59051214__59057054___TRIM37	0.091621	-3.44818	0.020098
chr17__59737453__59817773___VMP1	0.21201	-2.2378	0.031354
chr17__59910562__59926582___RPS6KB1	0.172798	-2.53284	0.031404
chr17__59935193__59936541___RPS6KB1	0.062322	-4.00411	0.018075
chr17__60198260__60214774___USP32	0.213175	-2.22989	0.042905
chr17__60271350__60288682___USP32	0.239534	-2.0617	0.038608
chr17__60299334__60301704___USP32	0.097874	-3.35293	0.023102
chr17__61015751__61040892___BCAS3	0.093618	-3.41708	0.022403

chr17__61776401__61781005___BRIP1	0.080292	-3.63861	0.019072
chr17__61965006__61968258___MED13	0.098808	-3.33923	0.022932
chr17__61972727__62063222___MED13	0.139712	-2.83947	0.038055
chr17__61984171__61995365___MED13	0.117877	-3.08465	0.028042
chr17__62536170__62565137___TLK2	0.097719	-3.35521	0.024332
chr17__62560016__62565137___TLK2	0.095781	-3.38412	0.020246
chr17__62578477__62586226___TLK2	0.200145	-2.32089	0.033493
chr17__63792412__63800617___DDX42	0.101677	-3.29793	0.023672
chr17__64052780__64053371___ERN1	0.09736	-3.36052	0.023894
chr17__67166478__67195470___HELZ	0.172622	-2.53432	0.038803
chr17__67891847__67894165___BPTF	0.107296	-3.22033	0.024309
chr17__68429996__68433575___WIPI1	0.087969	-3.50686	0.020098
chr17__73203000__73203793___COG1	0.133784	-2.90202	0.031491
chr17__76007060__76010543___EVPL	0.091511	-3.44991	0.020886
chr17__76738282__76776541___MFSD11	0.150335	-2.73375	0.025627
chr17__7945728__7945986___CNTROB	0.14222	-2.8138	0.034524
chr17__81667729__81670453___CCDC137	0.150526	-2.73192	0.038055
chr17__82464287__82472698___NARF	0.115049	-3.11968	0.026144
chr17__8443927__8460160___NDEL1	0.126796	-2.97942	0.032177
chr18__116842__118504___ROCK1P1	0.089949	-3.47476	0.019466
chr18__13012973__13019206___CEP192	0.088827	-3.49286	0.021477
chr18__22968806__22984990___RBBP8	0.099558	-3.32832	0.025546
chr18__23463967__23466276___RIOK3	0.173978	-2.52302	0.029199
chr18__23504371__23509279___C18orf8	0.102345	-3.28848	0.024309
chr18__23515856__23516423___C18orf8	0.101902	-3.29474	0.020098
chr18__26315229__26335231___TAF4B	0.149032	-2.74631	0.022932
chr18__2718158__2752552___SMCHD1	0.137847	-2.85886	0.036405
chr18__2732265__2762236___SMCHD1	0.222561	-2.16773	0.038488
chr18__36142281__36160015___ELP2	0.163539	-2.6123	0.034427
chr18__37066890__37067545___KIAA1328	0.103822	-3.26781	0.024487
chr18__39207685__39208789___LINC00669	0.140997	-2.82627	0.039379
chr18__45736456__45739662___SLC14A1	0.136413	-2.87395	0.038055
chr18__51046920__51049324___SMAD4	0.090347	-3.46838	0.020886
chr18__54271360__54287411___POLI	0.097618	-3.3567	0.024309
chr18__54877567__54884436___RAB27B	0.070127	-3.83388	0.018607
chr18__62138243__62163656___PIGN	0.079621	-3.65071	0.019072
chr18__62211153__62232427___KIAA1468	0.078537	-3.67048	0.019072
chr18__62539681__62544873___ZCCHC2	0.179433	-2.47848	0.026509
chr18__62539681__62556297___ZCCHC2	0.104057	-3.26456	0.024309
chr18__70047971__70075541___RTTN	0.088038	-3.50574	0.019072
chr18__79126267__79193263___ATP9B	0.283425	-1.81896	0.035288
chr18__9182382__9195698___ANKRD12	0.088882	-3.49197	0.029199
chr18__9182382__9216900___ANKRD12	0.132125	-2.92003	0.022932
chr18__9263790__9275667___ANKRD12	0.192935	-2.37381	0.049262
chr18__9522160__9522509___RALBP1	0.184233	-2.44039	0.037823
chr19__10166598__10173174___DNMT1	0.137797	-2.85939	0.034864

chr19__10173090__10182077___DNMT1	0.070928	-3.81751	0.018075
chr19__1090908__1091907___POLR2E	0.140255	-2.83387	0.038055
chr19__15268905__15273133___BRD4	0.095711	-3.38517	0.020813
chr19__17101660__17102557___MYO9B	0.078891	-3.66399	0.019577
chr19__17162350__17163122___MYO9B	0.131403	-2.92793	0.037679
chr19__19465345__19474118___GATAD2A	0.115184	-3.11799	0.023672
chr19__21447650__21463843___NA	0.262483	-1.9297	0.049858
chr19__29817137__29817541___CCNE1	0.066809	-3.90382	0.018075
chr19__34430576__34438766___UBA2	0.07631	-3.71198	0.019072
chr19__34431861__34467014___UBA2	0.101768	-3.29664	0.022108
chr19__34458769__34464131___UBA2	0.100801	-3.31042	0.025392
chr19__4354949__4355173___MPND	0.112329	-3.1542	0.031354
chr19__47094389__47094608___ZC3H4	0.055695	-4.1663	0.015563
chr19__48149763__48151339___LIG1	0.120925	-3.04782	0.031354
chr19__51133313__51134407___SIGLEC9	0.112712	-3.14929	0.030101
chr19__52383849__52385742___ZNF880	0.075786	-3.72193	0.018908
chr19__52618936__52635153___ZNF83	0.061844	-4.01523	0.018075
chr19__53148681__53153793___ZNF347	0.105788	-3.24075	0.028772
chr19__5653115__5657347___SAFB	0.06444	-3.95589	0.018075
chr19__56576713__56578278___ZNF470	0.104753	-3.25494	0.026625
chr19__8337795__8339167___KANK3	0.129688	-2.94688	0.034915
chr19__9652953__9653878___ZNF562	0.089898	-3.47557	0.020098
chr2__108451028__108475850___GCC2	0.085231	-3.55248	0.020246
chr2__108839185__108856970___CCDC138	0.092235	-3.43855	0.022213
chr2__110649234__110661841___BUB1	0.085817	-3.54259	0.020098
chr2__112074912__112107840___TMEM87B	0.129671	-2.94707	0.032384
chr2__11214357__11217169___ROCK2	0.195842	-2.35224	0.044172
chr2__112299849__112321865___ZC3H6	0.178318	-2.48747	0.034864
chr2__113934279__113942359___ACTR3	0.125442	-2.99491	0.020164
chr2__119920069__119955323___PTPN4	0.133305	-2.9072	0.036101
chr2__120285874__120289757___RALB	0.084281	-3.56865	0.020098
chr2__127763062__127771004___WDR33	0.243475	-2.03816	0.029366
chr2__127999741__128000454___SAP130	0.14202	-2.81584	0.038892
chr2__128097429__128116343___UGGT1	0.321101	-1.6389	0.041104
chr2__128170288__128173939___UGGT1	0.076467	-3.70902	0.018908
chr2__135769769__135772547___UBXN4	0.193908	-2.36655	0.020183
chr2__144424796__144425538___ZEB2	0.133644	-2.90354	0.033416
chr2__144464166__144486308___ZEB2	0.13608	-2.87747	0.033595
chr2__148178700__148342336___MBD5	0.066894	-3.90198	0.018075
chr2__148233245__148342336___MBD5	0.152684	-2.71138	0.026576
chr2__148761782__148765146___EPC2	0.088563	-3.49715	0.011892
chr2__151416561__151428922___RIF1	0.068067	-3.8769	0.018607
chr2__151438684__151461289___RIF1	0.114386	-3.12801	0.027771
chr2__151440027__151446575___RIF1	0.116419	-3.10261	0.028404
chr2__151441905__151443709___RIF1	0.102096	-3.29201	0.022213
chr2__151465854__151475219___RIF1	0.079768	-3.64805	0.019072

chr2__152657889__152659009___PRPF40A	0.136911	-2.86869	0.037563
chr2__15415546__15511350___NBAS	0.156744	-2.67352	0.041689
chr2__158603070__158621421___PKP4	0.128434	-2.9609	0.036598
chr2__158620990__158621421___PKP4	0.052034	-4.2644	0.014522
chr2__160281417__160284868___RBMS1	0.128763	-2.95722	0.0325
chr2__168063500__168075231___STK39	0.120488	-3.05304	0.030101
chr2__168074982__168129758___STK39	0.130347	-2.93957	0.035288
chr2__171011373__171028405___TLK1	0.193572	-2.36906	0.043177
chr2__171022872__171046362___TLK1	0.079666	-3.64989	0.019072
chr2__171117739__171132092___TLK1	0.105064	-3.25066	0.022475
chr2__171117739__171153527___TLK1	0.140959	-2.82666	0.039402
chr2__171337453__171339554___METTL8	0.301102	-1.73168	0.031404
chr2__171448681__171453213___DCAF17	0.120782	-3.04953	0.030579
chr2__171540808__171541793___CYBRD1	0.336023	-1.57337	0.020246
chr2__171690147__171692894___DYNC1I2	0.264501	-1.91866	0.044172
chr2__174378923__174387779___CIR1	0.065065	-3.94198	0.018075
chr2__17714861__17745951___SMC6	0.117648	-3.08745	0.026913
chr2__190655977__190673152___NAB1	0.110974	-3.17171	0.025392
chr2__200857973__200861862___CLK1	0.164862	-2.60067	0.028192
chr2__200920222__200937966___ORC2	0.087683	-3.51156	0.019788
chr2__200949554__200958133___ORC2	0.105181	-3.24906	0.025999
chr2__201149003__201154407___CFLARCFLAR-AS1	0.153903	-2.6999	0.045272
chr2__201307519__201364176___NA	0.162808	-2.61876	0.027676
chr2__201350711__201364173___NA	0.167667	-2.57633	0.038938
chr2__201392909__201399493___TRAK2	0.147122	-2.76491	0.039831
chr2__201392909__201407597___TRAK2	0.142099	-2.81503	0.04073
chr2__202206737__202220106___SUMO1	0.073576	-3.76462	0.018908
chr2__203278573__203292326___CYP20A1	0.099753	-3.3255	0.023102
chr2__206056198__206063244___INO80D	0.076373	-3.71079	0.018908
chr2__210104104__210154611___KANSL1L	0.065619	-3.92975	0.018075
chr2__210431725__210476412___LANCL1	0.150082	-2.73618	0.044213
chr2__218529956__218562813___USP37	0.064462	-3.9554	0.018075
chr2__218546919__218560883___USP37	0.054816	-4.18926	0.015563
chr2__218546919__218562813___USP37	0.115193	-3.11787	0.026625
chr2__222613811__222624775___FARSB	0.160774	-2.63689	0.048131
chr2__222613811__222634541___FARSB	0.128534	-2.95978	0.031013
chr2__222928862__222930812___ACSL3	0.121529	-3.04062	0.032177
chr2__224495832__224514772___CUL3	0.114766	-3.12323	0.030579
chr2__226837548__226867688___RHBDD1	0.087836	-3.50905	0.019072
chr2__227491547__227536993___AGFG1	0.113019	-3.14536	0.027784
chr2__229840822__229859574___TRIP12	0.108962	-3.1981	0.024487
chr2__23782869__23823569___ATAD2B	0.138128	-2.85592	0.034864
chr2__23867835__23875904___ATAD2B	0.112693	-3.14953	0.032177
chr2__23884765__23895970___ATAD2B	0.122076	-3.03415	0.032935
chr2__24060814__24068791___NA	0.101648	-3.29835	0.023799
chr2__241140521__241140753___PASK	0.171593	-2.54294	0.039729

chr2__24135119__24161613___FAM228B	0.151813	-2.71963	0.030725
chr2__24137909__24147086___FAM228B	0.158301	-2.65926	0.023008
chr2__24137909__24161613___FAM228B	0.073852	-3.75922	0.019072
chr2__241407537__241436538___FARP2	0.09494	-3.39684	0.019788
chr2__24270671__24271941___ITSN2	0.074678	-3.74317	0.019072
chr2__24536715__24584560___NCOA1	0.19302	-2.37318	0.043109
chr2__24564295__24673463___NCOA1	0.123376	-3.01887	0.028042
chr2__26254247__26263479___HADHB	0.135538	-2.88323	0.038584
chr2__26364302__26383347___EPT1	0.079194	-3.65846	0.019072
chr2__27382126__27387158___PPM1G	0.099044	-3.33579	0.024612
chr2__32377588__32380290___BIRC6	0.216108	-2.21018	0.049858
chr2__33128432__33222151___LTBP1	0.105313	-3.24724	0.023102
chr2__33300451__33301644___LTBP1	0.099975	-3.32229	0.024309
chr2__33523879__33534400___RASGRP3	0.10488	-3.25319	0.026576
chr2__33565246__33568187___NA	0.090831	-3.46067	0.020246
chr2__37032629__37041292___HEATR5B	0.122318	-3.0313	0.030951
chr2__37101923__37104132___NA	0.115369	-3.11567	0.028404
chr2__44174762__44180397___PPM1B	0.038367	-4.704	0.006314
chr2__44430281__44505730___CAMKMT	0.143669	-2.79918	0.039729
chr2__44443253__44444094___CAMKMT	0.18925	-2.40163	0.028772
chr2__44456568__44549728___CAMKMT	0.087435	-3.51565	0.019072
chr2__44484877__44505730___CAMKMT	0.032681	-4.93539	0.026542
chr2__47408401__47429941___MSH2	0.134212	-2.89742	0.038892
chr2__53887259__53893799___PSME4	0.089975	-3.47434	0.020623
chr2__55558775__55588956___SMEK2	0.117745	-3.08626	0.031404
chr2__55577315__55591575___SMEK2	0.123399	-3.0186	0.034864
chr2__55644637__55646486___PNPT1	0.149537	-2.74142	0.04363
chr2__61115979__61121276___KIAA1841	0.1026	-3.2849	0.022108
chr2__61178981__61187029___AHSA2	0.165937	-2.5913	0.034864
chr2__61220310__61223296___USP34	0.179167	-2.48062	0.047046
chr2__61223060__61281242___USP34	0.393616	-1.34514	0.04667
chr2__61492035__61497007___XPO1	0.205341	-2.28391	0.033324
chr2__61501996__61533903___XPO1	0.108803	-3.20021	0.030247
chr2__68513080__68545312___APLF	0.112805	-3.1481	0.024437
chr2__70224554__70230854___TIA1	0.086908	-3.52436	0.019788
chr2__71365429__71365706___ZNF638	0.064556	-3.9533	0.018075
chr2__71396141__71406262___ZNF638	0.107145	-3.22237	0.023672
chr2__8243565__8287558___LINC00299	0.073171	-3.77258	0.018908
chr2__86740927__86773435___RMND5A	0.144906	-2.78681	0.026144
chr2__8860613__8868549___MBOAT2	0.164454	-2.60425	0.018908
chr2__9344532__9350895___ASAP2	0.140716	-2.82914	0.037535
chr2__99064939__99104118___TSGA10	0.128407	-2.9612	0.031059
chr2__99078659__99117759___TSGA10	0.153573	-2.703	0.039387
chr2__99429840__99435941___REV1	0.079055	-3.66099	0.018908
chr20__13559008__13569586___TASP1	0.101743	-3.297	0.024487
chr20__1452493__1455132___NSFL1C	0.116702	-3.0991	0.019072

chr20__18543019__18554390___SEC23B	0.051759	-4.27203	0.014522
chr20__25632158__25634827___NA	0.071568	-3.80453	0.018075
chr20__2947982__2975241___PTPRA	0.114452	-3.12718	0.000491
chr20__35651264__35659014___RBM12	0.075742	-3.72276	0.019072
chr20__35655157__35659014___RBM12	0.132648	-2.91432	0.035327
chr20__35655202__35659014___CPNE1	0.203564	-2.29644	0.036144
chr20__35721740__35739017___RBM39	0.095265	-3.39191	0.021199
chr20__35863013__35869551___PHF20	0.073459	-3.76692	0.018075
chr20__38551071__38554076___RALGAPB	0.15537	-2.68622	0.041991
chr20__3963875__3974400___RNF24	0.127278	-2.97395	0.032867
chr20__41061394__41081240___TOP1	0.078135	-3.67788	0.019466
chr20__41061394__41084568___TOP1	0.088057	-3.50541	0.020246
chr20__41092472__41112925___TOP1	0.069319	-3.85061	0.018075
chr20__41112782__41115439___TOP1	0.179334	-2.47928	0.025392
chr20__4195282__4204704___NA	0.080958	-3.62669	0.019681
chr20__43635926__43642624___IFT52	0.131104	-2.93122	0.032177
chr20__44981829__44987296___STK4	0.204932	-2.28678	0.033362
chr20__44987132__44995257___STK4	0.11772	-3.08657	0.031404
chr20__47224317__47236516___ZMYND8	0.078766	-3.66628	0.019466
chr20__47228605__47229806___ZMYND8	0.074068	-3.75501	0.018607
chr20__47235924__47236516___ZMYND8	0.121954	-3.03559	0.030247
chr20__47236326__47249439___ZMYND8	0.14027	-2.83372	0.038499
chr20__47249287__47262428___ZMYND8	0.151613	-2.72153	0.04235
chr20__47262288__47276905___ZMYND8	0.130593	-2.93685	0.037734
chr20__47276314__47283648___ZMYND8	0.095623	-3.38651	0.020098
chr20__47290187__47347926___ZMYND8	0.096695	-3.37041	0.023008
chr20__48952705__48953790___ARFGEF2	0.12923	-2.95199	0.034864
chr20__49849579__49855581___SLC9A8	0.115158	-3.11832	0.025392
chr20__5557945__5567560___GPCPD1	0.147454	-2.76167	0.038055
chr20__5557945__5570239___GPCPD1	0.090303	-3.46909	0.019466
chr20__5559940__5565078___GPCPD1	0.111511	-3.16474	0.031515
chr20__5559940__5570239___GPCPD1	0.07619	-3.71425	0.018908
chr20__5565017__5604440___GPCPD1	0.075918	-3.71941	0.019072
chr20__62256057__62260125___OSBPL2	0.138851	-2.84839	0.040029
chr21__15777904__15842540___USP25	0.073472	-3.76667	0.018908
chr21__15808809__15831629___USP25	0.181862	-2.45909	0.037237
chr21__15860622__15877991___USP25	0.149961	-2.73734	0.040053
chr21__32737254__32759269___PAXBP1	0.158019	-2.66183	0.049265
chr21__33340999__33343676___IFNAR1	0.059994	-4.05903	0.018075
chr21__33559230__33559775___SON	0.069514	-3.84654	0.018908
chr21__33781461__33782133___ITSN1	0.103613	-3.27072	0.026106
chr21__36341399__36345031___MORC3	0.080357	-3.63743	0.019681
chr21__36359955__36364259___MORC3	0.095266	-3.3919	0.019788
chr21__36368988__36372531___MORC3	0.15573	-2.68288	0.031354
chr21__39209995__39215362___BRWD1	0.121567	-3.04018	0.036144
chr21__39224408__39229436___BRWD1	0.091884	-3.44404	0.019577

chr21__39224408__39232498___BRWD1	0.136677	-2.87115	0.045579
chr21__42994848__42995343___PKNOX1	0.099652	-3.32696	0.025392
chr21__44077693__44080127___TRAPPC10	0.176989	-2.49827	0.04196
chr22__20043355__20048328___TANGO2	0.117728	-3.08648	0.028883
chr22__20933779__20934244___CRKL	0.061485	-4.02363	0.018075
chr22__21805825__21807846___MAPK1	0.191652	-2.38344	0.027368
chr22__28694032__28719485___CHEK2	0.091526	-3.44968	0.020725
chr22__28710006__28725367___CHEK2	0.18602	-2.42647	0.045771
chr22__28710006__28734727___CHEK2	0.133841	-2.90141	0.032177
chr22__28724977__28725367___CHEK2	0.418187	-1.25778	0.035288
chr22__29137342__29142100___KREMEN1	0.100499	-3.31474	0.022213
chr22__29813430__29822464___ASCC2	0.087888	-3.50819	0.019466
chr22__32478981__32485209___FBXO7	0.315069	-1.66626	0.020725
chr22__41125864__41130003___EP300	0.16299	-2.61715	0.049194
chr22__42890947__42891182___PACSIN2	0.196465	-2.34766	0.03784
chr22__46626751__46637960___GRAMD4	0.108971	-3.19798	0.028772
chr3__100281742__100283811___TBC1D23	0.258162	-1.95365	0.038849
chr3__101656104__101660028___ZBTB11	0.236256	-2.08157	0.045338
chr3__112563385__112573956___SLC35A5	0.045527	-4.45714	0.011892
chr3__121498477__121498670___POLQ	0.116842	-3.09737	0.029366
chr3__121726913__121730973___GOLGB1	0.097469	-3.35892	0.023601
chr3__125451305__125460860___SNX4	0.101513	-3.30026	0.022213
chr3__125453810__125460860___SNX4	0.139039	-2.84644	0.0403
chr3__130992951__131001344___ATP2C1	0.105663	-3.24246	0.024309
chr3__131462749__131471279___MRPL3	0.082058	-3.60722	0.019577
chr3__132681914__132692818___NPHP3-ACAD11	0.097746	-3.35482	0.021835
chr3__134495296__134513465___CEP63	0.09791	-3.3524	0.020426
chr3__134495296__134537268___CEP63	0.14631	-2.7729	0.045327
chr3__134531845__134537268___CEP63	0.124993	-3.00008	0.031515
chr3__136398749__136477412___STAG1	0.102998	-3.27932	0.023641
chr3__136417885__136502779___STAG1	0.125179	-2.99793	0.036722
chr3__138209817__138210434___ARMC8	0.315416	-1.66467	0.048758
chr3__138209817__138237572___ARMC8	0.087383	-3.51651	0.019466
chr3__138500110__138532570___CEP70	0.129881	-2.94474	0.030951
chr3__138525490__138537347___CEP70	0.17951	-2.47787	0.040213
chr3__138621407__138629156___FAIM	0.099259	-3.33265	0.025508
chr3__138681967__138684803___PIK3CB	0.056531	-4.14481	0.018075
chr3__141512163__141540609___RASA2	0.083977	-3.57386	0.019788
chr3__141963812__141993585___TFDP2	0.118285	-3.07966	0.029366
chr3__141974048__141978682___TFDP2	0.142221	-2.8138	0.036604
chr3__141993538__141995141___TFDP2	0.079864	-3.6463	0.019072
chr3__142664202__142678113___PLS1	0.080982	-3.62625	0.019072
chr3__143985543__143989832___C3orf58	0.117913	-3.0842	0.030247
chr3__14443624__14447816___SLC6A6	0.121675	-3.03889	0.030101
chr3__148384760__148446998___NA	0.126011	-2.98838	0.036287
chr3__148582857__148592265___NA	0.096996	-3.36593	0.023641

chr3__149068240__149073322___HLTF	0.152777	-2.7105	0.048945
chr3__158646165__158653467___GFM1	0.092	-3.44222	0.019072
chr3__167704842__167725473___PDCD10	0.195655	-2.35361	0.048581
chr3__167720062__167725473___PDCD10	0.080219	-3.63991	0.019681
chr3__169975608__169983253___SEC62	0.232142	-2.10692	0.028404
chr3__172760156__172783909___ECT2	0.118442	-3.07775	0.026577
chr3__17372075__17384015___TBC1D5	0.082522	-3.59908	0.019466
chr3__17622648__17623913___TBC1D5	0.092368	-3.43646	0.020246
chr3__17622648__17733460___TBC1D5	0.06938	-3.84933	0.018075
chr3__179413412__179426242___GNB4	0.178886	-2.48289	0.033763
chr3__180947865__180951468___FXR1	0.07944	-3.65398	0.018908
chr3__182940359__182965753___NA	0.331248	-1.59402	0.036508
chr3__185675296__185689627___IGF2BP2	0.158472	-2.6577	0.048852
chr3__188406112__188524787___LPP	0.15158	-2.72185	0.04362
chr3__193657080__193695467___OPA1	0.083807	-3.57679	0.019072
chr3__196019880__196020735___LOC102723457	0.063199	-3.98396	0.018075
chr3__196053418__196069568___TFRC	0.116432	-3.10245	0.032177
chr3__196053418__196071498___TFRC	0.143901	-2.79685	0.0403
chr3__196064309__196072152___TFRC	0.362179	-1.46523	0.036144
chr3__196069455__196075360___TFRC	0.081046	-3.62511	0.018908
chr3__196885151__196886694___SENP5	0.072064	-3.79457	0.018983
chr3__196899666__196903610___SENP5	0.112252	-3.15519	0.025999
chr3__197814908__197832317___LRCH3	0.169151	-2.56362	0.037734
chr3__25604760__25620816___TOP2B	0.115653	-3.11213	0.026743
chr3__25609568__25618849___TOP2B	0.153635	-2.70242	0.049341
chr3__25635936__25645470___TOP2B	0.105775	-3.24093	0.026625
chr3__25751098__25778688___NGLY1	0.065764	-3.92656	0.018075
chr3__27411642__27452498___SLC4A7	0.143159	-2.80431	0.041935
chr3__28251712__28253765___CMC1	0.080546	-3.63404	0.019466
chr3__3156219__3174261___CRBN	0.393233	-1.34654	0.041935
chr3__32708670__32717237___CNOT10	0.157201	-2.66932	0.033293
chr3__37108637__37121691___LRRFIP2	0.116237	-3.10486	0.028772
chr3__37286014__37302332___GOLGA4	0.176147	-2.50515	0.045403
chr3__47037666__47057490___SETD2	0.153107	-2.70738	0.048538
chr3__47622207__47678311___SMARCC1	0.151621	-2.72146	0.047398
chr3__47675475__47678311___SMARCC1	0.100461	-3.3153	0.022108
chr3__50108070__50108304___RBM5	0.083008	-3.5906	0.019681
chr3__52411029__52414587___PHF7	0.148626	-2.75024	0.04919
chr3__52678500__52682233___PBRM1	0.049441	-4.33815	0.014522
chr3__56571181__56594028___CCDC66	0.166216	-2.58887	0.048481
chr3__56588862__56594028___CCDC66	0.152274	-2.71526	0.042954
chr3__56666260__56673725___FAM208A	0.261264	-1.93642	0.030247
chr3__56669700__56673725___FAM208A	0.239739	-2.06046	0.014522
chr3__57890041__57896932___SLMAP	0.257264	-1.95868	0.038608
chr3__60765524__60767098___FHIT	0.104746	-3.25504	0.023816
chr3__63898399__63952483___ATXN7	0.147295	-2.76322	0.045156

chr3__69027900__69028295___TMF1	0.1787	-2.48439	0.046017
chr3__69038564__69042912___TMF1	0.104923	-3.2526	0.02436
chr3__69039551__69044595___TMF1	0.119257	-3.06785	0.032934
chr3__69187770__69189952___FRMD4B	0.140463	-2.83174	0.041905
chr3__71041328__71112637___FOXP1	0.094775	-3.39935	0.021999
chr3__9969719__9977446___EMC3	0.127693	-2.96925	0.020442
chr4__102795426__102826636___UBE2D3	0.130865	-2.93385	0.028772
chr4__102801560__102802560___UBE2D3	0.13896	-2.84726	0.041935
chr4__103108803__103132896___CENPE	0.156158	-2.67892	0.031657
chr4__103174736__103181456___CENPE	0.126772	-2.9797	0.038488
chr4__106164392__106248306___TBCK	0.110378	-3.17947	0.028166
chr4__109513747__109520484___SEC24B	0.102926	-3.28032	0.027634
chr4__117575655__117575857___NA	0.083962	-3.57412	0.019788
chr4__127982939__128030672___C4orf29	0.118639	-3.07535	0.031515
chr4__128936655__128946152___SCLT1	0.086255	-3.53525	0.020164
chr4__128936655__128952840___SCLT1	0.131858	-2.92294	0.037602
chr4__128936655__128992237___SCLT1	0.098163	-3.34867	0.023906
chr4__128957026__129003876___SCLT1	0.04175	-4.58209	0.009368
chr4__129036278__129082373___SCLT1	0.144824	-2.78763	0.040212
chr4__129039041__129093167___SCLT1	0.143659	-2.79928	0.042279
chr4__139116649__139168042___ELF2	0.178901	-2.48276	0.033888
chr4__139137630__139168042___ELF2	0.225115	-2.15126	0.0403
chr4__143415477__143469277___GAB1	0.09385	-3.41351	0.020442
chr4__143433491__143440382___GAB1	0.093804	-3.41421	0.023102
chr4__143989877__144001283___NA	0.095886	-3.38253	0.020246
chr4__145162640__145171720___OTUD4	0.062806	-3.99296	0.018075
chr4__145823422__145849561___ZNF827	0.107128	-3.2226	0.028404
chr4__150467673__150491035___LRBA	0.078075	-3.679	0.019466
chr4__150798081__150831976___LRBA	0.156995	-2.67121	0.031354
chr4__152411303__152482673___FBXW7	0.096466	-3.37383	0.023404
chr4__153583190__153598732___KIAA0922	0.136046	-2.87783	0.034864
chr4__15711807__15718993___BST1	0.134197	-2.89758	0.031662
chr4__158713119__158715668___PPID	0.143769	-2.79818	0.025999
chr4__168998202__169007756___CBR4	0.129986	-2.94357	0.031515
chr4__169424553__169537911___NEK1	0.147183	-2.76432	0.041277
chr4__169477124__169508852___NEK1	0.116277	-3.10436	0.033888
chr4__169477432__169508331___NEK1	0.128369	-2.96163	0.037237
chr4__169507715__169537911___NEK1	0.091664	-3.4475	0.020442
chr4__169585349__169599197___NEK1	0.070237	-3.83163	0.018908
chr4__169585349__169602678___NEK1	0.08359	-3.58052	0.019466
chr4__169665757__169697734___CLCN3	0.118403	-3.07823	0.030973
chr4__183683975__183693147___TRAPPC11	0.091753	-3.4461	0.020246
chr4__184661774__184678394___PRIMPOL	0.114131	-3.13124	0.024437
chr4__185247294__185267155___SNX25	0.096599	-3.37184	0.020098
chr4__20704466__20727397___PACRGL	0.093528	-3.41846	0.02337
chr4__25154998__25159107___SEPSECS	0.107579	-3.21654	0.026106

chr4__25256543__25263849___PI4K2B	0.142769	-2.80824	0.036766
chr4__2689506__2690970___FAM193A	0.132256	-2.9186	0.033976
chr4__343782__344430___ZNF141	0.151714	-2.72058	0.049869
chr4__36210390__36214480___ARAP2	0.067743	-3.88379	0.018075
chr4__38089932__38118192___TBC1D1	0.157402	-2.66747	0.0498
chr4__39698223__39755739___UBE2K	0.13534	-2.88534	0.020246
chr4__39737420__39738131___UBE2K	0.094338	-3.40602	0.020246
chr4__39837478__39838208___PDS5A	0.083213	-3.58705	0.019466
chr4__39841948__39845880___PDS5A	0.082511	-3.59927	0.019162
chr4__40594258__40596800___RBM47	0.193821	-2.36721	0.044577
chr4__42001616__42023384___SLC30A9	0.234234	-2.09398	0.043489
chr4__42022838__42039053___SLC30A9	0.119776	-3.06159	0.028758
chr4__42616033__42627109___ATP8A1	0.125388	-2.99553	0.018908
chr4__4457191__4471706___STX18	0.064598	-3.95238	0.018075
chr4__48510059__48515275___FRYL	0.146715	-2.76891	0.044577
chr4__48534545__48542121___FRYL	0.150343	-2.73367	0.028277
chr4__48842636__48857365___OCIAD1	0.105116	-3.24995	0.025058
chr4__51860543__51899378___DCUN1D4	0.177753	-2.49205	0.039729
chr4__53145333__53145582___SCFD2	0.10782	-3.2133	0.023672
chr4__55403236__55417985___TMEM165	0.10396	-3.26591	0.027455
chr4__55959682__55985358___CEP135	0.102661	-3.28404	0.024402
chr4__55964274__55981379___CEP135	0.184511	-2.43822	0.031515
chr4__56017648__56019555___CEP135	0.112402	-3.15326	0.019072
chr4__7006632__7014557___TBC1D14	0.208255	-2.26358	0.048674
chr4__70942823__70975286___MOB1B	0.099239	-3.33295	0.020246
chr4__73085249__73097272___ANKRD17	0.105903	-3.23918	0.024487
chr4__75804134__75805303___USO1	0.110737	-3.17479	0.029199
chr4__76130656__76136412___NUP54	0.160137	-2.64262	0.030101
chr4__77862806__77909372___MRPL1	0.145093	-2.78495	0.040213
chr4__78842385__78865720___BMP2K	0.066724	-3.90565	0.018075
chr4__82878730__82881937___SEC31A	0.128244	-2.96303	0.033888
chr4__83439863__83448961___HELQ	0.124348	-3.00754	0.028772
chr4__84896911__84932363___WDFY3	0.173644	-2.52579	0.032065
chr4__88113303__88115058___ABCG2	0.103529	-3.27189	0.022546
chr4__88949326__88953934___FAM13A	0.132944	-2.91111	0.031657
chr4__89822246__89836789___SNCA	0.128922	-2.95543	0.045159
chr4__911673__913668___GAK	0.168846	-2.56622	0.039157
chr4__9641071__9641450___NA	0.085835	-3.54229	0.020246
chr4__98404477__98421394___RAP1GDS1	0.142169	-2.81432	0.04235
chr4__98574457__98578081___TSPAN5	0.057715	-4.11491	0.018075
chr5__10213491__10224061___NA	0.14083	-2.82797	0.040902
chr5__108341927__108348530___FBXL17	0.081254	-3.62142	0.020098
chr5__109781396__109823837___MAN2A1	0.1522	-2.71596	0.048758
chr5__112985835__113013536___DCP2	0.152303	-2.71498	0.041935
chr5__115866670__115902992___AP3S1	0.135089	-2.88802	0.037535
chr5__126804776__126832801___LMNB1	0.072702	-3.78187	0.018908

chr5__131504626__131510491___RAPGEF6	0.0808	-3.62951	0.019072
chr5__131698917__131709272___FNIP1	0.171712	-2.54194	0.031492
chr5__132587562__132589837___RAD50	0.24246	-2.04418	0.038892
chr5__133064980__133076898___HSPA4	0.151501	-2.7226	0.046459
chr5__134199086__134206131___PPP2CA	0.120014	-3.05873	0.030247
chr5__134686790__134688299___SEC24A	0.089668	-3.47927	0.020098
chr5__137942875__137949184___FAM13B	0.090211	-3.47055	0.019681
chr5__138006990__138019146___FAM13B	0.106078	-3.23681	0.022403
chr5__142885298__142913293___ARHGAP26	0.076346	-3.71131	0.019072
chr5__143295460__143314168___NR3C1	0.165595	-2.59427	0.049689
chr5__145587325__145670827___NA	0.150006	-2.73691	0.04363
chr5__145764931__145796547___PRELID2	0.136026	-2.87804	0.039936
chr5__145796442__145823134___PRELID2	0.205047	-2.28598	0.041935
chr5__146263491__146271058___RBM27	0.052129	-4.26178	0.014541
chr5__146269207__146271058___RBM27	0.139866	-2.83788	0.041245
chr5__146483540__146507207___TCERG1	0.138652	-2.85046	0.034864
chr5__14741827__14751239___ANKH	0.156112	-2.67935	0.04903
chr5__151452343__151479489___SLC36A1	0.172594	-2.53455	0.036508
chr5__151790323__151791062___G3BP1	0.142704	-2.80891	0.042905
chr5__154029489__154034967___FAM114A2	0.130045	-2.94291	0.034797
chr5__154790325__154794262___LARP1	0.16611	-2.58979	0.028413
chr5__154865442__154867792___CNOT8	0.097497	-3.3585	0.024309
chr5__160049514__160051183___TTC1	0.117764	-3.08603	0.027217
chr5__163473179__163475672___HMMR	0.104957	-3.25212	0.023102
chr5__168488602__168495436___RARS	0.23279	-2.1029	0.031515
chr5__168493894__168502105___RARS	0.219085	-2.19044	0.042905
chr5__168554951__168564065___NA	0.12938	-2.95031	0.034864
chr5__168559032__168566266___PANK3	0.141183	-2.82437	0.020164
chr5__173108624__173123202___CREBRF	0.170074	-2.55576	0.019681
chr5__176943335__176969706___UIMC1	0.126413	-2.98378	0.031404
chr5__177041126__177044533___ZNF346	0.118818	-3.07317	0.029199
chr5__177044389__177050936___ZNF346	0.120226	-3.05618	0.032065
chr5__32390275__32397338___ZFR	0.105845	-3.23997	0.026509
chr5__34919840__34923234___BRIX1	0.123651	-3.01565	0.028042
chr5__36950999__36962274___NIPBL	0.234216	-2.09409	0.031916
chr5__36984676__36995804___NIPBL	0.121944	-3.03571	0.030709
chr5__40764514__40777586___PRKAA1	0.286918	-1.80129	0.037823
chr5__43122039__43174494___ZNF131	0.203703	-2.29546	0.033416
chr5__43122044__43161931___ZNF131	0.125434	-2.995	0.028302
chr5__43675511__43677806___NNT	0.10682	-3.22675	0.021999
chr5__50399859__50411383___EMB	0.102463	-3.28683	0.025392
chr5__50750151__50778650___PARP8	0.086392	-3.53296	0.019072
chr5__53636856__53658624___NDUFS4	0.076887	-3.70111	0.018908
chr5__54280207__54282327___ARL15	0.124206	-3.0092	0.034755
chr5__55272087__55281515___DHX29	0.035304	-4.82402	0.004729
chr5__55645789__55656774___SLC38A9	0.133403	-2.90614	0.034915

chr5__64800248__64804386___CWC27	0.101327	-3.30291	0.025999
chr5__65521475__65542848___CENPK	0.198408	-2.33346	0.037884
chr5__65542802__65551636___CENPK	0.105612	-3.24315	0.023672
chr5__66012049__66028343___ERBB2IP	0.095387	-3.39006	0.022775
chr5__69197053__69208359___CENPH	0.111754	-3.1616	0.025392
chr5__69300012__69311204___CCDC125	0.102372	-3.2881	0.025284
chr5__69371035__69374711___RAD17	0.122378	-3.03058	0.031515
chr5__73051349__73052507___FCHO2	0.090708	-3.46263	0.022229
chr5__77053965__77055596___AGGF1	0.093047	-3.4259	0.020246
chr5__77463095__77464809___WDR41	0.108202	-3.2082	0.028054
chr5__79290121__79306461___JMY	0.093182	-3.4238	0.019681
chr5__79613011__79645192___PAPD4	0.148397	-2.75246	0.027112
chr5__79640851__79657001___PAPD4	0.106124	-3.23617	0.023672
chr5__79640851__79682061___PAPD4	0.089376	-3.48397	0.019466
chr5__79645123__79682061___PAPD4	0.117949	-3.08377	0.030579
chr5__83388148__83398290___NA	0.12517	-2.99804	0.035978
chr5__94649454__94654752___ANKRD32	0.194739	-2.36038	0.036144
chr5__94654630__94663908___ANKRD32	0.152814	-2.71015	0.045825
chr5__95748333__95763620___RHOBTB3	0.171865	-2.54065	0.041388
chr5__95906523__95932713___ELL2	0.075431	-3.72869	0.018908
chr5__98879552__98881375___CHD1	0.098959	-3.33702	0.02306
chr6__108854225__108858271___ARMC2	0.104936	-3.25242	0.023641
chr6__109140421__109150239___CEP57L1	0.091446	-3.45093	0.020246
chr6__110887505__110893662___AMD1	0.177604	-2.49326	0.045197
chr6__111472013__111474479___REV3L	0.168638	-2.568	0.021899
chr6__119188405__119204882___MAN1A1	0.112013	-3.15826	0.030155
chr6__119301988__119306992___MAN1A1	0.104787	-3.25446	0.021999
chr6__119361291__119363332___NA	0.137067	-2.86705	0.034247
chr6__133982568__133984671___TBPL1	0.136188	-2.87633	0.023513
chr6__134986066__134993875___HBS1L	0.13523	-2.88652	0.032177
chr6__135192324__135200415___MYB	0.181351	-2.46315	0.035121
chr6__13579451__13600949___SIRT5	0.115404	-3.11523	0.033416
chr6__13632370__13641307___RANBP9	0.108635	-3.20244	0.023906
chr6__136694140__136720589___MAP3K5	0.06109	-4.03293	0.018075
chr6__138907495__138914761___REPS1	0.094206	-3.40804	0.023102
chr6__149517042__149541586___PPIL4	0.140873	-2.82754	0.041784
chr6__149525143__149535738___PPIL4	0.102499	-3.28632	0.02436
chr6__149533458__149535738___PPIL4	0.177776	-2.49187	0.046975
chr6__149533458__149541586___PPIL4	0.131968	-2.92174	0.031404
chr6__149572285__149580723___GINM1	0.111311	-3.16733	0.023102
chr6__149579834__149580723___GINM1	0.130917	-2.93327	0.032177
chr6__149738643__149742570___NUP43	0.125341	-2.99607	0.030247
chr6__157592988__157595723___ZDHHC14	0.153158	-2.7069	0.04183
chr6__16274415__16290621___GMPR	0.155531	-2.68472	0.030709
chr6__24456498__24467274___GPLD1	0.138856	-2.84834	0.037795
chr6__24777222__24781621___GMNN	0.084363	-3.56725	0.019466

chr6__30021667__30035983___ZNRD1-AS1	0.078951	-3.6629	0.019466
chr6__35874233__35891013___SRPK1	0.141434	-2.8218	0.038608
chr6__36524341__36525642___STK38	0.066736	-3.9054	0.018075
chr6__36601708__36603173___SRSF3	0.206841	-2.2734	0.034864
chr6__36899426__36902434___C6orf89	0.066353	-3.9137	0.018075
chr6__42637011__42642481___UBR2	0.104399	-3.25982	0.027217
chr6__42650284__42658824___UBR2	0.139532	-2.84133	0.037563
chr6__42662184__42679832___UBR2	0.134473	-2.89461	0.037823
chr6__42673791__42684871___UBR2	0.169515	-2.56052	0.030449
chr6__42676056__42684871___UBR2	0.134123	-2.89837	0.040192
chr6__47533602__47544706___CD2AP	0.190427	-2.39269	0.041935
chr6__47533602__47554766___CD2AP	0.175431	-2.51103	0.019072
chr6__4854525__4892379___CDYL	0.105498	-3.24471	0.024437
chr6__49606848__49615771___RHAG	0.184657	-2.43708	0.021999
chr6__49611024__49615771___RHAG	0.090229	-3.47027	0.020164
chr6__49614687__49615771___RHAG	0.085341	-3.55062	0.019681
chr6__53505392__53509250___GCLC	0.170792	-2.54969	0.039729
chr6__53514204__53532766___GCLC	0.085685	-3.54481	0.019466
chr6__57124734__57150862___ZNF451	0.129615	-2.9477	0.036144
chr6__63646527__63680161___PHF3	0.177248	-2.49616	0.044213
chr6__63646527__63685911___PHF3	0.07981	-3.64729	0.019072
chr6__75621532__75647801___SENP6	0.349424	-1.51695	0.037224
chr6__75659262__75663518___SENP6	0.087635	-3.51235	0.019466
chr6__79015082__79043003___PHIP	0.161014	-2.63474	0.049921
chr6__79513212__79519085___LCA5	0.216655	-2.20653	0.049921
chr6__84169328__84186623___KIAA1009	0.120717	-3.0503	0.028042
chr6__87215903__87233527___ZNF292	0.073092	-3.77415	0.019072
chr6__87514428__87516880___RARS2	0.106347	-3.23315	0.026826
chr6__89846562__89855544___CASP8AP2	0.069511	-3.84661	0.018908
chr6__97267882__97273062___MMS22L	0.077933	-3.68161	0.019072
chr6__98875415__98905670___FBXL4	0.136078	-2.8775	0.034864
chr6__99476143__99510230___USP45	0.097675	-3.35586	0.022403
chr7__102399548__102404683___PRKRIP1LOC100630923	0.157381	-2.66766	0.04235
chr7__103103051__103128792___NAPEPLD	0.145636	-2.77956	0.046433
chr7__103182378__103184127___DPY19L2P2	0.139996	-2.83655	0.036058
chr7__103233800__103257724___DPY19L2P2	0.088314	-3.50122	0.019072
chr7__104161072__104188381___ORC5	0.120981	-3.04715	0.025999
chr7__105038126__105091314___KMT2E	0.094745	-3.3998	0.020246
chr7__105040839__105081797___KMT2E	0.081966	-3.60882	0.019681
chr7__105066727__105081797___KMT2E	0.184706	-2.43669	0.043277
chr7__112286873__112287074___ZNF277	0.226717	-2.14104	0.039877
chr7__112895569__112915447___C7orf60	0.111556	-3.16416	0.025615
chr7__116110708__116112038___NA	0.134516	-2.89415	0.023463
chr7__125329682__125347207___RP11-3B12.2	0.088626	-3.49613	0.019466
chr7__128641203__128648982___NA	0.107758	-3.21414	0.023102
chr7__129873855__129880971___UBE2H	0.175248	-2.51253	0.031515

chr7__131338841__131341532___MKLN1	0.099429	-3.33019	0.023008
chr7__131338841__131375493___MKLN1	0.124309	-3.008	0.028772
chr7__131373710__131399433___MKLN1	0.465789	-1.10225	0.024309
chr7__131387120__131388972___MKLN1	0.25718	-1.95915	0.028887
chr7__131387120__131445903___MKLN1	0.148989	-2.74672	0.042658
chr7__131437785__131445903___MKLN1	0.125708	-2.99185	0.031515
chr7__139371387__139409654___LUC7L2	0.125378	-2.99565	0.035803
chr7__140454603__140472011___MKRN1	0.010405	-6.58657	0.022234
chr7__148766561__148767749___CUL1	0.08985	-3.47633	0.020246
chr7__152220523__152238826___KMT2C	0.066867	-3.90256	0.018075
chr7__154967816__154998784___PAXIP1	0.111821	-3.16074	0.027676
chr7__155672867__155707068___RBM33	0.125042	-2.99951	0.030247
chr7__157382246__157385611___DNAJB6	0.105281	-3.24769	0.025999
chr7__16258390__16301466___ISPD	0.104397	-3.25985	0.023672
chr7__2229984__2230764___MAD1L1	0.091958	-3.44288	0.019951
chr7__24620052__24650712___MPP6	0.206787	-2.27378	0.043177
chr7__24623666__24641868___MPP6	0.09673	-3.36989	0.020246
chr7__26725428__26739964___SKAP2	0.104806	-3.25421	0.02337
chr7__27785163__27796219___TAX1BP1	0.121653	-3.03916	0.030008
chr7__30323642__30326497___ZNRF2	0.120904	-3.04807	0.028772
chr7__30563731__30574881___LOC401320	0.142689	-2.80905	0.038619
chr7__32869984__32879942___KBTBD2	0.114961	-3.12078	0.023906
chr7__33015670__33035988___NT5C3A	0.102805	-3.28201	0.025058
chr7__35890668__35898383___SEPT7	0.243647	-2.03714	0.035121
chr7__40092965__40094396___CDK13	0.127451	-2.97199	0.032177
chr7__48410520__48412583___ABCA13	0.06342	-3.97892	0.018075
chr7__48466953__48489344___ABCA13	0.066022	-3.92092	0.018075
chr7__48466956__48489344___ABCA13	0.145192	-2.78397	0.048571
chr7__48511084__48528345___ABCA13	0.089921	-3.4752	0.020246
chr7__6187050__6190531___CYTH3	0.066842	-3.9031	0.018075
chr7__6580555__6585260___ZDHHC4	0.084278	-3.5687	0.019466
chr7__66991137__66994282___SBDS	0.102436	-3.28721	0.02556
chr7__73462922__73466401___BAZ1B	0.085835	-3.54229	0.020164
chr7__77083887__77098951___NA	0.078814	-3.6654	0.019072
chr7__77109938__77113483___NA	0.083309	-3.58538	0.019727
chr7__80646652__80677271___CD36	0.101142	-3.30555	0.023816
chr7__848418__849603___SUN1	0.140167	-2.83478	0.039402
chr7__87884979__87888059___DBF4	0.091126	-3.45599	0.020246
chr7__90604218__90623543___CDK14	0.124412	-3.0068	0.034797
chr7__91941095__91995800___AKAP9	0.099856	-3.324	0.024383
chr7__91992885__92014328___AKAP9	0.127604	-2.97026	0.036246
chr7__92076855__92083655___AKAP9	0.199688	-2.32418	0.025284
chr7__92294889__92362273___ANKIB1	0.158357	-2.65875	0.025392
chr7__93252653__93297243___CCDC132	0.187496	-2.41507	0.023008
chr7__93257394__93259632___CCDC132	0.086616	-3.52922	0.020098
chr7__93259550__93311272___CCDC132	0.141101	-2.8252	0.043721

chr7__93271220__93311272___CCDC132	0.171895	-2.5404	0.027784
chr7__93303460__93334197___CCDC132	0.103852	-3.26741	0.026296
chr7__93334117__93341575___CCDC132	0.103832	-3.26768	0.024309
chr8__100264034__100300651___RNF19A	0.104385	-3.26002	0.026601
chr8__103040798__103042407___ATP6V1C1	0.072342	-3.78903	0.018908
chr8__105419144__105444381___ZFPM2	0.089975	-3.47433	0.019072
chr8__106679210__106684359___OXR1	0.207529	-2.26862	0.035577
chr8__119783381__119791459___TAF2	0.249035	-2.00558	0.033493
chr8__120693692__120693908___SNTB1	0.139728	-2.83931	0.037563
chr8__123077111__123128513___TBC1D31	0.109643	-3.18912	0.024309
chr8__123325893__123336532___ATAD2	0.09775	-3.35475	0.024309
chr8__130134296__130169067___ASAP1	0.14356	-2.80027	0.046294
chr8__130136951__130187285___ASAP1	0.105211	-3.24864	0.024309
chr8__130152736__130188183___ASAP1	0.122463	-3.02958	0.031515
chr8__130214556__130236994___ASAP1	0.184753	-2.43633	0.031354
chr8__132746942__132757294___TMEM71	0.136993	-2.86783	0.038336
chr8__132803819__132825371___PHF20L1	0.087612	-3.51272	0.019681
chr8__140347757__140360193___TRAPPC9	0.065373	-3.93517	0.018075
chr8__140539320__140541358___AGO2	0.114518	-3.12636	0.026509
chr8__140830472__140864399___PTK2	0.191358	-2.38565	0.04196
chr8__140879471__140890769___PTK2	0.118587	-3.07598	0.0354
chr8__143640579__143641432___ZNF623	0.145848	-2.77746	0.04817
chr8__17195523__17221975___ZDHHC2	0.138941	-2.84746	0.014522
chr8__18799295__18804898___PSD3	0.172512	-2.53523	0.039611
chr8__21991868__22004030___XPO7	0.129604	-2.94781	0.018075
chr8__23566108__23568378___SLC25A37	0.06423	-3.96062	0.018075
chr8__26360169__26363890___PPP2R2A	0.080506	-3.63477	0.019466
chr8__26408000__26408376___BNIP3L	0.203351	-2.29796	0.031515
chr8__26410909__26411069___BNIP3L	0.099548	-3.32847	0.023102
chr8__27748077__27748598___CCDC25	0.094555	-3.4027	0.023102
chr8__31087776__31091898___WRN	0.155282	-2.68704	0.044985
chr8__38321072__38348143___WHSC1L1	0.133989	-2.89981	0.032384
chr8__42957094__42964474___HOOK3	0.090555	-3.46506	0.019072
chr8__42964311__42974194___HOOK3	0.132409	-2.91693	0.038055
chr8__47279862__47294030___SPIDR	0.12227	-3.03186	0.031515
chr8__47900373__47930787___PRKDC	0.129251	-2.95175	0.029366
chr8__47927194__47930787___PRKDC	0.14578	-2.77813	0.04183
chr8__53795647__53829533___ATP6V1H	0.115292	-3.11664	0.027784
chr8__58565019__58572314___SDCBP	0.119162	-3.069	0.028758
chr8__60794986__60808272___CHD7	0.110931	-3.17227	0.024437
chr8__61618978__61644632___ASPH	0.212996	-2.2311	0.035009
chr8__67095293__67113862___CSPP1	0.098174	-3.34852	0.022775
chr8__67103037__67159137___CSPP1	0.123187	-3.02108	0.0354
chr8__70583164__70594590___TRAM1	0.075584	-3.72577	0.018075
chr8__73738284__73739868___STAU2	0.126215	-2.98604	0.030471
chr8__85109595__85126837___LRRCC1	0.113529	-3.13887	0.032065

chr8__85138035__85138475___LRRCC1	0.172235	-2.53755	0.04082
chr8__85336945__85338449___CA1	0.113746	-3.13612	0.032478
chr8__92916929__92929574___TRIQK	0.102231	-3.29009	0.024751
chr8__96834973__96880005___CPQ	0.07507	-3.73562	0.018908
chr8__99013760__99064287___VPS13B	0.117915	-3.08418	0.033416
chr8__99096312__99136752___VPS13B	0.069438	-3.84813	0.018075
chr8__99134632__99275254___VPS13B	0.112478	-3.15228	0.028772
chr8__99142974__99275254___VPS13B	0.110125	-3.18278	0.02556
chr8__99156549__99193057___VPS13B	0.070288	-3.83057	0.018075
chr8__99467414__99481802___VPS13B	0.113744	-3.13614	0.026625
chr8__99556450__99585517___VPS13B	0.117323	-3.09144	0.026577
chr8__99556450__99661491___VPS13B	0.097258	-3.36204	0.024309
chr9__107306379__107318879___RAD23B	0.072726	-3.78139	0.018908
chr9__107321983__107325004___RAD23B	0.081963	-3.60887	0.0192
chr9__111433233__111444494___KIAA0368	0.128872	-2.95598	0.032933
chr9__112098470__112157613___SUSD1	0.147226	-2.7639	0.04235
chr9__112250929__112276013___PTBP3	0.092829	-3.42928	0.020813
chr9__112438431__112441770___HSDL2	0.057613	-4.11746	0.018075
chr9__120408347__120409316___CDK5RAP2	0.134853	-2.89054	0.034915
chr9__120439399__120448126___CDK5RAP2	0.095915	-3.3821	0.023008
chr9__120550792__120568388___CDK5RAP2	0.096273	-3.37672	0.023102
chr9__120996240__121008498___C5	0.080877	-3.62813	0.019072
chr9__121167489__121175224___CNTRL	0.135426	-2.88442	0.037829
chr9__121460104__121463328___GGTA1P	0.100604	-3.31324	0.024309
chr9__122280443__122291840___MRRF	0.160068	-2.64325	0.047357
chr9__123158332__123184298___STRBP	0.128203	-2.9635	0.034915
chr9__123757703__123769563___DENND1A	0.12092	-3.04787	0.019681
chr9__125298890__125302826___GAPVD1	0.107397	-3.21897	0.024976
chr9__125301983__125302826___GAPVD1	0.163903	-2.60908	0.034442
chr9__125341177__125342299___GAPVD1	0.11523	-3.11742	0.030273
chr9__125915686__125929845___PBX3	0.110368	-3.1796	0.024309
chr9__128185547__128187934___CIZ1	0.125206	-2.99763	0.038055
chr9__128907157__128909321___LRRC8A	0.131741	-2.92423	0.037237
chr9__132400035__132402828___TTF1	0.180012	-2.47384	0.039644
chr9__133042087__133043926___GTF3C5	0.071977	-3.79632	0.018908
chr9__17330632__17416189___CNTLN	0.190316	-2.39353	0.04967
chr9__17388162__17395069___CNTLN	0.282676	-1.82278	0.045562
chr9__19060088__19096769___HAUS6	0.084409	-3.56646	0.019072
chr9__19078176__19089559___HAUS6	0.119969	-3.05926	0.030247
chr9__19093171__19096769___HAUS6	0.305888	-1.70892	0.046445
chr9__19288596__19316839___DENND4C	0.12699	-2.97721	0.028715
chr9__19423862__19424841___ACER2	0.107147	-3.22234	0.023672
chr9__20360742__20365744___MLLT3	0.105517	-3.24446	0.026601
chr9__26861066__26887513___CAAP1	0.106068	-3.23694	0.022213
chr9__26923178__26928408___PLAA	0.102726	-3.28313	0.020886
chr9__34306252__34311371___KIF24	0.108881	-3.19918	0.025392

chr9__3630938__3633465___NA	0.123436	-3.01816	0.03908
chr9__36372496__36376127___RNF38	0.075733	-3.72293	0.018908
chr9__36657241__36674937___MELK	0.204536	-2.28957	0.040827
chr9__36669310__36674937___MELK	0.134242	-2.8971	0.035009
chr9__3668263__3674648___RP11-509J21.1	0.137342	-2.86416	0.038898
chr9__37842089__37861235___DCAF10	0.176158	-2.50506	0.038283
chr9__40994633__41011730___LOC100132352	0.076914	-3.70062	0.018908
chr9__4823548__4860901___RCL1	0.128295	-2.96247	0.019577
chr9__4892405__4966194___NA	0.075592	-3.72563	0.019072
chr9__5050686__5055788___JAK2	0.099099	-3.33498	0.023102
chr9__5066678__5090911___JAK2	0.048283	-4.37234	0.014522
chr9__68727596__68728934___PIP5K1B	0.25072	-1.99585	0.036508
chr9__68876677__68940790___PIP5K1B	0.101497	-3.30049	0.023799
chr9__6984166__7011879___KDM4C	0.150731	-2.72995	0.043862
chr9__6984166__7015929___KDM4C	0.104144	-3.26334	0.021999
chr9__77238002__77252352___VPS13A	0.265033	-1.91576	0.029897
chr9__77337255__77345142___VPS13A	0.103816	-3.26791	0.024309
chr9__77794463__77931856___GNAQ	0.121428	-3.04182	0.030247
chr9__79704783__79709699___TLE4	0.105349	-3.24676	0.025999
chr9__83677727__83683066___UBQLN1	0.107284	-3.22049	0.023218
chr9__83679775__83686155___UBQLN1	0.430908	-1.21455	0.028772
chr9__85575315__85646435___AGTPBP1	0.143394	-2.80195	0.036753
chr9__85959793__85996577___NAA35	0.070122	-3.83399	0.018908
chr9__86305192__86319670___ZCCHC6	0.136681	-2.87111	0.039729
chr9__89418056__89475550___SEMA4D	0.132242	-2.91875	0.031657
chr9__93013852__93018215___FGD3	0.13708	-2.86691	0.031879
chr9__95978061__95979866___LOC101928170	0.087537	-3.51396	0.020098
chr9__96364464__96368305___SLC35D2	0.089747	-3.47799	0.020246
chrX__101101058__101148161___CENPI	0.052531	-4.25068	0.015732
chrX__101101058__101161569___CENPI	0.093388	-3.42062	0.021477
chrX__10860043__10883281___MID1-2	0.060009	-4.05867	0.018075
chrX__10944205__11110981___MID1-2	0.075632	-3.72487	0.018075
chrX__11055936__11110981___MID1-2	0.145713	-2.7788	0.04371
chrX__11367771__11370505___ARHGAP6	0.114025	-3.13257	0.033493
chrX__118396970__118398470___WDR44	0.102114	-3.29175	0.022932
chrX__118442244__118444494___WDR44	0.101288	-3.30346	0.024309
chrX__118584735__118590302___DOCK11	0.278342	-1.84507	0.047816
chrX__120237455__120240355___NKAPP1	0.131497	-2.9269	0.030725
chrX__123686548__123712908___THOC2	0.128679	-2.95815	0.029436
chrX__1288519__1290509___CSF2RA	0.098847	-3.33866	0.024309
chrX__131709498__131722364___FIRRE	0.110114	-3.18294	0.024309
chrX__132382178__132406392___MBNL3	0.124874	-3.00145	0.026601
chrX__134413488__134417302___PHF6	0.100351	-3.31688	0.02524
chrX__13744415__13751368___OFD1	0.158231	-2.65989	0.047453
chrX__150638943__150649901___MTM1	0.098371	-3.34562	0.020213
chrX__150814862__150831293___CD99L2	0.133682	-2.90312	0.020426

chrX__155277134__155299145___CLIC2	0.065937	-3.92277	0.018075
chrX__155399001__155419562___NA	0.092232	-3.43858	0.020098
chrX__16698236__16702941___CTPS2	0.116068	-3.10695	0.02556
chrX__17103718__17106052___REPS2	0.090019	-3.47363	0.020246
chrX__1770497__1771629___NA	0.088875	-3.49208	0.020246
chrX__20193487__20195145___RPS6KA3	0.067348	-3.89223	0.018075
chrX__24723155__24743329___POLA1	0.071685	-3.80219	0.018152
chrX__24775197__24843677___POLA1	0.117364	-3.09093	0.02792
chrX__44931938__44934553___KDM6A	0.150571	-2.73148	0.043277
chrX__68192919__68201710___OPHN1	0.102927	-3.28031	0.02337
chrX__68511849__68513405___YIPF6	0.150413	-2.733	0.049262
chrX__68513327__68521497___YIPF6	0.235846	-2.08408	0.043109
chrX__71367499__71460803___TAF1	0.080198	-3.64029	0.019072
chrX__77557451__77664778___ATRX	0.101629	-3.29862	0.02337
chrX__77589834__77600564___ATRX	0.1208	-3.04931	0.033416
chrX__77656560__77664778___ATRX	0.110828	-3.1736	0.028302
chrX__77681520__77685006___ATRX	0.194242	-2.36407	0.044981
chrX__77829031__77830895___MAGT1	0.069918	-3.83819	0.018908
chrX__77971621__77989958___ATP7A	0.148725	-2.74928	0.046319
chrX__77971621__78003236___ATP7A	0.406712	-1.29792	0.038892
chrX__78009102__78021079___ATP7A	0.098325	-3.34629	0.025392
chrX__80288906__80310233___CHMP1B2P	0.102504	-3.28625	0.025392
chrY__12709388__12722187___USP9Y	0.121956	-3.03557	0.031515
chrY__19041370__19045288___NA	0.117135	-3.09375	0.034864
chrY__20579608__20588105___EIF1AY	0.128749	-2.95736	0.034442

Appendix O

Approval

Human Research Ethics Committee

Federation UNIVERSITY • AUSTRALIA

Principal Researcher:	Professor Fergal Grace
Other/Student Researcher/s:	Professor Fadi Charchar Dr Brendan O'Brien
School/Section:	**School of Health Science & Psychology/Human Movement & Sports Science**
Project Number:	**A17-134**
Project Title:	**Characterisation of candidate epigenetic signatures that differentiate the response to strength and fitness training in athletes and novice exercisers.**
For the period:	04/12/2017 to 01/09/2018

Quote the Project No: A17-134 in all correspondence regarding this application.

Approval has been granted to undertake this project in accordance with the proposal submitted for the period listed above.

Please note: It is the responsibility of the Principal Researcher to ensure the Ethics Office is contacted immediately regarding any proposed change or any serious or unexpected adverse effect on participants during the life of this project.

In Addition: Maintaining Ethics Approval is contingent upon adherence to all Standard Conditions of Approval as listed on the final page of this notification

COMPLIANCE REPORTING DATES TO HREC:

Final project report:
1 October 2018

The combined annual/final report template is available at:
http://federation.edu.au/research-and-innovation/research-support/ethics/human-ethics/human-ethics3

Fiona Koop
Ethics Officer
4 December 2017
Please note the standard conditions of approval on Page 2:

Approval

Human Research Ethics Committee

Federation UNIVERSITY • AUSTRALIA

STANDARD CONDITIONS OF APPROVAL

1. Conduct the project strictly in accordance with the proposal submitted and granted ethics approval, including any amendments made to the proposal required by the HREC.

2. Advise (email: research.ethics@federation.edu.au) immediately of any complaints or other issues in relation to the project which may warrant review of the ethical approval of the project.

3. Where approval has been given subject to the submission of copies of documents such as letters of support or approvals from third parties, these are to be provided to the Ethics Office prior to research commencing at each relevant location.

4. Submission for approval of amendments to the approved project before implementing such changes. A combined amendment template covering the following is available on the HRE website: http://federation.edu.au/research/research-support/ethics/human-ethics/human-ethics3
   - Request for Amendments
   - Request for Extension. Note: Extensions cannot be granted retrospectively.
   - Changes to Personnel

5. Annual Progress reports on the anniversary of the approval date and a Final report within a month of completion of the project are to be submitted by the due date each year for the project to have continuing approval.

6. If, for any reason, the project does not proceed or is discontinued, advise the committee by completing the Final report form.

7. Notify the Ethics Office of any changes in contact details including address, phone number and email address for any member of the research team.

8. The HREC may conduct random audits and / or require additional reports concerning the research project as part of the requirements for monitoring, as set out in the National statement on Ethical Conduct in Human Research.

Failure to comply with the *National Statement on Ethical Conduct in Human Research* (2007) and with the conditions of approval will result in suspension or withdrawal of approval.